



University  
of Glasgow

Srivastava, Anubhav (2014) *Comparative metabolomics of erythroid lineage and Plasmodium life stages reveal novel host and parasite metabolism*. PhD thesis.

<http://theses.gla.ac.uk/5725/>

Copyright and moral rights for this thesis are retained by the author

A copy can be downloaded for personal non-commercial research or study, without prior permission or charge

This thesis cannot be reproduced or quoted extensively from without first obtaining permission in writing from the Author

The content must not be changed in any way or sold commercially in any format or medium without the formal permission of the Author

When referring to this work, full bibliographic details including the author, title, awarding institution and date of the thesis must be given

# Comparative metabolomics of erythroid lineage and *Plasmodium* life stages reveal novel host and parasite metabolism

Anubhav Srivastava, M.Sc.

This thesis is submitted in fulfilment of the requirements for the degree of Doctor of Philosophy

July 2014



University  
of Glasgow

Institute of Infection, Immunity & Inflammation

College of Medicine, Veterinary Medicine & Life Sciences

Wellcome Trust Centre for Molecular Parasitology

University of Glasgow, Glasgow, U.K.

## Abstract

Malaria, caused by the Apicomplexan parasite *Plasmodium* is a deadly disease which poses a huge health and economic burden over many populations in the world, mostly in sub-Saharan Africa and Asia. To design new intervention strategies and to improve upon existing drugs against malaria, it is important to understand the biochemistry of the *Plasmodium* parasite and its interaction with the host.

We used metabolomics to dissect the biology of the reticulocyte preferring rodent malaria parasite *Plasmodium berghei* and showed that metabolic reserves in the reticulocytes can aid in survival of malaria parasites when their metabolism is genetically or chemically disrupted, pointing towards a direct role of host cell metabolism in parasite survival. These results have implications for currently used ways of intermediation in malaria infections which target only parasite metabolism against the human malaria parasites, *Plasmodium vivax* which prefers to infect reticulocytes and *Plasmodium falciparum* which is capable of infecting all erythrocytes.

We also used metabolomics to show the biochemical differences between the asexual and sexual stages of *P. berghei* parasites and our data gave additional insights into the preparatory phase of the gametocyte stage at the metabolic level with the discovery of a phosphagen system which plays a role in gametogenesis. Targeted metabolomics of *P. berghei* life stages using isotopic labelling showed that TCA cycle metabolism is predominant in the mosquito stages. Discovery of a reductive arm of TCA metabolism in reticulocytes pointed towards the existence of rudimentary mitochondria in young erythrocytes. Another surprising discovery was the presence of up regulated  $\gamma$ -Aminobutyric acid (GABA) metabolism in the ookinete stage in *P. berghei* which may act as an energy source during the ookinete to oocyst transition in the mosquito. This pathway presented novel candidates for transmission blocking.

## Author's Declaration

I, Anubhav Srivastava hereby declare that I am the sole author of this thesis and I have performed all of the work presented here, with the following exceptions:

1. **Sections 2.6 and 2.7.** All samples for LC-MS analysis were run by the Glasgow Polyomics facility, University of Glasgow, Glasgow and all samples for GC-MS analysis were run by the Metabolomics Australia facility, University of Melbourne, Australia. LC-MS data analysis for untargeted metabolomics was done under the supervision of Dr. Darren Creek and in collaboration with Prof. Mike Barrett, University of Glasgow, Glasgow. GC-MS data analysis of isotopically labeled *P. berghei* parasites was under the supervision of Dr. Jim MacRae and in collaboration with Prof. Malcolm McConville from University of Melbourne, Australia.
2. **Section 6.2.1.** MS/MS analysis of phosphocreatine from *P. berghei* gametocyte extracts and commercially acquired phosphocreatine was done by Dr. Karl Burgess, Glasgow Polyomics facility, University of Glasgow, Glasgow.

## Acknowledgements

I am extremely grateful to Prof. Andy Waters for providing me the opportunity to undertake my PhD under his supervision and for his continuous support, valuable time and advice over the last few years. I want to thank my assessors Prof. Sylke Muller and Prof. Markus Meissner for their useful suggestions and helping me to focus on specific aspects in this study. I also wish to thank Prof. Mike Barrett for taking out the time to discuss my data, suggest experiments and proof-reading this thesis.

This work could not have been made possible without the great support system that is the entire Waters group. I want to thank Anne Graham and Rachael Cameron for their great help during the initial stages of the experiments and for always standing up to offer a hand when there is a need without even thinking twice, whether or not I realize it. Special thanks to Nisha Philip for numerous impromptu discussions, brainstorming ideas and very useful insights into the parasite biology which helped me shape my hypotheses. I also want to thank Sonya Taylor and Mhairi Stewart who made working in our office a lot of fun and answered my *Toxoplasma* or *Trypanosoma* related queries. I wish to thank Katie Hughes for always asking the most intriguing questions and helping with the initial flow cytometry set ups. I want to extend a big thank you to Agnieszka Religa for sharing her unpublished RNA Seq data and being the chirpy, ever-smiling herself in the gloomy Glasgow weather. I wish to thank Abhinav Sinha and Harshal Patil for helping me in the lab and the JRF and discussing both Biology and Bollywood. I also want to thank Angela McBride and Nicola Mamczur for brilliantly looking after the mosquitoes and providing material for experiments as and when required.

I wish to thank Darren Creek and Jim MacRae for patiently teaching me MS data analysis and Prof. Malcolm McConville for inviting me to the University of Melbourne to work with Metabolomics Australia. I wish to thank Tanita Casci and Karl Burgess for making sure all my samples ran smoothly and efficiently at the Glasgow Polyomics facility. I also wish to thank Colin, Margaret, Gary, David and Maurice for taking great care of the animals at the JRF and helping out on the weekends.

I wish to thank the University of Glasgow for providing me with the Staff Research Scholarship, Prof. Andy Waters for supporting my PhD tuition and EVIMalaR for two OzMalNet travel awards to travel to Australia.

A huge thank you to my parents and family who don't really get to see me a lot due to my work but without whose unending support, I wouldn't have been able to get this far.

And a big thanks to my lovely wife Sonya for being the pillar of support throughout my PhD and beyond. She reinstated the sense of motivation when I seemed to lose mine and sometimes her selfless love, care (and cheesecakes!) were all that kept me going.

Anubhav Srivastava

31<sup>st</sup> July 2014

## Table of Contents

Abstract .....	i
Author's declaration .....	ii
Acknowledgements .....	iii
Table of Contents .....	v
List of Figures .....	x
List of Tables .....	xiv
Abbreviations .....	xv
1 Introduction.....	1
1.1 Malaria .....	1
1.2 <i>Plasmodium berghei</i> as a model.....	4
1.2.1 Pre-erythrocytic development.....	5
1.2.2 Asexual blood stages .....	6
1.2.3 Gametocytes: the sexual precursor cells .....	6
1.2.4 Mosquito stages .....	7
1.3 Reticulocyte biology.....	7
1.3.1 Reticulocytes vs normocytes.....	7
1.3.2 Reticulocytes as the preferred host cell type for some <i>Plasmodium</i> species 7	
1.4 Metabolism in <i>Plasmodium</i> and host erythrocytes.....	8
1.4.1 Glycolysis .....	9
1.4.2 TCA cycle .....	10
1.4.3 Electron Transport Chain .....	10
1.4.4 Fatty Acid synthesis .....	11
1.4.5 Pentose Phosphate Pathway .....	12
1.5 Metabolomics.....	13
1.5.1 Metabolomics: a post genomics launch-pad .....	13
1.5.2 Metabolomics: what it has to offer? .....	13
1.5.3 Metabolomics: contributions in different biological systems .....	14
1.5.4 Metabolomics platforms .....	16
1.5.5 Metabolomics: Untargeted and Targeted approaches.....	17
1.5.6 Metabolomics: Data generation, storage and interpretation .....	18

1.5.7	Role of metabolomics in functional genomics.....	20
1.5.8	Role of metabolomics in systems biology .....	21
1.5.9	Metabolomics of protozoan parasites.....	22
1.5.10	Metabolomics in malaria research: a road just taken .....	23
1.6	Aims and objectives .....	25
1.6.1	Finding out metabolic differences between reticulocytes and normocytes.....	25
1.6.2	Elucidating the role of reticulocyte as a specialized host cell.....	25
1.6.3	Establishing key metabolic differences between <i>Plasmodium</i> asexual, gametocyte and mosquito stages .....	25
2	Methods.....	27
2.1	<i>P. berghei</i> methods.....	27
2.1.1	Infection of laboratory animals with <i>P. berghei</i> parasites .....	27
2.1.2	Transfection of <i>P. berghei</i> parasites.....	27
2.1.3	Selection of transfected parasites .....	28
2.1.4	Cryopreservation of blood stage parasites.....	28
2.1.5	Investigation of the course of parasitemia .....	28
2.1.6	Removal of leucocytes from blood or cultured parasites.....	28
2.1.7	Short term <i>in vitro</i> culture of asexual blood stage parasites for making schizonts .....	29
2.1.8	Purification of schizonts.....	29
2.1.9	Generation of knockout parasites.....	30
2.1.10	Cloning transfected parasite populations.....	30
2.1.11	Preparation of purified parasites for isolation of DNA and protein .	31
2.1.12	Genomic DNA extraction .....	31
2.1.13	Asexual growth competition assay .....	32
2.1.14	Lethality experiments in C57/B6 mice .....	32
2.1.15	Gametocyte conversion monitoring by FACS during blood stage growth	32
2.1.16	Exflagellation assay and DNA quantification by FACS .....	33
2.1.17	<i>in vitro</i> culture of ookinetes .....	33
2.1.18	<i>in vitro</i> sexual crosses.....	33
2.1.19	Mosquito transmission experiments.....	34
2.1.20	Determination of IC <sub>50</sub> value of <i>P. berghei</i> inhibitors <i>in vitro</i> .....	34
2.2	Determination of IC <sub>50</sub> value of <i>P. falciparum</i> asexual growth inhibition <i>in vitro</i> .....	36

2.3	Molecular biology .....	36
2.3.1	Preparation of DNA constructs.....	36
2.3.2	Checking for integration of transfectants by PCR .....	39
2.3.3	Western blot analysis .....	40
2.4	Immunofluorescence assay (IFA) .....	43
2.5	Reticulocyte methods.....	43
2.5.1	Enrichment of reticulocytes in mice and rats .....	43
2.5.2	Monitoring reticulocyte production .....	44
2.5.3	Obtaining a pure population of reticulocytes .....	44
2.6	Untargeted Metabolomics methods using LC-MS & GC-MS.....	45
2.6.1	Uninfected reticulocyte enriched and un-enriched red blood cell preparation .....	45
2.6.2	<i>P. berghei</i> schizonts (Gametocyte Producer and gametocyte non-producer) whole cells, lysed parasites and lysis supernatant preparation ..	46
2.6.3	<i>P. berghei</i> gametocytes: whole cell, lysed parasite and lysis supernatant preparation .....	47
2.6.4	Metabolite Extraction, drying and storage.....	48
2.6.5	LC-MS analysis.....	48
2.6.6	GC-MS analysis .....	49
2.7	Targeted metabolomics methods using GC-MS .....	50
2.7.1	Cultures using minimal media and labelled carbon source.....	50
2.7.2	Isotopic labelling of <i>P. berghei</i> asexual cultures .....	51
2.7.3	Isotopic labelling of <i>P. berghei</i> gametocytes <i>in vitro</i> .....	52
2.7.4	Isotopic labelling of <i>P. berghei</i> ookinete cultures .....	53
2.7.5	Metabolite Extraction, drying and storage.....	53
2.7.6	Targeted GC-MS analysis.....	54
3	Comparative metabolomics of erythroid lineage reveals that reticulocytes provide metabolic reserves for <i>Plasmodium</i> parasites.....	56
3.1	Introduction .....	56
3.2	Results.....	57
3.2.1	The reticulocyte metabolome is more complex and abundant than the mature erythrocyte .....	57
3.2.2	The reticulocyte metabolome reflects its ongoing developmental programme.....	60
3.2.3	Features of intermediary carbon metabolism (ICM) are dispensable in asexual blood stage <i>P. berghei</i> .....	63

3.2.4	Pyrimidine biosynthesis pathway can be disrupted in asexual <i>P. berghei</i> development.....	71
3.3	Discussion .....	82
3.3.1	Intermediary Carbon Metabolism (ICM) .....	83
3.3.2	Pyrimidine biosynthesis.....	84
3.3.3	Other metabolic pathways enriched in reticulocytes .....	87
3.3.4	Phylogenetic analyses of the key metabolic enzymes .....	90
3.4	Conclusions .....	90
4	<i>Plasmodium</i> metabolism is stage specific .....	92
4.1	Introduction .....	92
4.2	Results.....	93
4.2.1	<i>P. berghei</i> schizonts vs uninfected reticulocyte enriched erythrocytes .....	94
4.2.2	<i>P. berghei</i> gametocytes vs uninfected reticulocyte enriched erythrocytes .....	96
4.2.3	<i>P. berghei</i> gametocytes vs schizonts .....	97
4.3	Observations.....	98
5	Central Carbon metabolism in <i>Plasmodium</i> .....	101
5.1	Introduction .....	101
5.2	Results.....	104
5.2.1	Asexual blood stages .....	107
5.2.2	Gametocytes .....	119
5.2.3	Ookinetes .....	132
5.2.4	Evidence of a partial GABA shunt in <i>P. berghei</i> .....	144
5.3	Discussion .....	147
5.3.1	Asexual blood stages .....	147
5.3.2	Reductive carboxylation in reticulocytes during TCA metabolism ..	148
5.3.3	Gametocytes .....	149
5.3.4	Ookinetes .....	150
5.3.5	GABA as an energy source in ookinete stage .....	151
5.4	Conclusions .....	153
6	Phosphocreatine is a potential energy reserve in <i>P. berghei</i> gametocytes.	155
6.1	Introduction .....	155
6.1.1	Phosphagen energy system.....	155
6.1.2	Creatine kinase .....	156
6.2	Results.....	157

6.2.1	Gametocytes store phosphocreatine.....	157
6.2.2	Creatine kinase is not encoded by <i>P. berghei</i> .....	158
6.2.3	Creatine kinase enzyme activity is present in UIR and PBIR .....	159
6.2.4	Creatine kinase could not be detected using a specific antibody ..	160
6.2.5	Creatine kinase inhibition: effect on <i>P. berghei</i> development .....	162
6.3	Discussion .....	166
6.4	Conclusion .....	167
7	Summary .....	168
8	Future work .....	170
8.1	Pantothenate metabolism .....	170
8.2	Carnitine derivatives .....	172
8.3	<i>Plasmodium</i> specific metabolic pathways .....	173
9	Appendix .....	174
10	References .....	223
11	Publication .....	239

## List of Figures

Figure 1-1 Global distribution of malaria and percentage population at risk. ....	1
Figure 1-2 Distribution of reported malaria in patient deaths.....	1
Figure 1-3 Life cycle of malaria parasite .....	2
Figure 1-4 Distribution of <i>P. falciparum</i> and <i>P. vivax</i> in the world .....	3
Figure 2-1 Competition growth assay of <i>P. berghei</i> line using FACS analysis.....	32
Figure 2-2 Schematic representation of diagnostic PCR to detect correct integration in modified parasite genome .....	40
Figure 3-1 Dynamics of reticulocyte enrichment in peripheral blood <i>in vivo</i> followed by Phenylhydrazine-HCl treatment of mice. ....	58
Figure 3-2 Volcano plot showing distribution of putative metabolites according to their fold change in abundance in uninfected reticulocyte enriched erythrocytes vs uninfected normocyte enriched erythrocytes.....	60
Figure 3-3 Presence of mitochondrial signal in reticulocytes.....	61
Figure 3-4 Reticulocytes provide metabolic reserves to <i>P. berghei</i> parasites....	62
Figure 3-5 Fold change of metabolites of central carbon metabolism and pyrimidine biosynthesis in rodent reticulocytes compared to normocytes. ....	63
Figure 3-6 Schematic representation of intermediary carbon metabolism (ICM) in <i>Plasmodium</i> . ....	64
Figure 3-7 Schematic representation of gene deletion and confirmation by PCR for generating ICM mutants .....	66
Figure 3-8 Asexual stage phenotypic analyses of ICM mutants. ....	67
Figure 3-9 Effect on gametocytogenesis and gamete formation in ICM mutants.	68
Figure 3-10 <i>in vitro</i> ookinete conversion in ICM mutants.....	69
Figure 3-11 Mosquito infectivity of ICM mutants.....	70
Figure 3-12 Representative images of mosquito infectivity of ICM mutants....	71
Figure 3-13 Schematic representation of pyrimidine biosynthesis pathway in <i>Plasmodium</i> . ....	72
Figure 3-14 Schematic representation of gene deletion and confirmation by PCR for generating pyrimidine biosynthesis mutants .....	74
Figure 3-15 Asexual stage phenotypic analyses of Pyrimidine biosynthesis mutants. ....	75
Figure 3-16 Effect on gametocytogenesis and gamete formation in Pyrimidine biosynthesis mutants.....	76
Figure 3-17 <i>in vitro</i> ookinete conversion in Pyrimidine biosynthesis mutants....	77
Figure 3-18 Mosquito infectivity of Pyrimidine synthesis mutant parasites compared to wt. ....	78
Figure 3-19 Representative images of mosquito infectivity of Pyrimidine biosynthesis mutant parasites compared to wt. ....	79
Figure 3-20 Mosquito infectivity of <i>in vivo</i> crossed Pb270 x <i>oprt</i> <sup>-</sup> and Pb270 x <i>ompdc</i> <sup>-</sup> mutant parasites compared to wt .....	80
Figure 3-21 Genotypic analyses of transmitted parasites obtained after exposure of naïve mice to mosquitoes infected with <i>in vivo</i> crossed Pb270 x <i>oprt</i> <sup>-</sup> and Pb270 x <i>ompdc</i> <sup>-</sup> mutant parasites compared to wt.....	81

Figure 3-22 <i>P. berghei</i> and <i>P. falciparum</i> inhibition by Dihydroartemisinin (DHA) and 5-Fluoroorotic Acid (5FOA) <i>in vitro</i> .....	82
Figure 3-23 Schematic representation of Glutathione synthesis pathway in <i>Plasmodium</i> . ....	88
Figure 4-1 Volcano plot showing distribution of putative metabolites according to their fold change in abundance in <i>P. berghei</i> schizonts vs reticulocyte enriched erythrocytes.....	95
Figure 4-2 Volcano plot showing distribution of putative metabolites according to their fold change in abundance in <i>P. berghei</i> gametocytes vs uninfected reticulocyte enriched erythrocytes. ....	97
Figure 4-3 Volcano plot showing distribution of putative metabolites according to their fold change in abundance in Gametocytes vs Schizonts. ....	98
Figure 5-1 Schematic representation of Glycolysis .....	102
Figure 5-2 Schematic representation of TCA cycle .....	102
Figure 5-3 Schematic representation of the flow of carbon skeletons through the glycolytic and TCA cycle pathways. ....	105
Figure 5-4 Heat map showing enrichment .....	106
Figure 5-5 <sup>13</sup> C U-Glucose labelling of glycolytic intermediates in <i>P. berghei</i> asexual stages.....	111
Figure 5-7 Fraction labelling of TCA cycle isotopomers at the 24h time point in <i>P. berghei</i> infected reticulocyte enriched erythrocytes (PBIR)- schizont stage and similarly incubated uninfected reticulocyte enriched erythrocytes (UIR)cultured in the presence of <sup>13</sup> C U-Glucose.....	112
Figure 5-8 <sup>13</sup> C <sup>15</sup> N U-Glutamine labelling of glycolytic intermediates in <i>P. berghei</i> asexual stages.....	117
Figure 5-10 Fraction labelling of TCA cycle isotopomers at the 24h time point in <i>P. berghei</i> infected reticulocyte enriched erythrocytes (PBIR)- schizont stage and similarly incubated uninfected reticulocyte enriched erythrocytes (UIR)cultured in the presence of <sup>13</sup> C <sup>15</sup> N U-Glutamine. ....	118
Figure 5-11 <sup>13</sup> C U-Glucose labelling of glycolytic intermediates in purified <i>P. berghei</i> gametocytes during activation. ....	121
Figure 5-12 <sup>13</sup> C U-Glucose labelling of TCA cycle intermediates in <i>P. berghei</i> gametocytes during activation. ....	124
Figure 5-13 Fraction labelling of TCA cycle isotopomers in <i>P. berghei</i> gametocytes during activation in the presence of <sup>13</sup> C U-Glucose. ....	126
Figure 5-14 <sup>13</sup> C <sup>15</sup> N U-Glutamine labelling of glycolytic intermediates in <i>P. berghei</i> gametocytes during activation. ....	127
Figure 5-15 <sup>13</sup> C <sup>15</sup> N U-Glutamine labelling of TCA cycle intermediates in <i>P. berghei</i> gametocytes during activation. ....	130
Figure 5-16 Fraction labelling of TCA cycle isotopomers in <i>P. berghei</i> gametocytes during activation in the presence of <sup>13</sup> C <sup>15</sup> N U-Glutamine .....	132
Figure 5-17 <sup>13</sup> C U-Glucose labelling of glycolytic intermediates in purified <i>P. berghei</i> ookinetes and unfertilised female gametes. ....	133
Figure 5-18 <sup>13</sup> C U-Glucose labelling of TCA cycle intermediates in purified <i>P. berghei</i> ookinetes and unfertilised female gametes. ....	136

Figure 5-19 Fraction labelling of TCA cycle isotopomers in purified <i>P. berghei</i> ookinetes and unfertilised female gametes in the presence of $^{13}\text{C}$ U-Glucose. .	138
Figure 5-20 $^{13}\text{C}^{15}\text{N}$ U-Glutamine labelling of glycolytic intermediates in purified <i>P. berghei</i> ookinetes and unfertilised female gametes. ....	139
Figure 5-21 $^{13}\text{C}^{15}\text{N}$ U-Glutamine labelling of TCA cycle intermediates in purified <i>P. berghei</i> ookinetes and unfertilised female gametes. ....	142
Figure 5-22 Fraction labelling of TCA cycle isotopomers in purified <i>P. berghei</i> ookinetes and unfertilised female gametes in the presence of $^{13}\text{C}^{15}\text{N}$ U-Glutamine. ....	144
Figure 5-23 $^{13}\text{C}^{15}\text{N}$ U-Glutamine labelling of GABA in <i>P. berghei</i> asexual stages. ....	145
Figure 5-24 $^{13}\text{C}^{15}\text{N}$ U-Glutamine labelling of GABA in purified <i>P. berghei</i> gametocytes during activation. ....	146
Figure 5-25 $^{13}\text{C}^{15}\text{N}$ U-Glutamine labelling of GABA in purified <i>P. berghei</i> ookinetes and unfertilised female gametes. ....	147
Figure 5-26 Model of GABA metabolism in <i>P. berghei</i> ookinetes. ....	153
Figure 6-1 Creatine kinase interconverts phosphocreatine into creatine .....	156
Figure 6-2 Fold change of Creatine and Phosphocreatine as observed in different sample groups compared in the untargeted metabolomics study. ....	157
Figure 6-3 MS/MS fragmentation for identification of phosphocreatine. ....	158
Figure 6-4 Creatine kinase isoforms in <i>Mus musculus</i> .....	159
Figure 6-5 Creatine kinase activity assay. ....	160
Figure 6-6 Antibody ab76506 from Abcam was raised against a 91 amino acid fragment of human Mtck (in red) conserved in the mouse mitochondrial isoform. ....	161
Figure 6-7 Western blot analysis using ab76506 showing titration of protein content from positive controls. ....	162
Figure 6-8 Exflagellation inhibition and rescue. ....	163
Figure 6-9 Immunoflorescence assay .....	164
Figure 6-10 Effect of ATP/ADP translocase inhibition. ....	165
Figure 8-1 Fold change of Pantothenate and Phosphopantothenate as observed in different sample groups compared in the untargeted metabolomics study. ....	171
Figure 9-1 Volcano plot showing the distribution of abundance of all 4560 peaks detected in uninfected reticulocyte enriched erythrocytes as compared to uninfected normocyte enriched erythrocytes in rodent blood. ....	174
Figure 9-2 Volcano plot showing the distribution of abundance of all ~5000 peaks detected in <i>P. berghei</i> schizonts as compared to uninfected reticulocyte enriched erythrocytes. ....	174
Figure 9-3 Volcano plot showing the distribution of abundance of all ~5000 peaks detected in <i>P. berghei</i> gametocytes as compared to uninfected reticulocyte enriched erythrocytes. ....	175
Figure 9-4 Volcano plot showing the distribution of abundance of all ~5000 peaks detected in <i>P. berghei</i> gametocytes as compared to <i>P. berghei</i> schizonts. ....	175
Figure 9-5 Phylogenetic analyse of key metabolic enzymes in <i>Plasmodium</i> spp. ....	177

Figure 9-6 Schematic representation of gene deletion and confirmation by PCR  
for generation of *aconitase*<sup>-</sup> mutants..... 178

## List of Tables

Table 1 SDS-PAGE resolving and stacking gel composition .....	41
Table 2 Putative metabolites (PMs) represented in Figure 3-2 showing fold change in abundance in uninfected reticulocyte enriched erythrocytes compared to normocyte enriched erythrocytes. ....	179
Table 3 Putative metabolites (PMs) represented in Figure 4-1 showing fold change in abundance in mature schizonts compared to uninfected reticulocyte enriched erythrocytes. ....	187
Table 4 Putative metabolites (PMs) represented in Figure 4-2 showing fold change in abundance in Gametocytes compared to uninfected reticulocyte enriched erythrocytes. ....	198
Table 5 Putative metabolites (PMs) represented in Figure 4-3 showing fold change in abundance in <i>P. berghei</i> gametocytes compared to <i>P. berghei</i> schizonts. ....	209
Table 6 List of Primers used for PCR .....	220
Table 7 E-value for each metabolic enzyme compared between different species of <i>Plasmodium</i> after doing BLAST with the corresponding <i>P. berghei</i> amino acid sequence.....	221

## Abbreviations

°C	Degrees Celsius
μ	Micro
μg	Microgram
μl	Microliter
μM	Micromolar
μm	Micrometer
μmol	Micromoles
3' UTR	Three Prime Untranslated Region
5' UTR	Five Prime Untranslated Region
5-FC	5-Fluorocytosine
5FOA	5-Fluoroorotate
<i>aat</i>	Aspartate Amino Transferase
<i>act</i>	Aspartate Carbamoyltransferase
ADP	Adenosine Diphosphate
AMP	Adenosine Monophosphate
APC	Allophycocyanin
APS	Ammonium Per-Sulphate
ATP	Adenosine Tri Phosphate
BA	Bongrekic Acid
BBD	Butyrobetaine Dioxygenase
BCKDH	Branched Chain A-Keto Acid Dehydrogenase
bp	Base Pairs
BSA	Bovine Serum Albumin
CA	Carboxyatractyloside
CD71	Transferrin Receptor
CDP	Cytidine Diphosphate
CE	Capillary Electrophoresis
<i>ck</i>	Creatine Kinase

CoA	Coenzyme A
<i>cpsII</i>	Carbamoyl Phosphate Synthetase II
Cr	Creatine
Cyt-ck	Cytoplasmic Creatine Kinase
DAPI	4',6-Diamidino-2-Phenylindole
dCDP	Deoxycytidine Diphosphate
dCTP	Deoxycytidine Triphosphate
ddH <sub>2</sub> O	Double Distilled Water
DHFR/TS	Dihydrofolate Reductase-Thymidylate Synthase
<i>dhoase</i>	Dihydroorotase
<i>dhodh</i>	Dihydroorotate Dehydrogenase
DMSO	Dimethyl Sulphoxide
DNA	Deoxyribonucleic Acid
dNTP	Deoxynucleotide Triphosphate
DTT	Dithiothreitol
dTTP	Deoxythymidine Triphosphate
dUDP	Deoxyuridine Diphosphate
dUTP	Deoxyuridine Triphosphate
ECL	Enhanced Chemiluminescence
ECM	Experimental Cerebral Malaria
EDTA	Ethylene Diamine Tetraacetic Acid
EGTA	Ethylene Glycol Tetraacetic Acid
ePBS	Enriched Phosphate Buffered Saline
ETC	Electron Transport Chain
FACS	Fluorescence-Activated Cell Sorting
FAS II	Fatty Acid Synthesis Type II
FBS	Foetal Bovine Serum
FCS	Foetal Calf Serum
FDNB	1-Fluoro-2,4-Dinitrobenzene

g	Grams
g	Relative Centrifugal Force
G6PDH	Glucose-6-Phosphate Dehydrogenase
GABA	$\gamma$ -Aminobutyric Acid
GC	Gas Chromatography
gDNA	Genomic Deoxyribonucleic Acid
GFP	Green Fluorescent Protein
GOI	Gene Of Interest
GR	Glutathione Reductase
GS	Glutathione Synthetase
GSH	Glutathione (Reduced)
GSSG	Glutathione Disulphide (Oxidized)
GST	Glutathione-S-Transferase
<i>hdf</i>	Human Dihydrofolate Reductase
HEPES	4-(2-Hydroxyethyl)-1-Piperazineethanesulfonic Acid
HPLC	High Performance Liquid Chromatography
HRP	Horseradish Peroxidase
HTMLA	3-Hydroxy- N-Trimethyl-Lysine Aldolase
IC <sub>50</sub>	Inhibitory Concentration For 50 % Growth Inhibition
IFA	Immunofluorescence Assay
IPP	Isopentenyl Pyrophosphate
kb	Kilobases
kDa	Kilodaltons
KHCO <sub>3</sub>	Potassium Bicarbonate
ko	Knockout
LMRG	Leiden Malaria Research Group
m	Meter
m	Milli
M	Molar

MACS	Magnet Activated Cell Sorting
<i>mdh</i>	Malate Dehydrogenase
mg	Milligram
MgCl <sub>2</sub>	Magnesium Chloride
min	Minute
ml	Milliliter
mM	Millimolar
MR4	Malaria Research And Reference Reagent Resource Center
MS	Mass Spectrometry
MSI	Metabolomics Standards Initiative
MSPs	Merozoite Surface Proteins
<i>Mt-ck</i>	Mitochondrial Creatine Kinase
n	Nano
NaCl	Sodium Chloride
NAD <sup>+</sup>	Nicotinamide Adenine Dinucleotide (Oxidized)
NADH	Nicotinamide Adenine Dinucleotide (Reduced)
NADP	Nicotinamide Adenine Dinucleotide Phosphate
NADP <sup>+</sup>	Nicotinamide Adenine Dinucleotide Phosphate (Oxidized)
NADPH	Nicotinamide Adenine Dinucleotide Phosphate (Reduced)
ng	Nanogram
NH <sub>4</sub> Cl	Ammonium Chloride
nm	Nanometer
nM	Nanomolar
NMR	Nuclear Magnetic Resonance
N-terminal	Amino Terminal
OD	Optical Density
<i>ompdc</i>	Orotidine 5'-Monophosphate Decarboxylase
<i>oprt</i>	Orotate Phosphoribosyltransferase

ORF /orf	Open Reading Frame
PAGE	Polyacrylamide Gel Electrophoresis
PanK	Pantothenate Kinase
PBS	Phosphate Buffered Saline
PBIR	<i>P. berghei</i> infected reticulocyte enriched erythrocytes
PC	Phosphatidylcholine
PCR	Polymerase Chain Reaction
PCr	Phosphocreatine
PDH	Pyruvate Dehydrogenase
PE	Phosphatidylethanolamine
<i>pepc</i>	Phosphoenolpyruvate Carboxylase
PfEBAs	<i>P. falciparum</i> Erythrocyte Binding Antigens
phz	Phenylhydrazine-Hydrochloride
PL	Phospholipid
pmol	Picomole
PPP	Pentose Phosphate Pathway
PV	Parasitophorous Vacuole
RBC	Red Blood Cell
RBP	Reticulocyte Binding Protein
RFP	Red Fluorescent Protein
RNA	Ribonucleic Acid
ROS	Reactive Oxygen Species
SD	Standard Deviation
SDS	Sodium Dodecyl Sulphate
sec	Seconds
SM	Selectable Marker
TBE	Tris-Borate Containing EDTA
TCA cycle	Tri-Carboxylic Acid Cycle
TE	Tris Containing EDTA

TEMED	N,N,N',N'-Tetramethylethylenediamine
TMABA-DH	4-Tri-Methylaminobutyraldehyde Dehydrogenase
TMLD	N-Trimethyl-Lysine Dioxygenase
TO	Theilers Original
UIR	Uninfected reticulocyte enriched erythrocytes
UMP	Uridine Monophosphate
UTP	Uridine-5'-Triphosphate
UTR	Untranslated Region
V	Volt
v/v	Volume Per Volume
w/v	Weight Per Volume
WHO	World Health Organization
WT	Wild-Type
yfcu	Uridyl Phosphoribosyl Transferase
$\gamma$ GC	Gamma-Glutamylcysteine
$\gamma$ GCS	Gamma-Glutamylcysteine Synthetase

# 1 Introduction

## 1.1 Malaria

The *Plasmodium falciparum* parasite which causes malaria is a major killer in sub Saharan Africa and South East Asia. The World Health Organization (WHO) estimates that about 3.3 billion people (half of the world's population) are at risk of malaria (Figure 1-1).

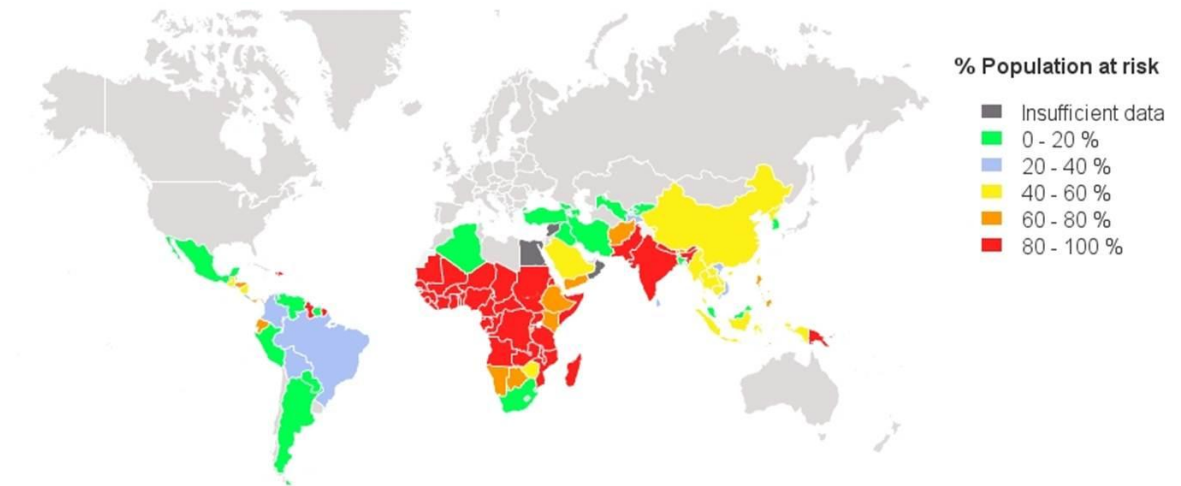


Figure 1-1 Global distribution of malaria and percentage population at risk (Mapper 2013, WHO 2013).

According to the 2013 WHO World Malaria Report (WHO 2013), in 2012, there were around 207 million reported cases of malaria and it accounted for almost 627,000 deaths. 90% of these deaths occurred in the WHO African region, mostly among young children under 5 years old (Figure 1-2).

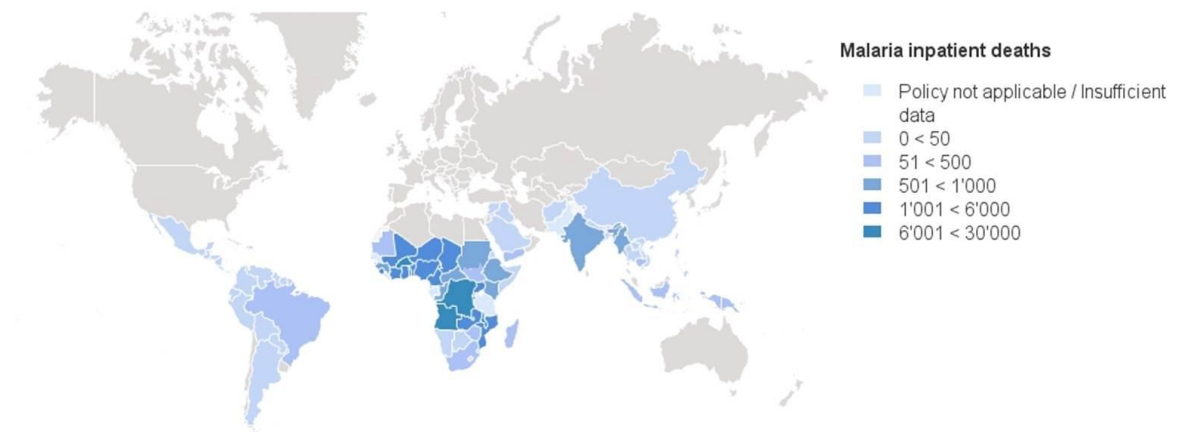


Figure 1-2 Distribution of reported malaria in patient deaths (Mapper 2013, WHO 2013)

However, the WHO relies on passive national reporting of malaria cases by governments and the number of cases could be up to 50% more than reported in Africa and up to 200% more in areas outside Africa (Snow, Guerra et al. 2005) and it is possible that we are underestimating the impact of malaria on the world population. Widespread resistance to drugs against malaria (Travassos and Laufer 2009) adds to the problem and there is an urgent need for vaccine development to ease the burden malaria imposes.

*Plasmodium* spp. parasites have a complex lifecycle (Figure 1-3) involving a mosquito vector and a mammalian host. Sexual development of the parasite takes place in the midgut of a female Anopheles mosquito where male and female gamete fusion leads to zygote formation, meiosis, ookinete development and subsequent oocyst and infective sporozoite formation which are transferred to a mammalian host with an Anopheline bite. It is the asexual development of parasites in the host, starting from an extra-erythrocytic cycle in the liver and then an erythrocytic invasion cycle that causes pathology.

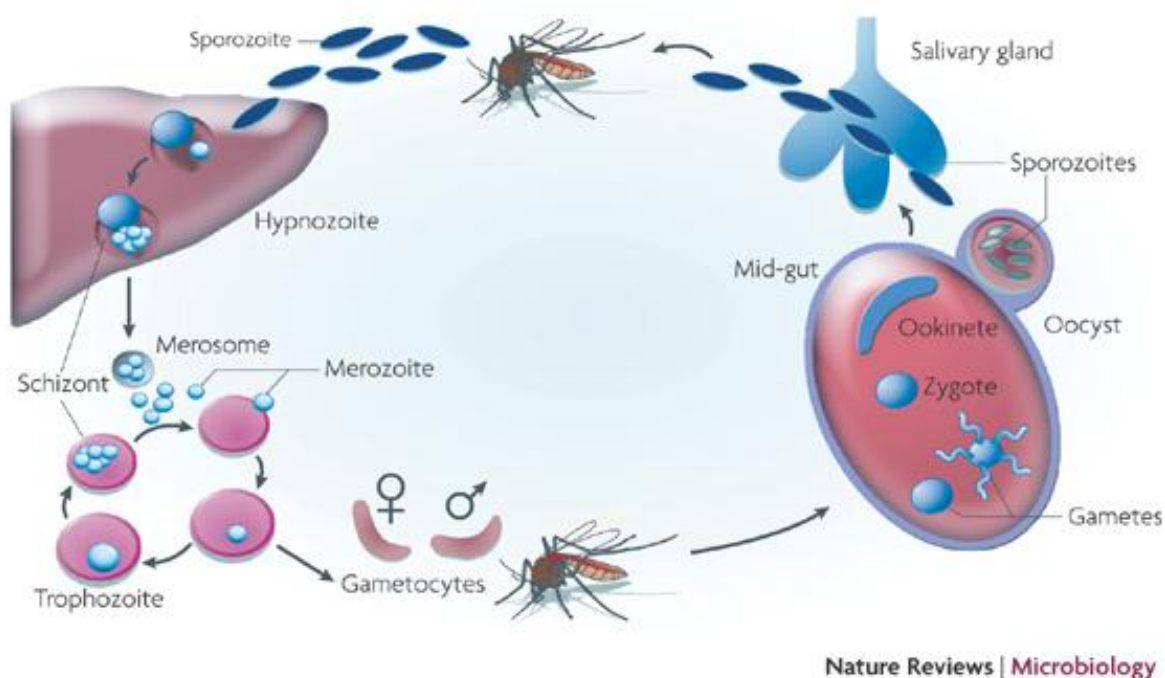


Figure 1-3 Life cycle of malaria parasite (Pain and Hertz-Fowler 2009)

*P. falciparum* is the most deadly species, although *Plasmodium vivax* is now well recognized as an important contributor to the economic toll of malaria (Reyes-Sandoval and Bachmann 2013) (Figure 1-4). *Plasmodium malariae*, *Plasmodium ovale* and *Plasmodium knowlesi* also account for a number of malaria cases and the latter commonly can be lethal.

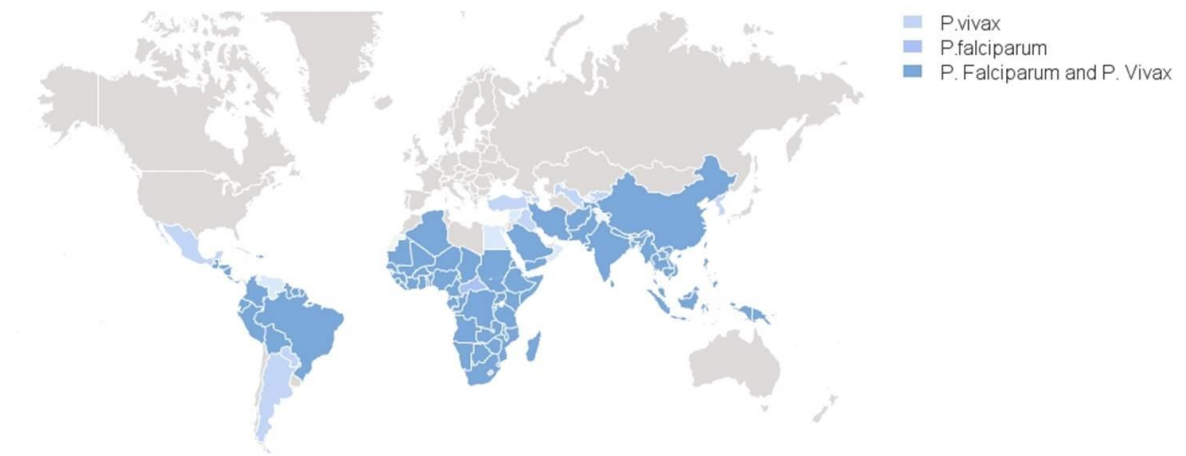


Figure 1-4 Distribution of *P. falciparum* and *P. vivax* in the world (Mapper 2013, WHO 2013)

It is not only important to study *Plasmodium* parasites because of their medical importance; they are also representative of the evolutionarily interesting group of protozoa, the Apicomplexans. They get their name from a specialized assembly of secretory and structural elements at the apical end called the apical complex, consisting of micronemes, rhoptries and dense granules (Baum, Gilberger et al. 2008, Gubbels and Duraisingh 2012). Another specialized organelle found in Apicomplexans is a rudimentary plastid called the apicoplast is a result of secondary endosymbiosis between a parasite ancestor and red algae (Fleige, Limenitakis et al. 2010). Having adopted an intracellular lifestyle, and being an obligatory mammalian pathogen, the apicomplexan parasite does not have the ability for photosynthesis but still the apicoplast is essential for parasite survival and harbors a number of important biosynthetic pathways more similar to plants and prokaryotes than to animals, which make it all the more fascinating (Baumeister, Winterberg et al. 2010). Also, recently it was shown that in *P. falciparum* parasites lacking a functional apicoplast, supplementation with isopentenyl pyrophosphate (IPP) rescued the parasites in *in vitro* cultures indicating that non-mevalonate isoprenoid precursor biosynthesis is the main function of apicoplast in this species during blood stage growth (Yeh and Derisi 2011). The parasite's life cycle presents itself within two different host-vector environments which - has ensured adaptation in the process, including reduced metabolic capacity (Kafsack and Llinas 2010), an ability to undergo tremendous change in its cellular makeup during and after transmission (Aly, Vaughan et al. 2009) and the development of strategies to avoid host defense mechanisms (Frevort 2004).

## 1.2 *Plasmodium berghei* as a model

The study of malaria parasites and their complex interactions with the human host and Anopheline vectors has challenged medical research for more than 100 years. One of the ways technology has evolved to address this problem is the use of animal models of malaria which facilitates studying topics such as drug resistance and new drug discovery, cytoadherence, gene expression and immunogenicity to vaccine candidates. Animal models provide controlled systems for *in vivo* investigation of host-parasite interactions across the various stages of the life-cycle and are an invaluable tool for research. *P. berghei* is one of the four widely studied rodent malaria species (the other three being *Plasmodium vinckei*, *Plasmodium chabaudi* and *Plasmodium yoelii*) which have been isolated from Central Africa and are useful malaria models with distinct morphological and developmental characteristics (LMRG Online Resource accessed August 2007). The natural mammalian host of these parasites is the Thicket Rat (*Grammomys surdaster*) but they can grow in a number of laboratory mouse and rat strains and are transmitted by Anopheline mosquito vectors.

The most deadly human malaria parasite *P. falciparum* has a genome of approximately 22.9 Mb with 14 chromosomes, a G+C content of approximately 19% and about 5,369 genes (Gardner, Hall et al. 2002). The other economically important human malaria parasite *P. vivax* has a genome of 28.6 Mb with 14 chromosomes, 42.3% G+C content and approximately 5,433 genes (Carlton, Adams et al. 2008). *P. berghei* has an estimated genome size of 18-20 Mb, with 14 chromosomes in the size range of 0.6 Mb to 3.8 Mb (Hall, Karras et al. 2005) with an average protein identity of 62.9%, average nucleotide identity of 70.3% and 3,890 orthologous gene pairs with *P. falciparum*. (Hall, Karras et al. 2005). More up to date and accurate information about the genome of *Plasmodium* spp. is available on PlasmoDB, a functional genomic database for malaria parasites (accessible from <http://PlasmoDB.org>). This database is updated regularly with every release and also contains additional information about transcription profiles, proteomics and protein function, population biology and field studies of malaria parasites (Aurrecochea, Brestelli et al. 2009). The similarity between rodent malaria causing species and important human parasites and easy availability of genetic manipulation strategies (de Koning-Ward, Janse et al. 2000, Janse, Ramesar et al. 2006) make them useful models. Resources such as the Malaria Research and Reference Reagent Resource Center (MR4), Rodent

Malaria genetically modified parasites database (RMgmDB) and the European Malaria Reagent Repository which archive useful plasmids and parasite lines with disrupted and tagged genes help make it an invaluable tool to study malaria under laboratory conditions.

### 1.2.1 Pre-erythrocytic development

The basic details of the life-cycle of *Plasmodium* spp. are conserved across the genus and *P. berghei* is described here as the model species used as the system of study here. A mosquito infected with *P. berghei* starts the pre-erythrocytic phase of the infection in a rodent as the sporozoite stage of the parasite is injected into the mammalian host when the mosquito takes the blood meal. In experimental conditions, upto 100 sporozoites are injected by a single mosquito bite and they are deposited mostly in the extra-cellular matrix of the skin where they move by gliding motility and then invade blood or lymphatic vessels (Menard, Tavares et al. 2013). The sporozoites enter into the blood circulation and reach the liver where they target Kupffer cells and endothelial cells lining the liver sinusoidal barrier and eventually invade hepatocytes (Tavares, Formaglio et al. 2013). Sporozoites then invade and migrate through multiple host cells before invading and settling in a hepatocyte by forming a parasitophorous vacuole (Mota, Pradel et al. 2001). In approximately 47-52 hours, after multiple rounds of DNA replication which starts around 20h post invasion and nuclear division, the sporozoite develops into a mature schizont which is a syncytial cell with up to 1,500-8,000 merozoites (Meis, Verhave et al. 1985). In *P. berghei* infected hepatocytes, membrane-bound vesicles devoid of host cell nuclei containing parasite merozoites are formed in detached infected cells called merozoites bulge into liver sinusoids and act as shuttles to ensure delivery of merozoites into blood circulation (Sturm, Amino et al. 2006). Such important findings have been results of work done in the animal model of malaria, *P. berghei* which is not possible to do in human malaria parasites and this underlines the usefulness of studying animal models of disease.

In some *Plasmodium* species which infect monkeys, *P. cynomolgi*, *P. fieldi* and *P. simiovale* and two which infect humans, *P. vivax* and *P. ovale*, a few *Plasmodium* infected hepatocytes do not develop after reaching the early hepatic trophozoite stage and exist in a state of dormancy in which they can

persist for many years (Dembеле, Gego et al. 2011). These forms are called hypnozoites and can cause recurring infections in the mammalian host.

### 1.2.2 Asexual blood stages

*P. berghei* merozoites, when released from an infected hepatocyte enter the peripheral circulation, invade erythrocytes and show a strong preference for young erythrocytes (reticulocytes) (Janse, Boorsma et al. 1989). Inside the erythrocyte, the merozoite grows into a trophozoite which devours the hemoglobin and other nutrients present inside the host cell and grows in size with an increase in cytoplasm. The parasites produce crystals of brown hemozoin which are characteristic pigment granules that are concentrated as the trophozoite matures which takes about 16 hours post-invasion. A mature trophozoite starts replicating its DNA and undergoing nuclear division, thus entering the schizont stage which is finished by 24 hours post invasion resulting in a syncytium containing 8-24 nuclei. Schizonts usually are not seen in peripheral circulation and sequester in the capillaries of inner organs (Franke-Fayard, Janse et al. 2005). This sequestration in the microvasculature of the brain in mammalian host is the main factor of cerebral malaria pathology in cases of *P. falciparum* infections in humans (Idro, Marsh et al. 2010). Models of experimental cerebral malaria (ECM) are also available for studies in *P. berghei* which although mechanistically different from *P. falciparum* (Ramos, Bullard et al. 2013) still provide a system to study the pathology in *in vivo* conditions indicated to be caused by similar sequestration of infected erythrocytes in brain (Baptista, Pamplona et al. 2010). Mature schizonts then rupture and release merozoites into the circulation. These invade more erythrocytes and the asexual development continues with a cyclic increase in parasitized erythrocytes.

### 1.2.3 Gametocytes: the sexual precursor cells

In each asexual developmental cycle in *P. berghei*, about 5-20% parasites stop asexual multiplication and develop into sexual precursor cells called gametocytes which take 26-30 hours to mature (Mons, Janse et al. 1985). Merozoites released from infected hepatocytes can also directly form gametocytes (Suhrbier, Janse et al. 1987). Gametocyte production is influenced by environmental and genetic factors (Janse, Ramesar et al. 1992) and gametocytes can be distinguished from mature trophozoites only after 18-22 hours post-invasion and characterized by a single enlarged nucleus and the

presence of pigment granules. A mature gametocyte occupies the complete host cell.

#### **1.2.4 Mosquito stages**

*Plasmodium* infected erythrocytes are taken up during a blood meal if a mosquito bites an infected host and only mature gametocytes undergo further development in a mosquito midgut. Gametocytes prepare themselves for a relatively hostile environment within the mosquito mid-gut where a drastic change in environment (e.g. low temperature, increased pH) and other mosquito factors like xanthurenic acid give them cues to form haploid gametes (Billker, Lindo et al. 1998). Female gametocytes differentiate into a single, spherical macrogamete whereas each male gametocyte undergoes three rapid rounds of nuclear division within 8-12 minutes and forms eight microgametes (Janse, Van der Klooster et al. 1986). The gametes fuse to form a diploid apolar zygote which undergoes meiosis within four hours and after 18-24 hours develops into an invasive motile polarized form called ookinete which then traverses the mid-gut wall of the mosquito and forms an oocyst on the basal lamina which then develops to form thousands of sporozoites (Sinden and Billingsley 2001). The sporozoites travel to the salivary glands of the mosquito ready for the next cycle of infection.

### **1.3 Reticulocyte biology**

#### **1.3.1 Reticulocytes vs normocytes**

Reticulocytes are young erythrocytes which are released from bone marrow into peripheral blood and undergo a lot of changes as they mature into normocytes in circulation. The maturation process has been found to be associated with simplification of the cell leading to the loss of a number of organelles such as mitochondria, ribosomes, vesicles and lysosomes, acquisition of a biconcave shape, increase in shear membrane resistance, change in membrane organisation of about 30 membrane proteins and about 20% loss of surface area and decrease in membrane cholesterol (Gronowicz, Swift et al. 1984, Liu, Guo et al. 2010).

#### **1.3.2 Reticulocytes as the preferred host cell type for some *Plasmodium* species**

Invasion of an erythrocyte is a prerequisite for establishment of infection by the malaria parasite and a number of parasite and host proteins have been studied

which facilitate this process. The most studied parasite proteins hypothesized to be involved in the invasion process in *P. falciparum* are merozoite surface proteins (MSPs), *P. falciparum* erythrocyte binding antigens or PfEBAs (which are related to *P. vivax* duffy binding protein) and PfRHs or *P. falciparum* reticulocyte binding protein (RBP) homologues (which are related to *P. vivax* RBPs) (Tham, Healer et al. 2012) (Harvey, Gilson et al. 2012). These proteins are stored in specialized organelles in the apical complex. MSPs are highly variable and their main function is adhesion to erythrocytes during the initial contact phase while PfEBAs and PfRHs are mobilized to the merozoite surface after the initial contact has been made. The exact mechanism of invasion is not completely understood and there is apparently a functional redundancy in erythrocyte invasion pathways as these parasite protein families are highly diverse (Wright and Rayner 2014). Erythrocyte surface proteins have also been studied to understand the interaction between the parasite surface and host proteins which facilitate invasion. *P. falciparum* merozoites have been shown to utilize sialic acid on glycoporphins (Maier, Duraisingh et al. 2003, Mayer, Cofie et al. 2009) and more recently, basigin (Crosnier, Bustamante et al. 2011) as erythrocyte receptors whereas *P. vivax*, which prefers to invade reticulocytes, has been shown to express reticulocyte binding proteins (Galinski, Medina et al. 1992) and require a host Duffy blood group glycoprotein for invasion (Barnwell, Nichols et al. 1989). The Duffy glycoprotein is present on both reticulocytes and normocytes and is not the reason for preferential invasion of reticulocytes by *P. vivax* parasites. Moreover, Duffy-negative populations have been shown to be susceptible to infection by *P. vivax* malaria (Mendes, Dias et al. 2011, Carvalho, Queiroz et al. 2012). The reason for this preferential invasion of reticulocytes could be more complicated than just surface protein interactions and is very intriguing. The *in vivo* model parasite *P. berghei* is 150 times more likely to invade reticulocytes in the presence of equal numbers of mature erythrocytes and reticulocytes (Cromer, Evans et al. 2006) although it can also invade mature erythrocytes.

#### **1.4 Metabolism in *Plasmodium* and host erythrocytes**

Due to their parasitic and largely intracellular life-style, *Plasmodium* spp. have a comparatively reduced metabolic capacity as compared to higher independent organisms. They seem to have completely lost the ability to synthesize purines and amino acids *de novo* (Booden and Hull 1973, Sherman 1977) but have

retained many central metabolic pathways like glycolysis (Homewood 1977), the citric acid cycle (Macrae, Dixon et al. 2013), lipid synthesis (Holz 1977), the pentose phosphate pathway (though they lack transaldolase) (Barrett 1997), pyrimidine biosynthesis (Hyde 2007) and glycosylation (Macedo, Schwarz et al. 2010). As *Plasmodium* parasites are intracellular, their metabolism is interlinked with the host cells and is dependent upon the availability of nutrients from the surrounding environment. Mature erythrocytes, which comprise of almost 98% of circulating red blood cells and are carriers of oxygen, have been shown to be metabolically active but somewhat simpler than the erythroid precursors present in the bone marrow (Chen, Liu et al. 2009). The major metabolic pathways in mature erythrocytes have been shown to be glycolysis (Chapman, Hennessey et al. 1962) and pentose phosphate pathway (Stromme and Eldjarn 1962).

#### 1.4.1 Glycolysis

The main pathway for generating energy in *Plasmodium* parasites has been long considered to be glycolysis and although it is not a very efficient process (generating only 2 molecules of ATP from one molecule of glucose); the practically unlimited supply of glucose in mammalian blood seems to make up for the inefficiency of this anaerobic process. Erythrocytes have been shown to utilize glucose exclusively for their energy requirements through the glycolytic pathway converting glucose to lactate (Chapman, Hennessey et al. 1962). Normal erythrocytes internalize glucose mainly using glucose transporter 1 (GLUT1) (Krishna, Woodrow et al. 2000) and consume glucose at a rate of 1-2 mmol (1 cell)<sup>-1 h<sup>-1</sup></sup>. In *Plasmodium* infected erythrocytes, the consumption of glucose increases by 50-100 fold as compared to uninfected erythrocytes, while most of the glucose still gets converted to lactate (Roth 1990) indicating the increased flux in the glycolytic pathway and ability of *Plasmodium* parasites to consume large quantities of glucose. All glycolytic enzymes are encoded by the *Plasmodium* genome and expressed during the intraerythrocytic blood stage development (Gardner, Hall et al. 2002) (Bozdech, Llinas et al. 2003). Recently, it has been proposed that with this reliance on unrestricted glycolysis, *Plasmodium* metabolism has evolved to support rapid biomass generation in addition to ATP production for fulfilling its energy needs during the proliferative asexual phase (Salcedo-Sora, Caamano-Gutierrez et al. 2014). In addition, the presence of *Plasmodium*-induced new permeability pathways (NPP) on the host

cell membrane (Kirk, Staines et al. 1999) allow a wide range of low molecular weight solutes to enter the infected cell.

*Plasmodium* parasites are neither capable of generating storage carbohydrates such as glycogen (Dasgupta 1960, Homewood 1977) nor of generating 6-carbon sugars like glucose from non-carbohydrate carbon substrates by gluconeogenesis as they lack the second last enzyme of gluconeogenesis- fructose-1-6-biphosphatase (Gardner, Hall et al. 2002). Hence, *Plasmodium* parasites have evolved to survive in the specific, glucose rich anaerobic niche of mammalian erythrocytes for most of their proliferative asexual cycle. Although, energy requirements in the mosquito stages may also be quite demanding, especially during the oocyst stage where a proliferation of sporozoites takes place, it has been shown that following a blood meal, the sugar contents of mosquito hemolymph increase by 4 fold (Mack, Samuels et al. 1979) and can support the growth of *Plasmodium* parasites.

#### 1.4.2 TCA cycle

The other glucose metabolism pathway, the tri-carboxylic acid (TCA) cycle which links cytosolic glycolysis to mitochondrial metabolism which is usually utilized by aerobic organisms to generate ATP from glycolytic end products, was long considered to be inactive in non-nucleated mature erythrocytes (Dajani and Orten 1958). The TCA cycle has recently been explored in some detail in *Plasmodium* (Macrae, Dixon et al. 2013) where in asexual stages, glycolysis and the TCA cycle pathways were found to be active although with a low flux in contrast to the gametocyte stage, where this pathway was found to be more active and essential for gametocyte maturation. The absence of a mitochondrial pyruvate dehydrogenase in *Plasmodium* doesn't seem to stop glycolytic carbon skeletons from entering the TCA cycle and it was recently proposed that a mitochondrion located branched chain  $\alpha$ -keto acid dehydrogenase (BCKDH) complex can catalyze the pyruvate (glycolytic end product) to acetyl-CoA (TCA cycle intermediate- entry point) conversion (Macrae, Dixon et al. 2013, Oppenheim, Creek et al. 2014).

#### 1.4.3 Electron Transport Chain

Although the TCA cycle generates 2 additional molecules of ATP after glycolysis for each molecule of glucose, it is the Electron Transport chain (ETC) which classically generates 34 molecules and is the site of oxidative phosphorylation.

Yet, in *Plasmodium* parasites the ETC is dispensable (Hino, Hirai et al. 2012) in asexual blood stages and serves only one metabolic function, that of regenerating ubiquinone which is required as an electron acceptor for dihydroorotate dehydrogenase (DHODH), a pyrimidine biosynthesis enzyme (Painter, Morrisey et al. 2007). This minimalistic utilization of glucose for energy generation in a glucose rich environment is representative of an obligatory parasitic lifestyle. Parasites deficient in a fully functional ETC are not able to complete development in the mosquito stages (Hino, Hirai et al. 2012) and fail to transmit, pointing towards a possible switch to oxidative phosphorylation in the mosquito vector where seemingly unlimited supply of glucose unlike mammalian blood is not present.

#### 1.4.4 Fatty Acid synthesis

The malaria parasite has at least three stages in its life-cycle where it undergoes asexual mitotic proliferation and produces numerous merozoites (in hepatocytes, it produces thousands of merozoites (Meis, Verhave et al. 1985), in asexual schizonts, it produces upto 36 merozoites depending on species (Cowman and Crabb 2006) and thousands of sporozoites in mature oocysts). The production of new daughter parasites requires the generation of copious quantities of membrane material, the main component of which are fatty acids. The parasite genome encodes all the enzymes which constitute the bacteria like Fatty Acid Synthesis type II (FAS II) pathway which are targeted to the apicoplast (Gardner, Hall et al. 2002). However, the FASII pathway has been shown to be essential only for liver stage development of the parasite and is dispensable in the blood stage where it is proposed that fatty acids can be scavenged from the host serum and cell (Vaughan, O'Neill et al. 2009). There is an important distinction between the rodent and human parasites here as in *P. berghei* and *Plasmodium yoelii* the FASII pathway is dispensable for sporozoites development as well while in *P. falciparum*, FAS II is essential for sporozoite development (van Schaijk, Kumar et al. 2013) indicating the presence of an undiscovered mechanism of fatty acid synthesis in mosquito stages in the rodent parasites. In the mature erythrocytes, fatty acid biosynthesis is not active but FAS type I has been shown to be present in immature erythrocytes (Pittman and Martin 1966).

### 1.4.5 Pentose Phosphate Pathway

Another important metabolic pathway in eukaryotes is the pentose phosphate pathway (PPP) which utilizes carbohydrates as carbon source but rather than following a catabolic route, it takes the sugars to an anabolic path where it generates 5-C sugars for nucleic acid synthesis, NADPH required for maintaining redox balance of the cell and cofactors for other biosynthetic reactions (Berg JM 2002). This pathway is present in erythrocytes (Stromme and Eldjarn 1962) and all enzymes of this pathway except transaldolase (which links the pentose phosphate pathway to glycolysis) are encoded by the *Plasmodium* genome (Gardner, Hall et al. 2002). It has been shown that the PPP activity of a *Plasmodium* infected erythrocyte is almost 78 times more than an uninfected cell and the pathway is most active at the trophozoite stage and slows down in mature schizonts indicating that this pathway is utilized for combating the oxidative stress generated by reactive oxygen species produced from hemoglobin digestion in a growing parasite (Atamna, Pascarmona et al. 1994). Another interesting point in this study was that 82% of the PPP activity present in an infected erythrocyte was shown to be derive from the parasite, showing that the parasite's pathway carried the major flux and also that the host PPP was increased by 24 times which is similar to when uninfected erythrocytes are subjected to oxidative stress.

Importantly, individuals deficient in glucose-6-phosphate dehydrogenase (G6PDH) - the first enzyme of the PPP, are resistant to clinical malaria. Such individuals carry an X-linked, hereditary genetic defect caused by mutations in the G6PD gene and suffer from neonatal jaundice and acute haemolytic anaemia (Cappellini and Fiorelli 2008). The actual mechanism of this resistance to malaria in such individuals is not entirely understood as *in vitro* studies and field studies have produced conflicting results. However, in areas where this mutation is common, the incidence of *P. falciparum* malaria is relatively low (Ruwende and Hill 1998). This implies that the parasite requires the host cell to be viable for as long as it stays there and an impaired capacity to maintain the redox balance due to loss of production of NADPH from the erythrocyte PPP affects the parasite's ability to establish a robust infection.

## 1.5 Metabolomics

### 1.5.1 Metabolomics: a post genomics launch-pad

The whole ‘omics’ technologies revolution has given us tools and means to develop a more comprehensive understanding of biological systems. Metabolomics is a powerful and unbiased approach to study these complex systems with a depth never measured before. It not only provides a way to look at the functional aspect of life right down to the cellular level but also paints a bigger picture of cellular dynamics of the same in most advanced forms. The need for a more holistic approach to understanding systems stems from the realization that traditional reductionist methods like molecular biology and biochemistry alone cannot analyze biological systems as a whole (Goodacre 2005). Metabolomics can contribute to our understanding of biological systems and typically, small molecule metabolites (less than 1500Da) constitute the ‘metabolome’ of a specific cell, body part or organism (Wishart, Tzur et al. 2007). Simply put, modern ‘metabolomics’ deals with the high through-put quantification and identification of small molecule metabolites, smaller than most proteins and other macromolecules, which usually exist in a living system. The origins of using metabolites to predict biological alterations date back to the middle ages when characteristics of body fluids like colour, smell and taste were linked to possible disease. A urine chart was published by German physician Ulrich Pinder in a book called *Epiphanie Medicorum* in 1506 which showed how disease could be diagnosed using these features of urine (Nicholson and Lindon 2008).

### 1.5.2 Metabolomics: what it has to offer?

Although the field of metabolomics has emerged from the groundwork done by numerous biochemists over many years, the ability to measure an enormous number of metabolites at once from very complex biological samples and to use them to construct the ‘metabolic profile’ as a means to identify potential biomarkers of disease or drug response is a big leap forward (Griffin and Vidal-Puig 2008). In spite of all the technological advances, the basic principle of functional metabolomics, i.e. finding a link between chemical patterns and biology is unchanged (Nicholson and Lindon 2008). A more modern take on the need for studying metabolomics is that it forms one of the pillars of systems biology and bridges the gaps between genome, transcriptome, proteome and the

ultimate phenotype of the organism studied. Being more downstream and closer to the actual phenotype of the organism it is a powerful tool for large scale functional analyses (Allen, Davey et al. 2003). Non targeted metabolic profiling is a rational progression that follows systematic analysis of DNA, RNA and protein in any organism (Weckwerth 2003) and if it is integrated with existing functional genomics information, the link between genotype and ultimate phenotype of an organism becomes clearer (Bino, Hall et al. 2004).

### 1.5.3 Metabolomics: contributions in different biological systems

The potential of metabolomics is now recognised across many disciplines in biological sciences and many experimental and model organisms have been metabolically profiled producing interesting data. The enormous metabolic complexity of one of the simplest model organisms, *E.coli*, has been well documented by Robert et al. (Robert M 2007) which only reiterates the fact that the existing biochemical knowledge about all life forms is far from complete.

In another study in an extremophilic Archaea species, *Pyrococcus furiosus* (Trauger, Kalisak et al. 2008), metabolic profiling revealed altered occurrence and abundance of metabolites in response to suboptimal growing conditions. This was correlated to changed mRNA and protein levels, showing down-regulation in a number of growth related genes, whereas other genes were up regulated. Another important finding of this study was the discovery of an alternative polyamine biosynthesis pathway which *P. furiosus* switched to during the suboptimal growth conditions. A non-Archaea bacterial species *Thermus thermophilus*, has the same pathway, providing clues for evolutionary links between two distinct species (Trauger, Kalisak et al. 2008). Phylogeny based on genome information has provided us with a lot of insight into how different species have evolved from common ancestors. A similar comprehensive comparison of metabolites and metabolic pathways across closely related or even diverse species can prove to be another stepping stone for evolutionary biologists. For example, *E.coli* and *Saccharomyces cerevisiae* are very divergent species which belong to different kingdoms and are very different in their cellular organization; yet metabolic responses to nutrient starvation are found to be conserved across the two species (Brauer, Yuan et al. 2006).

Plant phytochemistry has interested scientists for hundreds of years and plant metabolomics has attracted many inputs so far as compared to other biological

systems. This is partly because plants produce many potential therapeutic agents e.g. the oldest anti-malarial known, Quinine was discovered in the 17<sup>th</sup> century from the bark of *Cinchona* tree and almost 400 years after its discovery, it remains an important drug (Achan, Talisuna et al. 2011). *Artemisia annua* (a Chinese herb also known as sweet wormwood or Qinghao) is the source of Artemisinin, now the standard treatment worldwide for *P. falciparum* malaria (Enserink 2005). Over 35,000 plant species have had their constituents analysed for anti-cancer activity (Saito and Matsuda 2010). Metabolite analysis complemented by gene expression studies in *Arabidopsis* has shed light on pleiotropic responses to environmental changes (Huang, Bhinu et al. 2009). An *Arabidopsis* transgene expressed in tobacco leads to increased accumulation of a flavonoid 'rutin' conferring resistance against pests and this study has been validated by metabolite profiling and expression data (Misra, Pandey et al. 2010). A web portal for plant metabolomics now exists where scientists all over the world can access, explore and download *Arabidopsis* metabolome data which is cross referenced to genetics, biochemistry and metabolic pathways of the model plant species (Bais, Moon et al. 2010).

Pedersen et al. showed the effects of inbreeding on the physiology of a widely used model organism, *Drosophila melanogaster*, using metabolite profiling where fundamental metabolic processes are found to be different in inbred and outbred lines (Pedersen, Kristensen et al. 2008). Novel metabolites related to insulin resistance have been discovered using metabolome analysis of liver tissue and plasma in mice (Li, Hu et al. 2010). Since its first release in 2007, the number of fully annotated metabolites in the human metabolome database (HMDB accessible at <http://www.hmdb.ca/>) increased by 300% from 2000 metabolites (Wishart, Tzur et al. 2007) to close to 7000 metabolites in its second release (Wishart, Knox et al. 2009). The most recent release of HMDB (version 3.0) has significantly expanded and the number of annotated metabolite entries has grown to more than 40,000 - an almost 600% increase since the second release (Wishart, Jewison et al. 2013).

A number of protists of medical and economic importance are studied very extensively and attempts at complete metabolic profiling of some kinetoplastid and apicomplexan species have already been made (Coustou, Biran et al. 2008, Doyle, MacRae et al. 2009, Olszewski, Morrissey et al. 2009, Teng, Junankar et al.

2009, van Brummelen, Olszewski et al. 2009, Scheltema, Decuyper et al. 2010, Creek, Anderson et al. 2012). Such a widespread use of metabolomics underlines the importance of this field which has created new opportunities to look for new knowledge at the interface of genomics, biochemistry, biotechnology and chemical ecology (Dixon and Strack 2003).

#### 1.5.4 Metabolomics platforms

The main challenge in metabolomics research is the vast diversity of chemicals and metabolites produced and processed by any living system. As an example, in the plant kingdom alone, there are an estimated 1 million metabolites (Saito and Matsuda 2010) and considering the number of organisms being analyzed today, very high-throughput, sensitive, quantitative and accurate techniques are required to aid metabolomics research. Since the chemical composition and relative abundance of all metabolites within a system is very variable, it is very difficult to extract and quantify all of them together (Kell 2004). Because of this chemical diversity of metabolites, specific methods of extraction are required for different classes. Polar and semi polar compounds are usually extracted using water and methanol and non-polar compounds are extracted using chloroform (Saito and Matsuda 2010). Sample extraction is followed by metabolite separation, detection and identification.

It is because of detection technologies like Mass Spectrometry (MS) and Nuclear Magnetic Resonance (NMR) that the field of metabolomics has come of age today (Griffiths 2008). Use of NMR to study effects of a number of variables on biological fluids like urine has been well reviewed by Bollard et al. (Bollard, Stanley et al. 2005). A number of metabolites from *Cryptococcus neoformans* cultures were identified using NMR spectroscopy with a view to identify virulence factors underlying human pathogenesis (Bubb, Wright et al. 1999). NMR has been mostly done using <sup>1</sup>H (proton) - 1D spectroscopy, where spectral peaks usually give a direct indication of metabolite abundance and are easily acquired. However, spectral overlap is a big issue and more than one metabolite can sometimes give similar peaks. 2D NMR spectroscopy overcomes this problem but then spectra acquisition times are increased (Ludwig and Viant 2010).

Amongst the most popular metabolomics methodologies, GC (Gas Chromatography), HPLC (High Performance Liquid Chromatography) and CE

(Capillary Electrophoresis) are mainly used for molecule separation and mass spectrometry (MS) is the most suitable detection technique (Terabe 2007).

GC-MS has been a popular choice in metabolomics studies because of its ease to measure levels of primary metabolites such as sugars, amino acids and organic acids, since hydrophilic compounds like these can be easily derivatized (Lisec, Schauer et al. 2006). Tandem mass spectrometry (MS/MS) and GC-MS were used to quantitatively determine diagnostic markers for Phenylketonuria (Chace, Millington et al. 1993) which laid the foundation for use of tandem mass spectrometry for neo-natal clinical screening (Chace and Kalas 2005) and many laboratories around the world use GC-MS for diagnosis of metabolic diseases involving organic acids (Chace 2001), steroids and hormones (Want, Cravatt et al. 2005). But GC-MS has its limitations with regards to sample preparation and types of samples that can be analyzed. The samples need to be able to be made volatile (for gas phase) and polar, non-volatile molecules are not detected.

LC-MS overcomes some of the problems associated with using GC-MS alone. LC-MS enables detection of more diverse chemicals with variable polarity, size and volatility and has better reproducibility, sensitivity and easier sample preparation (Want, Cravatt et al. 2005). CE-MS is another method to detect ionic metabolites such as nucleotides and phosphates, amino acids and organic acids (Monton and Soga 2007). CE requires minimum sample amount (usually in the nanolitre range) and has a low running cost. However, reproducibility in quantification and concentration sensitivity is low (Terabe 2001), a problem which can be partially overcome when fitted with an accurate mass spectrometer (Monton and Soga 2007).

These technologies need to be used wisely and possibly in conjunction with each other to get a comprehensive dataset that has a lesser possibility of missing important metabolites in the system studied.

### **1.5.5 Metabolomics: Untargeted and Targeted approaches**

The potential of metabolomics technologies can be realized in more than one manner and the methodologies can be divided into two broad categories: untargeted metabolomics involves a comprehensive analysis of all measurable analytes, which may include unknown compounds in a given system. Targeted metabolomics involves identification of pre-characterized and biochemically

annotated metabolites (Roberts, Souza et al. 2012). Untargeted metabolomics provides an unbiased approach to profile a biological system and may be used to compare all possible differences between two related biological systems or when looking within the same system, changes induced due to inherent biological processes, chemical interventions or genetic manipulations. It provides a powerful tool to develop hypotheses based on these observed differences which can then be followed up using classical reverse genetics, analyzing the biochemistry and ultimately answering novel biological questions which would not even be raised if it wasn't for this extremely useful approach of metabolomics.

Targeted metabolomics approaches are usually hypothesis driven and aim to investigate a specific biochemical question and focus on a known metabolic pathway or pathways (Patti, Yanes et al. 2012). These approaches are effective in answering queries regarding drug metabolism pharmacokinetics and measuring the influence of therapeutics and genetic modifications on a specific enzyme (Nicholson, Connelly et al. 2002). Targeted metabolomics has played a vital role in the development of the field of metabolomics and there are numerous examples where using heavy isotope labelling of metabolites has led to qualitative and quantitative metabolite profiling leading to important biological discoveries ranging from apicomplexan biology (MacRae, Sheiner et al. 2012, Macrae, Dixon et al. 2013) to cancer (Chaneton, Hillmann et al. 2012) to novel disease biomarkers (Griffiths, Koal et al. 2010).

#### **1.5.6 Metabolomics: Data generation, storage and interpretation**

Metabolomics technologies generate large amounts of data and organizing and analyzing the data is as important a task as generating it. The fundamental aim in dealing with raw metabolomics data is to identify metabolites from mass spectrum/chromatogram, determining their abundance/concentration and linking them to the metabolic pathways they are products of or participate in (Kell 2004).

The post genomic era has seen the generation of enormous amounts of data and numerous databases have been set up for cataloguing and archiving this data for the scientific community across the globe. A number of genomic databases have been created for organisms whose genomes have been sequenced to date and protein coding genes are annotated using homology. The general conservation of

metabolic enzymes is such that it is possible to generate genome-scale models of metabolism in databases such as MPMP (Malaria Parasite Metabolic Pathways-accessible at <http://mpmp.huji.ac.il/>) (Ginsburg 2006), KEGG (Kyoto Encyclopedia of Genes and Genomes, accessible at <http://www.genome.jp/kegg/>) (Kanehisa, Goto et al. 2006) and MetaCyc (accessible at <http://metacyc.org/>) (Caspi, Altman et al. 2014). Recently, a metabolic model of *Plasmodium* integration information from functional genomic studies was published (Tymoshenko, Oppenheim et al. 2013). However, as some enzymes and their substrate specificities are not correctly annotated in the genome, many novel metabolites and pathways might exist which are yet to be discovered.

A big hold up in early metabolome studies was accurate and reproducible identification of correct peaks from obtained spectra. This has been improved with new software capable of dealing with raw data and able to generate matrices with all signals in an order of their intensities (Saito and Matsuda 2010) leading to better identification and quantification of molecules (Scheltema, Jankevics et al. 2011, Creek, Jankevics et al. 2012).

Just as genomics data is useful only when it is standardized, metabolomic data needs to be generated using standardized methods and operating conditions with properly calibrated instruments. Since the predicted number of compounds represented in a mass spectrum can easily run into thousands, in order to eliminate false positives and select the most likely and chemically correct compound, algorithms have been developed to filter the data and reduce noise (Kind and Fiehn 2007). It has been proposed that these approaches towards getting accurate information from the studied system can only be helped by proper standardization and common infrastructure development across metabolomics laboratories. The Metabolomics Society based in Ardmore, Oklahoma, USA has taken first steps to standardize the metabolic profiling strategies by recommending general 'workflow' models through The Metabolomics Standards Initiative (MSI) (Sansone, Fan et al. 2007). MSI has proposed to categorize reported metabolites using terms such as identified (previously characterized and reported in literature), putatively annotated (no chemical reference, based on physicochemical properties and comparison with spectral libraries), putatively characterized (based on characteristic

physicochemical properties of a chemical class or by spectral similarity to known compounds of a chemical class) and unknown (although unidentified, potentially quantifiable and differentiable using spectral data) (Sumner 2007).

KEGG initiated in 1995 (Kanehisa 1997) is an online resource with a number of different database components. The PATHWAY database component in KEGG consists of information in the form of maps representing metabolic pathways, genetic information flow, signal transduction and disease information (Kanehisa, Goto et al. 2006). ApiCyc, LeishCyc, MPMP (Malaria Parasite Metabolic Pathways) and the metaTiger KEGG interface are repositories of metabolomics data collected from parasites (Kafsack and Llinas 2010). The human metabolome database's current release (version 3.0) contains over 40,000 metabolites which includes both polar and non-polar molecules in nm to  $\mu\text{m}$  range and has links to KEGG, PubChem, MetaCyc, ChEBI, PDB, Swiss-Prot, and GenBank) (Wishart, Jewison et al. 2013). With such a rich source of information which is continuously growing, thanks to tremendous amount of work done in metabolomics laboratories all over the world, the application of metabolic information is beginning to show its true potential.

### **1.5.7 Role of metabolomics in functional genomics**

For the true understanding of a complex biological system, it is necessary that its endogenous behavior and response to environmental changes be studied at the level of RNA, proteins and metabolites together. This is important if we are to move ahead from prediction to experimental validation of gene function (Stitt and Fernie 2003). As discussed above, the role of metabolomics cannot be underestimated in functional genomics where a number of orphan genes can be assigned functions using metabolomics data and integrating it with the transcriptomic and proteomic platforms (Hollywood, Brison et al. 2006).

There is a current need to integrate different 'omics' datasets while addressing any computational issues that may arise. Efforts have been made in this direction with the development of methodologies like 'integrOmics', an R based portal which feeds in and analyses high dimensional data and gives graphical outputs which are easy to interpret (Le Cao, Gonzalez et al. 2009) and an excel based system called IDEOM which is a tool designed to help biologists visualize metabolomics data easily (Creek, Jankevics et al. 2012). Metabolic information of unknown or partially known pathways gained by using such platforms may also

lead to the discovery of genes which are not directly responsible for a particular function but may be associated with one already discovered (guilt-by-association) (Altshuler, Daly et al. 2000). It is plausible that a shared regulatory system can control the expression of the set of genes involved in a biological process and if an unknown gene is co-expressed with a known gene found linked to metabolite accumulation, the unknown gene may have some role to play in the same pathway (Saito, Hirai et al. 2008).

Once the gene to metabolite connection (whether direct or indirect) is established using the integrated 'omics' approach, experimental validation can be employed using reverse genetics or reverse biochemistry tools. For example, in a study done in an ascomycete, *Stagnospora nodorum*, the role of genes involved in arabitol metabolism and their functional redundancy was shown using reverse genetics approach coupled with metabolomics where mutant lines were created and MS analyses was done on them after exposure to similar environmental stress (Lowe, Lord et al. 2008).

Forward genetics studies using quantitative trait locus analysis combined with metabolite profiling (mQTL) have also been made possible where metabolite levels can be linked to specific loci on the genome and the function of the genes spanning the loci deciphered. In a study on a model plant genus *Populus*, four mQTLs associated with flavonoid biosynthesis were mapped, they were assigned functions based on the related metabolite and known flavonoid pathway and by looking for homologues of flavonoid biosynthesis genes in *Populus* genome the corresponding genes were identified (Morreel, Goeminne et al. 2006). More recently, using a similar mQTL analysis, reduced fitness of chloroquine-resistant *P. falciparum* parasites was shown to be linked to mutations in chloroquine resistance transporter which interfered with hemoglobin digestion (Lewis, Wacker et al. 2014).

### **1.5.8 Role of metabolomics in systems biology**

For decades, scientists have studied living systems by breaking down the different components and looking at them part by part, going right down to the molecular level. Biological systems' behavior, cannot be explained by studying discreet information obtained from molecular studies, but may be tractable by using the methods of systems biology (Goodacre 2005). A holistic view to study whole pathways from genes, transcripts, proteins to metabolites and their

interactions forms the basis of systems biology. It has the potential to bring out the information which may not be evident by studying individual components alone (Snyder and Gallagher 2009).

Metabolomics has a huge potential to push systems biology forward and two approaches have been proposed to enable this: data-driven and model-driven (Saito and Matsuda 2010). The data-driven approach stems from an integrated analysis of whatever information is at hand (gained from different omics datasets) and using it to construct metabolic networks. Enzymes involved in metabolic networks (proteins) form the nodes or components and their interactions with other molecules form the links or edges (Yamada and Bork 2009). Such metabolic networks can be constructed for a given living system and using functional genomics approaches as discussed above (e.g. using a mutant), metabolic perturbations can be compared at a large scale, spanning various nodes in a network, eventually getting leads for novel or missing components in the network.

Rather than correlating components in the metabolomic network, the system's behavior can also be predicted by constructing a mathematical model based on information from the system's components and generating computer simulations to mimic the possible outcomes. For example, in an oncology study, a mathematical model of *Ras* signaling was developed which when supported by experimental data gave new insights into cytosolic GTPases activation (Stites, Tramont et al. 2007). Similarly, a dynamic model of energy metabolism in *Trypanosoma brucei* was used to predict possible outcomes when PPP was added to the existing standalone glycolytic model (Kerkhoven, Achcar et al. 2013) showing the importance of a systems approach when dealing with metabolism.

### **1.5.9 Metabolomics of protozoan parasites**

Protozoan parasites are well known to cause serious infections in humans and animals which are often fatal. Malaria (*Plasmodium* spp.), Human African sleeping sickness (*Trypanosoma* spp.), Babesiosis (*Babesia* spp.), Cryptosporidiosis (*Cryptosporidium* spp.), Toxoplasmosis (*Toxoplasma* spp.) and Leishmaniasis (*Leishmania* spp.) are some of the life threatening parasitic diseases and pose a big burden on world economy. Toxoplasmosis and Cryptosporidiosis are very severe in immune-compromised patients and patients with HIV/AIDS suffer high mortality from these parasites (Abrahamsen,

Templeton et al. 2004, Kim and Weiss 2008). Trypanosomatid Parasites (*Trypanosoma* and *Leishmania*) are responsible for approximately 150,000 deaths every year and there is no vaccine but treatment solely depends on chemotherapeutic drugs which themselves have high toxicity related effects on patients (Nussbaum, Honek et al. 2010).

The possibilities of discovering unorthodox metabolic pathways constituting existing or novel or derived metabolites is tremendous and metabolomics is a key technology that can be transferred across a number of biological disciplines to study numerous cell types, organisms and living systems.

Protozoan parasites, particularly apicomplexans and kinetoplastids are now being studied using metabolomics approaches, and although in its infancy, the developments are rather encouraging (Besteiro, Vo Duy et al. 2009, Olszewski, Morrissey et al. 2009, Scheltema, Decuyper et al. 2010, Creek, Anderson et al. 2012, MacRae, Sheiner et al. 2012, Macrae, Dixon et al. 2013).

#### **1.5.10 Metabolomics in malaria research: a road just taken**

The *P. falciparum* genome was published twelve years ago (Gardner, Hall et al. 2002) which further led to the prediction of a number of biochemical pathways in the parasite. This information is available through various web accessible databases like PlasmoDB, Brenda, KEGG, ApiCyc, Metatiger, Reactome and MPMP (Besteiro, Vo Duy et al. 2009). However, automatic reconstruction of metabolic pathways done *in silico*, using programs to run gene identities using known enzymes, is not perfect (Ginsburg 2009) and does not represent the truly functional metabolic network of the parasite. Moreover, the gene to metabolite ratio is not always 1:1 and the number of metabolites predicted can be underestimated where cellular enzymes have more than one substrate (Besteiro, Vo Duy et al. 2009). A better approach will be to identify the metabolites experimentally and then draw conclusions about the presence or absence of metabolic pathways in conjunction with genomic, transcriptomic and proteomic data. Since enzymes within biochemical pathways are potential drug targets (Travassos and Laufer 2009), new candidates can be identified or development of resistance to existing drugs can be studied in more detail in *Plasmodium* parasites with the help of metabolomics.

Some of the metabolomics approaches like NMR have been used to find biomarkers of *Plasmodium* infection in the infected host (Li, Wang et al. 2008) where urine and plasma samples were analyzed using  $^1\text{H-NMR}$  from *P. berghei* infected mice and markers of general infection were observed along with pipercolic acid which was found specific to *P. berghei* infection. Isotope labeled precursor NMR ( $^{13}\text{C}$ ) was used for metabolite profiling of host cell free parasites which showed that glycerol and glycerol-3-phosphate are major glucose metabolites in *P. falciparum* grown in an oxygen limited environment (Lian, Al-Helal et al. 2009). A number of different extraction protocols were tested in another study where  $^1\text{H-NMR}$  was used to profile *P. falciparum* metabolites where surprisingly accumulation of a culture buffering agent HEPES was seen inside parasites and extractions with perchloric acid were found to be better quenching as compared to methanol, methanol/water or methanol/chloroform/water (Teng, Junankar et al. 2009). NMR and  $^{13}\text{C}$  glucose were used to study the effect of *Plasmodium* infection on glucose utilization by host erythrocytes which showed that host metabolic pathways are greatly affected by the parasite and this serves as an example of the host parasite interaction where even uninfected erythrocytes were seen to have reduced glycolytic activity when treated with *Plasmodium* conditioned medium (Mehta, Sonawat et al. 2006).

Mass-spectrometry based metabolomics was used to show why *P. falciparum* infected erythrocytes have elevated Nicotinamide adenine dinucleotide (NAD<sup>+</sup>) levels and study the parasite NAD<sup>+</sup> metabolic pathway in detail (O'Hara, Kerwin et al. 2014). A similar analysis has also been used to reveal host-parasite interactions in *P. falciparum* infected erythrocytes where it was shown that systemic arginine depletion by the parasite might play some role in cerebral malaria pathogenesis (Olszewski, Morrisey et al. 2009). Using targeted metabolomics, mitochondrial metabolism (Macrae, Dixon et al. 2013), anaplerotic  $\text{CO}_2$  fixation and maintenance of cytosolic and mitochondrial redox balance in *P. falciparum* (Storm, Sethia et al. 2014) have also been explored. Malaria host-parasite interactions can be very interesting to study because there is a constant interplay of metabolites between host and parasite (Kafsack and Llinas 2010) and this dual system presents difficult challenges to profile individual metabolomes. The collective characterization of host-parasite metabolites has been called a co-metabolome by Holmes et al (Holmes, Wilson

et al. 2008) and it can be useful if baseline metabolomics data of uninfected host is available for quantitative and qualitative comparisons.

Metabolomics has a lot to offer and malaria research can benefit greatly from untargeted and targeted approaches to identify metabolic pathways which can lead to novel intervention strategies or improvement of existing ones.

## **1.6 Aims and objectives**

### **1.6.1 Finding out metabolic differences between reticulocytes and normocytes**

It is known that the reticulocytes are the preferred host cells of *P. berghei* and *P. vivax in vivo* (Galinski, Medina et al. 1992, Cromer, Evans et al. 2006) and apparently have a more complex cellular structure than normocytes (Gronowicz, Swift et al. 1984, Liu, Guo et al. 2010). The anticipation that reticulocytes have a more complex metabolic profile than normocytes and have a lot to offer to the parasites in terms of their metabolic reserves was explored by performing an untargeted metabolomics study where the metabolic profiles of reticulocytes and normocytes was compared using LC-MS and GC-MS and the metabolic differences between the two cell types established.

### **1.6.2 Elucidating the role of reticulocyte as a specialized host cell**

The apparent differences between reticulocytes and normocytes were assessed based on the metabolic pathways found to be present, enriched or reduced in either cell type. Parasite metabolism was then studied to elucidate which specific metabolic reserves contribute towards reticulocytes being the preferred choice for invasion and establishment of infection.

### **1.6.3 Establishing key metabolic differences between *Plasmodium* asexual, gametocyte and mosquito stages**

Untargeted metabolomics was also performed to find out key metabolic differences between the asexual and sexual stages of *P. berghei* parasites with an emphasis on determining how a gametocyte may prepare itself for the hostile environment of a mosquito midgut at the metabolic level as previously seen at transcriptional and translational level (Mair, Braks et al. 2006).

A targeted approach was also used to establish energy metabolism mechanisms in different stages in the life cycle of *P. berghei*. These studies provide

knowledge about novel and important biochemical host and parasite metabolic pathways and their interplay that offer potential routes to new intervention strategies against malaria.

## 2 Methods

### 2.1 *P. berghei* methods

#### 2.1.1 Infection of laboratory animals with *P. berghei* parasites

Infection of laboratory rodents (TO female mice 26-30g or Wistar female rats 150-175 g) was performed with *P. berghei* infected reticulocyte enriched blood obtained from cryopreserved stocks or directly from heart or tail-blood, from other infected animals. As *P. berghei* has a preference for invading reticulocytes, 0.1 ml of phenylhydrazine-HCl (12.5 mg/ ml solution) was administered to the mice by intraperitoneal injection 2 days prior to infection. For infection from cryopreserved parasites into a mouse, the contents of one cryotube containing 0.5 ml blood suspension were thawed at room temperature and 0.02-0.5 ml of the suspension was injected intraperitoneally into a mouse. For mouse infection with blood stages obtained from an infected animal (also known as mechanical passage), one drop of tail blood (5  $\mu$ l) from an infected animal with a parasitemia of 5-15% was collected in 10 ml PBS and 0.1 ml of this suspension was injected intraperitoneally into a mouse. 4-7 days, after injection, the parasitemia would typically increase from 0.1 to 5-20%. For infecting rats with blood stages obtained from an infected animal, 5-8 drops of tail blood (30-40  $\mu$ l) were collected from an infected animal with a parasitemia of 5-15% in 1 ml PBS and the 1 ml suspension was injected intraperitoneally in a rat, usually 0.5 ml on both sides of the abdomen. On day 4 or 5 after injection the parasitemia would typically range between 0.5-3 percent.

#### 2.1.2 Transfection of *P. berghei* parasites

Transfection of *P. berghei* parasites has been described in great detail earlier (Janse, Ramesar et al. 2006). Briefly, *P. berghei* infected reticulocyte enriched blood was used to set up *in vitro* schizont cultures as described in 2.1.7 and schizonts were purified as described in 2.1.8. Transfection was carried out by mixing 100  $\mu$ l of Nucleofector® solution, 10  $\mu$ l of DNA solution containing 5-10  $\mu$ g DNA with the schizont pellet and transferring the suspension into an electroporation cuvette which was then placed in the Amaxa Nucleofector® device and program U-33 was used. Following this, 50  $\mu$ l of medium was immediately added to the suspension and it was injected into a the tail vein of a

mouse kept in a 37°C warm box so that the veins were more accessible for injection.

### **2.1.3 Selection of transfected parasites**

Since the selectable marker used for transformation of *P. berghei* parasites contains a pyrimethamine resistant form of the human DHFR/TS gene, animals were provided with drinking water containing pyrimethamine (at 70 µg/ ml), one day after transfected parasites were injected and this was continued for a period of 5-8 days.

### **2.1.4 Cryopreservation of blood stage parasites**

Blood stages of parasite lines and clones were stored in liquid nitrogen. To obtain these blood stages from infected mice and rats, blood was collected by cardiac puncture and mixed 50:50 with a solution of 30% glycerol/PBS solution containing 0.05 ml of Heparin stock-solution (200 units/ml) and aliquoted into specially designed cryovials (Catalogue no. LW3534, Alpha laboratories) for storage at extremely low temperatures.

### **2.1.5 Investigation of the course of parasitemia**

The course of parasitemia was determined in Giemsa stained blood films made from tail blood. For checking parasitemia every infected mouse was tail-pricked and a thin blood film was prepared from tail blood on a standard microscope slide. After the slide was air-dried, it was fixed with methanol for 5 seconds, dried again and then immersed in a Couplin jar containing 12% Giemsa solution for 15 minutes. The slide was then rinsed carefully with water, air-dried and observed under a standard light microscope with immersion oil and objective at 100X. A minimum of 30 fields were visualized and infected cells were scored using a cell counter.

### **2.1.6 Removal of leucocytes from blood or cultured parasites**

Leucocytes were removed from collected blood or cultured parasites using columns prepared by filling up a 20 ml syringe with just sufficient glass wool to gate the end or using a 10 ml Zeba Spin Column (Catalogue number PN89898, Fisher) and cellulose powder (Catalogue number C6288-100G, Sigma) filled up to the 3 ml mark. These columns were first washed with RPMI1640 culture medium or PBS, then blood or parasite culture was passed through the column and allowed to flow through by gravity and then the columns were washed using PBS

or RPMI1640 culture medium again. RPMI1640 culture medium was used in the filtering process if parasites were used for further *in vitro* cultivation. PBS was used if parasites were to be used for DNA extraction or protein preparation. For quick and time sensitive applications, leucocytes were removed by using Plasmodipur Filters (Catalogue number 8011Filter25u, EuroProxima) attached to a 10 or 20 ml syringe. The filter was prewashed with RPMI1640 culture medium or PBS and after infected blood was passed through it, eluted with RPMI1640 culture medium or PBS.

### **2.1.7 Short term *in vitro* culture of asexual blood stage parasites for making schizonts**

For preparing schizonts, 1 ml blood was collected from an infected mouse by cardiac puncture using a 2 ml syringe at a parasitemia of 1-3%. Blood was transferred to 5 ml of complete culture medium containing 0.3 ml of heparin stock solution (200units/ml). Cells were pelleted by centrifugation for 8 minutes at 450g and supernatant was removed. Cells were then resuspended in 100 ml of complete culture media in a flask (TC FLASK 150CM - Corning 430823) and gassed for 30 seconds with a gas mix containing 5% CO<sub>2</sub>, 5% O<sub>2</sub>, 90% N<sub>2</sub>. Similarly, when setting up big volume cultures from infected blood obtained from a rat, the cells were finally resuspended in 150 ml of complete culture media. The flask was then incubated overnight at 37°C on a shaker at a minimal speed just to keep the cells in suspension. The next morning, 0.5 ml of the suspension was taken and a Giemsa-stained smear made from it to check for presence of mature schizonts.

### **2.1.8 Purification of schizonts**

The culture suspension containing the schizonts was combined and spun for 8 minutes at 450g and most of the supernatant was removed to resuspend the pellet in a final volume of 35 ml. A 55% Nycodenz/PBS solution was prepared and 10 ml of the Nycodenz-solution was laid under the culture suspension carefully, so that a sharp contrasting division was visible between the two suspension layers. The suspensions were then centrifuged for 20 minutes without the use of the brake at 450g and the brown layer at the interphase between two suspensions containing schizonts and mature gametocytes was carefully collected. The schizonts and gametocytes were pelleted by centrifugation for 8 minutes at 450g and for this washing step 10 ml culture medium obtained from

top of the gradient was used. The schizont pellet was resuspended in 500 µl of culture medium.

### **2.1.9 Generation of knockout parasites**

*P. berghei* schizonts (from line RMgm-7 which expresses GFP constitutively under *eef1a* promoter and from line RMgm-164 which expresses GFP in male gametocytes and RFP in female gametocytes) were transfected with linear DNA constructs containing the *yfcu-hdhfr* selectable marker flanked by homology arms (generated using primers in Table 6) corresponding to 5'UTR and 3'UTR of the orf of the gene of interest respectively, injected intravenously in female Wistar rats and TO mice and selected by pyrimethamine in drinking water as described in (Janse, Ramesar et al. 2006). Resulting transfectants were analysed by PCR for 5' and 3' integration (using primers in Table 6) and cloned by limiting dilution and further confirmed by PCR by lack of orf in mutants. For further phenotypic analysis, due to reasons of cost effectiveness and ease of handling, all mutants generated in TO mice were used and experiments were done by obtaining parasites grown in TO mice.

### **2.1.10 Cloning transfected parasite populations**

After transfection and selection by pyrimethamine, most of the parasites which are present in a rodent host were usually transfectants but some wild-type parasites survived drug treatment and transfected parasites had to be cloned to obtain a homogenous parasite line arising from a single parent. To achieve this, cloning by limiting dilution was done in 10 mice where 0.5-0.8 parasites were injected per mouse resulting in an infection rate of 20-60% of the mice. Briefly, a donor mouse was infected with the cryopreserved mixed population from which clones were to be obtained as described in 2.1.1 and parasitaemia was monitored until it reached 0.5% or above. Then from this mouse, 5 µl of tail blood was collected and diluted in 1 ml of complete culture medium/PBS, mixed well and 10 µl of this suspension was used for red blood cell counting using a Bürker cell counter haemocytometer. The concentration of erythrocytes in the cell suspension was determined and the sample was diluted to a final concentration of 0.5-0.8 parasites/0.2 ml culture medium/PBS. 0.2 ml of the suspension was injected per mouse intravenously in 10 mice. At day 10 after infection the mice were checked for parasites and usually 20 - 60% of mice became infected with a parasitaemia of 0.3 - 10%. Infected blood was collected

by cardiac puncture and used for cryopreservation or DNA extraction as described in 2.1.4 and 2.1.12 respectively.

### **2.1.11 Preparation of purified parasites for isolation of DNA and protein**

For isolation of DNA, RNA or preparing protein lysate from the parasites, first leucocytes were removed from blood or culture as described in 2.1.6 and then cells were pelleted by centrifugation for 8 minutes at 450g and then resuspended in cold (4°C) 50 ml erythrocyte lysis buffer (15mM NH<sub>4</sub>Cl, 1mM KHCO<sub>3</sub>, 0.1mM EDTA). The suspension was incubated on ice for 3-5min and then parasites were spun down by centrifugation for 8 minutes at 450g.

### **2.1.12 Genomic DNA extraction**

Parasite pellet was resuspended in 700 µl TNE buffer (10 mM Tris pH 8.0, 5 mM EDTA pH 8.0, 100 mM NaCl) and to the suspension, 200 µg RNAase (ribonuclease A 20 µl of a 10 mg/ml solution, bovine pancreatic in origin, Invitrogen- 12091-021) and 1% (v/v) SDS (100 µl of a 10% solution) was added. The mixture was incubated for 10 minutes at 37°C. Then 200 µg Proteinase K (from *Tritirachium album*, 20 µl of a 10 mg/ml solution, Sigma- P6556) was added and mixture was incubated for 1 hour at 37°C. Buffered phenol (Sigma- P9346) was added up to 1.5 ml, tube was inverted several times and centrifuged for 5 minutes at maximum speed. The aqueous upper phase was transferred to a new tube and buffered phenol: chloroform: isoamylalcohol: 25:24:1 (Sigma- P2069) was added up to 1.5 ml. The tube was inverted several times and centrifuged for 5 minutes at maximum speed. The aqueous upper phase was transferred to a new tube and chloroform: isoamylalcohol: 24:1 (Sigma- 25666) was added up to 1.5 ml. The tube was inverted several times and centrifuge for 5 minutes at maximum speed. The aqueous upper phase was transferred to a new tube and 0.1 volume of 3 M Sodium acetate, pH 5.2, and 2 volumes of 96% ethanol was added to it. The tube was inverted several times and DNA was precipitated at -20°C overnight. Then the tube was centrifuged for 20 minutes at maximum speed at 4°C, supernatant removed and DNA pellet was washed by adding 500 µl 70% ethanol and centrifuged 10 minutes at maximum speed at 4°C. Supernatant was discarded, DNA pellet was air-dried and resuspended with 100 µl water.

### 2.1.13 Asexual growth competition assay

Equal number of parasites ( $10^6$ ) of wt population expressing RFP under constitutive promoter eef1a (RMgm-86) and mutant population made in a parent line expressing GFP under the same promoter (RMgm-7) were mixed and injected into a mouse on day 0 and peripheral blood from the infected mouse was monitored using FACS analyses for the proportion of RFP positive (wt) and GFP positive (mutant) parasites over the next 12 days. Representative FACS screenshots Figure 2-1 show left panel on day 0 when wt and mutant populations are roughly in equal proportions and right panel shows that over time (by days 6-12), wt population overgrows a slow growing mutant. Infected blood was passaged into a new mouse when multiple infected cells started to appear in smears to allow for optimal growth.

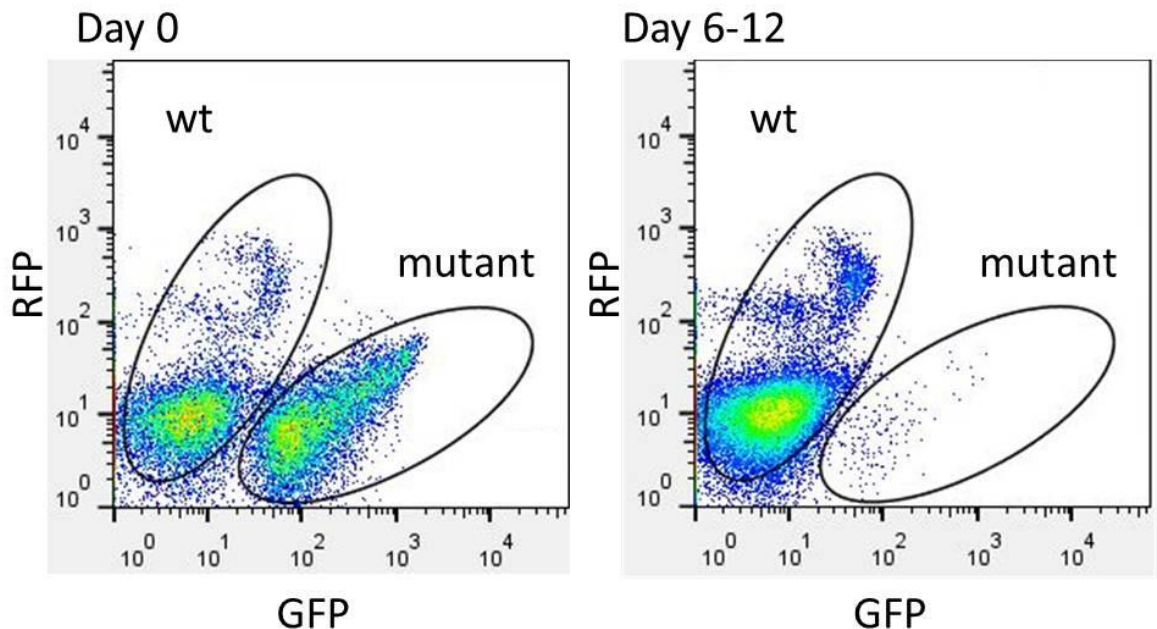


Figure 2-1 Competition growth assay of *P. berghei* wt line expressing RFP and a mutant line expressing GFP under eef1a promoter using FACS analysis

### 2.1.14 Lethality experiments in C57/B6 mice

$10^4$  iRBCs were injected intra-peritoneally into female 8-10 weeks old C57/B6 mice (n=5 per line) and parasitemia, disease pathology and mortality was monitored over 21 days.

### 2.1.15 Gametocyte conversion monitoring by FACS during blood stage growth

Mutants made in the RMgm-164 background which expresses GFP in male gametocytes and RFP in female gametocytes along with wt were grown in mice and peripheral blood was monitored by FACS analysis by checking for infected

erythrocytes (iRBCs) by Hoechst staining and the proportion of iRBCs expressing GFP and RFP, indicative of the presence of male and female gametocytes.

#### **2.1.16 Exflagellation assay and DNA quantification by FACS**

During exflagellation, male gametocytes undergo rapid endomitosis and DNA content is increased from  $n$  to  $8n$  within 8 minutes after activation. During this process, they pull a number of surrounding cells and form exflagellation centres which were counted on haemocytometer. DNA staining in exflagellating gametocytes was observed by fixing MACS-column purified activating gametocytes using 0.25% glutaraldehyde at 4 minute intervals, staining with 10  $\mu\text{M}$  Hoechst 33258 dye in PBS for 1 h at 37°C and doing FACS analysis on a CyAn ADP Analyser. UV excitation of Hoechst 33258 dye was performed with a violet laser (450/50 nm) and the gametocyte population was selected by gating on forward/side light scatter. The fluorescence intensity of a total of 100,000 cells was measured for each sample. The mean fluorescence intensity of the activating gametocyte is proportional to the mean DNA content of the parasites and activating male gametocytes and female gametocytes were gated based on DNA content at different time points based on the wt control. All data was plotted normalized to the controls.

#### **2.1.17 *in vitro* culture of ookinetes**

1 ml blood was collected from an infected mouse pre-treated with sulfadiazine in drinking water for 48 hours to remove asexual stages. This was done by cardiac puncture using a 2 ml syringe at a parasitemia (gametocytaemia) of 5-20%. The cells were diluted in a total volume of 30 ml of ookinete culture medium in a 75cm<sup>2</sup> flask. The ookinetes were cultured for 21 hours at 21°C. Ookinete production (ookinete conversion) rates, defined as the percentage of female gametes that develop into mature ookinetes, were determined by Giemsa-stained smears analysis.

#### **2.1.18 *in vitro* sexual crosses**

Equal numbers of gametocytes from two *P. berghei* lines obtained from infected TO mice treated with sulfadiazine in drinking water were taken and mixed in activation media. The suspension was then incubated at 21°C for 21 hours and giemsa smears were made for counting mature ookinetes and female gametes.

### 2.1.19 Mosquito transmission experiments

*P. berghei* infected reticulocyte enriched mice with a parasitemia of 5-10% were used to blood feed a cage of 250 mosquitoes for 10 minutes. Mature oocysts were counted in mosquito midguts between days 12-14 using a Leica M205 FA Fluorescence Stereomicroscope. Salivary gland sporozoites were checked between days 21-25. Infected mosquitoes were allowed to feed on naïve mice for 10 minutes between days 21-25 and these mice were observed for parasites by making giemsa stained blood smears between days 3-14 to check for successful transmission.

### 2.1.20 Determination of IC<sub>50</sub> value of *P. berghei* inhibitors *in vitro*

#### 2.1.20.1 Inhibition of asexual growth

Inhibitors were used to perform *in vitro* drug susceptibility tests in standard short-term cultures of synchronized *P. berghei* blood stages. Cultured and purified schizonts/merozoites of the reference ANKA strain of *P. berghei* line cl15cy1, obtained by Nycodenz density gradient purification were injected i.v. into the tail vein of a TO (Theilers Original outbred strain) mouse. Injected merozoites invade within 4h after injection and newly infected blood was collected from the mouse by heart puncture at 4h after the injection of the purified schizonts/merozoites. Infected blood was washed once (450 g, 8 min) with complete culture medium (RPMI1640 + 25% FCS, pH 7.5) followed by mixing of infected erythrocytes with serially diluted solutions of inhibitors in complete culture medium and incubated in 24-well plates in triplicate at a final concentration of 1% at 37°C for 24h under special gas mix of 5% CO<sub>2</sub>, 5% O<sub>2</sub>, 90% N<sub>2</sub>, conditions that permit ring forms to develop into mature schizonts. Parasite development was analysed by FACS after staining iRBCs with DNA-specific dye Hoechst-33258. The cells were pelleted by centrifugation (450 g, 8 min) and after removal of supernatant, cells were fixed with 0.25% glutaraldehyde/PBS solution and stained with 10 µM Hoechst-33258 solution in PBS for 1h at 37°C. Stained cells were analysed using MACSQuant analyser (Miltenyi Biotec, Germany). UV excitation of Hoechst-33258 dye was performed with a violet laser (450/50 nm) and the iRBC population was selected by gating on forward/sidelight scatter. A total of 100,000 cells per samples were analysed and mature schizonts were gated based on their fluorescence intensity and counted in each sample. For determination of growth inhibition, the number of mature schizonts observed was set to correspond to 100% growth for no drug

controls and percentage growth was calculated accordingly for the drug treated samples. 100% growth values were in the range 60-75% conversion of ring stage parasites to schizonts (15-20% of ring stage parasites committed to making gametocytes do not undergo DNA replication). Growth inhibitory curves were constructed in Graph pad Prism and based on data from three independent repeats, the IC<sub>50</sub> value for blood stage inhibition of *P. berghei* parasites were calculated. Giemsa stained smears from drug treated cultures were also checked to determine the stage at which parasites were growth arrested.

#### **2.1.20.2 Inhibition of gametocyte activation**

Gametocytes from the reference ANKA strain of *P. berghei* line cl15cy1 infected TO mouse which was treated with 30mg/L sulfadiazine in drinking water for 48 hours to kill asexual stages were obtained by cardiac puncture, suspended at 1% concentration in PBS (enriched with 20mM HEPES, 20mM Glucose, 4mM NaHCO<sub>3</sub>, 0.1% BSA, pH 7.25) mixed with different concentrations of inhibitors and incubated at 37 °C for 40 minutes in a 96 well-plate in triplicate samples. After this pre-treatment, cells were centrifuged at 400g for 5 min and supernatant was removed, washed twice with PBS and resuspended in fresh activation media (RPMI 1640 + 20% FCS +10µM Xanthurenic Acid, pH 7.5) at 1% concentration and incubated at 21 °C for 15 minutes. Exflagellation centres were counted in approximately 4000 visible cells on haemocytometer in triplicate. For calculation of exflagellation inhibition, the exflagellation percentage was set to 100% for no drug controls and was calculated accordingly for the drug treated samples. Inhibitory curves were constructed in Graph pad Prism. Based on counts from three independent repeats, the IC<sub>50</sub> value for exflagellation inhibition of *P. berghei* was determined.

#### **2.1.20.3 Inhibition of ookinete development**

Gametocytes from the reference ANKA strain of *P. berghei* line cl15cy1 infected TO mouse were obtained as above and infected blood was collected straight into ookinete growth medium (RPMI 1640 + 20% FCS +10µM Xanthurenic Acid, pH 7.5) at 1% concentration and incubated at 21 °C for 1 hour 30 minutes to allow for activation and fertilization without any inhibitors. Then inhibitors were added to this suspension in different concentrations in triplicates and incubated at 21 °C for a further 24 hours in 24 well plates. Then giemsa stained smears were made from all samples and slides were counted for mature ookinetes and female gametes. Approximately a combined total of minimum 100 ookinetes and female

gametes were counted per smear. To calculate ookinete conversion rates, number of mature ookinetes was divided by the combined total number of ookinetes and female gametes which was found to be in the range of 65-70% conversion of female gametes to mature ookinetes in no drug controls. For determining ookinete maturation inhibition, the ookinete conversion rate was set to 100% for no drug controls and was calculated accordingly for the drug treated samples. Inhibitory curves were constructed in Graph pad Prism. Based on counts from three independent repeats, the IC<sub>50</sub> value for ookinete maturation inhibition of *P. berghei* was determined.

## **2.2 Determination of IC<sub>50</sub> value of *P. falciparum* asexual growth inhibition *in vitro***

*P. falciparum* 3D7 strain was used for determining IC<sub>50</sub> values of inhibitors in *in vitro* cultures by measuring <sup>3</sup>H-Hypoxanthine incorporation in the presence of inhibitors in increasing concentrations as described (Desjardins, Canfield et al. 1979). Cultures were set up at 0.5 % parasitemia and approximately 2 % hematocrit in complete RPMI medium without hypoxanthine (IC<sub>50</sub> medium). A serial dilution of 2x required inhibitor concentration was prepared in a 96 well plate in similar IC<sub>50</sub> medium. In each well, 100 µl of inhibitor was mixed with 100 µl of cells, creating a 1 x final concentration of the inhibitor. Incorporation of <sup>3</sup>H-Hypoxanthine in uninfected erythrocytes and parasites incubated without inhibitor was also measured as negative control. Plates were incubated for 48 hours at 37°C in the presence of a specialized gas mix (5% CO<sub>2</sub>, 1% O<sub>2</sub>, 94% N<sub>2</sub>). After 48 hours of incubation, 100 µl of medium from each well was replaced with fresh medium containing 5 µCi <sup>3</sup>H-Hypoxanthine/ml. Plates were incubated for further 24 hours and then frozen at -20°C. Then the plates were defrosted and harvested using a Tomtec Mach III harvester and Wallac Printed Filter Mat- A filter mats. The filter mats were dried at 60°C for one hour and sealed in a plastic bag with 4 ml scintillation liquid. Radioactive decay was measured in a Wallac Trilux MicroBeta counter for 1 min per well. IC<sub>50</sub> values were calculated using GraphPad Prism software.

## **2.3 Molecular biology**

### **2.3.1 Preparation of DNA constructs**

DNA constructs for making knock out vectors were prepared using standard molecular biology techniques. For knock out constructs, homology arms

(approximately 1-2 kb upstream and downstream of the open reading frame of the gene to be knocked out) were amplified using PCR on wild type *P. berghei* genomic DNA where primers were designed with the appropriate restriction sites or overlapping sequence in place. The general protocol used for doing PCR was as follows.

PCR reaction mix:

Component	Volume ( $\mu$ l)	Final concentration
10 X PCR Buffer	5	1 X
25mM dNTPs	0.5	0.25mM
100 pmol/ $\mu$ l Sense primer	0.2	0.4 $\mu$ M
100 pmol/ $\mu$ l Anti-sense primer	0.2	0.4 $\mu$ M
50mM MgCl <sub>2</sub>	2.0	2mM
Taq Polymerase	0.2	1 unit
DNA template	1	(10-100ng per reaction)
MilliQ Water	Up to 50 $\mu$ l	

Thermo cycler program:

94 °C	94 °C	*Tm °C	72 °C	72 °C	4 °C
0:30 sec	0:30 sec	0:30 sec	**1min	10 min	$\infty$
30 cycles					

\*Tm- melting temperature of primer pair

\*\* 1 minute extension time is enough to amplify a 1kb fragment

The obtained PCR products were purified using Qiaquick PCR purification kit (Qiagen) following manufacturer's instructions. When doing molecular cloning, both PCR product and target plasmid were digested with appropriate restriction enzymes and then purified again either using Qiaquick PCR purification kit or by running on gel and extracting the appropriate band and purifying it using Qiaquick gel extraction kit (Qiagen) following manufacturer's instructions. The concentration of both the insert and the vector was determined by Nanodrop spectrophotometer and ligation reactions were set up in a vector to insert molar ratio of 1:3 using Rapid DNA ligation kit (Roche Diagnostics). The ligation mix was used to transform fusion-blue competent *E.coli* cells, by mixing 2  $\mu$ l ligation mix gently with cells and incubating them on ice for 30 minutes, followed by

heat-shock at 42°C for 45 seconds and incubation on ice for 1 minute. The bacteria were then incubated at 37°C with 400 µl LB broth for an hour and then the transformed bacteria were spread on pre-warmed LB agar plate with 100 µg/ml ampicillin and incubated overnight at 37°C. The next day, individual bacterial colonies were inoculated in 3 ml LB medium with ampicillin (100 µg/ml). After overnight incubation, the cultures were spun down and plasmid was extracted using the Qiaquick miniprep kit (Qiagen) following manufacturer's instructions. The obtained plasmids were analysed by restriction enzyme digestion. The plasmids were then linearized and appropriate fragments gel purified. 5-10 µg of the purified fragment was used for transfecting *P. berghei* schizonts.

When making PCR based knock-out vectors, homology arms were amplified using TaKaRa LA Taq® DNA Polymerase in the first reaction, cleaned as mentioned above and then used for a second (2 step) PCR reaction with TaKaRa LA Taq® DNA Polymerase where the overlapping ends complimentary to the selection cassette facilitated the amplification of the whole construct by a couple of external tag primers, ready for transfection which was then gel purified.

PCR 1 was set up as:

LA Taq	0.25µl (1.25 U)
LA PCR Buffer	2.5 µl
dNTP mix (2.5mM each)	4 µl
wt DNA	0.5 µl (50ng)
Water	12.75 µl
Primer 1 (10 pmol/µl)	2.5 µl
Primer 2 (10 pmol/µl)	2.5 µl
	25 µl

Thermo cycler program:

98°C	98°C	65°C	60°C	55°C	72°C	72°C	10°C
05:00	00:20	00:10	00:10	00:10	00:30	07:00	∞
30 cycles							

PCR2 was set up as:

Step1	
Upstream homology arm	100 ng
Downstream homology arm	100 ng
pL0048 containing selection cassette	100 ng
Buffer + MgCl <sub>2</sub>	5 µl
dNTPs (2.5mM each)	8 µl
LA Taq (2.5 U)	0.5 µl
Water	Upto 39 µl

Step 1 Thermo cycler program:

95°C	95°C	42°C	72°C	72°C	10°C
05:00	01:00	01:00	02:00	05:00	∞
15 cycles					

Step2: with primers

Then added to individual tubes were,

5 µl external tag primer 1 + 5 µl external tag primer 2 + 0.5 µl La Taq

Thermo cycler program:

94°C	94°C	50°C	68°C	94°C	50°C	68°C	68°C	10°C
02:00	00:15	00:30	04:30	00:15	00:30	4:30 + 5 sec/cycle	07:00	∞
15 cycles				20 cycles				

### 2.3.2 Checking for integration of transfectants by PCR

Primers were designed to anneal to the genomic region outside the two homology arms and then to check for integration, a corresponding reverse or forward primer was designed to anneal to the selection cassette. After correct integration of the homology arms and the selection cassette into the genome, both 5' and 3' integration PCRs were performed using the standard PCR protocol

and diagnostic gels were run to confirm integration in the right orientation (Figure 2-2).

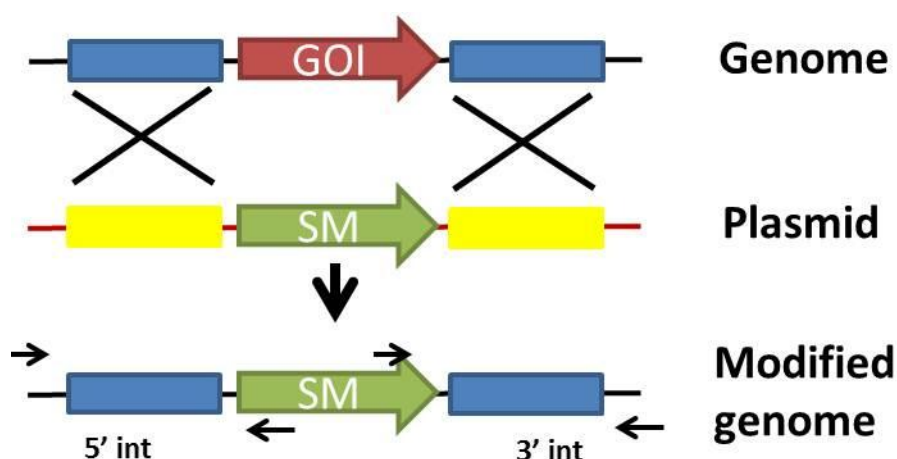


Figure 2-2 Schematic representation of diagnostic PCR to detect correct integration in modified parasite genome. GOI- Gene of interest, SM- Selectable Marker.

PCRs were also performed using primers which amplify the knocked out open reading frame (orf) in the wt control to see wt population background in the transfected lines and confirm clonality of new lines post cloning by limiting dilution.

### 2.3.3 Western blot analysis

Western blot analyses were performed on parasite pellets that were either freshly prepared or stored at  $-80^{\circ}\text{C}$  obtained either from an infected rodent host or overnight *in vitro* culture. Pellets were resuspended in 1x lysis buffer containing (1% Triton in PBS and protease inhibitors), stored on ice for 10 minutes, then mixed with 2x SDS gel-loading buffer (100 mM Tris-HCl pH 6.8; 200 mM dithiothreitol; 4% SDS; 0.2% bromophenol blue; 20% glycerol). The samples were then run on a SDS-PAGE gel and transferred to a Whatman® Protran® nitrocellulose membrane, which was subsequently probed with a primary antibody of choice and a compatible HRP-labelled secondary antibody detectable by an Enhanced Chemiluminescence (ECL) detection system (see below).

#### 2.3.3.1 Sodium dodecyl sulphate polyacrylamide gel electrophoresis (SDS-PAGE)

The Mini-PROTEAN® cell system (Bio-Rad) was used for gel preparation and running. A short-plate and a spacer-plate were cleaned with detergent, washed and then cleaned with ethanol and placed into the casting frame. The resolving

gel (12%) for standard protein analysis was prepared (Table 1) and cast. The top of the gel was cover with water saturated butanol and allowed to polymerise which took approximately 20 minutes. The stacking gel was prepared and following draining the water saturated butanol and a quick water washing, was immediately poured on the top. Then the comb was inserted and the gel was allowed to polymerise for 20 minutes.

Components	Resolving gel (12%)	Stacking gel
ddH <sub>2</sub> O	3.8 ml	2.03 ml
40% Acrylamide/Bis	3.0 ml	0.38 ml
Tris buffer	2.5 ml (1.5 M, pH 8.8)	0.38 ml (0.5 M, pH 6.8)
10% SDS	0.1 ml	0.03 ml
10% Ammonium per-	0.1 ml	0.03 ml
Glycerol	0.5 ml	0.15 ml
TEMED	4.0 $\mu$ l	3.0 $\mu$ l

**Table 1 SDS-PAGE resolving and stacking gel composition**

After the gel was polymerised, the gel cassette was removed from the casting frame and placed into the electrode assembly with the short plate facing inward and placed into the mini tank. The inner chamber was filled with approximately 100 ml of running buffer. Approximately 200 ml of running buffer was added to the mini tank (lower buffer chamber). After removing the comb, the wells were quickly washed and the protein samples were loaded into the wells. The gel was run at 120V for 1.5 - 2 hours.

### **2.3.3.2 Protein transfer onto the membrane**

The Trans-Blot<sup>®</sup> electrophoretic transfer cell system (Bio-Rad) was used for protein gel blotting onto a Whatman<sup>®</sup> Protran<sup>®</sup> nitrocellulose membrane in the following manner:

1. The transfer buffer (Tris 2.8g, Glycine 2.9 g, Methanol 200 ml, ddH<sub>2</sub>O upto 1 L) was chilled on ice 1 hour before blotting. The blot-cell was set up in the cold room.
2. 4 pieces of Whatman 3MM filter paper were cut with dimensions 9 x 7 cm and soaked together with fibre pads in transfer buffer.

3. A piece of Whatman® Protran® nitrocellulose membrane was cut to the same size as that of the protein gel.
4. The gel was removed from the electrophoresis apparatus and placed in transfer buffer.
5. The transfer cassette was assembled as follows (black side down): fibre pad, 2 layers of Whatman® filter paper, gel (upside down and without bubbles), Whatman® Protran® nitrocellulose membrane (without bubbles), 2 layers of Whatman filter paper, and fibre pad.
6. The cassette was placed in the transfer cell (black on black), ice element was inserted and transfer buffer was filled in.
7. The transfer cell was connected to the power source and run on 20V overnight in the cold room with the buffer stirring.

### **2.3.3.3 Immuno-detection**

After the membrane transfer, the antigen of interest was detected by an antigen specific primary monoclonal or polyclonal antibody, which was then recognised by a secondary anti-IgG antibody conjugated to horseradish peroxidase (HRP). The complex was visualised using the ECL Plus™ Western blotting detection reagents (Amersham Biosciences), which utilises a technology based on the enzymatic generation of acridinium ester intermediates. These intermediates react with peroxide under slight alkaline conditions to produce a sustained, high intensity chemiluminescence.

The Whatman® Protran® nitrocellulose membrane was first blocked in 2% non-fat dried milk/0.1% Tween in PBS for 1 hour at RT or 4°C overnight in order to block non-specific binding sites. The primary antibody was diluted in 2% non-fat dried milk/0.1% Tween in PBS (diluted 1:100 up to 1:5000 depending on the antibody; determined empirically) and the membrane was incubated overnight at 4°C (with rocking) with this diluted antibody milk solution. The membrane was briefly rinsed in 0.1% Tween in PBS, and washed 3x for 15 minutes in the same buffer at room temperature. The secondary HRP labelled antibody (Dako UK Ltd.) was diluted either 1:1000 or 1:3000 in 2% non-fat dried milk/0.1% Tween in PBS. The membrane was incubated for 1 hour at room temperature (with rocking). The membrane was again rinsed in 0.1% Tween in PBS and washed 3 times for 15 minutes at RT. The detection solution (Amersham Biosciences) was prepared by mixing solutions A and B in a ratio of 1:1. The

washed membrane was placed on a sheet of Saran Wrap and the detection solution was pipetted onto the membrane. Following 1 minute incubation the excess detection reagent was drained and the membrane wrapped in Saran Wrap. Finally the membrane was placed in an X-ray film cassette. Chemiluminescence detection was carried out in a dark room using an X-ray film. Exposure times varied according to the signal strength.

## **2.4 Immunofluorescence assay (IFA)**

IFAs were performed on fixed *P. berghei* infected reticulocyte enriched erythrocytes and mosquito stages. Smears from cultures were fixed with ice cold methanol for 10 minutes, washed twice in PBS and permeabilised with 0.1% Triton X-100/PBS for 10 minutes at room temperature. Slides were then blocked in 3% BSA/PBS for 1 hour at room temperature or overnight at 4°C. The primary antibody was diluted to a desired concentration in 3% BSA in PBS and pipetted on to the slides and covered with a piece of Parafilm to keep it from drying. Incubation was carried out for 2 hours at room temperature or overnight at 4°C. Slides were then washed three times in PBS for 10 minutes each to remove excess primary antibody. Secondary antibody was applied at 1:1000 to 1:2000 dilutions (in 3% BSA/PBS) and allowed to incubate for 1 hour at room temperature. Slides were washed three times for 10 min. in PBS. The slides were mounted in Vectashield® mounting medium with DAPI (Vector labs) and sealed with transparent nail polish to prevent drying. Fluorescence was analysed and images acquired using the DeltaVision Epifluorescence Microscope Imaging System and analysed by the SoftWoRx Explorer Suite software.

## **2.5 Reticulocyte methods**

### **2.5.1 Enrichment of reticulocytes in mice and rats**

Reticulocytes constitute 1-2% of RBCs in circulating peripheral blood. In mice and rats, the number of reticulocytes can be increased by depleting RBCs in blood inducing an erythropania which then leads to an accelerated erythropoiesis. This can be done either by controlled bleeding, erythropoietin administration or by administering phenylhydrazine-HCl which results in denaturation of haemoglobin and RBC lysis. Reticulocytosis evoked by phenylhydrazine-HCl administration is more rapid and is more easily controlled

for experimental purposes (Flanagan 1970), hence this method was used for experiments.

### **2.5.2 Monitoring reticulocyte production**

In all experimental animals, reticulocyte production was monitored whilst they were under procedures to make sure that they were bled on the day when number of reticulocytes was at its peak. A brief description of the procedure is as follows:

One female TO (Theilers Original) mouse (26-30 g) or a female Wistar rat (150-175 g) was injected intraperitoneally once with phenylhydrazine-HCl dissolved in 0.9% NaCl (w/v) at 100 mg/kg body weight and was monitored for production of reticulocytes for 9 days. Every day, 5  $\mu$ l of tail blood was taken in 500  $\mu$ l 0.1%BSA/PBS (kept on ice) and mixed well. Erythrocytes were stained with reticulocyte markers: either CD71 or sodium-potassium ATPase antibodies. Briefly, for CD71 staining, erythrocyte suspension received 3.1  $\mu$ l of 0.2 mg/ml CD71-APC (17-0711, Ebioscience) conjugated antibody and 2.5  $\mu$ l of 0.5 mg/ml Ter119 FITC (11-5921 Ebioscience) conjugated antibody, incubated on ice for 30 minutes, spun down for 15 seconds at 13000g, supernatant removed and resuspended in 0.1%BSA/PBS. For sodium-potassium ATPase staining, erythrocyte suspension received 5  $\mu$ l sodium-potassium ATPase antibody (AB76020, Abcam), incubated on ice for 30 minutes, spun down for 15 seconds at 13000g, supernatant removed, washed with 0.1%BSA/PBS and resuspended in 500  $\mu$ l 0.1%BSA/PBS with 2.5  $\mu$ l APC conjugated goat-anti-rabbit antibody (A-10931 Invitrogen). It was incubated on ice for 30 minutes, spun down, supernatant removed and resuspended in 500  $\mu$ l 0.1%BSA/PBS. Stained cells were analysed using a MACSQuant analyser (Miltenyi Biotec, Germany).

### **2.5.3 Obtaining a pure population of reticulocytes**

The highest number of reticulocytes in peripheral blood was observed on day 5 post single dose of phenylhydrazine-HCl. Hence reticulocytes were harvested on day 5 after phenylhydrazine-HCl injection for subsequent experiments. A pilot experiment was done to assess the number of reticulocytes which can be FACS sorted within a reasonable amount of time from a 42% CD71 positive population. Cells were prepared from a mouse treated with phenylhydrazine-HCl and cells stained with CD71 antibody as described in 2.5.2. Cells were sorted on BD FACS Aria cell sorter. Considering 2 continuous runs of about 1 hour 30 minutes, it was

found that from a 42% APC positive population, 4.5 to 5 million APC positive and 6.5 to 7 million APC low/negative cells can be obtained in 1 hour. Therefore, to sort  $10^7$  cells, approximately 2 to 2.5 hours of sorting time will be required. Sorting of  $10^8$  cells would require, approximately 20 hours during which time the reticulocytes continue to mature to normocytes. So being very time consuming, expensive and uncondusive to experimental design, FACS sorting was ruled out as a method to get pure populations of reticulocytes for metabolomics experiments as at least  $10^8$  cells are needed for each replicate. The metabolic signature of reticulocytes was deduced by comparing erythrocytes containing 98% or more normocytes to erythrocytes which were reticulocyte enriched (35% or more). Another way of obtaining pure reticulocytes could be in *in vitro culture* of CD34+ peripheral mouse stem cells and differentiating them into erythroid precursors. This method is not established in our laboratory yet and is being explored as a future possibility with some collaboration. See chapter 3 for details of reticulocyte metabolomics data.

## **2.6 Untargeted Metabolomics methods using LC-MS & GC-MS**

### **2.6.1 Uninfected reticulocyte enriched and un-enriched red blood cell preparation**

For collecting reticulocyte enriched red blood cells, three female Wistar rats were each injected with phenylhydrazine-HCl dissolved in 0.9% NaCl (w/v) at a dose of 100 mg/kg body weight and reticulocyte percentage in peripheral blood was monitored for 5 days as described in 2.5.2. In another three female Wistar rats, reticulocyte percentage in peripheral blood was monitored for five days as described in 2.5.2. On day five, all rats were bled by cardiac puncture and blood from each rat was collected in 10 ml RPMI1640 medium. Each suspension was passed through a prewashed Plasmodipur filter as described in 2.1.6. Cells were eluted with 10 ml RPMI1640, which gave a total volume of 20 ml which was divided into 2 falcon tubes with 10 ml each, tubes A and B. Both tubes were spun at 450g for 8 minutes (acceleration 9/ deceleration 2). Supernatant was removed from both the tubes. Pellet from tube A was resuspended in 100 ml complete media containing 75% RPMI1640 and 25% FCS, transferred to a 150cm flask, gassed for 60 seconds with a gas mix containing 5% CO<sub>2</sub>, 5% O<sub>2</sub>, 90% N<sub>2</sub>. The flask was then incubated for 24 hours at 37°C on a shaker at a minimal speed just to keep the cells in suspension. Pellet from tube B was resuspended in 40 ml

chilled enriched PBS (with 20 mM Hepes, 20 mM Glucose, 4 mM NaHCO<sub>3</sub>, and 0.1% BSA) and kept on ice. 20 µl of this suspension was put on a haemocytometer and cells were counted. From the suspension kept on ice, 4 tubes of 10<sup>8</sup> cells (total 12 tubes from all replicates) were prepared and kept on ice until metabolite extraction. Next day, after about 24 hours of incubation at 37°C, a thermometer was put in flask with sample A and the bottom of the flask was submerged in a dry ice ethanol bath and swirled around until temperature in thermometer read 8°C. The flask was then taken out immediately and divided equally into two pre-chilled falcon tubes kept on ice. Both tubes were spun at 450g at 4°C for 8 minutes (acceleration 9/deceleration 2). Supernatant was removed from both the tubes. Pellets from both tubes were resuspended in 40 ml chilled (4°C) enriched PBS and kept on ice. 20 µl of this suspension was put on a haemocytometer and cells were counted. From the suspension kept on ice, four tubes of 10<sup>8</sup> cells (total 12 tubes from all replicates) were prepared and kept on ice until metabolite extraction.

### **2.6.2 *P. berghei* schizonts (Gametocyte Producer and gametocyte non-producer) whole cells, lysed parasites and lysis supernatant preparation**

For schizonts from gametocyte producing and gametocyte non-producing parasites, three Wistar rats each were treated with phenylhydrazine-HCl as described in 2.5.1 on day one and next day were infected by mechanical passage of *P. berghei* parasites from mice infected with a gametocyte producing clone (820cl1m1cl1) and gametocyte non-producing clone (m9w21d) as described in 2.1.1. On day five, at parasitemia levels 7-12% all rats were bled by cardiac puncture and blood from each rat was collected in 10 ml RPMI1640 medium. Each suspension was passed through a prewashed Plasmodipur filter as described in 2.1.6. Cells were eluted with 10 ml RPMI1640 and spun at 450g for 8 minutes (acceleration 9/deceleration 2). Supernatant was removed and pellet was resuspended in 150 ml complete media containing 75% RPMI1640 and 25% FCS, transferred to a 150cm flask, gassed for 60 seconds with a gas mix containing 5% CO<sub>2</sub>, 5% O<sub>2</sub>, and 90% N<sub>2</sub>. The flask was then incubated for 24 hours at 37°C on a shaker at a minimal speed just to keep the cells in suspension. Next day after about 24 hours of incubation at 37°C, a thermometer was put in flask and the bottom of the flask was submerged in a dry ice ethanol bath and swirled around until the temperature in thermometer read 8°C. After this the flask was taken

out immediately and divided equally into four pre-chilled falcon tubes kept on ice. 10 ml chilled 55% Nycodenz was laid down carefully at bottom of tubes and tubes spun at 450g at 4°C for 20 min without using the brake. Schizonts were collected from the interface and pooled together from four tubes for each culture and topped up with culture medium up to 40 ml and kept on ice. 20 µl of this suspension was put on a haemocytometer and cells were counted. From the suspension kept on ice, four tubes of  $10^8$  cells (total 12 tubes from all replicates) were prepared and kept on ice until metabolite extraction. Another Falcon tube was prepared with  $4 \times 10^8$  cells and spun at 450g at 4°C for eight minutes. Supernatant was removed and cells were resuspended with 10 ml chilled erythrocyte lysis buffer and keep on ice for five min. The suspension was again spun at 450g at 4°C for eight minutes. Four tubes were prepared (total 12 tubes from all replicates) with 10 µl supernatant each and keep on ice until metabolite extraction. The rest of supernatant was then removed and the pellet was resuspended in chilled ePBS. The pellet was divided into four tubes with  $10^8$  cells (total 12 tubes from all replicates) and kept on ice until metabolite extraction.

### **2.6.3 *P. berghei* gametocytes: whole cell, lysed parasite and lysis supernatant preparation**

12 Wistar rats (three groups of four each) were treated with phenylhydrazine-HCl chloride as described in 2.5.1 on day 1 and next day were infected by mechanical passage of *P. berghei* parasites from a mouse infected with a gametocyte producing clone (820cl1m1cl1) as described in 2.1.1. At parasitemia levels of 7-12% at the end of day 5, the animals were given sulphadiazine in drinking water at 25 mg/liter to kill asexual stages. Animals were bled early morning on day 8 by cardiac puncture and blood from each rat was collected in 10 ml chilled enriched PBS. Each suspension was passed through a prewashed Plasmodipur filter as described in 2.1.6 and topped up with chilled enriched PBS to make a total volume of 35 ml per tube. 10 ml chilled 53% Nycodenz was laid down carefully at bottom of tubes and tubes were spun at 450g at 4°C for 20 min without brake. Gametocytes were collected from interphase and pooled together from four tubes for each group and topped up with enriched PBS up to 40 ml and kept on ice. 20 µl of this suspension was put on a haemocytometer and cells were counted. From the suspension kept on ice, 4 tubes of  $10^8$  cells (total 12 tubes from all replicates) were prepared and kept on ice until metabolite extraction. Another Falcon tube was prepared with  $4 \times 10^8$  cells and

spun at 450g at 4°C for 8 minutes (acceleration 9/deceleration 2). Supernatant was removed and cells were resuspended with 10 ml chilled erythrocyte lysis buffer and keep on ice for 5 min. the suspension was again spun at 450g at 4°C for 8 minutes (acceleration 9/deceleration 2). 4 tubes were prepared (total 12 tubes from all replicates) with 10 µl supernatant each and keep on ice until metabolite extraction. The rest of the supernatant was removed and pellet was resuspended into chilled ePBS. The pellet was divided into 4 tubes of 10<sup>8</sup> cells (total 12 tubes from all replicates) and kept on ice until metabolite extraction.

#### **2.6.4 Metabolite Extraction, drying and storage**

All the tubes were kept cold while doing extractions. Tubes with 10<sup>8</sup> cells each were centrifuged at 4°C for 10 minutes at 1300g and supernatant was removed. The pellet was resuspended with 500 µl cold enriched PBS and centrifuged at 4°C for five minutes at 2700g and supernatant removed again. Pellet was then resuspended in cold 200 µl of Chloroform/Methanol/Water (1:3:1) plus internal standards (5-fluorouridine, Cl-phenyl-cAMP, N-methyl glucamine, Canavanine, Piperazine all at 1 µM concentrations). The suspension was then mixed vigorously on cooled (4°C) shaker for one hour and sonicated for two min in ice cold water bath. This was followed by centrifugation for five minutes at 15,300g at 4°C. 180 µl supernatant was taken and split in two tubes separately for LC-MS runs in the Glasgow Polyomics facility at the University of Glasgow and GC-MS runs in Metabolomics Australia facility at the University of Melbourne. Tubes for the Melbourne lab were dried down under nitrogen flow, capped tightly and put at -80°C before shipment on dry ice. Tubes for the Glasgow lab were topped up with nitrogen, capped tightly and kept at -80°C.

#### **2.6.5 LC-MS analysis**

For LC-MS analysis, samples underwent hydrophilic interaction liquid chromatography-mass spectrometry with a 20mm x 2.1mm ZIC-HILIC guard column coupled to a 150 x 4.6mm ZIC-HILIC analytical column running at 300ul/min which was attached to an Orbitrap Exactive (Thermo Fisher). The gradient ran from 20% H<sub>2</sub>O 80% acetonitrile to 80% H<sub>2</sub>O, 20% acetonitrile in 30 minutes, followed by a wash at 5% acetonitrile, 95% H<sub>2</sub>O for 6 minutes, and equilibration at 20% H<sub>2</sub>O, 80% acetonitrile for 8 minutes. Raw mass spectrometry data was processed using the standard Glasgow Polyomics pipeline, consisting of XCMS for peak picking (Smith, Want et al. 2006), MzMatch for filtering and

grouping (Scheltema, Jankevics et al. 2011) and IDEOM for further filtering, post-processing and identification (Creek, Jankevics et al. 2012). Core putative metabolite identifications were validated against a panel of unambiguous standards by mass and retention time. Matched mass and retention time is acceptable as a tier 1 identification according to the Metabolomics Standards Initiative (MSI) (Sansone, Fan et al. 2007). Additional putative identifications were assigned by mass and predicted retention time followed by manual data filtration for removing duplicates and false positives and for including false rejections.

### 2.6.6 GC-MS analysis

For GC-MS, dried extracts were reconstituted with extraction solvent containing an additional internal standard (scyllo-Inositol SI 1 nmol) and dried in vacuum. Methoximation and derivatisation was done automatically with the help of an auto-sampling robot, first by adding 20  $\mu$ l of 20 mg/ml methoxyamine in pyridine and shaking at 37°C for 2 hours and then adding 20  $\mu$ l of BSTFA + 1% TMCS Silylation reagent and shaking at 37°C for 1 hour. Samples were then rested at room temperature for 1 hour and then 1  $\mu$ l was injected on an Agilent 7890A GC-5975 C mass-detector combination setup. Chromatography was done on a 30 m VF5-MS column with 0.25 mm inner diameter and helium as the carrier gas. The initial oven temperature was 70°C for 1 min, then 1°C/min oven temperature ramp to 76°C, then 5°C/min to 325°C and held for 10 min. Obtained raw data was fed through the Metabolomics Australia's in-house Metabolomics software PyMS (O'Callaghan, De Souza et al. 2012) which allowed for pre-processing of data by peak-finding, integration and alignment and generated a data matrix of candidate metabolites showing their intensity representing abundance of a metabolite in a given sample and its unique retention time. Then using the Agilent Chemstation software, the chromatograms were manually checked and the peaks corresponding to the retention times in the PyMS matrix were analysed for their Electron Ionisation (EI) spectrum. Metabolites were assigned putative identities by matching their spectra (with a cut-off score of  $\geq 90\%$ ) to Agilent Fiehn and NIST GC-MS Metabolomics libraries of metabolite GC-MS spectra which includes a searchable EI spectrum and retention index.

## 2.7 Targeted metabolomics methods using GC-MS

### 2.7.1 Cultures using minimal media and labelled carbon source

Based on the publications by Divo *et al* related to nutritional requirement of *Plasmodium* parasites in *in vitro* cultures (Divo, Geary et al. 1985, Geary, Divo et al. 1985, Geary, Divo et al. 1985), minimal media components were selected and prepared based on RPMI 1640 concentrations (Schuster 2002) using the following components available in the laboratory.

Salts and other components:

Components	mg/L (final concentration 1x)	mg/250 ml (for 10x stock)
Ca(NO <sub>3</sub> ) <sub>2</sub> .4H <sub>2</sub> O	100	250
KCl	400	1000
MgSO <sub>4</sub> (anhydrous)	48.8	122
NaCl	5300	13250
NaHCO <sub>3</sub>	2000	5000
Na <sub>2</sub> HPO <sub>4</sub> (anhydrous)	800	2000
Hypoxanthine	4.1	10.2
D-Glucose	2000	5000
Glutathione	1	3.3
HEPES	5958	14895
Phenol Red	5	12.5

All the components were mixed in ddH<sub>2</sub>O and stored at 4 °C.

Amino acids:

Amino acids	mg/L (final concentration 1x)	mg/250 ml (for 10x stock)
L-Cystine.2HCl	65	162.5
L-Glutamic Acid	20	50
L-Glutamine	300	750
L-Isoleucine	50	125
L-Methionine	15	37.5

L-Proline	20	50
L-Tyrosine.2Na.2H <sub>2</sub> O	29	75

All the components were mixed in ddH<sub>2</sub>O and stored at 4 °C.

Vitamins: Only Pantothenate was found to be essential by (Geary, Divo et al. 1985).

Vitamins	mg/L (final concentration 1x)	mg/ 10 ml (for 10,000x stock)
Ca-Pantothenate	0.25	25

Ca-Pantothenate was mixed in ddH<sub>2</sub>O and stored at 4 °C.

All components were mixed to 1x concentration and Pen-Strep antibiotic mix (1 ml/l) was added just before use. AlbuMAX® (Life Technologies- 11020-021) was added to a concentration of 5g/l, pH was adjusted to 7.3 and complete media was then sterile filtered using a 0.22µ filter. When a labelled carbon source was to be used for cultures (e.g. <sup>13</sup>C U-Glucose or <sup>13</sup>C<sup>15</sup>N U-Glutamine), the corresponding component was replaced with the isotopically labelled form.

### 2.7.2 Isotopic labelling of *P. berghei* asexual cultures

Parasites from the line 820m9w21dm1cl1 (gametocyte non-Producer) were used to grow a synchronous culture. 2 TO mice were bled (approximately 3 ml blood was obtained) 5 mins post invasion (after purified schizonts were injected i.v.) at a parasitemia of 6.5% (all very young rings). The mice were pre-treated with phz 5 days before to induce reticulocytosis. Blood was passed through two pre-washed Plasmodipur filters to remove leucocytes as described in 2.1.6. Blood from 2 mice was finally eluted in 30 ml ePBS. The suspension was observed by haemocytometer and then divided into 15 Falcon tubes such that each tube contained 6x10<sup>8</sup> RBCs. The tubes were spun at 450g for 8 mins, supernatant removed and cells were resuspended into 12 ml minimal media (plus albumax 5g/l) with 5 flasks containing <sup>13</sup>C U-Glucose (from Cambridge Isotope Laboratories), 5 flasks containing <sup>13</sup>C<sup>15</sup>N U-Glutamine (from Cambridge Isotope Laboratories) and 5 flasks containing unlabeled media components. The flasks were gassed and kept at 37 °C with slight shaking as described in 2.1.7. Each flask was harvested to collect samples for 0h, 6h, 12h, 18h, and 24h time points

(the first time point was collected after allowing for cells to equilibrate for 2 hours). 2 uninfected mice treated similarly were also bled at the same time and samples were processed exactly as for infected blood.

### **2.7.3 Isotopic labelling of *P. berghei* gametocytes *in vitro***

Parasites from line 820em1dcl2TBB (the parent producer line) were grown in 20 TO mice (infection was started by mechanical passage to ensure similar parasitaemias as described in 2.1.1). The mice were given sulfadiazine in drinking water (30 mg/L) when the parasitaemia reached ~30% and the mice were kept on sulfadiazine for 48 hours which led to killing of all asexual stage parasites and left mature circulating gametocytes at a parasitaemia of approximately 6%. All mice were then bled (approximately 1.5 ml blood from each mouse was obtained) into warm ePBS kept at 37°C to keep gametocytes unactivated. Blood was passed through two pre-washed Plasmodipur filters to remove leucocytes as described in 2.1.6. The suspension was then divided equally and passed through 16 prewashed MACS magnetic columns (Miltenyi Biotec, Germany) to get rid of uninfected cells, washed twice with 4 ml warm ePBS and eluted with warm ePBS by taking the column off the magnets and using a plunger twice. This whole process was done in the 37°C incubator. The suspension was observed on haemocytometer and then divided into 15 tubes so that each tube contains  $6 \times 10^8$  gametocytes. The tubes were then kept at 37°C and just before setting up according to the following scheme, spun at 450g for 8 mins, supernatant removed and resuspended.

For unactivated gametocytes, cells from 3 tubes prepared above were resuspended in 12 ml minimal media (plus albumax 5g/l) pre-warmed to 37°C with either  $^{13}\text{C}$  U-Glucose or with  $^{13}\text{C}^{15}\text{N}$  U-Glutamine or with unlabeled media components. Each suspension was allowed to equilibrate for 2 hours at 37°C before harvesting.

For activating gametocytes, cells from 4 tubes each prepared above were resuspended in 12 ml minimal media (plus 100  $\mu\text{M}$  Xanthurenic acid, albumax 5g/l) pre-warmed to 21°C with either  $^{13}\text{C}$  U-Glucose or with  $^{13}\text{C}^{15}\text{N}$  U-Glutamine or with unlabeled media components. Cells suspension were then incubated at 21°C and harvested at 1min, 10min, 20min and 30min time points.

#### 2.7.4 Isotopic labelling of *P. berghei* ookinete cultures

Parasites from line 820em1dcl2TBB (the parent producer line) and 137cl8 (48/45 ko which does not produce ookinetes but females are viable) were grown in 16 TO mice each (infection was started by mechanical passage to ensure similar parasitaemias as described in 2.1.1). The mice were given sulfadiazine in drinking water (30 mg/L) when the parasitaemia reached 30% and the mice were kept on sulfadiazine for 48 hours which led to killing of all asexual stage parasites and left mature circulating gametocytes at a parasitaemia of approximately 6%. All mice were then bled (approximately 1.5 ml blood from each mouse was obtained) into warm ePBS kept at 37°C to keep gametocytes unactivated. Blood was passed through two pre-washed Plasmodipur filters to remove leucocytes as described in 2.1.6. Cells were then spun at 450g for 8 mins and resuspended in 600 ml minimal media (plus 100 µM Xanthurenic acid, albumax 5g/l) pre-warmed to 21°C. After checking on haemocytometer, the suspension was divided into 6 flasks so that each flask had  $2 \times 10^{10}$  total cells ( $2 \times 6 \times 10^8$  gametocytes) in a final volume of 90 ml. The flasks were incubated at 21°C and harvested at 10h post activation and 21h post activation. 2 hours before harvesting, cells were spun at 450g for 8mins and supernatant was removed. The cells were resuspended with 12 ml minimal media (plus 100 µM Xanthurenic acid, albumax 5g/l) pre-warmed to 21°C with either  $^{13}\text{C}$  U-Glucose or with  $^{13}\text{C}^{15}\text{N}$  U-Glutamine or with unlabeled media components. Cells suspensions were then incubated again at 21°C. After harvesting, cells from each flask were then passed through prewashed MACS magnetic columns (Miltenyi Biotec, Germany) to get rid of uninfected cells, washed twice with 4 ml unlabeled complete minimal media and eluted with the same by taking the column off the magnets and using a plunger twice in the final volume of 12 ml. Metabolite extractions were then carried out on cells. At 21hours, the ookinete cultures from the producer line were found to have ~70% ookinete conversion rate whereas 137cl8 showed unfertilized female gametes only.

#### 2.7.5 Metabolite Extraction, drying and storage

At each time point, before harvesting, to quench metabolism, the tubes were immersed in a dry ice-ethanol bath. A thermometer was used to read the temperature and the flasks were taken out as soon as it reached 8°C on the scale. The culture suspension from each tube was then split to 6 tubes ( $10^8$  cells each) and the tubes were then spun at 1300g at 4°C and supernatant was

removed (10ul of this supernatant was used for extractions in 100ul extraction solvent- done for only 3 out of 6 tubes). The cells were washed once-resuspended in 500ul cold ePBS by pipetting up and down and spun again at 1300g at 4 °C and supernatant was removed. Then each pellet was resuspended in 150ul extraction solvent by pipetting up and down (Chloroform: methanol: water: 1:3:1 plus internal standards [5-fluorouridine, Cl-phenyl-cAMP, N-methyl glucamine, Canavanine, Piperazine all at 1uM concentrations]). The cells from unlabeled cultures were extracted in extraction solvent which also had labelled TCA cycle metabolites at following concentrations (U-<sup>13</sup>C-malic acid 5 mg/ ml; U-<sup>13</sup>C-fumaric acid 0.5 mg/ml; 1,4-<sup>13</sup>C-succinic acid 0.5 mg/ml; 2,4-<sup>13</sup>C-citric acid 1 mg/ml; 1,2,3,4-<sup>13</sup>C-ketoglutaric acid disodium, 5 mg/ml). The suspensions were mixed vigorously on shaker in cold room for 1 hour. This was done on a vortex with attachment for multiple tubes. The suspensions were sonicated for 10mins in ice-cold water bath. The suspensions were then centrifuged for 5 minutes at 15,300g at 4 °C. 50ul of the supernatant was then put into glass vials, dried under nitrogen flow at room temperature and stored at -80 °C before shipping to Metabolomics Australia.

### 2.7.6 Targeted GC-MS analysis

Samples were reconstituted, derivatized and run as described in 2.6.6. As a control, a mixture of known metabolites of glycolysis and TCA cycle at known concentrations was also derivatized and run with the samples to serve as a reference for retention time and spectrum during chromatographic separation. Data analysis was done manually on the Agilent Chemstation platform. First, every peak in the metabolite mix was checked against the Fiehn library and annotated with its retention time and major molecular ion post fragmentation. Then the major molecular ion for each metabolite of interest was worked out by looking at their possible fragmentations patterns and matched to this library. For doing individual ion extraction from the chromatogram of each sample, a molecular ion was chosen based on abundance and peak shape from the metabolite mix. Then for each sample, the chromatogram was scanned manually between the corresponding retention time ranges which were kept consistent at  $\pm 0.3$ min. The mass of the molecular ion of interest and all possible isotopes (depending on the number of C atoms) was queried in the specified retention time window. Retention time alignment for each isotope was observed for integration and individual peak areas were noted which were representative of

abundance of individual isotopic forms of the metabolite. Background correction for naturally occurring isotopes was done by calculating and subtracting the percentage labelling of ions in the control metabolite mix.

### **3 Comparative metabolomics of erythroid lineage reveals that reticulocytes provide metabolic reserves for *Plasmodium* parasites**

#### **3.1 Introduction**

The malaria causing apicomplexan parasite *Plasmodium* has a dynamic life cycle which is reflected in stage specific morphologies, transcriptomes, proteomes and most likely metabolomes (Bozdech, Llinas et al. 2003, Hall, Karras et al. 2005, Khan, Franke-Fayard et al. 2005, Llinas and del Portillo 2005, Olszewski, Morrisey et al. 2009, Kafsack and Llinas 2010). The latter reflects the type and extent of biochemical processes which take place in the parasite at any given time and in turn influences or is influenced by the host cell which may also be dynamic in its response to infection (Kafsack and Llinas 2010, Olszewski and Llinas 2011). Perhaps due to their parasitic life-style, *Plasmodium* spp. have a comparatively simplified and reduced metabolic capacity as compared to higher independent organisms. They are auxotrophic for purines and amino acids (Booden and Hull 1973, Sherman 1977) but have retained many central metabolic pathways like glycolysis (Homewood 1977), citric acid cycle (Macrae, Dixon et al. 2013), lipid synthesis (Holz 1977), pentose phosphate pathway (Barrett 1997), pyrimidine biosynthesis (Hyde 2007) and glycosylation (Macedo, Schwarz et al. 2010). As growing *Plasmodium* parasites are intracellular, their metabolism is interlinked with the host cells and is dependent upon the availability of external nutrients. As a result intracellular *Plasmodium* establish uptake systems such as the new permeation pathways with the purpose of accessing host cell and environmental nutrients (Landfear, 2011) with the parasite encoding >120 predicted membrane transport proteins (Martin, Goldberg, Kirk, 2009) a subset of which is located on the plasma membrane. Mature erythrocytes are also simplified cells which comprise almost 98% of the circulating red blood cells that are metabolically active but less complex than the erythroid precursors present in the bone marrow (Chen, Liu et al. 2009) and reticulocytes (maturing erythrocytes) present in peripheral circulation (Gronowicz, Swift et al. 1984). The major metabolic pathways in mature erythrocytes have been shown to be glycolysis (Chapman, Hennessey et al. 1962) and pentose phosphate pathway (Stromme and Eldjarn 1962).

Reticulocytes undergo many changes as they mature into normocytes. Maturation is associated with simplification of the cell leading to the loss of organelles (mitochondria, ribosomes, vesicles and lysosomes), acquisition of a biconcave shape with consequent increase in shear membrane resistance and loss or reduced abundance of 30 membrane proteins, 20% decrease in surface area and decreased cholesterol (Gronowicz, Swift et al. 1984, Liu, Guo et al. 2010). Reticulocytes are therefore, more complex than normocytes and should offer a more abundant and diverse nutrient base to an intracellular parasite than a normocyte which might be exploited by reticulocyte preferring *Plasmodium* spp.

To establish whether there are metabolic differences between reticulocytes and mature erythrocytes that mirror the great specialisation of the erythrocyte, a non-targeted metabolomics approach was taken. Small molecule metabolites (typically less than 1500Da) constitute the 'metabolome' of an organism or system and the characterization of a metabolome can give a snapshot of the physiology of the cell (Gomase, Changbhale et al. 2008). A discovery-based study to perform a comprehensive comparison of the metabolomes of uninfected rat and human reticulocytes and normocytes was undertaken to understand differences in intracellular host cell environments and the different opportunities afforded to intracellular parasites. The findings were then exploited using reverse genetics to disrupt parasite metabolism and establish the broad ability of *P. berghei* to utilise the products of host cell metabolism.

## 3.2 Results

### 3.2.1 The reticulocyte metabolome is more complex and abundant than the mature erythrocyte

Induction of reticulocytosis was achieved through administration of phenylhydrazine-HCl (PHZ, 100 mg/kg body weight) to Wistar rats and cells were harvested when reticulocyte percentage in peripheral blood reached its maximum level (~35% reticulocytes 5 days after treatment). This was monitored by FACS analysis using reticulocyte specific marker surface protein transferrin receptor (CD71) which is lost as they mature (Liu, Guo et al. 2010). Material was also collected for comparison with blood from non-enriched (~1% reticulocytes) animals (Figure 3-1).

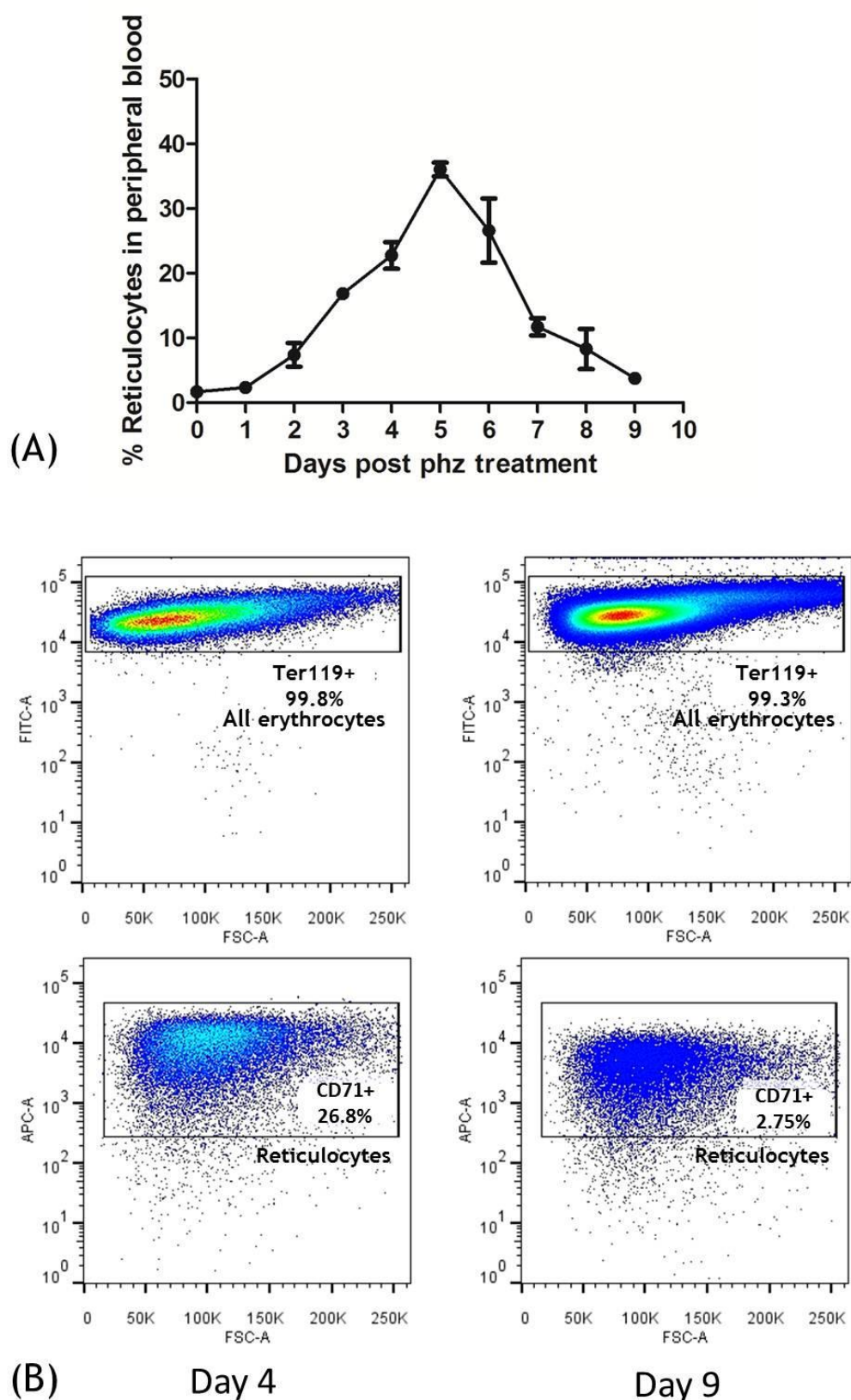


Figure 3-1 (A) Dynamics of reticulocyte enrichment in peripheral blood in vivo followed by Phenylhydrazine-HCl (phz) treatment of mice. Reticulocytes were harvested at day 5 post phz treatment. The error is given as the SD of  $n=3$  independent biological replicates. (B) CD71 (transferrin receptor) is a reticulocyte specific marker and is lost as RBCs mature. Left panels- day 4 post phz treatment, right panels- day 9 post phz treatment. Top panels show Ter119-FITC staining in RBCs which stains all erythroid cells. Bottom panels show CD71-APC staining in a subset of RBCs which stains only reticulocytes.

Metabolome analysis was performed using two independent and complementary approaches, Liquid Chromatography Mass Spectrometry (LC-MS) and Gas Chromatography Mass Spectrometry (GC-MS). Briefly, raw LC-MS data was processed using the standard Glasgow Polyomics pipeline, consisting of XCMS, MZMatch and IDEOM and raw GC-MS data was processed using the standard Metabolomics Australia pipeline consisting of PyMS matrix generation and Chemstation Electron Ionisation (EI) spectrum match analysis (sections 2.6.5 and 2.6.6). From a total number of 4560 peaks collected from the two platforms, 333 putative metabolites (PM) were robustly identified (minimum confidence value was set to 5/10 for LC-MS data analysis by IDEOM and minimum ion-spectra match was set to 90% to Agilent Fiehn and NIST GC-MS Metabolomics libraries for GC-MS data analysis by Chemstation) in all erythrocytes, although many more probable metabolites were detected but were not readily assigned an identity. For the purpose of description from hereon, uninfected reticulocyte enriched erythrocytes are referred to as ‘reticulocytes’ and uninfected normocyte enriched erythrocytes are referred to as ‘normocytes’. The volcano plot in Figure 3-2 shows the distribution of abundance of detected PMs in reticulocytes compared to normocytes.

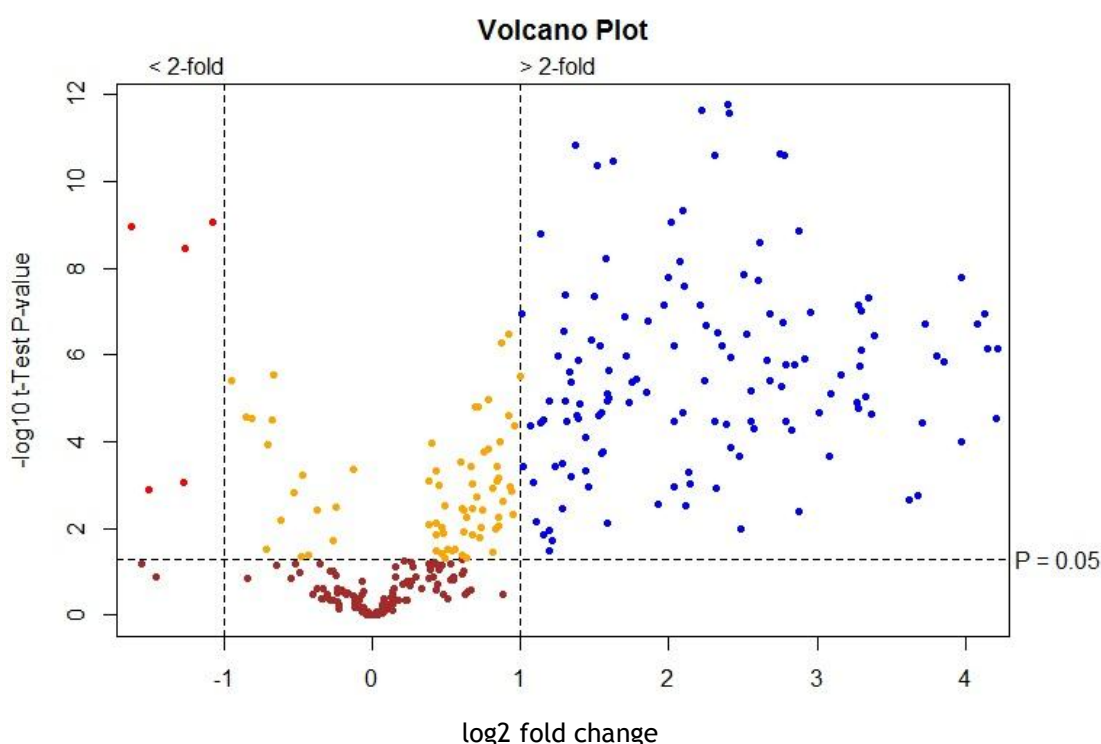


Figure 3-2 Volcano plot showing distribution of putative metabolites according to their fold change in abundance in uninfected reticulocyte enriched erythrocytes vs uninfected normocyte enriched erythrocytes. All significant changes are represented above the broken horizontal line. Coloured dots indicate metabolites which are: Blue- significantly up-regulated, Red- significantly down-regulated, Yellow- significant but little change, Brown- non-significant

Almost half of all detected PMs (149, ~45%) were found to be enriched in reticulocytes by more than 2 fold with a statistical significance of  $p < 0.05$  (

Figure 3-2, Table 2)

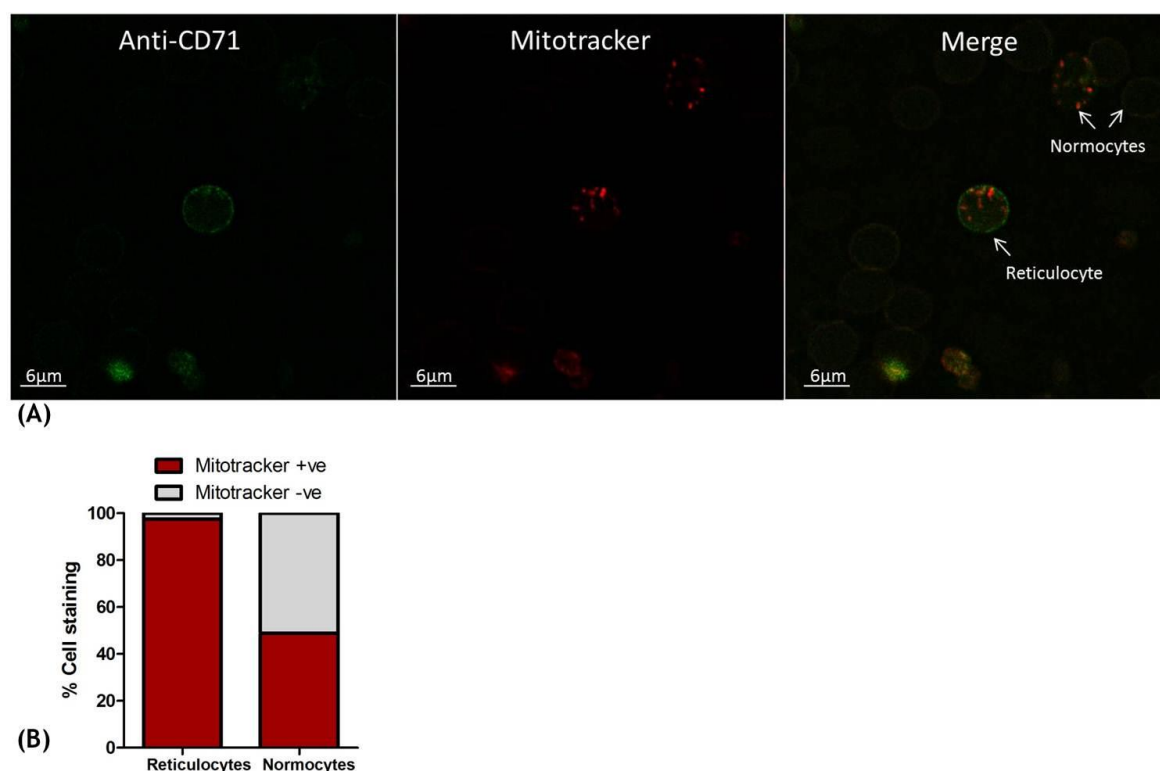
Only 5 (~1%) PMs were more abundant in mature erythrocytes by more than 2 fold with a statistical significance of  $p < 0.05$ , the majority being tri- peptides, amino acid and sugar derivatives. Of all the raw metabolomic peaks, including the unassigned ones, ~23% were also observed to be similarly enriched in reticulocytes and ~2% were found to be reduced and the remaining were unchanged between reticulocytes and normocytes (

Figure 9-1 in appendix). Importantly, as the rat reticulocyte-enriched samples contained 65% normocytes, the level of metabolite enrichment in reticulocytes was actually much greater and reflected in table 2. All identified metabolites were charted on known metabolic pathways using databases such as MPMP (Malaria Parasite Metabolic Pathways- accessible at <http://mpmp.huji.ac.il/>) (Ginsburg 2006), Pathos (A metabolomics tool from Glasgow Polyomics- accessible at <http://motif.gla.ac.uk/Pathos/>) (Leader, Burgess et al. 2011), KEGG (Kyoto Encyclopedia of Genes and Genomes, accessible at <http://www.genome.jp/kegg/>) (Kanehisa, Goto et al. 2006) and MetaCyc (accessible at <http://metacyc.org/>) (Caspi, Altman et al. 2014). Common key pathways in *Plasmodium* based on existing biochemistry of the malaria parasite (Kafsack and Llinas 2010, Olszewski and Llinas 2011), genomic data (Gardner, Hall et al. 2002) and mammalian host cell (based on data obtained in this study- Figure 3-2 and Table 2) were identified.

### 3.2.2 The reticulocyte metabolome reflects its ongoing developmental programme

Reticulocytes have been shown to possess mitochondria which are lost as the cells mature to normocytes (Gronowicz, Swift et al. 1984). We also found that almost all reticulocytes and a subset of normocytes (possibly erythrocytes which

have not reached terminal differentiation to normocytes yet) stain for Mitotracker® indicating the presence of mitochondria Figure 3-3.



**Figure 3-3** Presence of mitochondrial signal in reticulocytes. (A) IFA analysis of uninfected erythrocytes from peripheral rat blood shows presence of reticulocytes stained by anti-CD71 (green) and presence of a Mitotracker® signal (red) in both reticulocytes and some normocytes. (B) Flow cytometry analysis showed that all reticulocytes and almost half of normocytes stain for Mitotracker® signal indicating the presence of mitochondria.

In our metabolomics analysis in rat erythrocytes, we detected elevated TCA cycle intermediates in reticulocytes compared to normocytes which indicated the possibility of presence of a functional citric acid cycle and intermediary carbon metabolism in reticulocytes. Several intermediates in purine and pyrimidine metabolism were also found at elevated levels in reticulocytes compared to normocytes presumably originating either from biosynthesis in the preceding erythropoiesis stages or from catabolism of RNA to constituent nucleobases (Valentine and Paglia 1980). A number of metabolites of phospholipid (mainly phosphatidylcholines) metabolism were also observed in reticulocytes which were up regulated compared to normocytes. Many carnitine derivatives were also found to be up regulated in reticulocytes compared to normocytes which may relate to fatty acid breakdown by beta-oxidation in mitochondria or peroxisomes. Intermediates of pentose phosphate pathway, glutathione synthesis, arginine metabolism were notable among other pathways also found to be elevated in reticulocytes (Table 2)

Taken together the data demonstrated that the reticulocyte is a metabolically more complex cell than the erythrocyte. It possesses richer small molecule reserves which the invading malaria parasite may access and exploit. Furthermore there was a marked overlap in metabolic pathways observed in the reticulocyte and those predicted in the parasite. We hypothesised that common pathways between the parasite and reticulocyte might be uniquely dispensable to the parasite during the intra-reticulocytic development of *Plasmodium* compared with growth in a normocyte where the host metabolites for these pathways are less abundant. Also, parasites with such disrupted metabolism would probably be able to survive in the reticulocyte but not in the exo-erythrocytic stages such as in the mosquito (Figure 3-4).

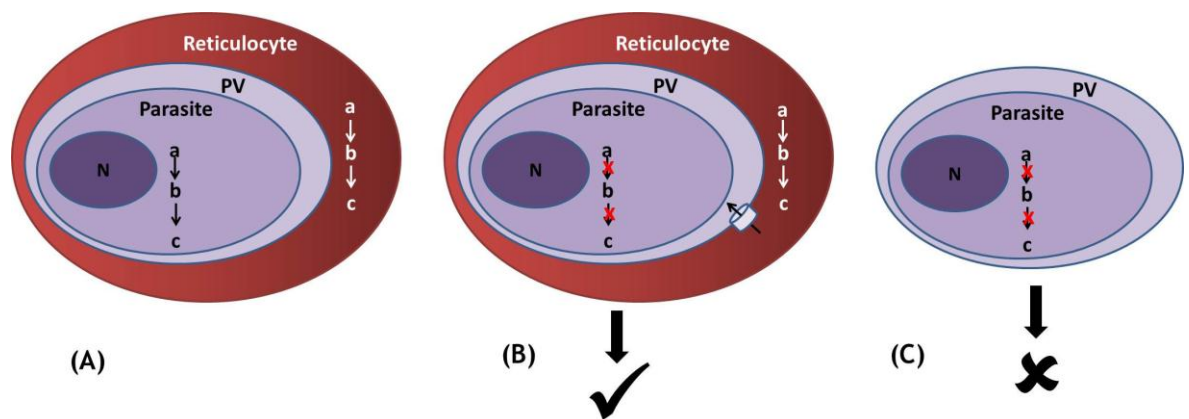


**Figure 3-4 Hypothesis: Reticulocytes provide metabolic reserves to *P. berghei* parasites.** (A) A reticulocyte is a complex cell with significant metabolic reserves and possibly active metabolism which overlaps with the malaria parasite and which it may exploit. (B) Key metabolic pathways which are common between the reticulocyte and the parasite may be dispensable in erythrocytic developmental stages in reticulocyte-resident *Plasmodium* spp. like *P. berghei* but not normocyte resident species e.g. *P. falciparum* *in vitro*. (C) However, disrupting parasite genes involved in these pathways might then affect parasite development at later stages of the life cycle (exo-erythrocytic mosquito stage development).

Therefore two metabolic pathways were targeted in *P. berghei* whose intermediates were significantly enriched in reticulocytes. These were intermediary carbon metabolism (ICM) and pyrimidine biosynthesis. The enrichment of metabolites involved in these pathways in reticulocytes as compared to normocytes was found to be significant (Figure 3-5, Table 2).

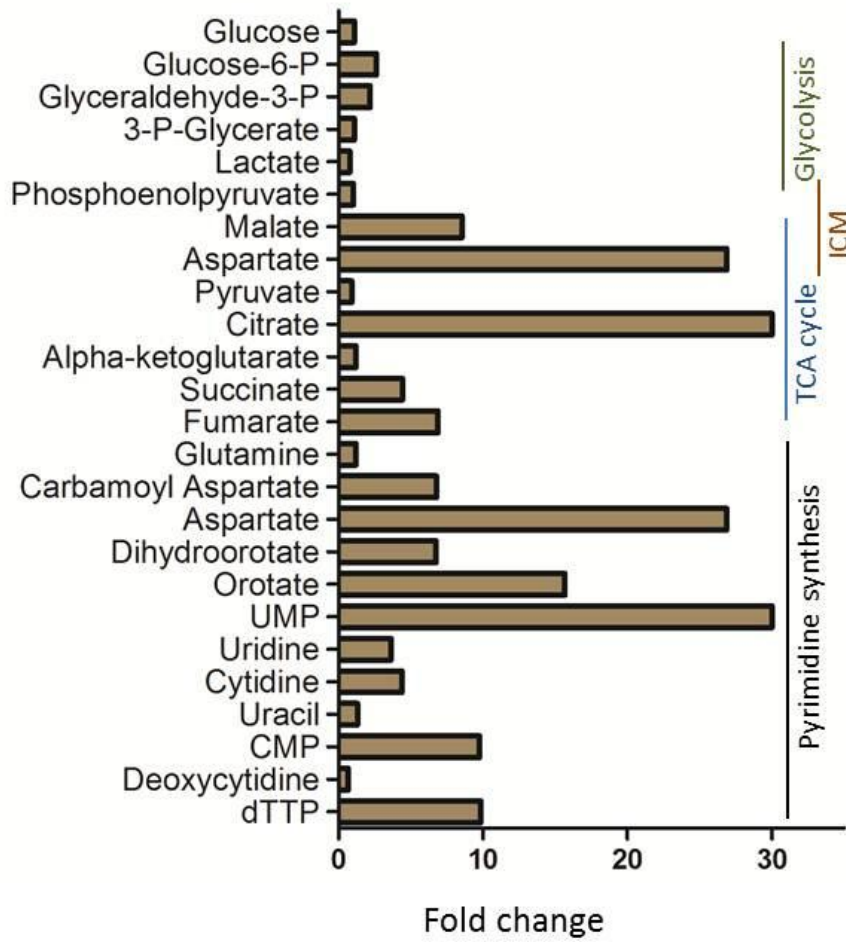


Figure 3-5 Fold change of metabolites of central carbon metabolism and pyrimidine biosynthesis in rodent reticulocytes compared to normocytes.

### 3.2.3 Features of intermediary carbon metabolism (ICM) are dispensable in asexual blood stage *P. berghei*

Carbon sources are catabolised by two major pathways in eukaryotes, glycolysis and TCA cycle. The presence of intermediary cytosolic enzymes such as Phosphoenolpyruvate Carboxylase (*pepc* PBANKA\_101790), Malate Dehydrogenase (*mdh* PBANKA\_111770) and Aspartate Amino Transferase (*aat* PBANKA\_030230) in *Plasmodium* spp. suggests the existence of an intermediary carbon metabolism (Figure 3-6).

## Intermediary carbon metabolism

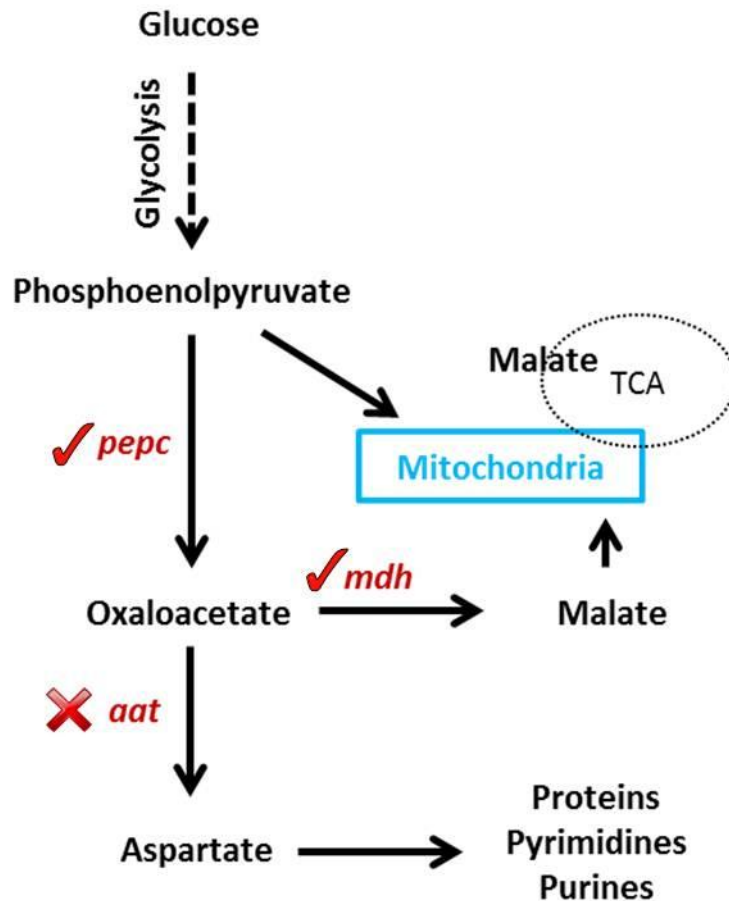


Figure 3-6 Schematic representation of intermediary carbon metabolism (ICM) in *Plasmodium*. Genes marked with (✓) were readily deleted in *P. berghei* blood stages and the ones marked with (✗) could not be deleted even after repeated attempts. *pepc*: Phosphoenolpyruvate Carboxylase (PBANKA\_101790), *mdh*: Malate Dehydrogenase (PBANKA\_111770), *aat*: Aspartate Amino Transferase (PBANKA\_030230).

Production of aspartate via this pathway is important as it feeds into protein and nucleic acid synthesis. Malate either enters mitochondria to participate in the TCA cycle or is excreted (Olszewski and Llinas 2011). In *in vitro* cultures of *P. falciparum*, *pepc* was found to be essential for normal intra-erythrocytic survival although mutants lacking *pepc* could be isolated in cultures that were supplemented by malate (Storm, Sethia et al. 2014). However, *mdh* and *aat* are essential in *P. falciparum* and cannot be deleted (personal communication Prof. Sylke Muller). Although the levels of glycolytic intermediates were not very different between reticulocytes and normocytes, metabolites involved in TCA

cycle and intermediary carbon metabolism (ICM) were found to be enriched in reticulocytes compared to normocytes (Figure 3-5, Table 2).

It has been shown that disruption of the TCA cycle in *P. berghei* blood stages through deletion of flavoprotein (Fp) subunit, *Pbsdha* (PBANKA\_051820) part of catalytic component for succinate dehydrogenase activity does not affect parasite viability in blood stage forms although ookinete development is impaired (Hino, Hirai et al. 2012). Attempts were made to delete the three genes which constitute the ICM, Phosphoenolpyruvate carboxylase, *pepc* (PBANKA\_101790), Malate dehydrogenase, *mdh* (PBANKA\_111770) and Aspartate amino Transferase, *aat* (PBANKA\_030230) encoding components of ICM (Figure 3-5). It proved possible to readily delete *pepc* and *mdh* (Figure 3-7), however *aat* proved refractory.

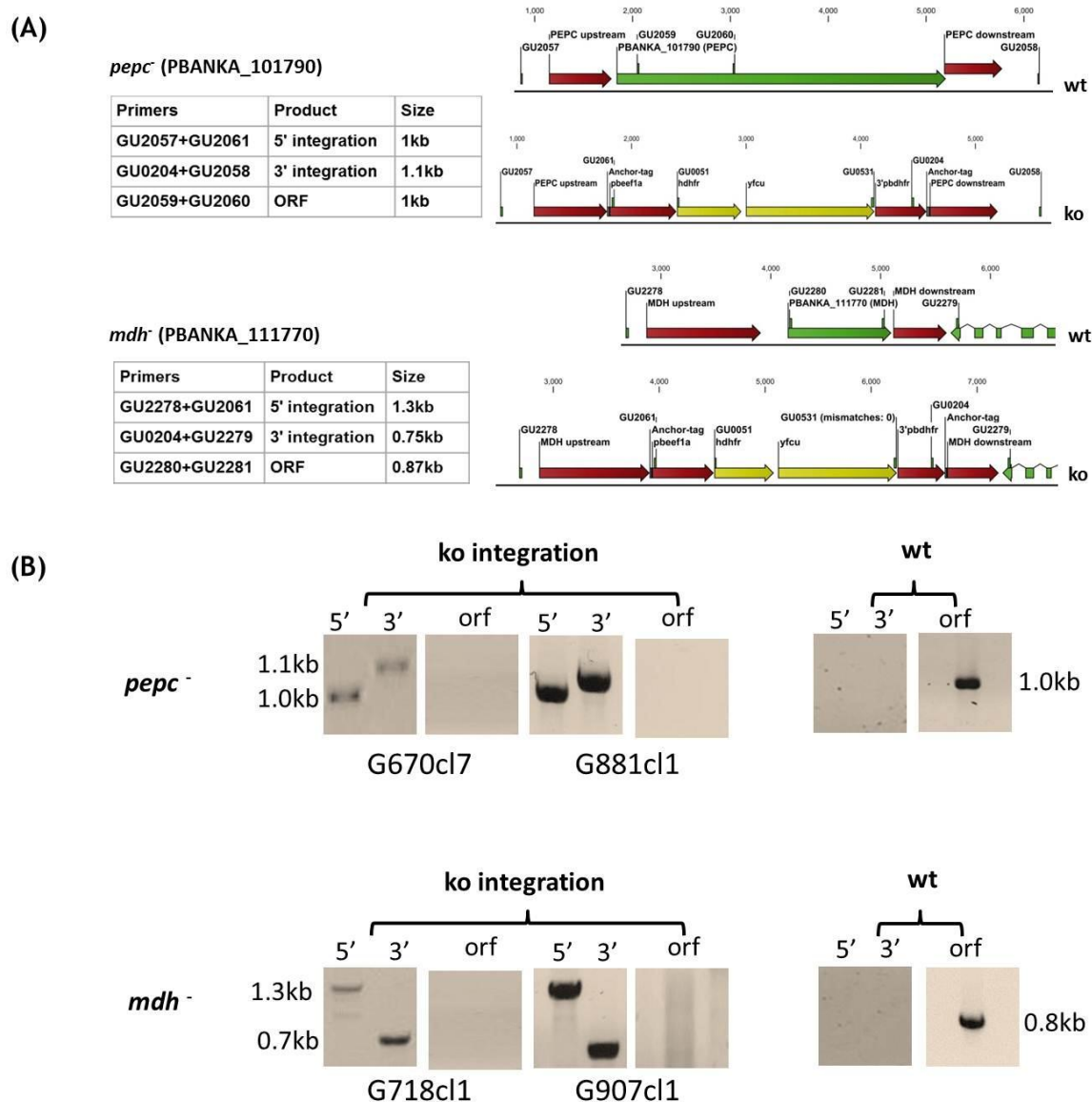
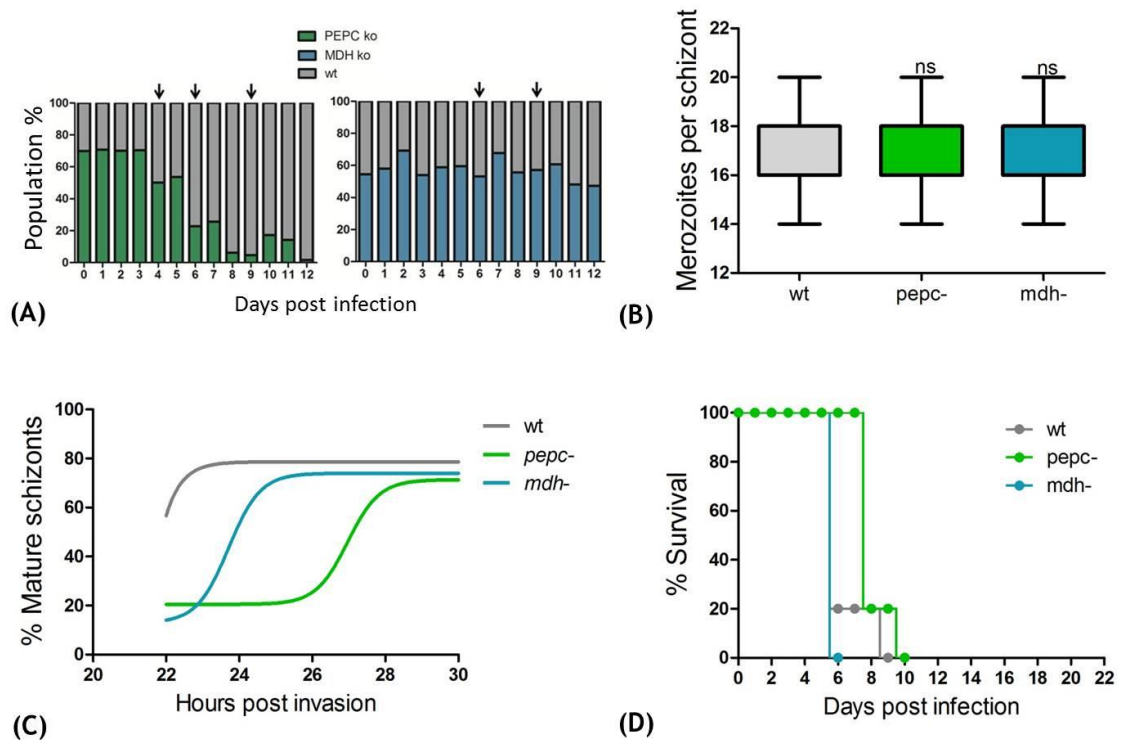


Figure 3-7 (A) Schematic representation of gene deletion strategy for (i) *pepc* (PBANKA\_101790) and (ii) *mdh* (PBANKA\_111770) in *P. berghei* parasites. (B) Gel electrophoresis of indicated PCR products to confirm integration of selection cassette, disruption of genes and clonality of mutant parasites. G670c17 and G718c11 were made in a wt parent line expressing GFP constitutively under the *eef1a* promoter (RMgm-7). G881c11 and G907c11 were made in a wt parent line which expresses GFP in male gametocytes under the dynein heavy chain promoter and RFP in female gametocytes under the LCCL domain-containing protein CCP2 promoter (RMgm-164).

### 3.2.3.1 Asexual stage phenotypic analyses of ICM mutant parasites

The mutant parasites survive in intra-erythrocytic stages but *pepc*<sup>-</sup> mutants were overgrown by the wt parasite in a competitive growth assay (performed as described in 2.1.13) in contrast to *mdh*<sup>-</sup> mutants which grew like wt (Figure 3-8 A). The number of merozoites observed in mature schizont stages in both *pepc* ko ( $17.02 \pm 1.76$ ) and *mdh* ko ( $17.41 \pm 1.68$ ) are statistically indistinguishable to wt ( $17.45 \pm 1.75$ ) (Figure 3-8B). The *pepc*<sup>-</sup> mutants take longer to develop in the asexual cycle (Figure 3-8C). However, both mutants cause severe cerebral

malaria in C57/B6 mouse model and the dynamics of their lethality is similar to wild type, killing all mice within 8-10 days post infection (Figure 3-8D).



**Figure 3-8 Asexual stage phenotypic analyses of ICM mutants.** (A) Competition growth assay using FACS analysis. Equal number of parasites wt population (RFP positive) and mutant population (GFP positive) were mixed and injected into a mouse on day 0 and peripheral blood from the infected mouse was monitored using FACS analyses over the next 12 days. *mdh*<sup>-</sup> parasites grow similar to wt but *pepc*<sup>-</sup> parasites were overgrown by wt by day 7. Arrows indicate mechanical passage into a new mouse (B) Number of merozoites per schizont grown in *in vitro* cultures as counted in giemsa stained smears. The error is given as the SD of  $n \geq 40$  schizonts. Data representative of 3 independent biological replicates. P-value: ns: not significant, unpaired two tailed t-test. (C) Time taken for asexual parasites to grow to mature schizont stage. Coloured lines indicate non-linear fit of percentage of mature schizonts observed in *in vitro* synchronous cultures of wt and mutant *P. berghei* parasites 22 hours post invasion.  $n=3$  independent biological replicates. (D) Lethality experiment in C57/B6 mice by wt and mutant *P. berghei* parasites.  $10^4$  parasites were injected intraperitoneally in mice ( $n=5$ ) on day 0 and they were monitored over 21 days. The mice were culled humanely when they showed severe malaria pathology. Both mutant parasites were found to be readily lethal to mice like wt.

### 3.2.3.2 Analyses of gametocytogenesis and gamete formation in ICM mutant parasites

The number of gametocytes formed in blood stages was found to be reduced in *pepc*<sup>-</sup> mutants by almost 50% but unaffected in *mdh* ko ( $p > 0.05$ ) compared to wt (Figure 3-9A). This defect in *pepc*<sup>-</sup> mutants was not found to be sex specific. Further phenotypic analyses of both *pepc*<sup>-</sup> mutants and *mdh*<sup>-</sup> mutants showed that exflagellation was also reduced in both mutants, more severely in *pepc*<sup>-</sup> mutants (84% less than wt,  $p < 0.0005$ ) than *mdh*<sup>-</sup> mutants (56% less than wt,

$p < 0.005$ ) (Figure 3-9B). DNA replication in male gametocytes as observed by FACS analysis was found to be delayed in both mutants (Figure 3-9C).

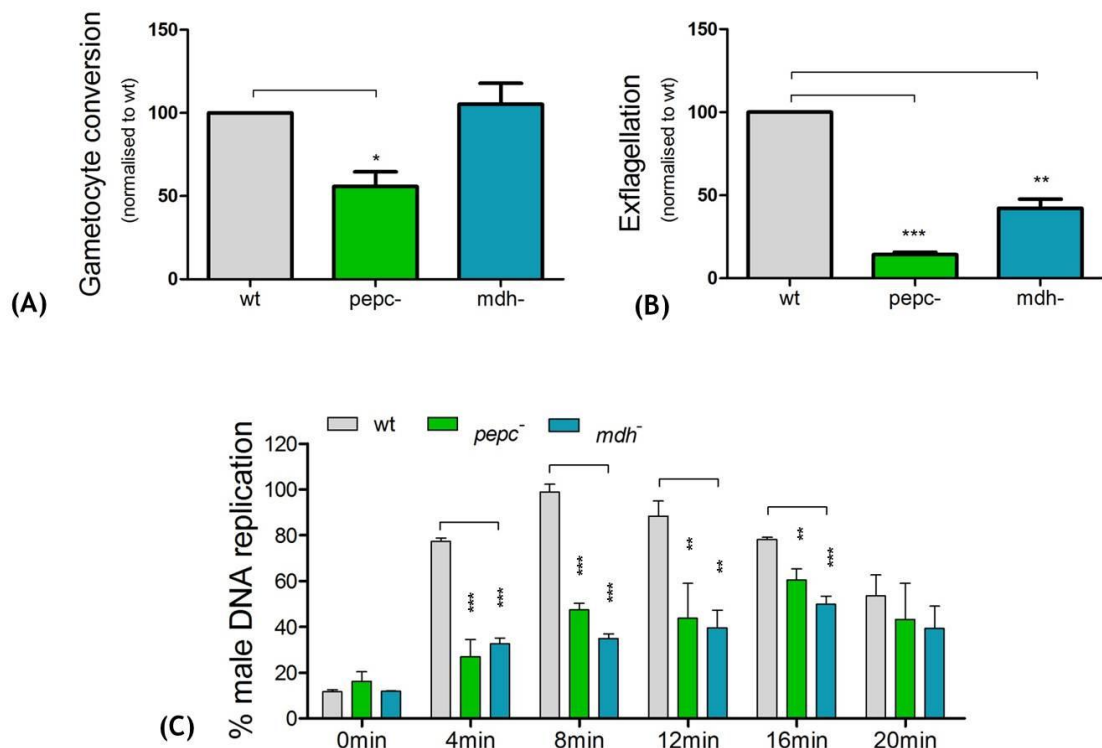


**Figure 3-9** Effect on gametocytogenesis and gamete formation in ICM mutants. (A) Gametocyte conversion normalised to wt during blood stages in mutant *P. berghei* parasites over 5 days post infection. The error is given as the SD of observed gametocyte conversion over 5 days. Data representative of  $n=2$  independent biological replicates. (Gametocyte conversion was observed using a wt parent line which has GFP expression in male gametocytes and RFP expression in female gametocytes (RMgm-164). *P. berghei* mutants were made in the same background and using FACS analysis, number of gametocytes was determined in infected blood. P-values: \* $p < 0.05$ , \*\* $p < 0.005$ , \*\*\* $p < 0.0005$ , paired two tailed t-test. (B) Exflagellation (male gamete formation) in mutant *P. berghei* parasites normalised to wt in *in vitro* activation assay. The error is given as the SD of  $n=3$  independent biological replicates. P-values: \*\* $p < 0.005$ , \*\*\* $p < 0.0005$ , paired two tailed t-test. (C) Determination of DNA content of male gametocytes over 20 minutes post activation by FACS analysis in mutant *P. berghei* parasites normalised to wt. DNA content was determined in Hoechst-33258-stained MACS purified gametocytes. Before activation (0mins) males show low DNA content with increasing amounts post activation reaching maximum levels between 8 to 12 minutes in wt. The error is given as the SD of  $n=3$  independent biological replicates. P-values: \*\* $p < 0.005$ , \*\*\* $p < 0.0005$ , unpaired two tailed t-test.

### 3.2.3.3 Analyses of *in vitro* fertilisation and ookinete development in ICM mutant parasites

Ookinete development in *in vitro* cultures of *pepc*<sup>-</sup> mutants was severely affected producing very few ookinetes, however in *mdh*<sup>-</sup> mutants, ookinetes were formed but the number was reduced by about 50% as compared to wt (Figure 3-10A). To determine if this defect was sex specific, crosses of *pepc*<sup>-</sup> and *mdh*<sup>-</sup> were done with *P. berghei* lines RMgm-348 (Pb270, *p47*) which produces viable male gametes but non-viable female gametes and RMgm-15 (Pb137,

*p48/45*<sup>-</sup>) which produces viable female gametes but non-viable male gametes. *pepc*<sup>-</sup> mutants were found to produce no ookinetes in either cross suggesting that gametes of both genders are affected. Similarly *mdh*<sup>-</sup> mutants crossing experiments showed that lack of *mdh* affected both genders and gave a parental phenotype producing 50% fewer mature ookinetes (Figure 3-10B).

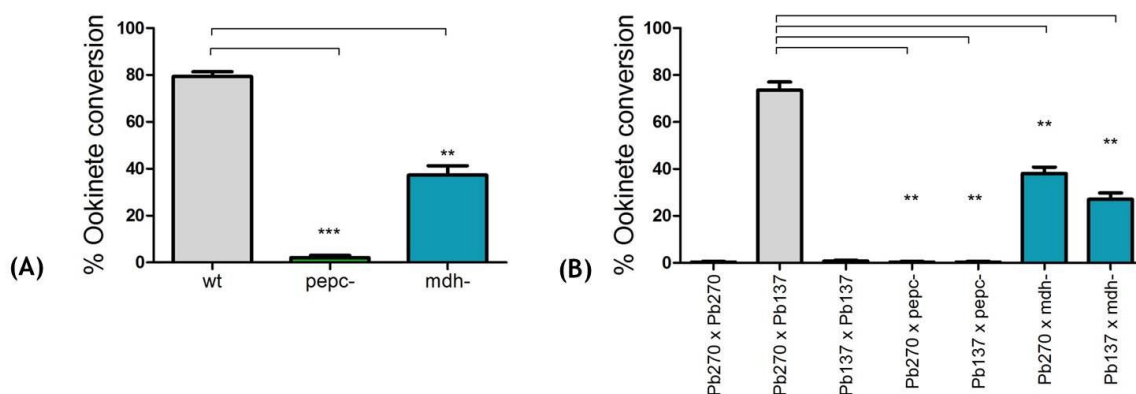


Figure 3-10 *in vitro* ookinete conversion in ICM mutants. (A) *in vitro* ookinete conversion of mutant *P. berghei* parasites as compared to wt. The error is given as the SD of n=3 independent biological replicates. P-values: \*\*p<0.005, \*\*\*p<0.0005, unpaired two tailed t-test. (B) *in vitro* ookinete conversion assay to measure fertility of mutant *P. berghei* gametocytes by analysing the capacity to form ookinetes by crossing gametes with RMgm-348 (Pb270, p47<sup>-</sup>) which produces viable male gametes but non-viable female gametes and RMgm-15 (Pb137, p48/45<sup>-</sup>) which produces viable female gametes but non-viable male gametes. The error is given as the SD of n=2 independent biological replicates. P-values: \*p<0.05, \*\*p<0.005, unpaired two tailed t-test.

### 3.2.3.4 Analyses of mosquito infectivity and transmission of ICM mutant parasites

Transmission of *pepc*<sup>-</sup> parasites through mosquitoes failed forming small numbers of oocysts in mosquito midguts and no salivary gland sporozoites. However, parasites lacking *mdh* could complete transmission through the mosquito and infect mice generating blood stage asexual forms in 48-72 hours like wt despite producing reduced numbers of oocysts when compared to wt (Figure 3-11 and Figure 3-12).

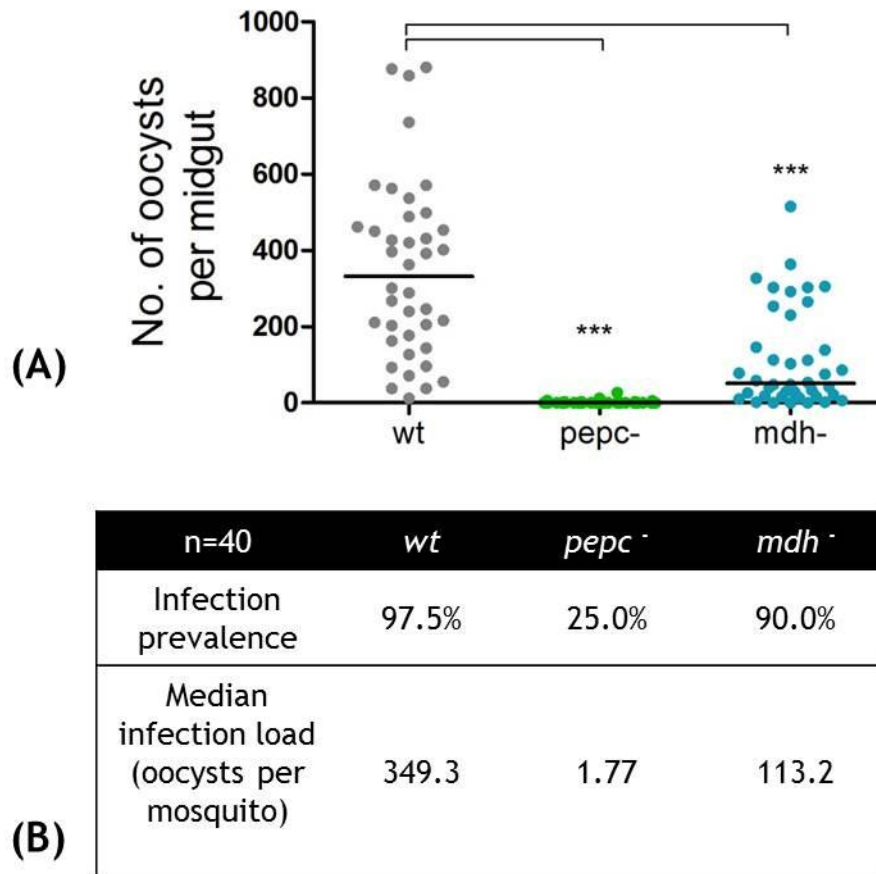


Figure 3-11 Mosquito infectivity of ICM mutant parasites compared to wt. (A) Number of mature oocysts at day 14 post infected blood feed in mosquito mid guts. n=40 mosquitoes cumulative of two independent biological replicates. \*\*\* $p < 0.0005$ , unpaired two tailed t-test. (B) Infection prevalence (percentage of observed mosquitoes found to be infected) and infection load (median of number of oocysts found per mosquito) in mutant *P. berghei* parasites compared to wt.

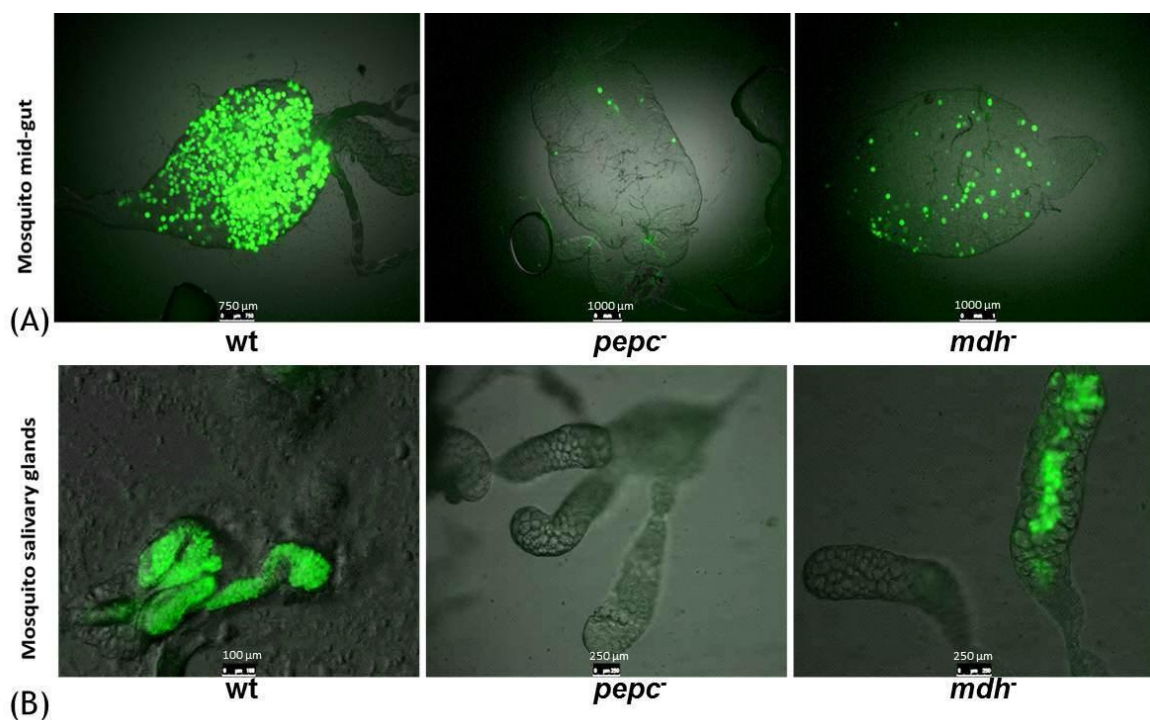


Figure 3-12 Representative images of mosquito infectivity of ICM mutant parasites compared to wt. (A) Mosquito mid guts showing mature oocysts at day 14 post infection in wt, *pepc*<sup>-</sup> and *mdh*<sup>-</sup> *P. berghei* infected reticulocyte enriched mosquitoes. (B) Mosquito salivary glands showing sporozoites at day 21 post infection in wt, *pepc*<sup>-</sup> and *mdh*<sup>-</sup> *P. berghei* infected reticulocyte enriched mosquitoes.

### 3.2.4 Pyrimidine biosynthesis pathway can be disrupted in asexual *P. berghei* development

*Plasmodium* undertakes rapid nucleic acid synthesis during blood stage asexual growth and is auxotrophic for purines, therefore the pyrimidine biosynthetic pathway has been considered a promising drug target. A schematic representation of pyrimidine biosynthesis pathway is given in Figure 3-13.

## Pyrimidine biosynthesis

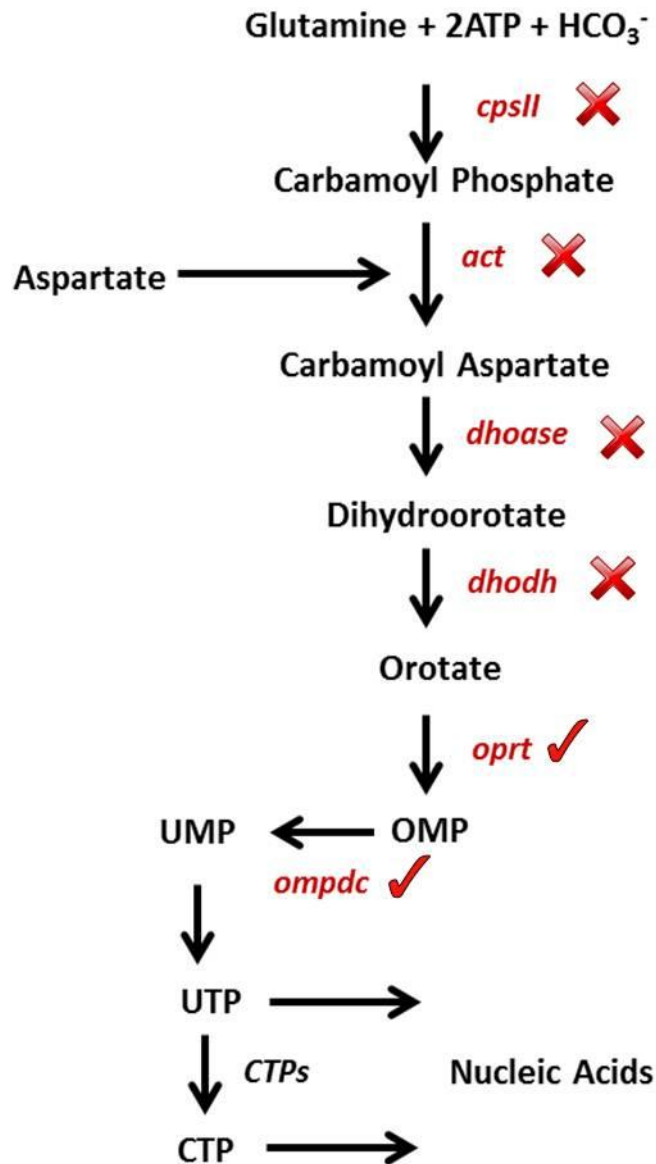


Figure 3-13 Schematic representation of pyrimidine biosynthesis pathway. Genes marked with (✓) were readily deleted in *P. berghei* blood stages and the ones marked with (✗) could not be deleted even after repeated attempts. *cpsII*: Carbamoyl phosphate synthetase II (PBANKA\_140670), *act*: Aspartate carbamoyltransferase (PBANKA\_135770), *dhase*: Dihydroorotase (PBANKA\_133610), *dhodh*: Dihydroorotate dehydrogenase (PBANKA\_010210), *oprT*: Orotate phosphoribosyltransferase (PBANKA\_111240), *ompdc*: Orotidine 5'-monophosphate decarboxylase (PBANKA\_050740).

Five out of six enzymes of this pathway have been shown to be potential targets against *P. falciparum* using inhibitors in standard *in vitro* cultures (Cassera, Zhang et al. 2011). However, most of these inhibitors have been markedly less potent in the *in vivo* model *P. berghei* and this difference has been attributed to reduced bio-availability of inhibitors in mice or apparent differences in target enzyme structure (Phillips, Gujjar et al. 2008, Gujjar, Marwaha et al. 2009).

Alternatively, the increased levels of pyrimidine biosynthesis intermediates observed in reticulocytes (Figure 3-5, Table 2) suggested that if *P. berghei* could access this resource it would be less affected by this class of inhibitors which work well on *P. falciparum in vitro* where host pyrimidine resources are low. Attempts to delete genes encoding enzymes involved in pyrimidine biosynthesis pathway carbamoyl phosphate synthetase II (*cpsII*) (PBANKA\_140670), aspartate carbamoyltransferase (*act*) (PBANKA\_135770), dihydroorotase (*dhoase*) (PBANKA\_133610), dihydroorotate dehydrogenase (*dhodh*) (PBANKA\_010210), orotate phosphoribosyltransferase (*oprt*) (PBANKA\_111240), orotidine 5'-monophosphate decarboxylase (*ompdc*) (PBANKA\_050740) were therefore made in *P. berghei* to see if reticulocyte pools of pyrimidine biosynthesis intermediates could compensate for the loss of *de novo* pyrimidine synthesis.

Only the genes encoding the final two steps of the pyrimidine biosynthesis pathway orotate phosphoribosyltransferase (*oprt*) and orotidine 5'-monophosphate decarboxylase (*ompdc*) genes were readily deleted (Figure 3-14) whereas the others could not be deleted even after repeated attempts (Figure 3-13).

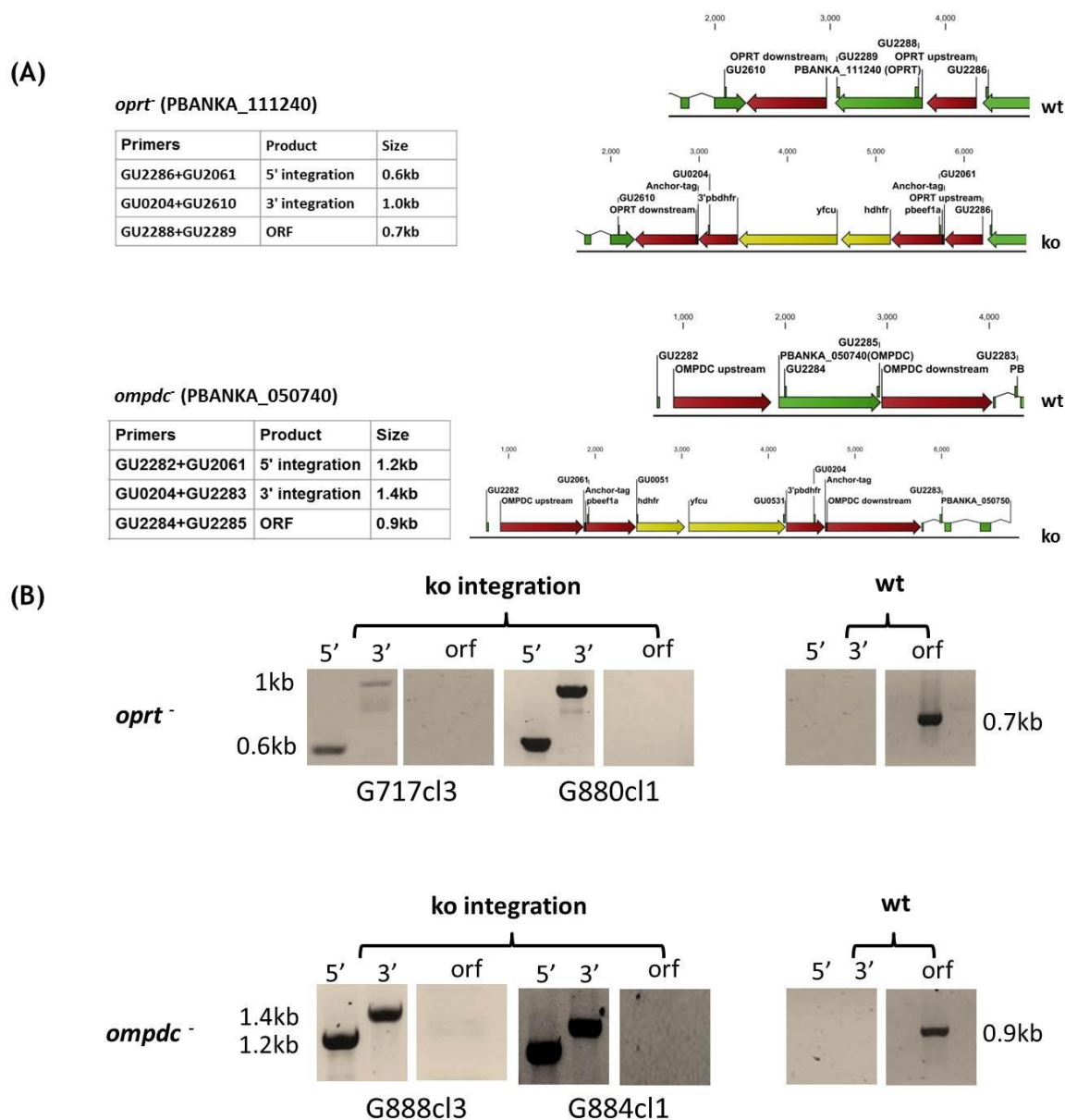
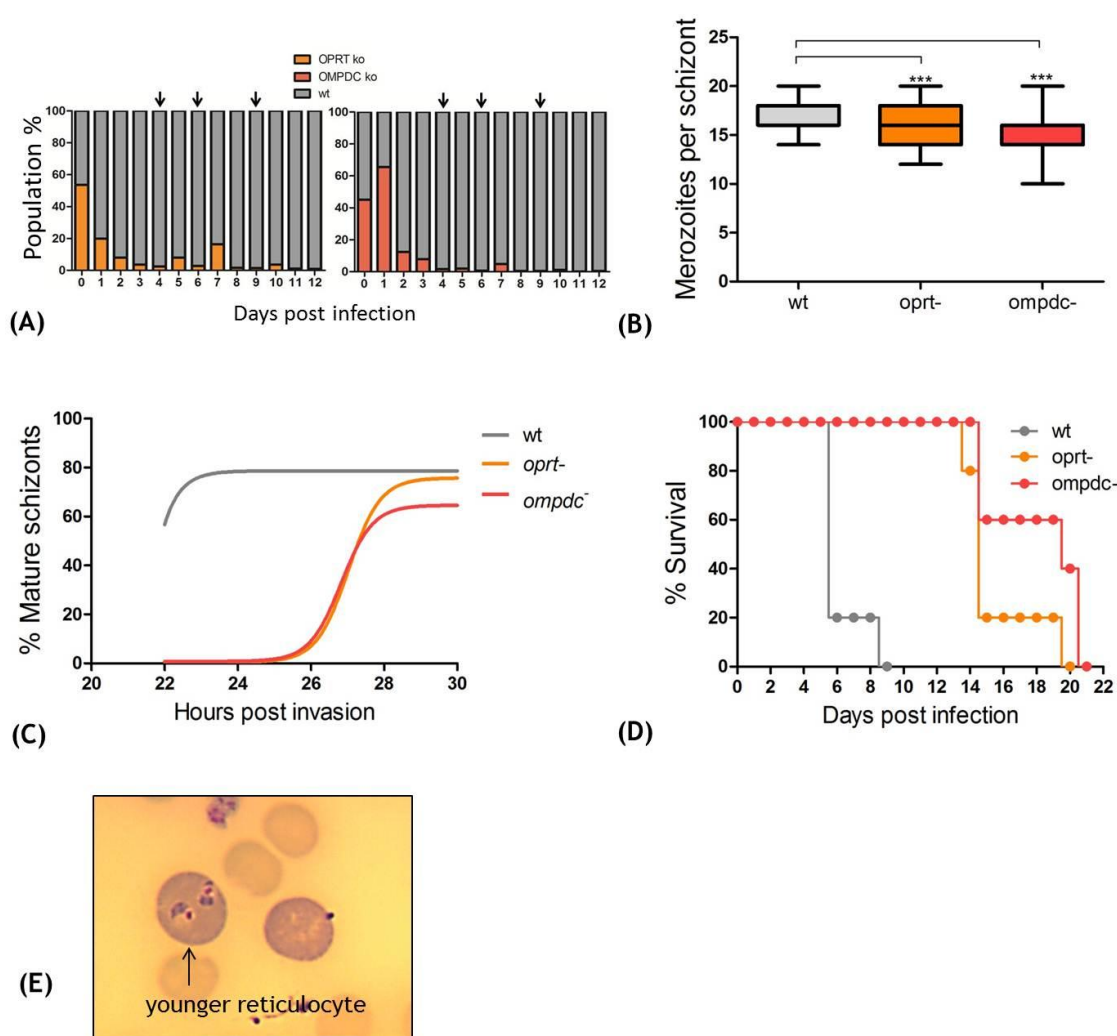


Figure 3-14 (A) Schematic representation of gene deletion strategy of (i) *opr*<sup>-</sup> (PBANKA\_111240) and (ii) *ompdc*<sup>-</sup> (PBANKA\_050740) in *P. berghei*. (B) Gel electrophoresis of indicated PCR products to confirm integration of selection cassette, disruption of genes and clonality of mutant. G717cl3 and G888cl3 were made in a wt parent line expressing GFP constitutively under the *eef1a* promoter (RMgm-7). G880cl1 and G884cl1 were made in a wt parent line which expresses GFP in male gametocytes under the dynein heavy chain promoter and RFP in female gametocytes under the LCCL domain-containing protein CCP2 promoter (RMgm-164).

### 3.2.4.1 Asexual stage phenotypic analyses of Pyrimidine synthesis mutant parasites

The *opr*<sup>-</sup> and *ompdc*<sup>-</sup> mutant parasites grow slowly and are rapidly outgrown in a competition growth assay with wt parasites (Figure 3-15A). Furthermore, both *opr*<sup>-</sup> mutants ( $15.90 \pm 2.04$ ,  $p < 0.0005$ ) and *ompdc*<sup>-</sup> mutants ( $15.17 \pm 2.45$ ,  $p < 0.0005$ ) were found to make, on average, significantly fewer merozoites than wt ( $17.45 \pm 1.75$ ) per schizont (Figure 3-15B) which took longer to mature (Figure 3-15C) as well. Both mutants showed altered lethality in the C57/B6 mouse

model as the mice infected with the mutants did not manifest symptoms of experimental cerebral malaria (ECM) but died between days 14-20 as a result of severe anaemia and hyperparasitemia (Figure 3-15D).



**Figure 3-15** Asexual stage phenotypic analyses of Pyrimidine biosynthesis mutants. (A) Competition growth assay using FACS analysis. Equal number of parasites wt population (RFP positive) and mutant population (GFP positive) were mixed and injected into a mouse on day 0 and peripheral blood from the infected mouse was monitored using FACS analyses over the next 12 days. Both *oprt*<sup>-</sup> and *ompdc*<sup>-</sup> parasites were overgrown by wt very quickly by day 3. Arrows indicate mechanical passage into a new mouse (B) Number of merozoites per schizont grown in *in vitro* cultures as counted in giemsa stained smears. The error is given as the SD of  $n \geq 40$  schizonts. Data representative of 3 independent biological replicates. P-value: ns: not significant, unpaired two tailed t-test. (C) Time taken for asexual parasites to grow to mature schizont stage. Coloured lines indicate non-linear fit of percentage of mature schizonts observed in *in vitro* synchronous cultures of wt and mutant *P. berghei* parasites 22 hours post invasion.  $n=3$  independent biological replicates. (D) Lethality experiment in C57/B6 mice by wt and mutant *P. berghei* parasites.  $10^4$  parasites were injected intraperitoneally in mice ( $n=5$ ) on day 0 and they were monitored over 21 days. The mice were culled humanely when they showed severe malaria pathology. Both mutant parasites were found to be lethal to mice although they did not show symptoms of ECM. (E) *oprt*<sup>-</sup> & *ompdc*<sup>-</sup> mutants invade the youngest reticulocytes which stain the darkest in Giemsa stained smears.

### 3.2.4.2 Analyses of gametocytogenesis and gamete formation in Pyrimidine biosynthesis mutant parasites

Gametocytaemia was slightly reduced only in *opr1*<sup>-</sup> parasites (Figure 3-16A) and unaffected in *ompdc*<sup>-</sup> mutants. There was no sex specific defect in production of gametocytes. Exflagellation (the production of male gametes) was found to be severely affected in *opr1*<sup>-</sup> and completely blocked in *ompdc*<sup>-</sup> parasites (Figure 3-16B) and DNA replication during male gametogenesis was severely reduced for both mutants (Figure 3-16C).

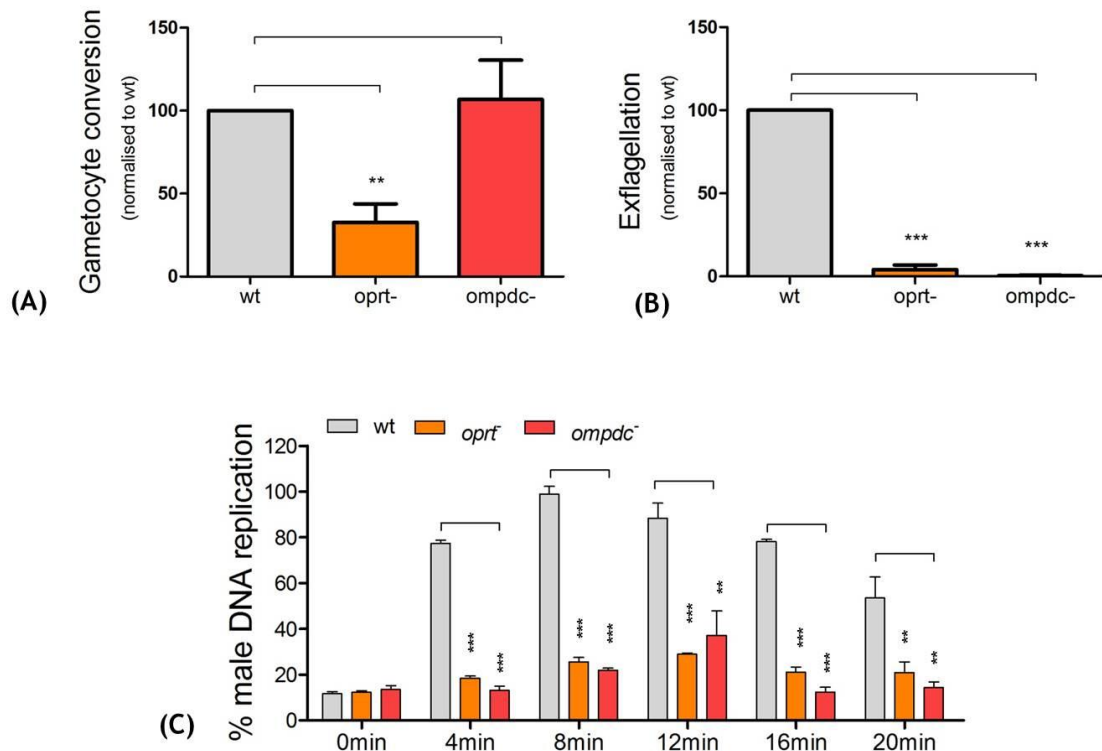


**Figure 3-16** Effect on gametocytogenesis and gamete formation in Pyrimidine biosynthesis mutants. (A) Gametocyte conversion normalised to wt during blood stages in mutant *P. berghei* parasites over 5 days post infection. The error is given as the SD of observed gametocyte conversion over 5 days. Data representative of n=2 independent biological replicates. (Gametocyte conversion was observed using a wt parent line which has GFP expression in male gametocytes and RFP expression in female gametocytes (RMgm-164). *P. berghei* mutants were made in the same background and using FACS analysis, number of gametocytes was determined in infected blood. P-values: \*p<0.05, \*\*p<0.005, \*\*\*p<0.0005, paired two tailed t-test. (B) Exflagellation (male gamete formation) in mutant *P. berghei* parasites normalised to wt in in vitro activation assay. The error is given as the SD of n=3 independent biological replicates. P-values: \*\*p<0.005, \*\*\*p<0.0005, paired two tailed t-test. (C) Determination of DNA content of male gametocytes over 20 minutes post activation by FACS analysis in mutant *P. berghei* parasites normalised to wt. DNA content was determined in Hoechst-33258-stained MACS purified gametocytes. Before activation (0mins) males show low DNA content with increasing amounts post activation reaching maximum levels between 8 to 12 minutes in wt. The error is given as the SD of n=3 independent biological replicates. P-values: \*\*p<0.005, \*\*\*p<0.0005, unpaired two tailed t-test.

### 3.2.4.3 Analyses of *in vitro* fertilisation and ookinete development in Pyrimidine biosynthesis mutant parasites

Consistent with the relative defects in male gametogenesis, very few ookinetes were formed in *in vitro* cultures in *opr<sup>t</sup>* parasites and no ookinetes were observed in *ompdc<sup>-</sup>* (Figure 3-17A). Genetic crosses of *opr<sup>t</sup>* and *ompdc<sup>-</sup>* mutants were performed with *P. berghei* lines RMgm-348 (Pb270, p47<sup>-</sup>) which produces viable male gametes but non-viable female gametes and RMgm-15 (Pb137, p48/45<sup>-</sup>) which produces viable female gametes but non-viable male gametes. This showed that interestingly RMgm-348 (Pb270) parasites were able to rescue the ookinete conversion defect in both mutant lines (Figure 3-17B) suggesting that viable male gamete formation is impaired in *opr<sup>t</sup>* and *ompdc<sup>-</sup>* mutant parasites while female gametes remain unaffected.

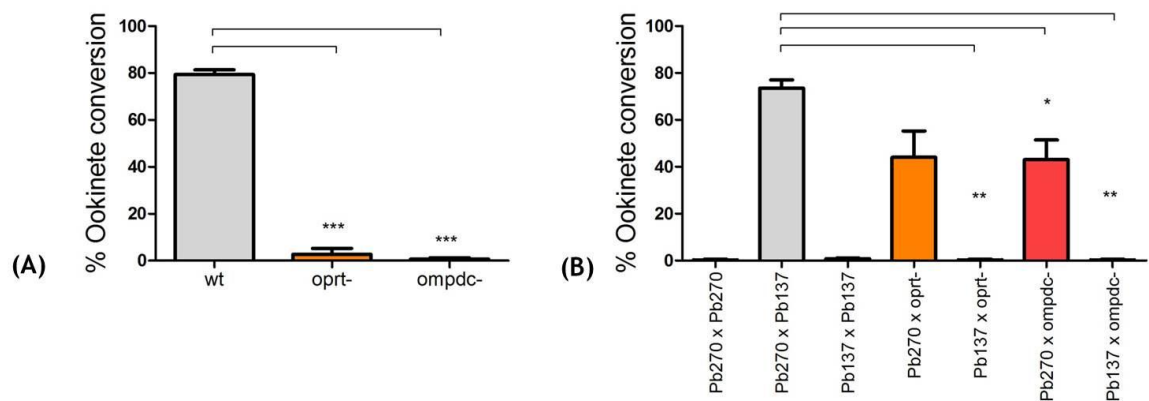


**Figure 3-17** *in vitro* ookinete conversion in Pyrimidine biosynthesis mutants. (A) *in vitro* ookinete conversion of mutant *P. berghei* parasites as compared to wt. The error is given as the SD of n=3 independent biological replicates. P-values: \*\*p<0.005, \*\*\*p<0.0005, unpaired two tailed t-test. (B) *in vitro* ookinete conversion assay to measure fertility of mutant *P. berghei* gametocytes by analysing the capacity to form ookinetes by crossing gametes with RMgm-348 (Pb270, p47<sup>-</sup>) which produces viable male gametes but non-viable female gametes and RMgm-15 (Pb137, p48/45<sup>-</sup>) which produces viable female gametes but non-viable male gametes. The error is given as the SD of n=2 independent biological replicates. P-values: \*p<0.05, \*\*p<0.005, unpaired two tailed t-test.

### 3.2.4.4 Analyses of mosquito infectivity and transmission of Pyrimidine biosynthesis mutant parasites

Infectivity to mosquito was significantly reduced in *opr<sup>t</sup>* and completely blocked in *ompdc<sup>-</sup>* mutants as seen by observing oocysts in infected mosquito midguts and salivary gland sporozoites (Figures 4 and S4) and infection to naïve mice was found to be completely blocked.

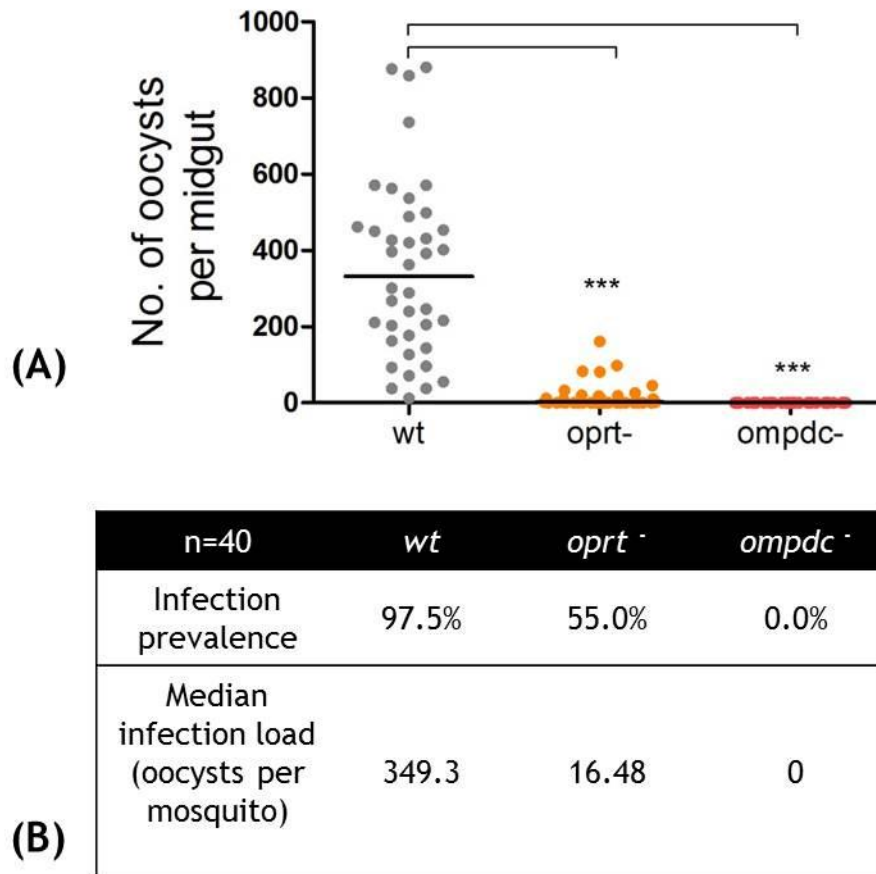


Figure 3-18 Mosquito infectivity of Pyrimidine synthesis mutant parasites compared to wt. (A) Number of mature oocysts at day 14 post infected blood feed in mosquito mid guts. n=40 mosquitoes cumulative of two independent biological replicates. \*\*\* $p < 0.0005$ , unpaired two tailed t-test. (B) Infection prevalence (percentage of observed mosquitoes found to be infected) and infection load (median of number of oocysts found per mosquito) in mutant *P. berghei* parasites compared to wt.

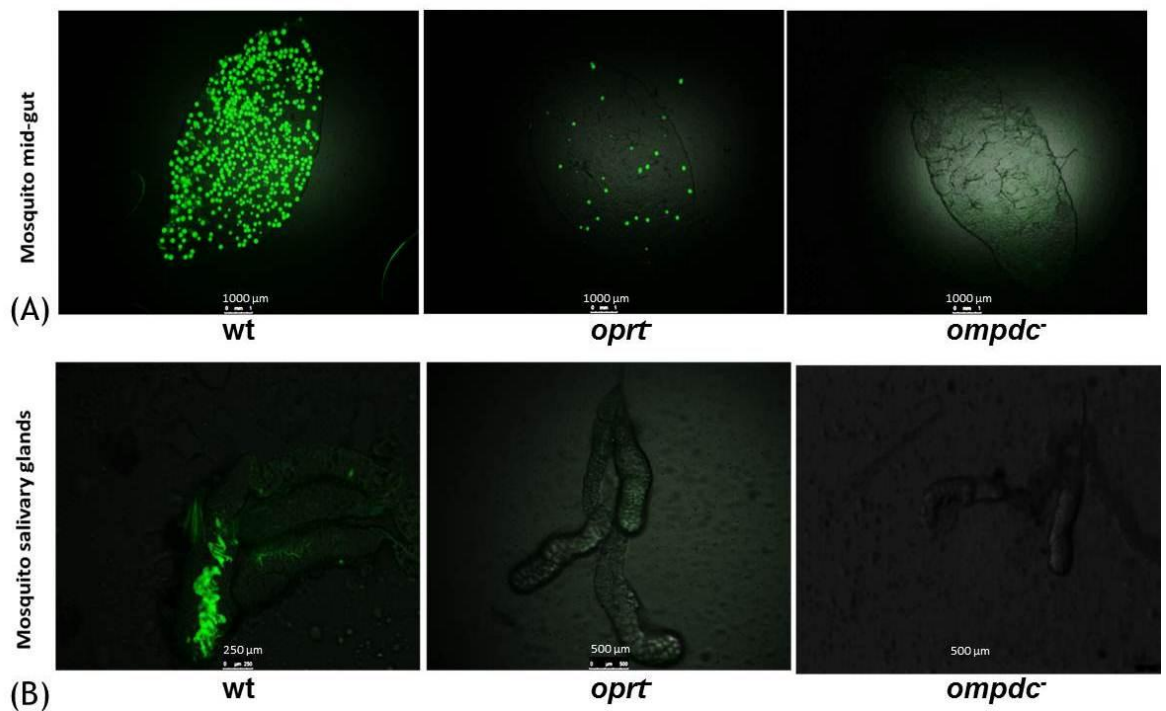


Figure 3-19 Representative images of mosquito infectivity of Pyrimidine biosynthesis mutant parasites compared to wt. (A) Mosquito mid guts showing mature oocysts at day 14 post infection in wt, *oprt*<sup>-</sup> and *ompdc*<sup>-</sup> *P. berghei* infected reticulocyte enriched mosquitoes. (B) Mosquito salivary glands showing sporozoites at day 21 post infection in wt, *oprt*<sup>-</sup> and *ompdc*<sup>-</sup> *P. berghei* infected reticulocyte enriched mosquitoes.

#### 3.2.4.5 Pb270 rescued *oprt*<sup>-</sup> and *ompdc*<sup>-</sup> ookinetes do not transmit through mosquito

Pb270 (p47<sup>-</sup>) crosses which rescued the ookinete stage phenotype in *oprt*<sup>-</sup> and *ompdc*<sup>-</sup> parasites pointing at male gamete specific defect (Figure 3-17B) were also performed *in vivo*. This was done by injecting mice with a mixed suspension of equal number (total 10<sup>4</sup>) of schizont stage parasites from Pb270 and either *oprt*<sup>-</sup> or *ompdc*<sup>-</sup> parasites and after 48 hours at approximately 3-5% parasitemia, allowing mosquitoes to feed on these mice. Exflagellation, fertilisation and ookinete development took place in mosquito midguts and mosquitoes were then dissected to look for presence of oocysts on day 12-14. As the Pb270 parasites were made in non-fluorescent background, any oocysts resulting from Pb270 self-fertilisation could not be observed quantitatively under the microscope. It was found that fluorescent oocyst production was blocked in both the crosses (Figure 3-20).

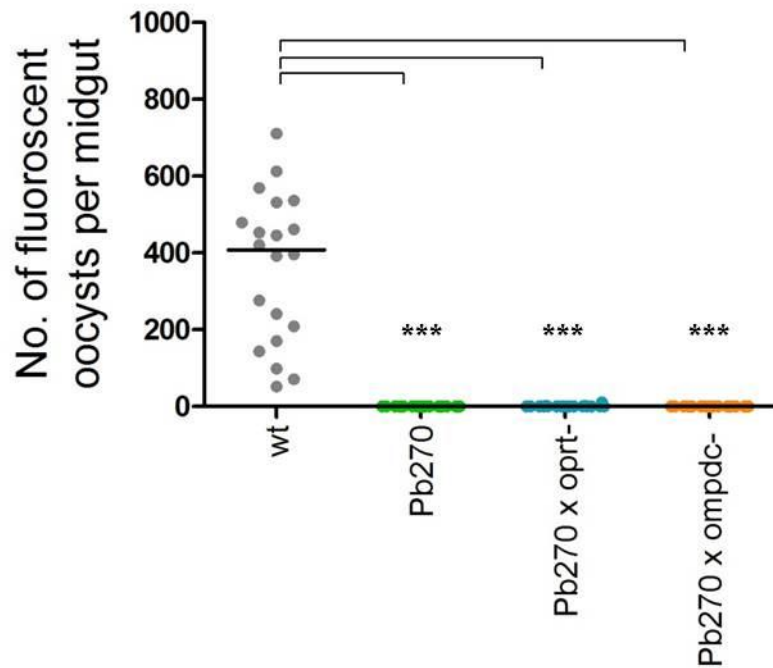
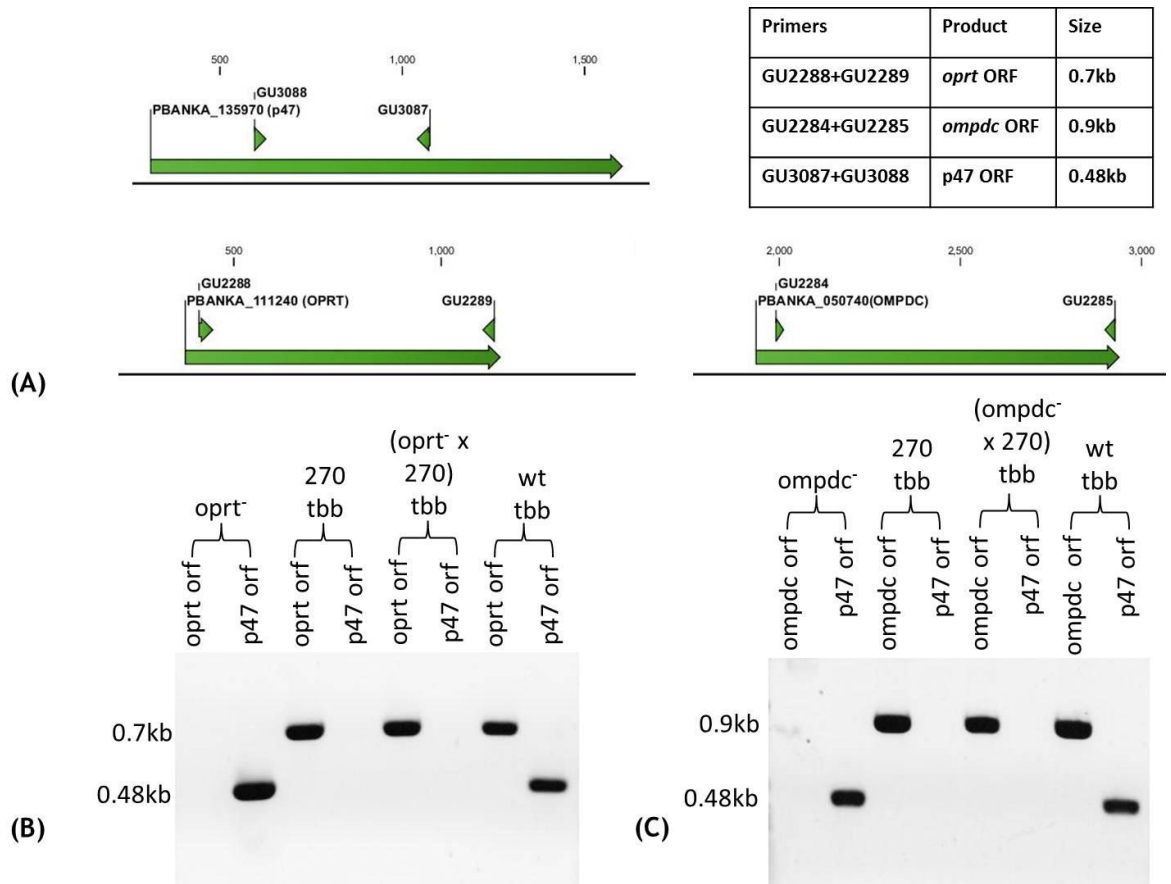


Figure 3-20 Mosquito infectivity as observed by counting mature fluorescent oocysts of *in vivo* crossed Pb270 x *opr*<sup>-</sup> and Pb270 x *ompdc*<sup>-</sup> mutant parasites compared to wt and self-fertilised Pb270 on day 14 post infected blood feed in mosquito mid guts. n=20 mosquitoes cumulative of two independent biological replicates. \*\*\*p<0.0005, unpaired two tailed t-test.

Also, no fluorescent sporozoites could be observed in salivary glands in these mosquitoes. These mosquitoes were then allowed to bite naïve mice on day 21 post infectious blood feed and mice were observed for parasites. By day 3-4, parasites could be observed in peripheral blood and were harvested to obtain genomic DNA to do genotypic characterisation. PCRs were performed to check for presence of *opr*, *ompdc* and p47 orfs in the transmitted parasites (tbb lines) and it was observed that only Pb270 (p47) parasites were transmitted (Figure 3-21).



**Figure 3-21 Genotypic analyses of transmitted parasites obtained after exposure of naïve mice to mosquitoes infected with *in vivo* crossed Pb270 x *opr*t<sup>-</sup> and Pb270 x *ompdc*<sup>-</sup> mutant parasites compared to wt and self-fertilised Pb270 (tbb: transmission bite back). (A) Schematic representation of expected PCR products for open reading frames indicating presence or absence of a gene. (B and C) p47 orf can be observed only in *opr*t<sup>-</sup>, *ompdc*<sup>-</sup> and wt tbb controls but not in self-fertilised Pb270 or crossed and transmitted [(Pb270 x *opr*t<sup>-</sup>)tbb and (Pb270 x *ompdc*<sup>-</sup>)tbb] parasites. Also, *opr*t orf and *ompdc* orf can be observed in the respective crossed and transmitted parasites. This indicates that only Pb270 parasites alone can successfully be transmitted.**

It has been observed before that Pb270 (p47<sup>-</sup>) parasites can form some ookinetes even though there is 10,000x reduction compared to wt and are able to transmit through mosquito (personal communication Chris Janse, LMRG). This implies that, not surprisingly, blocking the *de novo* pyrimidine biosynthesis in *opr*t<sup>-</sup> and *ompdc*<sup>-</sup> parasites also leads to defect in nucleotide synthesis in DNA replication required for establishment of a mature oocyst and complete sporogony in the mosquito.

### 3.2.4.6 Pyrimidine biosynthesis inhibition sensitivity is different in *P. berghei* and *P. falciparum*

We tested pyrimidine biosynthesis inhibition using a previously published inhibitor of this pathway in *P. falciparum* in parallel with *P. berghei* *in vitro* to test whether it had differential sensitivity between the species owing to *P. berghei* inhabiting reticulocytes which have metabolic reserves of the pyrimidine

biosynthesis pathway. This experiment was done in *in vitro* conditions to remove any discrepancy in findings which could potentially result from the issues of bioavailability of the inhibitor in mice if it were to be done *in vivo*. It is known that *oprt* can also use 5-fluoroorotate (5FOA) as an alternate substrate instead of orotate (Figure 3-13) and 5FOA has been shown to be an inhibitor of *P. falciparum* in *in vitro* cultures with very low  $IC_{50}$  in nano-molar range (Rathod, Khatri et al. 1989). We tested the activity of 5FOA against *P. berghei* and *P. falciparum* *in vitro* cultures (section 2.1.20.1 and 2.2) and found that the  $IC_{50}$  value was almost 90 fold higher in *P. berghei* inhibition (32.2nM) compared to *P. falciparum* inhibition (0.37nM) (Figure 3-22). Dihydroartemisinin (DHA) activity was used as a control and there wasn't any significant difference observed in its activity between *P. berghei* (6.6nM) and *P. falciparum* (2.8nM) Figure 3-22.

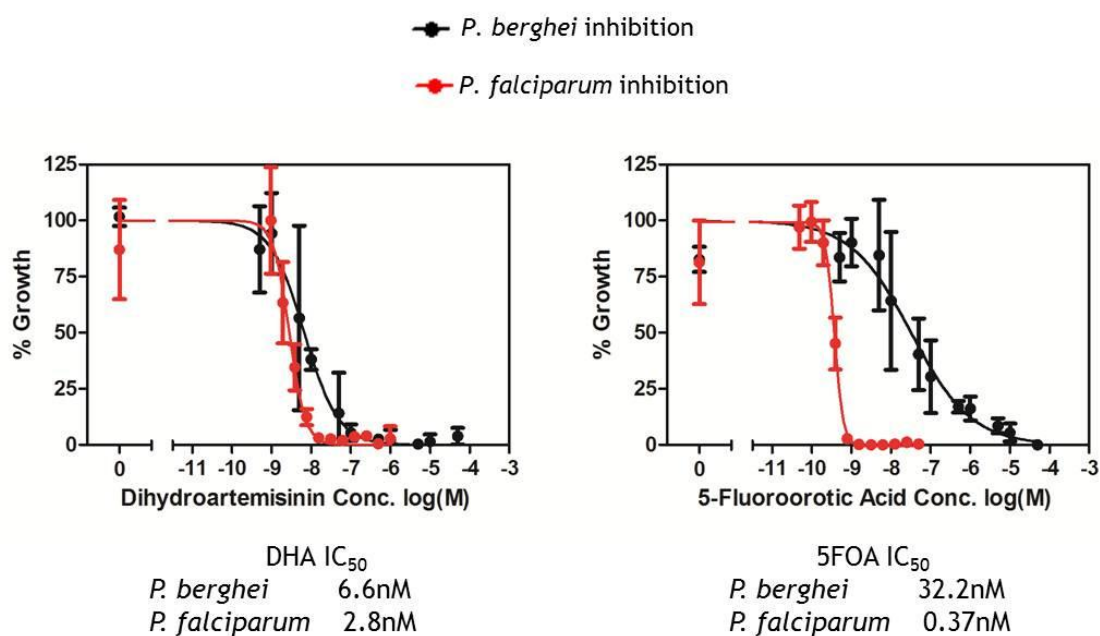


Figure 3-22 *P. berghei* and *P. falciparum* inhibition by Dihydroartemisinin (DHA) and 5-Fluoroorotic Acid (5FOA) *in vitro*. Error bars indicate SD from n=3 biological replicates.

### 3.3 Discussion

Protozoan parasites that live within their host cell are exquisitely adapted to derive maximum benefit from their intracellular niche. Most obviously blood stage malaria parasites import and catabolise haemoglobin and have developed sophisticated packaging systems to neutralise the potential damaging effects of the haem by-product. However a number of malaria parasites infectious to both

human (*P. vivax*) and rodents (*P. berghei*) exhibit a strong preference to colonise more complex reticulocytes rather than mature erythrocytes which might offer additional advantages to the parasite. The aims of this study were to investigate the anticipated metabolic differences between the two cell types and then to examine the possible functional consequences with regard to parasite survival and their exploitation of any differences.

The reticulocyte metabolome is both enriched and more complex than that of the mature erythrocyte and it was shown by disrupting two pathways (ICM and pyrimidine biosynthesis) in *P. berghei* blood stages which are essential in *P. falciparum* blood stages. The *P. berghei* mutants could not develop in the exo-erythrocytic mosquito stages, highlighting the importance of reticulocyte sourced metabolic reserves for their intracellular growth.

### 3.3.1 Intermediary Carbon Metabolism (ICM)

Glycolysis is the main pathway for carbon metabolism in erythrocytes (Chapman, Hennessey et al. 1962). Furthermore, there is proteomic evidence for residual TCA cycle and ICM enzymes in both human (Pasini, Kirkegaard et al. 2006) and rodent (Pasini, Kirkegaard et al. 2008) erythrocytes indicative of the more complex metabolism in the erythroid precursors which still has enzymatic footprints in erythrocytes which are devoid of nucleus and are released into peripheral circulation. The high levels of malate and aspartate in reticulocytes (Figure 3-5) could be a result of active production via ICM.

Gene deletions of both *pepc* and *mdh* in *P. berghei* gave a severe phenotype in post-erythrocytic mosquito stages as anticipated, however *pepc*<sup>-</sup> mutant was found to be more severely affected than the *mdh*<sup>-</sup> mutant (Figure 3-8, Figure 3-9, Figure 3-10, Figure 3-11 and Figure 3-12). This was because being an upstream gene in the pathway, *pepc*<sup>-</sup> mutant possibly had complete block in the production of both aspartate and malate via ICM (Figure 3-6) in mosquito stages in the extracellular parasite. Deleting *mdh* does not stop the development of all parasites in mosquito stages possibly because there are alternate ways of producing malate (e.g. TCA cycle). *mdh* has another function of generating reducing equivalents (NADH+H<sup>+</sup>) but there are other dehydrogenases in TCA cycle which can also generate them so this function is not exclusive to *mdh*. This further explains why *mdh*<sup>-</sup> mutants could still complete the life cycle.

Even after repeated attempts, *aat* could not be deleted in the blood stage (Figure 3-6). This could be because, the generation of aspartate is necessary not only for nucleic acid but also protein synthesis and this terminal step of intermediary carbon metabolism is critical in *in vivo* situations where aspartate levels are limiting (Olszewski and Llinas 2011). Failure to delete *aat* suggests that the apparent higher levels of aspartate observed in reticulocytes were not enough to meet all of the demands of a growing asexual stage parasite where a high turnover of nucleic acids and proteins is required and this can also explain the slow growth of asexual *pepc*<sup>-</sup> mutant parasites which seemed to take longer to develop.

### 3.3.2 Pyrimidine biosynthesis

DNA replication and RNA transcription require a continuously available and sufficient source of nucleotides in *Plasmodium* parasites whose lifecycle exhibits a wide variety of protein expression profiles and requires multiple replication steps both in mammalian host and mosquito vector. Both purines and pyrimidines make up the building blocks of these nucleotides and *Plasmodium* relies heavily on salvaging purines from the host as it doesn't encode any enzymes for *de novo* purine synthesis (Downie, Kirk et al. 2008). The purine salvage pathway is well characterised in *Plasmodium* (Riegelhaupt, Cassera et al. 2010) and once nucleosides are taken up by erythrocyte nucleoside transporters (Cassera, Zhang et al. 2011) inside the infected erythrocyte, non-selective pores with a large diameter on the parasitophorous vacuole allow them to be internalised (Downie, Kirk et al. 2008) (Desai, Krogstad et al. 1993), cross the parasite plasma membrane by PfNT1 and a yet to be characterised AMP transporters (Cassera, Hazleton et al. 2008) and interconverted to end products to be utilised for nucleic acid syntheses.

The situation is almost reverse when it comes to pyrimidines as it has been believed that unlike purines, pyrimidines exist in low concentrations in erythrocytes and *Plasmodium* encodes all enzymes necessary for *de novo* pyrimidine synthesis (Gardner, Hall et al. 2002), lacking transporters for salvage from the nutrient rich extra-cellular culture/host environment.

Other apicomplexan parasites are capable of pyrimidine salvage- e.g. *Cryptosporidium* spp. encode a bifunctional protein uridine kinase-uracil phosphoribosyltransferase-UK-UPRT (EC 2.7.1.48, EC 2.4.2.9) to salvage uridine,

uracil and cytidine and a thymidine kinase-TK (EC 2.7.1.21) to salvage thymidine. *Toxoplasma* spp. has partial salvage ability and has retained the monofunctional uracil phosphoribosyltransferase (UPRT) to take up uracil.

All these enzymes are not present in *Plasmodium* and hence *de novo* pyrimidine synthesis has been considered a promising drug target for malaria intervention. But there is an annotated UDP-N-acetyl glucosamine: UMP antiporter in *Plasmodium* (PBANKA\_110490) and such antiporters have been shown to transport nucleotide sugars in exchange for nucleotide monophosphates in human cells (Ishida and Kawakita 2004). This UMP antiporter is unique to *Plasmodium* spp. in apicomplexans as it does not have homologues in *Toxoplasma* or *Cryptosporidium* although they do have the usual UDP: sugar transporters (e.g. (TGVEG\_108800) and (cgd2\_590). Reticulocytes were found to have both UDP-N-acetyl glucosamine and UMP (Uridine monophosphate) in elevated amounts compared to normocytes (Table 2)

The first six steps of pyrimidine biosynthesis (Figure 3-13) lead to production of UMP which is the precursor of all pyrimidine nucleotides. As shown in Figure 3-5 and Table 2, in our metabolomics data, we found that a number of purine and pyrimidine biosynthesis intermediates were enriched in reticulocytes as compared to mature erythrocytes. As a reticulocyte resident parasite like *P. berghei* has ready access to these intermediates, we anticipated that the pyrimidine synthesis pathway may be dispensable for such a parasite in blood stages. Because 5 of the these 6 enzymes have been shown to be potential drug targets in normocyte cultured *P. falciparum*, we targeted these genes for deletion and managed to get the last two genes, *oprt* and *ompgc* knocked out in blood stages in the first attempt whereas the others could not be deleted (Figure 3-13).

The *oprt*<sup>-</sup> and *ompgc*<sup>-</sup> mutant parasites survived in intra-erythrocytic stages but seemed to grow slower than wt (Figure 3-15A). They also inhabited the youngest reticulocytes (Figure 3-15E) because younger reticulocytes presumably will have higher proportions of metabolic precursors. As these mutants were exclusively reliant on reticulocyte pools of pyrimidines, this possibly also led to a reduction in number of merozoites produced (Figure 3-15B). Although this reduction is small, it is still significant compared to wt and in evolutionary terms it seems to have a huge implication on asexual growth. These mutants were also found to

take longer to mature to schizont stage (Figure 3-15C). Although in *Plasmodium* spp., asexual development via schizogony differs considerably from the usual G1, S, G2 and M phases of the cell cycle observed in other eukaryotes, more than 550 proteins have been found to be associated with cell cycle regulation (Cai, Hong et al. 2013) indicating the presence of a tightly controlled cell cycle. It is thus possible that *opr1*<sup>-</sup> and *ompdc1*<sup>-</sup> mutants could be employing cell cycle check points which might limit the number of merozoites produced according to their ability to completely replicate their genomes, explaining their slower growth. Yet, in spite of a disrupted *de novo* pyrimidine synthesis pathway and slow growth, these mutants were able to cause disease and severe pathology and death in C57/B6 mice by hyperparasitemia and anaemia (Figure 3-15D).

*opr1* and *ompdc1* gene deletions gave a severe phenotype in post-erythrocytic stages as expected (Figure 3-16, Figure 3-17, Figure 3-18 and Figure 3-19). It is interesting to note that in both *Toxoplasma* and *Plasmodium* spp., *opr1* and *ompdc1* are mono-functional separate proteins but form a complex and catalyse the formation of UMP from orotate via Orotidine-mono-phosphate. The kinetic properties of this complex are different from that of a single protein in the mammalian host, UMP synthase which catalyses this whole inter-conversion (Krungrai, DelFraino et al. 2005).

The first defect in mosquito stages appeared to be in the process of viable male gamete formation which was severely impaired (Figure 3-16) and as quick DNA replication during the process of exflagellation requires rapid nucleotide synthesis and assembly, *de novo* pyrimidine synthesis becomes very crucial and reticulocyte pools of pyrimidines and their intermediates may not be enough for this process. This obviously had knock on effect on ookinete production as well (Figure 3-17A) which could be rescued when viable male gametes from Pb270 (p47<sup>-</sup>) *P. berghei* parasites were used for *in vitro* crosses pointing to a male gamete specific defect (Figure 3-17B). Mature oocyst production was severely reduced in both mutants (Figure 3-18 and Figure 3-19) and even the ookinetes formed by *in vitro* crosses with Pb270 parasites could not form mature oocysts (Figure 3-20). This and Figure 3-21 implied that *de novo* pyrimidine synthesis is required also for establishment of a mature oocyst and complete sporogony in the mosquito phase development of the parasite.

When the *oprt* inhibitor, 5-fluoroorotate (5FOA) was found to be less potent against *P. berghei* as compared to *P. falciparum in vitro* (Figure 3-22), it further supported the notion that reticulocytes can indeed protect the parasites in the intracellular blood stage from the effects of genetic or chemical disruption of the *de novo* pyrimidine biosynthesis pathway. As this protective environment is not present in the mosquito stages, the parasites are not able to fulfil their metabolic needs and don't survive.

Even after repeated attempts, *cpsII* (PBANKA\_140670), *act* (PBANKA\_135770), *dhoase* (PBANKA\_133610) and *dhodh* (PBANKA\_010210) could not be deleted (Figure 3-13). Although the first three genes are mono-functional in *Plasmodium*, their activities are included in a single tri-functional protein in the mammalian host (Hyde 2007). *cpsII* activity can be inhibited by a positive feedback mechanism by increased amounts of the end product UTP (Gero, Brown et al. 1984). Both *dhoase* and *dhodh* are bidirectional enzymes and could also play a role in the generation of additional aspartate required for protein synthesis by taking their respective reactions in the reverse direction. *dhodh* is also linked to ubiquinone (CoQ) as an electron acceptor and apart from converting dihydroorotate to orotate it also has a role in electron transport chain. Owing to the essentiality of these genes in these additional functions, it is not surprising that we could not delete them in asexual stage parasites.

It is also notable that homologues of some more downstream pyrimidine synthesis enzymes which eventually catalyse steps in the formation of UTP, CDP, dCTP and dTTP, namely Nucleoside diphosphate kinase B (NDK B) (PBANKA\_114240), CTP- CTP synthase (PBANKA\_103230), dCDP, dUDP and dUTP-Ribonucleotide Reductase (RNR) large subunit (PBANKA\_061160) have been found to be present in erythrocytes (Pasini, Kirkegaard et al. 2006, Pasini, Kirkegaard et al. 2008). This points towards the capability of the host cell in at least partially retaining some nucleotide synthesis pathways which the parasite can utilise.

### 3.3.3 Other metabolic pathways enriched in reticulocytes

#### 3.3.3.1 Glutathione biosynthesis pathway

*Plasmodium* spp. has to cope with oxidative stress caused by haemoglobin metabolism (formation of reactive oxygen species (ROS) and release of toxic ferriprotoporphyrin IX) and one of the ways it defends itself is by employing its

own fully functional Glutathione redox system (Muller 2004) and has a fully functional glutathione biosynthesis pathway (Figure 3-23A). Both gamma-glutamylcysteine synthetase ( $\gamma$ -GCS) and Glutathione Synthetase (GS) are essential for parasite survival in *P. falciparum* (Patzewitz, Wong et al. 2012).  $\gamma$ -GCS and Glutathione Reductase (GR) can be deleted in *P. berghei* and intra-erythrocytic asexual growth is unaffected but mosquito stage development is affected giving stunted oocysts and no sporozoites (Vega-Rodriguez, Franke-Fayard et al. 2009, Pastrana-Mena, Dinglasan et al. 2010). The reason for this apparent difference between the observations in *P. falciparum* and *P. berghei* was not clear.

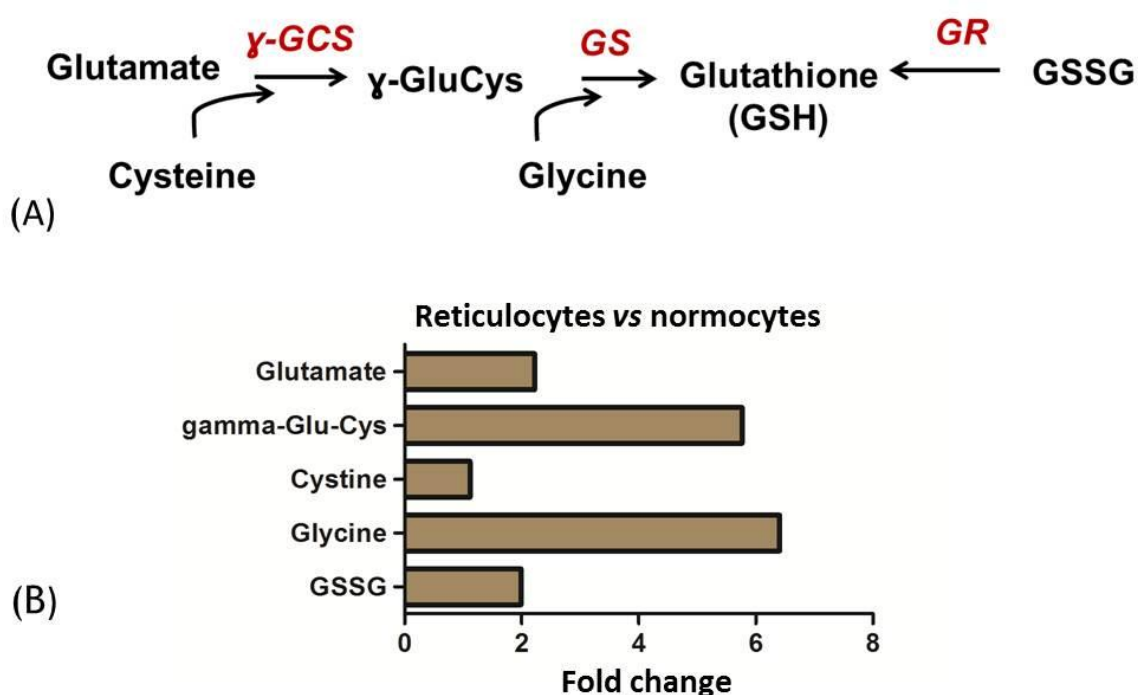


Figure 3-23 (A) Schematic representation of Glutathione synthesis pathway in *Plasmodium*.  $\gamma$ -GCS (gamma-glutamylcysteine synthetase), GS (Glutathione Synthetase), GR (Glutathione Reductase)  $\gamma$ -GluCys (gamma-L-Glutamyl-L-cysteine), GSSG (Glutathione di-sulphide). (B) Fold change of metabolites of Glutathione biosynthesis in rodent reticulocytes compared to normocytes.

Glutathione biosynthesis pathway has been shown previously to exist in erythrocytes (Majerus, Brauner et al. 1971) and the enzymes for this pathway have been shown to be present in both human (Pasini, Kirkegaard et al. 2006) and rodent (Pasini, Kirkegaard et al. 2008) erythrocytes. Our data demonstrated that the levels of glutathione synthesis intermediates were higher in reticulocytes than in mature erythrocytes (Figure 3-23B and Table 2). Although reduced glutathione (GSH) was not detected in our data (probably oxidised during sample storage), glutathione disulphide (GSSG) was detected and it was 2

fold higher in reticulocytes than normocytes. The high levels of glutathione biosynthesis pathway intermediates in reticulocytes suggested that these reserves in reticulocytes rescue the phenotype in *P. berghei*  $\gamma$ -GCS and GR mutant intra-erythrocytic asexual stages and the mosquito stages don't develop as they are exo-erythrocytic. This validated the metabolomics data against published observations and also lent weight to our hypothesis (Figure 3-4).

### 3.3.3.2 TCA cycle

As *Plasmodium* parasites rely on glycolysis (Homewood 1977) for energy production, TCA cycle has been expected to be non-essential in blood stages but has been found to be pivotal during mosquito stages (Hino, Hirai et al. 2012, Macrae, Dixon et al. 2013, Oppenheim, Creek et al. 2014) (See section 5 for detailed study of *P. berghei* TCA cycle metabolism). Reticulocytes contain mitochondria as explained above in section 3.2.2 and could potentially have a functional TCA cycle. It remains to be seen whether this would be a complete and canonical cycle or not (refer to section 5) as maturing reticulocytes are in the process of losing all their organelles and the mitochondria observed in them have been shown to be rudimentary (Gronowicz, Swift et al. 1984). However, if reticulocyte resident *Plasmodium* parasites required any metabolites resulting from the host TCA cycle, they have access to it.

### 3.3.3.3 Phosphatidylcholine and Phosphatidylethanolamine synthesis

The intermediates of Phospholipid (PL) (Phosphatidylcholine- PC and Phosphatidylethanolamine- PE) synthesis were observed to be enriched in reticulocytes compared to normocytes (Table 2). There is published evidence of phospholipid synthesis in reticulocytes (Ballas and Burka 1974) and as reticulocytes have been shown to remodel their membrane structure during maturation to normocytes (Gronowicz, Swift et al. 1984) (Liu, Guo et al. 2010), changes in the lipid profile were not unexpected. Interestingly, all PC and PE biosynthesis genes are essential in both *P. falciparum* and *P. berghei* blood stages and both these species have been shown to employ different methods of PC and PE synthesis, the most notable being the absence of a *PfPMT* orthologue (which converts phospho-ethanolamine to phospho-choline linking PE and PC synthesis in *P. falciparum*, thus providing an additional pathway to make PC) in *P. berghei* (Dechamps, Maynadier et al. 2010). However, this difference between the *P. falciparum* and *P. berghei* parasites cannot be attributed to the evolution of *P. berghei* to invade reticulocytes which have increased levels of PC and PE

intermediates because *P. vivax* which also invades reticulocytes possesses the *PfPMT* orthologue. Nevertheless, as *P. falciparum* has been shown to be susceptible to inhibitors of phospholipid (PL) synthesis (Ancelin, Calas et al. 2003), even though PL synthesis pathways have been shown to be essential in *P. berghei*, it could still be interesting to test these inhibitors on *P. berghei* given that reticulocytes have elevated levels of PL synthesis intermediates.

### 3.3.4 Phylogenetic analyses of the key metabolic enzymes

A phylogenetic comparison of enzymes of the predicted metabolic capacities of the different *Plasmodium* species for which whole genome data is available indicates that they are each expected to be capable of the same basic metabolic processes (Figure 9-5 and Table 7). Therefore the enriched environment of the reticulocyte does not appear to have exerted an obvious selection pressure on those parasites that preferentially develop within them.

## 3.4 Conclusions

It was hence found that reticulocytes are metabolically enriched with a significant overlap in the metabolic profile with *Plasmodium* spp. and some aspects of parasite metabolism can be redundant in blood stage parasites like *P. berghei*. Although data is not shown here (due to author declaration purposes), in collaboration with Creek et al. from Monash University, Australia, we have also observed a similar enrichment in human reticulocytes grown from CD34+ haematopoietic progenitor stem cells compared to normocytes. The metabolic profile between human and rodent reticulocytes was found to be very similar as well. Therefore it can be speculated that the human malaria parasite *P. vivax* would also be capable of accessing reticulocyte pools like it was observed for *P. berghei* in this study. This advantage of inhabiting a metabolically rich host cell may offer *P. vivax* parasites, an edge against drugs used to target their metabolism to clear infection in human populations. *P. vivax* parasites are already difficult to eradicate effectively using existing drugs owing to their ability to form hypnozoites and it is therefore not surprising that compared to *P. falciparum*, only a fraction of vaccine candidates are currently at trial stage against *P. vivax* (Reyes-Sandoval and Bachmann 2013).

*P. falciparum* parasites invade both reticulocytes and normocytes in the field and it is known that even in *in vitro* cultures, they grow better when using fresh blood which presumably has 1-2% reticulocytes (Personal communications Prof.

Lisa Ranford-Cartwright and Prof. Sylke Muller). It is thus possible that drugs targeting metabolism in *P. falciparum* that can be alleviated by scavenging of host reticulocyte metabolome might select for parasites that have developed a preference for invading reticulocytes and contribute to increase in resistance. Also, there is a possibility of recrudescence of parasites which can survive following a partially effective treatment by a metabolic inhibitor which could kill the parasites in the normocytes but not in the metabolically enriched younger reticulocytes.

The findings in this study therefore have potential implications for existing drug therapies against blood stage malaria that target only parasite metabolism which should differ according to the target host blood cell distributions of human malaria. Moreover, as it is evident that the parasite utilises its host cell to a great extent, both using it as a structural niche for asexual replication, as a source of nutrients and for small molecule metabolites to supplement its biochemical requirements, the useful elements of host cell metabolism could be targeted to kill the parasite as it has been done elsewhere (Sicard, Semblat et al. 2011). The great advantage of this approach is that the parasite would be less able to use mutations in its own genome to escape the indirect but deleterious effects of targeting host metabolism. However, one will have to be careful in designing such approaches so that essential metabolism in the host cell is disrupted only in parasitized cells, leaving the uninfected cells untouched, which can be challenging.

## 4 *Plasmodium* metabolism is stage specific

### 4.1 Introduction

Apicomplexans, which include the malaria parasite *Plasmodium*, belong to the phylum Chromalveolata which also contains ciliates and dinoflagellates, many of them photosynthetic. This phylum diverged from the main eukaryotic lineage very early and members differ substantially from yeast and other metazoans (Talevich, Tobin et al. 2012). Even though they contain a relict plastid, the loss of photosynthetic ability seems to have resulted from the emergence of a parasitic lifestyle for other apicomplexans and *Plasmodium* (Kalanon and McFadden 2010).

The *Plasmodium* parasite has a complex lifecycle (see section 1.2) where it resides in multiple environments, invades different cell types and undergoes asexual reproduction by mitotic division as well as sexual reproduction, fertilisation and meiosis. Across the life cycle, it uses a mosquito vector and a mammalian host with many different biochemical nutrient sources and ambient niches.

The life stage responsible for initiating the life cycle in the mosquito vector is the gametocyte stage and *P. berghei* undergoes systematic production of these sexual precursor cells (gametocytes) in every cycle (almost 20% of all cells) unlike *P. falciparum* where gametocytogenesis is apparently (stress-) inducible. The gametocytes in *Plasmodium* are different from asexual stages in morphology and cell structure. In *P. berghei*, the asexual cycle takes 22-24 hours whereas gametocyte development takes slightly longer, at 26-30 hours, after which mature gametocytes enter a post-mitotic G<sub>1</sub> stage and stay quiescent for up to further 24-30 hours before they degenerate and are removed from the circulation (Mons, Janse et al. 1985). Waiting to be picked up by a blood meal through a mosquito bite, gametocytes prepare themselves for a relatively hostile environment within the mosquito mid-gut where a drastic change in environment (e.g. low temperature, high pH) and other mosquito factors provide them with cues to form haploid gametes which fuse to form a diploid zygote. The apparently apolar zygote undergoes meiosis within 4 hours and after 18-24 hours develops into an invasive motile polar form called the ookinete which then traverses the midgut wall of the mosquito and forms an oocyst on the basal

lamina. The oocyst then develops to form thousands of sporozoites, ready for the next cycle of infection.

Gametocytes prepare themselves for such a dynamic change by employing strategies such as Conditional Translational Repression (CTR) which allows for a number of transcripts which encode proteins required for zygote development to be stored as mRNA-protein complexes within the female gametocytes (Mair, Braks et al. 2006). These mRNP complexes hold the transcripts and release them in a programmed fashion in response to environmental factors as the parasite develops.

It is anticipated that the preparation for the response to such a different environment and a dynamic structural remodelling should also be reflected at the metabolic level in the parasite. Comparing the metabolomes of gametocytes to asexual stages may thus give interesting insight into the metabolic machinery of a highly complex but conditionally terminally differentiated cell. Examples from other eukaryotic parasites like *Trypanosoma brucei* already exist where there is a shift in metabolism from glucose as a major carbon source in blood stages to proline in procyclic stages in the insect vector Tse-tse fly (Besteiro, Barrett et al. 2005). Identification of active metabolic pathways may provide alternate intervention strategies that the parasite is less able to evade.

Initially, an untargeted metabolomics approach was used (whose results are described below and one of the most interesting leads is discussed in section 6) to delineate and compare metabolomes of uninfected reticulocyte enriched erythrocytes (as host cell background), *P. berghei* purified asexual schizonts and purified gametocytes using Liquid Chromatography Mass Spectrometry (LC-MS) and Gas Chromatography Mass Spectrometry (GC-MS).

Also, a targeted metabolomics approach was used to study energy metabolism in different stages of *P. berghei* and the all the findings of this study are discussed in section 5.

## 4.2 Results

For the untargeted metabolomics study, briefly, raw LC-MS data was processed using the standard Glasgow Polyomics pipeline, consisting of XCMS, MZMatch and IDEOM and the raw GC-MS data was processed using the standard Metabolomics Australia pipeline consisting of PyMS matrix generation and Chemstation Electron

Ionisation (EI) spectrum match analysis (described in detail in section 2.6). The comparisons of metabolomes showed the following results:

#### 4.2.1 *P. berghei* schizonts vs uninfected reticulocyte enriched erythrocytes

From a total number of ~5000 peaks collected from the two platforms, 482 putative metabolites (PM) were robustly identified (minimum confidence value was set to 5/10 for LC-MS data analysis by IDEOM and minimum ion-spectra match was set to 90% to Agilent Fiehn and NIST GC-MS Metabolomics libraries for GC-MS data analysis by Chemstation- see sections 2.6.5 and 2.6.6) in this comparison group, although many more probable metabolites were detected but were not readily assigned an identity. Of these, 218 (~45%) were up-regulated by 2 fold or more in schizonts, 181 (~38%) were unchanged with 83 (~17%) down-regulated by more than 2 fold or absent as compared to uninfected reticulocyte enriched erythrocytes (

Figure 4-1 and Table 3).

Of all the raw metabolomic peaks, including the unassigned ones, ~ 15% were also observed to be similarly up-regulated in schizonts and ~24% were found to be downregulated and the remaining were unchanged between schizonts and uninfected reticulocyte enriched erythrocytes (

Figure 9-2).

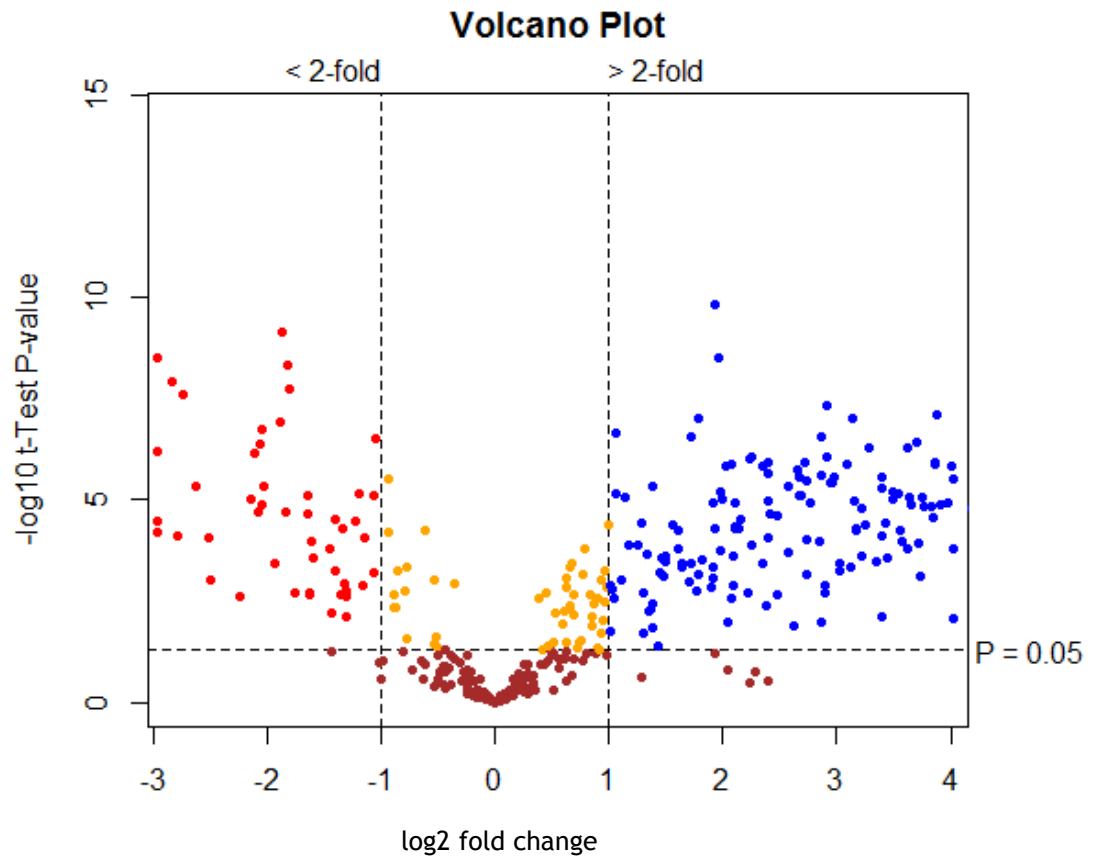


Figure 4-1 Volcano plot showing distribution of putative metabolites according to their fold change in abundance in *P. berghei* schizonts vs reticulocyte enriched erythrocytes. All significant changes are represented above the broken horizontal line. Coloured dots indicate metabolites which are: Blue- significantly up-regulated, Red- significantly down-regulated, Yellow- significant but little change, Brown- non-significant.

#### 4.2.2 *P. berghei* gametocytes vs uninfected reticulocyte enriched erythrocytes

From a total number of ~5000 peaks collected from the two platforms, 452 putative metabolites (PM) were robustly identified (identification parameters were set as above). Of these 190 (~42%) were found to be upregulated in gametocytes by 2 fold or more, 232 (~52%) were unchanged and 30 (~6%) were downregulated by more than 2 fold or absent as compared to uninfected reticulocytes (

Figure 4-2 and Table 4).

Of all the raw metabolomic peaks, including the unassigned ones, ~ 9% were also observed to be similarly up-regulated in gametocytes and ~18% were found to be downregulated and the remaining were unchanged between gametocytes and uninfected reticulocyte enriched erythrocytes (

Figure 9-3).

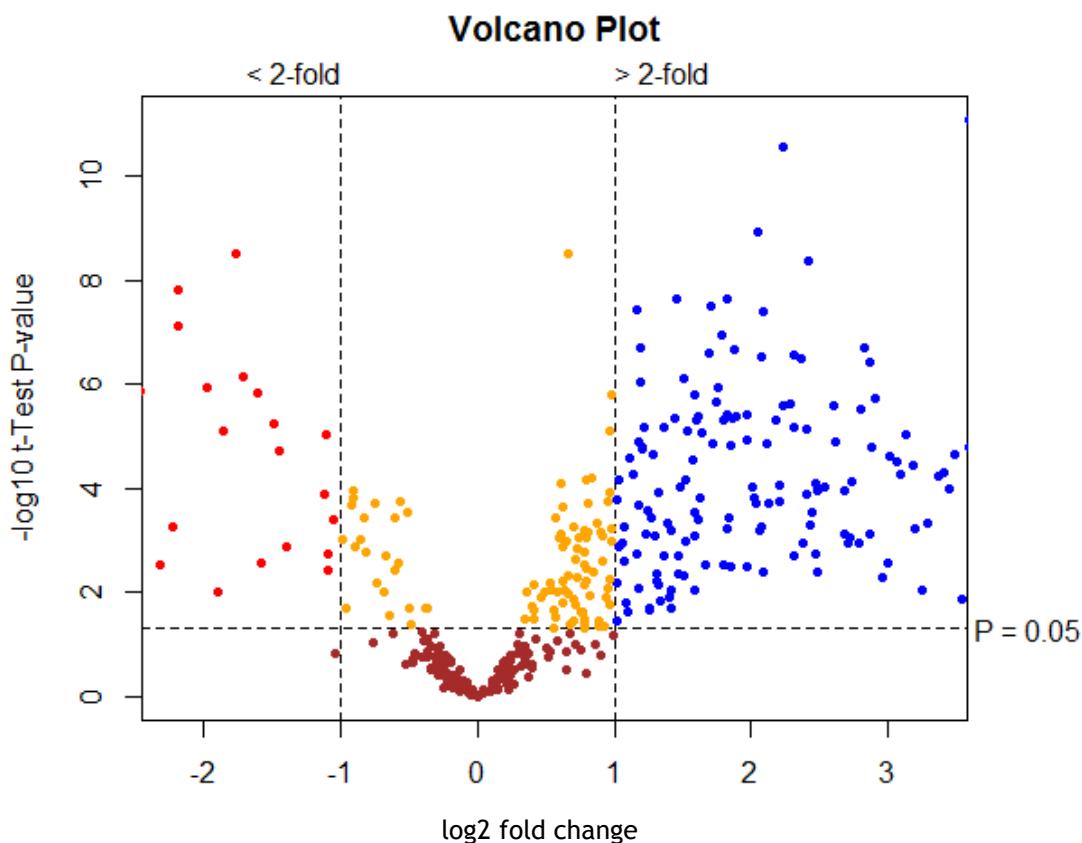


Figure 4-2 Volcano plot showing distribution of putative metabolites according to their fold change in abundance in *P. berghei* gametocytes vs uninfected reticulocyte enriched erythrocytes. All significant changes are represented above the broken horizontal line. Coloured dots indicate metabolites which are: Blue- significantly up-regulated, Red- significantly down-regulated, Yellow- significant but little change, Brown- non-significant.

#### 4.2.3 *P. berghei* gametocytes vs schizonts

From a total number of ~5000 peaks collected from the two platforms, 478 putative metabolites were identified (identification parameters were set as above) and compared and 116 (~24%) were found to be upregulated in gametocytes as compared to schizonts whereas 210 (~44%) were unchanged. 152 (~32%) putative metabolites were downregulated or absent in gametocytes as compared to schizonts (

Figure 4-3 and Table 5).

Of all the raw metabolomic peaks, including the unassigned ones, ~ 24% were also observed to be similarly up-regulated in gametocytes and ~17% were found to be downregulated and the remaining were unchanged between gametocytes and schizonts (

Figure 9-4).

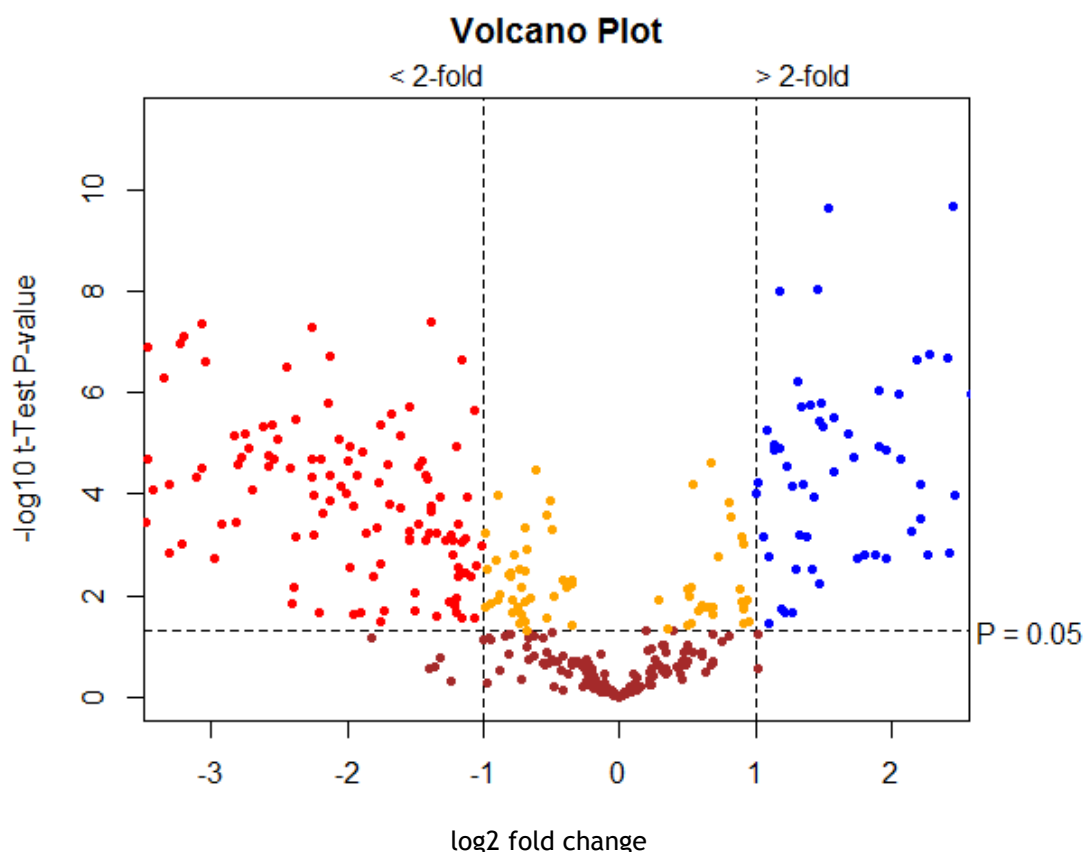


Figure 4-3 Volcano plot showing distribution of putative metabolites according to their fold change in abundance in Gametocytes vs Schizonts. All significant changes are represented above the broken horizontal line. Coloured dots indicate metabolites which are: Blue- significantly up-regulated, Red- significantly down-regulated, Yellow- significant but little change, Brown- non-significant.

### 4.3 Observations

The identified metabolites across these sample groups were then charted on to known metabolic pathways using metabolite search functions (which link a metabolite to the pathways it could potentially be a part of) on databases such as MPMP (Malaria Parasite Metabolic Pathways- accessible at <http://mpmp.huji.ac.il/>) (Ginsburg 2006), Pathos (A metabolomics tool from Glasgow Polyomics- accessible at <http://motif.gla.ac.uk/Pathos/>) (Leader, Burgess et al. 2011), KEGG (Kyoto Encyclopedia of Genes and Genomes, accessible at <http://www.genome.jp/kegg/>) (Kanehisa, Goto et al. 2006) and MetaCyc (accessible at <http://metacyc.org/>) (Caspi, Altman et al. 2014). This comprehensive comparison between the host and the parasite (at different life stages- sections 4.2.1 and 4.2.2) and within the parasite metabolome (at different life stages- section 4.2.3) revealed interesting insights into the

metabolism of the host cell and the parasite, some examples of which are given below.

It was found that in *P. berghei* parasites, metabolites of the TCA cycle were up regulated in gametocytes when compared to asexual schizonts (Table 5). As previously published RNA expression data has shown that the enzymes of the TCA cycle are up-regulated in gametocytes (Young, Fivelman et al. 2005), this was not surprising. The role of TCA cycle in central carbon metabolism was further elucidated in detail using targeted metabolomics and isotopically labelled  $^{13}\text{C}$  U-Glucose and  $^{13}\text{C}^{15}\text{N}$  U-Glutamine, the results of which are discussed in section 5.

Also, the discovery of elevated levels of phosphorylated creatine (phosphocreatine) in reticulocytes and gametocytes when compared to schizonts was extremely intriguing (Table 3, Table 4 and Table 5). Phosphocreatine serves as a rapidly mobilizable reserve of high-energy phosphates in higher organisms through a phosphagen system (Wallimann, Wyss et al. 1992) and this discovery indicated that gametocytes may store and employ the host phosphagen system to release energy at a later stage. The details of this study are discussed in section 6.

Another interesting observation was that the first two metabolites of Coenzyme-A synthesis were differentially abundant in *P. berghei* gametocyte and schizont stages (Table 5). The levels of non-phosphorylated pantothenate were up-regulated in gametocytes when compared to schizonts by about 13 fold and the levels of 4'-phospho-pantothenate were found to be up regulated in schizonts by about 8 fold when compared to gametocytes. The possibility that Coenzyme A synthesis is silent in unactivated gametocytes in the mammalian host and starts later in the mosquito stage is being queried at the moment (see section 8.1).

The data also showed elevated levels of acyl-carnitines in reticulocytes and gametocytes, compared to schizonts (Table 3, Table 4 and Table 5). As there are no annotated enzymes for  $\beta$ -oxidation of fatty acids in *Plasmodium* (Gardner, Hall et al. 2002), this suggested that gametocytes possibly store metabolites for fatty acid synthesis in the developing oocysts where new membranes are required for sporogony as the FASII pathway is dispensable for all stages of development except the liver stage and there is limited availability of fatty acids in the mosquito haemocoel compared to blood stage schizogony in a

mammalian host. This was not followed up further due to time constraints but has been considered for future work (see section 8.2).

## 5 Central Carbon metabolism in *Plasmodium*

### 5.1 Introduction

It has been widely accepted that the main energy generating pathway in *Plasmodium* parasites is glycolysis (Homewood 1977). By leading a parasitic life inside a host which has a practically unlimited supply of glucose, the intracellular parasite inside the mammalian host was thought to rely exclusively on glycolysis (Figure 5-1) for ATP generation. All enzymes involved in glycolysis are expressed during intraerythrocytic blood stage development in *Plasmodium* (Bozdech, Llinas et al. 2003).

Furthermore, the TCA cycle (Figure 5-2) which operates in the mitochondria and uses glycolytic end products generated in the cytoplasm has recently been explored into some detail in *Plasmodium* (Macrae, Dixon et al. 2013) where using metabolomics, it was shown that in asexual stages the classical link between glycolysis and the TCA cycle via glycolytic pyruvate was present although with a low flux in contrast to the gametocyte stage where the TCA cycle was found to be more active and essential for gametocyte maturation.

The role of anaplerosis (reactions involving intermediates of major metabolic pathways like glycolysis and TCA cycle) via the CO<sub>2</sub> fixing enzyme *pepc* has recently been dissected in detail in *P. falciparum* along with confirmation of operation of a canonical full TCA cycle (Storm, Sethia et al. 2014).

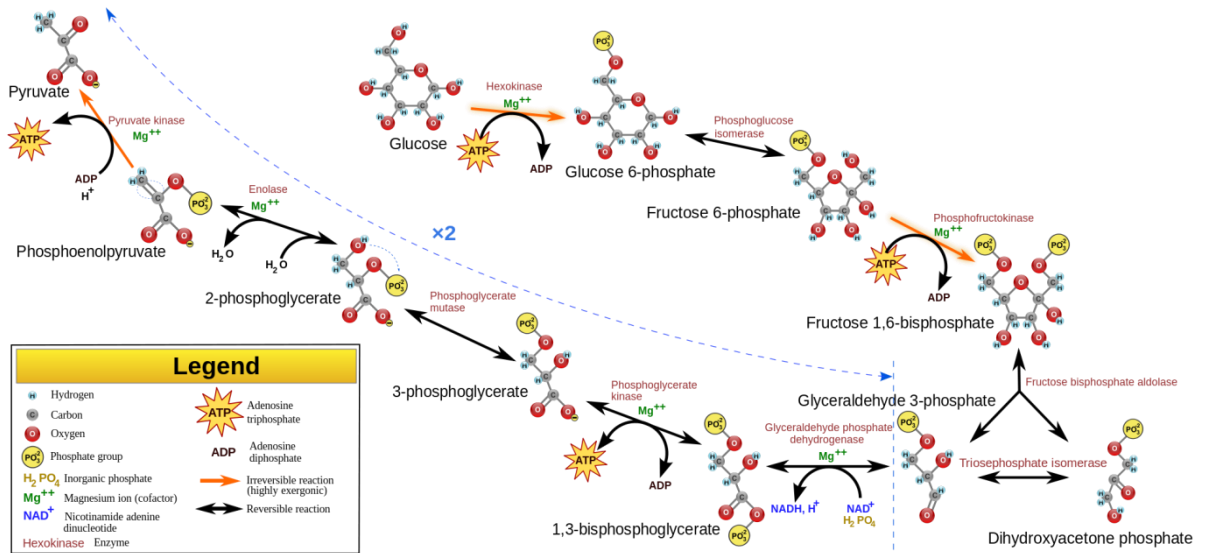


Figure 5-1 Schematic representation of Glycolysis (accessed from <http://en.wikipedia.org/wiki/File:Glycolysis2.svg>)

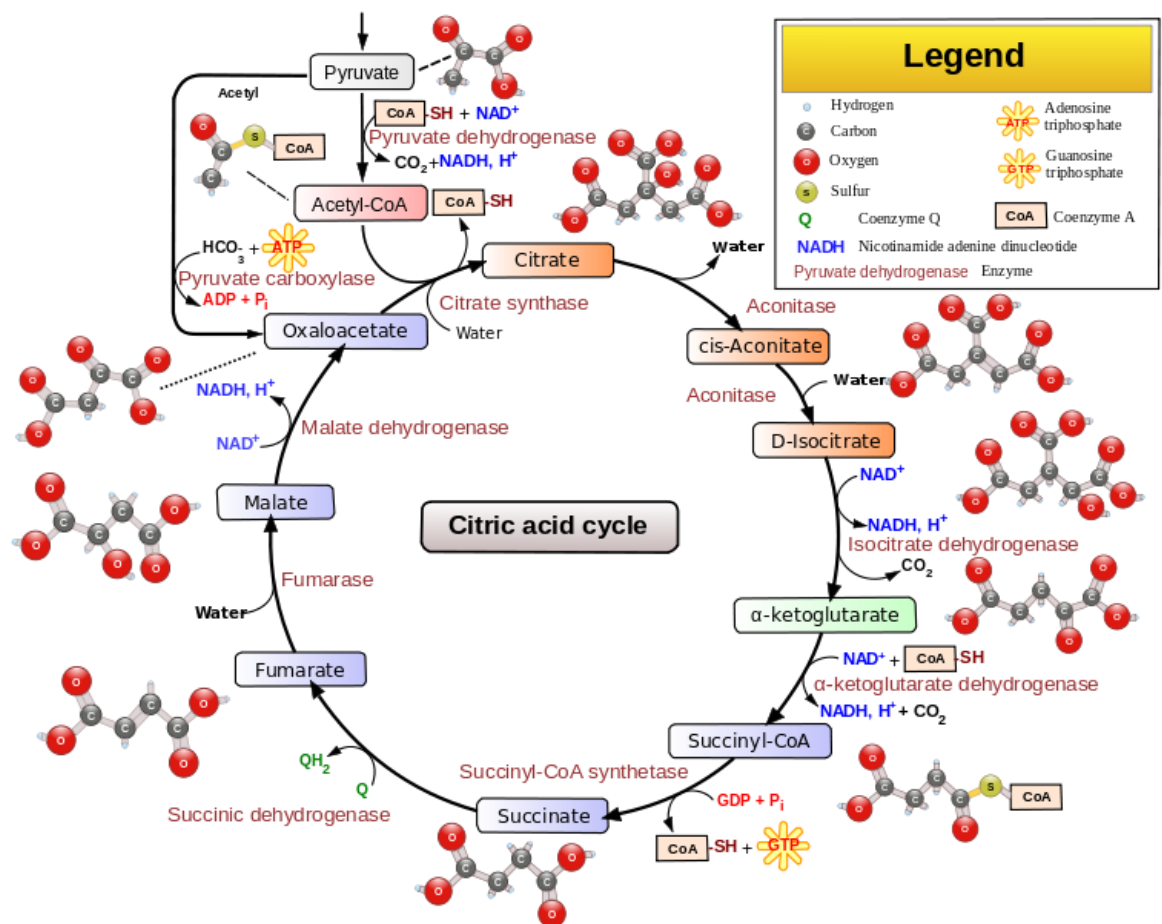


Figure 5-2 Schematic representation of TCA cycle (accessed from [http://en.wikipedia.org/wiki/File:Citric\\_acid\\_cycle\\_with\\_aconitate\\_2.svg](http://en.wikipedia.org/wiki/File:Citric_acid_cycle_with_aconitate_2.svg))

The asexual blood stages of *Plasmodium* have been shown to have a minimally cristate mitochondrion (Das, Syin et al. 1997) as compared to other apicomplexan parasites like *Toxoplasma gondii* (Sinai, Webster et al. 1997) and other free living microorganisms, indicating they might be metabolically inactive. However, mitochondrion retention has been associated with essentiality for survival, possibly as a site for the electron transport chain (ETC) which is necessary for transport of metabolites, re-oxidation of inner membrane dehydrogenases as well as pyrimidine biosynthesis (Krungskrai 1995).

Minimal oxygen consumption and CO<sub>2</sub> production and conversion of most of the consumed glucose to lactic acid by fermentation have been attributed to the fulfilment of energy needs of asexual stage parasites (Olszewski and Llinas 2011). However, the effectively unlimited supply of glucose present in the mammalian host is not available to the parasite in the mosquito vector, and as the parasite prepares itself for sexual reproduction in the mosquito mid-gut, there is predicted to be a switch from glycolysis to TCA cycle for energy production.

This theory has been recently supported by a study which showed that disrupting an enzyme involved in the TCA cycle and the electron transport chain led to decreased production of ookinetes and failure to form oocysts in mosquito stages of *P. berghei* (Hino, Hirai et al. 2012). There is evidence suggesting this process starts in mammalian host itself where gametocytes develop more complex tubular mitochondrial cristae required for mitochondrial function (Krungskrai 2004). RNA expression data also suggests that enzymes implicated in the TCA cycle are up-regulated in gametocytes (Young, Fivelman et al. 2005) and a proteomics study also found these enzymes to be present in gametocytes (Khan, Franke-Fayard et al. 2005) in keeping with the metabolomics studies (Macrae, Dixon et al. 2013).

Even though the mitochondrion is present in both male and female gametocytes, it is inherited only maternally (Creasey, Mendis et al. 1994, Okamoto, Spurck et al. 2009). Until recently, the role of the TCA cycle had not been studied in great detail in mosquito stages, but became of enhanced interest in light of a study (Olszewski, Mather et al. 2010), which proposed that the canonical TCA cycle does not exist in *P. falciparum* blood stages but rather takes a branched architecture and the 'reductive branch' produces acetyl co-A moieties whose

function and localisation remained unclear. However this paper was later retracted (Olszewski, Mather et al. 2013).

It is worth noting that a mitochondrial pyruvate dehydrogenase (PDH) is absent in *Plasmodium* (Oppenheim, Creek et al. 2014), yet glycolytic carbon skeletons enter the TCA cycle. This has been shown to occur via a mitochondrion-located, branched chain  $\alpha$ -keto acid dehydrogenase (BCKDH) complex that can catalyse pyruvate (glycolytic end product) to acetyl-CoA (TCA cycle intermediate entry point) conversion in *P. falciparum* and *P. berghei* (Macrae, Dixon et al. 2013, Oppenheim, Creek et al. 2014)

The complete role of the TCA cycle in *P. berghei* asexual and sexual stages is unresolved and the anticipated switch from glycolysis to the TCA cycle in mosquito stages is intriguing. In this study, the role of glycolysis and the TCA cycle in asexual stages, gametocytes and mosquito stages was investigated using targeted metabolomics.

## 5.2 Results

The central carbon metabolism of *P. berghei* asexual, gametocytes and ookinete stages was studied by performing metabolic labelling with  $^{13}\text{C}$  U-Glucose or  $^{13}\text{C}^{15}\text{N}$  U-Glutamine in cultures used to grow *P. berghei* parasites followed by analysis of isotopic enrichment in glycolysis and TCA cycle intermediates using GC-MS (see section 2.7 for details).

To understand isotopomer analysis it is important to understand the flow of carbon skeletons through the glycolytic and TCA cycle pathways which is described in Figure 5-3. The absolute abundance presented for each data set reflects the total concentration of metabolites in nmoles detected in the sample volume of 1 $\mu\text{l}$  injected in the GC-MS and is equivalent of extract from  $2.5 \times 10^6$  cells.

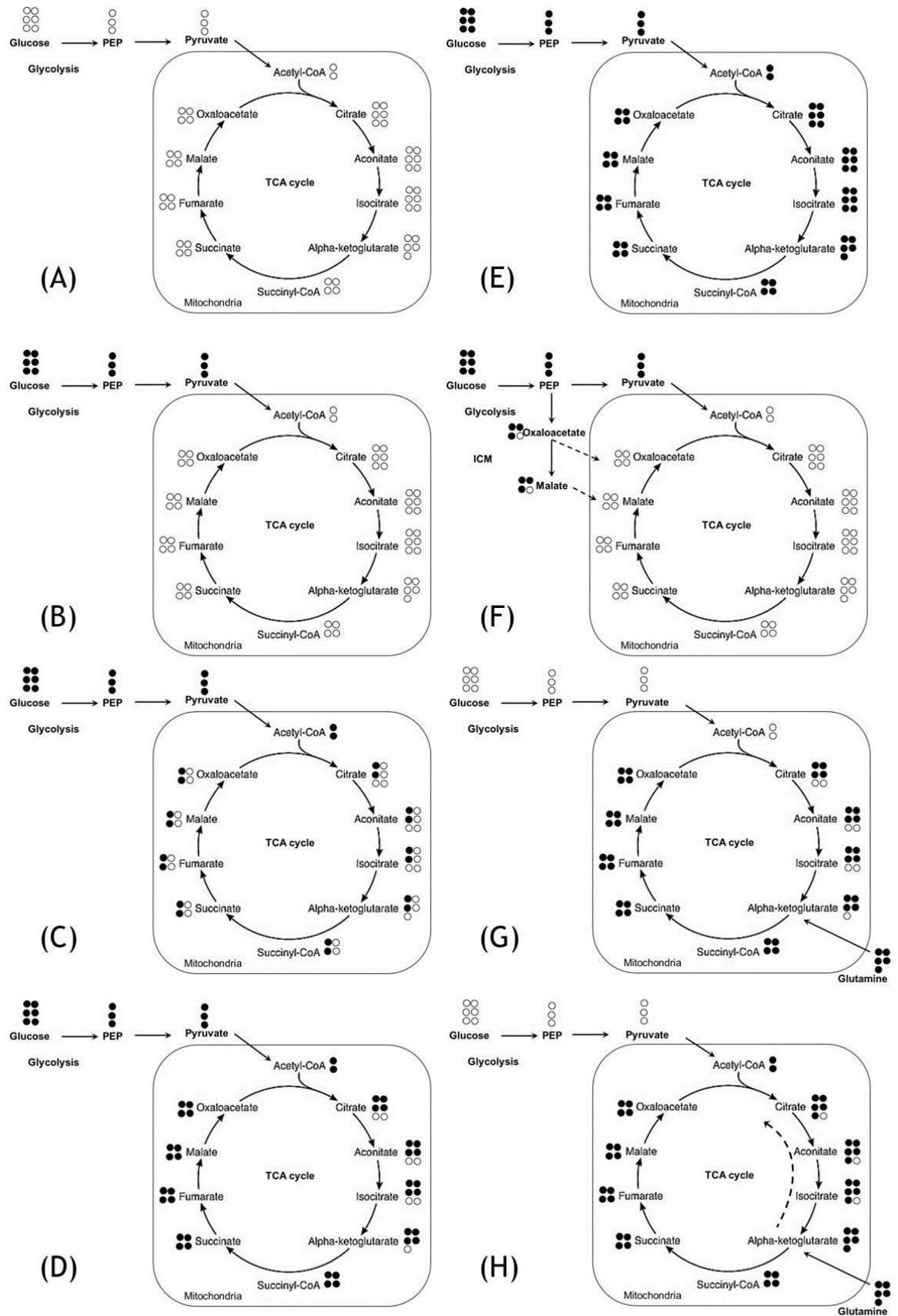


Figure 5-3 Schematic representation of the flow of carbon skeletons through the glycolytic and TCA cycle pathways. Open circles indicate unlabelled carbon atoms and closed circles indicate isotopically labelled carbon atoms.

While using  $^{13}\text{C}$  U-Glucose, provided the classical glycolysis to TCA cycle pathways operate in the canonical manner, starting from a completely labelled

6-C glucose molecule, all glycolytic intermediates should show a +6 or a +3 C labelling (Figure 5-3A and Figure 5-3B). All TCA cycle metabolites should then show a +2, +4 or +6 labelling (Figure 5-3C, Figure 5-3 D and Figure 5-3E). The expected abundance of +2 to +6 labelling will be in decreasing order as the carbon skeletons have to go round the TCA cycle three times to achieve maximal (+6) labelling. Anaplerotic reactions undergoing intermediary carbon metabolism in the cytosol should also give rise to +3 labelled intermediates (Figure 5-3F). While using  $^{13}\text{C}^{15}\text{N}$  U-Glutamine in cultures, as glutamine interconverts with the TCA cycle intermediate alpha-ketoglutarate, glycolytic metabolites should show no labelling and if the canonical TCA cycle is operative, TCA intermediates should show +4 labelling (Figure 5-3G). In case of a reductive carboxylation of alpha-ketoglutarate, it is also possible to see a +5 labelling of TCA cycle intermediates (Figure 5-3H).

A summary of the results is depicted in Figure 5-4.

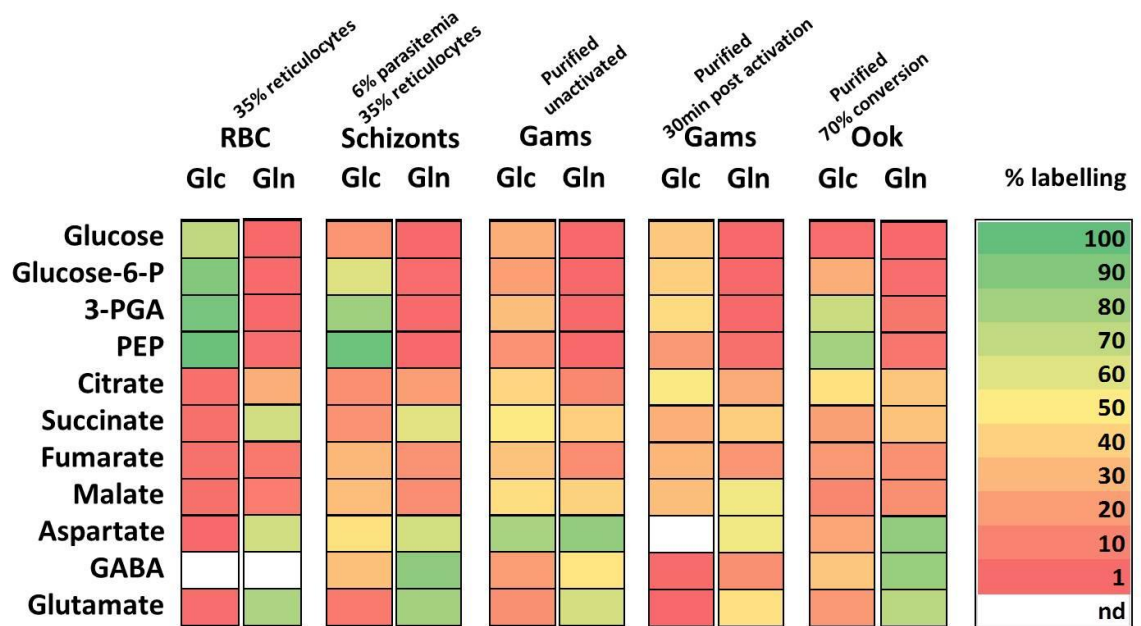


Figure 5-4 Heat map showing enrichment (% labelling containing one or more  $^{13}\text{C}$  carbons) after correction for natural abundance ( $n=3$ ). (Glc- $^{13}\text{C}$  U-Glucose, Gln- $^{13}\text{C}^{15}\text{N}$  U-Glutamine, RBC- uninfected reticulocyte enriched erythrocytes, Schizonts- 24h mature asexual schizonts, Gams-Purified Gametocytes, Ook- 21h mature ookinetes, nd-not detected)

### 5.2.1 Asexual blood stages

Uninfected RBCs and synchronised *P. berghei* gametocyte non-producer line (820m9w21dm1cl1) (Sinha, Hughes et al. 2014) ring stage infected RBCs (both enriched with ~35% reticulocytes prior to infection) were metabolically labelled with  $^{13}\text{C}$  U-Glucose or  $^{13}\text{C}^{15}\text{N}$  U-Glutamine for 24 hours in culture and cells were harvested at 0, 6, 12, 18 and 24 h time points for rapidly quenching metabolism, metabolite extraction and quantification of  $^{13}\text{C}$  enrichment by GC-MS (see section 2.7.2)

#### 5.2.1.1 $^{13}\text{C}$ U-Glucose labelling

In uninfected reticulocyte enriched erythrocytes (UIR) and *P. berghei* infected reticulocyte enriched erythrocytes (PBIR), it was found that  $^{13}\text{C}$  U-Glucose labelled glycolytic intermediates such as Glucose 6-phosphate (Glucose-6-P), 3-Phosphoglycerate (PGA) and Phosphoenolpyruvate (PEP) to a high level, almost ~70% or more. PEP was labelled almost 100% in both UIR and PBIR (Figure 5-5B, C and D). This suggested that there is active glycolysis in both UIR and PBIR as expected. However, the absolute abundance of glycolytic intermediates in UIR was higher than in PBIR and especially the glycolytic end product PEP was found to be almost double in UIR than in PBIR (Figure 5-5E). This indicated that in PBIR, glycolytic products are turned over rapidly by the parasite into downstream metabolites possibly into TCA cycle or intermediary carbon metabolism (ICM) or for biomass synthesis to support rapid proliferation and shizogony (Salcedo-Sora, Caamano-Gutierrez et al. 2014). Also, labelled glucose was consumed in PBIR more rapidly than in UIR as percentage labelling was only about 17% as compared to 70% in UIR (Figure 5-5A). As gluconeogenesis has not been reported in *Plasmodium* spp. to date, possibly due to the absence of a homologue of the enzyme fructose-1-6-biphosphatase, the presence of unlabelled glucose in these cultures could be due to gluconeogenesis in the host cell (reticulocytes) which seems to replenish the used up labelled glucose in infected cultures as there is no significant difference in absolute abundance of glucose in UIR and PBIR cultures at the 24 hour time point.

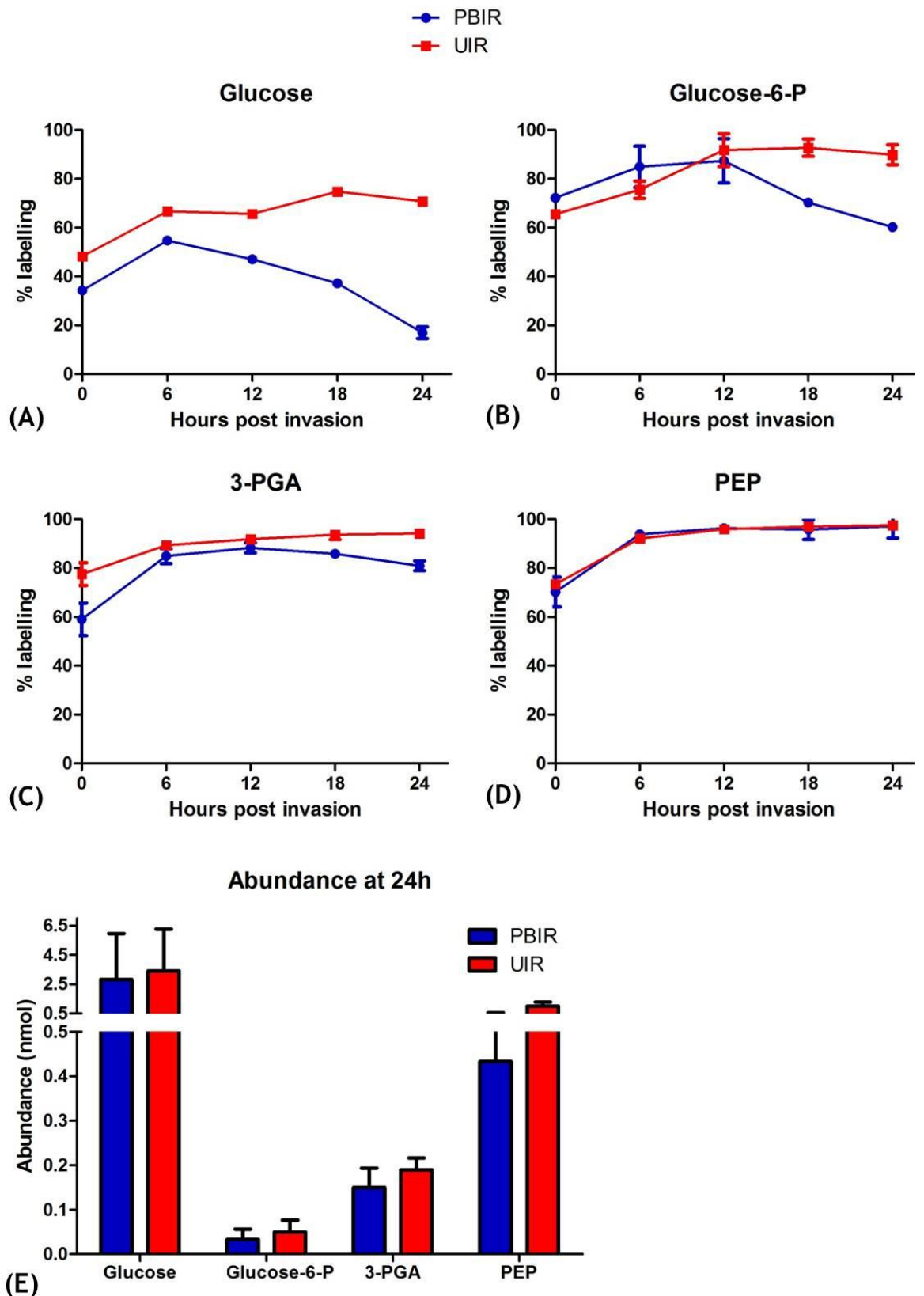
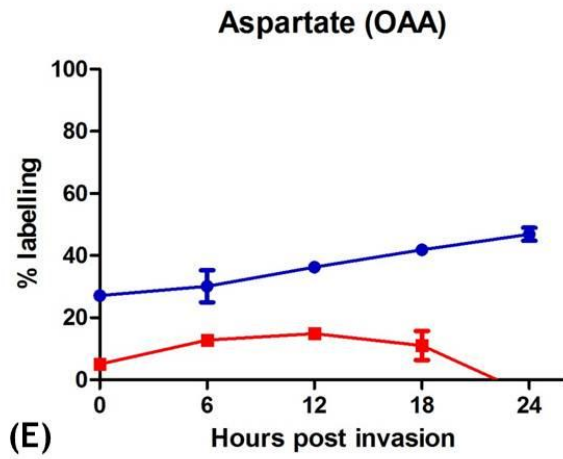
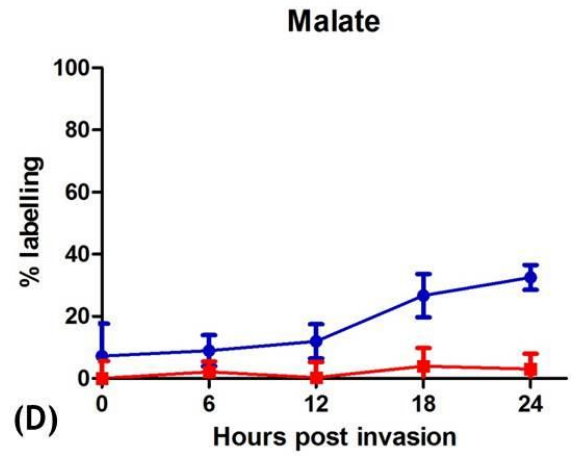
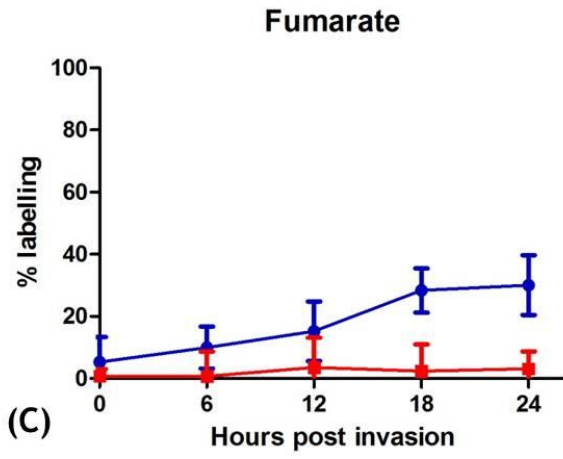
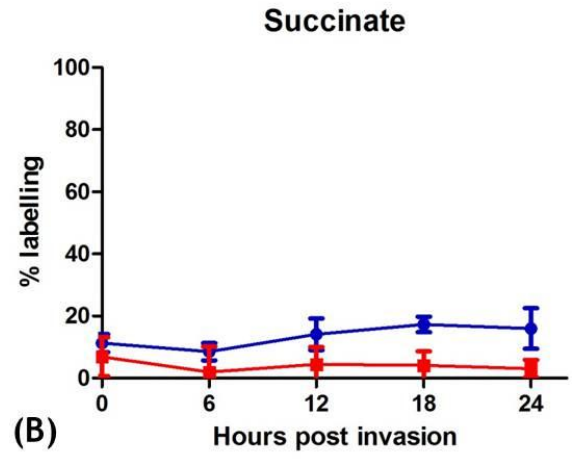
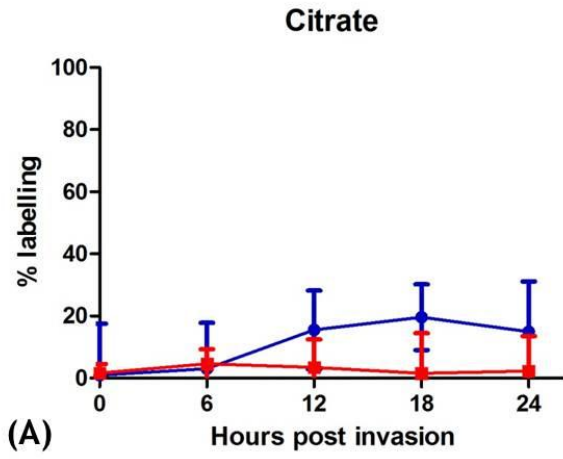


Figure 5-5 <sup>13</sup>C U-Glucose labelling of glycolytic intermediates in *P. berghei* asexual stages. Glycolytic intermediates were observed over the 24 hour asexual cycle (time points: 0, 6, 12, 18, 24h) of *P. berghei* infected reticulocyte enriched erythrocytes (PBIR) and similarly incubated uninfected reticulocyte enriched erythrocytes (UIR). Panels A, B, C and D show percentage labelling of Glucose, Glucose 6-phosphate (Glucose-6-P), 3-Phosphoglycerate (3-

PGA) and Phosphoenolpyruvate (PEP) respectively on the y-axis and time points on the x-axis. Panel E shows absolute abundance of these metabolites at 24h time point in nmol in  $2.5 \times 10^6$  cells in PBIR and UIR. Error bars indicate SD of n=3 biological replicates.

Looking at the TCA cycle metabolites, it was found that  $^{13}\text{C}$  U-Glucose labelled most TCA cycle intermediates actively as citrate, succinate, fumarate, malate and aspartate (proxy representative of oxaloacetate-OAA as they interconvert and OAA is not detected in GC-MS) were observed to be labelled in PBIR (Figure 5-6). This suggested that pyruvate from glycolysis does enter mitochondria in the absence of a mitochondrial pyruvate dehydrogenase, possibly through the BCKDH complex as shown by recent studies (Macrae, Dixon et al. 2013, Oppenheim, Creek et al. 2014). Although TCA intermediates were detected in UIR, their labelling and abundance with  $^{13}\text{C}$  U-Glucose was found to be much lower than PBIR.

● PBIR  
■ UIR



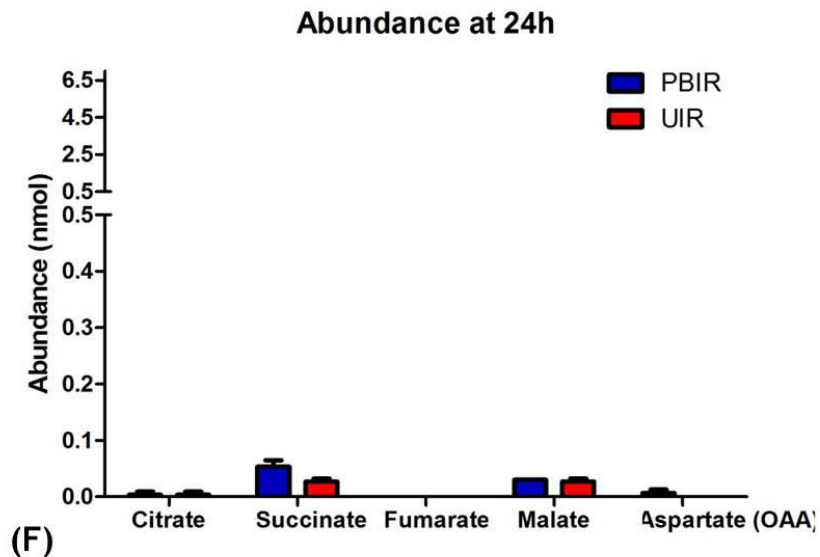


Figure 5-6  $^{13}\text{C}$  U-Glucose labelling of TCA cycle intermediates in *P. berghei* asexual stages. TCA cycle intermediates were observed over the 24 hour asexual cycle (time points: 0, 6, 12, 18, 24h) of *P. berghei* infected reticulocyte enriched erythrocytes (PBIR) and similarly incubated uninfected reticulocyte enriched erythrocytes (UIR). Panels A, B, C, D and E show percentage labelling of Citrate, Succinate, Fumarate, Malate and Aspartate (Oxalo-acetate) respectively on the y-axis and time points on the x-axis. Panel F shows absolute abundance of these metabolites at 24h time point in nmol in  $2.5 \times 10^6$  cells in PBIR and UIR. Error bars indicate SD of  $n=3$  biological replicates.

Isotopomer analysis of the TCA cycle metabolites at the 24 hour time point showed that the main isotopomers of citrate in  $^{13}\text{C}$  U-Glucose fed PBIR contained +2 and +4 labelled carbons indicating the presence of a canonical TCA cycle (Figure 5-7) where pyruvate feeds into the cycle via acetyl-coA as stated above. The absence of +6 labelled carbon atoms could be due to the accumulation of unlabelled glucose possibly from gluconeogenesis in the host reticulocytes and uninfected reticulocytes present in the cultures. Isotopomers containing +3 labelled carbons were also detected for fumarate, malate and aspartate (Figure 5-7C, D and E) suggesting the presence of intermediary carbon metabolism (Figure 3-6) and activity of *P. berghei* phosphoenolpyruvate carboxylase (*pepc*) which catalyses the carboxylation of  $^{13}\text{C}_3$ -PEP to  $^{13}\text{C}_3$ -oxaloacetate (Figure 5-3F). However the fraction labelling of these intermediates was found not to be very high - which could be due to the entry of other unlabelled carbon sources into the TCA cycle (possibly via the glutamine pathway - see section 5.2.1.2).

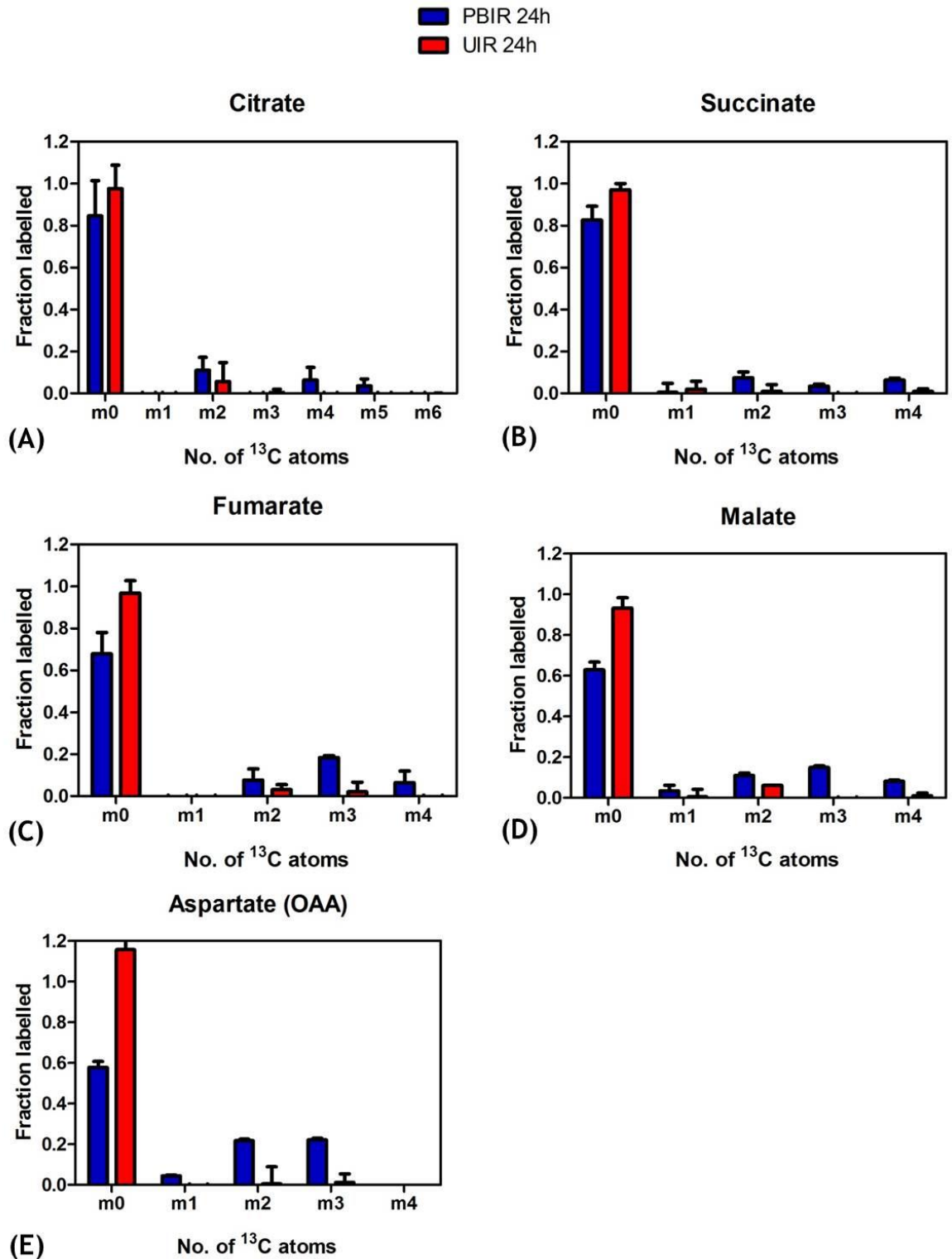


Figure 5-7 Fraction labelling of TCA cycle isotopomers at the 24h time point in *P. berghei* infected reticulocyte enriched erythrocytes (PBIR)- schizont stage and similarly incubated uninfected reticulocyte enriched erythrocytes (UIR) cultured in the presence of  $^{13}\text{C}$  U-Glucose. 'm (n)' on the x-axis indicates the number of  $^{13}\text{C}$  atoms in each metabolite. Panels A, B, C, D and E show fraction labelling of Citrate, Succinate, Fumarate, Malate and Aspartate (Oxalo-acetate) respectively on the y-axis. Error bars indicate SD of n=3 biological replicates.

#### 5.2.1.2 $^{13}\text{C}^{15}\text{N}$ U-Glutamine labelling

As expected,  $^{13}\text{C}^{15}\text{N}$  U-Glutamine did not label any glycolytic intermediates (Figure 5-8) as it enters TCA cycle directly via the intermediate alpha-ketoglutarate which feeds it into the TCA cycle (Olszewski, Mather et al. 2010, MacRae, Sheiner et al. 2012, Macrae, Dixon et al. 2013). The absolute abundance of glycolytic intermediates reflects their presence due to unlabelled glucose (Figure 5-8E).

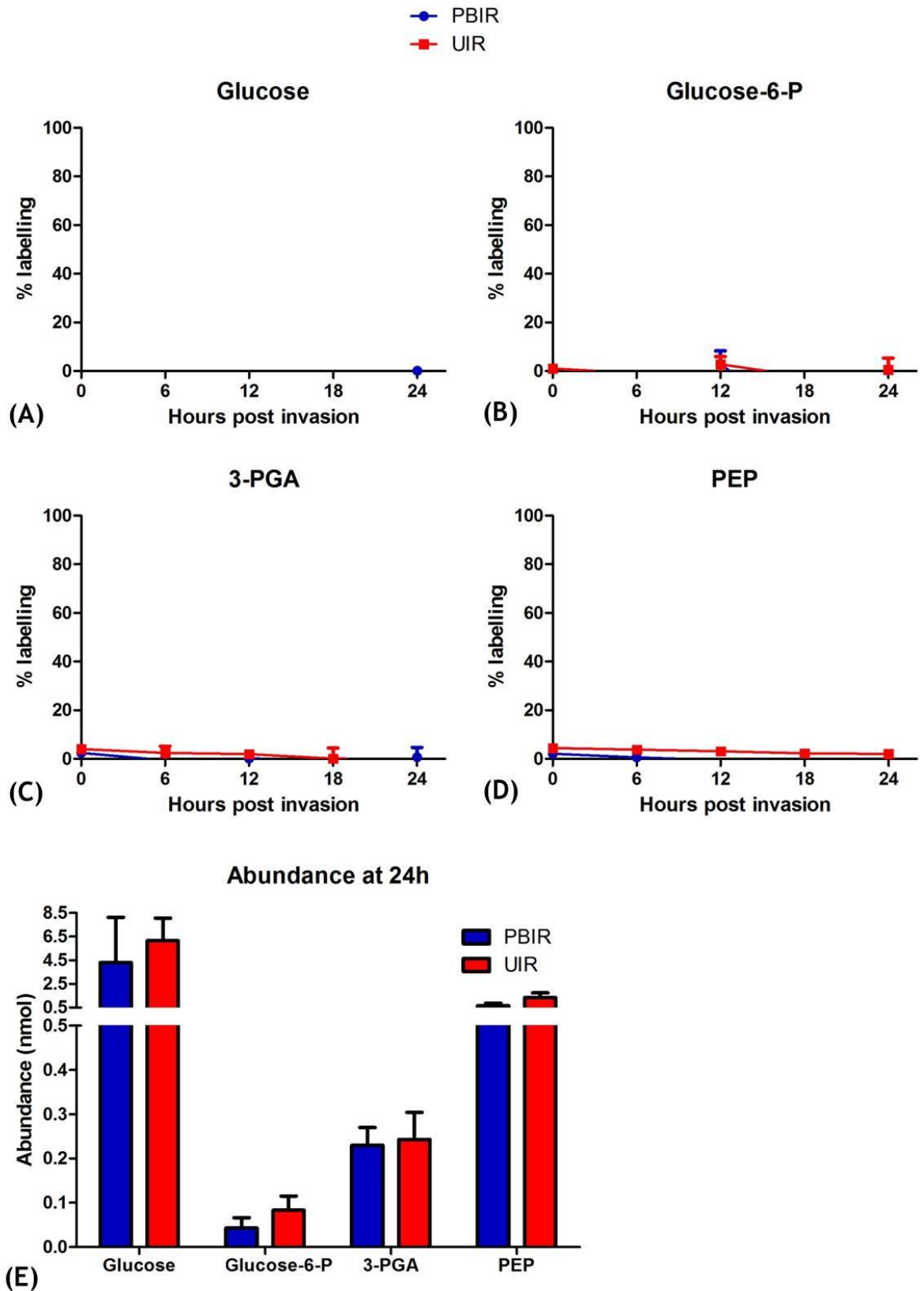


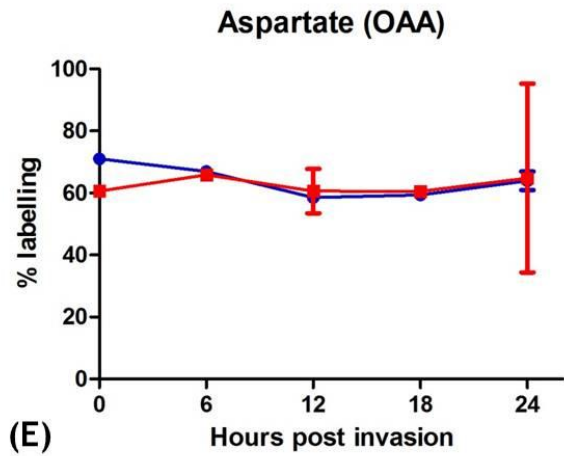
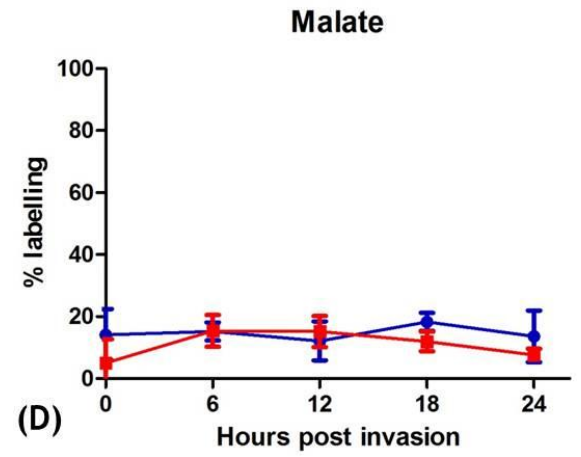
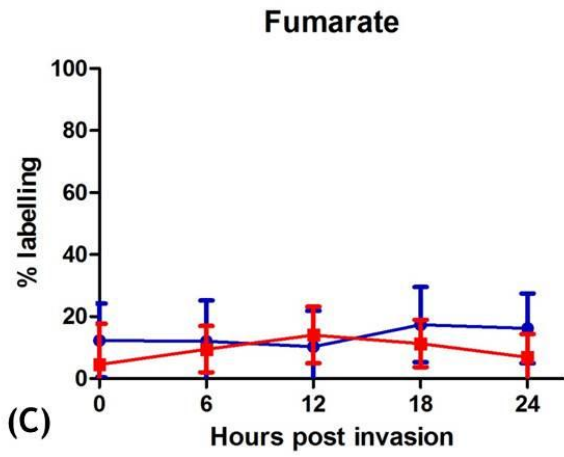
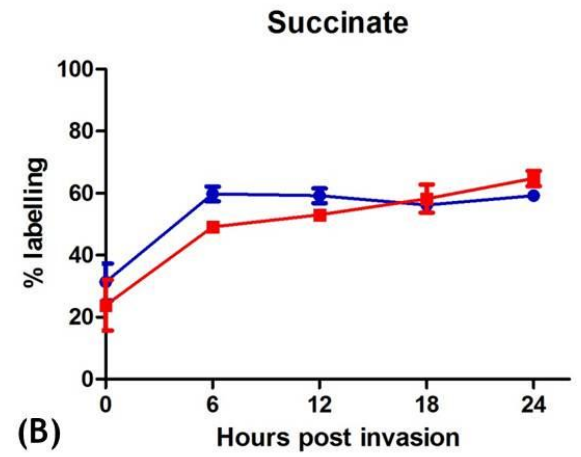
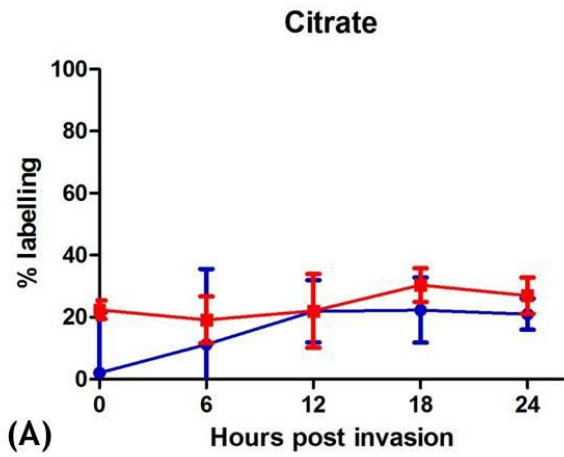
Figure 5-8  $^{13}\text{C}^{15}\text{N}$  U-Glutamine labelling of glycolytic intermediates in *P. berghei* asexual stages. Glycolytic intermediates were observed over the 24 hour asexual cycle (time points: 0, 6, 12, 18, 24h) of *P. berghei* infected reticulocyte enriched erythrocytes (PBIR) and similarly incubated uninfected reticulocyte enriched erythrocytes (UIR). Panels A, B, C and D show percentage labelling of Glucose, Glucose 6-phosphate (Glucose-6-P), 3-

Phosphoglycerate (3-PGA) and Phosphoenolpyruvate (PEP) respectively on the y-axis and time points on the x-axis. Panel E shows absolute abundance of these metabolites at 24h time point in nmol in  $2.5 \times 10^6$  cells in PBIR and UIR. Error bars indicate SD of n=3 biological replicates.

With  $^{13}\text{C}^{15}\text{N}$  U-Glutamine labelling, operation of a TCA cycle in *P. berghei* asexual stages was again confirmed as all TCA intermediates, citrate, succinate, fumarate, malate and aspartate (OAA) were found to be labelled (Figure 5-9). Labelling was also seen in UIR (which contained ~35% reticulocytes) and it was observed to be higher than what was seen with  $^{13}\text{C}$  U-Glucose (Figure 5-6). This is different from what has been shown for human normocytes which remain unlabelled in the presence of  $^{13}\text{C}^{15}\text{N}$  U-Glutamine (Macrae, Dixon et al. 2013). This was not surprising as mitochondria in UIR were found to be present (section 3.2.2) indicating that in reticulocytes, TCA metabolism might be operational but maximum flux comes from glutamine as the carbon source instead of glucose derived acetyl-coA.

Additionally, it was notable that in *P. berghei* asexual stages labelled with  $^{13}\text{C}^{15}\text{N}$  U-Glutamine, the labelling was found to be higher in succinate, aspartate (OAA), and to some extent, citrate compared to  $^{13}\text{C}$  U-Glucose labelling. This most probably was due to the presence of large cytoplasmic pools (as compared to mitochondrial) of unlabelled fumarate and malate coming from intermediary carbon metabolism (Figure 3-6) as the unlabelled glucose can also enter the cytoplasmic pools of malate and fumarate through the conversion of PEP to oxaloacetate via the cytoplasmic *pepc*, with succinate, oxaloacetate, and citrate being restricted to the mitochondrion (Figure 5-3F). This observation fitted well when looking at the  $^{13}\text{C}$  U-Glucose labelling data (Figure 5-6), where this difference was not seen and also explained the observed higher labelling in aspartate (OAA) compared to the other TCA intermediates.

● PBIR  
■ UIR



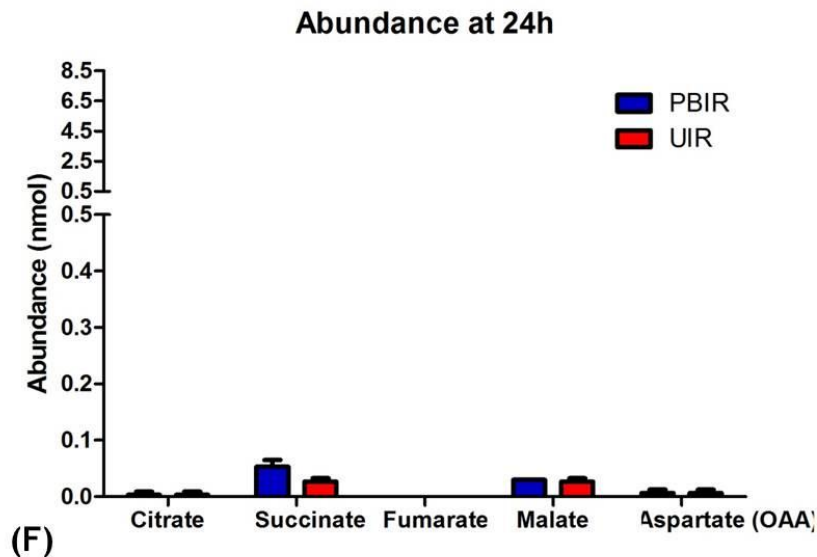


Figure 5-9  $^{13}\text{C}^{15}\text{N}$  U-Glutamine labelling of TCA cycle intermediates in *P. berghei* asexual stages. TCA cycle intermediates were observed over the 24 hour asexual cycle (time points: 0, 6, 12, 18, 24h) of *P. berghei* infected reticulocyte enriched erythrocytes (PBIR) and similarly incubated uninfected reticulocyte enriched erythrocytes (UIR). Panels A, B, C, D and E show percentage labelling of Citrate, Succinate, Fumarate, Malate and Aspartate (Oxalo-acetate) respectively on the y-axis and time points on the x-axis. Panel F shows absolute abundance of these metabolites at 24h time point in nmol in  $2.5 \times 10^6$  cells in PBIR and UIR. Error bars indicate SD of  $n=3$  biological replicates.

Isotopomer analysis of  $^{13}\text{C}^{15}\text{N}$  U-Glutamine labelled asexual *P. berghei* at 24 hours showed that all TCA cycle metabolites had the expected +2 and +4 labelling but not +6 labelling possibly due to the presence of unlabelled glucose feeding in to TCA cycle via the BCKDH complex and the extra cycle required for achieving maximal labelling. Surprisingly, citrate also showed +5 carbon labelling (Figure 5-10A). The observed +1 labelling in aspartate was due to the presence of an additional labelled  $^{15}\text{N}$  atom in  $^{13}\text{C}^{15}\text{N}$  U-Glutamine.

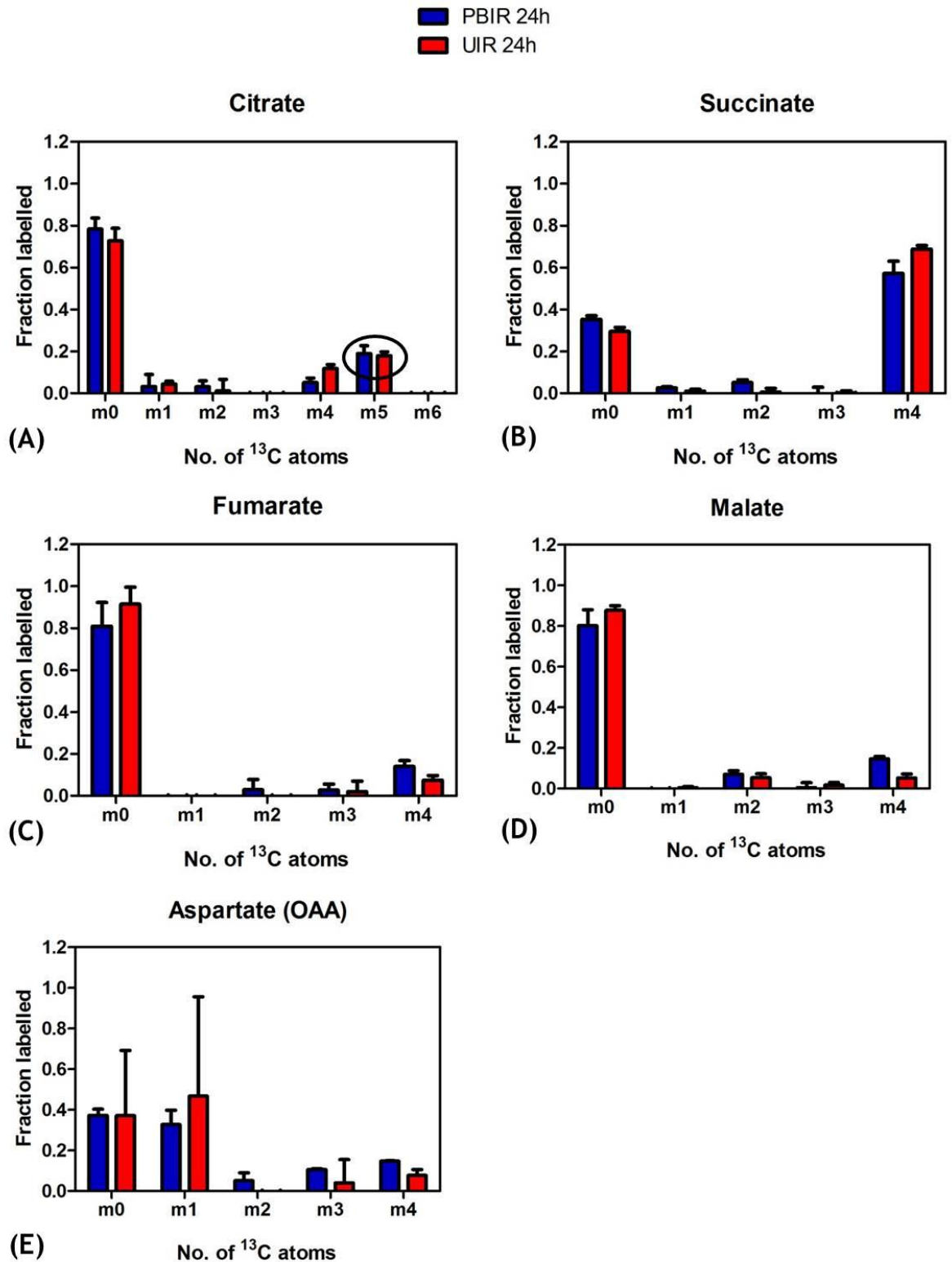


Figure 5-10 Fraction labelling of TCA cycle isotopomers at the 24h time point in *P. berghei* infected reticulocyte enriched erythrocytes (PBIR)- schizont stage and similarly incubated uninfected reticulocyte enriched erythrocytes (UIR) cultured in the presence of  $^{13}\text{C}^{15}\text{N}$  U-Glutamine. 'm (n)' on the x-axis indicates the number of  $^{13}\text{C}$  atoms in each metabolite (Additional  $^{15}\text{N}$  atom in the case of aspartate). Panels A, B, C, D and E show fraction labelling of Citrate (black circle emphasises +5 label), Succinate, Fumarate, Malate and Aspartate (Oxalo-acetate) respectively on the y-axis. Error bars indicate SD of n=3 biological replicates.

In the retracted (Olszewski, Mather et al. 2013) paper which hypothesised the presence of a branched architecture of TCA cycle in *Plasmodium* parasites (Olszewski, Mather et al. 2010), the main argument was based on a similar observation where they detected the presence of +5 labelled citrate from  $^{13}\text{C}^{15}\text{N}$  U-Glutamine fed cultures and assumed it to be coming from a ‘reductive arm’ of the TCA cycle of the parasite which supposedly takes alpha-ketoglutarate (interconverted from glutamine) into two different branches.

When looking at the isotopomer analysis of UIR incubated with  $^{13}\text{C}^{15}\text{N}$  U-Glutamine for 24 hours (Figure 5-10), it was discovered that the +5 citrate labelling was also present in UIR (Figure 5-10A), which constituted of ~35% reticulocytes containing apparently rudimentary mitochondria (Gronowicz, Swift et al. 1984). This probably means that there is indeed a ‘reductive arm’ of the TCA cycle present in reticulocytes which may explain the observation made by (Olszewski, Mather et al. 2010) as they used freshly obtained blood for culturing *P. falciparum* parasites which could have contained at least 1.5-2% reticulocytes. Reductive carboxylation like this has been observed before in cancer cells which have defective mitochondria (Mullen, Wheaton et al. 2012) or are under hypoxia (Metallo, Gameiro et al. 2012) and glutamine has specifically been shown to facilitate this reductive metabolism leading to production of lipogenic AcCoA (Fan, Kamphorst et al. 2013, Fendt, Bell et al. 2013).

### 5.2.2 Gametocytes

Magnetically purified *P. berghei* gametocytes (from gametocyte producer parent line 820em1dcl2TBB) were activated at 21°C in activation media (mimicking mosquito midgut conditions) where they were metabolically labelled with  $^{13}\text{C}$  U-Glucose or  $^{13}\text{C}^{15}\text{N}$  U-Glutamine in culture and cells were harvested at 1, 10, 20 and 30 min time points for rapidly quenching metabolism, metabolite extraction and quantification of  $^{13}\text{C}$  enrichment by GC-MS. The unactivated gametocytes were incubated for 2 hours with the labelled carbon sources to allow for equilibration of metabolism in the presence of labelled glucose or glutamine and then harvested as for other time points (see section 2.7.3). This was done as it was not possible to inject labelled carbon sources in mice and we wanted to analyse carbon metabolism in unactivated gametocytes as well. For the purpose of the time course analysis during activation, unactivated gametocytes were considered to be time point 0.

### 5.2.2.1 $^{13}\text{C}$ U-Glucose labelling

Using  $^{13}\text{C}$  U-Glucose, metabolic labelling of glycolytic intermediates was observed during the gametocyte activation process, however, the absolute levels of glycolytic intermediates were almost half of what was observed for the asexual stages (Figure 5-11) and the labelling of the glycolytic end product phosphoenolpyruvate (PEP) was not very strong compared to PBIR (section 5.2.1.1) suggesting that glycolytic flux was low in the observed samples. Not surprisingly, incubation of mature gametocytes with labelled glucose did not result in high labelling at any time point also suggesting that glucose consumption is not as upregulated in mature gametocytes as the growing asexual stages.

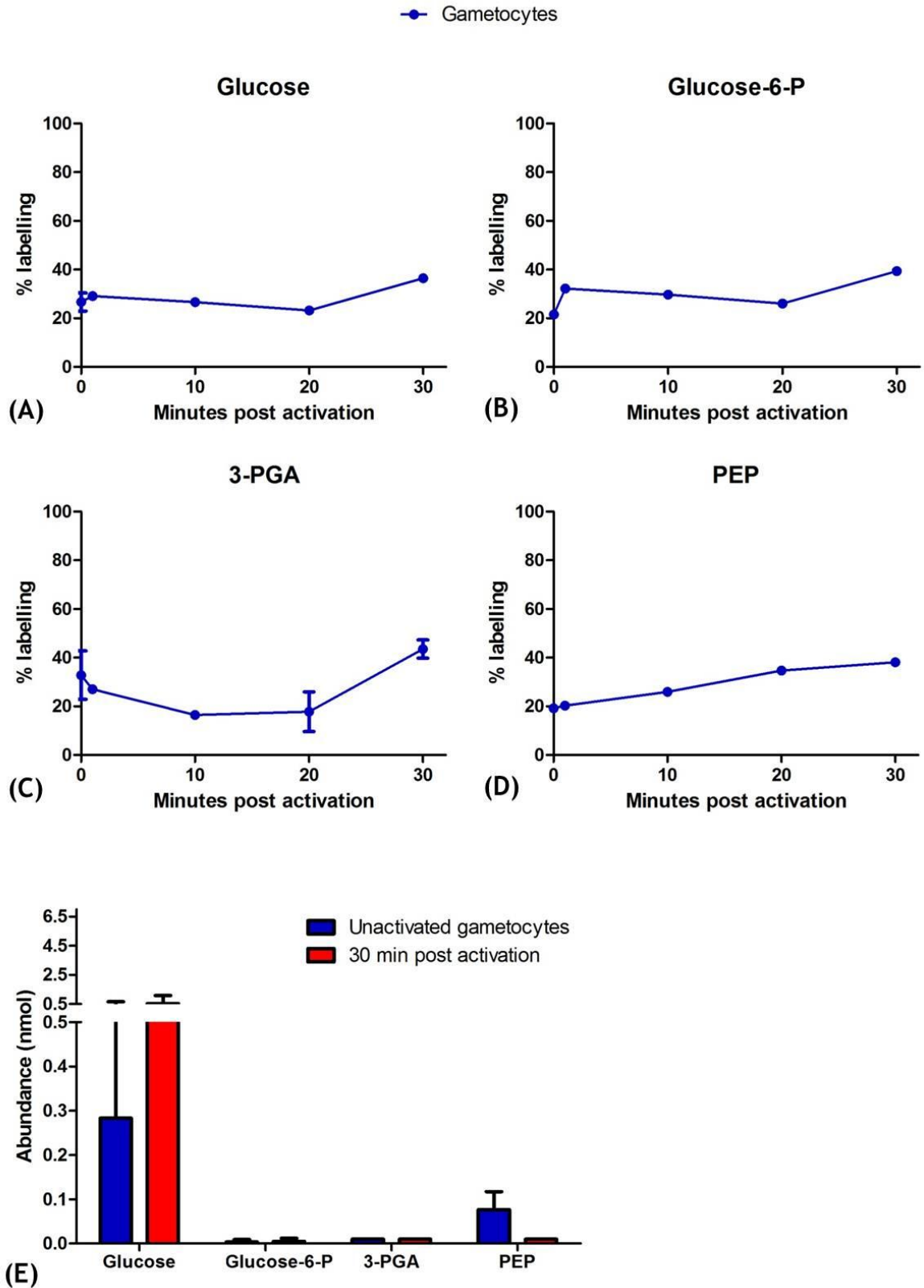
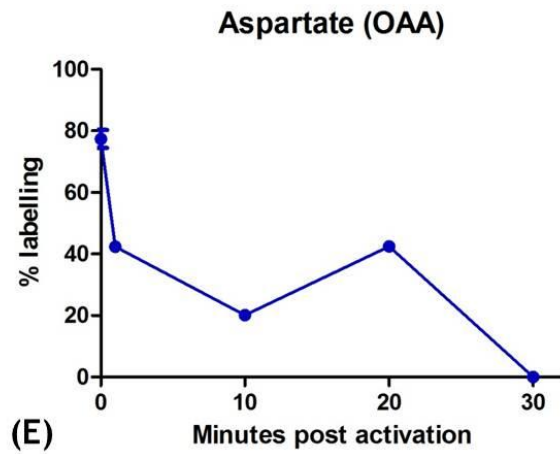
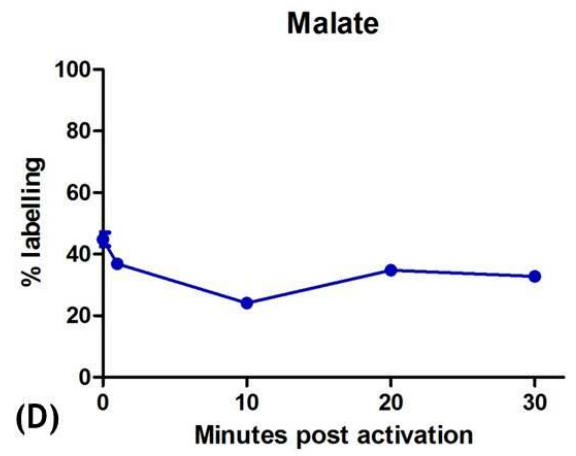
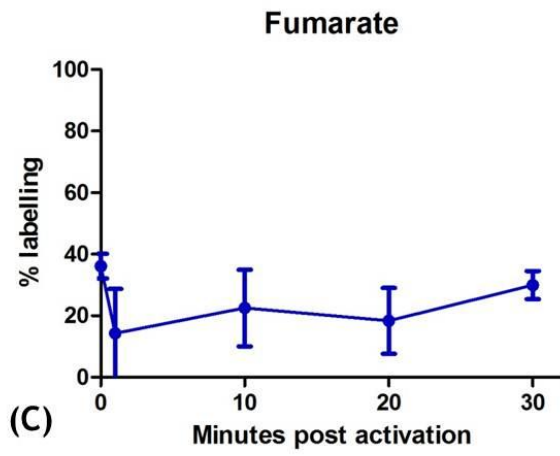
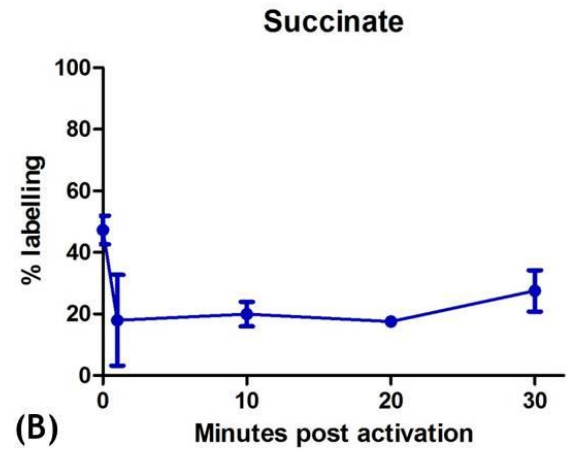
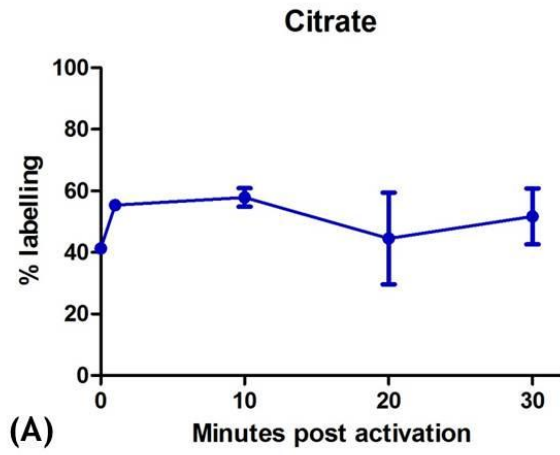


Figure 5-11  $^{13}\text{C}$  U-Glucose labelling of glycolytic intermediates in purified *P. berghei* gametocytes during activation. Glycolytic intermediates were observed over the 30min activation process (time points: 0, 1, 10, 20, 30 min). Panels A, B, C and D show percentage labelling of Glucose, Glucose 6-phosphate (Glucose-6-P), 3-Phosphoglycerate (3-PGA) and Phosphoenolpyruvate (PEP) respectively on the y-axis and time points on the x-axis. Panel E

shows absolute abundance of these metabolites in unactivated gametocytes and 30 minutes post activation in nmol in  $2.5 \times 10^6$  cells. Error bars indicate SD of n=3 biological replicates.

The TCA cycle intermediates during gametocyte activation in presence of  $^{13}\text{C}$  U-Glucose also showed labelling indicating the presence of a canonical TCA cycle and entry of glycolytic pyruvate into TCA cycle at this stage (Figure 5-12) as observed for the asexual stage. This was most probably facilitated through the BCKDH complex as shown in recent studies (Macrae, Dixon et al. 2013, Oppenheim, Creek et al. 2014). However the absolute abundance of the TCA cycle intermediates was very low as compared to that observed in the asexual stages.

● Gametocytes



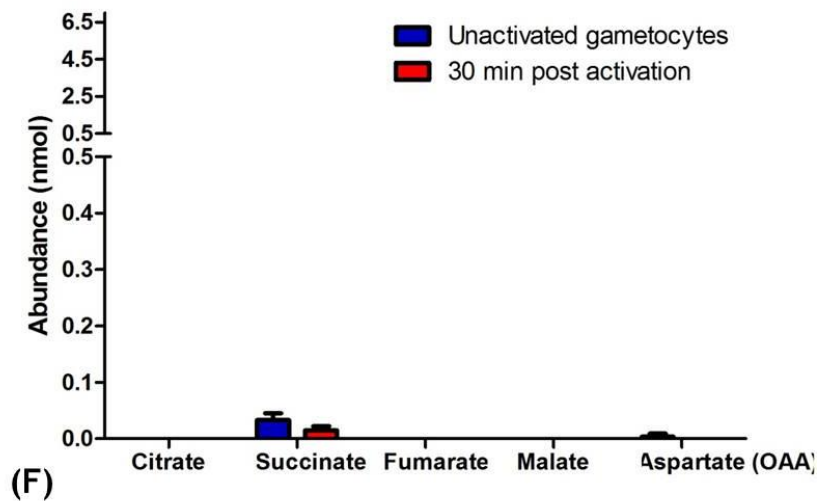


Figure 5-12  $^{13}\text{C}$  U-Glucose labelling of TCA cycle intermediates in *P. berghei* gametocytes during activation. TCA cycle intermediates were observed over the 30min activation process (time points: 0, 1,10,20,30 min). Panels A, B, C, D and E show percentage labelling of Citrate, Succinate, Fumarate, Malate and Aspartate (Oxalo-acetate) respectively on the y-axis and time points on the x-axis. Panel F shows absolute abundance of these metabolites in unactivated gametocytes and 30 minutes post activation in nmol in  $2.5 \times 10^6$  cells. Error bars indicate SD of  $n=3$  biological replicates.

Isotopomer analysis of gametocytes through the activation process showed that the main isotopomers were +2, +4 and +6 in case of citrate and +2 and +4 in case of other TCA intermediates indicating the presence of a canonical TCA cycle (Figure 5-13). Isotopomers containing +3 labelled carbons especially for fumarate and aspartate were also observed again indicating the presence of inter-conversions with the *pepc* mediated intermediary carbon metabolism (ICM) as observed for the asexual stages. Labelled aspartate disappears after 20 minutes and could be totally converted to malate and/or fumarate after this time by ICM as both of these metabolites have the +3 isotopomer as the main labelled ions at 30 minutes post activation.

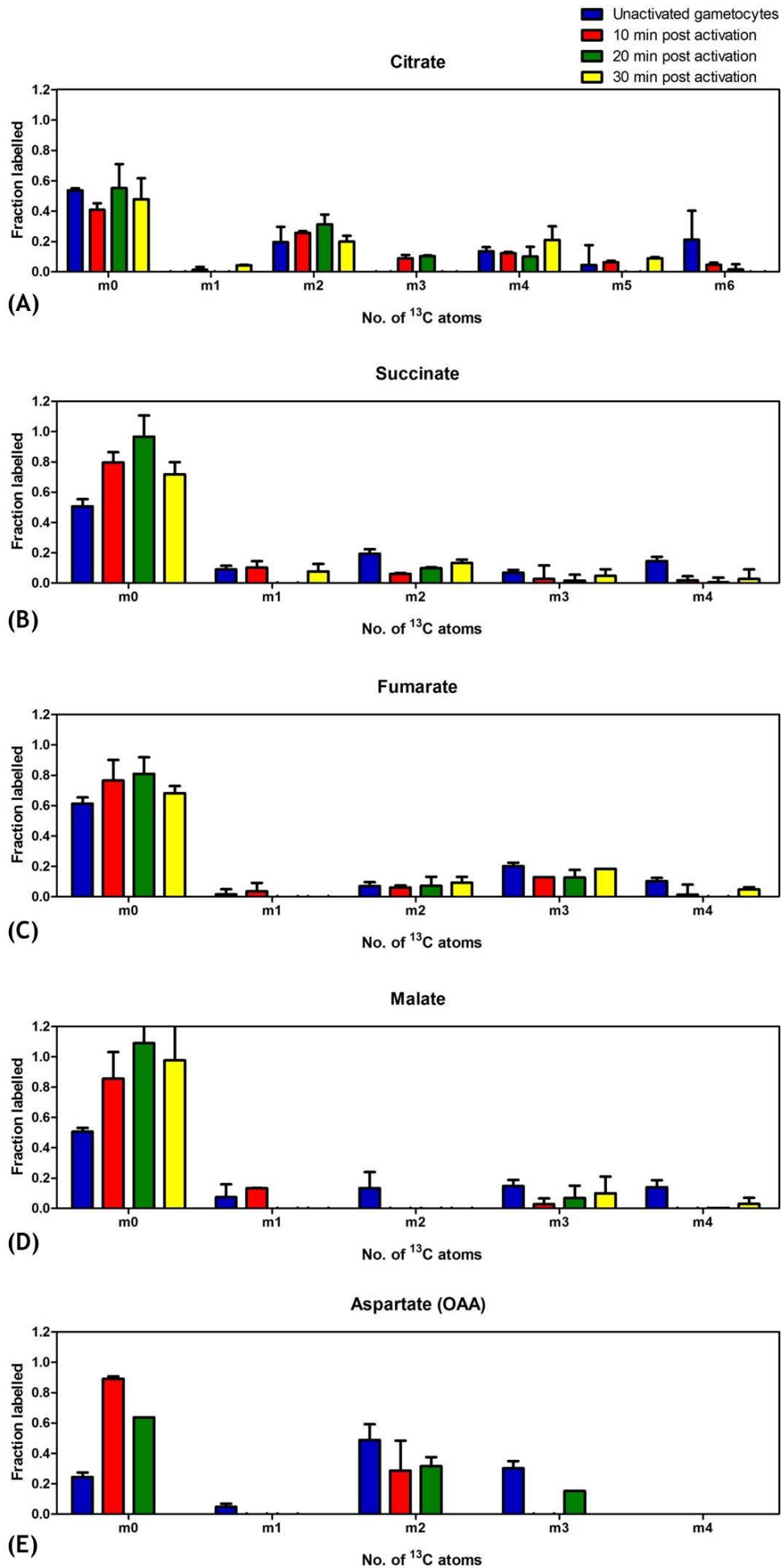


Figure 5-13 Fraction labelling of TCA cycle isotopomers in *P. berghei* gametocytes during activation in the presence of  $^{13}\text{C}$  U-Glucose. TCA cycle intermediates were observed over the 30min activation process (time points: 0, 1,10,20,30 min). 'm (n)' on the x-axis indicates the number of  $^{13}\text{C}$  atoms in each metabolite. Panels A, B, C, D and E show fraction labelling of Citrate, Succinate, Fumarate, Malate and Aspartate (Oxalo-acetate) respectively on the y-axis. Error bars indicate SD of n=3 biological replicates.

#### 5.2.2.2 $^{13}\text{C}^{15}\text{N}$ U-Glutamine labelling

Again, as expected,  $^{13}\text{C}^{15}\text{N}$  U-Glutamine did not label any glycolytic intermediates (Figure 5-14) during gametocyte activation just as was observed in asexual stages.

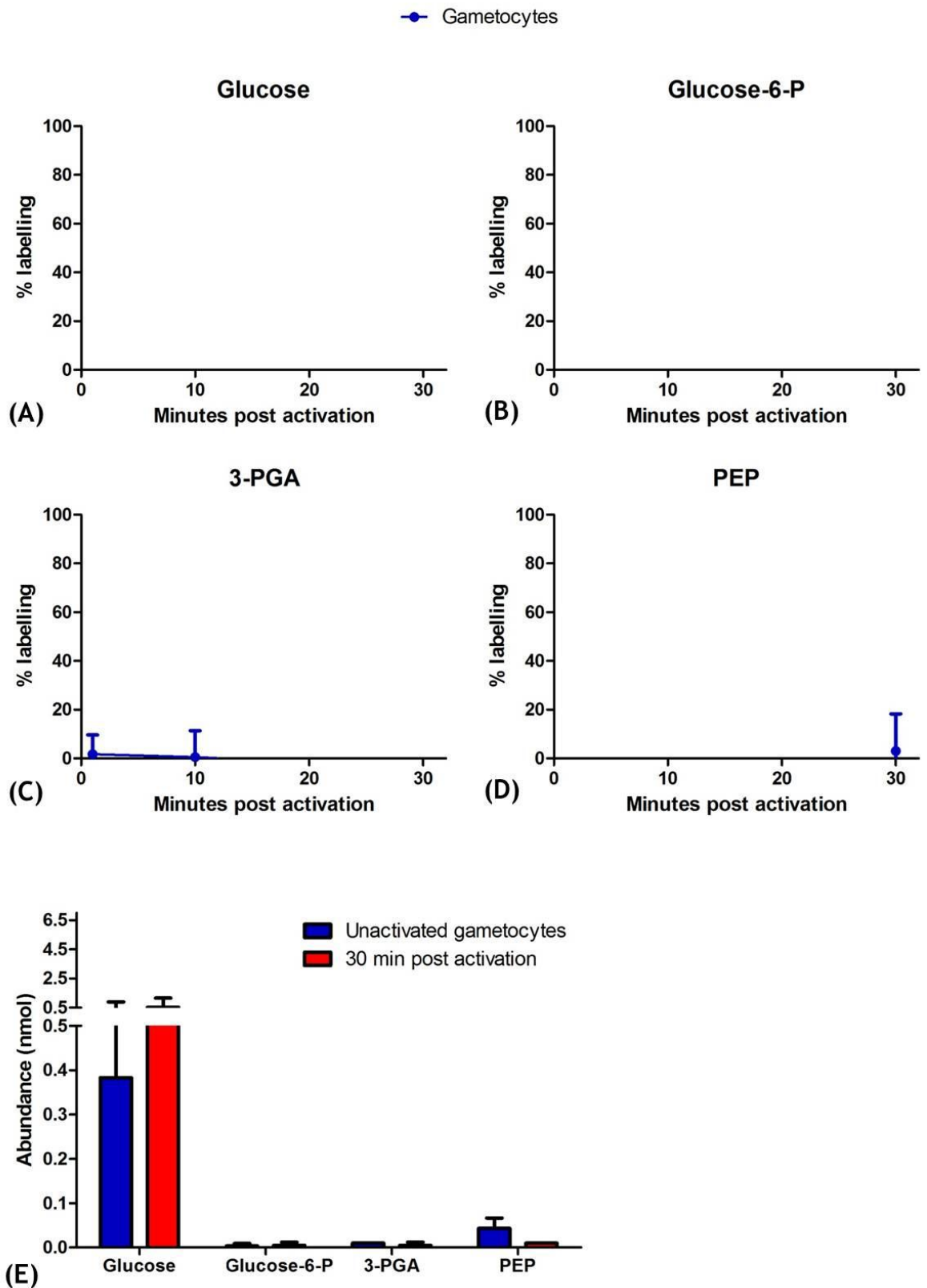
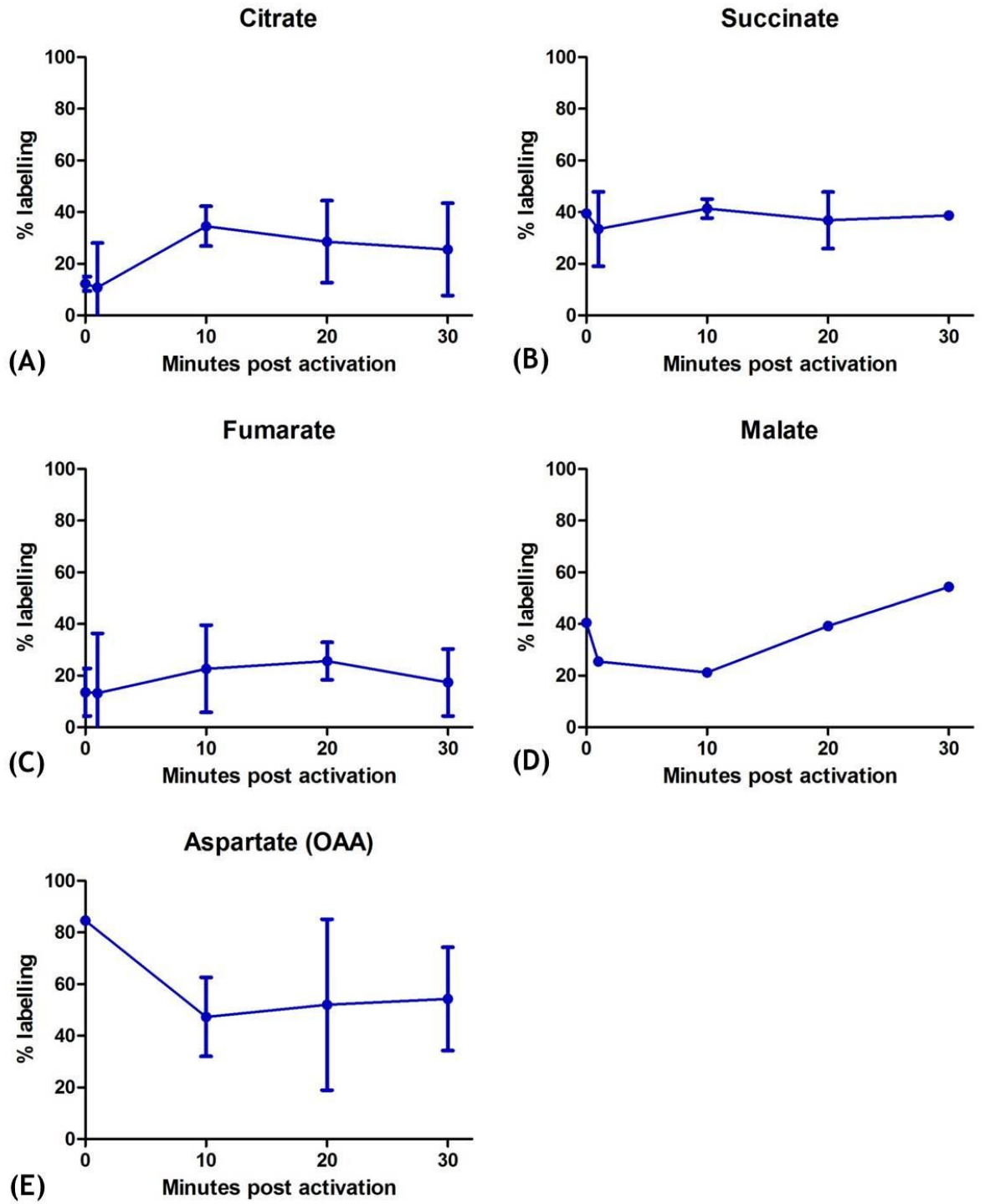


Figure 5-14  $^{13}\text{C}^{15}\text{N}$  U-Glutamine labelling of glycolytic intermediates in *P. berghei* gametocytes during activation. Glycolytic intermediates were observed over the 30min activation process (time points: 0, 1,10,20,30 min). Panels A, B, C and D show percentage labelling of Glucose, Glucose 6-phosphate (Glucose-6-P), 3-Phosphoglycerate (3-PGA) and Phosphoenolpyruvate (PEP) respectively on the y-axis and time points on the x-axis. Panel E

shows absolute abundance of these metabolites in unactivated gametocytes and 30 minutes post activation in nmol in  $2.5 \times 10^6$  cells. Error bars indicate SD of  $n=3$  biological replicates.

With  $^{13}\text{C}^{15}\text{N}$  U-Glutamine labelling, all TCA intermediates, citrate, succinate, fumarate, malate and aspartate (OAA) were found to be labelled (Figure 5-15) in activating gametocytes pointing towards the existence of a canonical TCA cycle with glutamine as a carbon source. However, the difference between succinate, aspartate (OAA), and citrate labelling on the one hand and malate and fumarate labelling on the other hand that was observed in asexual stages (where succinate, oxaloacetate, and citrate appeared to be restricted to the mitochondrion) was not seen in gametocytes. This suggested that ICM is present but is probably downregulated compared to asexual stages as unlabelled cytoplasmic pools of malate and fumarate (products of cytoplasmic glucose derived ICM) could not dilute the  $^{13}\text{C}^{15}\text{N}$  U-Glutamine derived mitochondrial produced malate and fumarate. However, the absolute abundance of TCA metabolites was found to be quite low.

● Gametocytes



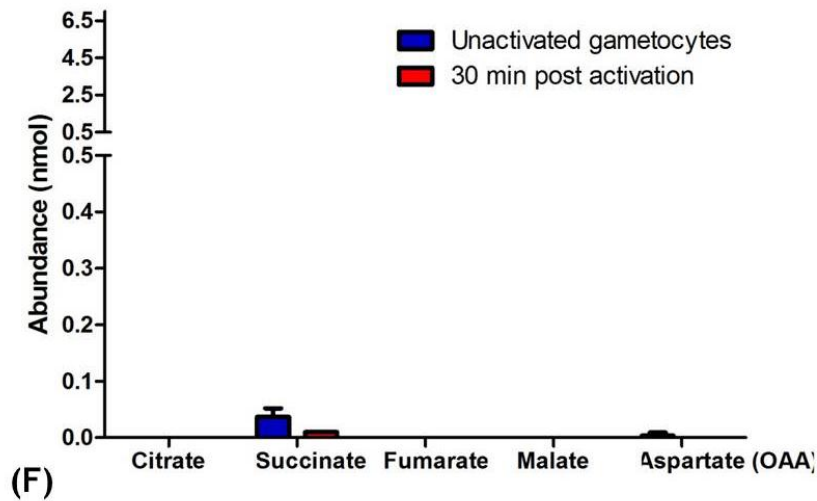


Figure 5-15  $^{13}\text{C}^{15}\text{N}$  U-Glutamine labelling of TCA cycle intermediates in *P. berghei* gametocytes during activation. TCA cycle intermediates were observed over the 30min activation process (time points: 0, 1, 10, 20, 30 min). Panels A, B, C, D and E show percentage labelling of Citrate, Succinate, Fumarate, Malate and Aspartate (Oxalo-acetate) respectively on the y-axis and time points on the x-axis. Panel F shows absolute abundance of these metabolites in unactivated gametocytes and 30 minutes post activation in nmol in  $2.5 \times 10^6$  cells. Error bars indicate SD of  $n=3$  biological replicates.

Isotopomer analysis of  $^{13}\text{C}^{15}\text{N}$  U-Glutamine labelled TCA cycle intermediates during gametocyte activation reiterated the presence of a canonical TCA cycle (Figure 5-16) as +2, +4 isotopomers of all TCA intermediates were seen. The absence of +3 isotopomers of fumarate and malate again suggested a down-regulated ICM during gametocyte activation, unlike the asexual stages. The low abundance of TCA cycle intermediates of this pathway pointed towards down regulation of TCA metabolism as well, compared to the asexual and ookinete stages (see later). The observed +1 labelling in aspartate was due to the presence of an additional labelled  $^{15}\text{N}$  atom in  $^{13}\text{C}^{15}\text{N}$  U-Glutamine.

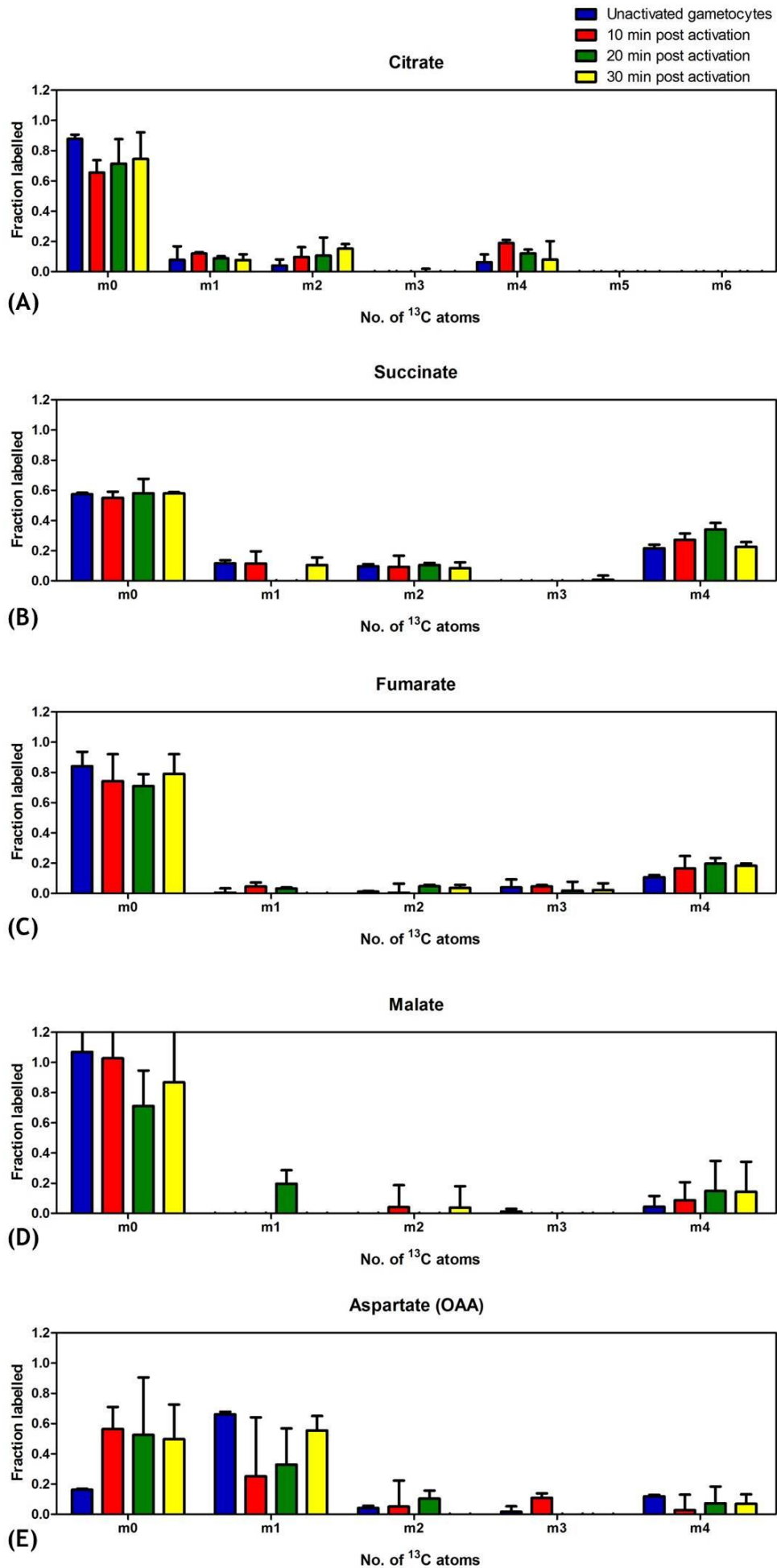


Figure 5-16 Fraction labelling of TCA cycle isotopomers in *P. berghei* gametocytes during activation in the presence of  $^{13}\text{C}^{15}\text{N}$  U-Glutamine. TCA cycle intermediates were observed over the 30min activation process (time points: 0, 1,10,20,30 min). 'm (n)' on the x-axis indicates the number of  $^{13}\text{C}$  atoms in each metabolite (Additional  $^{15}\text{N}$  atom in the case of aspartate). Panels A, B, C, D and E show fraction labelling of Citrate, Succinate, Fumarate, Malate and Aspartate (Oxalo-acetate) respectively on the y-axis. Error bars indicate SD of n=3 biological replicates.

### 5.2.3 Ookinetes

Gametocytes from line 820em1dcl2TBB (the parent gametocyte producer line) and Pb137 (48/45<sup>-</sup> which produces gametocytes but only female gametocytes are viable) were used for *in vitro* ookinete cultures. The latter line was used to resolve the difference between unfertilised and fertilised female gametes at the metabolic level. Samples were collected at two time points at 10 hours (retort stage) and 21 hours (mature ookinetes). Two hours prior to collection, UIR were removed using magnetic columns and cells were incubated in the presence of either  $^{13}\text{C}$  U-Glucose or  $^{13}\text{C}^{15}\text{N}$  U-Glutamine before rapidly quenching metabolism, metabolite extraction and quantification of  $^{13}\text{C}$  enrichment by GC-MS (see section 2.7.4).

#### 5.2.3.1 $^{13}\text{C}$ U-Glucose labelling

With  $^{13}\text{C}$  U-Glucose labelling, all glycolytic intermediates were found to be well labelled especially with the glycolytic end product PEP, where almost 80% labelling was observed both at 10 h and 21 h time points irrespective of fertilisation of female gametes. However, glucose labelling was quite low at 10 h and totally disappeared at the 21 hour time point suggesting a rapid turnover to downstream metabolites with time (Figure 5-17). The presence of unlabelled glucose in these cultures could be due to gluconeogenesis in the host cell (reticulocytes) present in the cultures as seen with the asexual stage data.

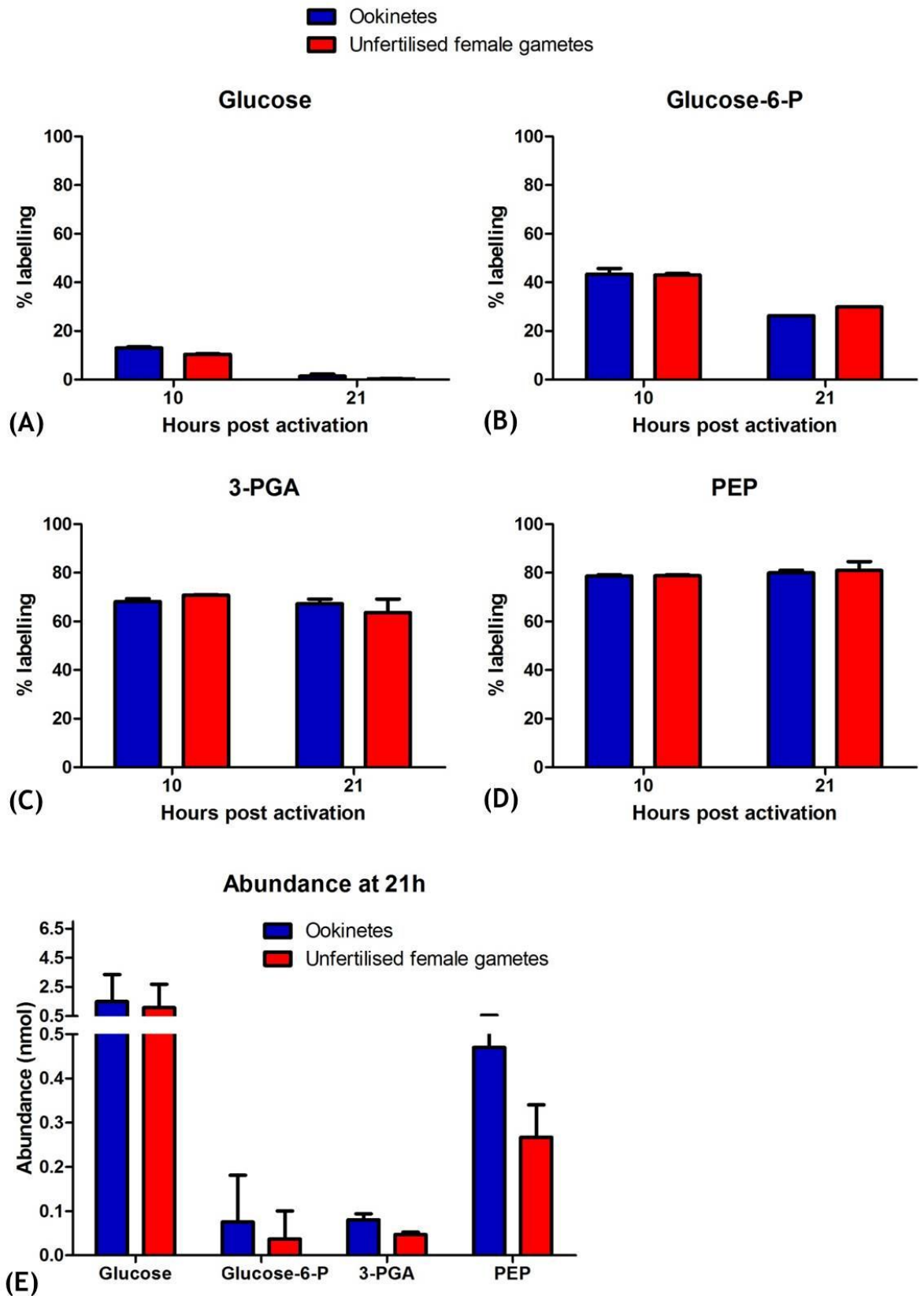
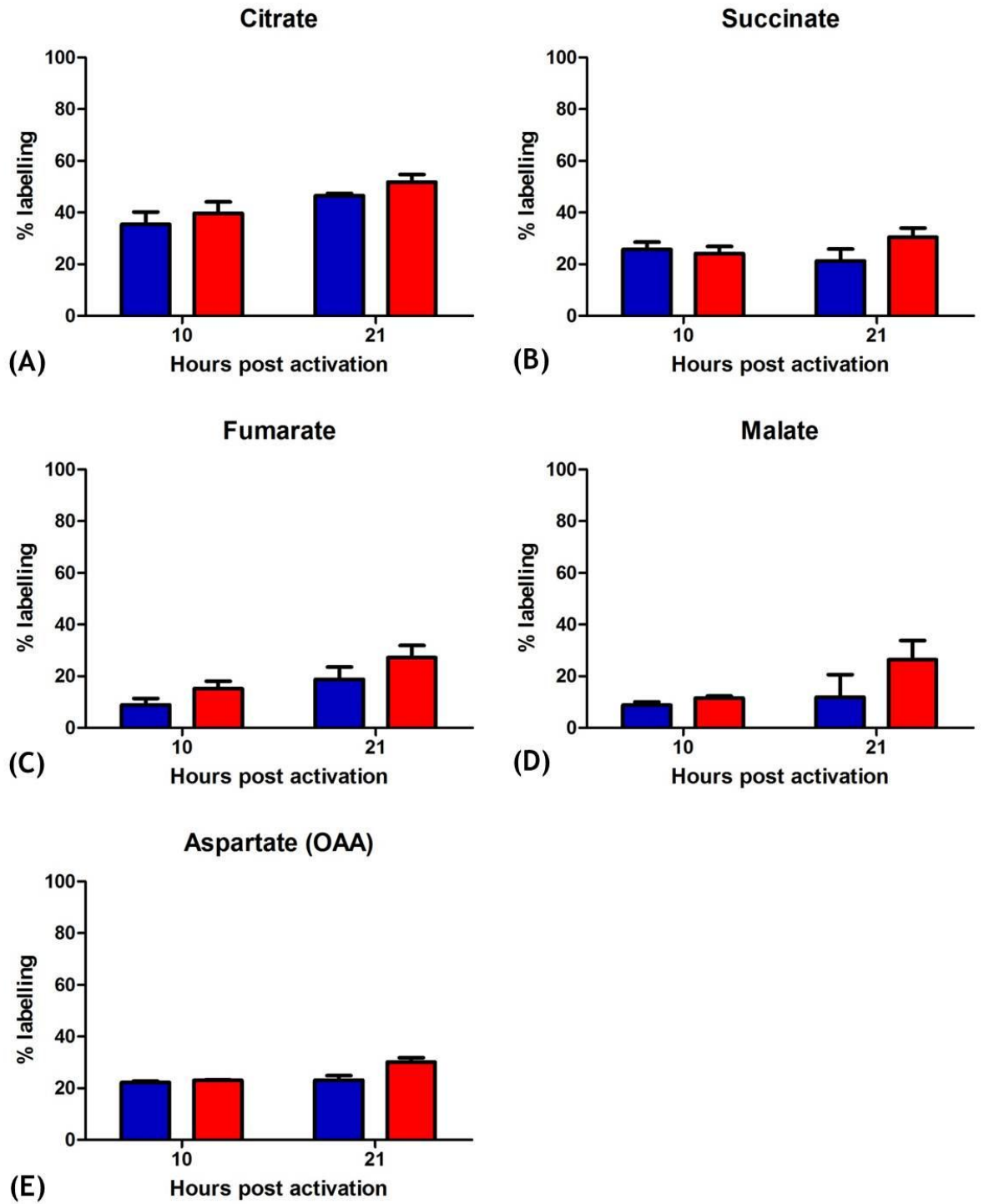


Figure 5-17 <sup>13</sup>C U-Glucose labelling of glycolytic intermediates in purified *P. berghei* ookinetes and unfertilised female gametes. Glycolytic intermediates were observed over 21 h ookinete maturation process (time points: 10 h and 21 h). Panels A, B, C and D show percentage labelling of Glucose, Glucose 6-phosphate (Glucose-6-P), 3-Phosphoglycerate (3-PGA) and Phosphoenolpyruvate (PEP) respectively on the y-axis and time points on the x-axis.

axis. Panel E shows absolute abundance of these metabolites in *P. berghei* ookinetes and unfertilised female gametes at the 21 h time point in nmol in  $2.5 \times 10^6$  cells. Error bars indicate SD of n=3 biological replicates.

All TCA cycle intermediates also seem to be labelled with  $^{13}\text{C}$  U-Glucose suggesting the presence of an active canonical TCA cycle (Figure 5-18). Labelling in citrate, succinate and aspartate (OAA) was found to be higher than in malate and fumarate, as seen in asexual stages and isotopomer analysis also suggested that apart from the usual +2, +4 and +6 isotopomers of TCA cycle intermediates, the presence of +3 labelled malate and fumarate suggested active ICM (Figure 5-19), especially at the 21 h time point where somewhat more label was seen in unfertilised female gametes than in mature ookinetes.

■ Ookinetes  
■ Unfertilised female gametes



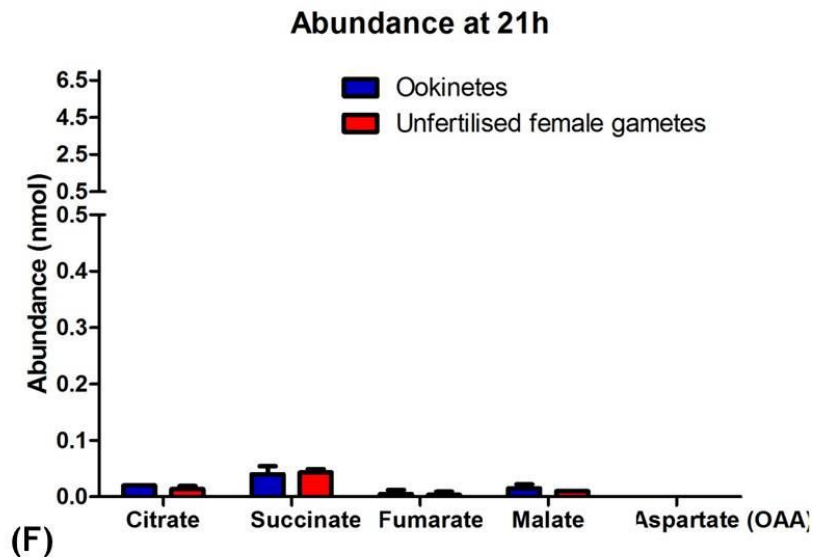


Figure 5-18  $^{13}\text{C}$  U-Glucose labelling of TCA cycle intermediates in purified *P. berghei* ookinetes and unfertilised female gametes. TCA cycle intermediates were observed over 21 h ookinete maturation process (time points: 10 h and 21 h). Panels A, B, C, D and E show percentage labelling of Citrate, Succinate, Fumarate, Malate and Aspartate (Oxalo-acetate) respectively on the y-axis and time points on the x-axis. Panel F shows absolute abundance of these metabolites in *P. berghei* ookinetes and unfertilised female gametes at the 21 h time point in nmol in  $2.5 \times 10^6$  cells. Error bars indicate SD of  $n=3$  biological replicates.

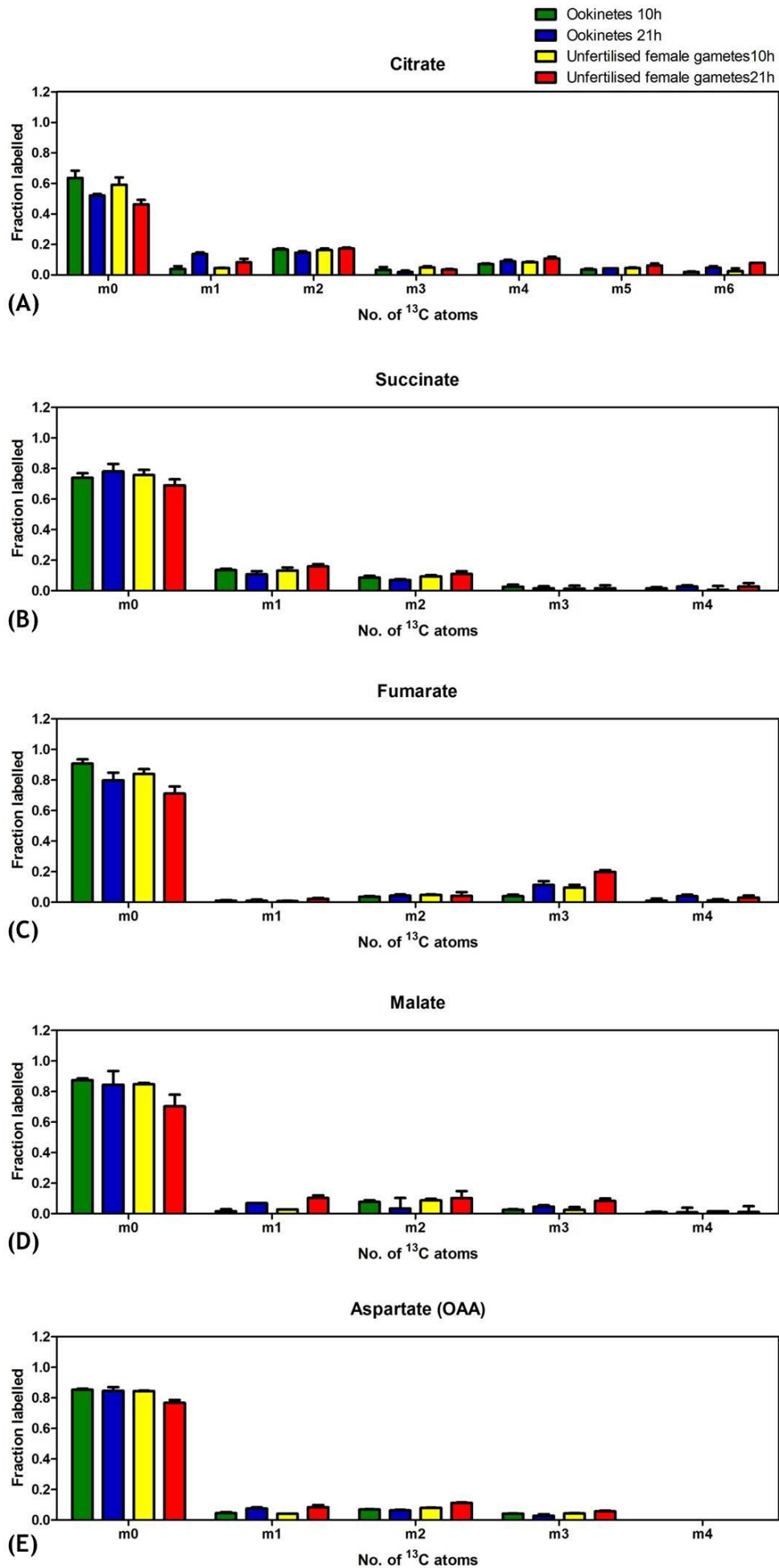


Figure 5-19 Fraction labelling of TCA cycle isotopomers in purified *P. berghei* ookinetes and unfertilised female gametes in the presence of  $^{13}\text{C}$  U-Glucose. TCA cycle intermediates were observed over 21 h ookinete maturation process (time points: 10 h and 21 h). 'm (n)' on the x-axis indicates the number of  $^{13}\text{C}$  atoms in each metabolite. Panels A, B, C, D and E show fraction labelling of Citrate, Succinate, Fumarate, Malate and Aspartate (Oxalo-acetate) respectively on the y-axis. Error bars indicate SD of n=3 biological replicates.

#### 5.2.3.2 $^{13}\text{C}^{15}\text{N}$ U-Glutamine labelling

$^{13}\text{C}^{15}\text{N}$  U-Glutamine does not label any glycolytic intermediates in ookinetes, as seen for other *P. berghei* stages described so far (Figure 5-20). Absolute abundance of glycolytic intermediates reflects their presence due to unlabelled glucose.

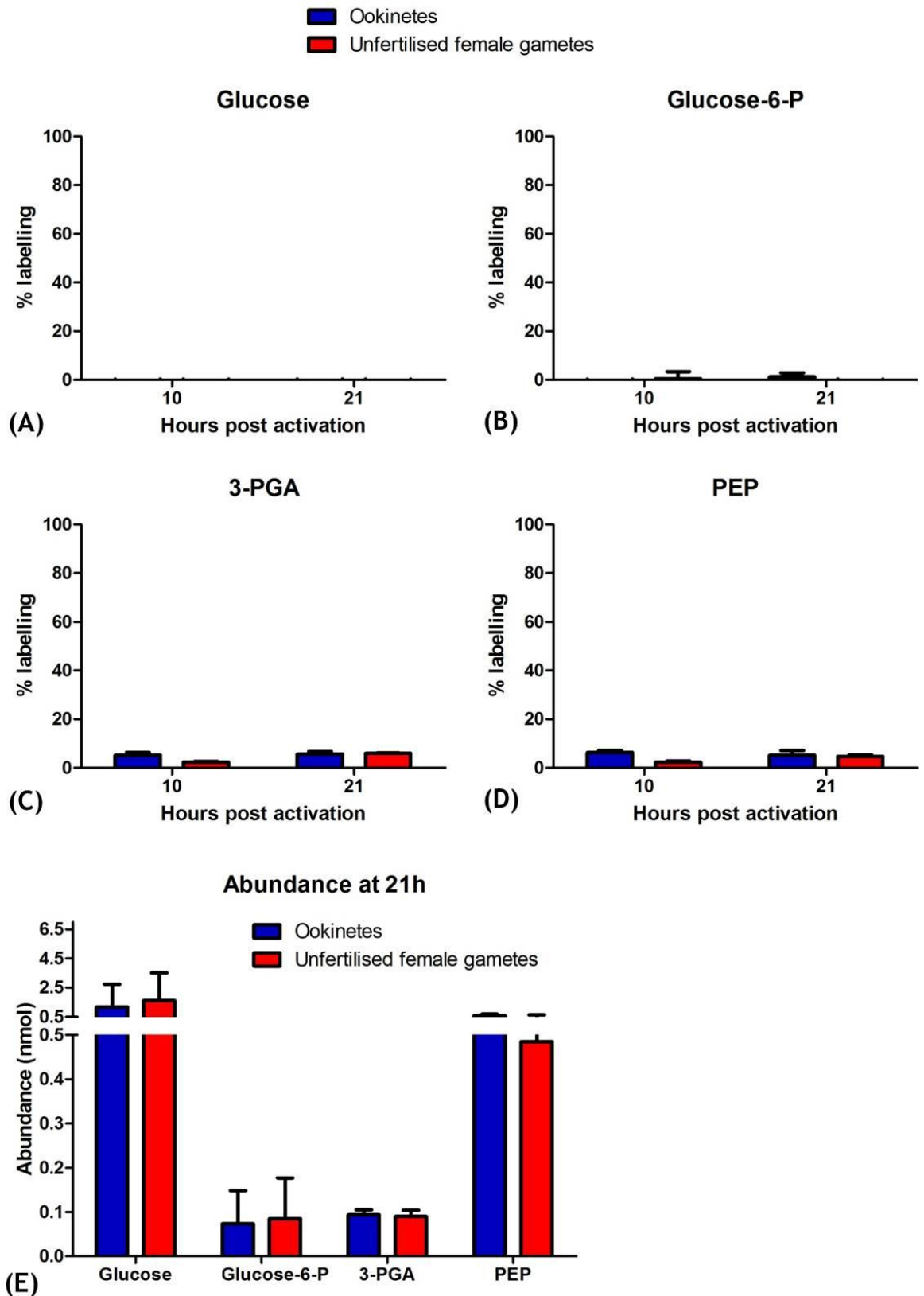
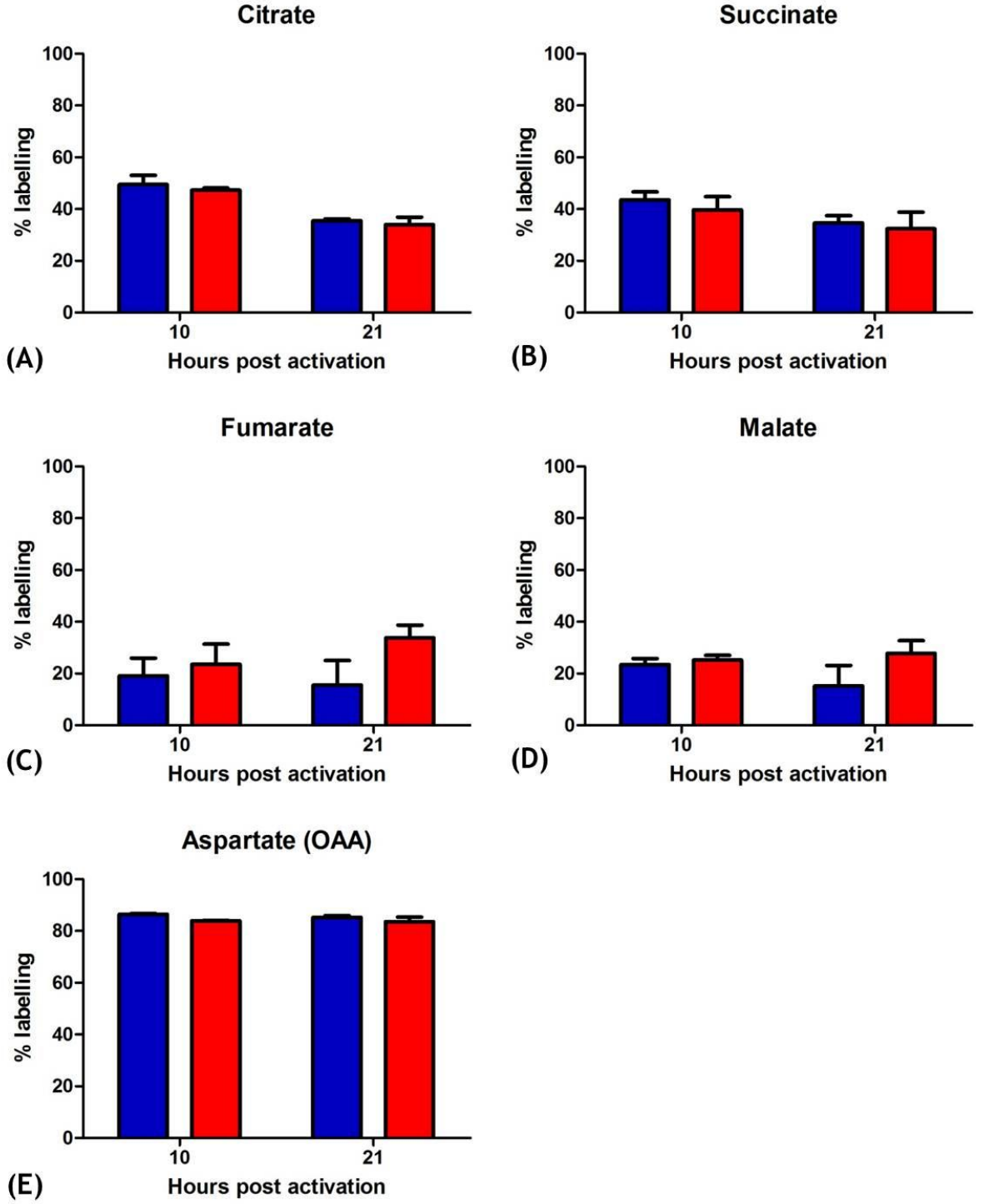


Figure 5-20  $^{13}\text{C}^{15}\text{N}$  U-Glutamine labelling of glycolytic intermediates in purified *P. berghei* ookinetes and unfertilised female gametes. Glycolytic intermediates were observed over 21 h ookinete maturation process (time points: 10 h and 21 h). Panels A, B, C and D show percentage labelling of Glucose, Glucose 6-phosphate (Glucose-6-P), 3-Phosphoglycerate (3-PGA) and Phosphoenolpyruvate (PEP) respectively on the y-axis and time points on the x-

axis. Panel E shows absolute abundance of these metabolites in *P. berghei* ookinetes and unfertilised female gametes at the 21 h time point in nmol in  $2.5 \times 10^6$  cells. Error bars indicate SD of n=3 biological replicates.

All TCA cycle intermediates showed labelling with  $^{13}\text{C}^{15}\text{N}$  U-Glutamine indicating the presence of an active TCA cycle obtaining its carbon from glutamine (Figure 5-21). Like asexual stages labelled with  $^{13}\text{C}^{15}\text{N}$  U-Glutamine, the proportion labelled was higher in succinate, aspartate (OAA), and citrate pointing towards cytoplasmic pools of unlabelled fumarate and malate coming from *pepc* mediated intermediary carbon metabolism (from unlabelled glucose) and mitochondrial restriction of succinate, oxaloacetate, and citrate. This was not observed with  $^{13}\text{C}$  U-Glucose labelling data (Figure 5-18). Isotopomer analysis of  $^{13}\text{C}^{15}\text{N}$  U-Glutamine labelling data showed the expected +2 and +4 isotopomers strengthening the likelihood of the presence of a canonical TCA cycle during ookinete development (Figure 5-22). The absence of +6 labelled carbon atoms could be due to the accumulation of unlabelled glucose possibly from gluconeogenesis in the uninfected reticulocytes present in the cultures. The observed +1 labelling in aspartate was due to the presence of an additional labelled  $^{15}\text{N}$  atom in  $^{13}\text{C}^{15}\text{N}$  U-Glutamine.

■ Ookinetes  
■ Unfertilised female gametes



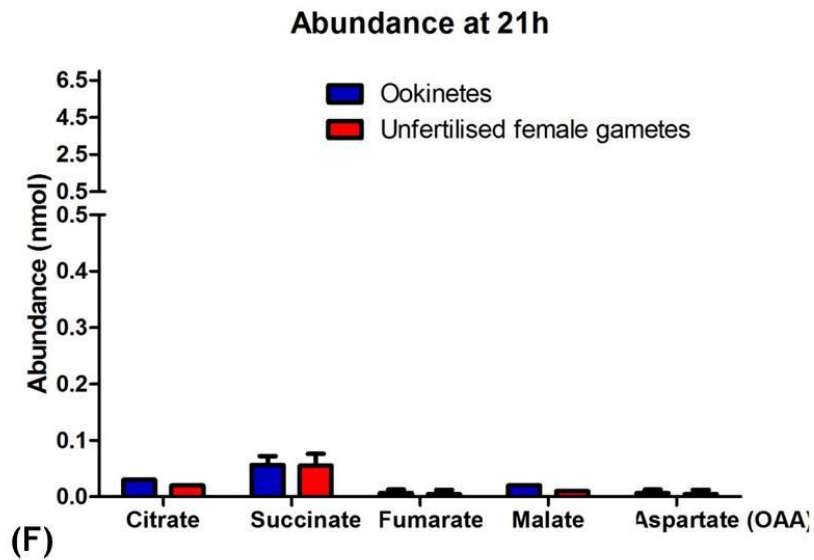


Figure 5-21  $^{13}\text{C}^{15}\text{N}$  U-Glutamine labelling of TCA cycle intermediates in purified *P. berghei* ookinetes and unfertilised female gametes. TCA cycle intermediates were observed over 21 h ookinete maturation process (time points: 10 h and 21 h). Panels A, B, C, D and E show percentage labelling of Citrate, Succinate, Fumarate, Malate and Aspartate (Oxalo-acetate) respectively on the y-axis and time points on the x-axis. Panel F shows absolute abundance of these metabolites in *P. berghei* ookinetes and unfertilised female gametes at the 21 h time point in nmol in  $2.5 \times 10^6$  cells. Error bars indicate SD of  $n=3$  biological replicates.

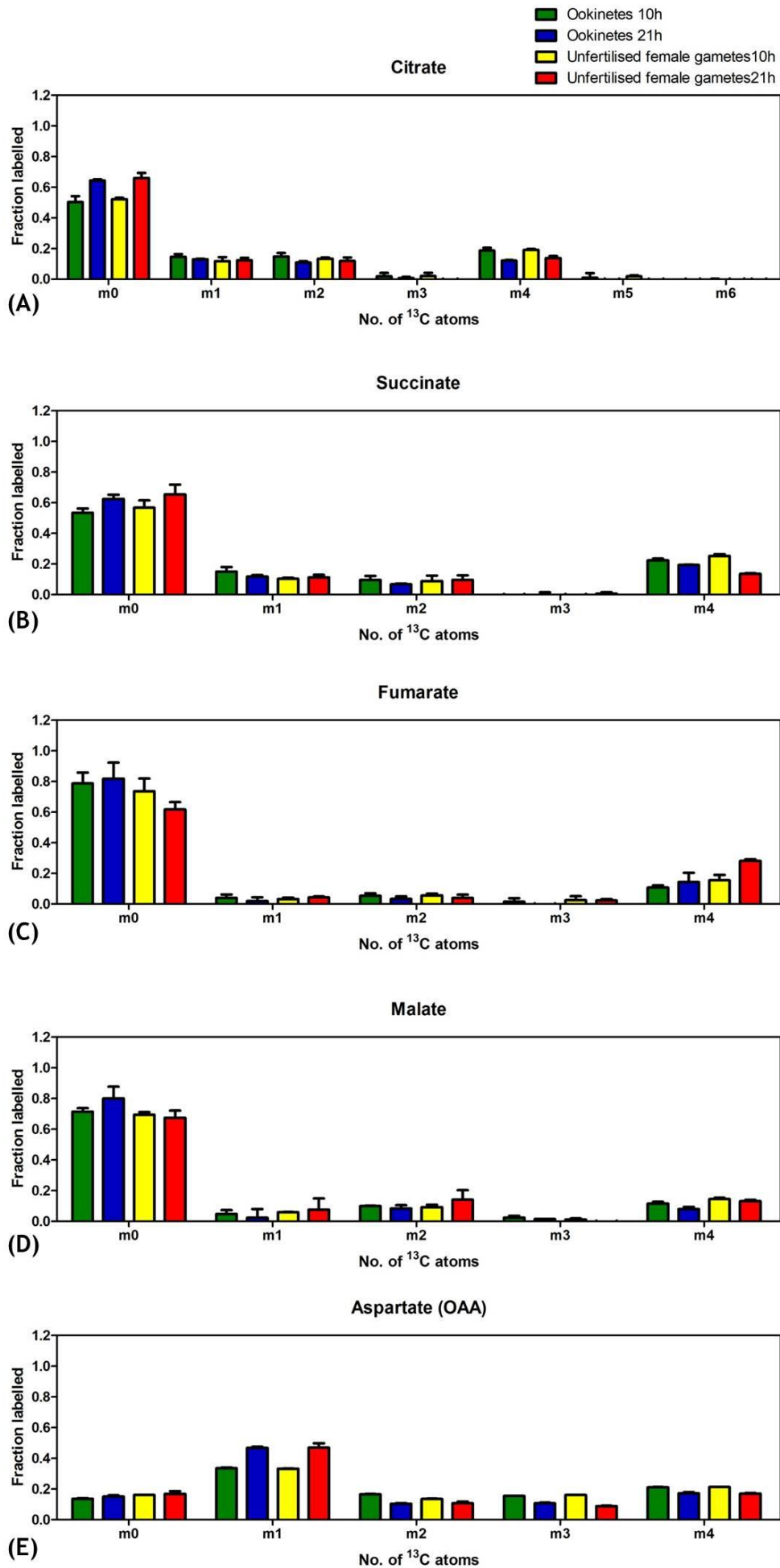


Figure 5-22 Fraction labelling of TCA cycle isotopomers in purified *P. berghei* ookinetes and unfertilised female gametes in the presence of  $^{13}\text{C}^{15}\text{N}$  U-Glutamine. TCA cycle intermediates were observed over 21 h ookinete maturation process (time points: 10 h and 21 h). 'm (n)' on the x-axis indicates the number of  $^{13}\text{C}$  atoms in each metabolite (Additional  $^{15}\text{N}$  atom in the case of aspartate). Panels A, B, C, D and E show fraction labelling of Citrate, Succinate, Fumarate, Malate and Aspartate (Oxalo-acetate) respectively on the y-axis. Error bars indicate SD of n=3 biological replicates.

#### 5.2.4 Evidence of a partial GABA shunt in *P. berghei*.

There is evidence in *Toxoplasma gondii* of existence of a partial GABA (gamma-Amino butyric acid) shunt as a means of energy storage (MacRae, Sheiner et al. 2012).  $^{13}\text{C}^{15}\text{N}$  U-Glutamine labelling of *P. berghei* parasites showed that during asexual development, only late stage and mature schizonts actively produce GABA and isotopomer analysis of these cells showed high level labelling of the +5 isotopomer of GABA (including the +1 from the Nitrogen atom in the carbon source  $^{13}\text{C}^{15}\text{N}$  U-Glutamine ) in the 24h schizont. No GABA was detected in UIR (Figure 5-23) indicating that the production of GABA was a parasite specific process. However absolute levels of GABA in asexual parasites were quite low compared to mosquito stages (see later).

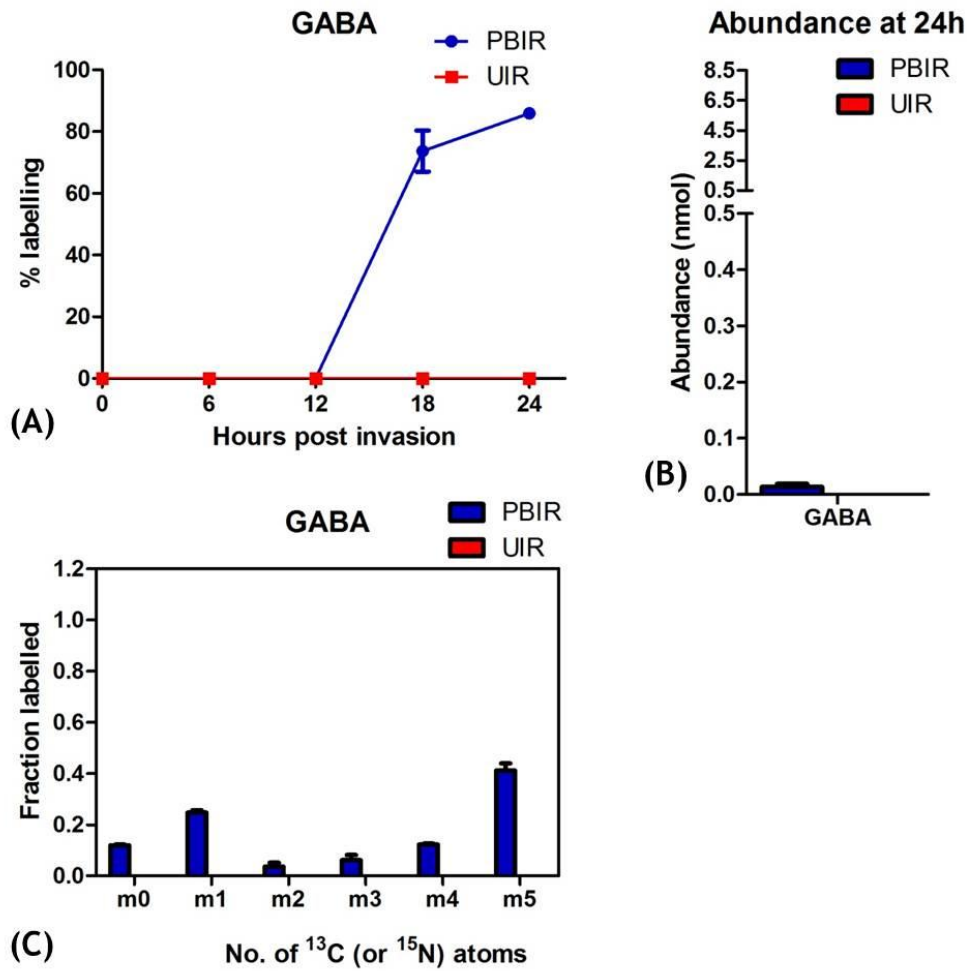


Figure 5-23  $^{13}\text{C}^{15}\text{N}$  U-Glutamine labelling of GABA in *P. berghei* asexual stages. (A) Labelling of GABA was observed over the 24 hour asexual cycle (time points: 0, 6, 12, 18, 24h) of *P. berghei* infected reticulocyte enriched erythrocytes (PBIR) and uninfected reticulocyte enriched erythrocytes (UIR). (B) Absolute abundance of GABA at the 24h time point in nmol in  $2.5 \times 10^6$  cells in PBIR and UIR. (C) Fraction labelling of GABA isotopomers observed at 24h stage in PBIR and UIR in the presence of  $^{13}\text{C}^{15}\text{N}$  U-Glutamine. 'm (n)' on the x-axis indicates the number of  $^{13}\text{C}$  or  $^{15}\text{N}$  atoms and the y-axis indicates fraction labelled. Error bars indicate SD of n=3 biological replicates.

Unactivated gametocytes showed almost 50% labelling of GABA in the presence of  $^{13}\text{C}^{15}\text{N}$  U-Glutamine but activating stages didn't label well and absolute levels of GABA were found to be much higher in unactivated gametocytes compared to activated gametocytes (Figure 5-24) or asexual stages seen above. However isotopomer analysis showed that +5 isotopomer was the most abundant species in both activated and unactivated gametocytes.

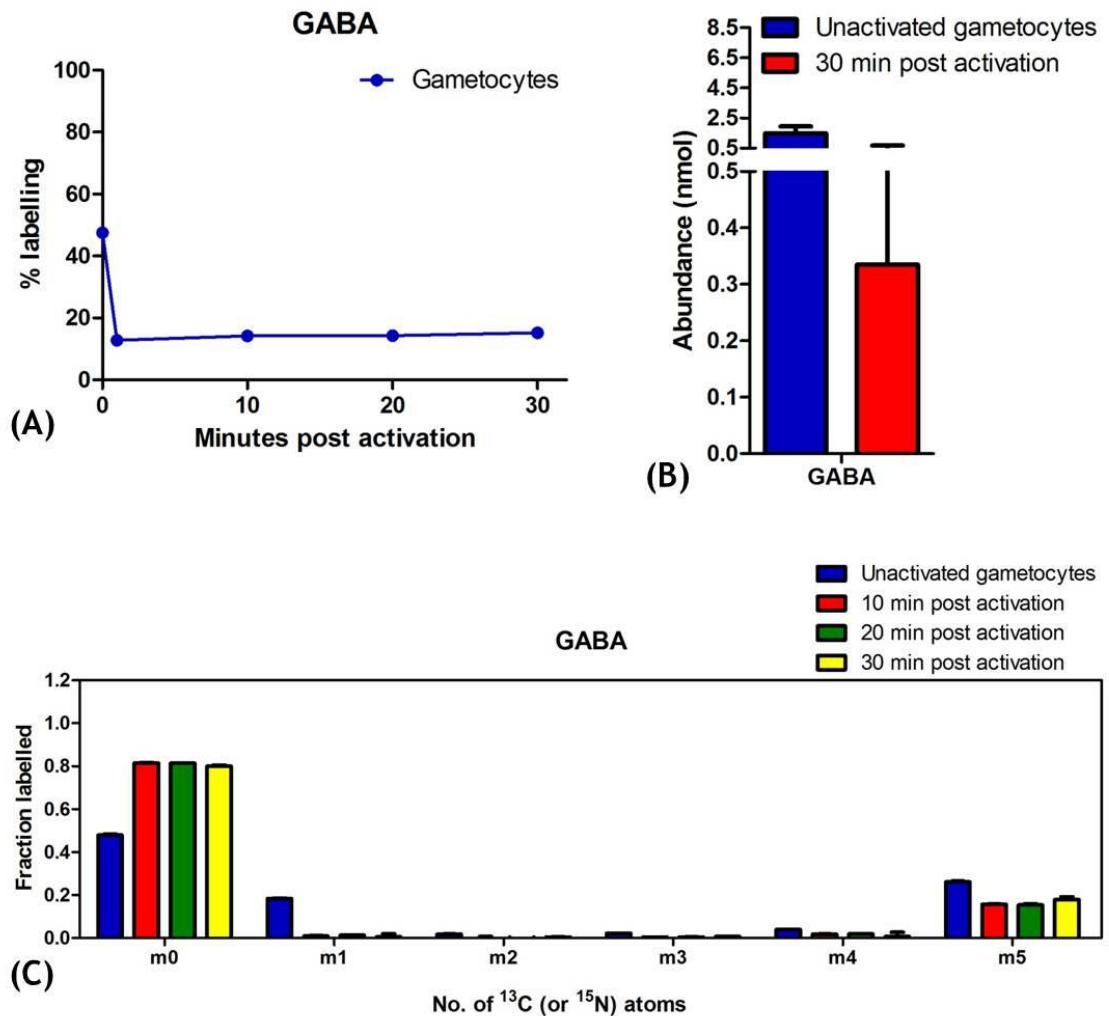


Figure 5-24  $^{13}\text{C}^{15}\text{N}$  U-Glutamine labelling of GABA in purified *P. berghei* gametocytes during activation. (A) GABA labelling was observed over the 30min activation process (time points: 0, 1,10,20,30 min) of *P. berghei* gametocytes. (B) Absolute abundance at 0min and 30min time points in nmol in  $2.5 \times 10^6$  purified *P. berghei* gametocytes. (C) Fraction labelling of GABA isotopomers observed over the 30min activation process (time points: 0, 1,10,20,30 min) of *P. berghei* gametocytes in the presence of  $^{13}\text{C}^{15}\text{N}$  U-Glutamine. 'm (n)' on the x-axis indicates the number of  $^{13}\text{C}$  or  $^{15}\text{N}$  atoms and the y-axis indicates fraction labelled. Error bars indicate SD of n=3 biological replicates.

The most abundant labelling of GABA by  $^{13}\text{C}^{15}\text{N}$  U-Glutamine was seen during the ookinete development stage of *P. berghei* where at the 21 h time point in both mature ookinetes and unfertilised activated female gametes, absolute levels of GABA were the highest in the life cycle (almost 8 fold higher than unactivated gametocytes and more than a hundred fold higher than the asexual stages - figure 2-25 a). Isotopomer analysis also showed the +5 labelled isotopomer of GABA to be present in both mature ookinetes and unfertilised, activated female gametes (Figure 5-25) b).

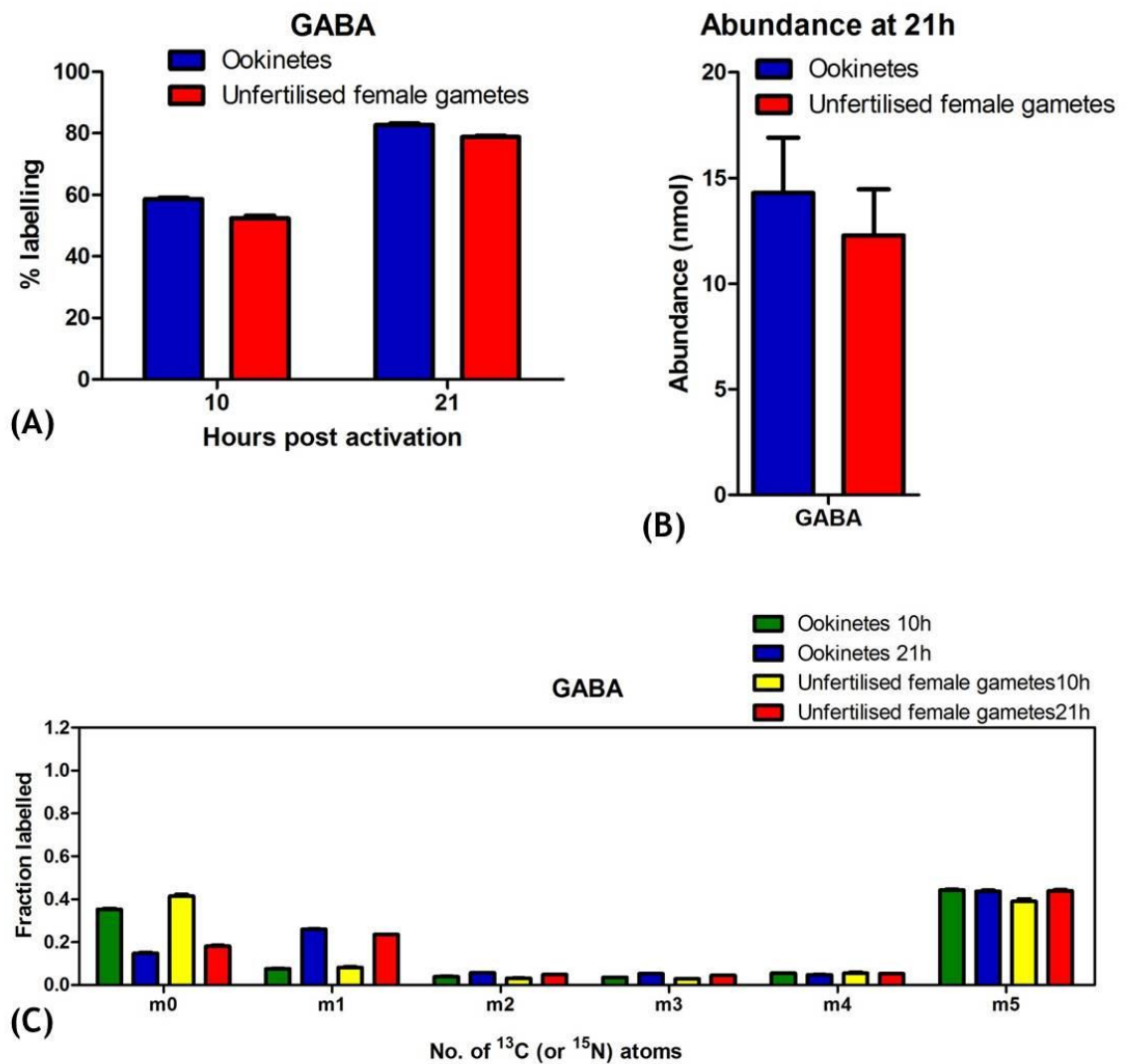


Figure 5-25  $^{13}\text{C}^{15}\text{N}$  U-Glutamine labelling of GABA in purified *P. berghei* ookinetes and unfertilised female gametes. GABA labelling was observed over the 21h ookinete maturation process (time points: 10h and 21h). (B) Absolute abundance at 21h in mature ookinetes and unfertilised female gametes in nmol in  $2.5 \times 10^6$  cells. (C) Fraction labelling of GABA isotopomers observed over 21h (time points: 10h and 21h) in purified *P. berghei* ookinetes and unfertilized female gametes in the presence of  $^{13}\text{C}^{15}\text{N}$  U-Glutamine. 'm (n)' on the x-axis indicates the number of  $^{13}\text{C}$  or  $^{15}\text{N}$  atoms and y-axis indicates the fraction labelled. Error bars indicate SD of n=3 biological replicates.

## 5.3 Discussion

### 5.3.1 Asexual blood stages

These results, amongst other interesting observations, confirmed the already known importance of glycolysis in *P. berghei* asexual stages as the main catabolic pathway to utilise glucose. Even though glycolysis was confirmed to be present in uninfected reticulocyte enriched erythrocytes (UIR),  $^{13}\text{C}$  U-Glucose

was found to be consumed in *P. berghei* infected reticulocyte enriched erythrocytes (PBIR) much more rapidly than in UIR. The absolute abundance of glycolytic intermediates in UIR was found to be higher than in PBIR which was most likely due to the rapid turnover of glycolytic end products in PBIR to downstream metabolites via the TCA cycle or intermediary carbon metabolism or for rapid biomass generation to help in proliferative shizogony as seen in some cancer cells (Salcedo-Sora, Caamano-Gutierrez et al. 2014).

Labelling of TCA cycle metabolites by  $^{13}\text{C}$  U-Glucose suggested the existence of a classical glycolysis to TCA cycle link via the glycolytic end product pyruvate, however, the absence of a mitochondrial pyruvate dehydrogenase (PDH) in *Plasmodium* spp. supported the proposed presence of a mitochondrion-located branched chain  $\alpha$ -keto acid dehydrogenase (BCKDH) complex which is present in all apicomplexans, except *Cryptosporidium* spp. (Seeber, Limenitakis et al. 2008). A very recent study confirmed that BCKDH indeed facilitates this process (Oppenheim, Creek et al. 2014).

Isotopomer analysis showed the activity of *pepc* mediated ICM with  $^{13}\text{C}_3$ -PEP becoming carboxylated to  $^{13}\text{C}_3$ -oxaloacetate but the low labelling of these intermediates pointed towards the possibility of other carbon sources entering into the TCA cycle (this was further resolved by  $^{13}\text{C}^{15}\text{N}$  U-Glutamine labelling of PBIR- see below). TCA cycle intermediates were also detected in UIR labelled with  $^{13}\text{C}$  U-Glucose (containing 35% reticulocytes) but their labelling and abundance was quite low. However, the importance of carbon metabolism in the host cell cannot be ignored, especially in the light of these data.

$^{13}\text{C}^{15}\text{N}$  U-Glutamine labelling showed that glutamine can be used as a carbon source in the TCA cycle during *P. berghei* asexual growth. Higher observed labelling in succinate, aspartate (OAA), and citrate suggested the presence of specific compartmentalisation of these metabolites to mitochondria as fumarate and malate, which can coexist in cytoplasmic pools made by *pepc* mediated ICM via PEP coming from unlabelled glucose, were shown to be present as labelled isotopomers of reduced abundance.

### 5.3.2 Reductive carboxylation in reticulocytes during TCA metabolism

With  $^{13}\text{C}^{15}\text{N}$  U-Glutamine, in UIR, labelling of TCA metabolites was found to be higher than that observed with  $^{13}\text{C}$  U-Glucose. Isotopomer analysis of  $^{13}\text{C}^{15}\text{N}$  U-Glutamine incubated UIR revealed the possibility of presence of a 'reductive

arm' of TCA metabolism and provided an explanation for the presence of +5 isotopomers of citrate in *Plasmodium* parasites as previously observed (Olszewski, Mather et al. 2010). Reductive carboxylation during TCA metabolism is a characteristic of cancerous cells with defective mitochondria (Mullen, Wheaton et al. 2012) or cells which are under stress (Metallo, Gameiro et al. 2012). Reticulocytes in the peripheral circulation are in a process of losing their organelles as they mature. The degeneration of mitochondria in reticulocytes takes place by a process of autolysis where they swell up, lose cristae and turn into single membrane bound vesicles, and then or fuse with lysosomes or are exocytosed (Gronowicz, Swift et al. 1984). It is also possible that these mitochondria in reticulocytes may use isoforms of NADP (+)/NADPH-dependent isocitrate dehydrogenase to produce glutamine-derived citrate and subsequently, acetyl-coenzyme A for lipid synthesis which is an active process in reticulocytes (Ballas and Burka 1974).

### 5.3.3 Gametocytes

Gametocyte activation is an energy demanding process and glycolysis has been considered to be the main energy contributor to male microgamete motility (Slavic, Delves et al. 2011) as with other parasite stages. During the activation process, female gametocytes differentiate into a single, spherical macrogamete whereas male gametocytes undergo three rapid rounds of nuclear division and within 8-12 minutes form eight microgametes each (Janse, Van der Klooster et al. 1986). Gametes then emerge from the host cells which is an active process.

Using  $^{13}\text{C}$  U-Glucose labelling, glycolytic intermediates in activating gametocytes were labelled but their absolute levels were found to be relatively low and the labelling of the glycolytic end product phosphoenolpyruvate (PEP) was found to be weak. Labelling of TCA cycle intermediates and their isotopomer analysis during gametocyte activation in the presence of  $^{13}\text{C}$  U-Glucose indicated the presence of a canonical TCA cycle.

TCA cycle intermediates were also labelled by  $^{13}\text{C}^{15}\text{N}$  U-Glutamine but the mitochondrial restriction of some metabolites as was observed in asexual stages was not seen in gametocytes. As +3 isotopomers of fumarate and malate were not detected, this also suggested a downregulated ICM during gametocyte activation, compared to the asexual stages. Although carbon skeletons from both, glucose and glutamine were found to enter the TCA cycle, the absolute

abundance of the intermediates of TCA cycle was quite low. However, as glucose derived glycolysis and subsequent TCA cycle operation is not the only manner in which activating gametocytes generate energy, there may be other pathways which facilitate this (section 0).

Overall, it was found that gametocytes were not very active metabolically as compared to asexual developmental stages (section 5.3.1) or ookinetes (section 5.3.4). Gametocytes are quiescent cells which when matured, reach a stable G1 cell cycle arrest stage (Lasonder, Ishihama et al. 2002) and circulate in the peripheral blood stream waiting to be picked up by the mosquito. Previous studies have also indicated that they are minimally active in terms of their metabolism (Sinden and Smalley 1979). This sexual precursor stage of the parasite is in a preparatory phase for development in the mosquito stage and although it does seem to store factors for later use (Mair, Braks et al. 2006) (section 0), there was little active metabolism observed through the central carbon pathways in this study in the short window of 30 minutes of activation.

#### 5.3.4 Ookinetes

The process of ookinete maturation leads to the formation of a motile parasite stage which traverses the midgut wall of the mosquito and forms an oocyst on the basal lamina of the midgut. Ookinete motility is an active process mediated by the actin-myosin motor complex (Siden-Kiamos, Ecker et al. 2006) which requires energy. It was concluded from our data that maturing ookinetes (and unfertilized female gametes) rapidly utilized glucose and turned it over to glycolytic intermediates with most labelling observed in the end product PEP with  $^{13}\text{C}$  U-Glucose labelling. All TCA cycle metabolites were also found to be labelled with  $^{13}\text{C}$  U-Glucose as a carbon source and the compartmentalization of citrate, succinate and oxaloacetate to mitochondria was observed, similar to asexual stages with fumarate and malate also present in the cytosol.

$^{13}\text{C}^{15}\text{N}$  U-Glutamine labelling also showed glutamine entering the TCA cycle as all intermediates were found to be labelled and operation of a canonical cycle. No +5 isotopomers of citrate were found in this exo-erythrocytic stage of the parasite, unlike the asexual stage, further strengthening the argument that the 'reductive arm' of TCA metabolism was reticulocyte specific. The flux coming from glutamine through the TCA cycle was found to be more than that coming from glucose as a carbon source. This was confirmed by almost 90% labelling of

aspartate (OAA) in  $^{13}\text{C}^{15}\text{N}$  U-Glutamine fed ookinete cultures compared to 20-30% in  $^{13}\text{C}$  U-Glucose fed cultures. Also, it was noted that unfertilized female gamete also undergoes similar metabolism as a fertilized ookinete, suggesting that fertilization is not a prerequisite for pre-programmed metabolism.

It has been shown that blocking the TCA cycle in *P. falciparum* asexual stages by the chemical inhibitor Sodium fluoroacetate (NaFAc) (which combines with coenzyme A to produce fluoroacetyl CoA in turn, reacting with citrate synthase to produce fluorocitrate which binds very tightly to aconitase stopping the citric acid cycle (Proudfoot, Bradberry et al. 2006)) did not have any effect on cell viability (Macrae, Dixon et al. 2013). Also, deletion of a gene of flavoprotein (Fp) subunit *Pbsdha* (PBANKA\_051820), one of the four components of complex II, a catalytic subunit for succinate dehydrogenase activity, did not have any effect on asexual growth in *P. berghei* (Hino, Hirai et al. 2012). However, in these studies, blocking aconitase stopped gametocytes from maturing and deletion of the succinate dehydrogenase subunit impaired the development of ookinetes and ookinete to oocyst transmission. It is possible that oxidative phosphorylation via the Electron Transport Chain (ETC), which is the most efficient step in producing ATP in the glycolysis→TCA cycle→ETC carbon flow and also takes part in heme biosynthesis is necessary for ookinete maturation and deleting the complex II subunit of succinate dehydrogenase (which also takes part in the TCA cycle and is a link between TCA cycle and ETC) compromises both, the TCA cycle and the ETC. It was surprising then that this did not have any effect on development of gametocytes in *P. berghei* (Hino, Hirai et al. 2012).

It was thought therefore that it would be interesting to delete aconitase in *P. berghei* to resolve this question. It was found that Aconitase (PBANKA\_135520) can indeed be deleted in *P. berghei* (Figure 9-6) and functional characterization of the mutant is underway.

### 5.3.5 GABA as an energy source in ookinete stage

One of the most important observations in this study was the labelling of GABA ( $\gamma$ -Amino Butyric Acid) observed in  $^{13}\text{C}^{15}\text{N}$  U-Glutamine enriched cultures in all *P. berghei* stages. GABA is stored as a short term energy reserve in the apicomplexan parasite *Toxoplasma gondii* where it takes part in a GABA shunt in which intermediates from the TCA cycle are used to synthesize glutamate, which

is subsequently decarboxylated to GABA which directly converts to succinate (MacRae, Sheiner et al. 2012).

In our data, we found that with  $^{13}\text{C}^{15}\text{N}$  U-Glutamine as the labelled carbon source, late stage and mature schizonts of *P. berghei* were found to label GABA, although the absolute levels in asexual stages were not very high. This was found to be exclusive to infected cells, ruling out this pathway in uninfected cells. Unactivated gametocytes seemed to accumulate GABA possibly in anticipation of the energy requirements during the mosquito stages. The most abundant and remarkable presence of GABA was seen in the ookinete developmental stages where 21 hours post activation, levels of GABA were the highest in the life cycle. Such high levels of GABA in the ookinete suggest a partial GABA shunt may operate in *P. berghei* as seen in *Toxoplasma gondii* and may play an important role in the mosquito stage transition and the establishment of the oocyst stage.

It should be noted that there is an important distinction between *Toxoplasma* and *Plasmodium* in GABA metabolism as *Toxoplasma* encodes for an enzyme succinate semi-aldehyde dehydrogenase, which is required for the direct conversion of GABA to the TCA-cycle intermediate succinate (MacRae, Sheiner et al. 2012) whereas *Plasmodium* does not encode for this enzyme (Gardner, Hall et al. 2002). Also, GABA is formed by decarboxylation of glutamate but the genes orthologous to those representing canonical versions of the enzyme which catalyzes this reaction, glutamate decarboxylase were not found in *Plasmodium* or *Toxoplasma* genomes. However, glutamate decarboxylases belong to an amino acid decarboxylase superfamily (Cook, Roos et al. 2007) and share conserved domains with other members of the same superfamily. A putative lysine decarboxylase (*ldc*) which usually converts lysine to cadaverine (not detected in our *P. berghei* metabolomics data or in *Toxoplasma* metabolomics data (MacRae, Sheiner et al. 2012)) is found in both *Plasmodium* (Gardner, Hall et al. 2002) and *Toxoplasma* genomes (Gajria, Bahl et al. 2008). *ldc* was shown to encode for a putative glutamate decarboxylase like protein (MacRae, Sheiner et al. 2012).

It is thus possible that deleting the *Plasmodium ldc* (PBANKA\_100340) will prevent the formation of GABA and show an ookinete stage phenotype. Potential transporters of GABA or glutamate to mitochondria e.g. Glutamate dehydrogenases (*gdha-1,2,3*) which are not required for asexual growth in *P.*

*falciparum* (Storm, Perner et al. 2011), amino acid transaminases (e.g. Ornithine amino transferase: PBANKA\_010740) and another putative transporter (PBANKA\_030670) (MacRae, Sheiner et al. 2012) could also be targeted to stop ookinete mitochondria from accessing GABA as a potential energy source and halt the parasite at this stage. RNA seq data from our lab (A.Religa, unpublished data) shows that *gdh1* is expressed at a high level in ookinetes and *ldc* shows high expression in the gametocyte stage. A simplistic possible model of GABA metabolism in *P. berghei* ookinete is represented in Figure 5-26.

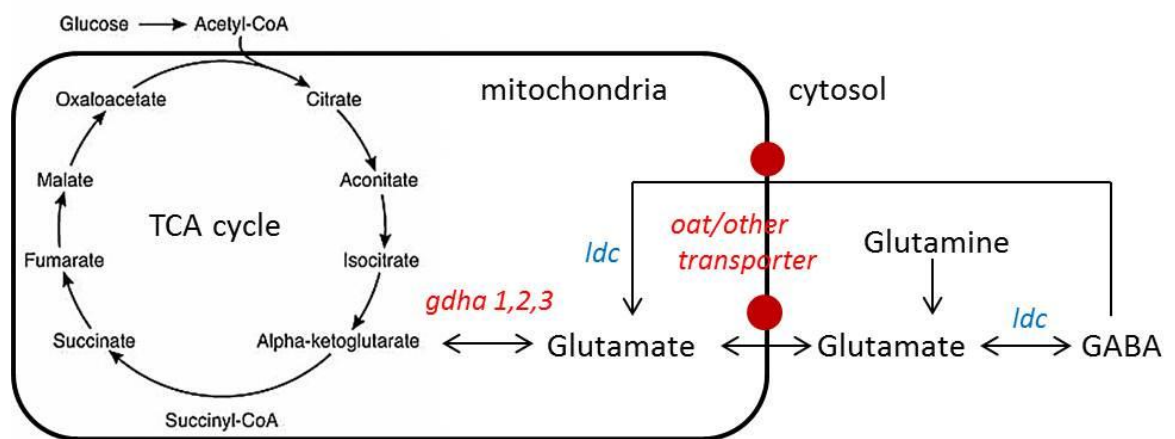


Figure 5-26 Model of GABA metabolism in *P. berghei* ookinetes. *gdha*- glutamate dehydrogenases: PBANKA\_102620 (*gdha1*) PBANKA\_101400 (*gdha2*) PBANKA\_122820 (*gdha3*), *oat*- Ornithine amino transferase (PBANKA\_010740), other transporter (PBANKA\_030670), *ldc*- Lysine decarboxylase (PBANKA\_100340)

## 5.4 Conclusions

This study elucidated the different roles of glucose and glutamine metabolism in *P. berghei* with both glycolysis and the TCA cycle found to be active in all stages although to varying degrees. The possibility of gluconeogenesis in reticulocytes was raised due to replenishment of unlabelled glucose in cultures and needs to be explored further. The observation that reticulocytes possess a reductive arm of TCA metabolism was intriguing and explains the observation of this pathway in *P. falciparum* cultures in which reticulocytes were present (Olszewski, Mather et al. 2013). The flux through the glutamine derived TCA cycle was found to dominate over the glycolytic pyruvate derived TCA cycle in all stages. An important similarity between the asexual and ookinete stages was the observed restriction of citrate and succinate to mitochondria and presence of fumarate, malate and oxaloacetate in both the cytosol (derived via the active ICM pathway) as well as the mitochondria. This compartmentalisation was not

observed in gametocytes which were found to be less active in terms of classical carbon metabolism. The characterisation of aconitase deficient *P. berghei* parasites would reveal the role of the canonical TCA cycle in gametocyte development and maturation.

The gametocytes did show GABA labelling by  $^{13}\text{C}^{15}\text{N}$  U-Glutamine and the observed absolute abundance of GABA in unactivated gametocytes was slightly higher than asexual stages which seemed to decrease 30 minutes post activation. This suggested that gametocyte might employ GABA metabolism during activation but the levels observed during ookinete maturation were at least 15 fold higher than unactivated gametocytes pointing towards ookinetes as the main stage for GABA metabolism in *P. berghei* life cycle. The proposed presence of alternative energy storage and generation system in gametocytes has been discussed in section 6.

The proposed role of GABA metabolism in the ookinete stage is of great interest with a number of genes implicated in this pathway as potential targets for dissecting the biology of energy metabolism at this stage. Extensive work to delete or conditionally knock out all the genes implicated in this pathway (Figure 5-26) is ongoing (we have successfully deleted five out of 6 genes- data not shown) which will be followed by phenotypic analyses and targeted metabolomics study of these mutants to further elucidate the role of GABA metabolism in *P. berghei* parasites.

## 6 Phosphocreatine is a potential energy reserve in *P. berghei* gametocytes

### 6.1 Introduction

The importance of energy metabolism in *P. berghei* has been emphasised in the previous chapter dealing with carbon metabolism. The gametocyte stage of *Plasmodium* parasites get ready for the hostile environment in the mosquito-mid gut and prepare themselves by using strategies like translational repression (Mair, Braks et al. 2006) to facilitate a quick turnover of proteins during development. The up-regulation of TCA function in gametocytes also reflects an anticipation of increased energy demands in female gametes which prepare themselves for the post-fertilization stages when they convert from a non-motile apolar zygote to a polar and motile ookinete stage, during which access to glucose in the mosquito midgut and hemolymph may be limited (Talman, Domarle et al. 2004). The energy requirements of the male gametocyte are high and specific to the first few minutes after the mosquito takes the blood meal when a drastic change in environment (e.g. low temperature, high pH) and other mosquito factors like xanthurenic acid give them cues to form haploid gametes (Muhia, Swales et al. 2001) (Arai, Billker et al. 2001). Female gametocytes differentiate into a single, spherical macrogamete whereas male gametocytes undergo three rapid rounds of nuclear division and within 8-12 minutes form eight microgametes each (Janse, Van der Klooster et al. 1986). During the formation of the male gametes, such rapid nuclear division and development of flagella which start beating violently to form exflagellation centers is one of the most spectacular events of the *Plasmodium* life cycle. It is a very active process, probably requiring a very rapid turnover of ATP production. Glycolysis has classically been considered to be the main pathway which facilitates this in *Plasmodium* (Slavic, Delves et al. 2011, Sinden, Carter et al. 2012).

#### 6.1.1 Phosphagen energy system

Apart from glycolysis, the TCA cycle and oxidative phosphorylation, another energy system called the phosphagen system has been described to operate in higher organisms and is described as the quickest way to resynthesize ATP (Wallimann, Wyss et al. 1992) without oxygen and does not produce lactic acid and hence can be described as alactic anaerobic energy generation. The phosphagen system utilises phosphocreatine (PCr) which is stored as a rapidly

mobilizable reserve of high energy phosphate in metazoans and releases ATP in the reversible reaction catalysed by the enzyme creatine kinase (*ck*) (Figure 6-1).

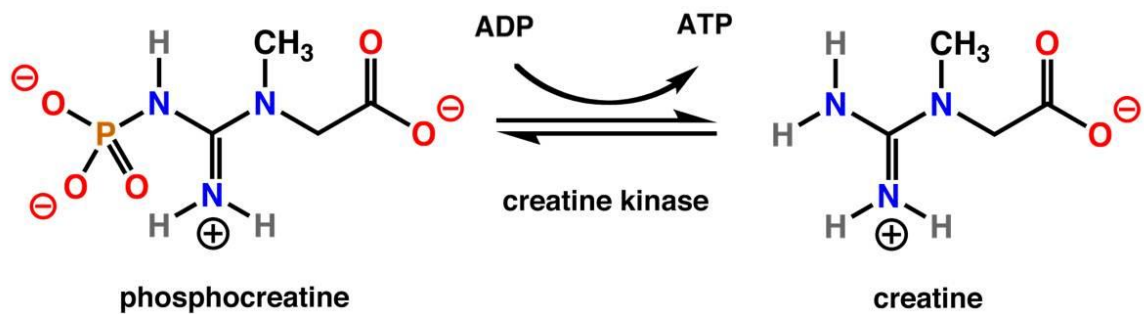


Figure 6-1 Creatine kinase interconverts phosphocreatine into creatine releasing ATP in a reversible reaction (accessed from [http://en.wikipedia.org/wiki/Creatine\\_kinase](http://en.wikipedia.org/wiki/Creatine_kinase))

In most muscles, the ATP regeneration capacity of *ck* is very high and considerably exceeds both ATP utilization as well as ATP replenishment by oxidative phosphorylation and glycolysis. For example, the maximal rate of ATP synthesis by the *ck* reaction in rat cardiac muscle (30  $\mu\text{mol/s/g}$ ) is much higher than the rate of ATP production by oxidative phosphorylation (2.5  $\mu\text{mol/s/g}$ ) (Wallimann, Wyss et al. 1992).

### 6.1.2 Creatine kinase

Creatine kinase (*ck*) belongs to a group of phosphagen kinases which has evolved by a gene duplication event from arginine kinase (followed by creatine specificity, quaternary structure and a mitochondrial targeting sequence for Mt isoforms) (Ellington and Suzuki 2007). There are four isoforms of this enzyme in vertebrates.

1. Mtck1- Mitochondrial UMtck found ubiquitously in mitochondria in vertebrates.
2. Mtck2- Mitochondrial SMtck found in sarcomeric mitochondria in vertebrates.
3. Cytck-M- Cytoplasmic M-ck Muscle type in muscle cells of vertebrates.
4. Cytck-B- Cytoplasmic B-ck Brain type in neuronal cells of vertebrates.

A flagellar isoform is also found in primitive spermatozoa of protochordates and marine sponges (Tombes and Shapiro 1987). *Plasmodium* parasites do not encode for any obvious *ck* isoforms.

## 6.2 Results

### 6.2.1 Gametocytes store phosphocreatine

Comparative untargeted metabolomics of *P. berghei* mature gametocytes and mature schizonts revealed that gametocyte infected erythrocytes contain almost 50 fold higher levels of phosphocreatine when compared to mature schizonts (Table 5). UIR were also found to store roughly 12 fold higher levels of phosphocreatine compared to normocytes (mature erythrocytes) (Table 2). The abundance of phosphocreatine in gametocyte infected reticulocytes was only marginally higher compared to uninfected reticulocytes (Table 4) and because it was detected in only whole cells and not lysed parasite pellets, it suggested that gametocytes probably store the host phosphocreatine for later use while schizonts seemed to have exhausted this resource (Figure 6-2).

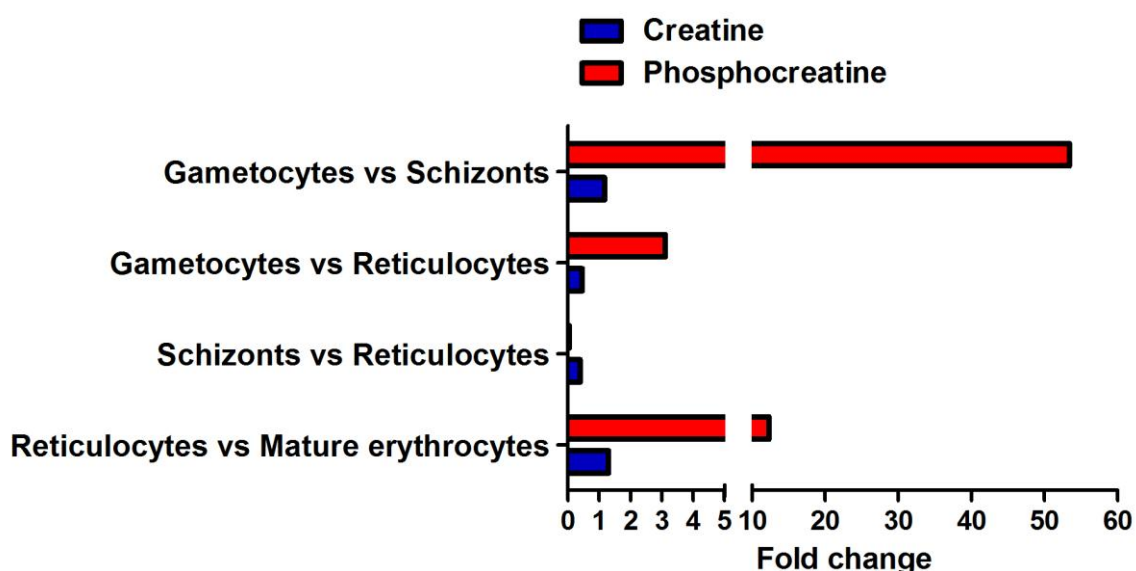
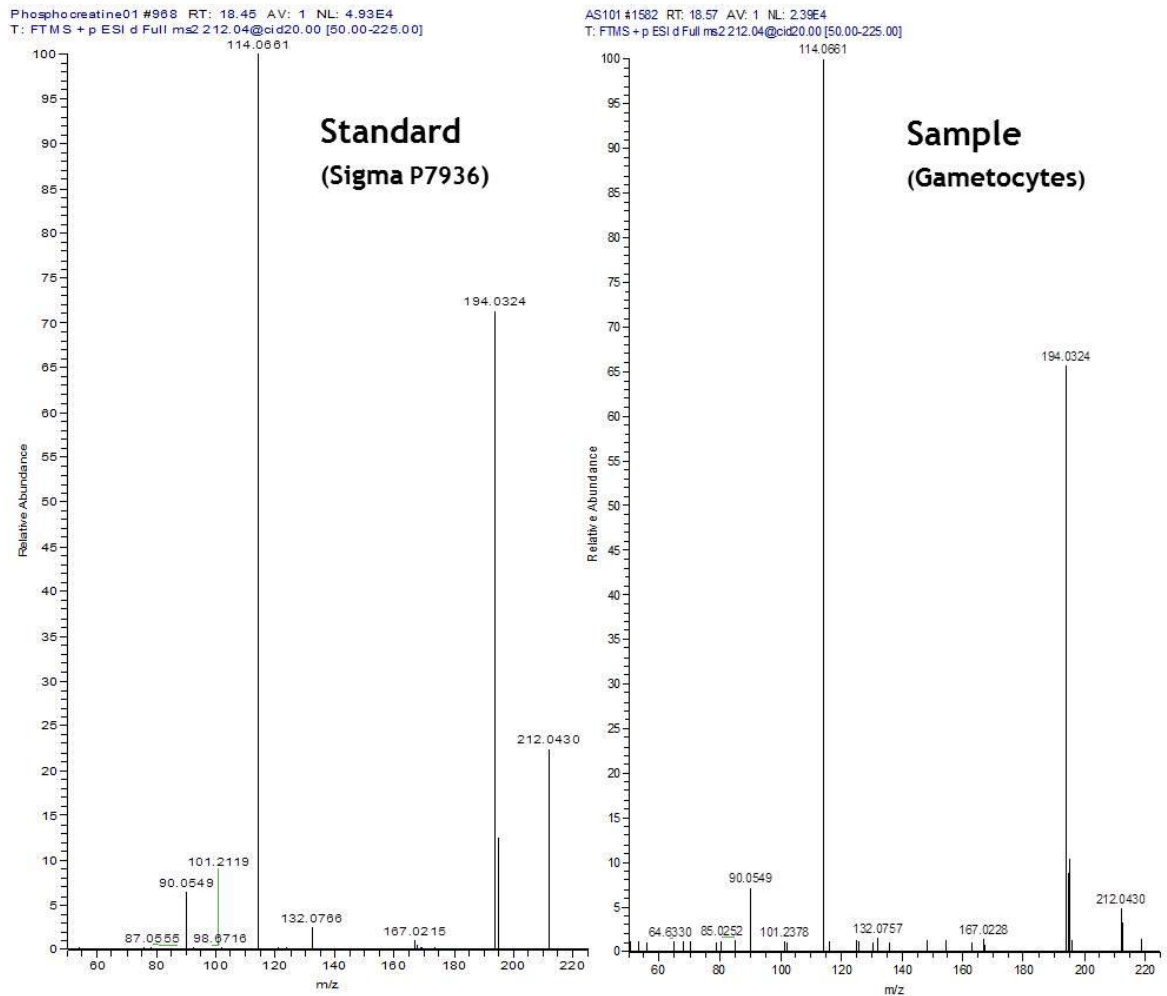


Figure 6-2 Fold change of Creatine and Phosphocreatine as observed in different sample groups compared in the untargeted metabolomics study.

The discovery of phosphocreatine in gametocytes was of interest. However, since mass alone is insufficient to prove identity, MS/MS was performed on gametocyte extracts and the fragmentation pattern of the putative phosphocreatine was matched to commercially acquired phosphocreatine (Sigma P7936) which confirmed the validity of the identification (Figure 6-3).



**Figure 6-3 MS/MS fragmentation for identification of phosphocreatine.** The x-axis shows m/z ratio and the y-axis shows relative abundance of fragmented ions. Detected Molar mass of phosphocreatine 211.0355823. Left panel: Commercially acquired standard phosphocreatine (sigma P7936) with retention time 18.45 min. Right panel: phosphocreatine detected in gametocyte extract at retention time 18.57 min. Six major fragmentation ions were found to match between the standard and sample (90.0549, 114.0661, 132.0766, 167.0215, 194.0324, and 212.0430) which confirmed the identification.

### 6.2.2 Creatine kinase is not encoded by *P. berghei*.

All creatine kinase isoforms in the *P. berghei* mammalian host, *Mus musculus* have two phosphagen kinase domains and two ATP binding domains. The two mitochondrial isoforms additionally contain one mitochondrial transit peptide and one cardiolipin binding domain each (Figure 6-4).

## Creatine kinase isoforms in *Mus musculus*

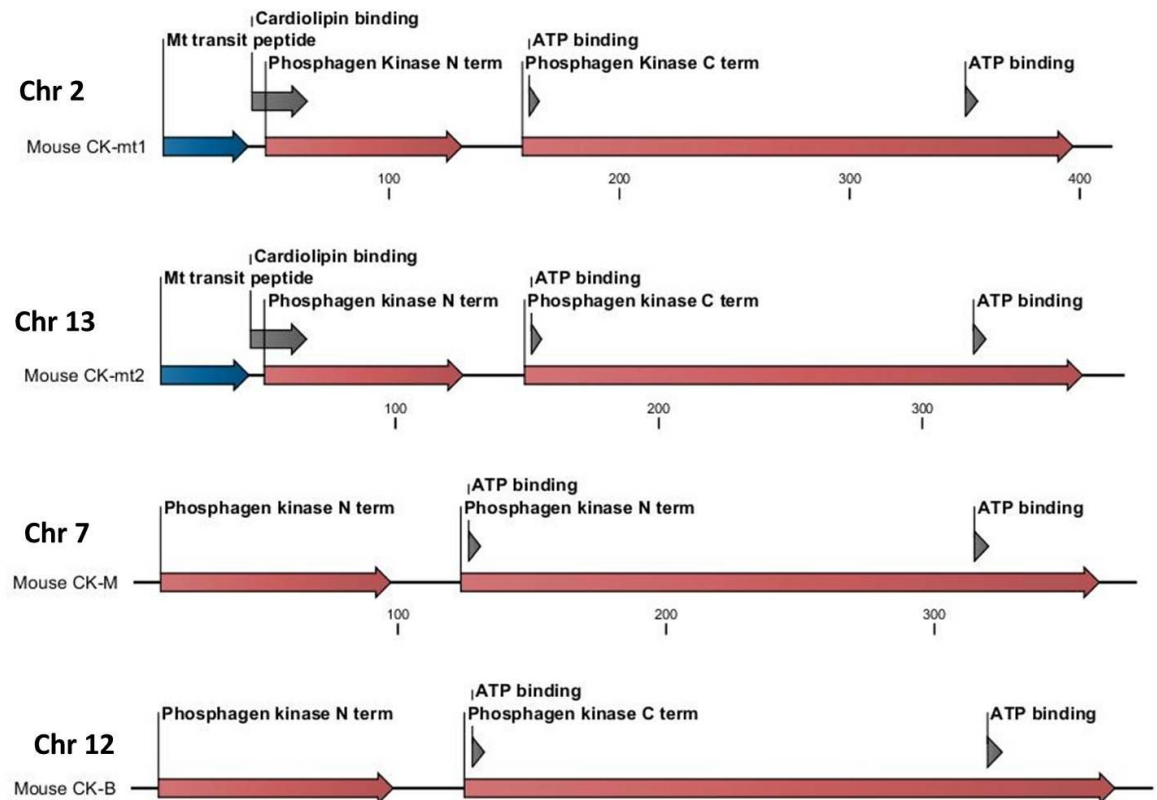


Figure 6-4 Creatine kinase isoforms in *Mus musculus*

Comprehensive bioinformatics analyses using whole enzyme isoform sequences and conserved phosphagen kinase and ATP binding domains failed to identify a closely related enzyme in *Plasmodium* spp. or other apicomplexans.

### 6.2.3 Creatine kinase enzyme activity is present in UIR and PBIR

The absence of *ck* enzyme in *Plasmodium* spp. suggested that if the parasites make use of the phosphagen system, they might hijack the enzyme from the host erythrocyte. To check for the presence of *ck* in erythrocytes, a *ck* activity assay was performed (using EnzyChrom™ Creatine Kinase Assay Kit ECPK-100 from BioAssay Systems according to the manufacturer's instructions) on uninfected erythrocytes (normocytes and reticulocyte enriched), purified schizonts (whole and lysed), purified gametocytes (whole, lysed and activated) and purified ookinetes. It showed the presence of *ck* activity in whole uninfected and infected erythrocytes but the activity was not detected in lysed parasites at either the schizont or gametocyte stage or in exoerythrocytic activated gametocytes or ookinete stages (Figure 6-5). However, the detected *ck* activity in these samples was at least 30 fold less than in positive controls (samples from

mouse muscle and brain homogenates where *ck* activity is supposed to be maximum).

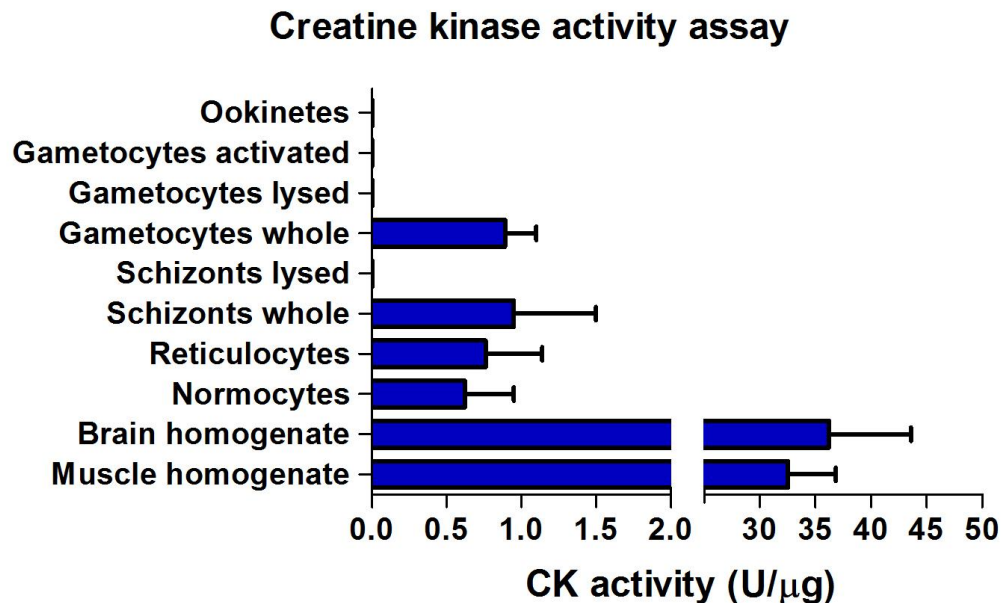


Figure 6-5 Creatine kinase activity assay. *ck* Activity was detected only in uninfected and infected whole erythrocytes. No *ck* activity was detected in lysed parasite pellet or activated gametocytes and ookinetes. Normalisation was done by matching protein concentration of positive controls (muscle and brain homogenates) to uninfected and infected erythrocytes and equal numbers of cells ( $1 \times 10^6$ ) were used for the lysate used for activity assay. Error bars indicate  $n=3$  biological replicates.

#### 6.2.4 Creatine kinase could not be detected using a specific antibody

An antibody (ab76506 Abcam) against a 91 amino acid fragment of human *Mtck* which was found to be conserved in a mouse *Mtck* isoform (Figure 6-6) was used for immuno-pull down and western blot analysis of uninfected erythrocytes (normocytes and reticulocytes), schizonts (whole and lysed), gametocytes (whole, lysed and activated) and ookinetes, however, the protein could not be detected in any of the samples despite detection of *ck* enzyme activity. The antibody detected the right sized band (46kDa) in brain and muscle homogenates of mouse which served as positive controls but a titration based on protein concentration showed that the limit of detection was quite high as lysate containing at least  $1 \mu\text{g}$  of protein from these homogenates had to be loaded on the gel to be able to see the chemi-luminescence signal (Figure 6-7). This suggested that *ck* might be present in very low quantities (enough to show

enzyme activity) in uninfected and infected erythrocytes but not enough to be detected by immuno-pulldowns or western blot analysis.

```

HumanCKmt      MAGPFSRLLSARPGRLRLLAGAGSLAAGFLLRPEPV-RAASERRRLYPSPAIEYDPLRKH 59
MusCKmt1_     MAGPFSRLLSARPGRLRLLAGAGSLTAGILLRPEVSGAAAERRLYPSPAIEYDPLRKH 60
MusCKmt2_     MASAFSKLLTGRNASLLFTTLGTALTTGYLLNRQKVSADAREQHKLFPPSADYDPLRKH 60
MusCK-M_      -----MPFGNTHNKFKLNYKPKQEYDPLSKH 26
MusCK-B_      -----MPFSNSHNTQKLRFPFAEDEFDPLSSH 26
                .           :   : .. : : * * * . *

HumanCKmt      NNCMASHLTPAVYARLCDKTTPTGWTLDQCIQTGVDPNGHPFIKTVGMVAGDEETYEYVFA 119
MusCKmt1_     NNCMASHLTPAVYARLCDKTTPTGWTLDQCIQTGVDPNGHPFIKTVGMVAGDEETYEYVFA 120
MusCKmt2_     NNCMAECLTPTIYAKLRNKMTPSGYTLDQCIQTGVDPNGHPFIKTVGMVAGDEESYEYVFA 120
MusCK-M_      NNHMAKVLTPLDLYNKLKDKETPSGFTLDDVIQTGVDPNGHPFIMTVGCVAGDEESYTVFK 86
MusCK-B_      NNHMAKVLTPELYAELRAKCTPSGFTLDDAIQTGVDPNGHPYIMTVGAVAGDEESYDVFK 86
                * * * . * * * : * . * * * : * * * : * * * * * * * * * * * * * * * * * * * *

HumanCKmt      DLFDPIQDRHNGYDPRMKTDLTDLASKIRSG-YFDERYVLSRVRTGRSIRGLSLPPA 178
MusCKmt1_     ELFDPIQDRHNGYDPRMKTDLTDLASKIRSG-YFDERYVLSRVRTGRSIRGLSLPPA 179
MusCKmt2_     DLFDPIQDRHNGYDPRVMKHTDLTDLASKITHG-QFDERYVLSRVRTGRSIRGLSLPPA 179
MusCK-M_      DLFDPIIQDRHGGYKP-TDKHKTDLNHNENLKGDDLDPNYVLSRVRTGRSIRKGYTLPPH 145
MusCK-B_      DLFDPIIEERHGGYQP-SDEHKTDLNDPNLQGGDDLDPNYVLSRVRTGRSIRGFCLPPH 145
                : * * * * * : * * * * * : * * * * * : * * * * * : * * * * * : * * * * *

HumanCKmt      CTRAERREVERVVVDALSGLKGLDLAGRYRLESEMTEAEQQQLIDDHFLFDKPVSPLLTAA 238
MusCKmt1_     CTRAERREVERVVVDALSGLKGLDLAGRYRLESEMTEAEQQQLIDDHFLFDKPVSPLLTAA 239
MusCKmt2_     CSRAERREVENVAITALEGLKGLDLAGRYRLESEMTEAEQQQLIDDHFLFDKPVSPLLTCA 239
MusCK-M_      CSRGERRAVEKLSVEALNSLTGEFKGKYPLKSMTEAEQQQLIDDHFLFDKPVSPLLLAS 205
MusCK-B_      CSRGERRAIEKLAVEALS SLDGDL SGRYYALKSMTEAEQQQLIDDHFLFDKPVSPLLLAS 205
                * : * . * * * : * : * : * * . * * : * : * * * * * * * * * * * * * * * * * :

HumanCKmt      GMARDWPDARGIWHNNEKSFLIWNNEEDHTRVISMEKGGNMKRVFERFCRGLKEVERLIQ 298
MusCKmt1_     GMARDWPDARGIWHNNEKSFLIWNNEEDHTRVISMEKGGNMKRVFERFCRGLKEVEKLIQ 299
MusCKmt2_     GMARDWPDARGIWHNYDKTFLIWIWNEEDHTRVISMEKGGNMKRVFERFCRGLKEVERLIQ 299
MusCK-M_      GMARDWPDARGIWHNDNKSFLVWVNEEDHLRVISMEKGGNMKEVFRFCVGLQKIBEIFK 265
MusCK-B_      GMARDWPDARGIWHNDNKTFLVWVNEEDHLRVISMQKGGNMKEVFRFCTGLTQIETLTK 265
                * * * * * * * * * * * * * * * * * * * * * * * * * * * * * * * * * * * * * * * * *

HumanCKmt      ERGWEFMWNERLGYILTCPSNLGTGLRAGVHIKLPKLSKDSRFPKILENLRQLQKRGTTGGV 358
MusCKmt1_     ERGWEFMWNERLGYILTCPSNLGTGLRAGVHIKLPKLSKDNRFPPKILENLRQLQKRGTTGGV 359
MusCKmt2_     ERGWEFMWNERLGYILTCPSNLGTGLRAGVHVRI PKLSKDPFRFSKILENLRQLQKRGTTGGV 359
MusCK-M_      KAGHPFMWNEHLGYVLTCPNSLGTGLRGGVHVKLANLSKHPKFEEILTRLRLQKRGTTGGV 325
MusCK-B_      SKNYEFMWNPGLGYILTCPSNLGTGLRAGVHIKLPKLSKHEKFEVSLKRLRLQKRGTTGGV 325
                . . * * * * : * * * : * * * * * * * * * * * * * * * * * * * * * * * * * *

HumanCKmt      DTAATGGVFDISNLDRLGKSEVELVQLVIDGVNYLIDCERRLERGQDIRIPTVHITKH- 417
MusCKmt1_     DTAATGGVFDISNLDRLGKSEVELVQLVIDGVNYLIDCERRLERGQDIRIPPLVHSHK- 418
MusCKmt2_     DTAAVADVYDISNIDRIGRSEVELVQLVIDGVNYLVDCEKLERGQDIKVPPLPQFGRK 419
MusCK-M_      DTAAVAVGFVDISNADRLGSSEVEVQLVVDGVKLMVEMEKLEKQGSIDDMI PAQK---- 381
MusCK-B_      DTAAVGGVFDVSNADRLGFSEVELVQMVVDGVKLLIEMEQRLEQQAIDDLMPAQK---- 381
                * * * * . * : * : * * * * * * * * * * * * * * * * * * * * * * * *

```

Figure 6-6 Antibody ab76506 from Abcam was raised against a 91 amino acid fragment of human Mtck (in red) conserved in the mouse mitochondrial isoform.

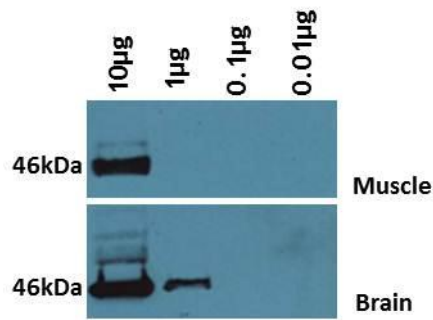


Figure 6-7 Western blot analysis using ab76506 showing titration of protein content from positive controls. Top panel- mouse muscle homogenate, bottom panel- mouse brain homogenate.

Since the relative specific activity in the erythrocytes was only one-thirtieth that in the control cells, it seems possible that the quantity of *ck* present in the erythrocytes is below the limit of detection.

### 6.2.5 Creatine kinase inhibition: effect on *P. berghei* development

The finding of phosphocreatine in gametocyte infected erythrocytes and its conversion to creatine with release of ATP during exflagellation indicated a possible role for this metabolite in the development of gametes. FDNB (1-fluoro-2,4-dinitrobenzene) is a membrane permeating reagent that forms a covalent derivative with a single cysteine residue to inactivate *ck* (Mahowald, Noltmann et al. 1962). As it is an amino and sulfhydryl group reagent (Sanger 1945) it has the potential to react with many targets (Tombes and Shapiro 1985). However, it has been shown that in specificity studies done in sea urchin sperm, ATPase and Myokinase activity as well as sperm respiration, motility and fertilisation were found to be totally resistant to FDNB even at concentrations of 20-50  $\mu\text{M}$  while it inhibited *ck* activity with an  $\text{IC}_{90}$  value of around 10  $\mu\text{M}$  (Tombes and Shapiro 1985). Also in a study done on rabbit *ck* isoforms, it was found that FDNB had specific activity with an  $\text{IC}_{90}$  value of 10  $\mu\text{M}$  and when calculated, the  $\text{IC}_{50}$  values for Cyt-*ck* and Mt-*ck* were found to be 101.8nM and 96.6nM respectively (Yang and Dubick 1977). Therefore FDNB can be used to inhibit *ck* specifically below 1  $\mu\text{M}$  range.

Standard *in vitro* inhibition tests against different *P. berghei* stages (Section 2.1.20) using FDNB showed that within the specificity range of under 1  $\mu\text{M}$ , schizogony and ookinete development are not affected but exflagellation (a rapid process where post-activation, male gametocytes undergo three rounds of

endomitosis and an axoneme assembly finally releasing eight microgametes in just 10-12 minutes) is highly impaired with an  $IC_{50}$  of 23.7 nM (Figure 6-8A). Addition of exogenous ATP (100 nM) during incubation with the inhibitor before activation and during activation rescued exflagellation (Figure 6-8B) induced by the inhibitor. This suggested that *ck* mediated conversion of phosphocreatine to ATP and creatine is necessary for complete exflagellation and male gamete formation and a possible ATP transport mechanism between the host, the parasite and the extra-cellular environment must play a role.

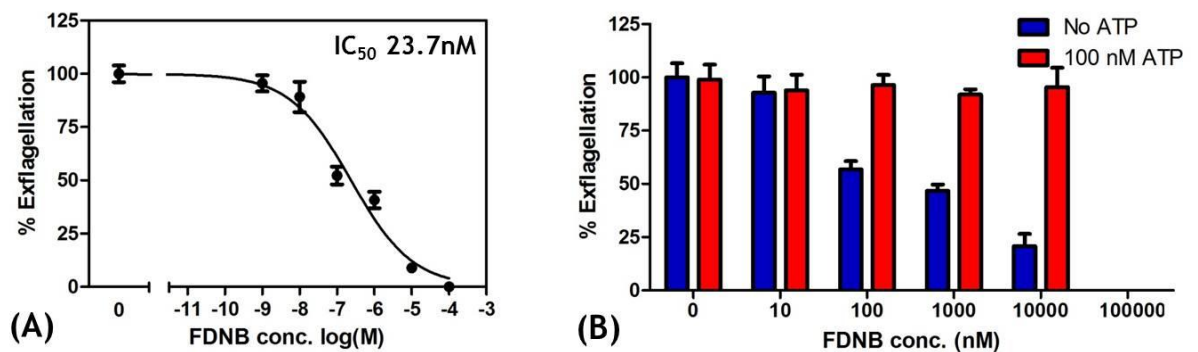


Figure 6-8 Exflagellation inhibition and rescue. (A) FDNB inhibits exflagellation with an  $IC_{50}$  23.7nM. (B) Addition of exogenous ATP rescues exflagellation inhibition by FDNB). Error bars indicate n=3 biological replicates.

Immunofluorescence staining was done using an anti-tubulin antibody to stain the male gametocytes and gametes and anti-Ter119 antibody to stain the erythrocyte surface to establish whether with *ck* inhibition, DNA replication takes place in male gametocytes post-activation and whether gametes emerge from the host erythrocyte. It showed that DNA replication is not affected by *ck* inhibition but the gametes did not emerge (Figure 6-9).

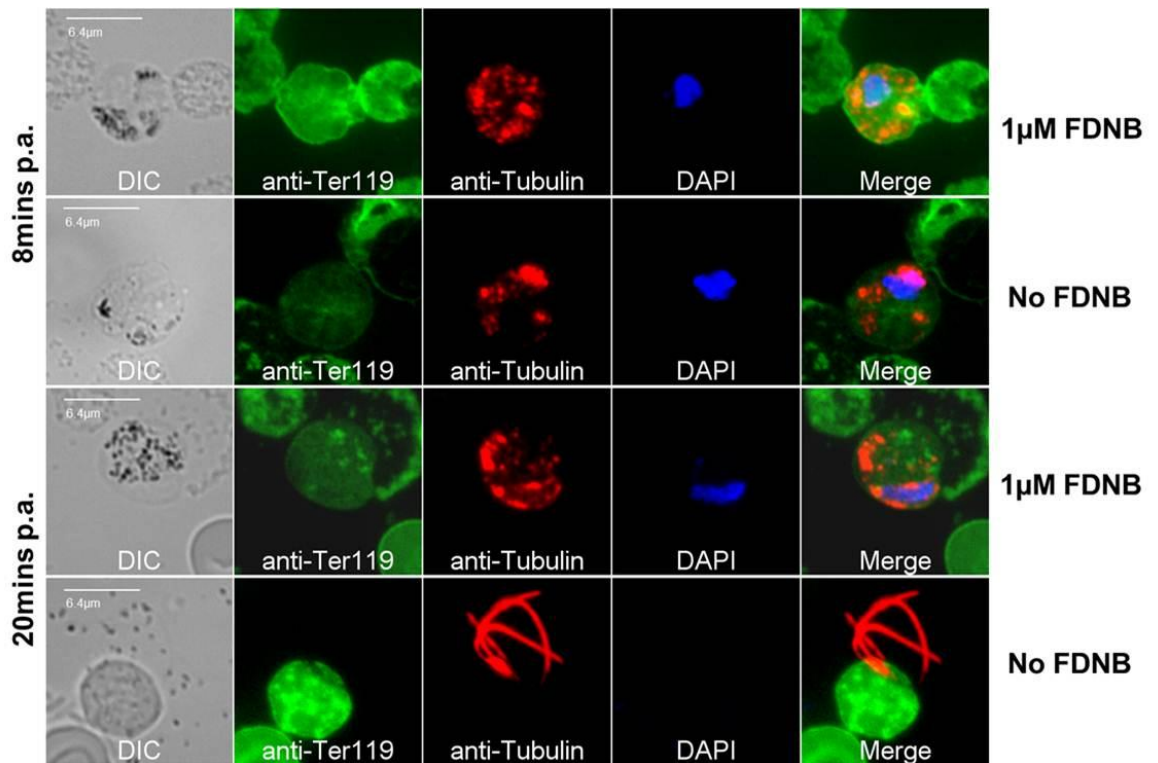


Figure 6-9 Immunofluorescence assay: *ck* inhibition during exflagellation. DIC (bright field), anti-Ter119 (green) stains the erythrocyte surface, anti-tubulin (red) stains male gametocytes and gametes, DAPI (blue) stains DNA. During exflagellation, DNA replication is completed by eight minutes and gametes emerge from host cell between 12-20 minutes. DAPI staining is not observed in 20mins p.a. no FDNB control because DNA is segregated into eight individual slender gametes.

The ATP mediated rescue of exflagellation inhibition by FDNB lead to investigation of ATP transport by the infected erythrocyte or parasite membrane. ATP-ADP translocase (usually present in the inner mitochondrial membrane) mediates ATP transport across the membrane. Bongrekinic Acid (BA) blocks the ATP-ADP translocase from the inner side of the membrane, while Carboxyatractyloside (CA) blocks the ATP-ADP translocase from the outer side of membrane (Kunji and Harding 2003). Neither BA nor CA affected the exflagellation process. However when tested in the presence of FDNB and exogenous ATP, adding CA reversed the exogenous ATP mediated rescue of FDNB induced exflagellation inhibition while adding BA did nothing (Figure 6-10).

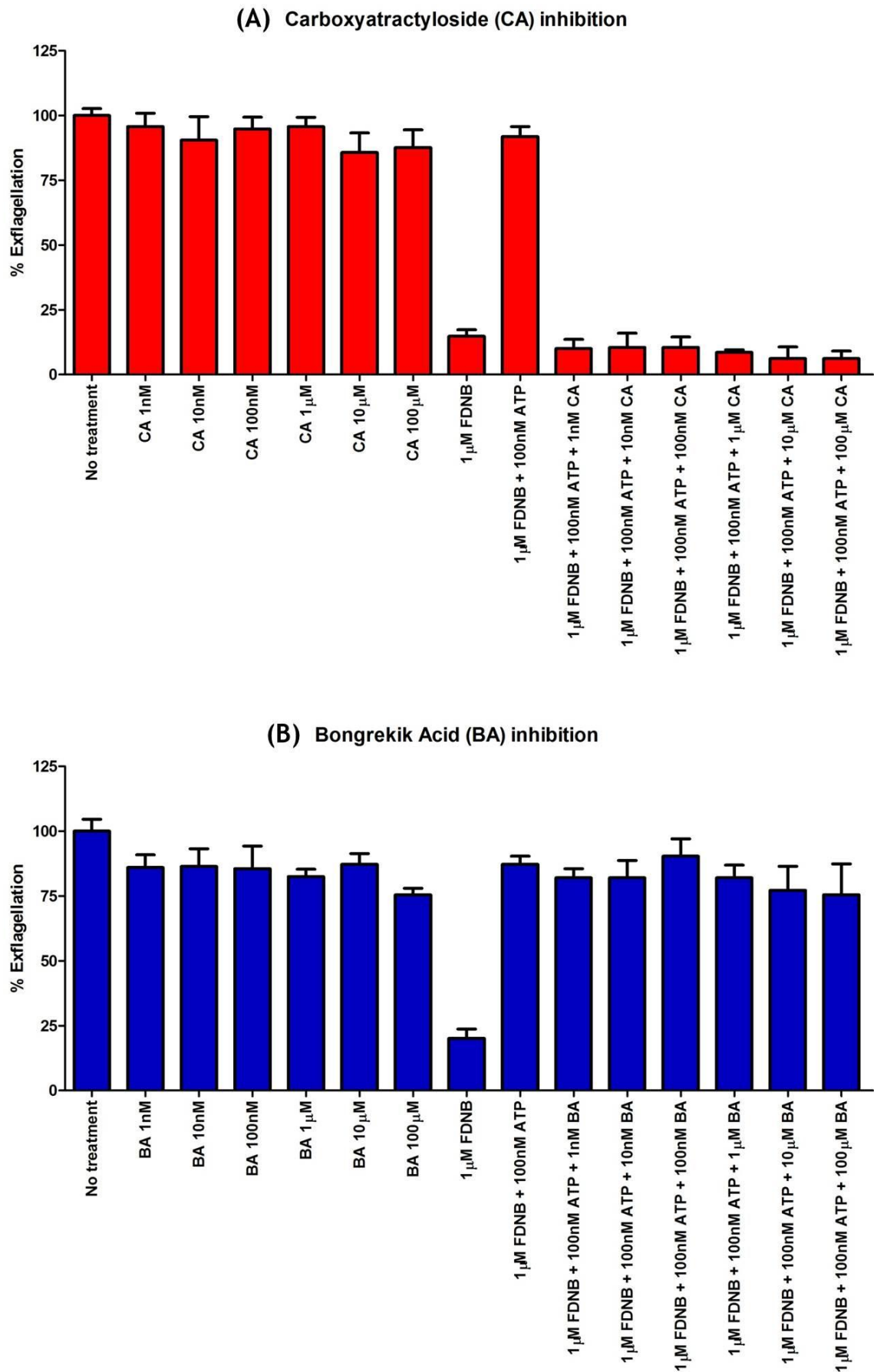


Figure 6-10 Effect of ATP/ADP translocase inhibition. (A) Carboxyatractyloside (CA) doesn't affect the process of exflagellation but reversed the exogenous ATP mediated rescue of

FDNB induced exflagellation inhibition. (B) Bongrekik Acid (BA) doesn't affect the process of exflagellation and could not reverse the exogenous ATP mediated rescue of FDNB induced exflagellation inhibition. Error bars indicate n=3 biological replicates.

### 6.3 Discussion

The confirmed discovery of high levels of phosphocreatine in reticulocytes and gametocytes when compared to schizonts was intriguing and pointed towards storage in the host compartment. The absence of a *ck* homologue in *Plasmodium* suggested that host *ck* may play a role in utilising the phosphagen system and enzyme activity assays in uninfected and infected whole cells confirmed *ck* activity although to a much lower level compared to muscle or brain tissue where it is a major contributor in energy metabolism. Although it was unexpected to find evidence of a phosphagen system in mammalian erythrocytes, it has been reported before in red blood cells of rainbow trout where significant *ck* activity was discovered, albeit at a lower level compared to glycolytic and TCA cycle enzymes (Walsh, Wood et al. 1990). One important similarity between trout erythrocytes (Tiano, Ballarini et al. 2000) and reticulocytes (Gronowicz, Swift et al. 1984) is the existence of mitochondria which are not present in mature normocytes and *ck* has two mitochondrial isoforms (Ellington and Suzuki 2007) and it is possible that this is the site of production of PCr in reticulocytes. *ck* is capable of phosphorylating creatine to produce phosphocreatine for storing energy derived from the ATP produced by the TCA cycle or oxidative phosphorylation. This Cr-PCr system has been shown to facilitate cellular energy transport from the site of ATP production to the site of ATP utilisation where *ck* can again release the phosphate group to transfer energy to demanding processes (Greenhaff 2001). It has been shown in our data in the previous section that reticulocytes are capable of both glycolysis and TCA cycle metabolism; whether they are capable of utilising the phosphagen system as well is unclear.

Inhibition of *ck* activity by FDNB only affected exflagellation and male gamete formation in the parasite life cycle within the specificity range of under 1  $\mu\text{M}$  the inhibitor FDNB (although schizogony and ookinete development were inhibited if FDNB was added at 10 $\mu\text{M}$  or more and off target effects cannot be ruled out). There was no notable effect on the emergence of female gametes either. Addition of exogenous ATP seemed to rescue exflagellation which was otherwise found to be inhibited by the *ck* inhibitor. This suggested either that

exflagellating cells need ATP beyond that which can be provided by glycolysis/the TCA cycle or that compartmentalisation of energy generation requires utilisation of host derived ATP for gamete emergence from the erythrocyte and host phosphagen system fulfils this need. It also pointed towards the existence of an ATP transporter in these cells. Experiments with CA showed that an ATP/ADP translocator may exist on the parasite membrane and while an adenylate translocase is present on the parasite mitochondrial membrane, its existence on the parasite membrane has also been previously speculated (Hatin, Jambou et al. 1992).

#### **6.4 Conclusion**

It was shown that gametocyte infected erythrocytes store phosphocreatine as a rapid-release energy source allowing exflagellation of male gametes during the mosquito stages. The high energy demanding process of exflagellation was shown to depend on this phosphagen system and targeting the host *ck* enzyme could be novel transmission blocking strategy as the parasite will not be able to develop resistance against host interventions. Such inhibitors will have to be designed so that they target only the infected host cells, possibly through the new permeability pathways as *ck* is indeed an important enzyme for host physiology in muscle and brain tissue.

## 7 Summary

Metabolomics is a great tool for unravelling the biochemistry of biological systems and in light of the presented data, it became clearer that it can reveal new information about the system studied and add functional information to the data obtained from other 'omics' technologies. One of the first challenges for us was the identification and quantification of metabolites in our samples which was done by existing software and data analysis platforms such as IDEOM (Creek, Jankevics et al. 2012) and Agilent Chemstation. There is room for improvement in terms of scale and user interface in these software and these technologies are constantly improving, which will hopefully make future analyses easier.

To establish the metabolite to pathway to gene connection was the next step which helped us focus on some very interesting aspects of host and parasite metabolism leading to new hypotheses generation and experimental validation using reverse genetics and/or reverse biochemistry experiments. One of the most exciting findings was the discovery of unexpected and novel metabolic pathways in the host reticulocytes and *P. berghei* gametocytes. The discovery of GABA metabolism in *P. berghei* ookinetes was another unexpected discovery which pointed towards the possibility of novel intervention strategies for transmission blocking.

The metabolic profile of reticulocytes was found to be more complex than normocytes and *P. berghei* parasites were shown to have overlapping metabolism with their preferred host cell types. A similar comparison study is being done with human reticulocytes and normocytes with our collaborators to be able to draw more conclusions about the biochemistry of the host-parasite interaction of the human reticulocyte preferring parasite *P. vivax*. However, the current difficulties in sustained *in vitro* culturing, genetic modification and phenotypic analyses of *P. vivax* parasites (Noulin, Borlon et al. 2013) are big challenges. Use of erythroid progenitor stem cells to generate laboratory adapted reticulocyte cultures which could be used for *P. vivax* propagation is being explored to help this (Panichakul, Sattabongkot et al. 2007, Noulin, Borlon et al. 2012). Nevertheless, it can still be concluded that because *P. vivax* parasites reside in a metabolically rich host cell, the host metabolism needs to be taken into consideration when designing new vaccines and drug targets. When it comes to *P. falciparum* which invade both reticulocytes and normocytes, our

data suggests that it is possible that targeting only parasite metabolism might put a selection pressure on parasites with a preference for invading reticulocytes and contribute to increased drug resistance.

The metabolic differences between the asexual and sexual stages of *P. berghei* parasites emphasised on how the gametocyte prepares itself for the hostile environment of the mosquito midgut at the metabolic level by possibly employing the host phosphagen system. However, the localisation of the key enzyme, creatine kinase, which facilitates this process, has proved elusive so far in the infected erythrocyte and the potential for designing new antibodies to localise it is being explored. The targeted metabolomics approach which was used to establish carbon metabolism in different stages in the life cycle of *P. berghei* surprisingly showed that GABA ( $\gamma$ -Aminobutyric acid) may act as an energy source during the ookinete stage and is being further investigated.

## 8 Future work

Apart from the above mentioned work currently being carried out to further the knowledge in studies described in the previous sections, other interesting leads which were identified in section 4 but which could not be worked on completely due to time constraints are listed below. These could form the basis for future studies in *Plasmodium* metabolism.

### 8.1 Pantothenate metabolism

Pantothenate has been shown to be essential for *P. falciparum* blood stage survival and is required for the synthesis of coenzyme A (CoA), an enzyme cofactor involved in numerous metabolic reactions in the cell. Pantothenate is converted to CoA via five universal enzyme-mediated steps and in the first step, *P. falciparum* uses Pantothenate kinases (PankKs) to trap, phosphorylate and commit pantothenate to CoA synthesis and accumulate it (Spry and Saliba 2009). This however is not the case for many mammalian cells which can accumulate pantothenate in its non-phosphorylated form (Spry, van Schalkwyk et al. 2010) .

There are two (PankKs) in *Plasmodium* and both are cytosolic.

1. PBANKA\_102260 (*P. falciparum* homologue PF3D7\_1420600)
2. PBANKA\_061140 (*P. falciparum* homologue PF3D7\_1437400)

By examining our metabolomics data (Table 5), it was found that the levels of a putative metabolite (PM) annotated as pantothenate were up-regulated in gametocytes when compared to schizonts by about 13 fold. However the levels of a PM annotated as 4'-phosphopantothenate were found to be downregulated in gametocytes by about 8 fold when compared to schizonts. Non-phosphorylated pantothenate was not detected in uninfected reticulocytes or normocytes. 4'-phosphopantothenate was detected in uninfected erythrocytes but their levels were not different between reticulocytes and normocytes (Figure 8-1).

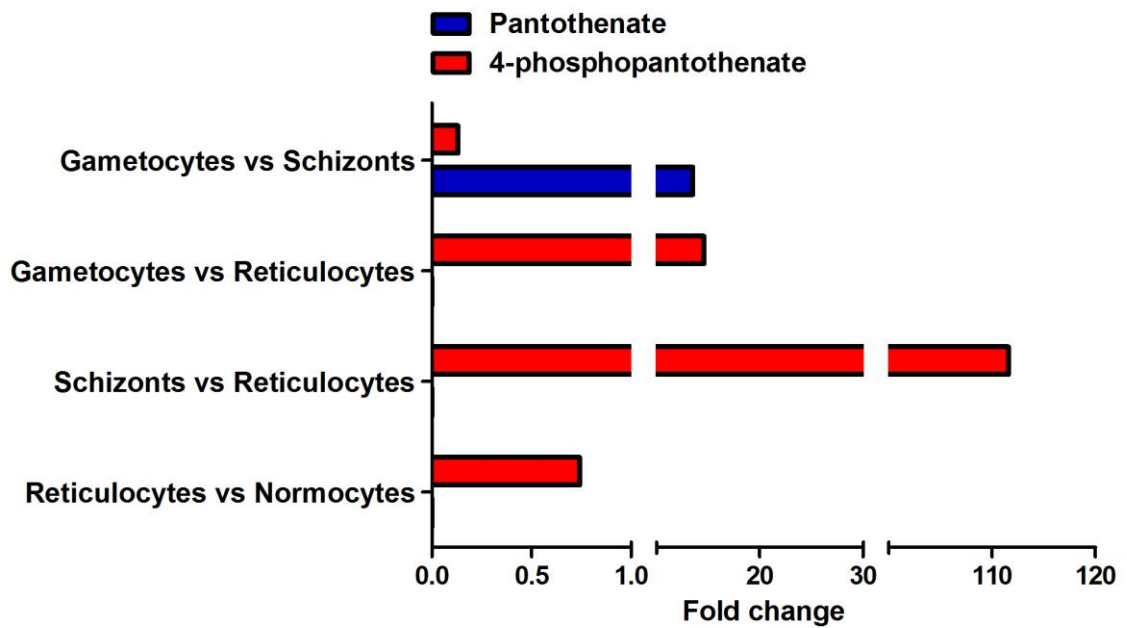


Figure 8-1 Fold change of Pantothenate and Phosphopantothenate as observed in different sample groups compared in the untargeted metabolomics study.

It was intriguing that gametocytes had more of the non-phosphorylated version of pantothenate whereas schizonts had the phosphorylated version of pantothenate. RNAseq data generated in our lab (unpublished, A. Religa personal communication), showed that in *P. berghei*, expression levels of Pank 1 (PBANKA\_102260) are low in all asexual stages but higher in gametocytes and ookinetes. Expression levels of Pank 2 (PBANKA\_061140) are low in the asexual ring stage and gametocytes but higher in late trophozoite and schizonts and highest in ookinetes. This implied that there could be an additional role of pantothenate kinases in mosquito stage development.

Preliminary experiments revealed that both pantothenate kinases could be readily deleted individually and a double knockout was also possible indicating that this enzyme activity is not required for blood stage development (data not shown). Gametocyte, gamete and ookinete production was similar to those achieved by wild type parasites, however, there was a defect observed in ookinete to oocyst transition resulting in a block in transmission in these mutant parasites (data not shown- not enough biological replicates done yet). This suggested that gametocytes could possibly phosphorylate pantothenate in mosquito stages where they utilise the co-A biosynthetic pathway during ookinete to oocyst transition. Phenotypic experiments with the double knock out and a planned targeted metabolomics experiment could reveal the extent of

dependence of gametocytes on pantothenate phosphorylation for mosquito transmission. We have also explored the possibility using PanK inhibitors as a malaria intervention strategy and are currently testing some of these inhibitors against the wt and PanK mutant *P. berghei* parasites.

## 8.2 Carnitine derivatives

Carnitine is synthesised from lysine and methionine in mammals in a four step pathway, the main enzymes for which are N-trimethyl-lysine dioxygenase (TMLD), 3-hydroxy- N-trimethyl-lysine aldolase (HTMLA), 4-trimethylaminobutyraldehyde dehydrogenase (TMABA-DH) and  $\gamma$ -butyrobetaine dioxygenase (BBD) (Vaz and Wanders 2002). The homologues of carnitine biosynthesis enzymes are not encoded by *Plasmodium* genome (Gardner, Hall et al. 2002). Carnitine helps in transport of fatty acids from the cytosol into the mitochondria during the breakdown of lipids for the generation of metabolic energy by their beta oxidation (Steiber, Kerner et al. 2004). Elevated levels of acyl-carnitine derivatives were detected in reticulocytes when compared to normocytes (Table 2) and in *P. berghei* gametocytes when they were compared to *P. berghei* schizonts (Table 5) in the untargeted metabolomics study. As there are no obvious homologues of enzymes that facilitate the transfer of these acyl-carnitine derivatives across the *Plasmodium* mitochondrial membrane (Carnitine palmitoyl transferases and translocases) or those which take part in  $\beta$ -oxidation in *Plasmodium* (Gardner, Hall et al. 2002), it is possible that, like phosphocreatine, these carnitine derivatives are host (reticulocyte) derived and are stored in gametocytes but not in schizonts. It is therefore likely that gametocytes may utilise these carnitine conjugated acyl moieties in the mosquito stages where serum fatty acids are limiting to make or extend fatty acids.

If the gametocytes are able to internalise these metabolites and carry them forward to the ookinete-oocyst stage, this could provide the answer to the long standing question of the source of fatty acid synthesis in *P. berghei* oocysts. In a newly formed oocyst on a mosquito basal lamina, after a growth phase, asexual mitotic replication results in the formation of a mature oocyst that contains thousands of daughter cells (sporozoites). The oocysts increase in size from 2-3  $\mu\text{m}$  in diameter to about 40  $\mu\text{m}$  within 10-13 days. All of the daughter cells need new membranes and hence, fatty acids. The FASII pathway is dispensable for

blood stage schizogony as fatty acids can be scavenged from host serum which is rich in these lipids (Vaughan, O'Neill et al. 2009) but not for liver stage schizogony - comparable to oocyst sporogony where again it is dispensable. This is not true for *P. falciparum* where FASII is essential for oocyst development (van Schaijk, Kumar et al. 2013), but as *P. falciparum* is not a reticulocyte preferring parasite, it probably does not have access to the acyl-carnitine derivatives seen in our *P. berghei* data.

Antibodies against specific acyl carnitine conjugates could be used to check for localisation in gametocytes, ookinetes and oocysts. Another way to test this hypothesis (although more difficult) would be to try labelling carnitines in the host animal by feeding heavy labelled methionine and lysine and infecting them with *P. berghei*, then doing a targeted metabolomics experiment with gametocyte and ookinete stages. It would still be very challenging to do any metabolomics studies on oocysts, due to logistical reasons and difficulty in getting enough material from mosquito dissections.

### **8.3 *Plasmodium* specific metabolic pathways**

A number of metabolites which were specific to *P. berghei* schizont and gametocyte stage and absent or reduced in uninfected erythrocytes (reticulocytes) were observed in the untargeted metabolomics data (Table 3 and Table 4). Most notable of these were fatty acids and their derivatives specific to the parasite, metabolites of arginine and proline metabolism, folate biosynthesis and energy metabolism. Of these, the metabolites implicated in energy metabolism were studied in great detail using targeted metabolomics and the data is described in section 5 above. All the metabolites which were putatively identified were previously known and no novel drug targets could be highlighted from this comparison. However, it is possible to go back to the raw MS data and look for metabolite peaks which were detected specifically in parasite samples but could not be identified. If such peaks could be identified and charted on to a metabolic pathway, there is a potential for finding new metabolic pathway(s) specific to the parasite.

This should however be done with caution as focussing on the parasite alone can lead to development of resistance and loss of efficacy of the potential inhibitor as from our data it is evident that host cell metabolism is of utmost importance.

## 9 Appendix

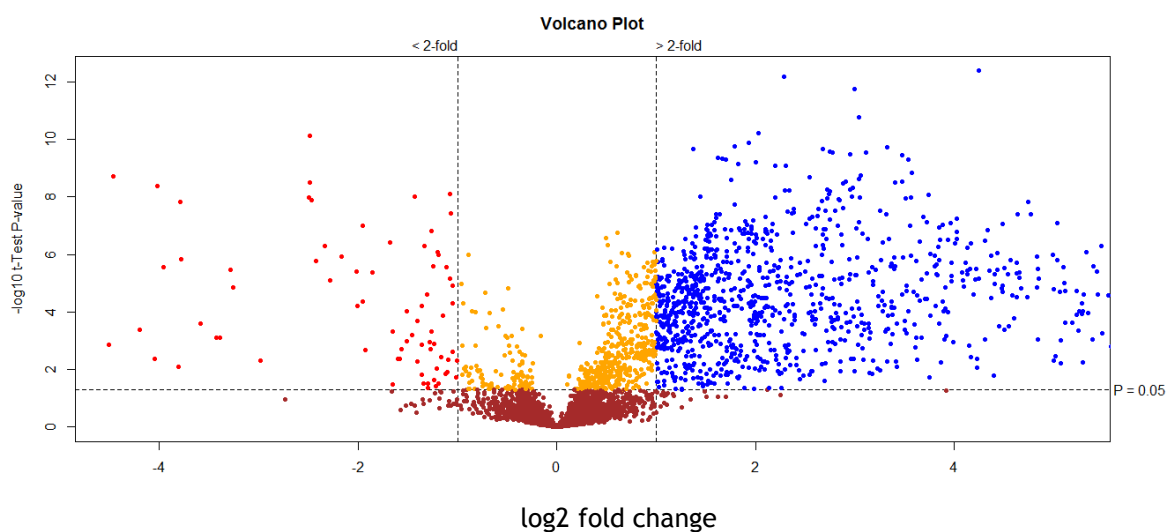


Figure 9-1 Volcano plot showing the distribution of abundance of all 4560 peaks detected in uninfected reticulocyte enriched erythrocytes as compared to uninfected normocyte enriched erythrocytes in rodent blood. All significant changes are represented above the broken horizontal line. Coloured dots indicate metabolites which are: Blue- significantly up-regulated, Red- significantly down-regulated, Yellow- significant but little change, Brown- non-significant.

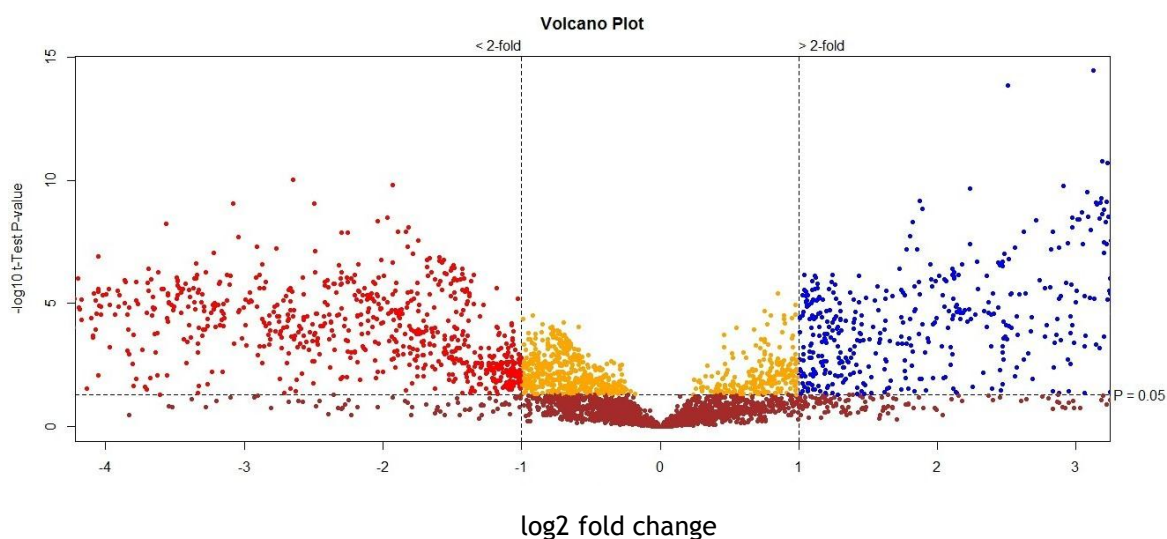
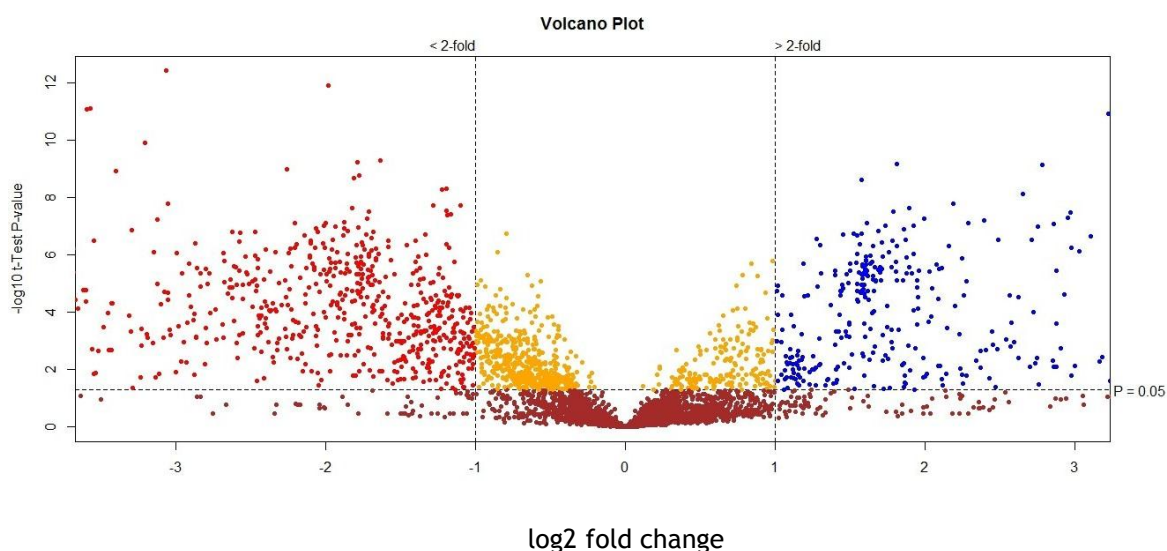
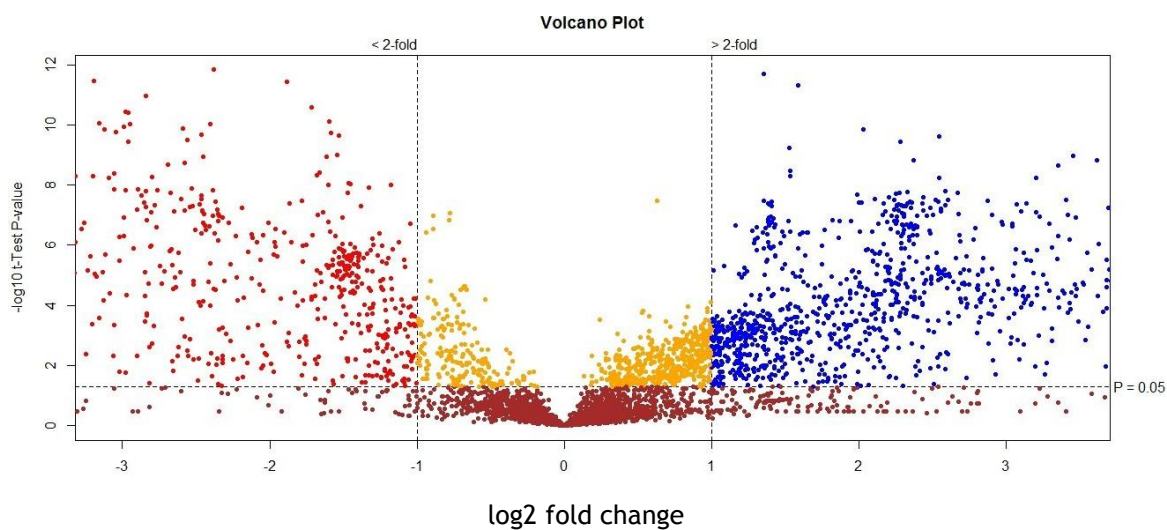


Figure 9-2 Volcano plot showing the distribution of abundance of all ~5000 peaks detected in *P. berghei* schizonts as compared to uninfected reticulocyte enriched erythrocytes. All significant changes are represented above the broken horizontal line. Coloured dots indicate metabolites which are: Blue- significantly up-regulated, Red- significantly down-regulated, Yellow- significant but little change, Brown- non-significant.



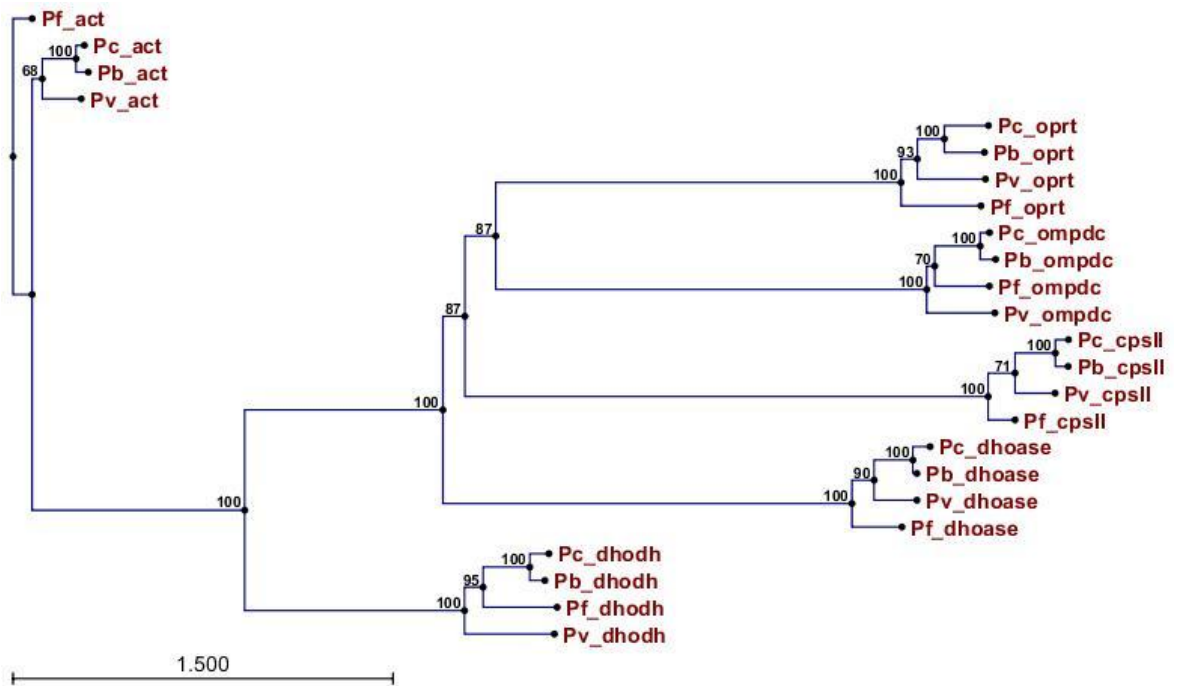
**Figure 9-3** Volcano plot showing the distribution of abundance of all ~5000 peaks detected in *P. berghei* gametocytes as compared to uninfected reticulocyte enriched erythrocytes. All significant changes are represented above the broken horizontal line. Coloured dots indicate metabolites which are: Blue- significantly up-regulated, Red- significantly down-regulated, Yellow- significant but little change, Brown- non-significant.



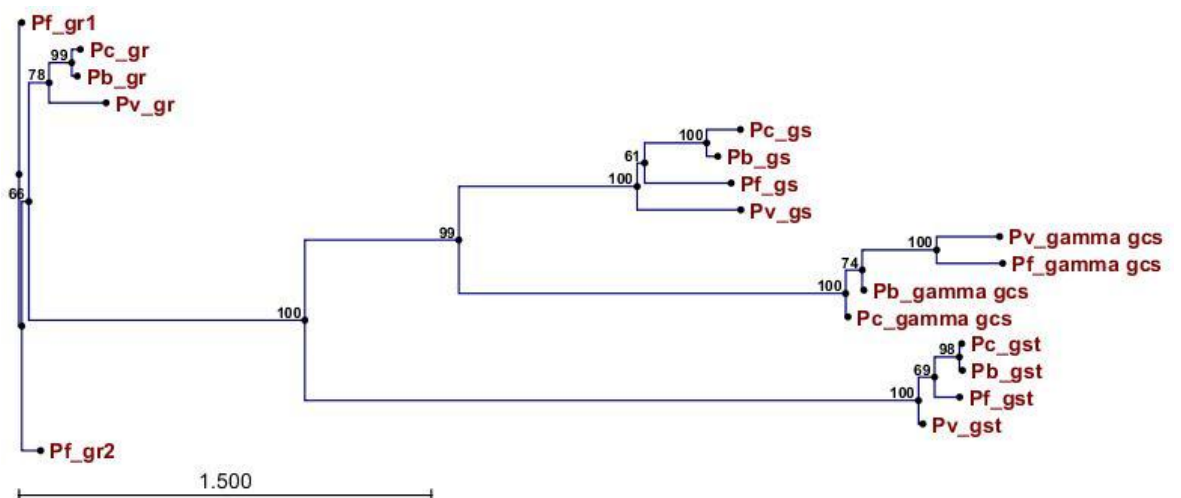
**Figure 9-4** Volcano plot showing the distribution of abundance of all ~5000 peaks detected in *P. berghei* gametocytes as compared to *P. berghei* schizonts. All significant changes are represented above the broken horizontal line. Coloured dots indicate metabolites which are: Blue- significantly up-regulated, Red- significantly down-regulated, Yellow- significant but little change, Brown- non-significant.



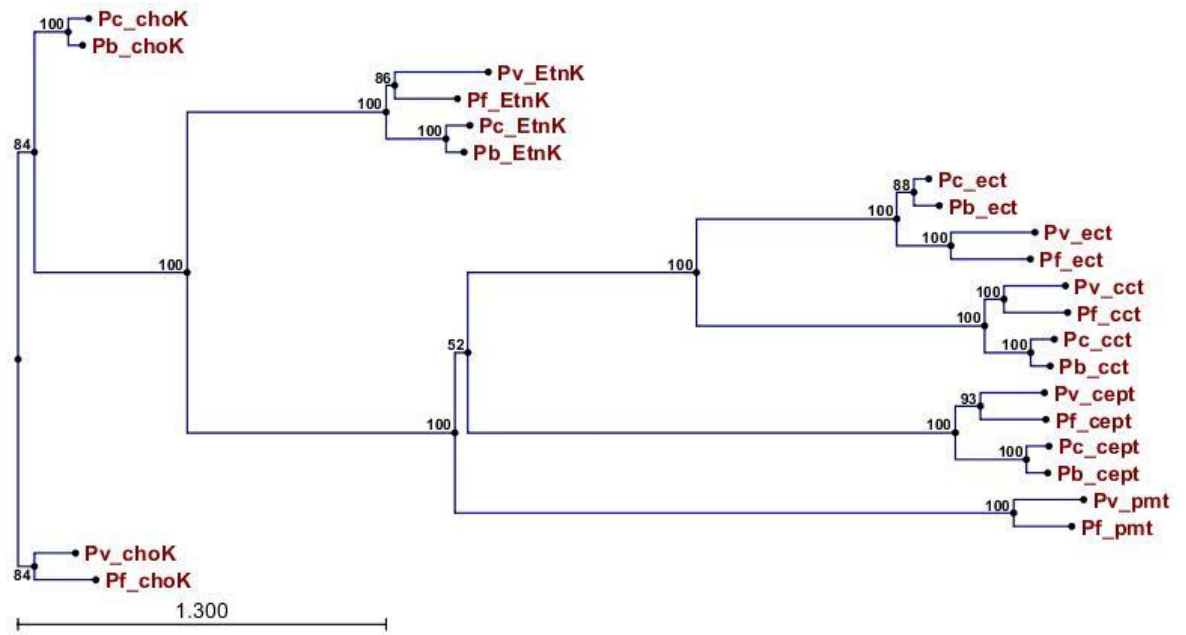
(A) ICM enzymes: amino acid sequence alignment tree



(B) Pyrimidine biosynthesis enzymes: amino acid sequence alignment tree



(C) Glutathione biosynthesis enzymes: amino acid sequence alignment tree



(D) Phospholipid biosynthesis enzymes: amino acid sequence alignment tree

Figure 9-5 Phylogenetic analyse of key metabolic enzymes in *Plasmodium* spp. Pb- *P. berghei*, Pc- *P. chabaudi*, Pf- *P. falciparum*, Pv- *P. vivax*. See Table 7 for the complete list of metabolic enzymes used in these analyses.

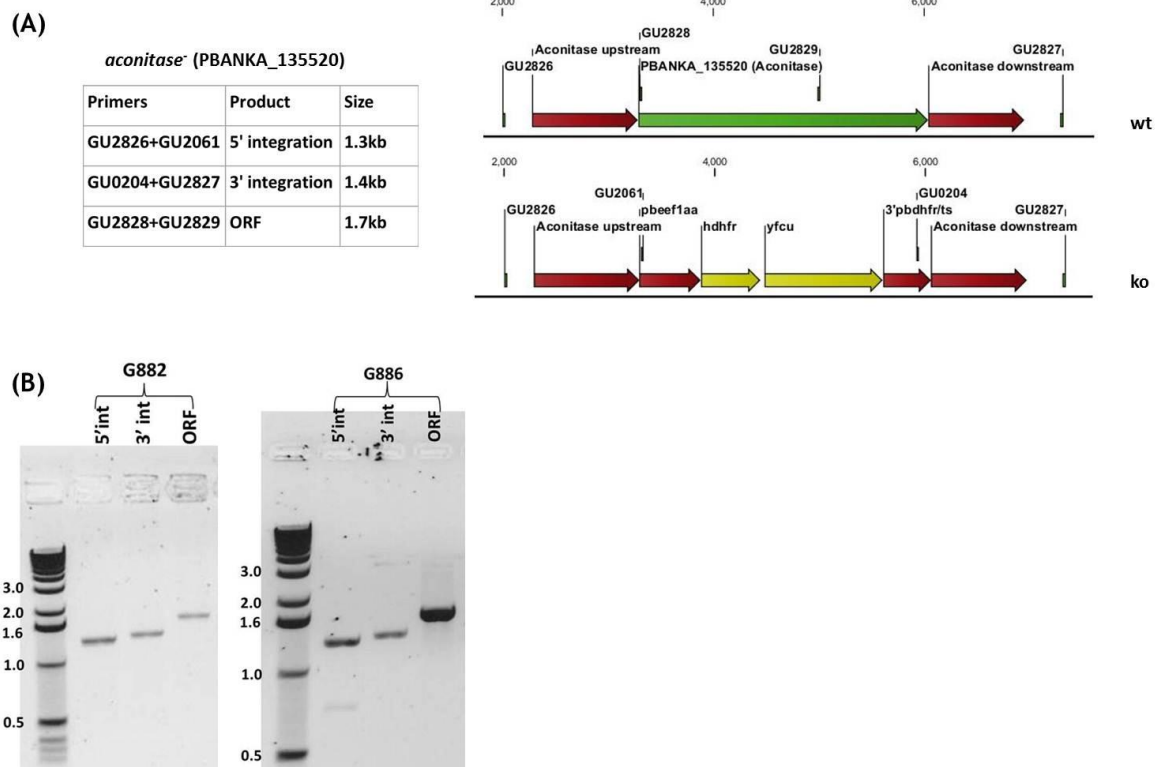


Figure 9-6 (A) Schematic representation of gene deletion strategy for *aconitase*<sup>-</sup> (PBANKA\_135520) in *P. berghei* parasites. (B) Gel electrophoresis of indicated PCR products to confirm integration of selection cassette, disruption of genes and clonality of mutant parasites. G882 was made in a wt parent line which expresses GFP in male gametocytes under the dynein heavy chain promoter and RFP in female gametocytes under the LCCL domain-containing protein CCP2 promoter (RMgm-164). G886 was made in a wt parent line expressing GFP constitutively under the *eef1a* promoter (RMgm-7). The presence of *orf* in both transfectants populations shows that the line is uncloned. Cloning and subsequent phenotypic characterisation of *aconitase*<sup>-</sup> *P. berghei* parasites is underway.

Table 2 Putative metabolites (PMs) represented in

Figure 3-2 showing fold change in abundance in uninfected reticulocyte enriched erythrocytes compared to normocyte enriched erythrocytes. Column 4 shows fold change corrected for the presence of 65% normocytes in uninfected reticulocyte enriched erythrocyte extracts. PMs are listed in order of decreasing abundance (metabolites identified with authentic standards are highlighted bold)

No.	Metabolite	Fold change	Fold change (corrected for presence of 65% normocytes)	P-value	Platform
1	Citric acid	>25 fold	>25 fold	9.65E-07	GC-MS
2	UMP	>25 fold	>25 fold	1.03E-02	GC-MS
3	Nonanoylcarnitine	>25 fold	>25 fold	8.40E-06	LC-MS
4	S-Methyl-L-methionine	>25 fold	>25 fold	1.01E-05	LC-MS
5	Ala-Val-Pro-Ser	>25 fold	>25 fold	1.64E-06	LC-MS
6	Dihydrobiopterin	>25 fold	>25 fold	9.59E-05	LC-MS
7	N-Acetyl-aspartyl-glutamate	>25 fold	>25 fold	3.80E-11	LC-MS
8	2-Amino-4-hydroxy-6-hydroxymethyl-7,8-dihydropteridine	>25 fold	>25 fold	3.98E-06	LC-MS
9	Aspartyl-L-proline	>25 fold	>25 fold	4.06E-05	LC-MS
10	sn-glycero-3-Phospho-1-inositol	>25 fold	>25 fold	2.48E-06	LC-MS
11	<b>L-Aspartate</b>	>25 fold	>25 fold	1.08E-05	LC-MS
12	Dodecanoylcarnitine	23.92	>25 fold	6.91E-06	LC-MS
13	CDP-choline	22.04	>25 fold	3.28E-04	LC-MS
14	UDP-N-acetyl-D-glucosamine	21.79	>25 fold	2.95E-08	LC-MS
15	O-Propanoylcarnitine	18.66	>25 fold	3.14E-06	LC-MS
16	Glycerophosphoglycerol	18.45	>25 fold	9.04E-05	LC-MS
17	<b>L-Carnitine</b>	17.81	>25 fold	3.18E-06	LC-MS
18	L-Octanoylcarnitine	17.47	>25 fold	5.88E-07	LC-MS
19	Glu-Asp	16.92	>25 fold	9.51E-07	LC-MS
20	N6-Acetyl-N6-hydroxy-L-lysine	15.71	>25 fold	2.71E-04	LC-MS
21	<b>Orotate</b>	15.68	>25 fold	1.00E-07	LC-MS
22	dCMP-ethanolamine	14.45	>25 fold	5.94E-06	LC-MS
23	Tetradecanoylcarnitine	13.99	>25 fold	4.84E-06	LC-MS
24	Sedoheptulose	13.30	>25 fold	1.02E-06	LC-MS
25	Gamma Glutamyl-glutamic acid	13.10	>25 fold	1.13E-04	LC-MS
26	Creatinine phosphate	12.79	>25 fold	3.60E-03	LC-MS
27	<b>Phosphocreatine</b>	12.32	24.64	4.50E-03	LC-MS
28	[GP (16:0)] 1-hexadecanoyl-2-sn-glycero-3-phosphate	10.43	20.86	1.81E-06	LC-MS
29	Glu-Pro	10.31	20.62	7.35E-05	LC-MS
30	L-Tyrosine methyl ester	10.15	20.3	2.82E-07	LC-MS
31	CDP-ethanolamine	10.03	20.06	3.21E-05	LC-MS
32	Ala-Asp-Asp	9.86	19.72	3.46E-06	LC-MS
33	dTTP	9.84	19.68	5.15E-07	LC-MS
34	<b>CMP</b>	9.75	19.5	7.49E-06	LC-MS
35	Prenyl-L-cysteine	9.73	19.46	5.95E-05	LC-MS
36	N2-Succinyl-L-ornithine	9.68	19.36	3.84E-07	LC-MS
37	N-(3S-hydroxydecanoyl)-L-serine	9.63	19.26	4.14E-05	LC-MS

38	Met-Thr-Asp	8.97	17.94	1.15E-05	LC-MS
39	<b>Malate</b>	8.55	17.1	2.82E-05	LC-MS
40	Ala-Ser-Tyr	8.46	16.92	5.50E-04	LC-MS
41	2,3,4,5-Tetrahydrodipicolinate	8.05	16.1	6.81E-05	LC-MS
42	<b>IMP</b>	7.75	15.5	5.83E-07	LC-MS
43	Ala-Cys	7.53	15.06	5.07E-06	LC-MS
44	<b>Xanthine</b>	7.36	14.72	1.10E-08	LC-MS
45	<b>Ribulose-5-phosphate</b>	7.33	14.66	7.69E-03	GC-MS
46	Acetylcholine	7.19	14.38	6.92E-06	LC-MS
47	<b>Choline phosphate</b>	7.10	14.2	1.59E-04	LC-MS
48	Glu-Gly	6.92	13.84	7.27E-06	LC-MS
49	<b>Fumarate</b>	6.90	13.8	1.03E-04	LC-MS
50	O-Butanoylcarnitine	6.84	13.68	2.96E-10	LC-MS
51	N-Acetyl-D-mannosamine	6.80	13.6	9.13E-07	LC-MS
52	N-Carbamoyl-L-aspartate	6.78	13.56	1.94E-05	LC-MS
53	Dihydroorotate	6.76	13.52	1.82E-06	LC-MS
54	Spermidine	6.71	13.42	2.74E-10	LC-MS
55	allylcysteine	6.42	12.84	6.51E-07	LC-MS
56	<b>Glycine</b>	6.41	12.82	1.50E-05	LC-MS
57	Thiomorpholine 3-carboxylate	6.35	12.7	5.69E-06	LC-MS
58	1-methylguanosine	6.11	12.22	1.89E-08	LC-MS
59	Gly-Pro	6.06	12.12	1.32E-07	LC-MS
60	Glu-Leu	5.95	11.9	1.50E-04	LC-MS
61	Leu-Thr	5.86	11.72	2.49E-05	LC-MS
62	Thr-Ala	5.85	11.7	1.05E-04	LC-MS
63	gamma-L-Glutamyl-L-cysteine	5.77	11.54	1.66E-06	LC-MS
64	1-Methyladenosine	5.69	11.38	9.08E-08	LC-MS
65	3-Hydroxy-N6,N6,N6-trimethyl-L-lysine	5.60	11.2	1.67E-02	LC-MS
66	O-hexanoyl-R-carnitine	5.54	11.08	5.41E-04	LC-MS
67	O-decanoyl-R-carnitine	5.35	10.7	5.33E-06	LC-MS
68	Malonylcarnitine	5.34	10.68	3.57E-04	LC-MS
69	<b>D-Ribose 5-phosphate</b>	5.29	10.58	3.61E-11	LC-MS
70	glucosamine-1,6-diphosphate	5.28	10.56	2.45E-11	LC-MS
71	N2-Acetyl-L-aminoadipate	5.24	10.48	1.24E-04	LC-MS
72	Leu-Pro	5.13	10.26	2.77E-06	LC-MS
73	2-Hydroxyadenine	5.02	10.04	1.52E-06	LC-MS
74	NG,NG-Dimethyl-L-arginine	4.99	9.98	2.55E-03	LC-MS
75	Fructoselysine 6-phosphate	4.95	9.9	2.90E-10	LC-MS
76	<b>D-Gluconic acid</b>	4.95	9.9	1.05E-04	LC-MS
77	D-Xylulose	4.77	9.54	1.06E-06	LC-MS
78	S-Methyl glutathione	4.72	9.44	1.54E-05	LC-MS
79	<b>sn-Glycerol 3-phosphate</b>	4.67	9.34	4.01E-11	LC-MS
80	Pseudouridine	4.64	9.28	3.97E-07	LC-MS
81	<b>Succinate</b>	4.41	8.82	2.10E-03	LC-MS
82	<b>Cytidine</b>	4.38	8.76	1.22E-03	LC-MS
83	Monomethyl-arginine	4.32	8.64	5.82E-03	LC-MS
84	Gamma-Aminobutyryl-lysine	4.30	8.6	1.56E-07	LC-MS

85	5-Methylcytidine	4.27	8.54	4.33E-09	LC-MS
86	Glu-Val	4.25	8.5	7.05E-05	LC-MS
87	Ala-Pro	4.22	8.44	5.39E-08	LC-MS
88	Pro-Pro	4.10	8.2	2.73E-06	LC-MS
89	[PC (16:0)] 1-hexadecanoyl-sn-glycero-3-phosphocholine	4.10	8.2	1.07E-04	LC-MS
90	-Hydroxy-eicosatetraenoic acid	4.10	8.2	2.54E-03	LC-MS
91	Xanthosine	4.05	8.1	8.44E-09	LC-MS
92	N-Acetyl-D-glucosamine 6-sulfate	4.00	8	1.12E-07	LC-MS
93	N-Acetyl-L-aspartate	3.91	7.82	4.80E-07	LC-MS
94	<b>Uridine</b>	3.63	7.26	8.83E-07	LC-MS
95	<b>3',5'-Cyclic AMP</b>	3.59	7.18	2.75E-05	LC-MS
96	N1-Acetylspermidine	3.44	6.88	1.54E-05	LC-MS
97	Glu-Ser	3.37	6.74	1.74E-05	LC-MS
98	<b>N-Acetylneuraminate</b>	3.33	6.66	4.47E-05	LC-MS
99	N-Acetyl-L-glutamate 5-semialdehyde	3.28	6.56	5.02E-06	LC-MS
100	Val-Val	3.25	6.5	7.95E-07	LC-MS
101	Asp-Asp	3.07	6.14	4.30E-10	LC-MS
102	Erythrose 1-phosphate	3.03	6.06	3.51E-05	LC-MS
103	Glu-Cys-Gln-Gln	3.01	6.02	9.51E-06	LC-MS
104	<b>Choline</b>	3.01	6.02	4.04E-05	LC-MS
105	N-Acetylserotonin	3.00	6	2.80E-05	LC-MS
106	Ala-Leu-Lys-Pro	2.99	5.98	1.31E-02	LC-MS
107	(1-Ribosylimidazole)-4-acetate	2.97	5.94	4.71E-08	LC-MS
108	O-Acetyl-L-homoserine	2.94	5.88	4.52E-04	LC-MS
109	1-Methylnicotinamide	2.93	5.86	4.96E-04	LC-MS
110	D-myo-Inositol 1,2-cyclic phosphate	2.92	5.84	7.41E-05	LC-MS
111	2-Carboxy-D-arabinitol 1-phosphate	2.91	5.82	2.91E-06	LC-MS
112	Glu-Thr	2.88	5.76	7.89E-05	LC-MS
113	<b>D-Erythrose 4-phosphate</b>	2.86	5.72	5.47E-10	LC-MS
114	Ala-Asp-Cys	2.82	5.64	3.04E-07	LC-MS
115	N3-(4-methoxyfumaroyl)-L-2,3-diaminopropanoate	2.78	5.56	2.32E-06	LC-MS
116	Ethanolamine phosphate	2.74	5.48	2.44E-03	LC-MS
117	Taurine	2.71	5.42	1.13E-03	LC-MS
118	Taurocyamine	2.70	5.4	2.20E-04	LC-MS
119	N-(L-Arginino)succinate	2.64	5.28	5.09E-05	LC-MS
120	<b>L-Arginine</b>	2.62	5.24	5.82E-06	LC-MS
121	<b>D-Glucose 6-phosphate</b>	2.61	5.22	9.22E-05	LC-MS
122	[SP] 3-dehydrosphinganine	2.60	5.2	8.90E-05	LC-MS
123	[SP] Sphing-4-enine-1-phosphate	2.59	5.18	2.21E-10	LC-MS
124	CMP-N-acetylneuraminate	2.53	5.06	1.72E-05	LC-MS
125	N2-(D-1-Carboxyethyl)-L-lysine	2.53	5.06	1.59E-03	LC-MS
126	Acetyl phosphate	2.51	5.02	1.02E-05	LC-MS
127	Hexose-phosphate	2.47	4.94	1.08E-04	LC-MS
128	Leucyl-leucine	2.46	4.92	4.24E-05	LC-MS
129	N-(octanoyl)-L-homoserine	2.46	4.92	2.88E-07	LC-MS
130	<b>Putrescine</b>	2.44	4.88	1.47E-06	LC-MS

131	<b>AMP</b>	2.44	4.88	6.68E-03	LC-MS
132	3-sulfopropanoate	2.42	4.84	8.40E-04	LC-MS
133	Leu-Val	2.39	4.78	4.89E-06	LC-MS
134	D-Methionine	2.35	4.7	9.33E-04	LC-MS
135	Ala-ala	2.31	4.62	3.03E-02	LC-MS
136	<b>Hypoxanthine</b>	2.29	4.58	4.84E-02	LC-MS
137	N5-Ethyl-L-glutamine	2.29	4.58	1.86E-02	LC-MS
138	N-Acetylglutamine	2.28	4.56	4.27E-05	LC-MS
139	<b>L-Glutamate</b>	2.22	4.44	1.01E-04	LC-MS
140	<b>L-Ornithine</b>	2.22	4.44	2.29E-02	LC-MS
141	Phe-Pro	2.20	4.4	1.27E-04	LC-MS
142	<b>DL-Glyceraldehyde 3-phosphate</b>	2.20	4.4	1.46E-08	LC-MS
143	<b>L-Cystathionine</b>	2.15	4.3	1.28E-02	LC-MS
144	Cys-Gly	2.12	4.24	1.98E-03	LC-MS
145	N-acetyl-(L)-arginine	2.09	4.18	1.33E-04	LC-MS
146	N-Acetyl-D-fucosamine	2.03	4.06	8.88E-04	LC-MS
147	Aminopropylcadaverine	2.01	4.02	6.77E-07	LC-MS
148	<b>Glutathione disulfide</b>	1.99	3.98	1.34E-05	LC-MS
149	<b>L-2-Aminoadipate</b>	1.94	3.88	1.42E-04	LC-MS
150	(R)-S-Lactoylglutathione	1.93	3.86	9.10E-03	LC-MS
151	pyrophosphate	1.91	3.82	3.05E-03	LC-MS
152	2-Hydroxyethanesulfonate	1.90	3.8	2.44E-03	LC-MS
153	<b>L-Asparagine</b>	1.90	3.8	8.75E-05	LC-MS
154	<b>GMP</b>	1.88	3.76	1.68E-06	LC-MS
155	Oleic acid	1.84	3.68	3.57E-01	GC-MS
156	beta-Alanine	1.84	3.68	4.79E-03	LC-MS
157	<b>Guanine</b>	1.83	3.66	2.80E-06	LC-MS
158	<b>NAD+</b>	1.82	3.64	2.96E-04	LC-MS
159	3-oxo-5S-amino-hexanoic acid	1.81	3.62	1.61E-03	LC-MS
160	<b>Sucrose</b>	1.80	3.6	1.00E-02	LC-MS
161	N2-(D-1-Carboxyethyl)-L-arginine	1.80	3.6	1.50E-02	LC-MS
162	succinamate	1.79	3.58	9.81E-04	LC-MS
163	Fructose	1.79	3.58	1.83E-03	GC-MS
164	Xanthosine 5'-phosphate	1.77	3.54	1.72E-02	LC-MS
165	N6-Methyl-L-lysine	1.75	3.5	2.56E-03	LC-MS
166	[FA trihydroxy(4:0)] 2,3,4-trihydroxy-butanoic acid	1.75	3.5	5.00E-02	LC-MS
167	<b>Guanosine</b>	1.72	3.44	4.32E-04	LC-MS
168	<b>S-Adenosyl-L-methionine</b>	1.72	3.44	4.04E-05	LC-MS
169	Asp-Gly	1.68	3.36	4.82E-04	LC-MS
170	Mannose	1.67	3.34	7.36E-03	GC-MS
171	LysoPC(17:0)	1.66	3.32	1.60E-02	LC-MS
172	1-Oleoylglycerophosphocholine	1.65	3.3	2.65E-02	LC-MS
173	Glycyl-leucine	1.63	3.26	6.03E-05	LC-MS
174	<b>L-Tryptophan</b>	1.62	3.24	3.93E-03	LC-MS
175	<b>D-Fructose 1,6-bisphosphate</b>	1.61	3.22	5.77E-05	LC-MS
176	Glu-Met	1.60	3.2	6.79E-03	LC-MS
177	<b>L-Tyrosine</b>	1.60	3.2	2.25E-02	LC-MS

178	<b>Adenosine</b>	1.59	3.18	2.09E-03	LC-MS
179	Glucopyranose	1.59	3.18	2.94E-01	LC-MS
180	2,7-Anhydro-alpha-N-acetylneuraminic acid	1.58	3.16	9.48E-04	LC-MS
181	<b>S-glutathionyl-L-cysteine</b>	1.57	3.14	3.31E-01	LC-MS
182	Trehalose	1.55	3.1	6.67E-02	GC-MS
183	Glu-Glu-Met	1.55	3.1	1.02E-02	LC-MS
184	palmitic acid	1.55	3.1	3.72E-01	LC-MS
185	3-Hydroxy-L-kynurenine	1.54	3.08	2.01E-02	LC-MS
186	talose	1.53	3.06	1.23E-01	LC-MS
187	<b>Allantoin</b>	1.53	3.06	7.03E-03	LC-MS
188	[PC (18:0)] 1-octadecanoyl-sn-glycero-3-phosphocholine	1.53	3.06	5.89E-02	LC-MS
189	<b>Inosine</b>	1.53	3.06	1.45E-01	LC-MS
190	Hypotaurine	1.52	3.04	7.01E-03	LC-MS
191	N-Methylnicotinate	1.52	3.04	7.37E-02	LC-MS
192	L-Glutamate 5-semialdehyde	1.51	3.02	7.86E-04	LC-MS
193	Hexadecasphinganine	1.47	2.94	4.54E-02	LC-MS
194	<b>5'-Methylthioadenosine</b>	1.46	2.92	1.83E-01	LC-MS
195	<b>N-methyl glucamine</b>	1.46	2.92	1.63E-01	LC-MS
196	(R)-2-Hydroxyglutarate	1.45	2.9	4.72E-02	LC-MS
197	<b>Deoxyadenosine</b>	1.44	2.88	1.83E-01	LC-MS
198	L-pyroglutamic acid	1.44	2.88	8.91E-02	GC-MS
199	<b>L-Proline</b>	1.42	2.84	4.43E-02	LC-MS
200	<b>L-Cystine</b>	1.42	2.84	4.56E-01	LC-MS
201	[PC (18:2)] 1-octadecadienoyl-sn-glycero-3-phosphocholine	1.41	2.82	6.86E-02	LC-MS
202	Thr-Asp-Ser	1.40	2.8	6.09E-03	LC-MS
203	<b>L-Phenylalanine</b>	1.40	2.8	2.19E-02	LC-MS
204	Mannitol	1.39	2.78	3.58E-01	GC-MS
205	Phosphoribosyl-AMP	1.39	2.78	9.82E-02	LC-MS
206	<b>L-Lysine</b>	1.38	2.76	1.62E-02	LC-MS
207	<b>L-Kynurenine</b>	1.38	2.76	5.58E-02	LC-MS
208	Trimethylamine N-oxide	1.36	2.72	2.34E-03	LC-MS
209	Malonate	1.36	2.72	1.18E-01	LC-MS
210	Ala-Asp-Ser	1.36	2.72	9.62E-02	LC-MS
211	<b>Adenine</b>	1.35	2.7	2.24E-01	LC-MS
212	2-Naphthylamine	1.35	2.7	4.76E-02	LC-MS
213	Methyloxaloacetate	1.34	2.68	1.31E-02	LC-MS
214	L-Methionine S-oxide	1.34	2.68	1.21E-03	LC-MS
215	(S)-Methylmalonate semialdehyde	1.34	2.68	2.26E-02	LC-MS
216	Asp-Ser-Ser	1.34	2.68	2.95E-01	LC-MS
217	Mannonic acid	1.34	2.68	8.58E-02	LC-MS
218	<b>N6,N6,N6-Trimethyl-L-lysine</b>	1.32	2.64	1.66E-01	LC-MS
219	<b>Uracil</b>	1.32	2.64	3.34E-04	LC-MS
220	D-Galactofuranose	1.31	2.62	8.79E-02	LC-MS
221	n-Pentadecanoic acid	1.31	2.62	9.48E-02	LC-MS
222	L-cysteine sulfinatate	1.31	2.62	1.16E-01	LC-MS
223	O-Palmitoyl-R-carnitine	1.30	2.6	1.69E-01	LC-MS

224	Creatine	1.30	2.6	8.74E-02	LC-MS
225	<b>L-Threonine</b>	1.30	2.6	1.43E-02	LC-MS
226	Xylitol	1.30	2.6	1.91E-03	LC-MS
227	Glu-Met-Thr	1.26	2.52	2.80E-01	LC-MS
228	tetracosahexanoic acid	1.22	2.44	1.62E-01	LC-MS
229	Methylmalonate	1.21	2.42	1.00E-01	LC-MS
230	alpha-ketoglutaric acid	1.20	2.4	2.01E-01	GC-MS
231	<b>L-Glutamine</b>	1.20	2.4	8.17E-02	LC-MS
232	Tyramine	1.19	2.38	2.40E-01	LC-MS
233	N-Methylethanolamine phosphate	1.18	2.36	4.96E-01	LC-MS
234	<b>L-Alanine</b>	1.17	2.34	2.07E-01	LC-MS
235	Arg-Gln-Ser-Ser	1.17	2.34	4.77E-01	LC-MS
236	L-1-Pyrroline-3-hydroxy-5-carboxylate	1.16	2.32	8.01E-02	LC-MS
237	Creatinine	1.15	2.3	2.32E-01	LC-MS
238	Maltose	1.13	2.26	4.76E-01	LC-MS
239	3-Oxopropanoate	1.12	2.24	1.02E-01	LC-MS
240	<b>L-serine</b>	1.11	2.22	1.58E-01	LC-MS
241	5-6-Dihydrouridine	1.11	2.22	2.74E-01	LC-MS
242	Ethyl (R)-3-hydroxyhexanoate	1.10	2.2	4.66E-01	LC-MS
243	Cortisone	1.10	2.2	7.89E-01	GC-MS
244	<b>D-glucose</b>	1.10	2.2	3.26E-01	LC-MS
245	Methylimidazoleacetic acid	1.10	2.2	3.58E-01	LC-MS
246	<b>Phenylacetyl glycine</b>	1.10	2.2	5.97E-01	LC-MS
247	D-Galactose	1.09	2.18	6.83E-01	LC-MS
248	<b>3-Phosphoglycerate</b>	1.09	2.18	4.29E-01	LC-MS
249	Propanoic acid	1.08	2.16	5.91E-01	LC-MS
250	Sulfoacetaldehyde	1.08	2.16	6.24E-01	LC-MS
251	Homocysteine	1.08	2.16	7.51E-01	LC-MS
252	<b>Orthophosphate</b>	1.06	2.12	8.22E-01	LC-MS
253	10-Hydroxydecanoic acid	1.05	2.1	4.54E-01	LC-MS
254	Glycodeoxycholate	1.05	2.1	7.75E-01	LC-MS
255	Dodecatetraenedioic acid	1.05	2.1	6.00E-01	LC-MS
256	2-C-Methyl-D-erythritol 4-phosphate	1.04	2.08	9.17E-01	LC-MS
257	Cys-Cys-His-His	1.04	2.08	7.96E-01	LC-MS
258	<b>phosphoenolpyruvic acid</b>	1.03	2.06	8.48E-01	LC-MS
259	5-Hydroxyindoleacetate	1.02	2.04	8.26E-01	LC-MS
260	Phe-Asp	1.01	2.02	9.49E-01	LC-MS
261	phosphoric acid	1.01	2.02	9.57E-01	LC-MS
262	N-Acetyl-D-glucosamine 6-phosphate	1.00	2	9.84E-01	LC-MS
263	Glu-Leu-Thr-His	-1.01	-2.02	9.61E-01	LC-MS
264	His-Phe-Val-Pro	-1.01	-2.02	9.66E-01	LC-MS
265	<b>Phenylpyruvate</b>	-1.02	-2.04	8.64E-01	LC-MS
266	hydroxy-octadecadienoic acid	-1.03	-2.06	8.40E-01	LC-MS
267	L-Noradrenaline	-1.03	-2.06	8.39E-01	LC-MS
268	di-n-Undecylamine	-1.03	-2.06	9.42E-01	LC-MS
269	Fructoselysine	-1.04	-2.08	6.75E-01	LC-MS
270	Acetamide, N,N-diethyl-	-1.05	-2.1	3.12E-01	GC-MS

271	3-Butenoic acid	-1.05	-2.1	1.99E-01	LC-MS
272	glycolic acid	-1.05	-2.1	3.77E-01	LC-MS
273	Myo-inositol-3-phosphate	-1.05	-2.1	8.44E-01	GC-MS
274	Erucic acid	-1.06	-2.12	7.49E-01	GC-MS
275	5-Hydroxypentanoate	-1.07	-2.14	4.88E-01	LC-MS
276	[FA (20:4)] 5Z,8Z,11Z,14Z-eicosatetraenoic acid	-1.07	-2.14	6.04E-01	LC-MS
277	Cholest-2-eno[2,3-b]indole, 1'-acetyl-6'-methoxy-	-1.08	-2.16	5.28E-01	GC-MS
278	N3-methylcytosine	-1.08	-2.16	6.50E-01	LC-MS
279	D-Threose	-1.08	-2.16	4.19E-01	LC-MS
280	4-Methylene-L-glutamine	-1.09	-2.18	6.82E-01	LC-MS
281	2-Phenylacetamide	-1.09	-2.18	5.21E-01	LC-MS
282	Pyruvate	-1.09	-2.18	1.13E-03	GC-MS
283	Heptanedioic acid	-1.10	-2.2	4.02E-01	LC-MS
284	methyl-dihydroxy-pentanoic acid	-1.12	-2.24	3.39E-01	LC-MS
285	dioxo-octanoic acid	-1.13	-2.26	3.67E-01	LC-MS
286	amino-undecanoic acid	-1.14	-2.28	3.49E-01	LC-MS
287	<b>L-Citrulline</b>	-1.17	-2.34	5.76E-01	LC-MS
288	<b>sn-glycero-3-Phosphocholine</b>	-1.17	-2.34	7.07E-01	LC-MS
289	Methanesulfonic acid	-1.18	-2.36	5.11E-01	LC-MS
290	Tetradecanedioic acid	-1.18	-2.36	3.52E-01	LC-MS
291	P-DPD	-1.18	-2.36	2.76E-01	LC-MS
292	Phthalic acid	-1.19	-2.38	6.18E-03	LC-MS
293	4-Acetamidobutanoate	-1.19	-2.38	1.49E-01	LC-MS
294	myo-Inositol	-1.20	-2.4	4.94E-01	LC-MS
295	Cyclododecane	-1.20	-2.4	3.07E-02	GC-MS
296	Gamma-Glutamylglutamine	-1.21	-2.42	1.26E-01	LC-MS
297	N4-acetyl-N4-hydroxy-1-aminopropane	-1.22	-2.44	4.86E-01	LC-MS
298	5-oxo-7-octenoic acid	-1.22	-2.44	1.24E-01	LC-MS
299	2-Acetolactate	-1.24	-2.48	3.78E-01	LC-MS
300	Urea	-1.26	-2.52	4.61E-01	GC-MS
301	Elaidicarnitine	-1.26	-2.52	2.77E-01	LC-MS
302	d-Xylose	-1.27	-2.54	4.61E-01	LC-MS
303	D-Glycerate	-1.28	-2.56	9.06E-02	LC-MS
304	<b>Lactate</b>	-1.29	-2.58	2.85E-01	LC-MS
305	2-acetamidoglucal	-1.30	-2.6	7.17E-03	LC-MS
306	Heme	-1.32	-2.64	3.71E-01	LC-MS
307	D-4'-Phosphopantothenate	-1.35	-2.7	5.89E-02	LC-MS
308	<b>Glycerol</b>	-1.39	-2.78	1.43E-03	LC-MS
309	Met-Ala-Gly	-1.40	-2.8	6.53E-02	LC-MS
310	Urate	-1.41	-2.82	1.34E-01	LC-MS
311	Stearic acid	-1.44	-2.88	8.78E-02	GC-MS
312	4-Guanidinobutanoate	-1.44	-2.88	3.24E-03	LC-MS
313	Deoxycytidine	-1.47	-2.94	1.75E-01	LC-MS
314	2-monooleoylglycerol	-1.53	-3.06	1.16E-02	LC-MS
315	6-[3]-ladderane-1-hexanol	-1.56	-3.12	9.22E-02	LC-MS
316	4-Hydroxy-L-threonine	-1.59	-3.18	1.30E-05	LC-MS

317	Val-Asp-Gly	-1.60	-3.2	1.09E-04	LC-MS
318	Ala-Ser	-1.64	-3.28	3.31E-04	LC-MS
319	Heptadecanoic acid	-1.64	-3.28	4.55E-02	GC-MS
320	Leu-Ala	-1.76	-3.52	1.04E-04	LC-MS
321	9,12-octadecadienal	-1.79	-3.58	1.70E-01	LC-MS
322	Thr-Ala-Asp	-1.80	-3.6	9.52E-05	LC-MS
323	N-Acetyl-D-glucosamine	-1.94	-3.88	1.55E-05	LC-MS
324	D-Sorbitol	-2.11	-4.22	8.20E-09	LC-MS
325	<b>L-Histidine</b>	-2.40	-4.8	2.99E-08	LC-MS
326	N-Ribosylnicotinamide	-2.42	-4.84	1.97E-03	LC-MS
327	octadecenamide	-2.76	-5.52	1.60E-01	LC-MS
328	Valine	-2.85	-5.7	2.69E-03	GC-MS
329	Cellobiose	-2.95	-5.9	9.12E-02	GC-MS
330	N5-(L-1-Carboxyethyl)-L-ornithine	-3.10	-6.2	1.01E-08	LC-MS
331	Hexose phosphate	-3.55	-7.1	5.65E-10	LC-MS
332	3-beta-D-Galactosyl-sn-glycerol	-5.38	-10.76	1.68E-06	LC-MS
333	Leu-Lys-Asp	-5.64	-11.28	1.04E-08	LC-MS

Table 3 Putative metabolites (PMs) represented in

Figure 4-1 showing fold change in abundance in mature schizonts compared to uninfected reticulocyte enriched erythrocytes. PMs are listed in order of decreasing abundance (metabolites identified with authentic standards are highlighted bold)

No.	Metabolites	Fold change (Schizonts/reticulocytes)	P-Value	Platform
1	Arg-Cys-Ser-Tyr	> 25 fold	4.76E-03	LC-MS
2	N-Acetyl-L-histidine	> 25 fold	4.38E-07	LC-MS
3	(S)-ATPA	> 25 fold	7.49E-05	LC-MS
4	CMP-N-trimethyl-2-aminoethylphosphonate	> 25 fold	1.03E-04	LC-MS
5	gamma-Glutamyl-gamma-aminobutyraldehyde	> 25 fold	1.09E-04	LC-MS
6	Carnosine	> 25 fold	3.70E-06	LC-MS
7	Proclavaminc acid	> 25 fold	1.33E-03	LC-MS
8	dTMP	> 25 fold	4.12E-05	LC-MS
9	Glu-Phe-Cys-Cys	> 25 fold	3.15E-05	LC-MS
10	UMP	> 25 fold	1.12E-03	GC-MS
11	Lys-Tyr	> 25 fold	1.05E-03	LC-MS
12	Ala-Gly-Pro	> 25 fold	1.35E-03	LC-MS
13	3-(Pyrazol-1-yl)-L-alanine	> 25 fold	5.14E-08	LC-MS
14	L-Rhamnose	> 25 fold	6.81E-06	LC-MS
15	Riboflavin	> 25 fold	2.75E-05	LC-MS
16	Propanoyl phosphate	> 25 fold	3.25E-06	LC-MS
17	Nalpha-Methylhistidine	> 25 fold	8.69E-06	LC-MS
18	<b>S-Adenosyl-L-methionine</b>	> 25 fold	2.61E-04	LC-MS
19	Volemitol	> 25 fold	1.04E-05	LC-MS
20	Glu-Asp-Pro	> 25 fold	1.25E-06	LC-MS
21	Trp-Pro	> 25 fold	3.02E-06	LC-MS
22	O-Phospho-L-serine	> 25 fold	3.46E-04	LC-MS
23	D-4'-Phosphopantothenate	> 25 fold	1.38E-04	LC-MS
24	[ST hydrox] N-(3alpha,7alpha-dihydroxy-5beta-cholan-24-oyl)-taurine	> 25 fold	6.20E-06	LC-MS
25	Ala-Leu-Asn-Ser	> 25 fold	4.71E-04	LC-MS
26	DL-Methionine sulfone	> 25 fold	2.17E-05	LC-MS
27	Asn-Asn-Asp	> 25 fold	3.93E-06	LC-MS
28	Hypusine	> 25 fold	9.86E-06	LC-MS
29	4,5-seco-dopa	> 25 fold	7.11E-06	LC-MS
30	<b>Choline phosphate</b>	> 25 fold	2.94E-05	LC-MS
31	Phe-Asp-Gln	> 25 fold	3.21E-04	LC-MS
32	1-(5-Phosphoribosyl)imidazole-4-acetate	> 25 fold	3.07E-06	LC-MS
33	Asn-Pro	> 25 fold	1.97E-05	LC-MS
34	Pyrimidine nucleoside	> 25 fold	9.12E-05	LC-MS
35	CDP-choline	> 25 fold	1.50E-03	LC-MS
36	Phosphonoacetaldehyde	> 25 fold	2.82E-06	LC-MS
37	Met-Ser	> 25 fold	1.78E-06	LC-MS
38	Ala-Pro	> 25 fold	2.55E-06	LC-MS
39	Lys-Pro	> 25 fold	9.13E-06	LC-MS
40	Cytidine 2'-phosphate	> 25 fold	3.79E-04	LC-MS

41	CDP-ethanolamine	> 25 fold	4.13E-04	LC-MS
42	L-rhamnitol	> 25 fold	2.74E-07	LC-MS
43	N-Ribosylnicotinamide	> 25 fold	1.22E-05	LC-MS
44	<b>Lactate</b>	> 25 fold	3.19E-05	LC-MS
45	2',3'-Cyclic UMP	> 25 fold	2.31E-03	LC-MS
46	Val-Asp-Gly	> 25 fold	1.74E-05	LC-MS
47	Pro-Pro	> 25 fold	2.34E-03	LC-MS
48	4,6-Dideoxy-4-oxo-dTDP-D-glucose	> 25 fold	2.43E-03	LC-MS
49	Glu-Glu-Gln-Pro	> 25 fold	2.40E-06	LC-MS
50	N(pi)-Methyl-L-histidine	> 25 fold	8.38E-04	LC-MS
51	D-Ribitol 5-phosphate	> 25 fold	1.86E-06	LC-MS
52	Leu-Asn-Asp	> 25 fold	2.58E-06	LC-MS
53	Cryogenine	> 25 fold	2.52E-05	LC-MS
54	<b>5'-Methylthioadenosine</b>	> 25 fold	2.22E-04	LC-MS
55	N1-Acetylspermidine	> 25 fold	1.91E-06	LC-MS
56	Sphinganine	> 25 fold	9.17E-04	LC-MS
57	Ethanolamine phosphate	> 25 fold	3.32E-04	LC-MS
58	<b>Adenine</b>	> 25 fold	5.04E-05	LC-MS
59	N2-(D-1-Carboxyethyl)-L-arginine	> 25 fold	1.85E-05	LC-MS
60	&alpha;-methylhistidine	> 25 fold	4.90E-03	LC-MS
61	<b>GMP</b>	24.46	1.31E-05	LC-MS
62	<b>L-Tyrosine</b>	23.83	2.66E-05	LC-MS
63	Fructoselysine	23.23	1.34E-05	LC-MS
64	Glu-Thr	23.09	8.13E-04	LC-MS
65	Folate	22.33	3.83E-06	LC-MS
66	CMP-2-aminoethylphosphonate	22.05	8.33E-06	LC-MS
67	Piperidine	21.57	1.29E-05	LC-MS
68	Sedoheptulose	20.72	4.65E-06	LC-MS
69	Glycylproline	20.01	2.49E-04	LC-MS
70	hydrogen iodide	19.5	9.46E-07	LC-MS
71	dAMP	19.47	1.89E-04	LC-MS
72	[SP (2:0)] sphinga-4E,14Z-dienine	19.02	2.79E-04	LC-MS
73	D-Methionine	18.17	1.69E-05	LC-MS
74	<b>L-Cystine</b>	16.34	8.07E-03	LC-MS
75	ADPribose 2'-phosphate	16.31	3.07E-06	LC-MS
76	<b>L-Histidine</b>	16.25	1.58E-04	LC-MS
77	<b>L-Ornithine</b>	16.02	1.41E-06	LC-MS
78	<b>L-Phenylalanine</b>	15.66	1.16E-05	LC-MS
79	gamma-L-Glutamyl-L-cysteinyl-beta-alanine	15	1.37E-05	LC-MS
80	phosphinomethylmalate	14.77	8.14E-08	LC-MS
81	<b>Putrescine</b>	14.56	1.14E-06	LC-MS
82	Met-Thr-Asp	14.5	1.39E-06	LC-MS
83	<b>L-Tryptophan</b>	14.34	2.74E-05	LC-MS
84	2-Hydroxyadenine	14.21	1.46E-05	LC-MS
85	Glycodeoxycholate	13.67	1.41E-05	LC-MS
86	Betaine	13.47	8.92E-06	LC-MS
87	Xanthosine 5'-phosphate	13.32	7.70E-04	LC-MS

88	<b>CMP</b>	13.16	1.14E-04	LC-MS
89	Glu-Met-Thr	12.94	3.75E-07	LC-MS
90	sn-glycero-3-Phospho-1-inositol	12.56	1.29E-05	LC-MS
91	1-methylguanosine	12.46	9.01E-06	LC-MS
92	Thr-Ala-Asp	12.34	1.55E-04	LC-MS
93	Methylimidazoleacetic acid	12.31	5.36E-07	LC-MS
94	N-hydroxy-N-isopropylloxamate	11.85	1.06E-04	LC-MS
95	Ala-Cys	11.72	5.48E-05	LC-MS
96	3-Oxopropanoate	11.65	6.80E-06	LC-MS
97	<b>Phenylacetyl glycine</b>	11.24	1.01E-05	LC-MS
98	Pyridoxamine phosphate	11.23	6.61E-06	LC-MS
99	<b>sn-glycero-3-Phosphocholine</b>	10.83	2.81E-04	LC-MS
100	N-Acetyl-aspartyl-glutamate	10.81	3.58E-05	LC-MS
101	Asp-Met-Asp-Gly	10.56	7.91E-03	LC-MS
102	<b>L-Glutamate</b>	10.53	2.83E-06	LC-MS
103	Ala-Ser	10.51	7.68E-05	LC-MS
104	N6-Methyl-L-lysine	10.5	5.30E-06	LC-MS
105	Leukotriene B4	10.13	3.28E-04	LC-MS
106	D-Sorbitol	9.71	5.26E-07	LC-MS
107	2,3,4,5-Tetrahydrodipicolinate	9.54	4.35E-05	LC-MS
108	GammaGlutamylglutamic acid	9.33	1.67E-05	LC-MS
109	succinamate	9.32	2.54E-04	LC-MS
110	L-Gulonate	9	4.94E-05	LC-MS
111	(S)-AMPA	8.99	5.43E-05	LC-MS
112	D-Glucuronate 1-phosphate	8.94	1.07E-05	LC-MS
113	dTDP-3-amino-2,3,6-trideoxy-D-threo-hexopyranos-4-ulose	8.76	9.52E-08	LC-MS
114	<b>IMP</b>	8.72	4.40E-04	LC-MS
115	DL-β;-hydroxynorvaline	8.47	1.31E-06	LC-MS
116	[Fv Hydroxy,trimethoxy(9:1)] 4'-Hydroxy-5,6,7-trimethoxyflavanone	8.16	3.74E-04	LC-MS
117	[FA hydroxy(20:4)] 15S-hydroxy-5Z,8Z,11Z,13E-eicosatetraenoic acid	8.1	5.77E-04	LC-MS
118	Phosphoribosyl-AMP	7.9	2.62E-06	LC-MS
119	<b>Adenosine</b>	7.77	3.63E-06	LC-MS
120	D-Sedoheptulose 1,7-bisphosphate	7.68	3.91E-06	LC-MS
121	<b>Choline</b>	7.54	8.54E-07	LC-MS
122	Retronecine	7.5	4.78E-08	LC-MS
123	<b>Guanosine</b>	7.47	1.91E-03	LC-MS
124	<b>Cytidine</b>	7.46	1.24E-03	LC-MS
125	Xylitol	7.3	1.06E-02	LC-MS
126	Ala-Leu-His-His	7.3	2.69E-07	LC-MS
127	alpha-aminopimelate	7.28	2.54E-06	LC-MS
128	<b>Uracil</b>	7.18	1.06E-04	LC-MS
129	Mevaldate	6.79	1.15E-05	LC-MS
130	<b>Uridine</b>	6.69	9.72E-05	LC-MS
131	Glycerone phosphate	6.67	3.38E-06	LC-MS
132	[SP] 3-dehydrosphinganine	6.63	6.66E-04	LC-MS
133	P-DPD	6.59	1.16E-06	LC-MS

134	<b>D-Gluconic acid</b>	6.42	7.81E-06	LC-MS
135	siroamide	6.38	2.83E-06	LC-MS
136	Ala-Leu-Lys-Pro	6.34	7.93E-06	LC-MS
137	4-Acetamidobutanoate	6.29	1.85E-06	LC-MS
138	Glu-Ser	6.16	1.25E-02	LC-MS
139	<b>NAD+</b>	5.94	2.01E-04	LC-MS
140	sn-glycero-3-Phosphoethanolamine	5.92	4.49E-06	LC-MS
141	NG,NG-Dimethyl-L-arginine	5.56	2.51E-05	LC-MS
142	(1-Ribosylimidazole)-4-acetate	5.54	2.29E-03	LC-MS
143	D-Alanyl-D-alanine	5.35	2.19E-05	LC-MS
144	Arg-Lys-Ser-Ser	5.27	1.14E-06	LC-MS
145	Pyrimidine 5'-deoxynucleotide	5.27	1.11E-05	LC-MS
146	N-Formimino-L-glutamate	5.26	8.75E-05	LC-MS
147	[FA (18:1)] 9Z-octadecenamide	5.26	3.09E-01	LC-MS
148	Ala-Lys-Met-Gln	5.25	2.19E-06	LC-MS
149	<b>Guanine</b>	5.2	3.93E-03	LC-MS
150	Cys-Glu-Glu-Pro	5.12	1.55E-06	LC-MS
151	N-Acetylglutamine	5.07	3.85E-04	LC-MS
152	[FA (18:2)] 9,12-octadecadienal	4.89	1.69E-01	LC-MS
153	Cys-Met-Ser-His	4.78	9.15E-07	LC-MS
154	Phe-Asp	4.76	1.25E-04	LC-MS
155	Palmiticamide	4.69	3.37E-01	LC-MS
156	<b>L-Kynurenine</b>	4.69	9.27E-07	LC-MS
157	[FA hydroxy,oxo(7:0/2:0)] 4-hydroxy-2-oxo-Heptanedioic acid	4.64	2.00E-03	LC-MS
158	Ala-Asp-Asp	4.47	2.90E-05	LC-MS
159	Glycerophosphoglycerol	4.4	5.28E-05	LC-MS
160	N-(Carboxyaminoethyl)urea	4.32	1.19E-05	LC-MS
161	Glycocholate	4.31	4.60E-05	LC-MS
162	Gamma-Glutamylglutamine	4.31	4.94E-05	LC-MS
163	<b>3',5'-Cyclic AMP</b>	4.28	1.28E-03	LC-MS
164	Sorbitol 6-phosphate	4.26	2.37E-04	LC-MS
165	[FA (20:4)] 5Z,8Z,11Z,14Z-eicosatetraenoic acid	4.21	2.64E-03	LC-MS
166	<b>N6,N6,N6-Trimethyl-L-lysine</b>	4.19	1.39E-06	LC-MS
167	N1-(5-Phospho-alpha-D-ribose)-5,6-dimethylbenzimidazole	4.14	1.03E-02	LC-MS
168	[FA (6:0)] 6-[3]-ladderane-1-hexanol	4.1	1.60E-01	LC-MS
169	5-Hydroxyindoleacetate	4.07	1.44E-06	LC-MS
170	<b>Xanthine</b>	3.97	1.01E-05	LC-MS
171	UDP-N-acetyl-D-glucosamine	3.93	1.73E-04	LC-MS
172	<b>L-Proline</b>	3.93	6.09E-06	LC-MS
173	L-Hypoglycin	3.89	3.24E-09	LC-MS
174	N2-(D-1-Carboxyethyl)-L-lysine	3.82	5.31E-05	LC-MS
175	Glu-Val	3.82	1.54E-10	LC-MS
176	(S)-2-Aminobutanoate	3.81	6.29E-02	LC-MS
177	2-Deoxy-D-ribose 5-phosphate	3.79	1.23E-05	LC-MS
178	<b>sn-Glycerol 3-phosphate</b>	3.79	4.40E-04	LC-MS
179	Glu-Pro	3.78	8.86E-04	LC-MS

180	N6-Acetyl-N6-hydroxy-L-lysine	3.71	1.44E-03	LC-MS
181	<b>AMP</b>	3.54	3.12E-04	LC-MS
182	L-Tyrosine methyl ester	3.45	6.84E-04	LC-MS
183	HEPES	3.44	9.39E-08	LC-MS
184	Acetylcholine	3.41	1.80E-03	LC-MS
185	[FA trihydroxy(4:0)] 2,3,4-trihydroxy-butanoic acid	3.31	2.67E-07	LC-MS
186	Glu-Leu	3.3	3.59E-04	LC-MS
187	2-Carboxy-D-arabinitol 1-phosphate	3.27	1.06E-03	LC-MS
188	Xanthosine	3.13	3.58E-04	LC-MS
189	L-Fucose 1-phosphate	3.11	4.48E-04	LC-MS
190	<b>Succinate</b>	3.07	1.55E-04	LC-MS
191	L-Glutamate 5-semialdehyde	3.04	5.88E-05	LC-MS
192	<b>Fumarate</b>	2.96	4.35E-05	LC-MS
193	Phe-Pro	2.83	2.33E-04	LC-MS
194	5-Acetamidopentanoate	2.83	3.23E-04	LC-MS
195	Arg-Gln-Ser-Ser	2.78	7.94E-04	LC-MS
196	[FA (7:0/2:0)] Heptanedioic acid	2.75	2.77E-04	LC-MS
197	<b>L-Cystathionine</b>	2.73	6.33E-04	LC-MS
198	Leu-Val	2.69	4.24E-02	LC-MS
199	S-Methyl-L-methionine	2.61	1.49E-02	LC-MS
200	N2-Acetyl-L-aminoadipate	2.61	3.65E-03	LC-MS
201	O-Acetyl-L-homoserine	2.6	4.86E-06	LC-MS
202	2-Aminoacrylate	2.58	4.90E-03	LC-MS
203	<b>Sucrose</b>	2.56	5.41E-03	LC-MS
204	Tiglic acid	2.52	2.20E-04	LC-MS
205	(-)-Salsolinol	2.47	1.89E-02	LC-MS
206	N-Dimethyl-2-aminoethylphosphonate	2.45	1.96E-03	LC-MS
207	3-Amino-2-oxopropyl phosphate	2.45	2.51E-01	LC-MS
208	<b>N-Acetylneuraminate</b>	2.43	3.64E-05	LC-MS
209	5-6-Dihydrouridine	2.38	1.33E-04	LC-MS
210	Sulfate	2.25	1.28E-04	LC-MS
211	D-Threose	2.2	8.51E-06	LC-MS
212	<b>L-Aspartate</b>	2.16	9.20E-04	LC-MS
213	5-Hydroxypentanoate	2.09	2.24E-07	LC-MS
214	1,3-benzenedisulfonate	2.08	7.09E-06	LC-MS
215	N5-Ethyl-L-glutamine	2.07	2.67E-03	LC-MS
216	(R)-AMAA	2.04	1.55E-03	LC-MS
217	Sulfoacetaldehyde	2.03	1.26E-03	LC-MS
218	allylcysteine	2.02	1.80E-02	LC-MS
219	<b>L-2-Aminoadipate</b>	1.99	4.32E-05	LC-MS
220	Hydroxymethylphosphonate	1.98	6.55E-02	LC-MS
221	(S)-3-Methyl-2-oxopentanoic acid	1.97	1.41E-03	LC-MS
222	L-Arabinonate	1.96	5.86E-04	LC-MS
223	L-Noradrenaline	1.94	3.42E-03	LC-MS
224	Val-Val	1.93	9.43E-03	LC-MS
225	Acetyl phosphate	1.91	9.46E-04	LC-MS
226	Thiomorpholine 3-carboxylate	1.9	1.98E-02	LC-MS

227	1-Oleoylglycerophosphocholine	1.89	4.93E-02	LC-MS
228	<b>S-glutathionyl-L-cysteine</b>	1.87	4.70E-02	LC-MS
229	N-Acetyl-D-glucosamine 6-phosphate	1.86	2.67E-03	LC-MS
230	Ala-Asp-Ser	1.84	6.40E-02	LC-MS
231	<b>L-Lysine</b>	1.82	3.86E-03	LC-MS
232	Vinylacetyl glycine	1.8	7.36E-03	LC-MS
233	Linamarin	1.8	1.29E-02	LC-MS
234	Thr-Asp-Ser	1.78	2.12E-03	LC-MS
235	L-Methionine S-oxide	1.74	5.85E-02	LC-MS
236	Asp-Gly	1.72	1.68E-04	LC-MS
237	<b>N-methyl glucamine</b>	1.71	9.10E-02	LC-MS
238	Biotin	1.7	7.00E-04	LC-MS
239	D-Aspartate	1.68	2.88E-02	LC-MS
240	<b>D-Ribose 5-phosphate</b>	1.67	3.38E-02	LC-MS
241	[SP hydroxy,hydroxy,methyl(10:2/2:0)] 6R-(8-hydroxydecyl)-2R-(hydroxymethyl)-piperidin-3R-ol	1.64	4.56E-02	LC-MS
242	D-Mannosylglycoprotein	1.61	8.52E-02	LC-MS
243	sodium chloride(aq)	1.61	6.92E-03	LC-MS
244	D-Glycerate	1.61	2.17E-03	LC-MS
245	D-Tryptophan	1.6	2.06E-01	LC-MS
246	Cys-Cys-His-His	1.59	3.68E-04	LC-MS
247	Fructoselysine 6-phosphate	1.58	4.70E-03	LC-MS
248	<b>L-Arginine</b>	1.57	4.37E-04	LC-MS
249	His-Phe-Val-Pro	1.57	3.93E-03	LC-MS
250	<b>L-Asparagine</b>	1.55	1.42E-03	LC-MS
251	Adipate	1.55	8.43E-04	LC-MS
252	Piperideine	1.54	3.40E-02	LC-MS
253	Leu-Lys-Asp	1.54	2.81E-01	LC-MS
254	Leu-Ala	1.54	5.47E-02	LC-MS
255	Prenyl-L-cysteine	1.53	8.28E-02	LC-MS
256	<b>L-Alanine</b>	1.53	5.39E-03	LC-MS
257	Gamma-Aminobutyryl-lysine	1.51	1.11E-02	LC-MS
258	8-keto-7-aminoperlagonate	1.47	8.56E-02	LC-MS
259	[FA hydroxy(18:2)] 9S-hydroxy-10E,12Z-octadecadienoic acid	1.47	8.16E-02	LC-MS
260	gamma-L-Glutamyl-L-cysteine	1.47	1.44E-01	LC-MS
261	Glu-Leu-Thr-His	1.44	6.27E-03	LC-MS
262	<b>3-Phosphoglycerate</b>	1.43	5.99E-02	LC-MS
263	N3-(4-methoxyfumaroyl)-L-2,3-diaminopropanoate	1.42	5.02E-01	LC-MS
264	2-monooleoylglycerol	1.42	3.33E-02	LC-MS
265	L-Threonine	1.41	6.86E-02	LC-MS
266	N2-Succinyl-L-ornithine	1.39	5.14E-02	LC-MS
267	<b>Malate</b>	1.39	8.90E-02	LC-MS
268	Glu-Gly	1.38	4.02E-02	LC-MS
269	L-1-Pyrroline-3-hydroxy-5-carboxylate	1.36	2.06E-03	LC-MS
270	N-Acetyl-D-glucosamine 6-sulfate	1.35	1.11E-01	LC-MS
271	[FA methyl,hydroxy(5:0)] 3R-methyl-3,5-	1.34	4.89E-02	LC-MS

	dihydroxy-pentanoic acid			
272	Pyridoxal phosphate	1.31	1.10E-01	LC-MS
273	Canavanine	1.31	2.71E-03	LC-MS
274	L-5-benzyl-hydantoin	1.28	4.72E-01	LC-MS
275	Heme	1.27	3.18E-01	LC-MS
276	<b>Orthophosphate</b>	1.26	2.09E-01	LC-MS
277	Homoarginine	1.24	4.31E-01	LC-MS
278	Leu-Thr	1.23	1.99E-01	LC-MS
279	Triethanolamine	1.22	4.24E-01	LC-MS
280	3-Hydroxy-L-kynurenine	1.22	5.85E-01	LC-MS
281	2-Naphthylamine	1.22	1.19E-01	LC-MS
282	Chelilutine	1.21	2.36E-01	LC-MS
283	Leucyl-leucine	1.21	2.40E-01	LC-MS
284	[GP (16:0)] 1-hexadecanoyl-2-sn-glycero-3-phosphate	1.21	4.26E-01	LC-MS
285	5-(chloromercuri)cytidine	1.2	5.52E-01	LC-MS
286	N-(octanoyl)-L-homoserine	1.19	1.13E-01	LC-MS
287	[FA (14:0/2:0)] Tetradecanedioic acid	1.18	2.87E-01	LC-MS
288	(R)-S-Lactoylglutathione	1.18	4.05E-01	LC-MS
289	Creatinine	1.17	3.07E-01	LC-MS
290	N-Acetyllactosamine	1.16	1.89E-01	LC-MS
291	Furfural diethyl acetal	1.14	4.95E-01	LC-MS
292	Aminopropylcadaverine	1.12	3.52E-01	LC-MS
293	[SP] Sphinganine-1-phosphate	1.12	5.52E-01	LC-MS
294	2-acetamidoglucal	1.12	2.55E-01	LC-MS
295	Methyl cinnamate	1.12	6.62E-01	LC-MS
296	Glu-Cys-Gln-Gln	1.11	4.57E-01	LC-MS
297	N-Acetyl-L-aspartate	1.1	6.35E-01	LC-MS
298	[FA (24:6)] 4,8,12,15,19,21-tetracosahexaenoic acid	1.09	4.78E-01	LC-MS
299	D-Lysine	1.09	6.37E-01	LC-MS
300	Maltose	1.08	5.25E-01	LC-MS
301	(R)-2-Hydroxyglutarate	1.07	7.77E-01	LC-MS
302	[FA oxo(8:0)] 5-oxo-7-octenoic acid	1.07	7.71E-01	LC-MS
303	(S)-Methylmalonate semialdehyde	1.06	8.19E-01	LC-MS
304	[FA dioxo(8:0)] 4,7-dioxo-octanoic acid	1.06	7.25E-01	LC-MS
305	Dodecanamide	1.06	7.47E-01	LC-MS
306	2-hydroxysuccinamate	1.06	6.16E-01	LC-MS
307	Sedoheptulose 7-phosphate	1.05	8.65E-01	LC-MS
308	allopurinol	1.05	8.77E-01	LC-MS
309	Cyclohex-2-enone	1.04	8.59E-01	GC-MS
310	Methylmalonate	1.04	6.89E-01	LC-MS
311	<b>L-Glutamine</b>	1.04	8.23E-01	LC-MS
312	L-Erythrulose	1.04	7.83E-01	LC-MS
313	[ST hydrox] 3alpha,7alpha-Dihydroxy-5beta-cholan-24-oic Acid	1.03	7.35E-01	LC-MS
314	[PC (18:2)] 1-(9Z,12Z-octadecadienoyl)-sn-glycero-3-phosphocholine	1.03	8.91E-01	LC-MS
315	[ST trihydrox] 3Alpha,7Alpha,12Alpha-trihydroxy-5Beta-cholan-24-oic acid	1.03	8.79E-01	LC-MS

316	Methyloxaloacetate	1.02	9.27E-01	LC-MS
317	4-Oxocyclohexanecarboxylate	1.01	9.16E-01	LC-MS
318	myristic amide	1.01	9.68E-01	LC-MS
319	Hippurate	1.01	9.66E-01	LC-MS
320	Mercaptoethanol	-1	9.91E-01	LC-MS
321	Asp-Asp	-1	9.74E-01	LC-MS
322	[ST hydroxy(3:0)] (5Z,7E)-(3S)-3-hydroxy-9,10-seco-5,7,10(19)-cholatrien-24-oic acid	-1.01	9.66E-01	LC-MS
323	&alpha;-(2,6-anhydro-3-deoxy-D-arabino-heptulopyranosid)onate 7-phosphate	-1.01	9.71E-01	LC-MS
324	Tyramine	-1.02	9.16E-01	LC-MS
325	&gamma;-aminobutyramide	-1.02	8.92E-01	LC-MS
326	Deoxyribonolactone	-1.03	8.07E-01	LC-MS
327	Tributyl phosphate	-1.03	8.32E-01	LC-MS
328	2-Acetolactate	-1.04	7.75E-01	LC-MS
329	N-Acetylserotonin	-1.04	8.41E-01	LC-MS
330	Furfural	-1.04	8.21E-01	LC-MS
331	Ethyl (R)-3-hydroxyhexanoate	-1.04	6.61E-01	LC-MS
332	gamma-Amino-gamma-cyanobutanoate	-1.05	7.71E-01	LC-MS
333	<b>Inosine</b>	-1.05	8.50E-01	LC-MS
334	3,4-Dihydroxy-trans-cinnamate	-1.06	7.69E-01	LC-MS
335	[PC (16:0)] 1-hexadecanoyl-sn-glycero-3-phosphocholine	-1.06	8.10E-01	LC-MS
336	Spermidine	-1.08	5.58E-01	LC-MS
337	[FA amino(11:0)] 11-amino-undecanoic acid	-1.08	7.46E-01	LC-MS
338	(4E)-2-Oxohexenoic acid	-1.09	6.88E-01	LC-MS
339	N-Acetylserotonin	-1.09	6.21E-01	LC-MS
340	[PK] 6-Methylsalicylic acid	-1.09	2.74E-01	LC-MS
341	Methanesulfonic acid	-1.1	6.24E-01	LC-MS
342	L-cysteine sulfinic acid	-1.1	4.95E-01	LC-MS
343	Urate	-1.11	6.75E-01	LC-MS
344	<b>Deoxyadenosine</b>	-1.11	6.73E-01	LC-MS
345	<b>Hypoxanthine</b>	-1.11	7.40E-01	LC-MS
346	2-Ethylhexyl phthalate	-1.12	5.03E-01	LC-MS
347	<b>L-Serine</b>	-1.14	2.87E-01	LC-MS
348	Monomethyl sulfate	-1.14	6.74E-01	LC-MS
349	MOPS	-1.16	1.71E-01	LC-MS
350	4-Hydroxybenzoate	-1.16	2.12E-01	LC-MS
351	Chlorate	-1.17	3.40E-01	LC-MS
352	N-(L-Arginino)succinate	-1.17	2.97E-01	LC-MS
353	<b>D-Erythrose 4-phosphate</b>	-1.18	3.05E-01	LC-MS
354	Glu-Asp	-1.18	2.70E-01	LC-MS
355	2-C-Methyl-D-erythritol 4-phosphate	-1.18	5.99E-01	LC-MS
356	3-Hydroxypropenoate	-1.18	1.50E-01	LC-MS
357	2',3'-Cyclic CMP	-1.18	4.51E-01	LC-MS
358	3-Methyleneoxindole	-1.19	6.91E-02	LC-MS
359	Erythrulose 1-phosphate	-1.2	2.65E-01	LC-MS
360	D-Mannose 1-phosphate	-1.21	1.70E-01	LC-MS
361	Hexadecasphinganine	-1.22	2.86E-01	LC-MS

362	2-Butyne-1,4-diol	-1.24	1.04E-01	LC-MS
363	[FA (12:4/2:0)] Dodecatetraenedioic acid	2E,4E,8E,10E- -1.28	1.12E-03	LC-MS
364	2-Hydroxyethanesulfonate	-1.28	8.08E-02	LC-MS
365	Asp-Ser-Ser	-1.3	3.68E-01	LC-MS
366	Allantoin	-1.31	6.54E-02	LC-MS
367	Phenylpyruvate	-1.32	1.42E-01	LC-MS
368	2,7-Anhydro-alpha-N-acetylneuraminic acid	-1.35	1.24E-01	LC-MS
369	D-myo-Inositol 1,2-cyclic phosphate	-1.35	5.19E-02	GC-MS
370	di-n-Undecylamine	-1.36	4.54E-01	LC-MS
371	olomoucine	-1.36	1.78E-01	LC-MS
372	LysoPC(17:0)	-1.36	1.40E-01	LC-MS
373	Diketogulonicacid	-1.36	3.74E-01	LC-MS
374	Aspartyl-L-proline	-1.37	1.28E-01	LC-MS
375	5-Methylcytidine	-1.4	1.82E-01	LC-MS
376	myo-Inositol	-1.41	2.62E-01	LC-MS
377	3-Methoxy-4-hydroxyphenylethyleneglycol	-1.41	4.41E-02	LC-MS
378	2,3,5-Trihydroxytoluene	-1.42	6.73E-02	LC-MS
379	D-Glucose 6-phosphate	-1.44	2.49E-02	LC-MS
380	DL-Glyceraldehyde 3-phosphate	-1.44	9.90E-04	LC-MS
381	CPA(18:1(11Z)/0:0)	-1.45	4.14E-01	LC-MS
382	Lotaustralin	-1.45	3.81E-02	LC-MS
383	L-thiazolidine-4-carboxylate	-1.53	1.10E-01	LC-MS
384	10-Hydroxydecanoic acid	-1.53	5.51E-05	LC-MS
385	3-Hydroxy-N6,N6,N6-trimethyl-L-lysine	-1.55	2.60E-01	LC-MS
386	D-Glucose	-1.57	9.40E-02	LC-MS
387	[ST] (5Z,7E)-9,10-seco-5,7,10(19)- cholestatriene	-1.66	1.50E-01	LC-MS
388	Taurine	-1.7	2.55E-02	LC-MS
389	4-Guanidinobutanoate	-1.72	4.74E-04	LC-MS
390	1-Aminocyclopropane-1-carboxylate	-1.73	1.86E-03	LC-MS
391	Miraxanthin-I	-1.75	5.27E-02	LC-MS
392	Leu-Pro	-1.82	5.73E-04	LC-MS
393	cis-(homo)2aconitate	-1.84	4.64E-03	LC-MS
394	beta-Alanine	-1.84	4.52E-03	LC-MS
395	N-Acetyl-D-fucosamine	-1.85	2.09E-03	LC-MS
396	Pseudouridine	-1.91	6.22E-05	LC-MS
397	beta-D-Fructose 2,6-bisphosphate	-1.92	2.92E-06	LC-MS
398	3,4',5-Trihydroxystilbene	-1.99	9.12E-02	LC-MS
399	Isocitrate	-1.99	2.69E-01	GC-MS
400	N5-(L-1-Carboxyethyl)-L-ornithine	-2.02	1.08E-01	LC-MS
401	glucosamine-1,6-diphosphate	-2.06	3.19E-07	LC-MS
402	Glutathione disulfide	-2.09	7.55E-06	LC-MS
403	Mesaconate	-2.1	6.29E-04	LC-MS
404	N-acetyl-(L)-arginine	-2.22	8.79E-05	LC-MS
405	Cys-Gly	-2.24	1.36E-03	LC-MS
406	Hypotaurine	-2.28	7.05E-06	LC-MS
407	CMP-N-acetylneuraminate	-2.34	3.30E-05	LC-MS

408	Malonate	-2.46	1.72E-03	LC-MS
409	Deoxycytidine	-2.47	7.94E-03	LC-MS
410	N-Methylethanolamine phosphate	-2.48	2.32E-03	LC-MS
411	Bis(glycerophospho)-glycerol	-2.5	1.13E-03	LC-MS
412	Creatine	-2.53	4.91E-05	LC-MS
413	1-Methylnicotinamide	-2.55	2.28E-03	LC-MS
414	4-Methylene-L-glutamine	-2.64	5.48E-04	LC-MS
415	N-Acetyl-D-mannosamine	-2.65	3.19E-05	LC-MS
416	(R)-Malate	-2.7	6.26E-03	LC-MS
417	3-beta-D-Galactosyl-sn-glycerol	-2.71	5.26E-02	LC-MS
418	<b>Glycine</b>	-2.72	1.69E-04	LC-MS
419	[PC (18:0)] 1-octadecanoyl-sn-glycero-3-phosphocholine	-3.01	2.85E-04	LC-MS
420	Tetradecanoylcarnitine	-3.06	1.10E-04	LC-MS
421	Elaidiccarnitine	-3.08	1.87E-03	LC-MS
422	[FA (6:0)] O-hexanoyl-R-carnitine	-3.09	2.20E-03	LC-MS
423	2-Phenylacetamide	-3.11	2.33E-05	GC-MS
424	gamma-Glutamyl-beta-cyanoalanine	-3.13	8.16E-06	LC-MS
425	DL-2-Aminooctanoicacid	-3.39	2.00E-03	LC-MS
426	Glycyl-leucine	-3.49	1.88E-08	LC-MS
427	N3-methylcytosine	-3.53	4.79E-09	LC-MS
428	Slaframine	-3.56	2.08E-05	LC-MS
429	O-Butanoylcarnitine	-3.67	6.94E-10	LC-MS
430	N-Acetyl-D-glucosaminatate	-3.71	1.21E-07	LC-MS
431	Homostachydrine	-3.83	3.73E-04	LC-MS
432	2,3-Dimethylmaleate	-4.1	4.61E-06	LC-MS
433	3-sulfopropoanate	-4.12	1.77E-07	LC-MS
434	4-Hydroxy-2-butynal	-4.14	1.29E-05	LC-MS
435	4-Hydroxy-L-threonine	-4.18	4.08E-07	LC-MS
436	<b>L-Carnitine</b>	-4.23	2.10E-05	LC-MS
437	D-Xylulose	-4.33	7.16E-07	LC-MS
438	Orotidine	-4.39	9.79E-06	LC-MS
439	N4-acetyl-N4-hydroxy-1-aminopropane	-4.74	2.53E-03	LC-MS
440	<b>L-Citrulline</b>	-5.64	9.10E-04	LC-MS
441	[FA hydroxy(10:0)] N-(3S-hydroxydecanoyl)-L-serine	-5.7	8.26E-05	LC-MS
442	N-Ethylglycocyanine	-6.15	4.62E-06	LC-MS
443	<b>Orotate</b>	-6.64	2.47E-08	LC-MS
444	Thr-Ala	-6.89	7.75E-05	LC-MS
445	Trimethylamine N-oxide	-7.12	1.18E-08	LC-MS
446	[FA] O-Palmitoyl-R-carnitine	-7.79	3.37E-05	LC-MS
447	(S)-Dihydroorotate	-7.82	6.48E-07	LC-MS
448	6-Acetyl-D-glucose	-7.83	6.06E-05	LC-MS
449	Ala-Asp-Cys	-7.84	3.28E-09	LC-MS
450	Met-Ala-Gly	-8.49	3.34E-06	LC-MS
451	[SP] Sphing-4-enine-1-phosphate	-8.71	3.67E-15	LC-MS
452	D-perosamine	-8.89	4.37E-06	LC-MS
453	Ala-Ser-Tyr	-8.91	5.41E-04	LC-MS

454	N-Acetyl-L-glutamate 5-semialdehyde	-8.91	7.25E-07	LC-MS
455	2-Phenylethanolglucuronide	-9.39	4.28E-06	LC-MS
456	[FA (10:0)] O-decanoyl-R-carnitine	-9.47	4.06E-06	LC-MS
457	2-Isopropylmaleate	-11.56	1.91E-06	LC-MS
458	Ergothioneine	-12.75	9.31E-09	LC-MS
459	O-Propanoylcarnitine	-13.46	3.85E-06	LC-MS
460	cis-Aconitate	-16.1	3.12E-05	LC-MS
461	<b>Phosphocreatine</b>	-17.16	3.85E-03	LC-MS
462	Stachydrine	-17.93	3.08E-04	LC-MS
463	L-Octanoylcarnitine	-18.16	6.64E-07	LC-MS
464	1,2-dioctanoyl-1-amino-2,3-propanediol	-19.83	7.85E-06	LC-MS
465	Dihydrobiopterin	-21.08	1.15E-04	LC-MS
466	indole carboxyl thiazole	-21.57	4.48E-08	LC-MS
467	(S)-2-Amino-3-(3-hydroxy-4-oxo-4H-pyridin-1-yl)propanoate	-22.56	3.04E-09	LC-MS
468	dTTP	<25 fold	2.52E-07	LC-MS
469	creatinine phosphate	<25 fold	2.60E-03	LC-MS
470	1-Methyladenosine	<25 fold	2.51E-08	LC-MS
471	N-Carbamoyl-L-aspartate	<25 fold	6.29E-06	LC-MS
472	IAA-phenylalanine	<25 fold	7.00E-07	LC-MS
473	Glu-Glu-Met	<25 fold	5.19E-08	LC-MS
474	Taurocyamine	<25 fold	4.20E-06	LC-MS
475	Ala-Val-Pro-Ser	<25 fold	1.63E-06	LC-MS
476	Glu-Met	<25 fold	2.86E-08	LC-MS
477	[FA oxo,amino(6:0)] 3-oxo-5S-amino-hexanoic acid	<25 fold	1.49E-06	LC-MS
478	2-6dimethylheptanoylcarnitine	<25 fold	8.34E-06	LC-MS
479	S-5-methylthiopentylhydroximoyl-L-cysteine	<25 fold	2.27E-08	LC-MS
480	2-Amino-4-hydroxy-6-hydroxymethyl-7,8-dihydropteridine	<25 fold	3.23E-06	LC-MS
481	2-Amino-4-hydroxy-6-(D-erythro-1,2,3-trihydroxypropyl)-7,8-dihydropteridine	<25 fold	1.22E-04	LC-MS
482	N-Methylnicotinate	<25 fold	7.96E-05	LC-MS

Table 4 Putative metabolites (PMs) represented in

Figure 4-2 showing fold change in abundance in Gametocytes compared to uninfected reticulocyte enriched erythrocytes. PMs are listed in order of decreasing abundance (metabolites identified with authentic standards are highlighted bold)

No.	Metabolites	Fold change (Gametocytes/ Reticulocytes)	P-Value	Platform
1	Arg-Cys-Ser-Tyr	> 25 fold	6.60E-03	LC-MS
2	dTMP	> 25 fold	8.39E-07	LC-MS
3	D-Ribitol 5-phosphate	> 25 fold	6.97E-08	LC-MS
4	Asp-Met-Asp-Gly	> 25 fold	2.48E-05	LC-MS
5	UMP	> 25 fold	6.00E-04	GC-MS
6	L-Gulonate	> 25 fold	3.38E-07	LC-MS
7	O-Phospho-L-serine	> 25 fold	1.05E-03	LC-MS
8	CMP-N-trimethyl-2-aminoethylphosphonate	> 25 fold	3.99E-05	LC-MS
9	Met-Ala-Asp	> 25 fold	8.98E-06	LC-MS
10	Lys-Tyr	> 25 fold	2.51E-03	LC-MS
11	Asn-Asn-Asp	> 25 fold	8.71E-05	LC-MS
12	Deoxyinosine	> 25 fold	2.12E-06	LC-MS
13	<b>D-Gluconic acid</b>	> 25 fold	1.83E-07	LC-MS
14	gamma-Glutamyl-gamma-aminobutyraldehyde	> 25 fold	2.27E-04	LC-MS
15	<b>sn-glycero-3-Phosphocholine</b>	> 25 fold	1.50E-09	LC-MS
16	Pyrimidine nucleoside	> 25 fold	1.34E-04	LC-MS
17	4,5-seco-dopa	> 25 fold	1.83E-05	LC-MS
18	Val-Asp-Gly	> 25 fold	5.19E-05	LC-MS
19	Hypusine	> 25 fold	1.59E-05	LC-MS
20	<b>Choline phosphate</b>	> 25 fold	2.76E-06	LC-MS
21	Ala-Leu-Asn-Ser	> 25 fold	9.01E-05	LC-MS
22	dAMP	> 25 fold	2.97E-04	LC-MS
23	Propanoyl phosphate	> 25 fold	3.59E-06	LC-MS
24	Phosphonoacetaldehyde	> 25 fold	3.94E-06	LC-MS
25	Ala-Ser-Tyr	20.4	3.02E-07	LC-MS
26	CDP-ethanolamine	19.99	1.60E-05	LC-MS
27	hydrogen iodide	19.83	1.45E-07	LC-MS
28	Leu-Asn-Asp	19.74	2.70E-06	LC-MS
29	Cytidine 2'-phosphate	19.73	1.04E-05	LC-MS
30	CDP-choline	18.57	2.01E-04	LC-MS
31	4,6-Dideoxy-4-oxo-dTDP-D-glucose	18.37	6.48E-06	LC-MS
32	Cryogenine	18.29	1.57E-04	LC-MS
33	Glu-Thr	17.09	1.11E-04	LC-MS
34	N-hydroxy-N-isopropylloxamate	16.51	2.87E-04	LC-MS
35	N-Ribosylnicotinamide	16.09	1.93E-04	LC-MS
36	2-Carboxy-D-arabinitol 1-phosphate	15.24	7.55E-05	LC-MS
37	D-4'-Phosphopantothenate	14.61	4.81E-05	LC-MS
38	<b>Inosine</b>	14.23	8.75E-07	LC-MS
39	succinamate	14.22	3.96E-04	LC-MS
40	<b>Hypoxanthine</b>	13.98	3.51E-08	LC-MS

41	Thr-Ala-Asp	12.54	7.21E-05	LC-MS
42	Ala-Gly-Pro	12.49	4.15E-06	LC-MS
43	Ethanolamine phosphate	12.35	2.32E-04	LC-MS
44	O-Acetyl-L-homoserine	12.12	1.70E-05	LC-MS
45	<b>Choline</b>	12.04	8.44E-12	LC-MS
46	Pro-Pro	11.67	1.40E-02	LC-MS
47	<b>3',5'-Cyclic AMP</b>	11.19	2.31E-05	LC-MS
48	GammaGlutamylglutamicacid	10.93	1.06E-04	LC-MS
49	Ala-Ser	10.65	4.91E-05	LC-MS
50	<b>Guanosine</b>	10.32	5.88E-05	LC-MS
51	N1-Acetylspermidine	9.83	4.67E-04	LC-MS
52	sn-glycero-3-Phosphoethanolamine	9.56	9.17E-03	LC-MS
53	[FA hydroxy(10:0)] N-(3S-hydroxydecanoyl)-L-serine	9.15	5.96E-04	LC-MS
54	Fructoselysine	9.11	3.53E-05	LC-MS
55	<b>GMP</b>	8.8	9.23E-06	LC-MS
56	Piperidine	8.57	5.28E-05	LC-MS
57	<b>CMP</b>	8.39	3.01E-05	LC-MS
58	D-Sedoheptulose 1,7-bisphosphate	8.08	2.40E-05	LC-MS
59	Lys-Pro	7.98	2.67E-03	LC-MS
60	Glu-Met-Thr	7.8	5.13E-03	LC-MS
61	Isocitrate	7.5	1.96E-06	GC-MS
62	Leukotriene B4	7.39	1.64E-05	LC-MS
63	&alpha;-methylhistidine	7.31	3.83E-07	LC-MS
64	Tetradecanoylcarnitine	7.29	7.36E-04	LC-MS
65	Glycerone phosphate	7.08	1.93E-07	LC-MS
66	Ala-Leu-Lys-Pro	6.95	3.02E-06	LC-MS
67	<b>Cytidine</b>	6.93	1.16E-03	LC-MS
68	Ala-Pro	6.66	7.71E-05	LC-MS
69	Glu-Gly	6.63	9.15E-04	LC-MS
70	[GP (16:0)] 1-hexadecanoyl-2-sn-glycero-3-phosphate	6.53	1.12E-03	LC-MS
71	Asn-Pro	6.44	1.14E-04	LC-MS
72	[FA (6:0)] O-hexanoyl-R-carnitine	6.41	7.86E-04	LC-MS
73	gamma-L-Glutamyl-L-cysteine	6.16	1.32E-05	LC-MS
74	Sedoheptulose	6.06	2.61E-06	LC-MS
75	[FA hydroxy(20:4)] 15S-hydroxy-5Z,8Z,11Z,13E-eicosatetraenoic acid	5.81	9.70E-05	LC-MS
76	Carnosine	5.58	4.02E-03	LC-MS
77	P-DPD	5.58	1.12E-04	LC-MS
78	UDP-N-acetyl-D-glucosamine	5.56	8.25E-05	LC-MS
79	<b>Guanine</b>	5.56	1.84E-03	LC-MS
80	<b>S-Adenosyl-L-methionine</b>	5.46	3.01E-04	LC-MS
81	Met-Thr-Asp	5.41	4.94E-04	LC-MS
82	2-Deoxy-D-ribose 5-phosphate	5.37	4.21E-09	LC-MS
83	Glu-Glu-Gln-Pro	5.32	1.35E-04	LC-MS
84	<b>L-Glutamate</b>	5.31	7.35E-06	LC-MS
85	<b>Putrescine</b>	5.21	1.10E-03	LC-MS
86	Diketogulonicacid	5.15	3.19E-07	LC-MS

87	Elaidiccarnitine	4.99	2.02E-03	LC-MS
88	cis-Aconitate	4.97	2.73E-07	LC-MS
89	D-Alanyl-D-alanine	4.95	6.71E-06	LC-MS
90	(S)-AMPA	4.87	2.44E-06	LC-MS
91	dTDP-3-amino-2,3,6-trideoxy-D-threo-hexopyranos-4-ulose	4.72	2.87E-11	LC-MS
92	Dihydrobiopterin	4.69	2.56E-06	LC-MS
93	gamma-L-Glutamyl-L-cysteinyl-beta-alanine	4.64	1.87E-04	LC-MS
94	N-Acetyl-aspartyl-glutamate	4.63	8.68E-05	LC-MS
95	5-(chloromercuri)cytidine	4.53	4.84E-06	LC-MS
96	N-Acetylglutamine	4.38	1.97E-04	LC-MS
97	Pyridoxamine phosphate	4.32	1.37E-05	LC-MS
98	<b>Lactate</b>	4.27	4.12E-08	LC-MS
99	Hydroxymethylphosphonate	4.27	3.94E-03	LC-MS
100	<b>sn-Glycerol 3-phosphate</b>	4.23	5.50E-04	LC-MS
101	[FA trihydroxy(4:0)] 2,3,4-trihydroxy-butanoic acid	4.22	2.89E-07	LC-MS
102	[PC (16:0)] 1-hexadecanoyl-sn-glycero-3-phosphocholine	4.18	6.64E-04	LC-MS
103	<b>L-Proline</b>	4.15	1.23E-09	LC-MS
104	CMP-2-aminoethylphosphonate	4.11	1.89E-04	LC-MS
105	D-Glucuronate 1-phosphate	4.07	1.51E-04	LC-MS
106	Ala-Cys	4.03	9.68E-05	LC-MS
107	2-Aminoacrylate	3.93	3.24E-03	LC-MS
108	<b>L-Cystathionine</b>	3.93	3.73E-06	LC-MS
109	DL-&beta;-hydroxynorvaline	3.91	1.15E-05	LC-MS
110	N-Acetyllactosamine	3.72	4.16E-06	LC-MS
111	<b>L-Tyrosine</b>	3.68	2.12E-07	LC-MS
112	Methylimidazoleacetic acid	3.65	4.43E-06	LC-MS
113	[FA] O-Palmitoyl-R-carnitine	3.62	3.25E-03	LC-MS
114	Ala-Asp-Asp	3.62	1.54E-05	LC-MS
115	N-Formimino-L-glutamate	3.56	3.68E-04	LC-MS
116	2,3,4,5-Tetrahydrodipicolinate	3.56	3.87E-06	LC-MS
117	N(pi)-Methyl-L-histidine	3.56	6.06E-04	LC-MS
118	Glu-Val	3.54	2.33E-08	LC-MS
119	[SP] Sphing-4-ene-1-phosphate	3.49	3.08E-03	LC-MS
120	2,3-Dimethylmaleate	3.47	4.85E-06	LC-MS
121	N2-Succinyl-L-ornithine	3.44	1.11E-07	LC-MS
122	4-Hydroxy-2-butyral	3.39	1.12E-06	LC-MS
123	Pyrimidine 5'-deoxynucleotide	3.36	2.14E-06	LC-MS
124	Mesaconate	3.29	1.41E-05	LC-MS
125	<b>L-Tryptophan</b>	3.27	3.11E-08	LC-MS
126	<b>L-Alanine</b>	3.23	2.51E-07	LC-MS
127	1-Oleoylglycerophosphocholine	3.19	2.99E-03	LC-MS
128	<b>Phosphocreatine</b>	3.11	8.81E-06	LC-MS
129	Bis(glycerophospho)-glycerol	3.08	1.48E-04	LC-MS
130	glucosamine-1,6-diphosphate	3.06	4.08E-04	LC-MS
131	3-Oxopropanoate	3.05	4.22E-06	LC-MS

132	sn-glycero-3-Phospho-1-inositol	3.04	5.05E-06	LC-MS
133	L-1-Pyrroline-3-hydroxy-5-carboxylate	3	1.65E-06	LC-MS
134	N-(octanoyl)-L-homoserine	3	2.96E-04	LC-MS
135	<b>AMP</b>	3	8.77E-03	LC-MS
136	O-Butanoylcarnitine	2.99	8.13E-04	LC-MS
137	<b>Glycine</b>	2.99	2.96E-05	LC-MS
138	creatinine phosphate	2.89	7.69E-06	LC-MS
139	[SP] 3-dehydrosphinganine	2.88	1.02E-03	LC-MS
140	<b>N-Acetylneuraminate</b>	2.87	7.00E-05	LC-MS
141	[PC (18:2)] 1-(9Z,12Z-octadecadienoyl)-sn-glycero-3-phosphocholine	2.86	4.93E-03	LC-MS
142	<b>L-Aspartate</b>	2.85	7.67E-07	LC-MS
143	L-Erythrulose	2.79	9.23E-05	LC-MS
144	[FA hydroxy(18:2)] 9S-hydroxy-10E,12Z-octadecadienoic acid	2.76	1.97E-03	LC-MS
145	[PC (18:0)] 1-octadecanoyl-sn-glycero-3-phosphocholine	2.76	4.53E-03	LC-MS
146	<b>Fumarate</b>	2.74	2.35E-08	LC-MS
147	Glycerophosphoglycerol	2.72	4.41E-06	LC-MS
148	[FA (18:1)] 9Z-octadecenamide	2.67	1.99E-02	LC-MS
149	[FA (10:0)] O-decanoyl-R-carnitine	2.67	9.41E-03	LC-MS
150	<b>Adenine</b>	2.66	6.42E-04	LC-MS
151	Sphinganine	2.64	1.21E-02	LC-MS
152	N6-Methyl-L-lysine	2.62	4.71E-04	LC-MS
153	N-Acetyl-L-glutamate 5-semialdehyde	2.58	6.96E-06	LC-MS
154	<b>IMP</b>	2.57	1.93E-03	LC-MS
155	N-Acetyl-D-glucosamine 6-phosphate	2.53	1.44E-02	LC-MS
156	Phe-Pro	2.5	1.22E-04	LC-MS
157	<b>5'-Methylthioadenosine</b>	2.49	7.08E-03	LC-MS
158	Gamma-Glutamylglutamine	2.48	4.35E-03	LC-MS
159	LysoPC(17:0)	2.48	5.86E-03	LC-MS
160	L-Fucose 1-phosphate	2.45	8.01E-04	LC-MS
161	Malonate	2.43	2.22E-05	LC-MS
162	(1-Ribosylimidazole)-4-acetate	2.42	3.75E-04	LC-MS
163	[ST hydroxy(3:0)] (5Z,7E)-(3S)-3-hydroxy-9,10-seco-5,7,10(19)-cholatrien-24-oic acid	2.4	2.24E-02	LC-MS
164	[ST trihydrox] 3Alpha,7Alpha,12Alpha-trihydroxy-5Beta-cholan-24-oic acid	2.38	2.11E-02	LC-MS
165	Fructoselysine 6-phosphate	2.37	2.63E-04	LC-MS
166	allylcysteine	2.36	7.81E-04	LC-MS
167	Erythrulose 1-phosphate	2.33	7.02E-06	LC-MS
168	N2-Acetyl-L-aminoadipate	2.3	1.82E-05	LC-MS
169	<b>Malate</b>	2.3	1.59E-05	LC-MS
170	4-Acetamidobutanoate	2.29	9.27E-07	LC-MS
171	<b>Uridine</b>	2.29	1.96E-07	LC-MS
172	D-Threose	2.26	2.08E-04	LC-MS
173	L-Octanoylcarnitine	2.26	8.68E-03	LC-MS
174	N3-methylcytosine	2.25	1.31E-05	LC-MS

175	<b>L-Phenylalanine</b>	2.24	3.72E-08	LC-MS
176	L-Tyrosine methyl ester	2.24	1.91E-03	LC-MS
177	Taurine	2.2	5.42E-05	LC-MS
178	Leu-Thr	2.17	2.69E-05	LC-MS
179	D-Methionine	2.16	2.61E-05	LC-MS
180	Prenyl-L-cysteine	2.14	2.33E-02	LC-MS
181	1,2-dioctanoyl-1-amino-2,3-propanediol	2.12	1.55E-02	LC-MS
182	[SP] Sphinganine-1-phosphate	2.12	1.63E-02	LC-MS
183	<b>D-Ribose 5-phosphate</b>	2.11	2.57E-03	LC-MS
184	Thr-Thr-Ser	2.1	5.52E-04	LC-MS
185	Thiomorpholine 3-carboxylate	2.08	1.15E-03	LC-MS
186	Lotaustralin	2.05	7.14E-05	LC-MS
187	5-6-Dihydrouridine	2.05	1.37E-03	LC-MS
188	D-Aspartate	2.02	1.60E-04	LC-MS
189	S-Methyl-L-methionine	2.02	6.59E-03	LC-MS
190	2-6dimethylheptanoylcarnitine	2.02	3.46E-02	LC-MS
191	Palmiticamide	1.99	6.89E-02	LC-MS
192	(R)-Malate	1.98	6.16E-04	LC-MS
193	<b>Adenosine</b>	1.97	1.06E-03	LC-MS
194	Betaine	1.97	1.58E-06	LC-MS
195	Glu-Leu	1.97	6.11E-04	LC-MS
196	D-perosamine	1.96	5.61E-03	LC-MS
197	Glu-Pro	1.96	1.16E-04	LC-MS
198	Aspartyl-L-proline	1.95	1.70E-02	LC-MS
199	Piperidine	1.95	7.97E-06	LC-MS
200	Sorbitol 6-phosphate	1.94	8.50E-03	LC-MS
201	Sedoheptulose 7-phosphate	1.93	1.84E-04	LC-MS
202	<b>Phenylacetyl glycine</b>	1.93	1.25E-02	LC-MS
203	2-Amino-4-hydroxy-6-hydroxymethyl-7,8-dihydropteridine	1.91	4.52E-02	LC-MS
204	Phosphoribosyl-AMP	1.89	2.62E-03	LC-MS
205	Xylitol	1.89	8.21E-04	LC-MS
206	&alpha;-(2,6-anhydro-3-deoxy-D-arabino-heptulopyranosid)onate 7-phosphate	1.87	7.18E-04	LC-MS
207	D-Tryptophan	1.87	1.65E-01	LC-MS
208	[FA (18:2)] 9,12-octadecadienal	1.85	3.45E-02	LC-MS
209	2-hydroxysuccinamate	1.85	4.68E-02	LC-MS
210	2-Isopropylmaleate	1.83	4.58E-04	LC-MS
211	DL-2-Aminooctanoicacid	1.82	1.01E-01	LC-MS
212	<b>D-Erythrose 4-phosphate</b>	1.81	4.23E-03	LC-MS
213	Glycylproline	1.78	6.18E-05	LC-MS
214	<b>Sucrose</b>	1.76	1.16E-02	LC-MS
215	<b>D-Glucose 6-phosphate</b>	1.76	2.03E-04	LC-MS
216	<b>3-Phosphoglycerate</b>	1.74	7.31E-04	LC-MS
217	D-myo-Inositol 1,2-cyclic phosphate	1.74	8.79E-04	GC-MS
218	L-Hypoglycin	1.74	6.23E-03	LC-MS
219	4-Hydroxybenzoate	1.74	3.62E-01	LC-MS

220	Asp-Asp	1.74	6.96E-05	LC-MS
221	N-(Carboxyaminoethyl)urea	1.73	3.59E-03	LC-MS
222	beta-D-Fructose 2,6-bisphosphate	1.72	1.70E-03	LC-MS
223	L-Methionine S-oxide	1.72	3.34E-02	LC-MS
224	Acetylcholine	1.72	7.21E-03	LC-MS
225	(R)-S-Lactoylglutathione	1.72	4.07E-02	LC-MS
226	Aminopropylcadaverine	1.71	3.00E-03	LC-MS
227	Retronecine	1.71	6.44E-04	LC-MS
228	Hypotaurine	1.71	4.80E-02	LC-MS
229	<b>DL-Glyceraldehyde 3-phosphate</b>	1.7	2.37E-02	LC-MS
230	Chelilutine	1.69	2.44E-02	LC-MS
231	allopurinol	1.69	1.23E-01	LC-MS
232	Acetyl phosphate	1.68	9.03E-04	LC-MS
233	L-Arabinonate	1.66	5.39E-03	LC-MS
234	D-Mannose 1-phosphate	1.66	1.45E-03	LC-MS
235	Glu-Met	1.65	1.70E-02	LC-MS
236	D-Glucono-1,5-lactone	1.65	9.69E-02	LC-MS
237	Pyridoxal phosphate	1.64	2.37E-03	LC-MS
238	Phe-Asp	1.63	3.62E-02	LC-MS
239	<b>NAD+</b>	1.63	1.33E-02	LC-MS
240	O-Propanoylcarnitine	1.62	5.64E-04	LC-MS
241	(-)-Salsolinol	1.6	4.14E-02	LC-MS
242	[FA (6:0)] 6-[3]-ladderane-1-hexanol	1.6	6.24E-02	LC-MS
243	<b>Allantoin</b>	1.58	1.06E-02	LC-MS
244	<b>Uracil</b>	1.58	3.06E-09	LC-MS
245	Glu-Asp	1.58	4.83E-03	LC-MS
246	5-Acetamidopentanoate	1.57	3.02E-01	LC-MS
247	beta-Alanine	1.57	1.04E-03	LC-MS
248	[Fv Hydroxy,trimethoxy(9:1)] 4'-Hydroxy-5,6,7-trimethoxyflavanone	1.57	1.41E-01	LC-MS
249	Thr-Ala	1.55	9.28E-03	LC-MS
250	Ala-Asp-Cys	1.54	1.64E-02	LC-MS
251	Leucyl-leucine	1.54	6.02E-03	LC-MS
252	Triethanolamine	1.54	2.31E-04	LC-MS
253	<b>L-Kynurenine</b>	1.53	1.31E-03	LC-MS
254	Leu-Val	1.52	7.32E-04	LC-MS
255	Trimethylamine N-oxide	1.52	8.14E-05	LC-MS
256	Val-Val	1.52	9.12E-04	LC-MS
257	Asp-Gly	1.5	9.75E-03	LC-MS
258	3-Amino-2-oxopropyl phosphate	1.49	8.31E-02	LC-MS
259	Glu-Glu-Met	1.49	3.09E-02	LC-MS
260	5-Hydroxypentanoate	1.48	3.75E-04	LC-MS
261	2-monooleoylglycerol	1.47	4.87E-02	LC-MS
262	Linamarin	1.47	2.25E-02	LC-MS
263	2-Phenylethanolglucuronide	1.46	9.32E-03	LC-MS
264	(R)-AMAA	1.45	9.26E-03	LC-MS
265	Vinylacetylglycine	1.45	6.39E-03	LC-MS
266	1-Methylnicotinamide	1.44	1.39E-01	LC-MS

267	Xanthosine 5'-phosphate	1.44	1.79E-01	LC-MS
268	N-Acetyl-L-aspartate	1.42	1.21E-01	LC-MS
269	Mevaldate	1.41	1.02E-02	LC-MS
270	Sulfate	1.39	1.25E-02	LC-MS
271	Chlorate	1.35	7.69E-02	LC-MS
272	5-Methylcytidine	1.33	2.19E-02	LC-MS
273	gamma-Glutamyl-beta-cyanoalanine	1.33	3.25E-02	LC-MS
274	Spermidine	1.32	7.42E-03	LC-MS
275	Tyramine	1.32	2.85E-01	LC-MS
276	HEPES	1.32	2.75E-01	LC-MS
277	4-Methylene-L-glutamine	1.31	2.43E-01	LC-MS
278	4-Guanidinobutanoate	1.31	1.94E-02	LC-MS
279	Arg-Gln-Ser-Ser	1.31	2.72E-01	LC-MS
280	N4-acetyl-N4-hydroxy-1-aminopropane	1.29	4.29E-01	LC-MS
281	[FA (14:0/2:0)] Tetradecanedioic acid	1.29	1.51E-01	LC-MS
282	5-Hydroxyindoleacetate	1.28	9.99E-03	LC-MS
283	<b>Glutathione disulfide</b>	1.28	3.27E-02	LC-MS
284	CMP-N-acetylneuraminate	1.27	1.08E-01	LC-MS
285	[FA methyl,hydroxy(5:0)] 3R-methyl-3,5-dihydroxy-pentanoic acid	1.27	2.11E-01	LC-MS
286	Gamma-Aminobutyryl-lysine	1.26	1.44E-01	LC-MS
287	N5-Ethyl-L-glutamine	1.25	2.60E-01	LC-MS
288	L-Threonine	1.24	6.33E-02	LC-MS
289	Cys-Gly	1.22	1.49E-01	LC-MS
290	N-Acetyl-D-fucosamine	1.22	9.69E-02	LC-MS
291	L-5-benzyl-hydantoin	1.21	6.06E-01	LC-MS
292	[FA (20:4) 5Z,8Z,11Z,14Z-eicosatetraenoic acid	1.2	3.13E-01	LC-MS
293	N-Acetylserotonin	1.19	3.12E-01	LC-MS
294	2-Amino-4-hydroxy-6-(D-erythro-1,2,3-trihydroxypropyl)-7,8-dihydropteridine	1.18	3.90E-01	LC-MS
295	4-Oxocyclohexanecarboxylate	1.18	1.67E-01	LC-MS
296	2-Naphthylamine	1.18	2.00E-01	LC-MS
297	1-Aminocyclopropane-1-carboxylate	1.17	2.39E-01	LC-MS
298	2-C-Methyl-D-erythritol 4-phosphate	1.17	7.12E-01	LC-MS
299	[SP hydroxy,hydroxy,methyl(10:2/2:0)] 6R-(8-hydroxydecyl)-2R-(hydroxymethyl)-piperidin-3R-ol	1.17	4.62E-01	LC-MS
300	[FA hydroxy,oxo(7:0/2:0)] 4-hydroxy-2-oxo-Heptanedioic acid	1.17	5.51E-01	LC-MS
301	(4E)-2-Oxohexenoic acid	1.17	4.23E-01	LC-MS
302	[FA (7:0/2:0)] Heptanedioic acid	1.16	3.16E-01	LC-MS
303	NG,NG-Dimethyl-L-arginine	1.16	4.99E-01	LC-MS
304	Glu-Ser	1.16	5.67E-01	LC-MS
305	Pseudouridine	1.15	2.13E-01	LC-MS
306	<b>L-Carnitine</b>	1.15	2.99E-01	LC-MS
307	Dodecanamide	1.15	3.87E-01	LC-MS
308	(S)-3-Methyl-2-oxopentanoic acid	1.13	2.19E-01	LC-MS

309	N-Ethylglycocyanine	1.12	4.03E-01	LC-MS
310	Furfural diethyl acetal	1.11	5.11E-01	LC-MS
311	<b>L-Serine</b>	1.11	3.11E-01	LC-MS
312	<b>L-Citrulline</b>	1.11	7.38E-01	LC-MS
313	Tiglic acid	1.11	4.11E-01	LC-MS
314	<b>L-Histidine</b>	1.11	6.77E-01	LC-MS
315	[FA dioxo(8:0)] 4,7-dioxo-octanoic acid	1.1	5.53E-01	LC-MS
316	Methylmalonate	1.1	4.58E-01	LC-MS
317	Methyl cinnamate	1.09	6.52E-01	LC-MS
318	2-Hydroxyadenine	1.08	5.03E-01	LC-MS
319	6-Acetyl-D-glucose	1.08	6.08E-01	LC-MS
320	(S)-2-Aminobutanoate	1.08	6.13E-01	LC-MS
321	<b>Deoxyadenosine</b>	1.07	7.65E-01	LC-MS
322	(R)-2-Hydroxyglutarate	1.07	7.72E-01	LC-MS
323	L-thiazolidine-4-carboxylate	1.06	7.85E-01	LC-MS
324	Taurocyamine	1.04	7.98E-01	LC-MS
325	Cys-Cys-His-His	1.04	7.81E-01	LC-MS
326	2-Acetolactate	1.03	8.37E-01	LC-MS
327	Orotidine	1.03	8.04E-01	LC-MS
328	3-Hydroxypropenoate	1.03	7.75E-01	LC-MS
329	Canavanine	1.03	7.61E-01	LC-MS
330	<b>Succinate</b>	1.01	9.73E-01	LC-MS
331	(S)-2-Amino-3-(3-hydroxy-4-oxo-4H-pyridin-1-yl)propanoate	1	9.85E-01	LC-MS
332	di-n-Undecylamine	1	9.95E-01	LC-MS
333	[PK] 6-Methylsalicylic acid	1	9.83E-01	LC-MS
334	Cyclohex-2-enone	1	9.95E-01	GC-MS
335	Glu-Leu-Thr-His	-1	9.86E-01	LC-MS
336	1,3-benzenedisulfonate	-1	9.79E-01	LC-MS
337	L-cysteine sulfinate	-1.01	9.58E-01	LC-MS
338	1-methylguanosine	-1.01	9.42E-01	LC-MS
339	<b>Orthophosphate</b>	-1.01	9.45E-01	LC-MS
340	[FA oxo(8:0)] 5-oxo-7-octenoic acid	-1.01	9.31E-01	LC-MS
341	3-Methyleneoxindole	-1.03	7.40E-01	LC-MS
342	Adipate	-1.03	8.19E-01	LC-MS
343	His-Phe-Val-Pro	-1.03	8.72E-01	LC-MS
344	sodium chloride(aq)	-1.04	8.92E-01	LC-MS
345	[ST] (5Z,7E)-9,10-seco-5,7,10(19)-cholestatriene	-1.04	9.05E-01	LC-MS
346	Leu-Ala	-1.04	8.26E-01	LC-MS
347	Tributyl phosphate	-1.04	7.99E-01	LC-MS
348	3,4-Dihydroxy-trans-cinnamate	-1.04	8.10E-01	LC-MS
349	D-Sorbitol	-1.05	5.17E-01	LC-MS
350	[FA oxo,amino(6:0)] 3-oxo-5S-amino-hexanoic acid	-1.06	6.67E-01	LC-MS
351	<b>N6,N6,N6-Trimethyl-L-lysine</b>	-1.06	7.77E-01	LC-MS
352	Thr-Asp-Ser	-1.06	7.33E-01	LC-MS
353	D-Glycerate	-1.06	6.75E-01	LC-MS

354	2-Butyne-1,4-diol	-1.07	5.56E-01	LC-MS
355	MOPS	-1.08	4.96E-01	LC-MS
356	Homoarginine	-1.08	7.58E-01	LC-MS
357	8-keto-7-aminoperlagonate	-1.08	6.42E-01	LC-MS
358	[FA (12:4/2:0)] 2E,4E,8E,10E-Dodecatetraenedioic acid	-1.09	2.98E-01	LC-MS
359	3-Hydroxy-N6,N6,N6-trimethyl-L-lysine	-1.09	7.87E-01	LC-MS
360	D-Xylulose	-1.11	4.32E-01	LC-MS
361	3-Methoxy-4-hydroxyphenylethyleneglycol	-1.12	4.79E-01	LC-MS
362	Miraxanthin-I	-1.13	6.65E-01	LC-MS
363	myristic amide	-1.14	4.03E-01	LC-MS
364	cis-(homo)2aconitate	-1.14	2.16E-01	LC-MS
365	N-Acetylisatin	-1.15	4.24E-01	LC-MS
366	Ethyl (R)-3-hydroxyhexanoate	-1.15	2.04E-01	LC-MS
367	<b>L-2-Aminoadipate</b>	-1.16	1.96E-01	LC-MS
368	<b>L-Ornithine</b>	-1.17	5.28E-01	LC-MS
369	[FA (24:6)] 4,8,12,15,19,21-tetracosahexaenoic acid	-1.18	1.57E-01	LC-MS
370	N-Acetyl-D-glucosamine 6-sulfate	-1.18	3.45E-01	LC-MS
371	N2-(D-1-Carboxyethyl)-L-arginine	-1.18	4.03E-01	LC-MS
372	Leu-Pro	-1.19	2.68E-01	LC-MS
373	Furfural	-1.19	3.66E-01	LC-MS
374	3-Hydroxy-L-kynurenine	-1.19	6.90E-01	LC-MS
375	2,3,5-Trihydroxytoluene	-1.19	2.57E-01	LC-MS
376	Deoxyribonolactone	-1.2	1.92E-01	LC-MS
377	phosphinomethylmalate	-1.21	1.13E-01	LC-MS
378	Ala-Asp-Ser	-1.22	3.09E-01	LC-MS
379	2-Ethylhexyl phthalate	-1.22	1.38E-01	LC-MS
380	<b>N-methyl glucamine</b>	-1.23	4.00E-01	LC-MS
381	<b>L-Lysine</b>	-1.23	1.93E-01	LC-MS
382	N-(L-Arginino)succinate	-1.23	1.59E-01	LC-MS
383	[FA amino(11:0)] 11-amino-undecanoic acid	-1.24	2.25E-01	LC-MS
384	2-acetamidoglucal	-1.24	6.34E-02	LC-MS
385	Methanesulfonic acid	-1.26	2.75E-01	LC-MS
386	Slaframine	-1.26	1.10E-01	LC-MS
387	N1-(5-Phospho-alpha-D-ribosyl)-5,6-dimethylbenzimidazole	-1.27	3.04E-01	LC-MS
388	<b>Phenylpyruvate</b>	-1.29	1.35E-01	LC-MS
389	[ST hydrox] 3alpha,7alpha-Dihydroxy-5beta-cholan-24-oic Acid	-1.29	2.10E-02	LC-MS
390	Sulfoacetaldehyde	-1.29	1.76E-01	LC-MS
391	N3-(4-methoxyfumaroyl)-L-2,3-diaminopropanoate	-1.29	7.76E-02	LC-MS
392	2',3'-Cyclic CMP	-1.3	1.99E-02	LC-MS
393	Maltose	-1.31	8.75E-02	LC-MS
394	2-Hydroxyethanesulfonate	-1.33	5.70E-02	LC-MS
395	Hexadecaspheganine	-1.33	1.81E-01	LC-MS
396	Monomethyl sulfate	-1.37	1.46E-01	LC-MS

397	Heme	-1.38	2.25E-01	LC-MS
398	Stachydrine	-1.39	1.87E-01	LC-MS
399	N-Dimethyl-2-aminoethylphosphonate	-1.4	4.25E-02	LC-MS
400	IAA-phenylalanine	-1.41	2.08E-02	LC-MS
401	10-Hydroxydecanoic acid	-1.43	2.97E-04	LC-MS
402	Mercaptoethanol	-1.44	2.39E-01	LC-MS
403	<b>Xanthine</b>	-1.47	1.76E-04	LC-MS
404	4-Hydroxy-L-threonine	-1.49	2.77E-03	LC-MS
405	Xanthosine	-1.53	3.83E-04	LC-MS
406	N-acetyl-(L)-arginine	-1.53	3.81E-03	LC-MS
407	N-Methylethanolamine phosphate	-1.54	6.29E-02	LC-MS
408	N2-(D-1-Carboxyethyl)-L-lysine	-1.57	2.80E-02	LC-MS
409	<b>L-Glutamine</b>	-1.59	2.04E-03	LC-MS
410	Glycodeoxycholate	-1.6	9.74E-03	LC-MS
411	2-Phenylacetamide	-1.67	6.71E-03	GC-MS
412	gamma-Amino-gamma-cyanobutanoate	-1.69	2.02E-04	LC-MS
413	<b>D-Glucose</b>	-1.69	9.16E-02	LC-MS
414	Creatinine	-1.77	1.71E-03	LC-MS
415	γ-aminobutyramide	-1.77	3.70E-04	LC-MS
416	(S)-Methylmalonate semialdehyde	-1.81	9.47E-04	LC-MS
417	N-Acetyl-D-mannosamine	-1.87	1.36E-03	LC-MS
418	L-Glutamate 5-semialdehyde	-1.87	1.49E-04	LC-MS
419	<b>L-Asparagine</b>	-1.88	1.12E-04	LC-MS
420	Methyloxaloacetate	-1.9	2.12E-04	LC-MS
421	Urate	-1.95	2.01E-02	LC-MS
422	olomoucine	-1.98	9.51E-04	LC-MS
423	<b>S-glutathionyl-L-cysteine</b>	-2.07	1.49E-01	LC-MS
424	Ergothioneine	-2.07	4.01E-04	LC-MS
425	D-Lysine	-2.13	3.82E-03	LC-MS
426	Creatine	-2.14	1.89E-03	LC-MS
427	3-sulfopropanoate	-2.15	9.59E-06	LC-MS
428	2,7-Anhydro-alpha-N-acetylneuraminic acid	-2.17	1.30E-04	LC-MS
429	Homostachydrine	-2.64	1.37E-03	LC-MS
430	1-Methyladenosine	-2.72	1.85E-05	LC-MS
431	N5-(L-1-Carboxyethyl)-L-ornithine	-2.8	5.71E-06	LC-MS
432	Leu-Lys-Asp	-2.99	2.70E-03	LC-MS
433	<b>L-Arginine</b>	-3.05	1.52E-06	LC-MS
434	<b>Orotate</b>	-3.27	7.45E-07	LC-MS
435	N-Acetyl-D-glucosamine	-3.39	3.25E-09	LC-MS
436	3-beta-D-Galactosyl-sn-glycerol	-3.62	7.84E-06	LC-MS
437	myo-Inositol	-3.74	1.02E-02	LC-MS
438	Biotin	-3.94	1.18E-06	LC-MS
439	Hippurate	-4.55	7.47E-08	LC-MS
440	Glycyl-leucine	-4.56	1.61E-08	LC-MS
441	N-Methylnicotinate	-4.69	5.59E-04	LC-MS
442	3,4',5-Trihydroxystilbene	-5	3.03E-03	LC-MS

443	Glu-Cys-Gln-Gln	-5.54	1.37E-06	LC-MS
444	S-5-methylthiopentylhydroximoyl-L-cysteine	-9.82	4.56E-08	LC-MS
445	dTTP	-11.11	2.32E-07	LC-MS
446	(S)-Dihydroorotate	-11.57	9.64E-07	LC-MS
447	N-Carbamoyl-L-aspartate	-15.49	9.06E-06	LC-MS
448	indole carboxyl thiazole	-18.71	4.24E-08	LC-MS
449	Met-Ala-Gly	<25 fold	3.84E-07	LC-MS
450	L-Noradrenaline	<25 fold	1.33E-09	LC-MS
451	Ala-Val-Pro-Ser	<25 fold	1.63E-06	LC-MS
452	Deoxycytidine	<25 fold	1.82E-04	LC-MS

Table 5 Putative metabolites (PMs) represented in

Figure 4-3 showing fold change in abundance in *P. berghei* gametocytes compared to *P. berghei* schizonts. PMs are listed in order of decreasing abundance (metabolites identified with authentic standards are highlighted bold)

No.	Metabolites	Fold change (Gametocytes/ Schizonts)	P-Value	Platform
1	2-Amino-4-hydroxy-6-(D-erythro-1,2,3-trihydroxypropyl)-7,8-dihydropteridine	> 25 fold	5.66E-07	LC-MS
2	2-Amino-4-hydroxy-6-hydroxymethyl-7,8-dihydropteridine	> 25 fold	5.29E-04	LC-MS
3	Ala-Ser-Tyr	> 25 fold	2.23E-07	LC-MS
4	2-6dimethylheptanoylcarnitine	> 25 fold	5.13E-04	LC-MS
5	N-Methylnicotinate	> 25 fold	4.47E-12	LC-MS
6	Dihydrobiopterin	> 25 fold	5.97E-07	LC-MS
7	Glu-Met	> 25 fold	1.78E-05	LC-MS
8	Met-Ala-Asp	> 25 fold	9.28E-06	LC-MS
9	cis-Aconitate	> 25 fold	9.60E-08	LC-MS
10	creatinine phosphate	> 25 fold	2.09E-08	LC-MS
11	Glu-Glu-Met	> 25 fold	9.25E-06	LC-MS
12	Deoxyinosine	> 25 fold	2.21E-06	LC-MS
13	<b>Phosphocreatine</b>	> 25 fold	1.53E-07	LC-MS
14	[FA hydroxy(10:0)] N-(3S-hydroxydecanoyl)-L-serine	> 25 fold	2.82E-04	LC-MS
15	[FA oxo,amino(6:0)] 3-oxo-5S-amino-hexanoic acid	> 25 fold	5.61E-09	LC-MS
16	Asp-Met-Asp-Gly	> 25 fold	2.92E-05	LC-MS
17	1,2-dioctanoyl-1-amino-2,3-propanediol	> 25 fold	2.25E-04	LC-MS
18	L-Octanoylcarnitine	> 25 fold	1.56E-04	LC-MS
19	Taurocyamine	> 25 fold	4.15E-06	LC-MS
20	[SP] Sphing-4-ene-1-phosphate	> 25 fold	3.36E-04	LC-MS
21	[FA] O-Palmitoyl-R-carnitine	> 25 fold	4.08E-04	LC-MS
22	[FA (10:0)] O-decanoyl-R-carnitine	> 25 fold	5.10E-04	LC-MS
23	IAA-phenylalanine	22.74	2.68E-07	LC-MS
24	Tetradecanoylcarnitine	22.31	3.36E-04	LC-MS
25	(S)-2-Amino-3-(3-hydroxy-4-oxo-4H-pyridin-1-yl)propanoate	22.09	5.31E-04	LC-MS
26	O-Propanoylcarnitine	21.84	1.97E-08	LC-MS
27	2-Isopropylmaleate	21.19	4.72E-07	LC-MS
28	[FA (6:0)] O-hexanoyl-R-carnitine	19.8	3.23E-04	LC-MS
29	N-Acetyl-L-glutamate 5-semialdehyde	18.22	1.97E-07	LC-MS
30	D-perosamine	17.43	3.24E-05	LC-MS
31	<b>Hypoxanthine</b>	15.58	4.25E-08	LC-MS
32	Elaidiccarnitine	15.37	6.51E-04	LC-MS
33	D-Ribitol 5-phosphate	15.06	1.24E-07	LC-MS
34	<b>Inosine</b>	14.98	7.36E-07	LC-MS
35	2,3-Dimethylmaleate	14.21	5.97E-07	LC-MS
36	Isocitrate	14.05	2.08E-06	GC-MS
37	4-Hydroxy-2-butyral	14.04	1.84E-07	LC-MS
38	L-Gulonate	12.99	5.96E-07	LC-MS

39	Stachydrine	12.91	1.19E-05	LC-MS
40	Ala-Asp-Cys	12.08	1.07E-05	LC-MS
41	2-Phenylethanolglucuronide	11.7	1.02E-07	LC-MS
42	<b>D-Gluconic acid</b>	11.18	3.53E-07	LC-MS
43	O-Butanoylcarnitine	10.98	6.52E-05	LC-MS
44	Trimethylamine N-oxide	10.83	3.61E-09	LC-MS
45	Thr-Ala	10.71	3.52E-07	LC-MS
46	6-Acetyl-D-glucose	8.45	1.58E-09	LC-MS
47	S-5-methylthiopentylhydroximoyl-L-cysteine	8.33	2.24E-06	LC-MS
48	[PC (18:0)] 1-octadecanoyl-sn-glycero-3-phosphocholine	8.31	4.45E-04	LC-MS
49	<b>Glycine</b>	8.12	3.27E-06	LC-MS
50	N3-methylcytosine	7.95	1.23E-07	LC-MS
51	Bis(glycerophospho)-glycerol	7.69	1.81E-05	LC-MS
52	Thr-Thr-Ser	7.03	1.64E-08	LC-MS
53	Diketogulonicacid	7.02	4.88E-07	LC-MS
54	Mesaconate	6.92	2.87E-06	LC-MS
55	N-Ethylglycocamine	6.88	4.09E-07	LC-MS
56	glucosamine-1,6-diphosphate	6.31	5.96E-05	LC-MS
57	<b>L-Citrulline</b>	6.24	4.08E-03	LC-MS
58	DL-2-Aminooctanoicacid	6.17	4.78E-03	LC-MS
59	Ergothioneine	6.15	2.48E-03	LC-MS
60	N4-acetyl-N4-hydroxy-1-aminopropane	6.12	4.12E-03	LC-MS
61	Malonate	5.99	1.06E-06	LC-MS
62	Piperideine	5.55	1.01E-04	LC-MS
63	<b>sn-glycero-3-Phosphocholine</b>	5.51	2.17E-10	LC-MS
64	[GP (16:0)] 1-hexadecanoyl-2-sn-glycero-3-phosphate	5.39	1.47E-03	LC-MS
65	(R)-Malate	5.33	1.99E-07	LC-MS
66	<b>L-Carnitine</b>	4.85	1.75E-07	LC-MS
67	Glu-Gly	4.81	1.52E-03	LC-MS
68	2-Carboxy-D-arabinitol 1-phosphate	4.66	2.94E-04	LC-MS
69	O-Acetyl-L-homoserine	4.66	6.64E-05	LC-MS
70	Orotidine	4.54	2.20E-07	LC-MS
71	[PC (16:0)] 1-hexadecanoyl-sn-glycero-3-phosphocholine	4.44	5.59E-04	LC-MS
72	gamma-L-Glutamyl-L-cysteine	4.19	2.02E-05	LC-MS
73	gamma-Glutamyl-beta-cyanoalanine	4.15	1.10E-06	LC-MS
74	Hypotaurine	3.9	1.92E-03	LC-MS
75	D-Xylulose	3.89	1.30E-05	LC-MS
76	5-(chloromercuri)cytidine	3.77	1.11E-05	LC-MS
77	Taurine	3.74	9.33E-07	LC-MS
78	1-Methylnicotinamide	3.69	1.62E-03	LC-MS
79	4-Methylene-L-glutamine	3.48	1.58E-03	LC-MS
80	LysoPC(17:0)	3.37	1.91E-03	LC-MS
81	beta-D-Fructose 2,6-bisphosphate	3.3	1.93E-05	LC-MS
82	N-Acetyllactosamine	3.21	6.66E-06	LC-MS
83	Lotaustralin	2.98	3.10E-06	LC-MS

84	CMP-N-acetylneuraminate	2.98	3.62E-05	LC-MS
85	beta-Alanine	2.89	2.31E-10	LC-MS
86	Slaframine	2.82	4.82E-06	LC-MS
87	Erythrose 1-phosphate	2.8	1.59E-06	LC-MS
88	4-Hydroxy-L-threonine	2.78	3.78E-06	LC-MS
89	[PC (18:2)] 1-(9Z,12Z-octadecadienyl)-sn-glycero-3-phosphocholine	2.77	5.80E-03	LC-MS
90	Cys-Gly	2.74	9.35E-09	LC-MS
91	L-Erythrulose	2.69	1.15E-04	LC-MS
92	Aspartyl-L-proline	2.68	3.06E-03	LC-MS
93	<b>Glutathione disulfide</b>	2.66	1.76E-06	LC-MS
94	<b>3',5'-Cyclic AMP</b>	2.61	6.64E-04	LC-MS
95	dTMP	2.55	6.57E-05	LC-MS
96	<b>D-Glucose 6-phosphate</b>	2.53	1.85E-06	LC-MS
97	N-(octanoyl)-L-homoserine	2.51	6.52E-04	LC-MS
98	N2-Succinyl-L-ornithine	2.47	6.05E-07	LC-MS
99	<b>DL-Glyceraldehyde 3-phosphate</b>	2.45	3.00E-03	LC-MS
100	[ST hydroxy(3:0)] (5Z,7E)-(3S)-3-hydroxy-9,10-seco-5,7,10(19)-cholatrien-24-oic acid	2.41	2.09E-02	LC-MS
101	N-Carbamoyl-L-aspartate	2.4	7.01E-05	LC-MS
102	D-myo-Inositol 1,2-cyclic phosphate	2.35	2.82E-05	GC-MS
103	[ST trihydrox] 3Alpha,7Alpha,12Alpha-trihydroxy-5Beta-cholan-24-oic acid	2.32	2.10E-02	LC-MS
104	Asp-Ser-Ser	2.29	1.85E-02	LC-MS
105	N-Acetyl-D-fucosamine	2.26	1.01E-08	LC-MS
106	4-Guanidinobutanoate	2.26	1.24E-05	LC-MS
107	Pseudouridine	2.2	1.40E-05	LC-MS
108	L-1-Pyrroline-3-hydroxy-5-carboxylate	2.2	1.06E-05	LC-MS
109	Hydroxymethylphosphonate	2.15	3.67E-02	LC-MS
110	<b>D-Erythrose 4-phosphate</b>	2.13	1.77E-03	LC-MS
111	<b>L-Alanine</b>	2.11	5.40E-06	LC-MS
112	<b>Allantoin</b>	2.08	6.66E-04	LC-MS
113	1-Aminocyclopropane-1-carboxylate	2.03	5.77E-05	LC-MS
114	<b>Orotate</b>	2.03	5.97E-02	LC-MS
115	4-Hydroxybenzoate	2.02	2.83E-01	LC-MS
116	D-Mannose 1-phosphate	2.01	9.48E-05	LC-MS
117	dAMP	1.94	3.29E-02	LC-MS
118	3-sulfopropanoate	1.92	1.18E-02	LC-MS
119	[SP] Sphinganine-1-phosphate	1.89	3.65E-02	LC-MS
120	&alpha;-(2,6-anhydro-3-deoxy-D-arabinoheptulopyranosid)onate 7-phosphate	1.89	9.65E-04	LC-MS
121	[FA hydroxy(18:2)] 9S-hydroxy-10E,12Z-octadecadienoic acid	1.88	1.88E-02	LC-MS
122	5-Methylcytidine	1.88	1.44E-02	LC-MS
123	Glu-Asp	1.87	7.04E-04	LC-MS
124	2-Phenylacetamide	1.86	1.30E-02	GC-MS
125	Sedoheptulose 7-phosphate	1.85	7.75E-03	LC-MS
126	Leu-Thr	1.77	2.80E-04	LC-MS
127	2-hydroxysuccinamate	1.75	6.46E-02	LC-MS

128	Asp-Asp	1.74	1.40E-04	LC-MS
129	1-Oleoylglycerophosphocholine	1.68	7.84E-02	LC-MS
130	<b>Malate</b>	1.66	1.75E-03	LC-MS
131	allopurinol	1.61	2.06E-01	LC-MS
132	L-thiazolidine-4-carboxylate	1.61	5.83E-02	LC-MS
133	sn-glycero-3-Phosphoethanolamine	1.61	2.16E-01	LC-MS
134	N-Methylethanolamine phosphate	1.61	2.43E-02	LC-MS
135	cis-(homo)2aconitate	1.61	1.66E-02	LC-MS
136	[ST] (5Z,7E)-9,10-seco-5,7,10(19)-cholestatriene	1.6	2.33E-01	LC-MS
137	<b>Choline</b>	1.6	2.37E-05	LC-MS
138	Chlorate	1.57	1.67E-02	LC-MS
139	Miraxanthin-I	1.55	3.13E-01	LC-MS
140	Leu-Pro	1.53	1.72E-02	LC-MS
141	Aminopropylcadaverine	1.53	1.53E-02	LC-MS
142	succinamate	1.53	1.28E-01	LC-MS
143	2-Aminoacrylate	1.52	1.53E-01	LC-MS
144	Fructoselysine 6-phosphate	1.5	1.96E-02	LC-MS
145	(R)-S-Lactoylglutathione	1.45	1.28E-01	LC-MS
146	N-acetyl-(L)-arginine	1.45	6.46E-05	LC-MS
147	Homostachydrine	1.45	6.79E-03	LC-MS
148	<b>L-Cystathionine</b>	1.44	3.42E-02	LC-MS
149	Spermidine	1.43	1.06E-02	LC-MS
150	3-Hydroxy-N6,N6,N6-trimethyl-L-lysine	1.42	3.97E-02	LC-MS
151	N-Acetyl-D-mannosamine	1.42	2.05E-01	LC-MS
152	UDP-N-acetyl-D-glucosamine	1.42	9.29E-02	LC-MS
153	2-Deoxy-D-ribose 5-phosphate	1.41	7.65E-03	LC-MS
154	Prenyl-L-cysteine	1.4	2.30E-01	LC-MS
155	Chelilutine	1.4	1.31E-01	LC-MS
156	N-hydroxy-N-isopropylloxamate	1.39	2.00E-01	LC-MS
157	2-C-Methyl-D-erythritol 4-phosphate	1.38	4.41E-01	LC-MS
158	<b>Guanosine</b>	1.38	2.05E-01	LC-MS
159	N-Acetyl-D-glucosamine 6-phosphate	1.36	2.37E-01	LC-MS
160	di-n-Undecylamine	1.36	3.37E-01	LC-MS
161	Tyramine	1.34	2.60E-01	LC-MS
162	<b>L-Aspartate</b>	1.32	5.11E-02	LC-MS
163	N-Acetyl-L-aspartate	1.28	3.24E-01	LC-MS
164	[FA trihydroxy(4:0)] 2,3,4-trihydroxybutanoic acid	1.28	4.35E-02	LC-MS
165	Leucyl-leucine	1.27	1.31E-01	LC-MS
166	<b>D-Ribose 5-phosphate</b>	1.27	2.74E-01	LC-MS
167	(4E)-2-Oxohexenoic acid	1.27	3.38E-01	LC-MS
168	3-Methoxy-4-hydroxyphenylethyleneglycol	1.26	2.71E-01	LC-MS
169	<b>L-Serine</b>	1.26	9.32E-02	LC-MS
170	Triethanolamine	1.26	2.80E-01	LC-MS
171	Pyridoxal phosphate	1.25	9.83E-02	LC-MS
172	N-Acetylserotonin	1.24	2.97E-01	LC-MS
173	<b>3-Phosphoglycerate</b>	1.22	2.27E-01	LC-MS

174	3-Hydroxypropenoate	1.22	1.21E-02	LC-MS
175	D-Aspartate	1.2	1.87E-01	LC-MS
176	2,3,5-Trihydroxytoluene	1.19	3.92E-01	LC-MS
177	<b>Deoxyadenosine</b>	1.19	3.79E-01	LC-MS
178	<b>N-Acetylneuraminate</b>	1.18	2.75E-01	LC-MS
179	Creatine	1.18	5.78E-01	LC-MS
180	[FA (12:4/2:0)] 2E,4E,8E,10E-Dodecatetraenedioic acid	1.17	1.08E-01	LC-MS
181	GammaGlutamylglutamicacid	1.17	4.45E-01	LC-MS
182	allylcysteine	1.17	4.79E-01	LC-MS
183	D-Tryptophan	1.17	5.63E-01	LC-MS
184	4-Oxocyclohexanecarboxylate	1.16	3.28E-01	LC-MS
185	3-Methyleneoxindole	1.15	1.19E-01	LC-MS
186	2-Butyne-1,4-diol	1.15	5.08E-02	LC-MS
187	<b>sn-Glycerol 3-phosphate</b>	1.12	6.17E-01	LC-MS
188	[PK] 6-Methylsalicylic acid	1.1	4.18E-01	LC-MS
189	Ala-Leu-Lys-Pro	1.1	5.62E-01	LC-MS
190	Thiomorpholine 3-carboxylate	1.1	6.60E-01	LC-MS
191	L-cysteine sulfinat	1.09	4.05E-01	LC-MS
192	N-Acetyl-D-glucosaminat	1.09	7.51E-01	LC-MS
193	[FA (14:0/2:0)] Tetradecanedioic acid	1.09	6.31E-01	LC-MS
194	Dodecanamide	1.08	6.58E-01	LC-MS
195	Pyrimidine nucleoside	1.08	7.57E-01	LC-MS
196	10-Hydroxydecanoic acid	1.07	5.60E-01	LC-MS
197	MOPS	1.07	3.62E-01	LC-MS
198	2-Acetolactate	1.07	6.46E-01	LC-MS
199	<b>Guanine</b>	1.07	8.26E-01	LC-MS
200	Val-Asp-Gly	1.07	7.57E-01	LC-MS
201	Glycerone phosphate	1.06	6.42E-01	LC-MS
202	Methylmalonate	1.06	6.10E-01	LC-MS
203	<b>L-Proline</b>	1.05	6.36E-01	LC-MS
204	D-Sedoheptulose 1,7-bisphosphate	1.05	7.63E-01	LC-MS
205	2-monooleoylglycerol	1.04	8.38E-01	LC-MS
206	[FA dioxo(8:0)] 4,7-dioxo-octanoic acid	1.03	8.52E-01	LC-MS
207	D-Threose	1.03	8.28E-01	LC-MS
208	<b>Phenylpyruvate</b>	1.03	8.99E-01	LC-MS
209	hydrogen iodide	1.02	8.96E-01	LC-MS
210	Thr-Ala-Asp	1.02	9.43E-01	LC-MS
211	3,4-Dihydroxy-trans-cinnamate	1.02	9.49E-01	LC-MS
212	Ala-Ser	1.01	9.50E-01	LC-MS
213	(R)-2-Hydroxyglutarate	1	9.90E-01	LC-MS
214	Tributyl phosphate	-1.01	9.65E-01	LC-MS
215	L-Methionine S-oxide	-1.02	9.55E-01	LC-MS
216	Methyl cinnamate	-1.03	9.15E-01	LC-MS
217	Furfural diethyl acetal	-1.03	8.86E-01	LC-MS
218	2-Naphthylamine	-1.03	7.74E-01	LC-MS
219	2-Hydroxyethanesulfonate	-1.04	7.07E-01	LC-MS
220	Cyclohex-2-enone	-1.04	8.74E-01	GC-MS

221	N-Acetylisatin	-1.05	7.81E-01	LC-MS
222	N-(L-Arginino)succinate	-1.06	7.19E-01	LC-MS
223	[FA methyl,hydroxy(5:0)] 3R-methyl-3,5-dihydroxy-pentanoic acid	-1.06	7.55E-01	LC-MS
224	L-5-benzyl-hydantoin	-1.06	6.77E-01	LC-MS
225	<b>Cytidine</b>	-1.08	7.96E-01	LC-MS
226	Glu-Val	-1.08	3.56E-01	LC-MS
227	D-Alanyl-D-alanine	-1.08	6.46E-01	LC-MS
228	<b>D-Glucose</b>	-1.08	7.50E-01	LC-MS
229	[FA oxo(8:0)] 5-oxo-7-octenoic acid	-1.08	7.48E-01	LC-MS
230	<b>Fumarate</b>	-1.08	5.29E-01	LC-MS
231	Hexadecasphinganine	-1.09	6.66E-01	LC-MS
232	2-Ethylhexyl phthalate	-1.1	5.76E-01	LC-MS
233	2',3'-Cyclic CMP	-1.1	7.24E-01	LC-MS
234	Ethyl (R)-3-hydroxyhexanoate	-1.1	1.41E-01	LC-MS
235	CPA(18:1(11Z)/0:0)	-1.1	7.98E-01	LC-MS
236	Asn-Asn-Asp	-1.13	5.41E-01	LC-MS
237	N2-Acetyl-L-aminoadipate	-1.13	5.31E-01	LC-MS
238	Phe-Pro	-1.13	4.58E-01	LC-MS
239	Acetyl phosphate	-1.14	3.75E-01	LC-MS
240	L-Threonine	-1.14	4.47E-01	LC-MS
241	Furfural	-1.14	4.69E-01	LC-MS
242	O-Phospho-L-serine	-1.14	6.62E-01	LC-MS
243	[FA amino(11:0)] 11-amino-undecanoic acid	-1.14	6.48E-01	LC-MS
244	Asp-Gly	-1.15	2.81E-01	LC-MS
245	myristic amide	-1.15	6.03E-01	LC-MS
246	Methanesulfonic acid	-1.15	4.70E-01	LC-MS
247	N-Acetylglutamine	-1.16	5.11E-01	LC-MS
248	5-6-Dihydrouridine	-1.17	3.41E-01	LC-MS
249	Deoxyribonolactone	-1.17	2.20E-01	LC-MS
250	L-Arabinonate	-1.18	1.80E-01	LC-MS
251	<b>AMP</b>	-1.18	5.03E-01	LC-MS
252	P-DPD	-1.18	3.17E-01	LC-MS
253	Monomethyl sulfate	-1.2	6.49E-01	LC-MS
254	Gamma-Aminobutyryl-lysine	-1.2	2.62E-01	LC-MS
255	Linamarin	-1.23	2.18E-01	LC-MS
256	Ala-Asp-Asp	-1.23	2.02E-01	LC-MS
257	Vinylacetyl glycine	-1.25	1.96E-01	LC-MS
258	L-Fucose 1-phosphate	-1.27	2.33E-01	LC-MS
259	Canavanine	-1.27	5.01E-03	LC-MS
260	<b>Orthophosphate</b>	-1.27	5.76E-03	LC-MS
261	Val-Val	-1.27	2.04E-01	LC-MS
262	[FA (24:6)] 4,8,12,15,19,21-tetracosahexaenoic acid	-1.28	3.88E-02	LC-MS
263	S-Methyl-L-methionine	-1.29	3.59E-01	LC-MS
264	Glycyl-leucine	-1.31	6.85E-03	LC-MS
265	[ST hydrox] 3alpha,7alpha-Dihydroxy-5beta-cholan-24-oic Acid	-1.33	4.75E-03	LC-MS

266	3-beta-D-Galactosyl-sn-glycerol	-1.34	7.50E-01	LC-MS
267	Homoarginine	-1.34	1.61E-01	LC-MS
268	Glu-Thr	-1.35	2.96E-01	LC-MS
269	Leukotriene B4	-1.37	1.91E-01	LC-MS
270	2-acetamidoglucal	-1.39	1.06E-02	LC-MS
271	[FA hydroxy(20:4)] 15S-hydroxy-5Z,8Z,11Z,13E-eicosatetraenoic acid	-1.39	1.96E-01	LC-MS
272	N5-(L-1-Carboxyethyl)-L-ornithine	-1.4	6.25E-01	LC-MS
273	(R)-AMAA	-1.41	5.28E-02	LC-MS
274	[SP hydroxy,hydroxy,methyl(10:2/2:0)] 6R-(8-hydroxydecyl)-2R-(hydroxymethyl)-piperidin-3R-ol	-1.41	1.78E-01	LC-MS
275	5-Hydroxypentanoate	-1.41	4.98E-04	LC-MS
276	Maltose	-1.42	1.35E-04	LC-MS
277	Mercaptoethanol	-1.43	2.14E-01	LC-MS
278	Glu-Leu-Thr-His	-1.44	2.58E-04	LC-MS
279	3-Hydroxy-L-kynurenine	-1.45	2.66E-02	LC-MS
280	<b>Sucrose</b>	-1.45	1.32E-01	LC-MS
281	olomoucine	-1.46	2.33E-01	LC-MS
282	N-Formimino-L-glutamate	-1.48	6.79E-02	LC-MS
283	(S)-Dihydroorotate	-1.48	2.10E-01	LC-MS
284	Cys-Cys-His-His	-1.53	3.29E-05	LC-MS
285	L-Tyrosine methyl ester	-1.54	6.20E-02	LC-MS
286	(-)-Salsolinol	-1.54	1.50E-01	LC-MS
287	<b>CMP</b>	-1.57	5.98E-02	LC-MS
288	Pyrimidine 5'-deoxynucleotide	-1.57	1.13E-02	LC-MS
289	8-keto-7-aminoperlagonate	-1.58	7.04E-02	LC-MS
290	UMP	-1.59	1.78E-01	GC-MS
291	Adipate	-1.6	1.18E-03	LC-MS
292	N-Acetyl-D-glucosamine 6-sulfate	-1.6	4.83E-02	LC-MS
293	Leu-Ala	-1.6	5.06E-02	LC-MS
294	2,7-Anhydro-alpha-N-acetylneuraminic acid	-1.61	1.00E-01	LC-MS
295	gamma-Amino-gamma-cyanobutanoate	-1.61	3.22E-02	LC-MS
296	Glycerophosphoglycerol	-1.62	1.32E-02	LC-MS
297	Sulfate	-1.62	3.26E-03	LC-MS
298	His-Phe-Val-Pro	-1.62	4.59E-04	LC-MS
299	3-Amino-2-oxopropyl phosphate	-1.64	4.43E-01	LC-MS
300	<b>L-Glutamine</b>	-1.65	2.33E-02	LC-MS
301	N5-Ethyl-L-glutamine	-1.65	6.71E-03	LC-MS
302	Glu-Met-Thr	-1.66	3.55E-02	LC-MS
303	sodium chloride(aq)	-1.67	2.97E-03	LC-MS
304	Glu-Leu	-1.68	1.74E-02	LC-MS
305	D-Glycerate	-1.71	1.59E-03	LC-MS
306	Gamma-Glutamylglutamine	-1.73	1.26E-02	LC-MS
307	&gamma;-aminobutyramide	-1.73	2.14E-02	LC-MS
308	(S)-3-Methyl-2-oxopentanoic acid	-1.74	4.29E-03	LC-MS
309	Leu-Asn-Asp	-1.75	3.59E-03	LC-MS
310	Heme	-1.75	5.96E-02	LC-MS

311	Urate	-1.75	5.98E-02	LC-MS
312	Phosphonoacetaldehyde	-1.76	3.83E-03	LC-MS
313	Leu-Val	-1.76	1.43E-01	LC-MS
314	5-Acetamidopentanoate	-1.8	6.42E-02	LC-MS
315	N3-(4-methoxyfumaroyl)-L-2,3-diaminopropanoate	-1.84	3.10E-01	LC-MS
316	(S)-AMPA	-1.85	9.28E-03	LC-MS
317	Cryogenine	-1.85	1.26E-02	LC-MS
318	dTDP-3-amino-2,3,6-trideoxy-D-threo-hexopyranos-4-ulose	-1.86	1.01E-04	LC-MS
319	Thr-Asp-Ser	-1.88	1.98E-03	LC-MS
320	(S)-Methylmalonate semialdehyde	-1.92	7.49E-02	LC-MS
321	Glu-Pro	-1.93	1.41E-02	LC-MS
322	Methyloxaloacetate	-1.94	7.08E-02	LC-MS
323	[FA (18:1)] 9Z-octadecenamide	-1.97	5.33E-01	LC-MS
324	4,5-seco-dopa	-1.97	2.98E-03	LC-MS
325	<b>L-Glutamate</b>	-1.98	6.09E-04	LC-MS
326	Acetylcholine	-1.98	1.75E-02	LC-MS
327	4,6-Dideoxy-4-oxo-dTDP-D-glucose	-2	7.42E-02	LC-MS
328	D-Mannosylglycoprotein	-2.03	1.04E-03	LC-MS
329	Creatinine	-2.07	2.66E-03	LC-MS
330	<b>N-methyl glucamine</b>	-2.09	2.79E-02	LC-MS
331	1,3-benzenedisulfonate	-2.09	2.23E-06	LC-MS
332	Arg-Gln-Ser-Ser	-2.12	4.17E-03	LC-MS
333	DL-&beta;-hydroxynorvaline	-2.16	1.18E-04	LC-MS
334	D-Glucuronate 1-phosphate	-2.2	7.65E-04	LC-MS
335	Sorbitol 6-phosphate	-2.2	3.59E-03	LC-MS
336	<b>L-Lysine</b>	-2.24	8.66E-04	LC-MS
337	L-Hypoglycin	-2.24	2.16E-07	LC-MS
338	Ala-Asp-Ser	-2.24	2.66E-02	LC-MS
339	Tiglic acid	-2.28	3.74E-04	LC-MS
340	D-Lysine	-2.28	4.34E-03	LC-MS
341	<b>Choline phosphate</b>	-2.29	2.69E-03	LC-MS
342	(1-Ribosylimidazole)-4-acetate	-2.29	2.13E-02	LC-MS
343	[SP] 3-dehydrosphinganine	-2.3	1.10E-02	LC-MS
344	<b>L-2-Aminoadipate</b>	-2.3	1.19E-05	LC-MS
345	CDP-ethanolamine	-2.33	1.55E-02	LC-MS
346	Met-Ser	-2.33	8.41E-04	LC-MS
347	N-Acetyl-aspartyl-glutamate	-2.33	1.56E-03	LC-MS
348	Ethanolamine phosphate	-2.35	1.29E-02	LC-MS
349	[FA (7:0/2:0)] Heptanedioic acid	-2.36	6.15E-04	LC-MS
350	Palmiticamide	-2.36	4.79E-01	LC-MS
351	Cytidine 2'-phosphate	-2.37	1.34E-02	LC-MS
352	Hypusine	-2.42	8.14E-04	LC-MS
353	N-(Carboxyaminoethyl)urea	-2.5	1.16E-04	LC-MS
354	3,4',5-Trihydroxystilbene	-2.5	1.65E-01	LC-MS
355	Fructoselysine	-2.55	5.99E-04	LC-MS
356	Lys-Tyr	-2.55	2.62E-02	LC-MS

357	[FA (6:0)] 6-[3]-ladderane-1-hexanol	-2.56	2.52E-01	LC-MS
358	Pyridoxamine phosphate	-2.6	1.77E-04	LC-MS
359	HEPES	-2.61	4.02E-08	LC-MS
360	Sulfoacetaldehyde	-2.61	2.21E-04	LC-MS
361	N-Ribosylnicotinamide	-2.63	5.90E-04	LC-MS
362	[FA (18:2)] 9,12-octadecadienal	-2.64	2.77E-01	LC-MS
363	myo-Inositol	-2.66	4.82E-05	LC-MS
364	2,3,4,5-Tetrahydrodipicolinate	-2.68	7.94E-04	LC-MS
365	Met-Thr-Asp	-2.68	4.29E-05	LC-MS
366	4-Acetamidobutanoate	-2.75	2.25E-05	LC-MS
367	<b>GMP</b>	-2.78	3.81E-04	LC-MS
368	<b>Putrescine</b>	-2.79	2.79E-05	LC-MS
369	Ala-Leu-Asn-Ser	-2.83	8.83E-03	LC-MS
370	CDP-choline	-2.84	1.94E-02	LC-MS
371	Ala-Cys	-2.91	7.81E-04	LC-MS
372	<b>L-Asparagine</b>	-2.91	1.86E-06	LC-MS
373	Phe-Asp	-2.91	5.27E-04	LC-MS
374	<b>Uridine</b>	-2.93	7.64E-04	LC-MS
375	<b>Succinate</b>	-3.04	1.83E-04	LC-MS
376	<b>L-Kynurenine</b>	-3.06	6.92E-06	LC-MS
377	5-Hydroxyindoleacetate	-3.19	2.71E-06	LC-MS
378	gamma-L-Glutamyl-L-cysteinyl-beta-alanine	-3.23	1.58E-04	LC-MS
379	N1-Acetylspermidine	-3.25	2.60E-05	LC-MS
380	Pro-Pro	-3.32	1.95E-02	LC-MS
381	Methylimidazoleacetic acid	-3.37	4.34E-06	LC-MS
382	Arg-Cys-Ser-Tyr	-3.37	3.39E-02	LC-MS
383	<b>IMP</b>	-3.39	2.32E-03	LC-MS
384	Sedoheptulose	-3.42	5.76E-05	LC-MS
385	N-Dimethyl-2-aminoethylphosphonate	-3.44	4.70E-04	LC-MS
386	[FA (20:4)] 5Z,8Z,11Z,14Z-eicosatetraenoic acid	-3.51	4.08E-03	LC-MS
387	(S)-2-Aminobutanoate	-3.54	6.97E-02	LC-MS
388	<b>NAD+</b>	-3.64	5.72E-04	LC-MS
389	alpha-aminopimelate	-3.72	1.45E-05	LC-MS
390	alpha;-methylhistidine	-3.75	2.19E-02	LC-MS
391	3-Oxopropanoate	-3.82	4.19E-05	LC-MS
392	<b>S-glutathionyl-L-cysteine</b>	-3.87	1.66E-04	LC-MS
393	Xylitol	-3.87	2.31E-02	LC-MS
394	<b>Adenosine</b>	-3.94	1.17E-05	LC-MS
395	[FA hydroxy,oxo(7:0/2:0)] 4-hydroxy-2-oxo-Heptanedioic acid	-3.97	2.81E-03	LC-MS
396	N6-Methyl-L-lysine	-4.01	2.26E-05	LC-MS
397	siroamide	-4.03	9.37E-05	LC-MS
398	sn-glycero-3-Phospho-1-inositol	-4.13	6.84E-05	LC-MS
399	Phosphoribosyl-AMP	-4.18	8.00E-06	LC-MS
400	Glycocholate	-4.37	4.35E-05	LC-MS
401	Retronecine	-4.38	1.95E-07	LC-MS
402	<b>L-Tryptophan</b>	-4.38	1.37E-04	LC-MS

403	<b>N6,N6,N6-Trimethyl-L-lysine</b>	-4.43	1.64E-06	LC-MS
404	<b>Uracil</b>	-4.54	2.43E-04	LC-MS
405	Hippurate	-4.58	2.10E-05	LC-MS
406	Leu-Lys-Asp	-4.62	2.19E-02	LC-MS
407	CMP-N-trimethyl-2-aminoethylphosphonate	-4.76	6.51E-04	LC-MS
408	Xanthosine	-4.77	1.03E-04	LC-MS
409	NG,NG-Dimethyl-L-arginine	-4.79	4.45E-05	LC-MS
410	<b>L-Arginine</b>	-4.79	5.02E-08	LC-MS
411	Mevaldate	-4.82	2.08E-05	LC-MS
412	[Fv Hydroxy,trimethoxy(9:1)] 4'-Hydroxy-5,6,7-trimethoxyflavanone	-5.2	6.93E-04	LC-MS
413	Glu-Asp-Pro	-5.22	3.47E-06	LC-MS
414	N1-(5-Phospho-alpha-D-ribose)-5,6-dimethylbenzimidazole	-5.26	7.02E-03	LC-MS
415	Glu-Ser	-5.32	1.49E-02	LC-MS
416	CMP-2-aminoethylphosphonate	-5.36	2.99E-05	LC-MS
417	Biotin	-5.47	3.10E-07	LC-MS
418	L-Glutamate 5-semialdehyde	-5.69	8.28E-06	LC-MS
419	<b>Phenylacetyl glycine</b>	-5.84	2.00E-05	LC-MS
420	<b>Xanthine</b>	-5.85	4.33E-06	LC-MS
421	Lys-Pro	-5.96	2.73E-05	LC-MS
422	N2-(D-1-Carboxyethyl)-L-lysine	-5.98	1.72E-05	LC-MS
423	Glu-Cys-Gln-Gln	-6.16	4.58E-06	LC-MS
424	<b>L-Tyrosine</b>	-6.48	7.87E-05	LC-MS
425	Propanoyl phosphate	-6.63	1.26E-05	LC-MS
426	Glu-Glu-Gln-Pro	-6.73	6.63E-06	LC-MS
427	Betaine	-6.84	1.86E-05	LC-MS
428	<b>L-Phenylalanine</b>	-6.98	2.61E-05	LC-MS
429	gamma-Glutamyl-gamma-aminobutyraldehyde	-7.05	3.61E-04	LC-MS
430	Ala-Pro	-7.15	7.11E-06	LC-MS
431	D-4'-Phosphopantothenate	-7.64	3.95E-04	LC-MS
432	Ala-Ala-Ala	-7.89	1.78E-03	LC-MS
433	Arg-Lys-Ser-Ser	-8.23	2.35E-07	LC-MS
434	Cys-Met-Ser-His	-8.4	4.31E-08	LC-MS
435	D-Methionine	-8.42	3.16E-05	LC-MS
436	Asn-Pro	-8.66	4.67E-05	LC-MS
437	Cys-Glu-Glu-Pro	-9.2	7.82E-08	LC-MS
438	Xanthosine 5'-phosphate	-9.28	9.97E-04	LC-MS
439	Ala-Lys-Met-Gln	-9.36	1.10E-07	LC-MS
440	<b>Lactate</b>	-9.9	6.59E-05	LC-MS
441	N(pi)-Methyl-L-histidine	-9.91	1.47E-03	LC-MS
442	D-Sorbitol	-10.25	4.87E-07	LC-MS
443	<b>Adenine</b>	-10.8	8.48E-05	LC-MS
444	Piperidine	-11.07	1.98E-05	LC-MS
445	Ala-Leu-His-His	-11.1	1.21E-07	LC-MS
446	Glycylproline	-11.25	3.49E-04	LC-MS
447	Sphinganine	-11.63	1.38E-03	LC-MS

448	1-methylguanosine	-12.57	8.79E-06	LC-MS
449	2-Hydroxyadenine	-13.14	1.56E-05	LC-MS
450	ADPribose 2'-phosphate	-13.32	2.98E-06	LC-MS
451	<b>5'-Methylthioadenosine</b>	-13.36	3.22E-04	LC-MS
452	<b>L-Histidine</b>	-14.71	1.64E-04	LC-MS
453	Proclavaminc acid	-15.02	2.09E-03	LC-MS
454	Folate	-16.57	4.10E-06	LC-MS
455	phosphinomethylmalate	-17.86	7.66E-08	LC-MS
456	Ala-Gly-Pro	-18.19	1.94E-03	LC-MS
457	<b>L-Ornithine</b>	-18.75	1.45E-06	LC-MS
458	Trp-Pro	-20.44	3.46E-06	LC-MS
459	Glycodeoxycholate	-21.9	1.10E-05	LC-MS
460	2',3'-Cyclic UMP	<25 fold	2.42E-03	LC-MS
461	Nalpha-Methylhistidine	<25 fold	1.00E-05	LC-MS
462	L-Rhamnose	<25 fold	8.06E-06	LC-MS
463	<b>S-Adenosyl-L-methionine</b>	<25 fold	3.18E-04	LC-MS
464	N2-(D-1-Carboxyethyl)-L-arginine	<25 fold	1.76E-05	LC-MS
465	L-rhamnitol	<25 fold	2.91E-07	LC-MS
466	[ST hydrox] N-(3alpha,7alpha-dihydroxy-5beta-cholan-24-oyl)-taurine	<25 fold	7.00E-06	LC-MS
467	Deoxycytidine	<25 fold	9.19E-05	LC-MS
468	(S)-ATPA	<25 fold	8.75E-05	LC-MS
469	1-(5-Phosphoribosyl)imidazole-4-acetate	<25 fold	3.21E-06	LC-MS
470	Phe-Asp-Gln	<25 fold	3.30E-04	LC-MS
471	Carnosine	<25 fold	4.08E-06	LC-MS
472	L-Noradrenaline	<25 fold	1.08E-05	LC-MS
473	Volemitol	<25 fold	1.06E-05	LC-MS
474	Riboflavin	<25 fold	2.77E-05	LC-MS
475	3-(Pyrazol-1-yl)-L-alanine	<25 fold	5.23E-08	LC-MS
476	Glu-Phe-Cys-Cys	<25 fold	3.17E-05	LC-MS
477	DL-Methionine sulfone	<25 fold	2.06E-05	LC-MS
478	N-Acetyl-L-histidine	<25 fold	4.39E-07	LC-MS

Table 6 List of Primers used for PCR

Primer	Sequence
GU2051	GATAATGTCCTACTTTTTCTTTG
GU2052	TATATAGCTGCTTGAGACAC
GU2053	GCAAAATACCGGATAACTC
GU2054	TTTAGGAAACCAATCAAAGAG
GU2057	GGGCTTTATACTATTTTTTTGTC
GU2058	TATCGTGGTAGAGTAAACTG
GU2059	CATGATTTATCCGAAAAATATAGTG
GU2060	GTGCTTTATATACATATACAACAC
GU2198	GGAATTATAATTCTTAACCCTAACATTTTAACCTCTC
GU2199	CTTGTCGTATATGCACTCGGTGTTGG
GU2200	CCTTAAAATGGATAGTCAAATTGATCGTACACAACCTAA
GU2201	CATCTCTAATTCGTTAGAATTTATTATAGACTACG
GU2278	CCACTGTAATCATAGAACAGTTCAACTAC
GU2279	CAAGATTAGTACACATTGGATTAATGGG
GU2280	CATTAATAGGAAGTGGCCAAATAGGG
GU2281	GATAGCAAGCTTGTTCTTCTTCTGTC
GU2190	CCTTTTCCTTTTGTTTTATCCATCCATTTA
GU2191	AATCTCAAATTGTGAAATAAACAATAAAAAATTTTGTC
GU2192	CTGAGTTCTGTATTTACTTTTCATAAGTTTTTAAACG
GU2193	CCCACATAAGTAAATATACATACACATATTATTATGC
GU2286	CTTAAATTAGCATTACTGCGTACATCCC
GU2610	GAGCTAGCTGAAAGTTGCAAT
GU2288	GATGAAGAATTACACAAAAATACAATGAATTATGC
GU2289	GTGAAATATCTTCTTCATAATTAAGGATGC
GU2194	GATGCTCTCTCGTATATCCGTTTAAATTAC
GU2195	GCTAGCTATGAATTTTAGTTGATAGATTTTTTATTG
GU2196	GAATACATTGAGTTTAAACGGAACCTCAATTTAATAGCC
GU2197	GCATGCAATATTGGCAATACATGAAAACGAATTAATAT
GU2282	GCACCCATATTTATATCAACATTTCTATCAG
GU2283	GCACAATTTTACATATCGATATATGTACAATG
GU2284	GTATTGGGTTGGATCCTGATGAAG
GU2285	CTTGTTCAATATTACCACATTTTCTATGTC
GU2826	CAATCCGGGCAGTATTGTATATAGTAAAG
GU2827	GAGGAAAATATCGAATATAATAATAGTCTTCG
GU2828	GCTGGTGTGAATTTTCACTAATATGTC
GU2829	CTAAAGCTGGAGAAGCTAAATAATTTGC
GU2061	GTAAACTTAAGCATAAAGAGCTCG
GU0204	GTCTCTTCAATGATTCATAAATAG

**Table 7 E-value for each metabolic enzyme compared between different species of *Plasmodium* after doing BLAST with the corresponding *P. berghei* amino acid sequence**

Query: <i>P. berghei</i> amino acid sequence			<i>P. berghei</i>		<i>P. chabaudi</i>		<i>P. vivax</i>		<i>P. falciparum</i>	
Metabolic pathway	Enzyme	OrthoMCL Group	Accession no.	E-value	Accession no.	E-value	Accession no.	E-value	Accession no.	E-value
Intermediary Carbon Metabolism	<i>pepc</i>	OG5_130145	PBANKA_101790	0.00	PCHAS_101870	0.00	PVX_085200	0.00	PF3D7_1426700	0.00
	<i>mdh</i>	OG5_126911	PBANKA_111770	0.00	PCHAS_111720	0.00	PVX_114050	e-177	PF3D7_0618500	e-158
	<i>aat</i>	OG5_126737	PBANKA_030230	0.00	PCHAS_030450	0.00	PVX_003655	0.00	PF3D7_0204500	0.00
Pyrimidine biosynthesis	<i>cpsII</i>	OG5_126835	PBANKA_140670	0.00	PCHAS_140860	0.00	PVX_122240	0.00	PF3D7_1308200	0.00
	<i>act</i>	OG5_128535	PBANKA_135770	0.00	PCHAS_136230	0.00	PVX_083135	0.00	PF3D7_1344800	0.00
	<i>dhoase</i>	OG5_130129	PBANKA_133610	0.00	PCHAS_134070	0.00	PVX_116830	0.00	PF3D7_1472900	e-172
	<i>dhodh</i>	OG5_127289	PBANKA_010210	0.00	PCHAS_010280	0.00	PVX_113330	0.00	PF3D7_0603300	0.00
	<i>oprT</i>	OG5_126793	PBANKA_111240	0.00	PCHAS_111200	e-131	PVX_080605	e-110	PF3D7_0512700	0.00
	<i>ompdc</i>	OG5_126793	PBANKA_050740	0.00	PCHAS_050750	0.00	PVX_111555	e-139	PF3D7_1023200	e-141
Glutathione biosynthesis	<i>γ-gcs</i>	OG5_128698	PBANKA_081980	0.00	PCHAS_082010	0.00	PVX_099360	0.00	PF3D7_0918900	0.00
	<i>gs</i>	OG5_128131	PBANKA_111180	0.00	PCHAS_111140	0.00	PVX_080630	0.00	PF3D7_0512200	0.00
	<i>gst</i>	OG5_128352	PBANKA_102390	e-151	PCHAS_102470	e-148	PVX_085515	e-125	PF3D7_1419300	e-124
	<i>gr</i>	OG5_126785	PBANKA_102340	0.00	PCHAS_102420	0.00	PVX_085490	0.00	PF3D7_1419800.1 PF3D7_1419800.2	& 0.00 (for both <i>PfGR1</i> & <i>PfGR2</i> )
Phospholipid synthesis	<i>etnk</i>	OG5_127649	PBANKA_092370	0.00	PCHAS_092070	0.00	PVX_091845	e-178	PF3D7_1124600	0.00

<i>chok</i>	OG5_127835	PBANKA_104010	0.00	PCHAS_104090	0.00	PVX_086340	0.00	PF3D7_1401800	0.00
<i>ect</i>	OG5_127671	PBANKA_136050	0.00	PCHAS_136510	0.00	PVX_083280	0.00	PF3D7_1347700	0.00
<i>cct</i>	OG5_128351	PBANKA_141510	0.00	PCHAS_141690	0.00	PVX_122650	0.00	PF3D7_1316600	0.00
<i>cept</i>	OG5_126828	PBANKA_112700	0.00	PCHAS_112650	0.00	PVX_114515	e-154	PF3D7_0628300	e-147
<i>pmt</i> (PfpMT as query sequence)	OG5_132295	Not present		Not present		PVX_083045	e-128	PF3D7_1343000	0.00

## 10 References

- Abrahamsen, M. S., T. J. Templeton, S. Enomoto, J. E. Abrahante, G. Zhu, C. A. Lancto, M. Deng, C. Liu, G. Widmer, S. Tzipori, G. A. Buck, P. Xu, A. T. Bankier, P. H. Dear, B. A. Konfortov, H. F. Spriggs, L. Iyer, V. Anantharaman, L. Aravind and V. Kapur (2004). "Complete genome sequence of the apicomplexan, *Cryptosporidium parvum*." *Science* **304**(5669): 441-445.
- Achan, J., A. O. Talisuna, A. Erhart, A. Yeka, J. K. Tibenderana, F. N. Baliraine, P. J. Rosenthal and U. D'Alessandro (2011). "Quinine, an old anti-malarial drug in a modern world: role in the treatment of malaria." *Malar J* **10**: 144.
- Allen, J., H. M. Davey, D. Broadhurst, J. K. Heald, J. J. Rowland, S. G. Oliver and D. B. Kell (2003). "High-throughput classification of yeast mutants for functional genomics using metabolic footprinting." *Nat Biotechnol* **21**(6): 692-696.
- Altshuler, D., M. Daly and L. Kruglyak (2000). "Guilt by association." *Nat Genet* **26**(2): 135-137.
- Aly, A. S., A. M. Vaughan and S. H. Kappe (2009). "Malaria parasite development in the mosquito and infection of the mammalian host." *Annu Rev Microbiol* **63**: 195-221.
- Ancelin, M. L., M. Calas, V. Vidal-Sailhan, S. Herbute, P. Ringwald and H. J. Vial (2003). "Potent inhibitors of Plasmodium phospholipid metabolism with a broad spectrum of in vitro antimalarial activities." *Antimicrob Agents Chemother* **47**(8): 2590-2597.
- Arai, M., O. Billker, H. R. Morris, M. Panico, M. Delcroix, D. Dixon, S. V. Ley and R. E. Sinden (2001). "Both mosquito-derived xanthurenic acid and a host blood-derived factor regulate gametogenesis of Plasmodium in the midgut of the mosquito." *Mol Biochem Parasitol* **116**(1): 17-24.
- Atamna, H., G. Pascarmona and H. Ginsburg (1994). "Hexose-monophosphate shunt activity in intact Plasmodium falciparum-infected erythrocytes and in free parasites." *Mol Biochem Parasitol* **67**(1): 79-89.
- Aurrecochea, C., J. Brestelli, B. P. Brunk, J. Dommer, S. Fischer, B. Gajria, X. Gao, A. Gingle, G. Grant, O. S. Harb, M. Heiges, F. Innamorato, J. Iodice, J. C. Kissinger, E. Kraemer, W. Li, J. A. Miller, V. Nayak, C. Pennington, D. F. Pinney, D. S. Roos, C. Ross, C. J. Stoeckert, Jr., C. Treatman and H. Wang (2009). "PlasmoDB: a functional genomic database for malaria parasites." *Nucleic Acids Res* **37**(Database issue): D539-543.
- Bais, P., S. M. Moon, K. He, R. Leitao, K. Dreher, T. Walk, Y. Sucaet, L. Barkan, G. Wohlgemuth, M. R. Roth, E. S. Wurtele, P. Dixon, O. Fiehn, B. M. Lange, V. Shulaev, L. W. Sumner, R. Welti, B. J. Nikolau, S. Y. Rhee and J. A. Dickerson (2010). "PlantMetabolomics.org: A web portal for Plant Metabolomics Experiments." *Plant Physiol*.
- Ballas, S. K. and E. R. Burka (1974). "Pathways of de novo phospholipid synthesis in reticulocytes." *Biochim Biophys Acta* **337**(2): 239-247.
- Baptista, F. G., A. Pamplona, A. C. Pena, M. M. Mota, S. Pied and A. M. Vigario (2010). "Accumulation of Plasmodium berghei-infected red blood cells in the brain is crucial for the development of cerebral malaria in mice." *Infect Immun* **78**(9): 4033-4039.
- Barnwell, J. W., M. E. Nichols and P. Rubinstein (1989). "In vitro evaluation of the role of the Duffy blood group in erythrocyte invasion by Plasmodium vivax." *J Exp Med* **169**(5): 1795-1802.
- Barrett, M. P. (1997). "The pentose phosphate pathway and parasitic protozoa." *Parasitol Today* **13**(1): 11-16.

- Baum, J., T. W. Gilberger, F. Frischknecht and M. Meissner (2008). "Host-cell invasion by malaria parasites: insights from Plasmodium and Toxoplasma." Trends Parasitol **24**(12): 557-563.
- Baumeister, S., M. Winterberg, J. M. Przyborski and K. Lingelbach (2010). "The malaria parasite Plasmodium falciparum: cell biological peculiarities and nutritional consequences." Protoplasma **240**(1-4): 3-12.
- Berg JM, T. J., Stryer L (2002). Biochemistry. 5th edition. New York, W H Freeman.
- Besteiro, S., M. P. Barrett, L. Riviere and F. Bringaud (2005). "Energy generation in insect stages of Trypanosoma brucei: metabolism in flux." Trends Parasitol **21**(4): 185-191.
- Besteiro, S., S. Vo Duy, C. Perigaud, I. Lefebvre-Tournier and H. J. Vial (2009). "Exploring metabolomic approaches to analyse phospholipid biosynthetic pathways in Plasmodium." Parasitology: 1-14.
- Billker, O., V. Lindo, M. Panico, A. E. Etienne, T. Paxton, A. Dell, M. Rogers, R. E. Sinden and H. R. Morris (1998). "Identification of xanthurenic acid as the putative inducer of malaria development in the mosquito." Nature **392**(6673): 289-292.
- Bino, R. J., R. D. Hall, O. Fiehn, J. Kopka, K. Saito, J. Draper, B. J. Nikolau, P. Mendes, U. Roessner-Tunali, M. H. Beale, R. N. Trethewey, B. M. Lange, E. S. Wurtele and L. W. Sumner (2004). "Potential of metabolomics as a functional genomics tool." Trends Plant Sci **9**(9): 418-425.
- Bollard, M. E., E. G. Stanley, J. C. Lindon, J. K. Nicholson and E. Holmes (2005). "NMR-based metabolomic approaches for evaluating physiological influences on biofluid composition." NMR Biomed **18**(3): 143-162.
- Booden, T. and R. W. Hull (1973). "Nucleic acid precursor synthesis by Plasmodium lophurae parasitizing chicken erythrocytes." Exp Parasitol **34**(2): 220-228.
- Bozdech, Z., M. Llinas, B. L. Pulliam, E. D. Wong, J. Zhu and J. L. DeRisi (2003). "The transcriptome of the intraerythrocytic developmental cycle of Plasmodium falciparum." PLoS Biol **1**(1): E5.
- Brauer, M. J., J. Yuan, B. D. Bennett, W. Lu, E. Kimball, D. Botstein and J. D. Rabinowitz (2006). "Conservation of the metabolomic response to starvation across two divergent microbes." Proc Natl Acad Sci U S A **103**(51): 19302-19307.
- Bubb, W. A., L. C. Wright, M. Cagney, R. T. Santangelo, T. C. Sorrell and P. W. Kuchel (1999). "Heteronuclear NMR studies of metabolites produced by Cryptococcus neoformans in culture media: identification of possible virulence factors." Magn Reson Med **42**(3): 442-453.
- Cai, H., C. Hong, T. G. Lilburn, A. L. Rodriguez, S. Chen, J. Gu, R. Kuang and Y. Wang (2013). "A novel subnetwork alignment approach predicts new components of the cell cycle regulatory apparatus in Plasmodium falciparum." BMC Bioinformatics **14 Suppl 12**: S2.
- Cappellini, M. D. and G. Fiorelli (2008). "Glucose-6-phosphate dehydrogenase deficiency." Lancet **371**(9606): 64-74.
- Carlton, J. M., J. H. Adams, J. C. Silva, S. L. Bidwell, H. Lorenzi, E. Caler, J. Crabtree, S. V. Angiuoli, E. F. Merino, P. Amedeo, Q. Cheng, R. M. Coulson, B. S. Crabb, H. A. Del Portillo, K. Essien, T. V. Feldblyum, C. Fernandez-Becerra, P. R. Gilson, A. H. Gueye, X. Guo, S. Kang'a, T. W. Kooij, M. Korsinczky, E. V. Meyer, V. Nene, I. Paulsen, O. White, S. A. Ralph, Q. Ren, T. J. Sargeant, S. L. Salzberg, C. J. Stoeckert, S. A. Sullivan, M. M. Yamamoto, S. L. Hoffman, J. R. Wortman, M. J. Gardner, M. R. Galinski, J. W. Barnwell and C. M. Fraser-Liggett (2008). "Comparative genomics of the neglected human malaria parasite Plasmodium vivax." Nature **455**(7214): 757-763.

- Carvalho, T. A., M. G. Queiroz, G. L. Cardoso, I. G. Diniz, A. N. Silva, A. Y. Pinto and J. F. Guerreiro (2012). "Plasmodium vivax infection in Anajas, State of Para: no differential resistance profile among Duffy-negative and Duffy-positive individuals." Malar J **11**: 430.
- Caspi, R., T. Altman, R. Billington, K. Dreher, H. Foerster, C. A. Fulcher, T. A. Holland, I. M. Keseler, A. Kothari, A. Kubo, M. Krummenacker, M. Latendresse, L. A. Mueller, Q. Ong, S. Paley, P. Subhraveti, D. S. Weaver, D. Weerasinghe, P. Zhang and P. D. Karp (2014). "The MetaCyc database of metabolic pathways and enzymes and the BioCyc collection of Pathway/Genome Databases." Nucleic Acids Res **42**(Database issue): D459-471.
- Cassera, M. B., K. Z. Hazleton, P. M. Riegelhaupt, E. F. Merino, M. Luo, M. H. Akabas and V. L. Schramm (2008). "Erythrocytic adenosine monophosphate as an alternative purine source in Plasmodium falciparum." J Biol Chem **283**(47): 32889-32899.
- Cassera, M. B., Y. Zhang, K. Z. Hazleton and V. L. Schramm (2011). "Purine and pyrimidine pathways as targets in Plasmodium falciparum." Curr Top Med Chem **11**(16): 2103-2115.
- Chace, D. H. (2001). "Mass spectrometry in the clinical laboratory." Chem Rev **101**(2): 445-477.
- Chace, D. H. and T. A. Kalas (2005). "A biochemical perspective on the use of tandem mass spectrometry for newborn screening and clinical testing." Clin Biochem **38**(4): 296-309.
- Chace, D. H., D. S. Millington, N. Terada, S. G. Kahler, C. R. Roe and L. F. Hofman (1993). "Rapid diagnosis of phenylketonuria by quantitative analysis for phenylalanine and tyrosine in neonatal blood spots by tandem mass spectrometry." Clin Chem **39**(1): 66-71.
- Chaneton, B., P. Hillmann, L. Zheng, A. C. Martin, O. D. Maddocks, A. Chokkathukalam, J. E. Coyle, A. Jankevics, F. P. Holding, K. H. Vousden, C. Frezza, M. O'Reilly and E. Gottlieb (2012). "Serine is a natural ligand and allosteric activator of pyruvate kinase M2." Nature **491**(7424): 458-462.
- Chapman, R. G., M. A. Hennessey, A. M. Waltersdorff, F. M. Huennekens and B. W. Gabrio (1962). "Erythrocyte metabolism. V. Levels of glycolytic enzymes and regulation of glycolysis." J Clin Invest **41**: 1249-1256.
- Chen, K., J. Liu, S. Heck, J. A. Chasis, X. An and N. Mohandas (2009). "Resolving the distinct stages in erythroid differentiation based on dynamic changes in membrane protein expression during erythropoiesis." Proc Natl Acad Sci U S A **106**(41): 17413-17418.
- Cook, T., D. Roos, M. Morada, G. Zhu, J. S. Keithly, J. E. Feagin, G. Wu and N. Yarlett (2007). "Divergent polyamine metabolism in the Apicomplexa." Microbiology **153**(Pt 4): 1123-1130.
- Coustou, V., M. Biran, M. Breton, F. Guegan, L. Riviere, N. Plazolles, D. Nolan, M. P. Barrett, J. M. Franconi and F. Bringaud (2008). "Glucose-induced remodeling of intermediary and energy metabolism in procyclic Trypanosoma brucei." J Biol Chem **283**(24): 16342-16354.
- Cowman, A. F. and B. S. Crabb (2006). "Invasion of red blood cells by malaria parasites." Cell **124**(4): 755-766.
- Creasey, A., K. Mendis, J. Carlton, D. Williamson, I. Wilson and R. Carter (1994). "Maternal inheritance of extrachromosomal DNA in malaria parasites." Molecular and biochemical parasitology **65**(1): 95-98.
- Creek, D. J., J. Anderson, M. J. McConville and M. P. Barrett (2012). "Metabolomic analysis of trypanosomatid protozoa." Mol Biochem Parasitol **181**(2): 73-84.

- Creek, D. J., A. Jankevics, K. E. Burgess, R. Breitling and M. P. Barrett (2012). "IDEOM: an Excel interface for analysis of LC-MS-based metabolomics data." *Bioinformatics* **28**(7): 1048-1049.
- Cromer, D., K. J. Evans, L. Schofield and M. P. Davenport (2006). "Preferential invasion of reticulocytes during late-stage *Plasmodium berghei* infection accounts for reduced circulating reticulocyte levels." *Int J Parasitol* **36**(13): 1389-1397.
- Crosnier, C., L. Y. Bustamante, S. J. Bartholdson, A. K. Bei, M. Theron, M. Uchikawa, S. Mboup, O. Ndir, D. P. Kwiatkowski, M. T. Duraisingh, J. C. Rayner and G. J. Wright (2011). "Basigin is a receptor essential for erythrocyte invasion by *Plasmodium falciparum*." *Nature* **480**(7378): 534-537.
- Dajani, R. M. and J. M. Orten (1958). "[A study of the citric acid cycle in erythrocytes]." *J Biol Chem* **231**(2): 913-924.
- Das, A., C. Syin, H. Fujioka, H. Zheng, N. Goldman, M. Aikawa and N. Kumar (1997). "Molecular characterization and ultrastructural localization of *Plasmodium falciparum* Hsp 60." *Molecular and biochemical parasitology* **88**(1-2): 95-104.
- Dasgupta, B. (1960). "Polysaccharides in the different stages of the life-cycles of certain sporozoa." *Parasitology* **50**: 509-514.
- de Koning-Ward, T. F., C. J. Janse and A. P. Waters (2000). "The development of genetic tools for dissecting the biology of malaria parasites." *Annu Rev Microbiol* **54**: 157-185.
- Dechamps, S., M. Maynadier, S. Wein, L. Gannoun-Zaki, E. Marechal and H. J. Vial (2010). "Rodent and nonrodent malaria parasites differ in their phospholipid metabolic pathways." *J Lipid Res* **51**(1): 81-96.
- Dembele, L., A. Gego, A. M. Zeeman, J. F. Franetich, O. Silvie, A. Rametti, R. Le Grand, N. Dereuddre-Bosquet, R. Sauerwein, G. J. van Gemert, J. C. Vaillant, A. W. Thomas, G. Snounou, C. H. Kocken and D. Mazier (2011). "Towards an in vitro model of *Plasmodium* hypnozoites suitable for drug discovery." *PLoS One* **6**(3): e18162.
- Desai, S. A., D. J. Krogstad and E. W. McCleskey (1993). "A nutrient-permeable channel on the intraerythrocytic malaria parasite." *Nature* **362**(6421): 643-646.
- Desjardins, R. E., C. J. Canfield, J. D. Haynes and J. D. Chulay (1979). "Quantitative assessment of antimalarial activity in vitro by a semiautomated microdilution technique." *Antimicrob Agents Chemother* **16**(6): 710-718.
- Divo, A. A., T. G. Geary, N. L. Davis and J. B. Jensen (1985). "Nutritional requirements of *Plasmodium falciparum* in culture. I. Exogenously supplied dialyzable components necessary for continuous growth." *The Journal of protozoology* **32**(1): 59-64.
- Dixon, R. A. and D. Strack (2003). "Phytochemistry meets genome analysis, and beyond." *Phytochemistry* **62**(6): 815-816.
- Downie, M. J., K. Kirk and C. B. Mamoun (2008). "Purine salvage pathways in the intraerythrocytic malaria parasite *Plasmodium falciparum*." *Eukaryot Cell* **7**(8): 1231-1237.
- Doyle, M. A., J. I. MacRae, D. P. De Souza, E. C. Saunders, M. J. McConville and V. A. Likic (2009). "LeishCyc: a biochemical pathways database for *Leishmania major*." *BMC Syst Biol* **3**: 57.
- Ellington, W. R. and T. Suzuki (2007). "Early evolution of the creatine kinase gene family and the capacity for creatine biosynthesis and membrane transport." *Sub-cellular biochemistry* **46**: 17-26.
- Enserink, M. (2005). "Infectious diseases. Source of new hope against malaria is in short supply." *Science* **307**(5706): 33.

- Fan, J., J. J. Kamphorst, J. D. Rabinowitz and T. Shlomi (2013). "Fatty acid labeling from glutamine in hypoxia can be explained by isotope exchange without net reductive isocitrate dehydrogenase (IDH) flux." J Biol Chem **288**(43): 31363-31369.
- Fendt, S. M., E. L. Bell, M. A. Keibler, B. A. Olenchock, J. R. Mayers, T. M. Wasylenko, N. I. Vokes, L. Guarente, M. G. Vander Heiden and G. Stephanopoulos (2013). "Reductive glutamine metabolism is a function of the alpha-ketoglutarate to citrate ratio in cells." Nat Commun **4**: 2236.
- Flanagan, J. P. L., Milton A. (1970). "Controlled Phenylhydrazine-Induced Reticulocytosis in the Rat." Ohio Journal of Science **Volume 70**(Issue 5 (September, 1970)): 300-304.
- Fleige, T., J. Limenitakis and D. Soldati-Favre (2010). "Apicoplast: keep it or leave it." Microbes Infect **12**(4): 253-262.
- Franke-Fayard, B., C. J. Janse, M. Cunha-Rodrigues, J. Ramesar, P. Buscher, I. Que, C. Lowik, P. J. Voshol, M. A. den Boer, S. G. van Duinen, M. Febbraio, M. M. Mota and A. P. Waters (2005). "Murine malaria parasite sequestration: CD36 is the major receptor, but cerebral pathology is unlinked to sequestration." Proc Natl Acad Sci U S A **102**(32): 11468-11473.
- Frevert, U. (2004). "Sneaking in through the back entrance: the biology of malaria liver stages." Trends Parasitol **20**(9): 417-424.
- Gajria, B., A. Bahl, J. Brestelli, J. Dommer, S. Fischer, X. Gao, M. Heiges, J. Iodice, J. C. Kissinger, A. J. Mackey, D. F. Pinney, D. S. Roos, C. J. Stoeckert, Jr., H. Wang and B. P. Brunk (2008). "ToxoDB: an integrated Toxoplasma gondii database resource." Nucleic Acids Res **36**(Database issue): D553-556.
- Galinski, M. R., C. C. Medina, P. Ingravallo and J. W. Barnwell (1992). "A reticulocyte-binding protein complex of Plasmodium vivax merozoites." Cell **69**(7): 1213-1226.
- Gardner, M. J., N. Hall, E. Fung, O. White, M. Berriman, R. W. Hyman, J. M. Carlton, A. Pain, K. E. Nelson, S. Bowman, I. T. Paulsen, K. James, J. A. Eisen, K. Rutherford, S. L. Salzberg, A. Craig, S. Kyes, M. S. Chan, V. Nene, S. J. Shallom, B. Suh, J. Peterson, S. Angiuoli, M. Pertea, J. Allen, J. Selengut, D. Haft, M. W. Mather, A. B. Vaidya, D. M. Martin, A. H. Fairlamb, M. J. Fraunholz, D. S. Roos, S. A. Ralph, G. I. McFadden, L. M. Cummings, G. M. Subramanian, C. Mungall, J. C. Venter, D. J. Carucci, S. L. Hoffman, C. Newbold, R. W. Davis, C. M. Fraser and B. Barrell (2002). "Genome sequence of the human malaria parasite Plasmodium falciparum." Nature **419**(6906): 498-511.
- Geary, T. G., A. A. Divo, L. C. Bonanni and J. B. Jensen (1985). "Nutritional requirements of Plasmodium falciparum in culture. III. Further observations on essential nutrients and antimetabolites." The Journal of protozoology **32**(4): 608-613.
- Geary, T. G., A. A. Divo and J. B. Jensen (1985). "Nutritional requirements of Plasmodium falciparum in culture. II. Effects of antimetabolites in a semi-defined medium." The Journal of protozoology **32**(1): 65-69.
- Gero, A. M., G. V. Brown and W. J. O'Sullivan (1984). "Pyrimidine de novo synthesis during the life cycle of the intraerythrocytic stage of Plasmodium falciparum." J Parasitol **70**(4): 536-541.
- Ginsburg, H. (2006). "Progress in in silico functional genomics: the malaria Metabolic Pathways database." Trends Parasitol **22**(6): 238-240.
- Ginsburg, H. (2009). "Caveat emptor: limitations of the automated reconstruction of metabolic pathways in Plasmodium." Trends Parasitol **25**(1): 37-43.
- Gomase, V. S., S. S. Changbhale, S. A. Patil and K. V. Kale (2008). "Metabolomics." Curr Drug Metab **9**(1): 89-98.

- Goodacre, R. V., S. and Harrigan, G.G. (2005). "Metabolome Analyses: Strategies for Systems Biology." Springer Science: 1-4.
- Greenhaff, P. L. (2001). "The creatine-phosphocreatine system: there's more than one song in its repertoire." J Physiol **537**(Pt 3): 657.
- Griffin, J. L. and A. Vidal-Puig (2008). "Current challenges in metabolomics for diabetes research: a vital functional genomic tool or just a ploy for gaining funding?" Physiol Genomics **34**(1): 1-5.
- Griffiths, W. J. (2008). "Metabolomics, Metabonomics and Metabolite Profiling." The Royal Society of Chemistry Publishing: 1-4.
- Griffiths, W. J., T. Koal, Y. Wang, M. Kohl, D. P. Enot and H. P. Deigner (2010). "Targeted metabolomics for biomarker discovery." Angew Chem Int Ed Engl **49**(32): 5426-5445.
- Gronowicz, G., H. Swift and T. L. Steck (1984). "Maturation of the reticulocyte in vitro." J Cell Sci **71**: 177-197.
- Gubbels, M. J. and M. T. Duraisingh (2012). "Evolution of apicomplexan secretory organelles." Int J Parasitol **42**(12): 1071-1081.
- Gujjar, R., A. Marwaha, F. El Mazouni, J. White, K. L. White, S. Creason, D. M. Shackelford, J. Baldwin, W. N. Charman, F. S. Buckner, S. Charman, P. K. Rathod and M. A. Phillips (2009). "Identification of a metabolically stable triazolopyrimidine-based dihydroorotate dehydrogenase inhibitor with antimalarial activity in mice." J Med Chem **52**(7): 1864-1872.
- Hall, N., M. Karras, J. D. Raine, J. M. Carlton, T. W. Kooij, M. Berriman, L. Florens, C. S. Janssen, A. Pain, G. K. Christophides, K. James, K. Rutherford, B. Harris, D. Harris, C. Churcher, M. A. Quail, D. Ormond, J. Doggett, H. E. Trueman, J. Mendoza, S. L. Bidwell, M. A. Rajandream, D. J. Carucci, J. R. Yates, 3rd, F. C. Kafatos, C. J. Janse, B. Barrell, C. M. Turner, A. P. Waters and R. E. Sinden (2005). "A comprehensive survey of the Plasmodium life cycle by genomic, transcriptomic, and proteomic analyses." Science **307**(5706): 82-86.
- Harvey, K. L., P. R. Gilson and B. S. Crabb (2012). "A model for the progression of receptor-ligand interactions during erythrocyte invasion by Plasmodium falciparum." Int J Parasitol **42**(6): 567-573.
- Hatin, I., R. Jambou, H. Ginsburg and G. Jaureguiberry (1992). "Single or multiple localization of ADP/ATP transporter in human malarial Plasmodium falciparum." Biochem Pharmacol **43**(1): 71-75.
- Hino, A., M. Hirai, T. Q. Tanaka, Y. Watanabe, H. Matsuoka and K. Kita (2012). "Critical roles of the mitochondrial complex II in oocyst formation of rodent malaria parasite Plasmodium berghei." Journal of biochemistry **152**(3): 259-268.
- Hollywood, K., D. R. Brison and R. Goodacre (2006). "Metabolomics: current technologies and future trends." Proteomics **6**(17): 4716-4723.
- Holmes, E., I. D. Wilson and J. K. Nicholson (2008). "Metabolic phenotyping in health and disease." Cell **134**(5): 714-717.
- Holz, G. G., Jr. (1977). "Lipids and the malarial parasite." Bull World Health Organ **55**(2-3): 237-248.
- Homewood, C. A. (1977). "Carbohydrate metabolism of malarial parasites." Bull World Health Organ **55**(2-3): 229-235.
- Huang, J., V. S. Bhinu, X. Li, Z. Dallal Bashi, R. Zhou and A. Hannoufa (2009). "Pleiotropic changes in Arabidopsis f5h and sct mutants revealed by large-scale gene expression and metabolite analysis." Planta **230**(5): 1057-1069.
- Hyde, J. E. (2007). "Targeting purine and pyrimidine metabolism in human apicomplexan parasites." Curr Drug Targets **8**(1): 31-47.
- Idro, R., K. Marsh, C. C. John and C. R. Newton (2010). "Cerebral malaria: mechanisms of brain injury and strategies for improved neurocognitive outcome." Pediatr Res **68**(4): 267-274.

- Ishida, N. and M. Kawakita (2004). "Molecular physiology and pathology of the nucleotide sugar transporter family (SLC35)." *Pflugers Arch* **447**(5): 768-775.
- Janse, C. J., E. G. Boorsma, J. Ramesar, M. J. Grobbee and B. Mons (1989). "Host cell specificity and schizogony of *Plasmodium berghei* under different in vitro conditions." *Int J Parasitol* **19**(5): 509-514.
- Janse, C. J., J. Ramesar, F. M. van den Berg and B. Mons (1992). "*Plasmodium berghei*: in vivo generation and selection of karyotype mutants and non-gametocyte producer mutants." *Exp Parasitol* **74**(1): 1-10.
- Janse, C. J., J. Ramesar and A. P. Waters (2006). "High-efficiency transfection and drug selection of genetically transformed blood stages of the rodent malaria parasite *Plasmodium berghei*." *Nat Protoc* **1**(1): 346-356.
- Janse, C. J., P. F. Van der Klooster, H. J. Van der Kaay, M. Van der Ploeg and J. P. Overdulve (1986). "Rapid repeated DNA replication during microgametogenesis and DNA synthesis in young zygotes of *Plasmodium berghei*." *Trans R Soc Trop Med Hyg* **80**(1): 154-157.
- Kafsack, B. F. and M. Llinas (2010). "Eating at the table of another: metabolomics of host-parasite interactions." *Cell Host Microbe* **7**(2): 90-99.
- Kalanon, M. and G. I. McFadden (2010). "Malaria, *Plasmodium falciparum* and its apicoplast." *Biochem Soc Trans* **38**(3): 775-782.
- Kanehisa, M. (1997). "A database for post-genome analysis." *Trends Genet* **13**(9): 375-376.
- Kanehisa, M., S. Goto, M. Hattori, K. F. Aoki-Kinoshita, M. Itoh, S. Kawashima, T. Katayama, M. Araki and M. Hirakawa (2006). "From genomics to chemical genomics: new developments in KEGG." *Nucleic Acids Res* **34**(Database issue): D354-357.
- Kell, D. B. (2004). "Metabolomics and systems biology: making sense of the soup." *Curr Opin Microbiol* **7**(3): 296-307.
- Kerkhoven, E. J., F. Achcar, V. P. Alibu, R. J. Burchmore, I. H. Gilbert, M. Trybilo, N. N. Driessen, D. Gilbert, R. Breitling, B. M. Bakker and M. P. Barrett (2013). "Handling Uncertainty in Dynamic Models: The Pentose Phosphate Pathway in *Trypanosoma brucei*." *PLoS Comput Biol* **9**(12): e1003371.
- Khan, S. M., B. Franke-Fayard, G. R. Mair, E. Lasonder, C. J. Janse, M. Mann and A. P. Waters (2005). "Proteome analysis of separated male and female gametocytes reveals novel sex-specific *Plasmodium* biology." *Cell* **121**(5): 675-687.
- Kim, K. and L. M. Weiss (2008). "Toxoplasma: the next 100years." *Microbes Infect* **10**(9): 978-984.
- Kind, T. and O. Fiehn (2007). "Seven Golden Rules for heuristic filtering of molecular formulas obtained by accurate mass spectrometry." *BMC Bioinformatics* **8**: 105.
- Kirk, K., H. M. Staines, R. E. Martin and K. J. Saliba (1999). "Transport properties of the host cell membrane." *Novartis Found Symp* **226**: 55-66; discussion 66-73.
- Krishna, S., C. J. Woodrow, R. J. Burchmore, K. J. Saliba and K. Kirk (2000). "Hexose transport in asexual stages of *Plasmodium falciparum* and kinetoplastidae." *Parasitol Today* **16**(12): 516-521.
- Krungskrai, J. (1995). "Purification, characterization and localization of mitochondrial dihydroorotate dehydrogenase in *Plasmodium falciparum*, human malaria parasite." *Biochim Biophys Acta* **1243**(3): 351-360.
- Krungskrai, J. (2004). "The multiple roles of the mitochondrion of the malarial parasite." *Parasitology* **129**(Pt 5): 511-524.
- Krungskrai, S. R., B. J. DelFraino, J. A. Smiley, P. Prapunwattana, T. Mitamura, T. Horii and J. Krungskrai (2005). "A novel enzyme complex of orotate phosphoribosyltransferase and orotidine 5'-monophosphate decarboxylase in

- human malaria parasite *Plasmodium falciparum*: physical association, kinetics, and inhibition characterization." *Biochemistry* **44**(5): 1643-1652.
- Kunji, E. R. and M. Harding (2003). "Projection structure of the atractyloside-inhibited mitochondrial ADP/ATP carrier of *Saccharomyces cerevisiae*." *J Biol Chem* **278**(39): 36985-36988.
- Lasonder, E., Y. Ishihama, J. S. Andersen, A. M. Vermunt, A. Pain, R. W. Sauerwein, W. M. Eling, N. Hall, A. P. Waters, H. G. Stunnenberg and M. Mann (2002). "Analysis of the *Plasmodium falciparum* proteome by high-accuracy mass spectrometry." *Nature* **419**(6906): 537-542.
- Le Cao, K. A., I. Gonzalez and S. Dejean (2009). "integrOmics: an R package to unravel relationships between two omics datasets." *Bioinformatics* **25**(21): 2855-2856.
- Leader, D. P., K. Burgess, D. Creek and M. P. Barrett (2011). "Pathos: a web facility that uses metabolic maps to display experimental changes in metabolites identified by mass spectrometry." *Rapid Commun Mass Spectrom* **25**(22): 3422-3426.
- Lewis, I. A., M. Wacker, K. L. Olszewski, S. A. Cobbold, K. S. Baska, A. Tan, M. T. Ferdig and M. Llinas (2014). "Metabolic QTL analysis links chloroquine resistance in *Plasmodium falciparum* to impaired hemoglobin catabolism." *PLoS Genet* **10**(1): e1004085.
- Li, J. V., Y. Wang, J. Saric, J. K. Nicholson, S. Dirnhofer, B. H. Singer, M. Tanner, S. Wittlin, E. Holmes and J. Utzinger (2008). "Global metabolic responses of NMRI mice to an experimental *Plasmodium berghei* infection." *J Proteome Res* **7**(9): 3948-3956.
- Li, L. O., Y. F. Hu, L. Wang, M. Mitchell, A. Berger and R. A. Coleman (2010). "Early hepatic insulin resistance in mice: a metabolomics analysis." *Mol Endocrinol* **24**(3): 657-666.
- Lian, L. Y., M. Al-Helal, A. M. Roslaini, N. Fisher, P. G. Bray, S. A. Ward and G. A. Biagini (2009). "Glycerol: an unexpected major metabolite of energy metabolism by the human malaria parasite." *Malar J* **8**: 38.
- Lisec, J., N. Schauer, J. Kopka, L. Willmitzer and A. R. Fernie (2006). "Gas chromatography mass spectrometry-based metabolite profiling in plants." *Nat Protoc* **1**(1): 387-396.
- Liu, J., X. Guo, N. Mohandas, J. A. Chasis and X. An (2010). "Membrane remodeling during reticulocyte maturation." *Blood* **115**(10): 2021-2027.
- Llinas, M. and H. A. del Portillo (2005). "Mining the malaria transcriptome." *Trends Parasitol* **21**(8): 350-352.
- LMRG (Online Resource accessed August 2007) "P.berghei- model of Malaria." [Leiden Malaria Research Group](#).
- Lowe, R. G., M. Lord, K. Rybak, R. D. Trengove, R. P. Oliver and P. S. Solomon (2008). "A metabolomic approach to dissecting osmotic stress in the wheat pathogen *Stagonospora nodorum*." *Fungal Genet Biol* **45**(11): 1479-1486.
- Ludwig, C. and M. R. Viant (2010). "Two-dimensional J-resolved NMR spectroscopy: review of a key methodology in the metabolomics toolbox." *Phytochem Anal* **21**(1): 22-32.
- Macedo, C. S., R. T. Schwarz, A. R. Todeschini, J. O. Previato and L. Mendonca-Previato (2010). "Overlooked post-translational modifications of proteins in *Plasmodium falciparum*: N- and O-glycosylation -- a review." *Mem Inst Oswaldo Cruz* **105**(8): 949-956.
- Mack, S. R., S. Samuels and J. P. Vanderberg (1979). "Hemolymph of *Anopheles stephensi* from noninfected and *Plasmodium berghei*-infected mosquitoes. 3. Carbohydrates." *J Parasitol* **65**(2): 217-221.

- Macrae, J. I., M. W. Dixon, M. K. Dearnley, H. H. Chua, J. M. Chambers, S. Kenny, I. Bottova, L. Tilley and M. J. McConville (2013). "Mitochondrial metabolism of sexual and asexual blood stages of the malaria parasite *Plasmodium falciparum*." BMC Biol **11**(1): 67.
- MacRae, J. I., L. Sheiner, A. Nahid, C. Tonkin, B. Striepen and M. J. McConville (2012). "Mitochondrial metabolism of glucose and glutamine is required for intracellular growth of *Toxoplasma gondii*." Cell Host Microbe **12**(5): 682-692.
- Mahowald, T. A., E. A. Noltmann and S. A. Kuby (1962). "Studies on adenosine triphosphate transphosphorylases. III. Inhibition reactions." J Biol Chem **237**: 1535-1548.
- Maier, A. G., M. T. Duraisingh, J. C. Reeder, S. S. Patel, J. W. Kazura, P. A. Zimmerman and A. F. Cowman (2003). "*Plasmodium falciparum* erythrocyte invasion through glycophorin C and selection for Gerbich negativity in human populations." Nat Med **9**(1): 87-92.
- Mair, G. R., J. A. Braks, L. S. Garver, J. C. Wiegant, N. Hall, R. W. Dirks, S. M. Khan, G. Dimopoulos, C. J. Janse and A. P. Waters (2006). "Regulation of sexual development of *Plasmodium* by translational repression." Science **313**(5787): 667-669.
- Majerus, P. W., M. J. Brauner, M. B. Smith and V. Minnich (1971). "Glutathione synthesis in human erythrocytes. II. Purification and properties of the enzymes of glutathione biosynthesis." The Journal of clinical investigation **50**(8): 1637-1643.
- Mapper, G. m. (2013). "GMP project Management: William Ryan O'Neil for GMP and MMV project Management: Maud Lugand & Raphaëlle Bessette for MMV." from <http://www.worldmalariaepidemiology.org/node/13>.
- Mayer, D. C., J. Cofie, L. Jiang, D. L. Hartl, E. Tracy, J. Kabat, L. H. Mendoza and L. H. Miller (2009). "Glycophorin B is the erythrocyte receptor of *Plasmodium falciparum* erythrocyte-binding ligand, EBL-1." Proc Natl Acad Sci U S A **106**(13): 5348-5352.
- Mehta, M., H. M. Sonawat and S. Sharma (2006). "Glycolysis in *Plasmodium falciparum* results in modulation of host enzyme activities." J Vector Borne Dis **43**(3): 95-103.
- Meis, J. F., J. P. Verhave, P. H. Jap and J. H. Meuwissen (1985). "Transformation of sporozoites of *Plasmodium berghei* into exoerythrocytic forms in the liver of its mammalian host." Cell Tissue Res **241**(2): 353-360.
- Menard, R., J. Tavares, I. Cockburn, M. Markus, F. Zavala and R. Amino (2013). "Looking under the skin: the first steps in malarial infection and immunity." Nat Rev Microbiol **11**(10): 701-712.
- Mendes, C., F. Dias, J. Figueiredo, V. G. Mora, J. Cano, B. de Sousa, V. E. do Rosario, A. Benito, P. Berzosa and A. P. Arez (2011). "Duffy negative antigen is no longer a barrier to *Plasmodium vivax*--molecular evidences from the African West Coast (Angola and Equatorial Guinea)." PLoS Negl Trop Dis **5**(6): e1192.
- Metallo, C. M., P. A. Gameiro, E. L. Bell, K. R. Mattaini, J. Yang, K. Hiller, C. M. Jewell, Z. R. Johnson, D. J. Irvine, L. Guarente, J. K. Kelleher, M. G. Vander Heiden, O. Iliopoulos and G. Stephanopoulos (2012). "Reductive glutamine metabolism by IDH1 mediates lipogenesis under hypoxia." Nature **481**(7381): 380-384.
- Misra, P., A. Pandey, M. Tiwari, K. Chandrashekar, O. P. Sidhu, M. H. Asif, D. Chakrabarty, P. K. Singh, P. K. Trivedi, P. Nath and R. Tuli (2010). "Modulation of transcriptome and metabolome of tobacco by *Arabidopsis* transcription factor, AtMyb12, leads to insect resistance." Plant Physiol.

- Mons, B., C. J. Janse, E. G. Boersma and H. J. Van der Kaay (1985). "Synchronized erythrocytic schizogony and gametocytogenesis of *Plasmodium berghei* in vivo and in vitro." *Parasitology* **91** ( Pt 3): 423-430.
- Monton, M. R. and T. Soga (2007). "Metabolome analysis by capillary electrophoresis-mass spectrometry." *J Chromatogr A* **1168**(1-2): 237-246; discussion 236.
- Morreel, K., G. Goeminne, V. Storme, L. Sterck, J. Ralph, W. Coppieters, P. Breyne, M. Steenackers, M. Georges, E. Messens and W. Boerjan (2006). "Genetical metabolomics of flavonoid biosynthesis in *Populus*: a case study." *Plant J* **47**(2): 224-237.
- Mota, M. M., G. Pradel, J. P. Vanderberg, J. C. Hafalla, U. Frevort, R. S. Nussenzweig, V. Nussenzweig and A. Rodriguez (2001). "Migration of *Plasmodium* sporozoites through cells before infection." *Science* **291**(5501): 141-144.
- Muhia, D. K., C. A. Swales, W. Deng, J. M. Kelly and D. A. Baker (2001). "The gametocyte-activating factor xanthurenic acid stimulates an increase in membrane-associated guanylyl cyclase activity in the human malaria parasite *Plasmodium falciparum*." *Mol Microbiol* **42**(2): 553-560.
- Mullen, A. R., W. W. Wheaton, E. S. Jin, P. H. Chen, L. B. Sullivan, T. Cheng, Y. Yang, W. M. Linehan, N. S. Chandel and R. J. DeBerardinis (2012). "Reductive carboxylation supports growth in tumour cells with defective mitochondria." *Nature* **481**(7381): 385-388.
- Muller, S. (2004). "Redox and antioxidant systems of the malaria parasite *Plasmodium falciparum*." *Molecular microbiology* **53**(5): 1291-1305.
- Nicholson, J. K., J. Connelly, J. C. Lindon and E. Holmes (2002). "Metabonomics: a platform for studying drug toxicity and gene function." *Nat Rev Drug Discov* **1**(2): 153-161.
- Nicholson, J. K. and J. C. Lindon (2008). "Systems biology: Metabonomics." *Nature* **455**(7216): 1054-1056.
- Noulin, F., C. Borlon, J. Van Den Abbeele, U. D'Alessandro and A. Erhart (2013). "1912-2012: a century of research on *Plasmodium vivax* in vitro culture." *Trends Parasitol* **29**(6): 286-294.
- Noulin, F., C. Borlon, P. van den Eede, L. Boel, C. M. Verfaillie, U. D'Alessandro and A. Erhart (2012). "Cryopreserved reticulocytes derived from hematopoietic stem cells can be invaded by cryopreserved *Plasmodium vivax* isolates." *PLoS One* **7**(7): e40798.
- Nussbaum, K., J. Honek, C. M. Cadmus and T. Efferth (2010). "Trypanosomatid Parasites Causing Neglected Diseases." *Curr Med Chem*.
- O'Callaghan, S., D. P. De Souza, A. Isaac, Q. Wang, L. Hodgkinson, M. Olshansky, T. Erwin, B. Appelbe, D. L. Tull, U. Roessner, A. Bacic, M. J. McConville and V. A. Likić (2012). "PyMS: a Python toolkit for processing of gas chromatography-mass spectrometry (GC-MS) data. Application and comparative study of selected tools." *BMC Bioinformatics* **13**: 115.
- O'Hara, J. K., L. J. Kerwin, S. A. Cobbold, J. Tai, T. A. Bedell, P. J. Reider and M. Llinas (2014). "Targeting NAD<sup>+</sup> Metabolism in the Human Malaria Parasite *Plasmodium falciparum*." *PLoS One* **9**(4): e94061.
- Okamoto, N., T. P. Spurck, C. D. Goodman and G. I. McFadden (2009). "Apicoplast and mitochondrion in gametocytogenesis of *Plasmodium falciparum*." *Eukaryotic cell* **8**(1): 128-132.
- Olszewski, K. L. and M. Llinas (2011). "Central carbon metabolism of *Plasmodium* parasites." *Molecular and biochemical parasitology* **175**(2): 95-103.
- Olszewski, K. L., M. W. Mather, J. M. Morrissey, B. A. Garcia, A. B. Vaidya, J. D. Rabinowitz and M. Llinas (2010). "Branched tricarboxylic acid metabolism in *Plasmodium falciparum*." *Nature* **466**(7307): 774-778.

- Olszewski, K. L., M. W. Mather, J. M. Morrissey, B. A. Garcia, A. B. Vaidya, J. D. Rabinowitz and M. Llinas (2013). "Retraction: Branched tricarboxylic acid metabolism in *Plasmodium falciparum*." *Nature* **497**(7451): 652.
- Olszewski, K. L., J. M. Morrissey, D. Wilinski, J. M. Burns, A. B. Vaidya, J. D. Rabinowitz and M. Llinas (2009). "Host-parasite interactions revealed by *Plasmodium falciparum* metabolomics." *Cell Host Microbe* **5**(2): 191-199.
- Oppenheim, R. D., D. J. Creek, J. I. Macrae, K. K. Modrzynska, P. Pino, J. Limenitakis, V. Polonais, F. Seeber, M. P. Barrett, O. Billker, M. J. McConville and D. Soldati-Favre (2014). "BCKDH: The Missing Link in Apicomplexan Mitochondrial Metabolism Is Required for Full Virulence of *Toxoplasma gondii* and *Plasmodium berghei*." *PLoS Pathog* **10**(7): e1004263.
- Pain, A. and C. Hertz-Fowler (2009). "Plasmodium genomics: latest milestone." *Nat Rev Microbiol* **7**(3): 180-181.
- Painter, H. J., J. M. Morrissey, M. W. Mather and A. B. Vaidya (2007). "Specific role of mitochondrial electron transport in blood-stage *Plasmodium falciparum*." *Nature* **446**(7131): 88-91.
- Panichakul, T., J. Sattabongkot, K. Chotivanich, J. Sirichaisinthop, L. Cui and R. Udomsangpetch (2007). "Production of erythropoietic cells in vitro for continuous culture of *Plasmodium vivax*." *Int J Parasitol* **37**(14): 1551-1557.
- Pasini, E. M., M. Kirkegaard, P. Mortensen, H. U. Lutz, A. W. Thomas and M. Mann (2006). "In-depth analysis of the membrane and cytosolic proteome of red blood cells." *Blood* **108**(3): 791-801.
- Pasini, E. M., M. Kirkegaard, D. Salerno, P. Mortensen, M. Mann and A. W. Thomas (2008). "Deep coverage mouse red blood cell proteome: a first comparison with the human red blood cell." *Mol Cell Proteomics* **7**(7): 1317-1330.
- Pastrana-Mena, R., R. R. Dinglasan, B. Franke-Fayard, J. Vega-Rodriguez, M. Fuentes-Caraballo, A. Baerga-Ortiz, I. Coppens, M. Jacobs-Lorena, C. J. Janse and A. E. Serrano (2010). "Glutathione reductase-null malaria parasites have normal blood stage growth but arrest during development in the mosquito." *The Journal of biological chemistry* **285**(35): 27045-27056.
- Patti, G. J., O. Yanes and G. Siuzdak (2012). "Innovation: Metabolomics: the apogee of the omics trilogy." *Nat Rev Mol Cell Biol* **13**(4): 263-269.
- Patzewitz, E. M., E. H. Wong and S. Muller (2012). "Dissecting the role of glutathione biosynthesis in *Plasmodium falciparum*." *Molecular microbiology* **83**(2): 304-318.
- Pedersen, K. S., T. N. Kristensen, V. Loeschcke, B. O. Petersen, J. O. Duus, N. C. Nielsen and A. Malmendal (2008). "Metabolomic signatures of inbreeding at benign and stressful temperatures in *Drosophila melanogaster*." *Genetics* **180**(2): 1233-1243.
- Phillips, M. A., R. Gujjar, N. A. Malmquist, J. White, F. El Mazouni, J. Baldwin and P. K. Rathod (2008). "Triazolopyrimidine-based dihydroorotate dehydrogenase inhibitors with potent and selective activity against the malaria parasite *Plasmodium falciparum*." *J Med Chem* **51**(12): 3649-3653.
- Pittman, J. G. and D. B. Martin (1966). "Fatty acid biosynthesis in human erythrocytes: evidence in mature erythrocytes for an incomplete long chain fatty acid synthesizing system." *J Clin Invest* **45**(2): 165-172.
- Proudfoot, A. T., S. M. Bradberry and J. A. Vale (2006). "Sodium fluoroacetate poisoning." *Toxicol Rev* **25**(4): 213-219.
- Ramos, T. N., D. C. Bullard, M. M. Darley, K. McDonald, D. F. Crawford and S. R. Barnum (2013). "Experimental cerebral malaria develops independently of endothelial expression of intercellular adhesion molecule-1 (icam-1)." *J Biol Chem* **288**(16): 10962-10966.

- Rathod, P. K., A. Khatri, T. Hubbert and W. K. Milhous (1989). "Selective activity of 5-fluoroorotic acid against *Plasmodium falciparum* in vitro." *Antimicrob Agents Chemother* **33**(7): 1090-1094.
- Reyes-Sandoval, A. and M. F. Bachmann (2013). "Plasmodium vivax malaria vaccines: Why are we where we are?" *Hum Vaccin Immunother* **9**(12).
- Riegelhaupt, P. M., M. B. Cassera, R. F. Frohlich, K. Z. Hazleton, J. J. Hefter, V. L. Schramm and M. H. Akabas (2010). "Transport of purines and purine salvage pathway inhibitors by the *Plasmodium falciparum* equilibrative nucleoside transporter PfENT1." *Mol Biochem Parasitol* **169**(1): 40-49.
- Robert M, S. T., Tomita M (2007). "E.coli Metabolomics: capturing the complexity of a 'simple' model." *Topics in Current Genetics* **18**: 1-46.
- Roberts, L. D., A. L. Souza, R. E. Gerszten and C. B. Clish (2012). "Targeted metabolomics." *Curr Protoc Mol Biol Chapter 30*: Unit 30 32 31-24.
- Roth, E., Jr. (1990). "Plasmodium falciparum carbohydrate metabolism: a connection between host cell and parasite." *Blood Cells* **16**(2-3): 453-460; discussion 461-456.
- Ruwende, C. and A. Hill (1998). "Glucose-6-phosphate dehydrogenase deficiency and malaria." *J Mol Med (Berl)* **76**(8): 581-588.
- Saito, K., M. Y. Hirai and K. Yonekura-Sakakibara (2008). "Decoding genes with coexpression networks and metabolomics - 'majority report by precogs'." *Trends Plant Sci* **13**(1): 36-43.
- Saito, K. and F. Matsuda (2010). "Metabolomics for Functional Genomics, Systems Biology, and Biotechnology." *Annu Rev Plant Biol*.
- Salcedo-Sora, J. E., E. Caamano-Gutierrez, S. A. Ward and G. A. Biagini (2014). "The proliferating cell hypothesis: a metabolic framework for *Plasmodium* growth and development." *Trends Parasitol* **30**(4): 170-175.
- Sanger, F. (1945). "The free amino groups of insulin." *Biochem J* **39**(5): 507-515.
- Sansone, S. A., T. Fan, R. Goodacre, J. L. Griffin, N. W. Hardy, R. Kaddurah-Daouk, B. S. Kristal, J. Lindon, P. Mendes, N. Morrison, B. Nikolau, D. Robertson, L. W. Sumner, C. Taylor, M. van der Werf, B. van Ommen and O. Fiehn (2007). "The metabolomics standards initiative." *Nat Biotechnol* **25**(8): 846-848.
- Scheltema, R. A., S. Decuypere, R. T'Kindt, J. C. Dujardin, G. H. Coombs and R. Breitling (2010). "The potential of metabolomics for *Leishmania* research in the post-genomics era." *Parasitology*: 1-12.
- Scheltema, R. A., A. Jankevics, R. C. Jansen, M. A. Swertz and R. Breitling (2011). "PeakML/mzMatch: a file format, Java library, R library, and tool-chain for mass spectrometry data analysis." *Anal Chem* **83**(7): 2786-2793.
- Schuster, F. L. (2002). "Cultivation of plasmodium spp." *Clinical microbiology reviews* **15**(3): 355-364.
- Seeber, F., J. Limenitakis and D. Soldati-Favre (2008). "Apicomplexan mitochondrial metabolism: a story of gains, losses and retentions." *Trends Parasitol* **24**(10): 468-478.
- Sherman, I. W. (1977). "Amino acid metabolism and protein synthesis in malarial parasites." *Bull World Health Organ* **55**(2-3): 265-276.
- Sicard, A., J. P. Semblat, C. Doerig, R. Hamelin, M. Moniatte, D. Dorin-Semblat, J. A. Spicer, A. Srivastava, S. Retzlaff, V. Heussler, A. P. Waters and C. Doerig (2011). "Activation of a PAK-MEK signalling pathway in malaria parasite-infected erythrocytes." *Cell Microbiol* **13**(6): 836-845.
- Siden-Kiamos, I., A. Ecker, S. Nyback, C. Louis, R. E. Sinden and O. Billker (2006). "Plasmodium berghei calcium-dependent protein kinase 3 is required for ookinete gliding motility and mosquito midgut invasion." *Mol Microbiol* **60**(6): 1355-1363.

- Sinai, A. P., P. Webster and K. A. Joiner (1997). "Association of host cell endoplasmic reticulum and mitochondria with the *Toxoplasma gondii* parasitophorous vacuole membrane: a high affinity interaction." *J Cell Sci* **110** (Pt 17): 2117-2128.
- Sinden, R. E. and P. F. Billingsley (2001). "Plasmodium invasion of mosquito cells: hawk or dove?" *Trends Parasitol* **17**(5): 209-212.
- Sinden, R. E., R. Carter, C. Drakeley and D. Leroy (2012). "The biology of sexual development of Plasmodium: the design and implementation of transmission-blocking strategies." *Malar J* **11**: 70.
- Sinden, R. E. and M. E. Smalley (1979). "Gametocytogenesis of *Plasmodium falciparum* in vitro: the cell-cycle." *Parasitology* **79**(2): 277-296.
- Sinha, A., K. R. Hughes, K. K. Modrzynska, T. D. Otto, C. Pfander, N. J. Dickens, A. A. Religa, E. Bushell, A. L. Graham, R. Cameron, B. F. Kafack, A. E. Williams, M. Llinas, M. Berriman, O. Billker and A. P. Waters (2014). "A cascade of DNA-binding proteins for sexual commitment and development in *Plasmodium*." *Nature* **507**(7491): 253-257.
- Slavic, K., M. J. Delves, M. Prudencio, A. M. Talman, U. Straschil, E. T. Derbyshire, Z. Xu, R. E. Sinden, M. M. Mota, C. Morin, R. Tewari, S. Krishna and H. M. Staines (2011). "Use of a selective inhibitor to define the chemotherapeutic potential of the plasmodial hexose transporter in different stages of the parasite's life cycle." *Antimicrob Agents Chemother* **55**(6): 2824-2830.
- Smith, C. A., E. J. Want, G. O'Maille, R. Abagyan and G. Siuzdak (2006). "XCMS: processing mass spectrometry data for metabolite profiling using nonlinear peak alignment, matching, and identification." *Anal Chem* **78**(3): 779-787.
- Snow, R. W., C. A. Guerra, A. M. Noor, H. Y. Myint and S. I. Hay (2005). "The global distribution of clinical episodes of *Plasmodium falciparum* malaria." *Nature* **434**(7030): 214-217.
- Snyder, M. and J. E. Gallagher (2009). "Systems biology from a yeast omics perspective." *FEBS Lett* **583**(24): 3895-3899.
- Spry, C. and K. J. Saliba (2009). "The human malaria parasite *Plasmodium falciparum* is not dependent on host coenzyme A biosynthesis." *The Journal of biological chemistry* **284**(37): 24904-24913.
- Spry, C., D. A. van Schalkwyk, E. Strauss and K. J. Saliba (2010). "Pantothenate utilization by *Plasmodium* as a target for antimalarial chemotherapy." *Infect Disord Drug Targets* **10**(3): 200-216.
- Steiber, A., J. Kerner and C. L. Hoppel (2004). "Carnitine: a nutritional, biosynthetic, and functional perspective." *Mol Aspects Med* **25**(5-6): 455-473.
- Stites, E. C., P. C. Trampont, Z. Ma and K. S. Ravichandran (2007). "Network analysis of oncogenic Ras activation in cancer." *Science* **318**(5849): 463-467.
- Stitt, M. and A. R. Fernie (2003). "From measurements of metabolites to metabolomics: an 'on the fly' perspective illustrated by recent studies of carbon-nitrogen interactions." *Curr Opin Biotechnol* **14**(2): 136-144.
- Storm, J., J. Perner, I. Aparicio, E. M. Patzewitz, K. Olszewski, M. Llinas, P. C. Engel and S. Muller (2011). "*Plasmodium falciparum* glutamate dehydrogenase is dispensable and not a drug target during erythrocytic development." *Malar J* **10**: 193.
- Storm, J., S. Sethia, G. J. Blackburn, A. Chokkathukalam, D. G. Watson, R. Breitling, G. H. Coombs and S. Muller (2014). "Phosphoenolpyruvate carboxylase identified as a key enzyme in erythrocytic *Plasmodium falciparum* carbon metabolism." *PLoS Pathog* **10**(1): e1003876.

- Stromme, J. H. and L. Eldjarn (1962). "The role of the pentose phosphate pathway in the reduction of methaemoglobin in human erythrocytes." Biochem J **84**: 406-410.
- Sturm, A., R. Amino, C. van de Sand, T. Regen, S. Retzlaff, A. Rennenberg, A. Krueger, J. M. Pollok, R. Menard and V. T. Heussler (2006). "Manipulation of host hepatocytes by the malaria parasite for delivery into liver sinusoids." Science **313**(5791): 1287-1290.
- Suhrbier, A., C. Janse, B. Mons, S. L. Fleck, J. Nicholas, C. S. Davies and R. E. Sinden (1987). "The complete development in vitro of the vertebrate phase of the mammalian malarial parasite *Plasmodium berghei*." Trans R Soc Trop Med Hyg **81**(6): 907-909.
- Sumner, L. W. (2007). "Proposed minimum reporting standards for chemical analysis." Metabolomics.
- Talevich, E., A. B. Tobin, N. Kannan and C. Doerig (2012). "An evolutionary perspective on the kinome of malaria parasites." Philos Trans R Soc Lond B Biol Sci **367**(1602): 2607-2618.
- Talman, A. M., O. Domarle, F. E. McKenzie, F. Ariey and V. Robert (2004). "Gametocytogenesis: the puberty of *Plasmodium falciparum*." Malar J **3**: 24.
- Tavares, J., P. Formaglio, S. Thiberge, E. Mordelet, N. Van Rooijen, A. Medvinsky, R. Menard and R. Amino (2013). "Role of host cell traversal by the malaria sporozoite during liver infection." J Exp Med **210**(5): 905-915.
- Teng, R., P. R. Junankar, W. A. Bubb, C. Rae, P. Mercier and K. Kirk (2009). "Metabolite profiling of the intraerythrocytic malaria parasite *Plasmodium falciparum* by (1)H NMR spectroscopy." NMR Biomed **22**(3): 292-302.
- Terabe (2001). "Capillary Electrophoretic Technique toward the metabolome analysis."
- Terabe, S. (2007). "Editorial on "Metabolome analysis by capillary electrophoresis-mass spectrometry" by M.R.N. Monton and T. Soga " Journal of Chromatography A **1168**(1-2): 236.
- Tham, W. H., J. Healer and A. F. Cowman (2012). "Erythrocyte and reticulocyte binding-like proteins of *Plasmodium falciparum*." Trends Parasitol **28**(1): 23-30.
- Tiano, L., P. Ballarini, G. Santoni, M. Wozniak and G. Falcioni (2000). "Morphological and functional changes of mitochondria from density separated trout erythrocytes." Biochim Biophys Acta **1457**(3): 118-128.
- Tombes, R. M. and B. M. Shapiro (1985). "Metabolite channeling: a phosphorylcreatine shuttle to mediate high energy phosphate transport between sperm mitochondrion and tail." Cell **41**(1): 325-334.
- Tombes, R. M. and B. M. Shapiro (1987). "Enzyme termini of a phosphocreatine shuttle. Purification and characterization of two creatine kinase isozymes from sea urchin sperm." The Journal of biological chemistry **262**(33): 16011-16019.
- Trauger, S. A., E. Kalisak, J. Kalisiak, H. Morita, M. V. Weinberg, A. L. Menon, F. L. Poole, 2nd, M. W. Adams and G. Siuzdak (2008). "Correlating the transcriptome, proteome, and metabolome in the environmental adaptation of a hyperthermophile." J Proteome Res **7**(3): 1027-1035.
- Travassos, M. A. and M. K. Laufer (2009). "Resistance to antimalarial drugs: molecular, pharmacologic, and clinical considerations." Pediatr Res **65**(5 Pt 2): 64R-70R.
- Tymoshenko, S., R. D. Oppenheim, D. Soldati-Favre and V. Hatzimanikatis (2013). "Functional genomics of *Plasmodium falciparum* using metabolic modelling and analysis." Brief Funct Genomics **12**(4): 316-327.
- Valentine, W. N. and D. E. Paglia (1980). "Erythrocyte disorders of purine and pyrimidine metabolism." Hemoglobin **4**(5-6): 669-681.

- van Brummelen, A. C., K. L. Olszewski, D. Wilinski, M. Llinas, A. I. Louw and L. M. Birkholtz (2009). "Co-inhibition of Plasmodium falciparum S-adenosylmethionine decarboxylase/ornithine decarboxylase reveals perturbation-specific compensatory mechanisms by transcriptome, proteome, and metabolome analyses." *J Biol Chem* **284**(7): 4635-4646.
- van Schaijk, B. C., T. R. Kumar, M. W. Vos, A. Richman, G. J. van Gemert, T. Li, A. G. Eappen, K. C. Williamson, B. J. Morahan, M. Fishbaugher, M. Kennedy, N. Camargo, S. M. Khan, C. J. Janse, K. L. Sim, S. L. Hoffman, S. H. Kappe, R. W. Sauerwein, D. A. Fidock and A. M. Vaughan (2013). "Type II fatty acid biosynthesis is essential for Plasmodium falciparum sporozoite development in the midgut of Anopheles mosquitoes." *Eukaryot Cell*.
- Vaughan, A. M., M. T. O'Neill, A. S. Tarun, N. Camargo, T. M. Phuong, A. S. Aly, A. F. Cowman and S. H. Kappe (2009). "Type II fatty acid synthesis is essential only for malaria parasite late liver stage development." *Cell Microbiol* **11**(3): 506-520.
- Vaz, F. M. and R. J. Wanders (2002). "Carnitine biosynthesis in mammals." *Biochem J* **361**(Pt 3): 417-429.
- Vega-Rodriguez, J., B. Franke-Fayard, R. R. Dinglasan, C. J. Janse, R. Pastrana-Mena, A. P. Waters, I. Coppens, J. F. Rodriguez-Orengo, P. Srinivasan, M. Jacobs-Lorena and A. E. Serrano (2009). "The glutathione biosynthetic pathway of Plasmodium is essential for mosquito transmission." *PLoS pathogens* **5**(2): e1000302.
- Wallimann, T., M. Wyss, D. Brdiczka, K. Nicolay and H. M. Eppenberger (1992). "Intracellular compartmentation, structure and function of creatine kinase isoenzymes in tissues with high and fluctuating energy demands: the 'phosphocreatine circuit' for cellular energy homeostasis." *The Biochemical journal* **281** ( Pt 1): 21-40.
- Walsh, P. J., C. M. Wood, S. Thomas and S. F. Perry (1990). "Characterization of red blood cell metabolism in rainbow trout." *J Exp Biol* **154**: 475-489.
- Want, E. J., B. F. Cravatt and G. Siuzdak (2005). "The expanding role of mass spectrometry in metabolite profiling and characterization." *ChemBiochem* **6**(11): 1941-1951.
- Weckwerth, W. (2003). "Metabolomics in systems biology." *Annu Rev Plant Biol* **54**: 669-689.
- WHO (2013) "World Malaria Report 2013." 284.
- Wishart, D. S., T. Jewison, A. C. Guo, M. Wilson, C. Knox, Y. Liu, Y. Djoumbou, R. Mandal, F. Aziat, E. Dong, S. Bouatra, I. Sinelnikov, D. Arndt, J. Xia, P. Liu, F. Yallou, T. Bjorn Dahl, R. Perez-Pineiro, R. Eisner, F. Allen, V. Neveu, R. Greiner and A. Scalbert (2013). "HMDB 3.0--The Human Metabolome Database in 2013." *Nucleic Acids Res* **41**(Database issue): D801-807.
- Wishart, D. S., C. Knox, A. C. Guo, R. Eisner, N. Young, B. Gautam, D. D. Hau, N. Psychogios, E. Dong, S. Bouatra, R. Mandal, I. Sinelnikov, J. Xia, L. Jia, J. A. Cruz, E. Lim, C. A. Sobsey, S. Shrivastava, P. Huang, P. Liu, L. Fang, J. Peng, R. Fradette, D. Cheng, D. Tzur, M. Clements, A. Lewis, A. De Souza, A. Zuniga, M. Dawe, Y. Xiong, D. Clive, R. Greiner, A. Nazyrova, R. Shaykhtudinov, L. Li, H. J. Vogel and I. Forsythe (2009). "HMDB: a knowledgebase for the human metabolome." *Nucleic Acids Res* **37**(Database issue): D603-610.
- Wishart, D. S., D. Tzur, C. Knox, R. Eisner, A. C. Guo, N. Young, D. Cheng, K. Jewell, D. Arndt, S. Sawhney, C. Fung, L. Nikolai, M. Lewis, M. A. Coutouly, I. Forsythe, P. Tang, S. Shrivastava, K. Jeroncic, P. Stothard, G. Amegbey, D. Block, D. D. Hau, J. Wagner, J. Miniaci, M. Clements, M. Gebremedhin, N. Guo, Y. Zhang, G. E. Duggan, G. D. Macinnis, A. M. Weljie, R. Dowlatabadi, F. Bamforth, D. Clive, R. Greiner, L. Li, T. Marrie, B. D. Sykes, H. J. Vogel and L.

- Querengesser (2007). "HMDB: the Human Metabolome Database." Nucleic Acids Res **35**(Database issue): D521-526.
- Wright, G. J. and J. C. Rayner (2014). "Plasmodium falciparum erythrocyte invasion: combining function with immune evasion." PLoS Pathog **10**(3): e1003943.
- Yamada, T. and P. Bork (2009). "Evolution of biomolecular networks: lessons from metabolic and protein interactions." Nat Rev Mol Cell Biol **10**(11): 791-803.
- Yang, W. C. and M. Dubick (1977). "Inhibition of cardiac creatine phosphokinase by fluorodinitrobenzene." Life Sci **21**(8): 1171-1177.
- Yeh, E. and J. L. Derisi (2011). "Chemical Rescue of Malaria Parasites Lacking an Apicoplast Defines Organelle Function in Blood-Stage Plasmodium falciparum." PLoS biology **9**(8): e1001138.
- Young, J. A., Q. L. Fivelman, P. L. Blair, P. de la Vega, K. G. Le Roch, Y. Zhou, D. J. Carucci, D. A. Baker and E. A. Winzeler (2005). "The Plasmodium falciparum sexual development transcriptome: a microarray analysis using ontology-based pattern identification." Molecular and biochemical parasitology **143**(1): 67-79.

## 11 Publication

Host reticulocytes provide metabolic reservoirs that can be exploited by malaria parasites

(see enclosed manuscript)

## Article title

Host reticulocytes provide metabolic reservoirs that can be exploited by malaria parasites

## Short title

Reticulocyte metabolism and malaria

## Author list

Anubhav Srivastava<sup>1,2</sup>, Darren J. Creek<sup>1-3,6</sup>, Krystal J. Evans<sup>5</sup>, David De Souza<sup>4</sup>, Louis Schofield<sup>5,7</sup>, Sylke Müller<sup>2</sup>, Michael P. Barrett<sup>1,2</sup>, Malcolm J. McConville<sup>3,4</sup> and Andrew P. Waters<sup>1,2</sup>

## Author Affiliations

<sup>1</sup>Wellcome Trust Centre for Molecular Parasitology, <sup>2</sup>Institute of Infection, Immunity & Inflammation, , College of Medical, Veterinary and Life Sciences, University of Glasgow, Scotland, UK.

<sup>3</sup>Department of Biochemistry and Molecular Biology, <sup>4</sup>Metabolomics Australia, Bio21 Molecular Science and Biotechnology Institute, University of Melbourne, Parkville, Victoria, 3010, Australia.

<sup>5</sup>Walter and Eliza Hall Institute of Medical Research, Melbourne, Australia.

<sup>6</sup>Drug Delivery Disposition and Dynamics, Monash Institute of Pharmaceutical Sciences, Monash University, Parkville, Australia.

<sup>7</sup>Australian Institute of Tropical Health and Medicine, James Cook University, Townsville, Australia.

## Corresponding author

Andrew P. Waters  
Institute of Infection, Immunity and Inflammation,  
College of Medical Veterinary & Life Sciences,  
University of Glasgow,  
120 University Place,  
Glasgow, G12 8TA, UK  
Email: [Andy.Waters@glasgow.ac.uk](mailto:Andy.Waters@glasgow.ac.uk)  
Phone: +44 (0)141 330 8720  
Fax: +44 (0)141 330 5422

## Details of the manuscript

Abstract word count: 194

Text word count: 3951 (excluding abstract, acknowledgements, authorship, references and figure legends)

Number of main figures: 5

Number of references: 53

## Scientific section designation RED CELLS, IRON, AND ERYTHROPOIESIS

## Key points

- Erythroid metabolism can ameliorate the impact of genetic or chemical disruption of metabolism in reticulocyte resident *Plasmodium* spp.
- Blood stage malaria intervention strategies targeting parasite metabolism should be formulated according to the target host erythrocyte.

## Abstract

Human malaria parasites proliferate in different erythroid cell types during infection. Whilst *Plasmodium vivax* exhibits a strong preference for immature erythrocytes (reticulocytes), the more pathogenic *P.falciparum* primarily infects mature erythrocytes (normocytes). In order to assess if these two host erythrocyte cell types offer different growth conditions and relate them to parasite preference, we compared the metabolomes of human and rodent reticulocytes with those of their normocyte counterparts. Reticulocytes were found to have a more complex, enriched metabolic profile than normocytes, indicating a higher level of metabolic redundancy between reticulocyte resident parasite stages and their host cell. This was further assessed by generating a panel of mutants of the reticulocyte preferent rodent malaria parasite *P.berghei* with defects in intermediary carbon metabolism (ICM) and pyrimidine biosynthesis known to be important for *P.falciparum* growth and survival *in vitro* in normocytes. Aspects of both pathways proved redundant producing generally slow growing, virulent *P.berghei* that committed to sexual development yet failed to complete transmission. These findings imply that malaria parasites can partially salvage pyrimidines from host red blood cells and drug therapies that target blood stage *Plasmodium* metabolism should be specifically formulated according to *Plasmodium* red blood cell tropism.

## Introduction

*Plasmodium* parasites have a dynamic life cycle which is reflected in stage-specific morphologies, transcriptomes, proteomes and metabolomes<sup>1-7</sup>. Due to their parasitic life-style, *Plasmodium* spp. have a reduced metabolic capacity compared to higher organisms. They are auxotrophic for purines and amino acids<sup>8,9</sup>, but have retained some central metabolic pathways including glycolysis<sup>10</sup>, citric acid cycle<sup>7,11</sup>, lipid synthesis<sup>12</sup>, pentose phosphate pathway<sup>13</sup>, pyrimidine biosynthesis<sup>14</sup> and glycosylation<sup>15</sup>. Being obligate intracellular parasites, their metabolism is linked to the host erythrocyte and heavily dependent on the availability of external nutrients. As a result, they establish systems such as the new permeation pathways with the purpose of accessing host cell and environmental nutrients<sup>16</sup>.

Normocytes (mature erythrocytes) comprise almost 98% of the circulating erythrocytes and can be considered “simplified” cells compared to the erythroid precursors present in the bone marrow<sup>17</sup> and reticulocytes (maturing erythrocytes) present in peripheral circulation<sup>18</sup>. The major metabolic pathways active in normocytes are glycolysis<sup>19</sup> and pentose phosphate pathway<sup>20</sup>. Reticulocytes undergo many changes in peripheral circulation as they mature into normocytes. Maturation is associated with a decrease in surface area, acquisition of a biconcave shape, increase in shear membrane resistance, loss of organelles (mitochondria, ribosomes, vesicles and lysosomes), reduction of up to 30 membrane proteins and decrease in membrane cholesterol<sup>18,21</sup>. As this process is likely associated with a general streamlining of cellular metabolism, reticulocytes are expected to contain a richer repertoire of nutrients than normocytes which might be exploited or even required by reticulocyte preferent *Plasmodium* parasites.

To establish whether there are metabolic differences between reticulocytes and normocytes, we undertook a non-targeted analysis of the metabolomes of these erythrocytes. Comparison of the metabolomes of uninfected rat and human reticulocytes and normocytes revealed major differences that could be exploited by intracellular parasite stages. This was tested using reverse genetics to disrupt parasite metabolism and establish the broad ability of *P.berghei* to utilise the products of reticulocyte metabolism.

## Methods

### Metabolomics of rodent erythrocytes

Induction of reticulocytosis was achieved through administration of phenylhydrazine-HCl (PHZ, 100 mg/kg body weight) to Wistar rats and cells were harvested when reticulocyte percentage in peripheral blood reached its maximum level (~35% reticulocytes 5 days after treatment). This was monitored by FACS analysis using the reticulocyte surface marker surface protein transferrin receptor (CD71), which is lost as reticulocytes mature to normocytes<sup>21</sup>. Material was also collected for comparison with blood from non-enriched (~1% reticulocytes) animals (Figures 1A and S1A). All samples were depleted of leucocytes. Metabolite extraction was done by using chloroform/methanol/water (1:3:1 v/v) and samples were analysed using LC-MS and GC-MS.

### Metabolomics of human CD34+ stem cell grown erythrocytes

CD34+ cells obtained from blood from human volunteers were cultured in a three-stage protocol based on published methods<sup>22</sup>. Cultured reticulocytes and normocytes from matching donors were used for metabolite extraction with chloroform/methanol/water (1:3:1 v/v) and samples were analysed using LC-MS.

### ***P.berghei* methods**

Infection of laboratory mice, asexual culture of *P.berghei* stages and generation of knockout parasites was done as before<sup>23</sup>. Asexual growth competition assay was done by mixing wt and mutant parasites expressing different fluorescent markers and performing co-infections in recipient mice and monitoring the growth of the two populations by flow cytometry as done before<sup>24</sup>. Lethality of mutant *P.berghei* parasites was checked by injecting infected RBCs (10<sup>4</sup>) into C57/B6 mice and monitoring parasitaemia, disease pathology and mortality over 21 days. Gametocyte conversion was monitored by flow cytometry in mutants generated in parent line (820cl1m1cl1) expressing GFP in male gametocytes and RFP in female gametocytes<sup>25</sup>. DNA quantification during exflagellation was also monitored by flow cytometry in mutant *P.berghei* parasites. Development of ookinetes in wild type, mutants and sexual crosses was observed in standard *in vitro* cultures maintained at 21°C. Mosquito transmission experiments were done in 5-8 days old mosquitoes used for infected blood feeds at 21°C and monitored for oocyst and sporozoite development using a Leica M205 FA fluorescence stereomicroscope.

### **Determination of IC<sub>50</sub> value of inhibitors *in vitro***

Inhibitors were used to perform *in vitro* drug susceptibility tests in standard cultures of synchronized *P.berghei* and *P.falciparum* blood stages. For testing *P.berghei* inhibition, inhibitors were used at increasing concentrations to culture ring stage *P.berghei* for 24 hours and parasite development to schizont stage was analyzed by flow cytometry after staining iRBCs with DNA-specific dye Hoechst-33258. *P.falciparum* 3D7 strain was used for determining IC<sub>50</sub> values of inhibitors in *in vitro* cultures by measuring <sup>3</sup>H-Hypoxanthine incorporation in the presence of inhibitors in increasing concentrations.

## **Results**

### **The reticulocyte metabolome is more complex than the mature erythrocyte**

Metabolite extracts from normocytes and reticulocyte-enriched erythrocyte populations (35% reticulocytes, Figure 1A) were analyzed in parallel by liquid chromatography mass spectrometry (LC-MS) and gas chromatography mass spectrometry (GC-MS), with both platforms providing overlapping, as well as complementary coverage of their metabolomes. LC-MS data was processed using XCMS, MZMatch and IDEOM while GC-MS data was processed using PyMS matrix generation and Chemstation Electron Ionisation (EI) spectrum match analysis. A total of 333 metabolites were provisionally identified from a total of 4560 mass features and peaks. Almost half of all detected metabolites were found to be more than 2-fold more abundant in reticulocytes and similar changes were observed when all mass features and peaks were included in the analyses (Figures 1B, S1B & C,

Table S1). Importantly, as the rat reticulocyte-enriched samples contained 65% normocytes, the level of metabolite enrichment in reticulocytes was actually much greater. The top 20 metabolites up-regulated in rodent reticulocytes showed a similar trend towards up-regulation in human reticulocytes grown *in vitro* from CD34+ stem cells analysed using LC-MS (Figure 1C). All identified metabolites were charted on metabolic pathways known to exist in *Plasmodium* and mammalian host cell from biochemical studies<sup>6,7,11,26,27</sup> and genomic data<sup>28</sup>.

### **The reticulocyte metabolome reflects its ongoing developmental programme**

Fractions enriched in rodent reticulocytes contained elevated levels of glycolytic, pentose phosphate pathway and TCA cycle intermediates (Table S1). The presence of the latter indicates that reticulocytes have a functional tricarboxylic acid (TCA) and associated intermediary carbon metabolism, consistent with the presence of a residual population of mitochondria in reticulocytes that are lost in normocytes<sup>18</sup>. Increases in the levels of intermediates of the purine and pyrimidine metabolic pathways in reticulocytes presumably originate either from biosynthesis in the preceding erythropoiesis stages or from catabolism of nucleic acid to constituent nucleobases<sup>29</sup>. A number of intermediates of phospholipid metabolism were also elevated in reticulocytes compared to normocytes. In addition, many carnitine derivatives were found to be up-regulated in rodent (although interestingly not in human) reticulocytes which may relate to fatty acid catabolism by  $\beta$ -oxidation in the mitochondria or peroxisomes of these cells. Other notable changes included elevated levels of intermediates in glutathione and arginine metabolism in reticulocytes.

Taken together these data demonstrate that the reticulocyte contains elevated levels of many metabolites that could potentially be used by the invading malaria parasite. Furthermore there was a marked overlap in metabolic pathways observed in the reticulocyte and those predicted in the parasite<sup>27,28</sup>. Common pathways might therefore be uniquely dispensable to *Plasmodium* during its growth in the reticulocyte compared with that in normocytes where many host metabolites are depleted. To test this hypothesis, we used reverse genetics to target several metabolic pathways in intermediary metabolism and pyrimidine biosynthesis in *P.berghei* whose intermediates were significantly up-regulated in reticulocytes.

### **Features of intermediary carbon metabolism are dispensable in asexual blood stage *P.berghei***

Asexual red blood cell stages of *Plasmodium* spp. express the cytosolic enzymes, phosphoenolpyruvate carboxylase (*pepc*, PBANKA\_101790), malate dehydrogenase (*mdh*, PBANKA\_111770) and aspartate amino transferase (*aat*, PBANKA\_030230) and are thought to

catabolize glucose via the intermediary carbon metabolic pathways depicted in figure 2A. Production of aspartate via this pathway is likely to be important for protein and nucleic acid synthesis as it has been shown that the  $\alpha$ -amino group from aspartate is utilised in purine salvage and the carbon skeleton is used as a precursor in pyrimidine biosynthesis<sup>30</sup> while inhibition of *aat* has been shown to be lethal to *P.falciparum*<sup>31</sup>. Malate produced by these pathways either enters mitochondria to participate in the TCA cycle or is excreted<sup>7,26</sup>.

Metabolites involved in TCA cycle and intermediary carbon metabolism (ICM), including malate and aspartate, were found to be substantially higher in reticulocytes compared to normocytes (Figure 2A). The elevated levels of these intermediates may possibly explain the previous observation that disruption of the TCA cycle in *P.berghei* blood stages through deletion of flavoprotein (Fp) subunit, *pbsdha* (PBANKA\_051820) part of the catalytic component for succinate dehydrogenase activity had little effect on parasite viability in blood stage forms, although ookinete development is impaired<sup>32</sup>. To further explore the possibility that *P.berghei*, a reticulocyte resident parasite has potential access to the anapleurotic substrates of host cell ICM, attempts were made to delete *pepc*, *mdh* and *aat* in *P.berghei* and assess the importance of these parasite enzymes throughout the life cycle (Figure 2A). It proved possible to delete *pepc* and *mdh* (Figures S2A and S2B), however *aat* proved refractory. The *pepc*<sup>-</sup> and *mdh*<sup>-</sup> mutant parasites survive in intra-erythrocytic stages but the *pepc*<sup>-</sup> mutants were overgrown by the wt parasite in a sensitive single host competitive growth assay. This was not the case when monitoring the growth of the *mdh*<sup>-</sup> mutants, which did not display a growth phenotype at this stage of their development (Figures 3A and S3A). Scrutiny of the growth phenotype detected in the *pepc*<sup>-</sup> mutants showed that they have a prolonged asexual cycle although there was no difference in merozoite numbers in mature schizonts (Figures S3B and S3C). However, both mutants cause severe cerebral malaria in CD57/B6 mouse model and the dynamics of their lethality is similar to wt, killing all mice within 8-10 days post infection (Figure 3B). The number of gametocytes formed in blood stages was reduced in *pepc*<sup>-</sup> mutants by almost 50% but unaffected in *mdh*<sup>-</sup> (Figure 3C). Further phenotypic analyses showed reduction in exflagellation (the production of mature male gametes) and delay in DNA replication during this process which was more pronounced in the *pepc*<sup>-</sup> mutant (figures 3D, 3E and S3D). Ookinete development in *in vitro* cultures of *pepc*<sup>-</sup> mutants was also severely affected while in *mdh*<sup>-</sup> mutants, ookinetes were formed but the number was reduced by about 50% compared to wt (Figure 4A). To determine if this defect was sex specific, crosses of *pepc*<sup>-</sup> and *mdh*<sup>-</sup> were performed with *P.berghei* lines RMgm-348 (Pb270, *p47*) which produces viable male gametes but non-viable female gametes and RMgm-15 (Pb137, *p48/45*) which produces viable female gametes but non-viable male gametes<sup>33</sup>. Mutants of *pepc*<sup>-</sup> were found to produce severely reduced number of ookinetes in either cross suggesting that gametes of both genders are affected

and that the activity of the protein is essential for gamete formation. This was not the case for *mdh*<sup>-</sup> mutants where although crossing experiments showed that lack of MDH protein affected both genders, they mimicked the parental phenotype producing 50% fewer mature ookinetes (Figure 4B). Transmission of *pepc*<sup>-</sup> parasites through mosquitoes failed forming small numbers of oocysts in mosquito midguts and no salivary gland sporozoites. However, parasites lacking *mdh* could complete transmission through the mosquito and infect mice generating blood stage asexual forms in 48-72 hours similar to wt despite producing reduced numbers of oocysts when compared to wt (Figures 4C, 4D and S4). Overall, these results suggest that two key enzymes in *P.berghei* ICM are at least partially redundant during stages of infection in which the parasites resides primarily in reticulocytes, but that they become essential as the parasite differentiates and proliferates within other host or vector cell types.

### Pyrimidine biosynthesis can be partially disrupted in reticulocyte-preferent *P.berghei*

*Plasmodium* spp. are heavily dependent on nucleic acid synthesis during blood stage asexual growth and either salvage (i.e purines) or synthesize (i.e pyrimidines) the requisite bases. A schematic representation of the pyrimidine biosynthesis pathway is given in Figure 2B. Five out of six enzymes of this pathway have been shown to be potential targets against *P.falciparum* using parasite specific inhibitors in standard *in vitro* cultures<sup>34</sup>. However, most of these inhibitors have been markedly less potent in the *in vivo* *P.berghei* model and this difference has been attributed to reduced bio-availability of inhibitors in mice or apparent differences in target enzyme structures<sup>35,36</sup>. Alternatively, our study showing increased levels of all pyrimidine biosynthesis intermediates observed in reticulocytes (bar glutamine, Figure 2B) raised the possibility that if *P.berghei* could access this resource through pyrimidine salvage pathways leading to reduced dependency on *de novo* synthesis it would be less affected by this class of inhibitors compared to *P.falciparum* residing in mature normocytes<sup>14,34</sup>. Attempts to delete 6 genes encoding enzymes involved in the pyrimidine biosynthesis pathway in *P.berghei* such as carbamoyl phosphate synthetase II (*cpsII*, PBANKA\_140670), aspartate carbamoyltransferase (*act*, PBANKA\_135770), dihydroorotase (*dhoase*, PBANKA\_133610), dihydroorotate dehydrogenase (*dhodh*, PBANKA\_010210), orotate phosphoribosyltransferase (*oprt*, PBANKA\_111240) and orotidine 5'-monophosphate decarboxylase (*ompdc*, PBANKA\_050740) were therefore made to see if reticulocyte pools of pyrimidine biosynthesis intermediates could compensate for the loss of *de novo* pyrimidine synthesis in the parasites.

Only the genes encoding the enzymes of the final two steps of the pyrimidine biosynthesis pathway, *oprt* and *ompdc* could be deleted (Figures S2A and S2B). The *oprt*<sup>-</sup> and *ompdc*<sup>-</sup> mutant parasites are rapidly outgrown in a competition growth assay with wt parasites (Figure 3A), grow slowly (figure

S3B), produce significantly fewer merozoites than wt (figure S3C), and seem to invade very young reticulocytes (figure S3E). Both mutants showed altered lethality in the CD57/B6 mouse model as the mice infected with the mutants did not manifest the symptoms of experimental cerebral malaria (ECM) but died between days 14-20 as a result of severe anaemia and hyperparasitemia (Figure 3B). The process of transmission was also affected by the loss of *ompdc* and *opr*. Gametocytemia was significantly reduced only in *opr* parasites (Figure 3C). Exflagellation was found to be severely affected in *opr* and completely blocked in *ompdc* parasites (Figure 3D) and DNA replication during male gametogenesis was severely reduced (Figure 3E). Consistent with the defects in male gametogenesis, very few ookinetes were formed in *in vitro* cultures in *opr* parasites and no ookinetes were observed in *ompdc* (Figure 4A). Genetic crosses of *opr* and *ompdc* mutants were performed as above with *P.berghei* lines RMgm-348 and RMgm-15 which showed that viable male gametes were able to rescue the ookinete conversion defect in both mutant lines suggesting that formation of male gametes is impaired in both *opr* and *ompdc* mutant parasites while female gametes remain unaffected (Figure 4B). Infectivity to the mosquito was significantly reduced in *opr* and completely blocked in *ompdc* mutants as seen by observing oocysts in infected mosquito midguts and salivary gland sporozoites (Figures 4C, D and S4) and infection to naïve mice was found to be completely blocked. However, when ookinetes from *p47* x *opr* or *ompdc* crosses were fed to mosquitoes, they failed to develop into mature oocysts and did not complete sporogony and those mosquitoes could not infect naïve mice (data not shown).

We also tested the effect of a previously published inhibitor of pyrimidine biosynthesis (5-fluoroorotate, 5FOA<sup>37</sup> in both *P.falciparum* and *P.berghei*. This was done to assess whether there is differential sensitivity towards interfering with pyrimidine biosynthesis between the species due to the reticulocyte preference of the latter. The comparisons were carried out *in vitro* to prevent bioavailability of the inhibitor confounding *in vivo* data in mice. We tested the activity and found that the IC<sub>50</sub> value of 5FOA *in vitro* was almost 90-fold higher in *P.berghei* (32.2 ± 0.9 nM) compared to *P.falciparum* (0.37 ± 0.01 nM) (Figure 5). A dihydroartemisinin control showed no major difference in inhibition between *P.berghei* (6.6 ± 0.1 nM) and *P.falciparum* (2.8 ± 0.2 nM). These data strongly support our hypothesis that *P.berghei* can access pyrimidine precursors from the reticulocyte.

## Discussion

Our data established that reticulocytes have a much more complex metabolome than normocytes, adding to previously well documented changes that occur during reticulocyte to normocyte differentiation in the peripheral circulation<sup>18,21</sup>. We predicted that malaria parasites infectious to

both human (*P. vivax*) and rodents (*P. berghei*) which exhibit a strong tropism for reticulocytes rather than normocytes may be more tolerant to the loss of key metabolic pathways because of redundancy with host pathways. Conversely, the down-regulation of key metabolic pathways in normocytes compared to reticulocytes may explain why several of the corresponding pathways in asexual blood stages of *P. falciparum* appear to be essential *in vitro*. Our data strongly suggest that reticulocytes do indeed provide a highly enriched host cell niche for some *Plasmodium* species, with important implications for drug discovery strategies.

Whilst glycolysis is the main pathway for carbon metabolism in erythrocytes<sup>19</sup>, both human<sup>38</sup> and rodent<sup>39</sup> erythrocytes retain a residual proteomic signature of TCA cycle and ICM enzymes and our metabolomics data suggests that these pathways are much more active in reticulocytes. The increased availability of these metabolites in reticulocytes likely explains the non-essentiality of the *P. berghei pepc* and *mdh* genes, which are involved in regulating intracellular levels of oxaloacetate and malate. In contrast, PEPC is essential for normal intra-erythrocytic survival of *P. falciparum in vitro*, although this can be by-passed by nutrient supplementation of *P. falciparum* infected normocytes<sup>26</sup>. It should be noted that the *pbpepc*<sup>-</sup> mutant still showed a significant growth defect compared with wt parasites (similar to the *P. falciparum* mutant) in the asexual blood stage cycle as revealed by our sensitive single host competitive growth assay. It would be interesting to use this assay to compare asexual growth dynamics of other available metabolic mutants such as the *pbsdha*<sup>-</sup> with wt which might reveal additional defects to those reported<sup>32</sup>. The *P. berghei pepc*<sup>-</sup> mutant also failed to complete transmission through mosquitoes as a result of defects in gametocyte production, male gamete formation, female gamete viability resulting in trace oocyst formation and failure to enter sporogony, which extends our understanding of the importance of this metabolic enzyme for parasite development beyond the asexual blood stages previously investigated<sup>26</sup>. A possible explanation for this phenotype is that the *pepc*<sup>-</sup> mutant is unable to generate sufficient aspartate for nucleotide biosynthesis and is unable to scavenge aspartate from other host cells infected during its sexual and asexual life cycle (Figure 2A).

In line with this suggestion is the repeated failure to delete *P. berghei aat* which generates aspartate, an essential precursor for nucleic acid and protein synthesis. The essential nature of *aat* suggests that either the apparently higher levels of aspartate in reticulocytes are insufficient to meet the demands of a growing asexual stage parasite or that, as in *P. falciparum* intra-erythrocytic stages, *P. berghei* is not readily able to access host cytoplasmic pools of aspartate<sup>40</sup>. Production of aspartate in *Plasmodium pepc*<sup>-</sup> mutants can still be achieved through generation of the oxaloacetic acid precursor by mitochondrial malate:quinone oxidoreductase (MQO) or the reverse reaction of

cytosolic MDH. However, this is apparently a suboptimal solution for the *pepc*<sup>-</sup> parasite resulting in slow growth in the blood and failure to develop in the mosquito. *Plasmodium* AAT can also generate methionine from aspartate, glutamate and other amino acids which can act as effective amino donors<sup>41</sup> and regulate glutamine/glutamate metabolism. These functions may not be rescued by simple aspartate salvage from the host and further support the essentiality of *aat* as a key enzyme for the parasite.

The *P.falciparum* gene encoding MDH has proved refractory to deletion, suggesting that it is essential for these parasites. In marked contrast, the *P.berghei* mutants lacking *mdh* were readily generated, suggesting that this species may scavenge reticulocyte pools of malate. The *mdh*<sup>-</sup> mutant exhibited a very modest growth phenotype and was able to develop into mosquito-infective stages, despite producing 1/3 fewer oocysts than wt. The continued viability of the *mdh*<sup>-</sup> mutants during transmission in the absence of reticulocyte-based compensatory sources of the metabolite can be explained by continued TCA derived production of malate and NADH+ H<sup>+</sup> reducing equivalents given the increased flux through the TCA metabolism in gametocytes and probably later sexual stages<sup>7,11</sup>. Conditional silencing or disruption of *P.falciparum mdh* or degradation of MDH in mature gametocytes or later stages of *P.falciparum* would establish if MDH is required for transmission of the human parasite.

*Plasmodium* spp. salvage their purine requirements from the host cell, but retain the ability to synthesise pyrimidines<sup>42</sup>. Purine nucleosides are taken up by the parasite PfNT1 and other, as yet, unidentified AMP transporters<sup>43</sup> after they are delivered to the parasitophorous vacuole via the action of erythrocyte nucleoside transporters<sup>34,44</sup> and a non-selective transport process<sup>42,45</sup>. In contrast, while other Apicomplexa (i.e *Cryptosporidium* spp., *Toxoplasma* spp.) retain the capacity to salvage pyrimidines<sup>14</sup>, *Plasmodium* spp. are thought to lack transporters required for host pyrimidine salvage<sup>28</sup> and to be completely dependent on *de novo* pyrimidine synthesis for asexual growth<sup>34</sup>.

The survival of *P.berghei oprt* and *ompdc*- mutants has two possible explanations which are not mutually exclusive: 1. Exclusive reliance on reticulocyte pools of pyrimidines (also leading to a reduction in number of merozoites produced). 2. Conversion of parasite-produced orotate to UMP by host UMP synthase. Both outcomes require transport of nucleosides or nucleotides from the host cytoplasm to the parasite. It is notable that *Plasmodium* spp., uniquely amongst the apicomplexa, contain an annotated UDP-N-acetyl glucosamine: UMP antiporter (PBANKA\_110490, PF3D7\_0505300) which might partially fulfil this need as such antiporters have been shown to transport nucleotide sugars in exchange for nucleotide monophosphates in human cells<sup>46</sup> although location of this antiporter in *Plasmodium* is not yet clear. Both pyrimidine biosynthesis mutants

survive only in the youngest reticulocytes which might reflect either adequacy of supply of host UMP (or derivatives) or the capacity of the youngest reticulocytes to convert parasite-derived orotate. Indeed enzymes involved in the later stages of pyrimidine biosynthesis, nucleoside diphosphate kinase B, CTP synthase and ribonucleotide reductase large subunit have been identified in rodent and human erythrocytes<sup>38,39</sup>. The possibility that host pyrimidine enzymes may have redundant functions with the parasite enzymes catalyzing late steps in pyrimidine biosynthesis is supported by the apparent essentiality of the *P.berghei* genes encoding the first five steps of pyrimidine biosynthesis.

The reticulocyte metabolome also explains other species-specific differences between *P.berghei* and *P.falciparum*. Glutathione biosynthesis occurs in erythrocytes<sup>38,39,47,48</sup> and *Plasmodium* (Figure S5A)<sup>49</sup> where it is essential in blood stage *P.falciparum*<sup>50</sup> but not *P.berghei*<sup>51,52</sup>. We demonstrated increased levels of glutathione synthesis intermediates in reticulocytes (Figure S5B) and that 10 fold excess of the IC<sub>50</sub> for *P.falciparum* (~60µM)<sup>50</sup> of buthionine sulphoximine an inhibitor of γ-glutamylcysteine synthetase had no inhibitory effect on *P.berghei* parasites (figure S5C). This is consistent with the reticulocyte-mediated rescue of chemical disruption of the glutathione synthesis pathway in *P.berghei*.

Enzymes involved in *Plasmodium* intermediary carbon metabolism<sup>11,26</sup> and pyrimidine biosynthesis<sup>34</sup> are considered attractive targets for drug development. The metabolome surveys and drug inhibition data presented here provide reasons to be cautious about extrapolating conclusions regarding gene essentiality in reticulocyte preferent parasites such as *P.berghei* as part of any drug discovery pathway that has been based initially upon screens in normocytes. Bioavailability in mouse models and/or difference in target enzyme structures between species have been proposed as reasons for the relative ineffectiveness of drugs when tested *in vivo* using *P.berghei*<sup>35,36</sup>. Our data shows that the reticulocyte metabolome may provide a reservoir of metabolites downstream of the point of action of a drug rendering the drug less effective. This has a number of consequences:

1. Good drug candidates for *P.falciparum* might be (or already have been) eliminated from further development due to misleading data from *in vivo P.berghei* testing.
2. Normocyte preferent rodent parasites (e.g. *P. yoelii* YM)<sup>53</sup> might provide a more accurate model to test drug candidates for *P.falciparum* malaria.
3. *P.berghei* could provide an accurate model for the development of drugs against reticulocyte preferent *P. vivax*.

4. Recrudescence of *P.falciparum* infection during treatment with antimalarials that target parasite metabolism might result from their survival in a 'protective' reticulocyte niche, the existence of which cannot be predicted by standard *in vitro* cultures.
5. Reticulocyte resident parasites exposed to anti-metabolites at levels determined by *in vitro* culture would be sub-optimal with the subsequent risk of being more conducive for the selection of drug resistant progeny.

## Acknowledgements

We would like to thank Dr. Karl Burgess for helping in running LC-MS samples, Marco Biddau for providing 3D7 *P.falciparum* parasites for drug assays and Anne Graham and Rachael Orr for helping in sample harvesting for metabolomics analysis. MJM is a NHMRC Principal Research Fellow. DJC is a NHMRC CJ Martin Training Fellow. APW is a Wellcome Trust Principal Research Fellow.

## Authorship contributions

AS designed experiments, generated and analysed the rodent erythroid metabolome data, performed the gene deletions, phenotypic analyses and drug sensitivity assays in *P.berghei* and *P.falciparum*, analysed the data and wrote the manuscript. DJC helped with LC-MS data analysis of rodent samples, provided human LC-MS data and advised on identification of metabolites. KJE cultured human reticulocytes and provided human erythroid LC-MS data. DDS generated GC-MS data for rodent samples. LS provided human erythroid LCMS data. SM facilitated the *P.falciparum* drug sensitivity assays, interpreted data and wrote the manuscript. MPB helped in study design, facilitated metabolomics studies and interpreted data. MJM interpreted data, facilitated metabolomics studies and wrote the manuscript. APW conceived, designed and supervised the study, interpreted data and wrote the manuscript.

## Conflict of Interest disclosure

The authors declare no competing financial interests.

## References

1. Bozdech Z, Llinas M, Pulliam BL, Wong ED, Zhu J, DeRisi JL. The transcriptome of the intraerythrocytic developmental cycle of *Plasmodium falciparum*. *PLoS Biol*. 2003;1(1):E5.
2. Llinas M, del Portillo HA. Mining the malaria transcriptome. *Trends Parasitol*. 2005;21(8):350-352.
3. Khan SM, Franke-Fayard B, Mair GR, et al. Proteome analysis of separated male and female gametocytes reveals novel sex-specific *Plasmodium* biology. *Cell*. 2005;121(5):675-687.
4. Hall N, Karras M, Raine JD, et al. A comprehensive survey of the *Plasmodium* life cycle by genomic, transcriptomic, and proteomic analyses. *Science*. 2005;307(5706):82-86.
5. Olszewski KL, Morrisey JM, Wilinski D, et al. Host-parasite interactions revealed by *Plasmodium falciparum* metabolomics. *Cell Host Microbe*. 2009;5(2):191-199.

6. Kafsack BF, Llinas M. Eating at the table of another: metabolomics of host-parasite interactions. *Cell Host Microbe*. 2010;7(2):90-99.
7. Macrae JI, Dixon MW, Dearnley MK, et al. Mitochondrial metabolism of sexual and asexual blood stages of the malaria parasite *Plasmodium falciparum*. *BMC Biol*. 2013;11(1):67.
8. Booden T, Hull RW. Nucleic acid precursor synthesis by *Plasmodium lophurae* parasitizing chicken erythrocytes. *Exp Parasitol*. 1973;34(2):220-228.
9. Sherman IW. Amino acid metabolism and protein synthesis in malarial parasites. *Bull World Health Organ*. 1977;55(2-3):265-276.
10. Homewood CA. Carbohydrate metabolism of malarial parasites. *Bull World Health Organ*. 1977;55(2-3):229-235.
11. Oppenheim RD, Creek DJ, Macrae JI, et al. BCKDH: The Missing Link in Apicomplexan Mitochondrial Metabolism Is Required for Full Virulence of *Toxoplasma gondii* and *Plasmodium berghei*. *PLoS Pathog*. 2014;10(7):e1004263.
12. Holz GG, Jr. Lipids and the malarial parasite. *Bull World Health Organ*. 1977;55(2-3):237-248.
13. Barrett MP. The pentose phosphate pathway and parasitic protozoa. *Parasitol Today*. 1997;13(1):11-16.
14. Hyde JE. Targeting purine and pyrimidine metabolism in human apicomplexan parasites. *Curr Drug Targets*. 2007;8(1):31-47.
15. Macedo CS, Schwarz RT, Todeschini AR, Previato JO, Mendonca-Previato L. Overlooked post-translational modifications of proteins in *Plasmodium falciparum*: N- and O-glycosylation -- a review. *Mem Inst Oswaldo Cruz*. 2010;105(8):949-956.
16. Landfear SM. Nutrient transport and pathogenesis in selected parasitic protozoa. *Eukaryot Cell*. 2011;10(4):483-493.
17. Chen K, Liu J, Heck S, Chasis JA, An X, Mohandas N. Resolving the distinct stages in erythroid differentiation based on dynamic changes in membrane protein expression during erythropoiesis. *Proc Natl Acad Sci U S A*. 2009;106(41):17413-17418.
18. Gronowicz G, Swift H, Steck TL. Maturation of the reticulocyte in vitro. *J Cell Sci*. 1984;71:177-197.
19. Chapman RG, Hennessey MA, Waltersdorff AM, Huennekens FM, Gabrio BW. Erythrocyte metabolism. V. Levels of glycolytic enzymes and regulation of glycolysis. *J Clin Invest*. 1962;41:1249-1256.
20. Stromme JH, Eldjarn L. The role of the pentose phosphate pathway in the reduction of methaemoglobin in human erythrocytes. *Biochem J*. 1962;84:406-410.
21. Liu J, Guo X, Mohandas N, Chasis JA, An X. Membrane remodeling during reticulocyte maturation. *Blood*. 2010;115(10):2021-2027.
22. Douay L, Giarratana MC. Ex vivo generation of human red blood cells: a new advance in stem cell engineering. *Methods Mol Biol*. 2009;482:127-140.
23. Janse CJ, Ramesar J, Waters AP. High-efficiency transfection and drug selection of genetically transformed blood stages of the rodent malaria parasite *Plasmodium berghei*. *Nat Protoc*. 2006;1(1):346-356.
24. Sinha A, Hughes KR, Modrzynska KK, et al. A cascade of DNA-binding proteins for sexual commitment and development in *Plasmodium*. *Nature*. 2014;507(7491):253-257.
25. Ponzi M, Siden-Kiamos I, Bertuccini L, et al. Egress of *Plasmodium berghei* gametes from their host erythrocyte is mediated by the MDV-1/PEG3 protein. *Cell Microbiol*. 2009;11(8):1272-1288.
26. Storm J, Sethia S, Blackburn GJ, et al. Phosphoenolpyruvate carboxylase identified as a key enzyme in erythrocytic *Plasmodium falciparum* carbon metabolism. *PLoS Pathog*. 2014;10(1):e1003876.
27. Ginsburg H. Progress in in silico functional genomics: the malaria Metabolic Pathways database. *Trends Parasitol*. 2006;22(6):238-240.

28. Gardner MJ, Hall N, Fung E, et al. Genome sequence of the human malaria parasite *Plasmodium falciparum*. *Nature*. 2002;419(6906):498-511.
29. Valentine WN, Paglia DE. Erythrocyte disorders of purine and pyrimidine metabolism. *Hemoglobin*. 1980;4(5-6):669-681.
30. Bulusu V, Jayaraman V, Balaram H. Metabolic fate of fumarate, a side product of the purine salvage pathway in the intraerythrocytic stages of *Plasmodium falciparum*. *J Biol Chem*. 2011;286(11):9236-9245.
31. Wrenger C, Muller IB, Schifferdecker AJ, Jain R, Jordanova R, Groves MR. Specific inhibition of the aspartate aminotransferase of *Plasmodium falciparum*. *J Mol Biol*. 2011;405(4):956-971.
32. Hino A, Hirai M, Tanaka TQ, Watanabe Y, Matsuoka H, Kita K. Critical roles of the mitochondrial complex II in oocyst formation of rodent malaria parasite *Plasmodium berghei*. *Journal of biochemistry*. 2012;152(3):259-268.
33. van Dijk MR, Janse CJ, Thompson J, et al. A central role for P48/45 in malaria parasite male gamete fertility. *Cell*. 2001;104(1):153-164.
34. Cassera MB, Zhang Y, Hazleton KZ, Schramm VL. Purine and pyrimidine pathways as targets in *Plasmodium falciparum*. *Curr Top Med Chem*. 2011;11(16):2103-2115.
35. Gujjar R, Marwaha A, El Mazouni F, et al. Identification of a metabolically stable triazolopyrimidine-based dihydroorotate dehydrogenase inhibitor with antimalarial activity in mice. *J Med Chem*. 2009;52(7):1864-1872.
36. Phillips MA, Gujjar R, Malmquist NA, et al. Triazolopyrimidine-based dihydroorotate dehydrogenase inhibitors with potent and selective activity against the malaria parasite *Plasmodium falciparum*. *J Med Chem*. 2008;51(12):3649-3653.
37. Rathod PK, Khatri A, Hubbert T, Milhous WK. Selective activity of 5-fluoroorotic acid against *Plasmodium falciparum* in vitro. *Antimicrob Agents Chemother*. 1989;33(7):1090-1094.
38. Pasini EM, Kirkegaard M, Mortensen P, Lutz HU, Thomas AW, Mann M. In-depth analysis of the membrane and cytosolic proteome of red blood cells. *Blood*. 2006;108(3):791-801.
39. Pasini EM, Kirkegaard M, Salerno D, Mortensen P, Mann M, Thomas AW. Deep coverage mouse red blood cell proteome: a first comparison with the human red blood cell. *Mol Cell Proteomics*. 2008;7(7):1317-1330.
40. Martin RE, Kirk K. Transport of the essential nutrient isoleucine in human erythrocytes infected with the malaria parasite *Plasmodium falciparum*. *Blood*. 2007;109(5):2217-2224.
41. Berger LC, Wilson J, Wood P, Berger BJ. Methionine regeneration and aspartate aminotransferase in parasitic protozoa. *J Bacteriol*. 2001;183(15):4421-4434.
42. Downie MJ, Kirk K, Mamoun CB. Purine salvage pathways in the intraerythrocytic malaria parasite *Plasmodium falciparum*. *Eukaryot Cell*. 2008;7(8):1231-1237.
43. Cassera MB, Hazleton KZ, Riegelhaupt PM, et al. Erythrocytic adenosine monophosphate as an alternative purine source in *Plasmodium falciparum*. *J Biol Chem*. 2008;283(47):32889-32899.
44. Quashie NB, Ranford-Cartwright LC, de Koning HP. Uptake of purines in *Plasmodium falciparum*-infected human erythrocytes is mostly mediated by the human equilibrative nucleoside transporter and the human facilitative nucleobase transporter. *Malar J*. 2010;9:36.
45. Desai SA, Krogstad DJ, McCleskey EW. A nutrient-permeable channel on the intraerythrocytic malaria parasite. *Nature*. 1993;362(6421):643-646.
46. Ishida N, Kawakita M. Molecular physiology and pathology of the nucleotide sugar transporter family (SLC35). *Pflugers Arch*. 2004;447(5):768-775.
47. Minnich V, Smith MB, Brauner MJ, Majerus PW. Glutathione biosynthesis in human erythrocytes. I. Identification of the enzymes of glutathione synthesis in hemolysates. *The Journal of clinical investigation*. 1971;50(3):507-513.
48. Majerus PW, Brauner MJ, Smith MB, Minnich V. Glutathione synthesis in human erythrocytes. II. Purification and properties of the enzymes of glutathione biosynthesis. *The Journal of clinical investigation*. 1971;50(8):1637-1643.

49. Muller S. Redox and antioxidant systems of the malaria parasite *Plasmodium falciparum*. *Molecular microbiology*. 2004;53(5):1291-1305.
50. Patzewitz EM, Wong EH, Muller S. Dissecting the role of glutathione biosynthesis in *Plasmodium falciparum*. *Molecular microbiology*. 2012;83(2):304-318.
51. Vega-Rodriguez J, Franke-Fayard B, Dinglasan RR, et al. The glutathione biosynthetic pathway of *Plasmodium* is essential for mosquito transmission. *PLoS pathogens*. 2009;5(2):e1000302.
52. Pastrana-Mena R, Dinglasan RR, Franke-Fayard B, et al. Glutathione reductase-null malaria parasites have normal blood stage growth but arrest during development in the mosquito. *The Journal of biological chemistry*. 2010;285(35):27045-27056.
53. Walliker D, Sanderson A, Yoeli M, Hargreaves BJ. A genetic investigation of virulence in a rodent malaria parasite. *Parasitology*. 1976;72(2):183-194.

## Figure legends

### Figure 1. Comparison of reticulocytes and normocytes reveals metabolite enrichment in rodent and human reticulocytes.

- A. Dynamics of reticulocyte enrichment in peripheral blood *in vivo* followed by Phenylhydrazine-HCl (phz) treatment of mice. Reticulocytes were harvested at day 5 post phz treatment. The error is given as the standard deviation (S.D.) of 3 independent biological replicates.
- B. Volcano plot showing distribution of putative metabolites according to their fold change in abundance in reticulocyte enriched erythrocytes vs normocyte enriched erythrocytes in rodent blood. All significant changes are represented above the broken horizontal line. Coloured dots indicate metabolites which are: Blue- significantly up-regulated, Red- significantly down-regulated, Yellow- significant but little change, Brown- non-significant. n=3 independent biological replicates (with four internal technical replicates each). Significance tested by Welch's T-test ( $\alpha < 0.05$ ). Almost half of all detected metabolites (147, ~45%) were found to be more than 2-fold more abundant in reticulocytes. Only 5 (~1%) metabolites were more than 2-fold more abundant in normocytes than in reticulocytes. The rest of the metabolites did not show a significant difference between reticulocytes and normocytes. See figure S1C and table S1 in supplementary data for the complete list of detected metabolites and their respective abundance fold changes.
- C. Representative metabolites up-regulated in reticulocytes compared to normocytes in human and rodent erythrocytes. Relative levels (peak intensities) are expressed as fold change observed in reticulocyte vs normocytes. Dotted line indicates no change and error bars

indicate R.S.D. (Relative Standard Deviation) of peak intensities from reticulocyte samples multiplied to the fold change values from n=3 independent biological replicates.

**Figure 2. Metabolites of intermediary carbon metabolism (ICM) and pyrimidine biosynthesis are up-regulated in reticulocytes.**

- A. Top panel: Fold change of relative levels (peak intensities) of metabolites of carbon metabolism in rodent reticulocytes compared to normocytes. Dotted line indicates no change and error bars indicate R.S.D. (Relative Standard Deviation) of peak intensities from reticulocyte samples multiplied to the fold change values from n=3 independent biological replicates. Bottom panel: Schematic representation of intermediary carbon metabolism (ICM) in *Plasmodium*. Genes marked with (✓) were deleted in *P.berghei* blood stages and the ones marked with (✖) could not be deleted even after repeated attempts. *pepc*: Phosphoenolpyruvate Carboxylase (PBANKA\_101790), *mdh*: Malate Dehydrogenase (PBANKA\_111770), *aat*: Aspartate Amino Transferase (PBANKA\_030230).
- B. Top panel: Fold change of relative levels (peak intensities) of metabolites of pyrimidine biosynthesis in rodent reticulocytes compared to normocytes. Dotted line indicates no change and error bars indicate R.S.D. (Relative Standard Deviation) of peak intensities from reticulocyte samples multiplied to the fold change values from n=3 independent biological replicates. Bottom panel: Schematic representation of pyrimidine biosynthesis pathway. Genes marked with (✓) were deleted in *P.berghei* blood stages and the ones marked with (✖) could not be deleted even after repeated attempts. *cpsII*: Carbamoyl phosphate synthetase II (PBANKA\_140670), *act*: Aspartate carbamoyltransferase (PBANKA\_135770), *dhoase*: Dihydroorotase (PBANKA\_133610), *dhodh*: Dihydroorotate dehydrogenase (PBANKA\_010210), *oprt*: Orotate phosphoribosyltransferase (PBANKA\_111240), *ompdc*: Orotidine 5'-monophosphate decarboxylase (PBANKA\_050740).

(Also see Figures S2 A and B for gene deletion strategy and confirmation)

**Figure 3. Phenotypic analyses of blood stage mutant *P.berghei* parasites.**

- A. *in vivo* growth assay of mutants in mixed infections in competition with wild type parasites over 12 days. Coloured lines represent non-linear fit of percentage of mutant parasites in total parasite population. Data representative of n=3 independent biological replicates. (Also see Figure S3 A, B and C)

- B. Lethality experiment in C57/B6 mice by wt and mutant *P.berghei* parasites.  $10^4$  parasites were injected intra-peritoneally in mice (n=5) on day 0 and they were monitored for 21 days. The mice were culled humanely when they showed severe malaria pathology. All mutant parasites were found to be lethal to mice.
- C. Gametocyte conversions during blood stages in mutant *P.berghei* parasites over 5 days post infection. Data from 2 independent observed gametocyte conversion experiments are shown  $\pm$  S.D. Gametocyte conversion was observed using a wt parent line which expresses GFP in male gametocytes and RFP in female gametocytes (RMgm-164). *P.berghei* mutants were generated in the same genetic background and analysed using FACS determining the number of gametocytes in infected blood. P-values: \*p<0.05, \*\*p<0.005, \*\*\*p<0.0005, paired two tailed t-test.
- D. Exflagellation (male gamete formation) in mutant *P.berghei* parasites normalised to wt in *in vitro* activation assay. The error is given as the SD of n=3 independent biological replicates. P-values: \*\*p<0.005, \*\*\*p<0.0005, paired two tailed t-test.
- E. Determination of DNA content of male gametocytes over 20 minutes post activation by FACS analysis in mutant *P.berghei* parasites normalised to wt. DNA content was determined in Hoechst-33258-stained MACS purified gametocytes. Before activation (0mins) males show low DNA content with increasing amounts post activation reaching maximum levels between 8 to 12 minutes in wt. Data from 3 independent biological replicates are given  $\pm$  S.D. P-values: \*\*p<0.005, \*\*\*p<0.0005, unpaired two tailed t-test. DNA replication in mutant *P.berghei* parasites was reduced by 50% compared to wt at the 8 minute time point and further delayed taking up to 16 minutes to complete. (Also see figure S3 D)

**Figure 4. Mosquito stage development of *P.berghei* mutant parasites** (Also see figure S4).

- A. *in vitro* ookinete conversion of mutant *P.berghei* parasites as compared to wt. The error is given as the S.D. of n=3 independent biological replicates. P-values: \*\*p<0.005, \*\*\*p<0.0005, unpaired two tailed t-test.
- B. *in vitro* ookinete conversion assay to measure fertility of mutant *P.berghei* gametocytes. Fertility of mutant *P.berghei* gametocytes was analysed by their capacity to form ookinetes by crossing gametes with RMgm-348 (Pb270, p47) which produces viable male gametes but non-viable female gametes and RMgm-15 (Pb137, p48/45) which produces viable female gametes but non-viable male gametes. The error is given as the S.D. of n=2 independent biological replicates. P-values: \*p<0.05, \*\*p<0.005, unpaired two tailed t-test.

- C. Number of mature oocysts at day 14 post infected blood feed in mosquito mid guts. n=40 mosquitoes cumulative of two independent biological replicates. \*\*\*p<0.0005, unpaired two tailed t-test.
- D. Infection prevalence (percentage of observed mosquitoes found to be infected) and infection load (median of number of oocysts found per mosquito) in mutant *P.berghei* parasites compared to wt.

**Figure 5. *P.berghei* and *P.falciparum* inhibition by dihydroartemisinin (DHA) and 5-fluoroorotic acid (5FOA) *in vitro*.** Error bars indicate S.D. from n=3 biological replicates.

Figures

Figure 1

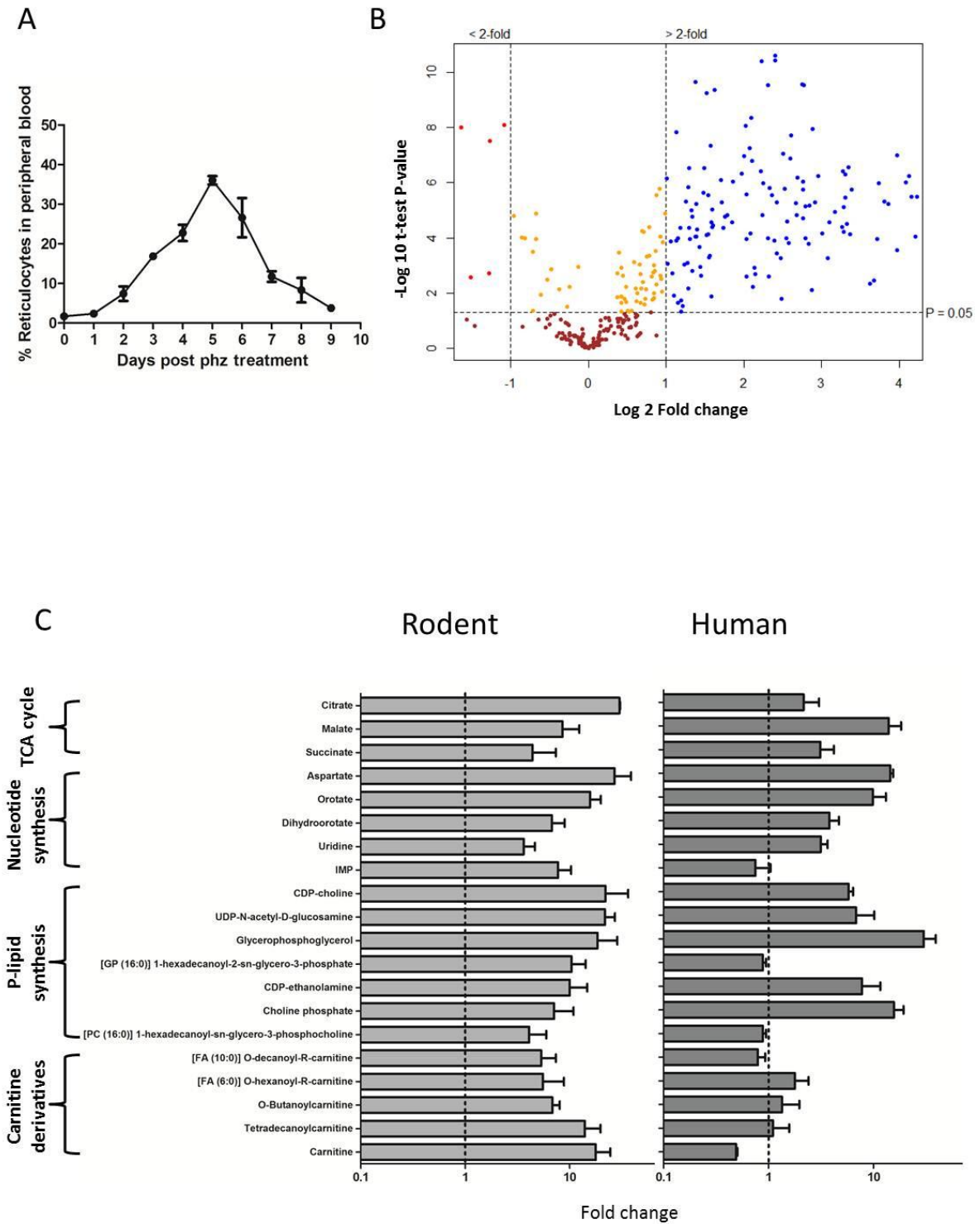


Figure 2

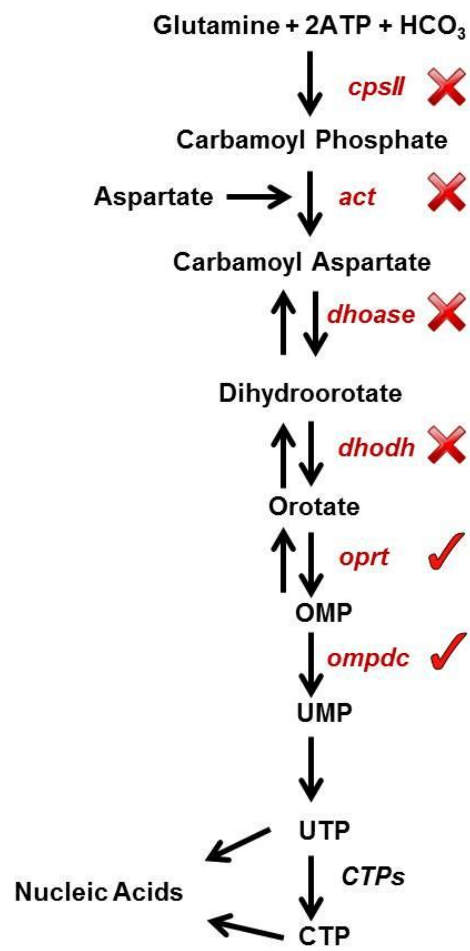
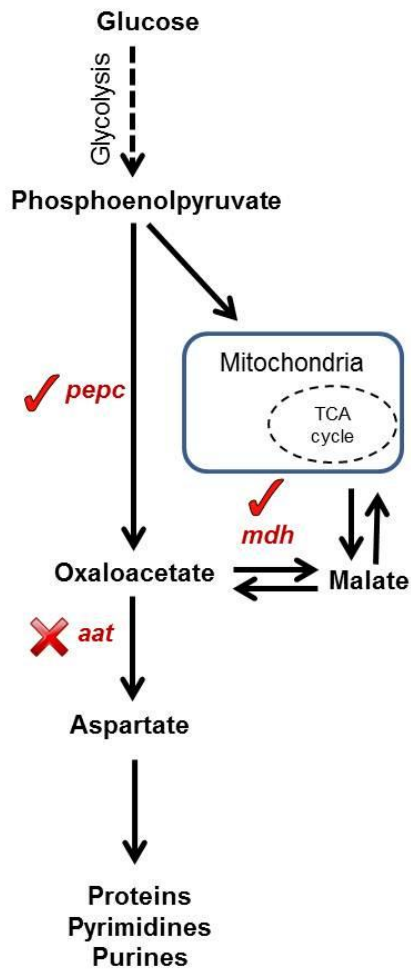
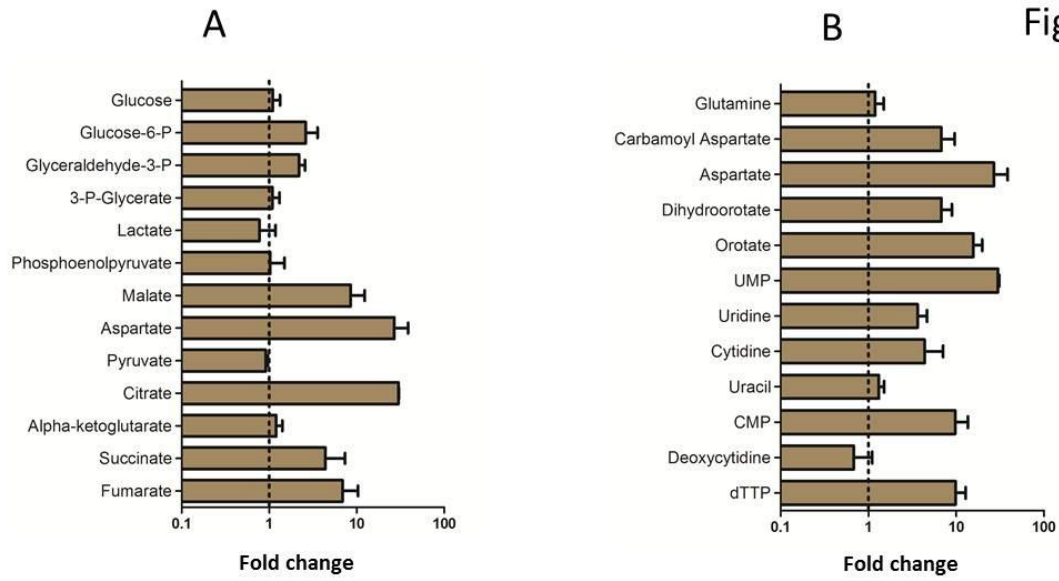


Figure 3

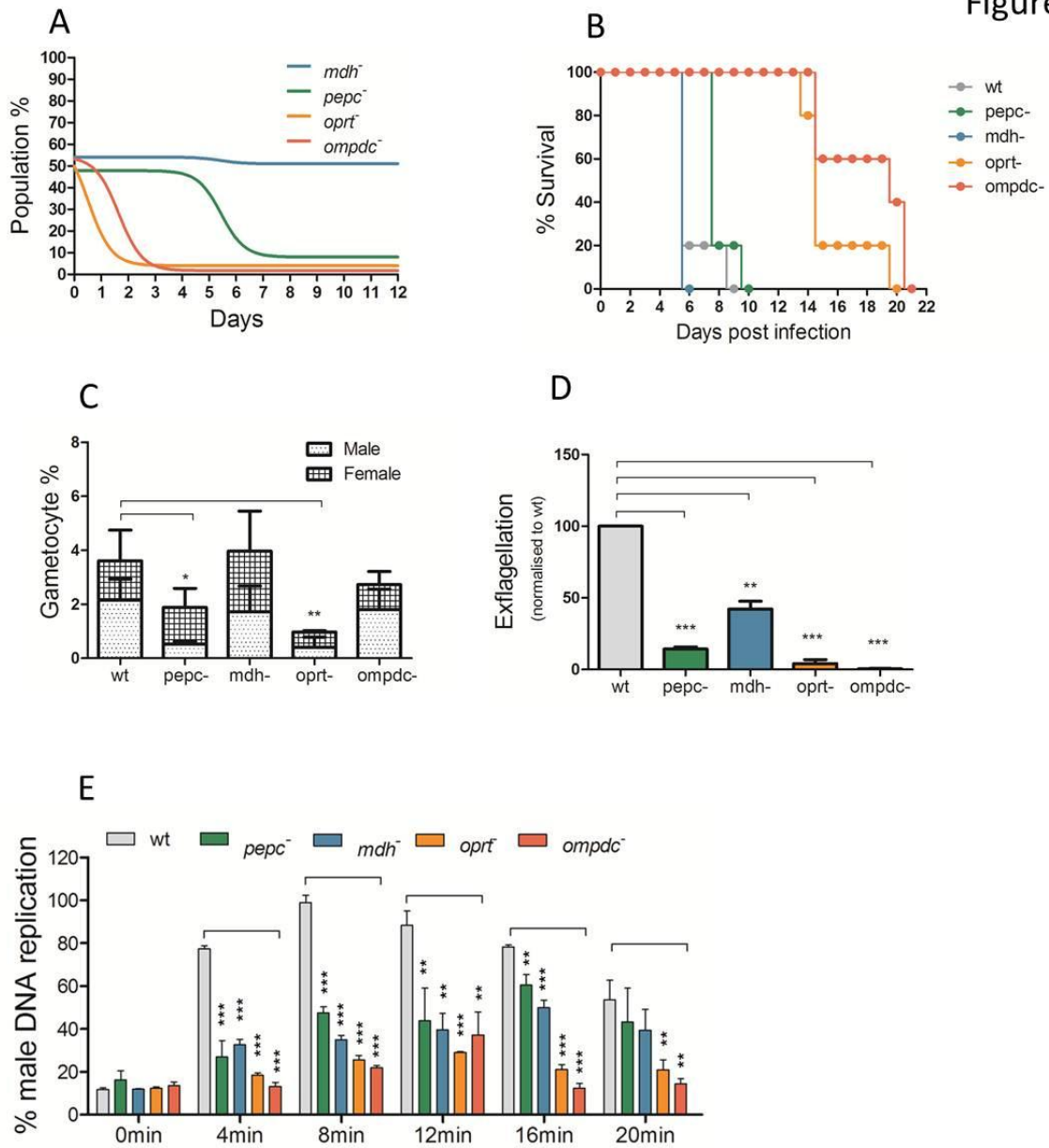


Figure 4

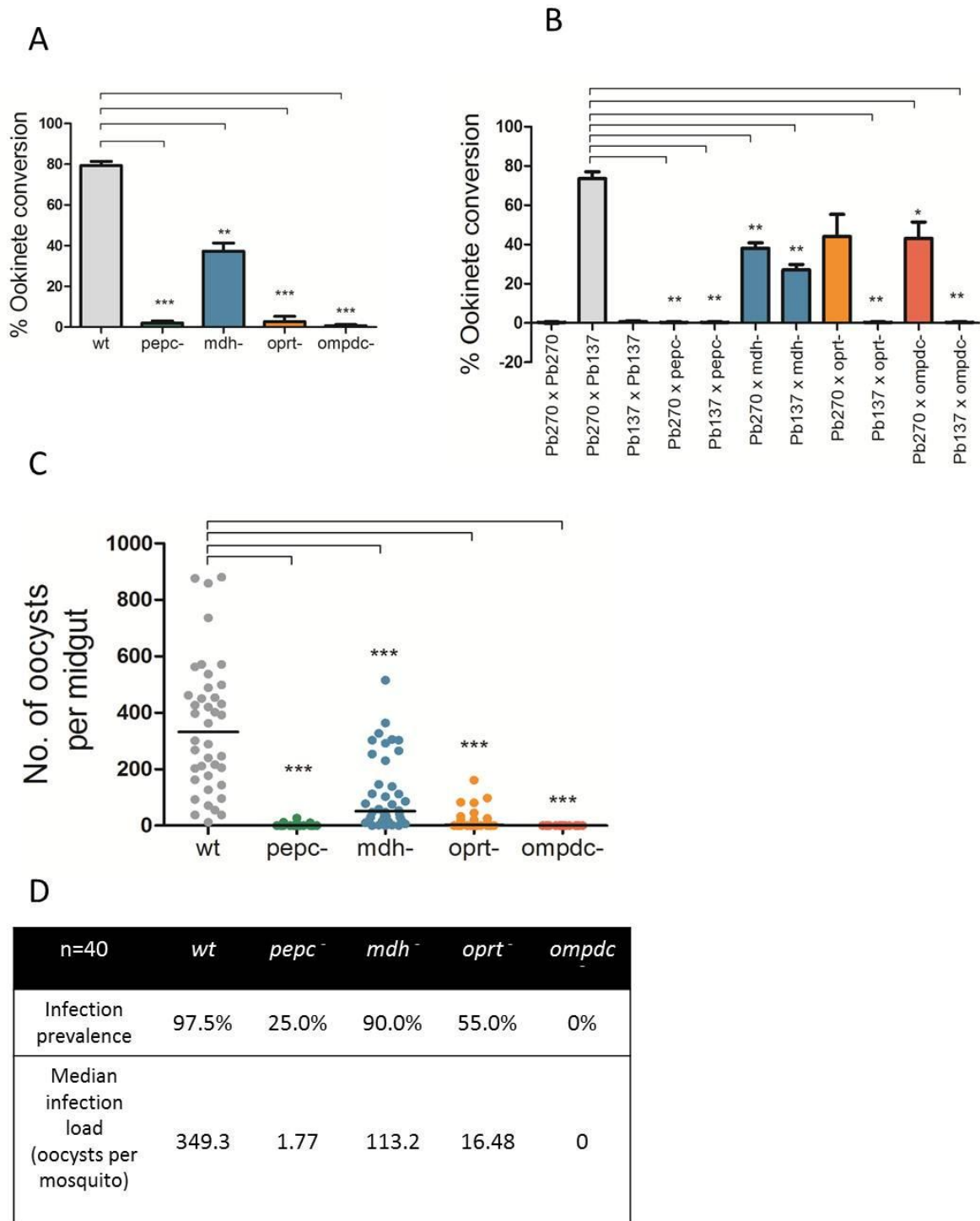
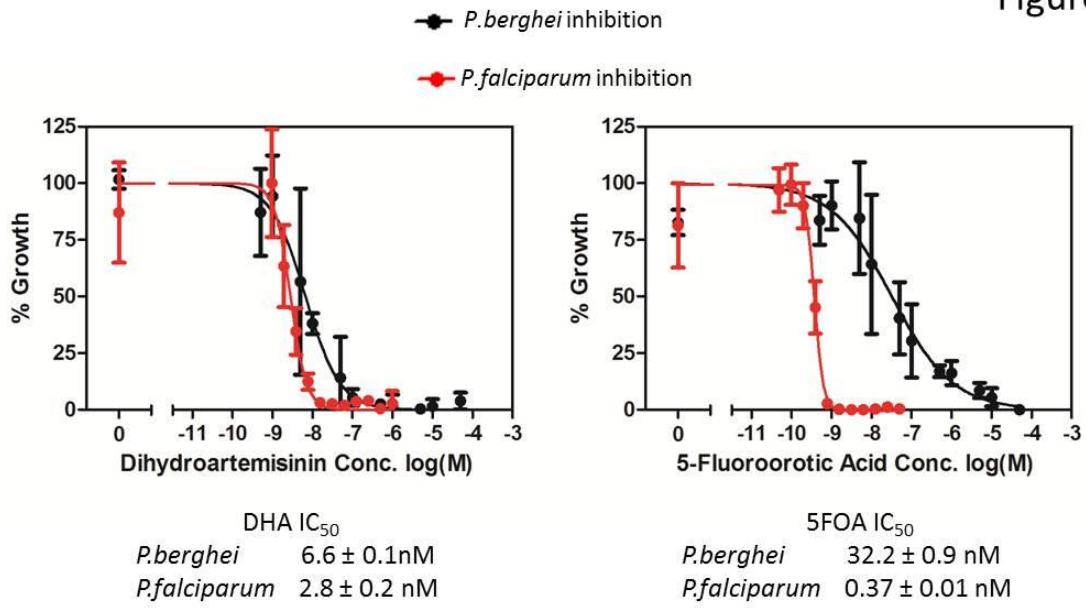


Figure 5



## Supplementary methods

### Rodent erythrocyte sample preparation for metabolomics

For collecting reticulocyte enriched red blood cells, 3 female Wistar rats were each injected with phenylhydrazine-HCl dissolved in 0.9% NaCl (w/v) at a dose of 100 mg/kg body weight and reticulocyte percentage in peripheral blood was monitored using reticulocyte marker CD71-APC antibody by FACS analysis performed on a MACSQuant analyser (Miltenyi Biotec, Germany). On day 5, all rats showed reticulocyte population to be around 30-35% and were bled by cardiac puncture and blood from each rat was collected in RPMI1640 medium. Non reticulocyte enriched normocyte containing samples (with ~1.5% reticulocytes) were prepared similarly without phenylhydrazine-HCl treatment. Each suspension was quickly passed through a prewashed Plasmodipur filter to remove leucocytes and eluted with RPMI1640 medium. A thermometer was put in the bottom of the suspension and the tube submerged in a dry-ice ethanol bath with gentle agitation until the temperature reached 8°C, at which point the tube was immediately immersed in an ice bucket. Using this protocol, the temperature of the cell suspension reached 0°C within 10-12 seconds. The chilled suspension was centrifuged at 450 g for 8 minutes, supernatant was removed and the volumes of equal number of reticulocyte enriched and un-enriched erythrocytes were found to be the same. The cell pellets were resuspended in ice-cold enriched PBS (containing 20 mM Hepes, 20 mM Glucose, 4 mM NaHCO<sub>3</sub>, and 0.1% BSA). The cell density of the suspension was determined using a haemocytometer and replicates containing 1 x 10<sup>8</sup> cells were prepared in enriched PBS (up to 2ml per tube) and kept on ice until metabolite extraction. After first wash (centrifugation at 4°C for 10 min at 1,300g) the pellet was resuspended with 500 µl cold enriched PBS for the second wash (centrifugation at 4°C for 5 minutes at 2,700g) and supernatant was removed again. Finally, the washed pellets were suspended in cold 200 µl of chloroform/methanol/water (1:3:1 v/v) containing internal standards (5-fluorouridine, Cl-phenyl-cAMP, N-methyl glucamine, canavanine and piperazine) at 1 µM concentration. After vigorous mixing in a cooled (4°C) shaker for 1 hour and sonication (2 min, 0°C), the suspension was centrifuged (at 4°C for 5 min at 15,300 g) and equal aliquots (90 µl) of the supernatant were transferred to separate tubes for LC-MS and GC-MS analyses. Tubes for LC-MS analyses were topped up with nitrogen, capped tightly and kept at -80°C before running. Tubes for GC-MS analyses were dried down under nitrogen flow, capped tightly and put at -80°C before reconstitution with chloroform/methanol/water (1:3:1 v/v) prior to derivatization. All experiments were performed according to the Home Office licence regulations and the local ethical committees.

### Metabolomic analysis of rodent erythrocytes

For LC-MS analysis, samples underwent hydrophilic interaction liquid chromatography (HILIC) (UltiMate 3000 RSLC, Thermo Fisher) with a 20mm x 2.1mm ZIC-HILIC guard column coupled to a 150 x 4.6mm ZIC-HILIC analytical column running at 300  $\mu$ l/min, coupled to an Exactive Orbitrap mass spectrometer (Thermo Fisher). The LC-MS method is based on a previously published HILIC method (Creek, Jankevics et al. 2011) with a gradient starting at 20% H<sub>2</sub>O with 0.1% formic acid (A) and 80% acetonitrile with 0.1% formic acid (B), decreasing to 20% B at 30 minutes, followed by a wash at 5% B for 6 minutes, and equilibration at 80% B for 8 minutes. Raw mass spectrometry data was processed using the standard Glasgow Polyomics pipeline, consisting of XCMS for peak picking (Smith, Want et al. 2006), MzMatch for filtering and grouping (Scheltema, Jankevics et al. 2011) and IDEOM for further filtering, post-processing and identification (Creek, Jankevics et al. 2012). Core metabolite identifications were validated against a panel of unambiguous standards by mass and retention time. Additional putative identifications were assigned by mass and predicted retention time (Creek, Jankevics et al. 2011). Automatic metabolite identification was followed by manual data filtration for removing false positives and duplicate identifications and including false rejections.

For GC-MS, dried samples were suspended in chloroform/methanol/water (1:3:3 v/v) and the upper methanol-water phase containing polar metabolites was retained for this study. Samples were dried under nitrogen and subjected to automated methoximation and TMS derivatisation using an Gerstal autosampler/sample preparation robot fitted to an Agilent- 7890A GC-5975 MSD instrument. Briefly, samples were methoximated in 20 mg/ml methoxyamine in pyridine (20  $\mu$ l) with shaking at 37°C for 2 hours and then derivitized by addition of BSTFA + 1% TMCS (20 $\mu$ l) silylation reagent and shaking at 37°C for 1 hr. After incubation at room temperature for 1 hour, sample (1 $\mu$ l) was analyzed on an Agilent 7890A GC -5975 C mass-detector instrument, equipped with a VF5-MS column (30 m, 0.25 mm inner diameter) and helium as the carrier gas. The oven temperature was held at 70°C (1min), then ramped at 1°C/min to 76°C, then 5°C/min to 325°C and held for 10 min. GC/MS peaks were aligned using the Metabolomics software PyMS (O'Callaghan, De Souza et al. 2012) which generated a data matrix of candidate metabolites showing their intensity representing abundance of a metabolite in a given sample and its unique retention time. Chromatograms were manually checked using Agilent Chemstation software and the peaks corresponding to the retention times in the PyMS matrix were identified based on their Electron Ionisation (EI) spectrum. Metabolites were assigned putative identities by matching their spectra (with a cut-off score of  $\geq$ 90%) to Agilent Fiehn and NIST GC-MS Metabolomics libraries of metabolite GC-MS spectra.

From a total number of 4560 peaks collected from the two platforms, 333 metabolites were putatively annotated in erythrocytes, with identification in LC-MS data based on accurate mass and predicted retention time (minimum confidence value of 5/10 in IDEOM) (Creek, Jankevics et al. 2012) and GC-MS based on spectral matching to Agilent Fiehn (Kind, Wohlgemuth et al. 2009) and NIST (National Institute of Standards and Technology, Gaithersburg, MD, USA) spectral libraries (minimum spectral match score of 90% in Chemstation). It is noted that many more probable metabolites were detected but were not readily assigned an identity according to these parameters. From all 333 metabolites, 293 metabolites were identified by LC-MS and 40 metabolites were identified by GC-MS, with 17 metabolites identified by both platforms (Table S1). Of the overlapping metabolites measured on both platforms, the fold-change values in abundance observed between reticulocytes and normocytes were found to be consistent in both direction and magnitude on both platforms. These metabolites were quantitated using the LC-MS data in order to avoid duplication.

### **Metabolomics analysis of Human CD34+ stem cell grown erythrocytes**

Blood from human volunteers was supplied by the Australian Red Cross Blood Service and experiments approved by the Walter and Eliza Hall Institute Human Research Ethics Committee. Peripheral blood mononucleated cells were obtained from blood by Percoll density purification and CD34+ hemopoietic progenitor cells were isolated by magnetic bead separation according to the manufacturer's instructions (Miltenyi Biotec). CD34+ cells were cultured in a three-stage protocol based on the methods of (Douay and Giarratana 2009). Initially cells were cultured at 37°C in a humid atmosphere of 5% CO<sub>2</sub> at a density of  $1 \times 10^4$  cells/mL and then maintained in the range of  $2 \times 10^4$  to  $10^5$  cells/mL in IMDM (LifeTech) containing 5% (v/v) AB Serum (Interstate Companies Laboratories), 10 µg/ml Insulin (Sigma), 3U/ml heparin (Pfizer), 200 µg/ml Transferrin (Prospec), 3U/ml EPO (Eprex). During stage one (days 0-8) this was supplemented with 10ng/ml SCF (GenScript) and 1ng/ml IL-3 (R&D systems); during stage two (days 8-11) with 10ng/ml SCF and additional 800 µg/ml transferrin and stage 3 (days 11-18) with 3U/ml EPO and additional 800 µg/ml transferrin. Cultured reticulocytes (cRetics) were filtered at day 18 using a PALL WBF leukocyte filter. Isogenic control red blood cells (RBCs) were retained from donor blood, washed in IMDM and stored in saline-adenine-glucose-mannitol solution (SAG-M) at 4°C prior to use.

Cells were washed and cultured overnight in stage 3-supplemented IMDM (as outlined above). Metabolism was quenched by immersion of cultures in an ethanol/dry ice bath to 0-4 °C. Cells were pelleted by centrifugation (10,000 rpm for 1 minute) and washed in cold PBS (1 mL). Metabolites were extracted from  $1 \times 10^8$  RBCs and  $0.5 \times 10^8$  cRetics by addition of 300 µL chloroform/methanol/water (1:3:1 v/v) containing internal standards (CHAPS, CAPS, PIPES and TRIS; 1 µM) and left for 30 min at 4 °C with periodic mixing and sonication. Cellular debris was removed by

centrifugation (16,000 rpm for 10 min) and the supernatant was dried under nitrogen gas prior to analysis. Samples were reconstituted in 80% acetonitrile for analysis by high resolution LC-MS with minor adjustments to the previously described ZIC-pHILIC-AC method (Zhang, Creek et al. 2012). The chromatography utilized a 4.6 x 150 mm, 5  $\mu$ m ZIC-pHILIC column (Sequant) with 10 mM ammonium carbonate (A) and acetonitrile (B) mobile phase at a flow rate of 300  $\mu$ L/min. The gradient ran from 80% B (0 min) to 40% B (20 min), then to 5% B for 3 minutes (23-26 mins) followed by re-equilibration at 80% B for 9 minutes (29-38 mins). Mass detection was performed on an Agilent Q-TOF 6550 (Agilent Technologies) operating in negative mode electrospray ionisation with capillary voltage 3.5 kV and fragmenter voltage 175 V. Initial data analysis was conducted with the IDEOM package as described above (Creek, Jankevics et al. 2012) and peak areas for selected metabolites were extracted based on accurate mass and retention time and manually verified with the MassHunter software. Comparison of the average and median peak heights from all detected cellular metabolites demonstrated no significant difference between reticulocytes and normocytes, confirming that the cell number based normalization, with adjustment for cell size (i.e. twice as many normocytes than reticulocytes per sample), was appropriate. Two experiments were performed in triplicate, using cells (cRetics and corresponding isogenic RBCs) from two independent donors.

### **Infection of laboratory animals with *P. berghei* parasites**

For mouse infections, female Theilers Original (TO) outbred mice of body weight 26-30g were used. Cryopreserved blood stages were thawed at room temperature and 0.02-0.5 ml of the suspension was injected intraperitoneally into a mouse. For mouse infection with blood stages obtained from an infected mouse (mechanical passage), one droplet of tail blood (5  $\mu$ l) was collected from an infected animal with a parasitemia of 5-15% in 10 ml PBS and 0.1 ml of the suspension was injected intraperitoneally into a mouse. On day 4-7 after injection the parasitemia increased from 0.1 to 5-20%. For rat infection, female Wistar rats of body weight 150-175 g were used. To infect these, 5-8 droplets of tail blood (30-40  $\mu$ l) were collected from an infected animal with a parasitemia of 5-15% in 1ml PBS and the 1ml suspension was injected intraperitoneally. On day 4 or 5 after injection the parasitemia ranged between 0.5-3%.

### **Asexual cultures of *P. berghei***

*P. berghei* cultures were maintained for one cycle using standard methods. RPMI1640 (containing 5 g/L of Albumax II<sup>®</sup>) were used as the growing medium and flasks were gassed for 30 seconds with a gas mix containing 5% CO<sub>2</sub>, 5% O<sub>2</sub>, 90% N<sub>2</sub> and incubated overnight at 37°C on a shaker at a minimal speed just to keep the cells in suspension. Maturation of schizonts and number of merozoites per schizonts were analysed in Giemsa stained smears made from *in vitro* cultures.

### Generation of knockout parasites and cloning

*P. berghei* schizonts (from line RMgm-7 which expresses GFP constitutively under *eef1a* promoter and from line RMgm-164 which expresses GFP in male gametocytes and RFP in female gametocytes) were transfected with linear DNA constructs containing the *yfcu-hdhfr* selectable marker flanked by homology arms (generated using primers in table S2) corresponding to 5'UTR and 3'UTR of the orf of the gene of interest respectively, injected intravenously in female Wistar rats and TO mice and selected by pyrimethamine in drinking water as described in (Janse, Ramesar et al. 2006). Resulting transfectants were analysed by PCR for 5' and 3' integration (using primers in table S2), cloned by limiting dilution and the absence of open reading frame in the mutants confirmed by PCR. For further phenotypic analysis, due to reasons of cost effectiveness and ease of handling, all mutants generated in TO mice were used and experiments were done by obtaining parasites grown in TO mice.

### Asexual growth competition assay

Equal numbers of mutant parasites ( $10^6$  cells) made in RMgm-7 background expressing GFP constitutively under *eef1a* promoter were mixed with wt parasites ( $10^6$  cells) (RMgm-86) expressing RFP under the same promoter and the mixture was injected into a mouse. The population of infected erythrocytes (iRBCs) was monitored by Hoechst staining and the proportion of iRBCs expressing GFP and RFP was recorded by FACS analysis over the course of two weeks. Infected blood from first mouse was sequentially passage into two or three mice to avoid multiple infections over this period.

### Lethality experiments in C57/B6 mice

iRBCs ( $10^4$ ) were injected intra-peritoneally into female 8-10 weeks old C57/B6 mice (n=5 per line) and parasitemia, disease pathology and mortality was monitored over 21 days.

### Gametocyte conversion monitoring by FACS during blood stage growth

Mutants made in the RMgm-164 background which expresses GFP in male gametocytes and RFP in female gametocytes along with wt were grown in mice and peripheral blood was monitored by FACS analysis by checking for infected erythrocytes (iRBCs) by Hoechst staining and the proportion of iRBCs expressing GFP and RFP, indicative of the presence of male and female gametocytes.

### Exflagellation assay and DNA quantification by FACS

During gametogenesis, male gametocytes undergo rapid endomitosis and DNA content is increased from 1n to 8n within 8 minutes after activation and adherent clumps of erythrocytes are formed around the activating gametocytes called exflagellation centres which were counted on haemocytometer. DNA staining in exflagellating gametocytes was observed by fixing MACS-column

purified activating gametocytes using 0.25% glutaraldehyde at 4 minute intervals, staining with 10  $\mu$ M Hoechst 33258 dye in PBS for 1 h at 37°C and doing FACS analysis on a CyAn ADP Analyser. UV excitation of Hoechst 33258 dye was performed with a violet laser (405 nm) and the gametocyte population was selected by gating on forward/side light scatter. The fluorescence intensity of a total of 100,000 cells was measured for each sample. The mean fluorescence intensity of the activating gametocyte is proportional to the mean DNA content of the parasites and activating male gametocytes and female gametocytes were gated based on DNA content at different time points based on the wt control. All data was plotted normalised to the controls.

### **Ookinete cultures of *P. berghei* and conversions**

Mice infected with *P. berghei* were given sulfadiazine in drinking water which killed all asexual stage parasites in 48 hours and circulating gametocytes remain in blood. Mice were bled and infected blood was collected in RPMI1640 containing 5 g/L Albumax II® and 100  $\mu$ M xanthurenic acid to activate gametocytes. Cultures were incubated at 21°C for 21 hours and giemsa smears were made for counting mature ookinetes and female gametes whose cumulative ratio to female gametes only gave the ookinete conversion rate.

### ***in vitro* sexual crosses**

Equal numbers of gametocytes from two *P. berghei* lines obtained from infected TO mice treated with sulfadiazine in drinking water were taken and mixed in activation media. The suspension was then incubated at 21°C for 21 hours and Giemsa smears were made for counting mature ookinetes and female gametes

### **Mosquito transmission experiments**

*P. berghei* infected mice with a parasitemia of 5-10% were used to blood feed a cage of 250 mosquitoes for 10 minutes. Mature oocysts were counted in mosquito midguts between days 12-14 using a Leica M205 FA Fluorescence Stereomicroscope. Salivary gland sporozoites were checked between days 21-25. Infected mosquitoes were allowed to feed on naïve mice for 10 minutes between days 21-25 and these mice were observed for parasites by making giemsa stained blood smears between days 3-14 to check for successful transmission.

### **Determination of IC<sub>50</sub> value of *P. berghei* inhibitors *in vitro***

Inhibitors were used to perform *in vitro* drug susceptibility tests in standard short-term cultures of synchronized *P. berghei* blood stages. Cultured and purified schizonts/merozoites of the reference ANKA strain of *P. berghei* line cl15cy1, obtained by Nycodenz density gradient purification were injected i.v. into the tail vein of a TO mouse. Injected merozoites invade within 4h after injection and newly infected blood was collected from the mouse by heart puncture at 4h after the injection of

the purified schizonts/merozoites. Infected blood was washed once (450 g, 8 min) with complete culture medium (RPMI1640 + 25% FCS, pH 7.5) followed by mixing of infected erythrocytes with serially diluted solutions of inhibitors in complete culture medium and incubated in 24-well plates in triplicate at a final parasitaemia of 1% at 37°C for 24h under special gas mix of 5% CO<sub>2</sub>, 5% O<sub>2</sub>, 90% N<sub>2</sub>, conditions that permit ring forms to develop into mature schizonts. Parasite development was analysed by FACS after staining iRBCs with DNA-specific dye Hoechst-33258. The cells were pelleted by centrifugation (450 g, 8 min) and after removal of supernatant, cells were fixed with 0.25% glutaraldehyde/PBS solution and stained with 10 µM Hoechst-33258 solution in PBS for 1h at 37°C. Stained cells were analysed using MACSQuant analyser (Miltenyi Biotec, Germany). UV excitation of Hoechst-33258 dye was performed with a violet laser (450/50 nm) and the iRBC population was selected by gating on forward/sidelight scatter. A total of 100,000 cells per samples were analysed and mature schizonts were gated based on their fluorescence intensity and counted in each sample. For determination of growth inhibition, the number of mature schizonts observed was set to correspond to 100% growth for no drug controls and percentage growth was calculated accordingly for the drug treated samples. 100% growth values were in the range 60-75% conversion of ring stage parasites to schizonts (15-20% of ring stage parasites committed to making gametocytes do not undergo DNA replication). Growth inhibitory curves were constructed in Graph pad Prism and based on data from three independent repeats, the IC<sub>50</sub> value for blood stage inhibition of *P. berghei* parasites were calculated. Giemsa stained smears from drug treated cultures were also checked to determine the stage at which parasites were growth arrested.

### **Determination of IC<sub>50</sub> value of *P. falciparum* asexual growth inhibition *in vitro***

*P. falciparum* 3D7 strain was used for determining IC<sub>50</sub> values of inhibitors in *in vitro* cultures by measuring <sup>3</sup>H-Hypoxanthine incorporation in the presence of inhibitors in increasing concentrations as described (Desjardins, Canfield et al. 1979). Cultures were set up at 0.5 % parasitaemia and approximately 2% hematocrit in complete RPMI medium without hypoxanthine (IC<sub>50</sub> medium). Human erythrocytes were washed and stored in RPMI1640 (without AlbumaxII®) at 4°C for not more than a week. A serial dilution of 2 times of the required inhibitor concentration was prepared in a 96 well plate in similar IC<sub>50</sub> medium. In each well, 100 µl of inhibitor was mixed with 100 µl of cells, creating a 1 times final concentration of the inhibitor. Incorporation of <sup>3</sup>H-hypoxanthine (1Ci/ ml, specific activity 20Ci/ mmol) in uninfected erythrocytes and parasites incubated without inhibitor was also measured as negative control. Plates were incubated for 48 hours at 37°C in the presence of a specialized gas mix (5% CO<sub>2</sub>, 1% O<sub>2</sub>, 94% N<sub>2</sub>). After 48 hours of incubation, 100 µl of medium from each well was replaced with fresh medium containing 0.4 µCi <sup>3</sup>H-hypoxanthine per well. Plates

were incubated for further 24 hours and then frozen at -20°C. Then the plates were defrosted and harvested using a Tomtec Mach III harvester and Wallac Printed Filter Mat- A filter mats. The filter mats were dried at 60°C for one hour and sealed in a plastic bag with 4 ml scintillation liquid. Radioactive decay was measured in a Wallac Trilux MicroBeta counter for 1 min per well. IC<sub>50</sub> values were calculated using GraphPad Prism software.

## Supplementary tables

Table S1. Metabolites represented in Figure 1B showing fold change in abundance in uninfected reticulocyte enriched erythrocytes compared to normocyte enriched erythrocytes. Metabolites are listed in order of decreasing abundance. Metabolites identified with authentic standards are highlighted bold, others are considered putative identifications.

No.	Metabolite	Fold change	P-value	Platform
1	Citric acid	>25 fold	9.65E-07	GC-MS
2	UMP	>25 fold	1.03E-02	GC-MS
3	Nonanoylcarnitine	>25 fold	8.40E-06	LC-MS
4	S-Methyl-L-methionine	>25 fold	1.01E-05	LC-MS
5	Ala-Val-Pro-Ser	>25 fold	1.64E-06	LC-MS
6	Dihydrobiopterin	>25 fold	9.59E-05	LC-MS
7	N-Acetyl-aspartyl-glutamate	>25 fold	3.80E-11	LC-MS
8	2-Amino-4-hydroxy-6-hydroxymethyl-7,8-dihydropteridine	>25 fold	3.98E-06	LC-MS
9	Aspartyl-L-proline	>25 fold	4.06E-05	LC-MS
10	sn-glycero-3-Phospho-1-inositol	>25 fold	2.48E-06	LC-MS
11	<b>L-Aspartate</b>	>25 fold	1.08E-05	LC-MS
12	Dodecanoylcarnitine	23.92	6.91E-06	LC-MS
13	CDP-choline	22.04	3.28E-04	LC-MS
14	UDP-N-acetyl-D-glucosamine	21.79	2.95E-08	LC-MS
15	O-Propanoylcarnitine	18.66	3.14E-06	LC-MS
16	Glycerophosphoglycerol	18.45	9.04E-05	LC-MS
17	<b>L-Carnitine</b>	17.81	3.18E-06	LC-MS
18	L-Octanoylcarnitine	17.47	5.88E-07	LC-MS
19	Glu-Asp	16.92	9.51E-07	LC-MS
20	N6-Acetyl-N6-hydroxy-L-lysine	15.71	2.71E-04	LC-MS
21	<b>Orotate</b>	15.68	1.00E-07	LC-MS
22	dCMP-ethanolamine	14.45	5.94E-06	LC-MS
23	Tetradecanoylcarnitine	13.99	4.84E-06	LC-MS
24	Sedoheptulose	13.30	1.02E-06	LC-MS
25	Gamma Glutamyl-glutamic acid	13.10	1.13E-04	LC-MS
26	Creatinine phosphate	12.79	3.60E-03	LC-MS
27	Phosphocreatine	12.32	4.50E-03	LC-MS

28	[GP (16:0)] 1-hexadecanoyl-2-sn-glycero-3-phosphate	10.43	1.81E-06	LC-MS
29	Glu-Pro	10.31	7.35E-05	LC-MS
30	L-Tyrosine methyl ester	10.15	2.82E-07	LC-MS
31	CDP-ethanolamine	10.03	3.21E-05	LC-MS
32	Ala-Asp-Asp	9.86	3.46E-06	LC-MS
33	dTTP	9.84	5.15E-07	LC-MS
34	<b>CMP</b>	9.75	7.49E-06	LC-MS
35	Prenyl-L-cysteine	9.73	5.95E-05	LC-MS
36	N2-Succinyl-L-ornithine	9.68	3.84E-07	LC-MS
37	N-(3S-hydroxydecanoyl)-L-serine	9.63	4.14E-05	LC-MS
38	Met-Thr-Asp	8.97	1.15E-05	LC-MS
39	<b>Malate</b>	8.55	2.82E-05	LC-MS
40	Ala-Ser-Tyr	8.46	5.50E-04	LC-MS
41	2,3,4,5-Tetrahydrodipicolinate	8.05	6.81E-05	LC-MS
42	<b>IMP</b>	7.75	5.83E-07	LC-MS
43	Ala-Cys	7.53	5.07E-06	LC-MS
44	<b>Xanthine</b>	7.36	1.10E-08	LC-MS
45	<b>Ribulose-5-phosphate</b>	7.33	7.69E-03	GC-MS
46	Acetylcholine	7.19	6.92E-06	LC-MS
47	<b>Choline phosphate</b>	7.10	1.59E-04	LC-MS
48	Glu-Gly	6.92	7.27E-06	LC-MS
49	<b>Fumarate</b>	6.90	1.03E-04	LC-MS
50	O-Butanoylcarnitine	6.84	2.96E-10	LC-MS
51	N-Acetyl-D-mannosamine	6.80	9.13E-07	LC-MS
52	N-Carbamoyl-L-aspartate	6.78	1.94E-05	LC-MS
53	Dihydroorotate	6.76	1.82E-06	LC-MS
54	Spermidine	6.71	2.74E-10	LC-MS
55	allylcysteine	6.42	6.51E-07	LC-MS
56	<b>Glycine</b>	6.41	1.50E-05	LC-MS
57	Thiomorpholine 3-carboxylate	6.35	5.69E-06	LC-MS
58	1-methylguanosine	6.11	1.89E-08	LC-MS
59	Gly-Pro	6.06	1.32E-07	LC-MS
60	Glu-Leu	5.95	1.50E-04	LC-MS
61	Leu-Thr	5.86	2.49E-05	LC-MS
62	Thr-Ala	5.85	1.05E-04	LC-MS
63	gamma-L-Glutamyl-L-cysteine	5.77	1.66E-06	LC-MS
64	1-Methyladenosine	5.69	9.08E-08	LC-MS
65	3-Hydroxy-N6,N6,N6-trimethyl-L-lysine	5.60	1.67E-02	LC-MS
66	O-hexanoyl-R-carnitine	5.54	5.41E-04	LC-MS
67	O-decanoyl-R-carnitine	5.35	5.33E-06	LC-MS
68	Malonylcarnitine	5.34	3.57E-04	LC-MS
69	<b>D-Ribose 5-phosphate</b>	5.29	3.61E-11	LC-MS
70	glucosamine-1,6-diphosphate	5.28	2.45E-11	LC-MS
71	N2-Acetyl-L-aminoadipate	5.24	1.24E-04	LC-MS

72	Leu-Pro	5.13	2.77E-06	LC-MS
73	2-Hydroxyadenine	5.02	1.52E-06	LC-MS
74	NG,NG-Dimethyl-L-arginine	4.99	2.55E-03	LC-MS
75	Fructoselysine 6-phosphate	4.95	2.90E-10	LC-MS
76	<b>D-Gluconic acid</b>	4.95	1.05E-04	LC-MS
77	D-Xylulose	4.77	1.06E-06	LC-MS
78	S-Methyl glutathione	4.72	1.54E-05	LC-MS
79	<b>sn-Glycerol 3-phosphate</b>	4.67	4.01E-11	LC-MS
80	Pseudouridine	4.64	3.97E-07	LC-MS
81	<b>Succinate</b>	4.41	2.10E-03	LC-MS
82	<b>Cytidine</b>	4.38	1.22E-03	LC-MS
83	Monomethyl-arginine	4.32	5.82E-03	LC-MS
84	Gamma-Aminobutyryl-lysine	4.30	1.56E-07	LC-MS
85	5-Methylcytidine	4.27	4.33E-09	LC-MS
86	Glu-Val	4.25	7.05E-05	LC-MS
87	Ala-Pro	4.22	5.39E-08	LC-MS
88	Pro-Pro	4.10	2.73E-06	LC-MS
89	[PC (16:0)] 1-hexadecanoyl-sn-glycero-3-phosphocholine	4.10	1.07E-04	LC-MS
90	-Hydroxy-eicosatetraenoic acid	4.10	2.54E-03	LC-MS
91	Xanthosine	4.05	8.44E-09	LC-MS
92	N-Acetyl-D-glucosamine 6-sulfate	4.00	1.12E-07	LC-MS
93	N-Acetyl-L-aspartate	3.91	4.80E-07	LC-MS
94	<b>Uridine</b>	3.63	8.83E-07	LC-MS
95	<b>3',5'-Cyclic AMP</b>	3.59	2.75E-05	LC-MS
96	N1-Acetylspermidine	3.44	1.54E-05	LC-MS
97	Glu-Ser	3.37	1.74E-05	LC-MS
98	<b>N-Acetylneuraminate</b>	3.33	4.47E-05	LC-MS
99	N-Acetyl-L-glutamate 5-semialdehyde	3.28	5.02E-06	LC-MS
100	Val-Val	3.25	7.95E-07	LC-MS
101	Asp-Asp	3.07	4.30E-10	LC-MS
102	Erythrulose 1-phosphate	3.03	3.51E-05	LC-MS
103	Glu-Cys-Gln-Gln	3.01	9.51E-06	LC-MS
104	<b>Choline</b>	3.01	4.04E-05	LC-MS
105	N-Acetylserotonin	3.00	2.80E-05	LC-MS
106	Ala-Leu-Lys-Pro	2.99	1.31E-02	LC-MS
107	(1-Ribosylimidazole)-4-acetate	2.97	4.71E-08	LC-MS
108	O-Acetyl-L-homoserine	2.94	4.52E-04	LC-MS
109	1-Methylnicotinamide	2.93	4.96E-04	LC-MS
110	D-myo-Inositol 1,2-cyclic phosphate	2.92	7.41E-05	LC-MS
111	2-Carboxy-D-arabinitol 1-phosphate	2.91	2.91E-06	LC-MS
112	Glu-Thr	2.88	7.89E-05	LC-MS
113	<b>D-Erythrose 4-phosphate</b>	2.86	5.47E-10	LC-MS
114	Ala-Asp-Cys	2.82	3.04E-07	LC-MS
115	N3-(4-methoxyfumaroyl)-L-2,3-diaminopropanoate	2.78	2.32E-06	LC-MS

116	Ethanolamine phosphate	2.74	2.44E-03	LC-MS
117	Taurine	2.71	1.13E-03	LC-MS
118	Taurocyamine	2.70	2.20E-04	LC-MS
119	N-(L-Arginino)succinate	2.64	5.09E-05	LC-MS
120	<b>L-Arginine</b>	2.62	5.82E-06	LC-MS
121	<b>D-Glucose 6-phosphate</b>	2.61	9.22E-05	LC-MS
122	[SP] 3-dehydrosphinganine	2.60	8.90E-05	LC-MS
123	[SP] Sphing-4-enine-1-phosphate	2.59	2.21E-10	LC-MS
124	CMP-N-acetylneuraminate	2.53	1.72E-05	LC-MS
125	N2-(D-1-Carboxyethyl)-L-lysine	2.53	1.59E-03	LC-MS
126	Acetyl phosphate	2.51	1.02E-05	LC-MS
127	Hexose-phosphate	2.47	1.08E-04	LC-MS
128	Leucyl-leucine	2.46	4.24E-05	LC-MS
129	N-(octanoyl)-L-homoserine	2.46	2.88E-07	LC-MS
130	<b>Putrescine</b>	2.44	1.47E-06	LC-MS
131	<b>AMP</b>	2.44	6.68E-03	LC-MS
132	3-sulfopropanoate	2.42	8.40E-04	LC-MS
133	Leu-Val	2.39	4.89E-06	LC-MS
134	D-Methionine	2.35	9.33E-04	LC-MS
135	Ala-ala	2.31	3.03E-02	LC-MS
136	<b>Hypoxanthine</b>	2.29	4.84E-02	LC-MS
137	N5-Ethyl-L-glutamine	2.29	1.86E-02	LC-MS
138	N-Acetylglutamine	2.28	4.27E-05	LC-MS
139	<b>L-Glutamate</b>	2.22	1.01E-04	LC-MS
140	<b>L-Ornithine</b>	2.22	2.29E-02	LC-MS
141	Phe-Pro	2.20	1.27E-04	LC-MS
142	<b>DL-Glyceraldehyde 3-phosphate</b>	2.20	1.46E-08	LC-MS
143	<b>L-Cystathionine</b>	2.15	1.28E-02	LC-MS
144	Cys-Gly	2.12	1.98E-03	LC-MS
145	N-acetyl-(L)-arginine	2.09	1.33E-04	LC-MS
146	N-Acetyl-D-fucosamine	2.03	8.88E-04	LC-MS
147	Aminopropylcadaverine	2.01	6.77E-07	LC-MS
148	<b>Glutathione disulfide</b>	1.99	1.34E-05	LC-MS
149	<b>L-2-Amino adipate</b>	1.94	1.42E-04	LC-MS
150	(R)-S-Lactoylglutathione	1.93	9.10E-03	LC-MS
151	pyrophosphate	1.91	3.05E-03	LC-MS
152	2-Hydroxyethanesulfonate	1.90	2.44E-03	LC-MS
153	<b>L-Asparagine</b>	1.90	8.75E-05	LC-MS
154	<b>GMP</b>	1.88	1.68E-06	LC-MS
155	Oleic acid	1.84	3.57E-01	GC-MS
156	beta-Alanine	1.84	4.79E-03	LC-MS
157	<b>Guanine</b>	1.83	2.80E-06	LC-MS
158	<b>NAD+</b>	1.82	2.96E-04	LC-MS
159	3-oxo-5S-amino-hexanoic acid	1.81	1.61E-03	LC-MS

160	<b>Sucrose</b>	1.80	1.00E-02	LC-MS
161	N2-(D-1-Carboxyethyl)-L-arginine	1.80	1.50E-02	LC-MS
162	succinamate	1.79	9.81E-04	LC-MS
163	Fructose	1.79	1.83E-03	GC-MS
164	Xanthosine 5'-phosphate	1.77	1.72E-02	LC-MS
165	N6-Methyl-L-lysine	1.75	2.56E-03	LC-MS
166	[FA trihydroxy(4:0)] 2,3,4-trihydroxy-butanoic acid	1.75	5.00E-02	LC-MS
167	<b>Guanosine</b>	1.72	4.32E-04	LC-MS
168	<b>S-Adenosyl-L-methionine</b>	1.72	4.04E-05	LC-MS
169	Asp-Gly	1.68	4.82E-04	LC-MS
170	Mannose	1.67	7.36E-03	GC-MS
171	LysoPC(17:0)	1.66	1.60E-02	LC-MS
172	1-Oleoylglycerophosphocholine	1.65	2.65E-02	LC-MS
173	Glycyl-leucine	1.63	6.03E-05	LC-MS
174	<b>L-Tryptophan</b>	1.62	3.93E-03	LC-MS
175	<b>D-Fructose 1,6-bisphosphate</b>	1.61	5.77E-05	LC-MS
176	Glu-Met	1.60	6.79E-03	LC-MS
177	<b>L-Tyrosine</b>	1.60	2.25E-02	LC-MS
178	<b>Adenosine</b>	1.59	2.09E-03	LC-MS
179	Glucopyranose	1.59	2.94E-01	LC-MS
180	2,7-Anhydro-alpha-N-acetylneuraminic acid	1.58	9.48E-04	LC-MS
181	<b>S-glutathionyl-L-cysteine</b>	1.57	3.31E-01	LC-MS
182	Trehalose	1.55	6.67E-02	GC-MS
183	Glu-Glu-Met	1.55	1.02E-02	LC-MS
184	palmitic acid	1.55	3.72E-01	LC-MS
185	3-Hydroxy-L-kynurenine	1.54	2.01E-02	LC-MS
186	talose	1.53	1.23E-01	LC-MS
187	<b>Allantoin</b>	1.53	7.03E-03	LC-MS
188	[PC (18:0)] 1-octadecanoyl-sn-glycero-3-phosphocholine	1.53	5.89E-02	LC-MS
189	<b>Inosine</b>	1.53	1.45E-01	LC-MS
190	Hypotaurine	1.52	7.01E-03	LC-MS
191	N-Methylnicotinate	1.52	7.37E-02	LC-MS
192	L-Glutamate 5-semialdehyde	1.51	7.86E-04	LC-MS
193	Hexadecasphinganine	1.47	4.54E-02	LC-MS
194	<b>5'-Methylthioadenosine</b>	1.46	1.83E-01	LC-MS
195	<b>N-methyl glucamine</b>	1.46	1.63E-01	LC-MS
196	(R)-2-Hydroxyglutarate	1.45	4.72E-02	LC-MS
197	<b>Deoxyadenosine</b>	1.44	1.83E-01	LC-MS
198	L-pyroglutamic acid	1.44	8.91E-02	GC-MS
199	<b>L-Proline</b>	1.42	4.43E-02	LC-MS
200	<b>L-Cystine</b>	1.42	4.56E-01	LC-MS
201	[PC (18:2)] 1-octadecadienoyl-sn-glycero-3-phosphocholine	1.41	6.86E-02	LC-MS
202	Thr-Asp-Ser	1.40	6.09E-03	LC-MS

203	<b>L-Phenylalanine</b>	1.40	2.19E-02	LC-MS
204	Mannitol	1.39	3.58E-01	GC-MS
205	Phosphoribosyl-AMP	1.39	9.82E-02	LC-MS
206	<b>L-Lysine</b>	1.38	1.62E-02	LC-MS
207	<b>L-Kynurenine</b>	1.38	5.58E-02	LC-MS
208	Trimethylamine N-oxide	1.36	2.34E-03	LC-MS
209	Malonate	1.36	1.18E-01	LC-MS
210	Ala-Asp-Ser	1.36	9.62E-02	LC-MS
211	<b>Adenine</b>	1.35	2.24E-01	LC-MS
212	2-Naphthylamine	1.35	4.76E-02	LC-MS
213	Methyloxaloacetate	1.34	1.31E-02	LC-MS
214	L-Methionine S-oxide	1.34	1.21E-03	LC-MS
215	(S)-Methylmalonate semialdehyde	1.34	2.26E-02	LC-MS
216	Asp-Ser-Ser	1.34	2.95E-01	LC-MS
217	Mannonic acid	1.34	8.58E-02	LC-MS
218	<b>N6,N6,N6-Trimethyl-L-lysine</b>	1.32	1.66E-01	LC-MS
219	<b>Uracil</b>	1.32	3.34E-04	LC-MS
220	D-Galactofuranose	1.31	8.79E-02	LC-MS
221	n-Pentadecanoic acid	1.31	9.48E-02	LC-MS
222	L-cysteine sulfinic acid	1.31	1.16E-01	LC-MS
223	O-Palmitoyl-R-carnitine	1.30	1.69E-01	LC-MS
224	Creatine	1.30	8.74E-02	LC-MS
225	<b>L-Threonine</b>	1.30	1.43E-02	LC-MS
226	Xylitol	1.30	1.91E-03	LC-MS
227	Glu-Met-Thr	1.26	2.80E-01	LC-MS
228	tetracosahexanoic acid	1.22	1.62E-01	LC-MS
229	Methylmalonate	1.21	1.00E-01	LC-MS
230	alpha-ketoglutaric acid	1.20	2.01E-01	GC-MS
231	<b>L-Glutamine</b>	1.20	8.17E-02	LC-MS
232	Tyramine	1.19	2.40E-01	LC-MS
233	N-Methylethanolamine phosphate	1.18	4.96E-01	LC-MS
234	<b>L-Alanine</b>	1.17	2.07E-01	LC-MS
235	Arg-Gln-Ser-Ser	1.17	4.77E-01	LC-MS
236	L-1-Pyrroline-3-hydroxy-5-carboxylate	1.16	8.01E-02	LC-MS
237	Creatinine	1.15	2.32E-01	LC-MS
238	Maltose	1.13	4.76E-01	LC-MS
239	3-Oxopropanoate	1.12	1.02E-01	LC-MS
240	<b>L-serine</b>	1.11	1.58E-01	LC-MS
241	5-6-Dihydrouridine	1.11	2.74E-01	LC-MS
242	Ethyl (R)-3-hydroxyhexanoate	1.10	4.66E-01	LC-MS
243	Cortisone	1.10	7.89E-01	GC-MS
244	<b>D-glucose</b>	1.10	3.26E-01	LC-MS
245	Methylimidazoleacetic acid	1.10	3.58E-01	LC-MS
246	<b>Phenylacetyl glycine</b>	1.10	5.97E-01	LC-MS

247	D-Galactose	1.09	6.83E-01	LC-MS
248	<b>3-Phosphoglycerate</b>	1.09	4.29E-01	LC-MS
249	Propanoic acid	1.08	5.91E-01	LC-MS
250	Sulfoacetaldehyde	1.08	6.24E-01	LC-MS
251	Homocysteine	1.08	7.51E-01	LC-MS
252	<b>Orthophosphate</b>	1.06	8.22E-01	LC-MS
253	10-Hydroxydecanoic acid	1.05	4.54E-01	LC-MS
254	Glycodeoxycholate	1.05	7.75E-01	LC-MS
255	Dodecatetraenedioic acid	1.05	6.00E-01	LC-MS
256	2-C-Methyl-D-erythritol 4-phosphate	1.04	9.17E-01	LC-MS
257	Cys-Cys-His-His	1.04	7.96E-01	LC-MS
258	<b>phosphoenolpyruvic acid</b>	1.03	8.48E-01	LC-MS
259	5-Hydroxyindoleacetate	1.02	8.26E-01	LC-MS
260	Phe-Asp	1.01	9.49E-01	LC-MS
261	phosphoric acid	1.01	9.57E-01	LC-MS
262	N-Acetyl-D-glucosamine 6-phosphate	1.00	9.84E-01	LC-MS
263	Glu-Leu-Thr-His	-1.01	9.61E-01	LC-MS
264	His-Phe-Val-Pro	-1.01	9.66E-01	LC-MS
265	<b>Phenylpyruvate</b>	-1.02	8.64E-01	LC-MS
266	hydroxy-octadecadienoic acid	-1.03	8.40E-01	LC-MS
267	L-Noradrenaline	-1.03	8.39E-01	LC-MS
268	di-n-Undecylamine	-1.03	9.42E-01	LC-MS
269	Fructoselysine	-1.04	6.75E-01	LC-MS
270	Acetamide, N,N-diethyl-	-1.05	3.12E-01	GC-MS
271	3-Butenoic acid	-1.05	1.99E-01	LC-MS
272	glycolic acid	-1.05	3.77E-01	LC-MS
273	Myo-inositol-3-phosphate	-1.05	8.44E-01	GC-MS
274	Erucic acid	-1.06	7.49E-01	GC-MS
275	5-Hydroxypentanoate	-1.07	4.88E-01	LC-MS
276	[FA (20:4)] 5Z,8Z,11Z,14Z-eicosatetraenoic acid	-1.07	6.04E-01	LC-MS
277	Cholest-2-eno[2,3-b]indole, 1'-acetyl-6'-methoxy-	-1.08	5.28E-01	GC-MS
278	N3-methylcytosine	-1.08	6.50E-01	LC-MS
279	D-Threose	-1.08	4.19E-01	LC-MS
280	4-Methylene-L-glutamine	-1.09	6.82E-01	LC-MS
281	2-Phenylacetamide	-1.09	5.21E-01	LC-MS
282	Pyruvate	-1.09	1.13E-03	GC-MS
283	Heptanedioic acid	-1.10	4.02E-01	LC-MS
284	methyl-dihydroxy-pentanoic acid	-1.12	3.39E-01	LC-MS
285	dioxo-octanoic acid	-1.13	3.67E-01	LC-MS
286	amino-undecanoic acid	-1.14	3.49E-01	LC-MS
287	<b>L-Citrulline</b>	-1.17	5.76E-01	LC-MS
288	<b>sn-glycero-3-Phosphocholine</b>	-1.17	7.07E-01	LC-MS
289	Methanesulfonic acid	-1.18	5.11E-01	LC-MS
290	Tetradecanedioic acid	-1.18	3.52E-01	LC-MS

291	P-DPD	-1.18	2.76E-01	LC-MS
292	Phthalic acid	-1.19	6.18E-03	LC-MS
293	4-Acetamidobutanoate	-1.19	1.49E-01	LC-MS
294	myo-Inositol	-1.20	4.94E-01	LC-MS
295	Cyclododecane	-1.20	3.07E-02	GC-MS
296	Gamma-Glutamylglutamine	-1.21	1.26E-01	LC-MS
297	N4-acetyl-N4-hydroxy-1-aminopropane	-1.22	4.86E-01	LC-MS
298	5-oxo-7-octenoic acid	-1.22	1.24E-01	LC-MS
299	2-Acetolactate	-1.24	3.78E-01	LC-MS
300	Urea	-1.26	4.61E-01	GC-MS
301	Elaidiccarnitine	-1.26	2.77E-01	LC-MS
302	d-Xylose	-1.27	4.61E-01	LC-MS
303	D-Glycerate	-1.28	9.06E-02	LC-MS
304	<b>Lactate</b>	-1.29	2.85E-01	LC-MS
305	2-acetamidoglucal	-1.30	7.17E-03	LC-MS
306	Heme	-1.32	3.71E-01	LC-MS
307	D-4'-Phosphopantothenate	-1.35	5.89E-02	LC-MS
308	<b>Glycerol</b>	-1.39	1.43E-03	LC-MS
309	Met-Ala-Gly	-1.40	6.53E-02	LC-MS
310	Urate	-1.41	1.34E-01	LC-MS
311	Stearic acid	-1.44	8.78E-02	GC-MS
312	4-Guanidinobutanoate	-1.44	3.24E-03	LC-MS
313	Deoxycytidine	-1.47	1.75E-01	LC-MS
314	2-monooleoylglycerol	-1.53	1.16E-02	LC-MS
315	6-[3]-ladderane-1-hexanol	-1.56	9.22E-02	LC-MS
316	4-Hydroxy-L-threonine	-1.59	1.30E-05	LC-MS
317	Val-Asp-Gly	-1.60	1.09E-04	LC-MS
318	Ala-Ser	-1.64	3.31E-04	LC-MS
319	Heptadecanoic acid	-1.64	4.55E-02	GC-MS
320	Leu-Ala	-1.76	1.04E-04	LC-MS
321	9,12-octadecadienal	-1.79	1.70E-01	LC-MS
322	Thr-Ala-Asp	-1.80	9.52E-05	LC-MS
323	N-Acetyl-D-glucosamine	-1.94	1.55E-05	LC-MS
324	D-Sorbitol	-2.11	8.20E-09	LC-MS
325	<b>L-Histidine</b>	-2.40	2.99E-08	LC-MS
326	N-Ribosylnicotinamide	-2.42	1.97E-03	LC-MS
327	octadecenamide	-2.76	1.60E-01	LC-MS
328	Valine	-2.85	2.69E-03	GC-MS
329	Cellobiose	-2.95	9.12E-02	GC-MS
330	N5-(L-1-Carboxyethyl)-L-ornithine	-3.10	1.01E-08	LC-MS
331	Hexose phosphate	-3.55	5.65E-10	LC-MS
332	3-beta-D-Galactosyl-sn-glycerol	-5.38	1.68E-06	LC-MS
333	Leu-Lys-Asp	-5.64	1.04E-08	LC-MS

Table S2. List of primers.

Primer	Sequence	Comments
GU2051	GATAATGTCTACTTTTTCTTTG	<i>pepc</i> 5'homology arm forward
GU2052	TATATAGCTGCTTGAGACAC	<i>pepc</i> 5' homology arm reverse
GU2053	GCAAAATACCGGATAACTC	<i>pepc</i> 3'homology arm forward
GU2054	TTTAGGAAACCAATCAAAGAG	<i>pepc</i> 3' homology arm reverse
GU2057	GGGCTTTATACTATTTTTTTGTC	<i>pepc</i> ko 5' integration forward
GU2058	TATCGTGGTAGAGTAAAACCTG	<i>pepc</i> ko 3' integration reverse
GU2059	CATGATTTATCCGAAAAATATAGTG	<i>pepc</i> orf forward
GU2060	GTGCTTTATATACATATAACAACAC	<i>pepc</i> orf reverse
GU2198	GGAATTATAATTCTTAACCCTAACATTTAACCTCTC	<i>mdh</i> 5'homology arm forward
GU2199	CTTGTCGTATATGCACTCGGTGTTGG	<i>mdh</i> 5' homology arm reverse
GU2200	CCTTAAATGGATAGTCAAATTGATCGTACACAATAA	<i>mdh</i> 3'homology arm forward
GU2201	CATCTCTAATTCGTTAGAATTTATTATAGACTACG	<i>mdh</i> 3' homology arm reverse
GU2278	CCACTGTAATCATAGAACAGTTCAACTAC	<i>mdh</i> ko 5' integration forward
GU2279	CAAGATTAGTACACATTGGATTAATGGG	<i>mdh</i> ko 3' integration reverse
GU2280	CATTAATAGGAAGTGGCCAAATAGGG	<i>mdh</i> orf forward
GU2281	GATAGCAAGCTTGTTCTTCTCTGTC	<i>mdh</i> orf reverse
GU2190	CCTTTTCCTTTTGTTTTATCCATCCATTTA	<i>opr</i> t 5'homology arm forward
GU2191	AATCTCAAATTGTGAAATAACAATAAAAAATTTTGTC	<i>opr</i> t 5' homology arm reverse
GU2192	CTGAGTTCTGTATTTACTTTTCATAAGTTTTAAACG	<i>opr</i> t 3'homology arm forward
GU2193	CCCACATAAGTAAATATACATACATATTATTATGC	<i>opr</i> t 3' homology arm reverse
GU2286	CTTAAATTAGCATTACTGCGTACATCCC	<i>opr</i> t ko 5' integration forward
GU2610	GAGCTAGCTGAAAGTTGCAAT	<i>opr</i> t ko 3' integration reverse
GU2288	GATGAAGAATTACACAAAAAATACAATGAATTATGC	<i>opr</i> t orf forward
GU2289	GTGAAATATCTTCTTCATAATTAAGGATGC	<i>opr</i> t orf reverse
GU2194	GATGCTCTCTCGTATATCCGTTTAAATTAC	<i>ompdc</i> 5'homology arm forward
GU2195	GCTAGCTATGAATTTTAGTTGATAGATTTTTTATTTG	<i>ompdc</i> 5' homology arm reverse
GU2196	GAATACATTGAGTTTAAACGGAACCTCAATTTAATAGCC	<i>ompdc</i> 3'homology arm forward
GU2197	GCATGCAATATTGGCAATACATGAAAACGAATTAATAT	<i>ompdc</i> 3' homology arm reverse
GU2282	GCACCCATATTTATATCAACATTTCTATCAG	<i>ompdc</i> ko 5' integration forward
GU2283	GCACAATTTTACATATCGATATATGTACAATG	<i>ompdc</i> ko 3' integration reverse
GU2284	GTATTGGGTTGGATCCTGATGAAG	<i>ompdc</i> orf forward
GU2285	CTTGTTCAATATTACCACCATTTTCTATGTC	<i>ompdc</i> orf reverse
GU2061	GTAAACTTAAGCATAAAGAGCTCG	5' integration reverse (in plasmid)
GU0204	GTCTCTTCAATGATTCATAAATAG	3' integration forward (in plasmid)

## Supplementary figures

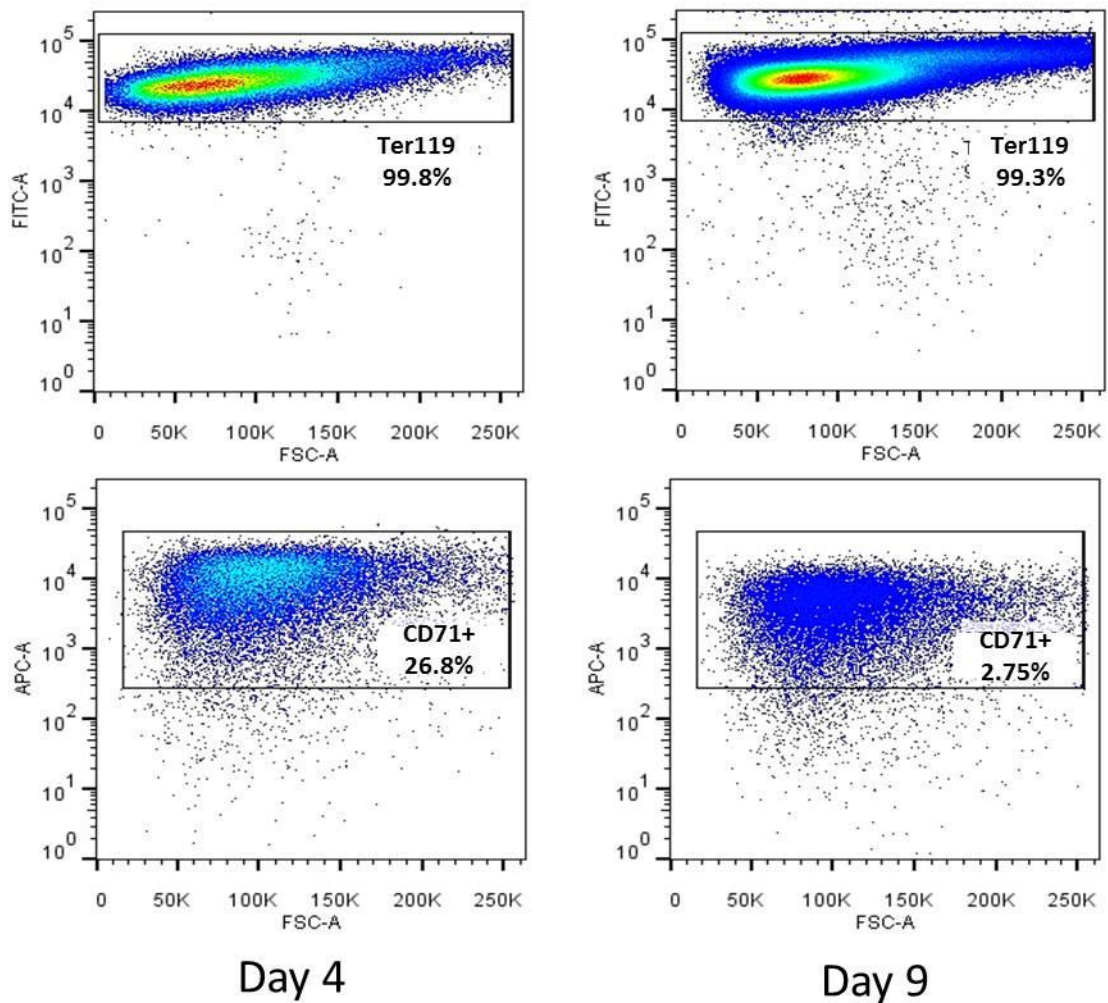


**Figure S1A. Characterisation of the enriched reticulocyte population induced by Phenylhydrazine-HCl (PHZ) by FACS analysis.** CD71 (transferrin receptor) is a reticulocyte specific marker and is lost as erythrocytes mature. Left panels- day 4 post phz treatment, right panels- day 9 post phz treatment. Top panels show Ter119-FITC staining in RBCs which stains all erythroid cells. Bottom panels show CD71-APC staining in RBCs which stains only reticulocytes.

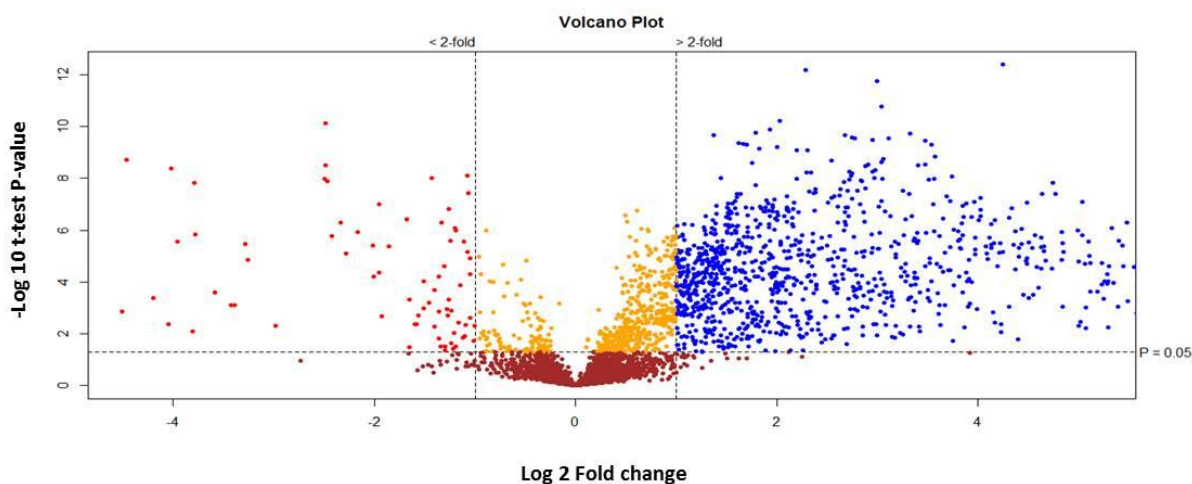


**Figure S1B.** Volcano plot showing the distribution of abundance of all ~4560 peaks detected across both LC-MS and GC-MS platforms in reticulocytes as compared to normocytes in rodent blood. All significant changes are represented above the broken horizontal line. Coloured dots indicate peaks which are: Blue- significantly up-regulated, Red- significantly down-regulated, Yellow- significant but little change, Brown- non-significant. n=3 independent biological replicates (with four internal technical replicates each). Significance tested by Welch's T-test ( $\alpha < 0.05$ ). Of the ~4,230 unassigned mass features/peaks, 1051 (~23%) were up-regulated and 91 peaks (~2%) downregulated in the reticulocyte-enriched fraction.

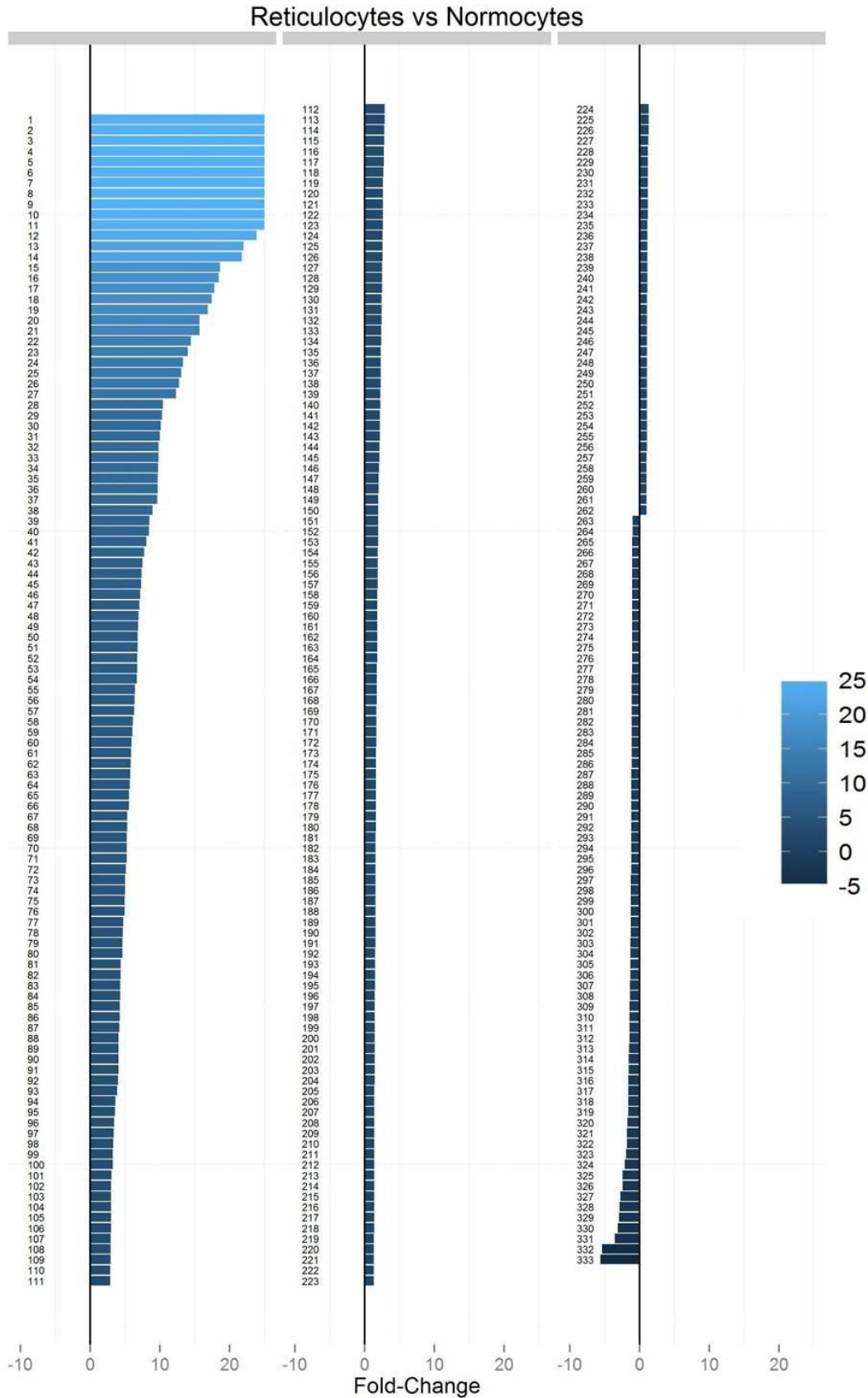
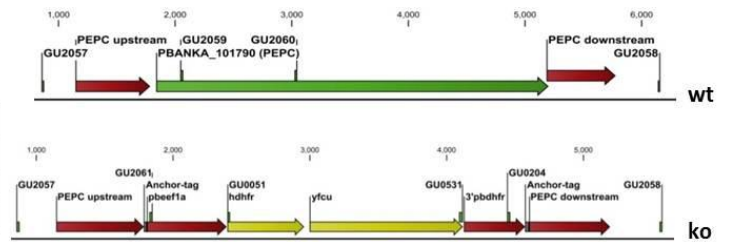


**Figure S1C. Fold change of metabolite abundance in rodent reticulocytes as compared to normocytes. See table S1 for metabolite names corresponding to numbers**

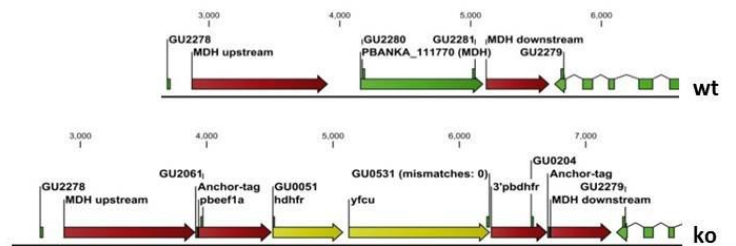
(i) *pepc* (PBANKA\_101790)

Primers	Product	Size
GU2057+GU2061	5' integration	1kb
GU0204+GU2058	3' integration	1.1kb
GU2059+GU2060	ORF	1kb



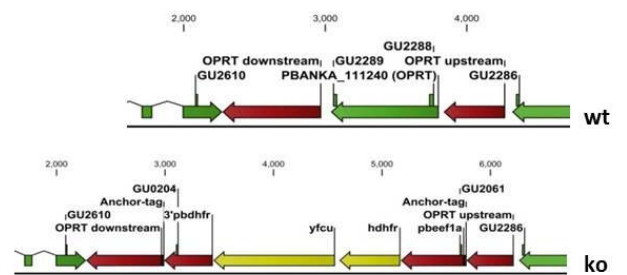
(ii) *mdh* (PBANKA\_111770)

Primers	Product	Size
GU2278+GU2061	5' integration	1.3kb
GU0204+GU2279	3' integration	0.75kb
GU2280+GU2281	ORF	0.87kb



(iii) *opr* (PBANKA\_111240)

Primers	Product	Size
GU2286+GU2061	5' integration	0.6kb
GU0204+GU2610	3' integration	1.0kb
GU2288+GU2289	ORF	0.7kb



(iv) *ompdc* (PBANKA\_050740)

Primers	Product	Size
GU2282+GU2061	5' integration	1.2kb
GU0204+GU2283	3' integration	1.4kb
GU2284+GU2285	ORF	0.9kb

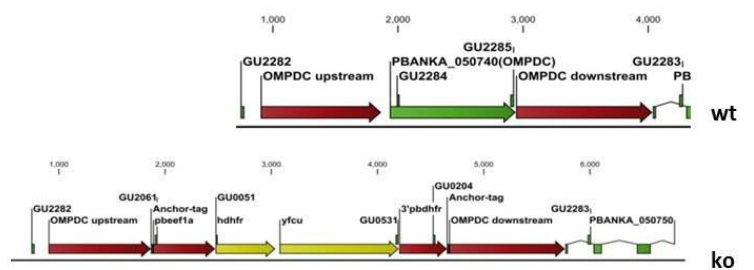
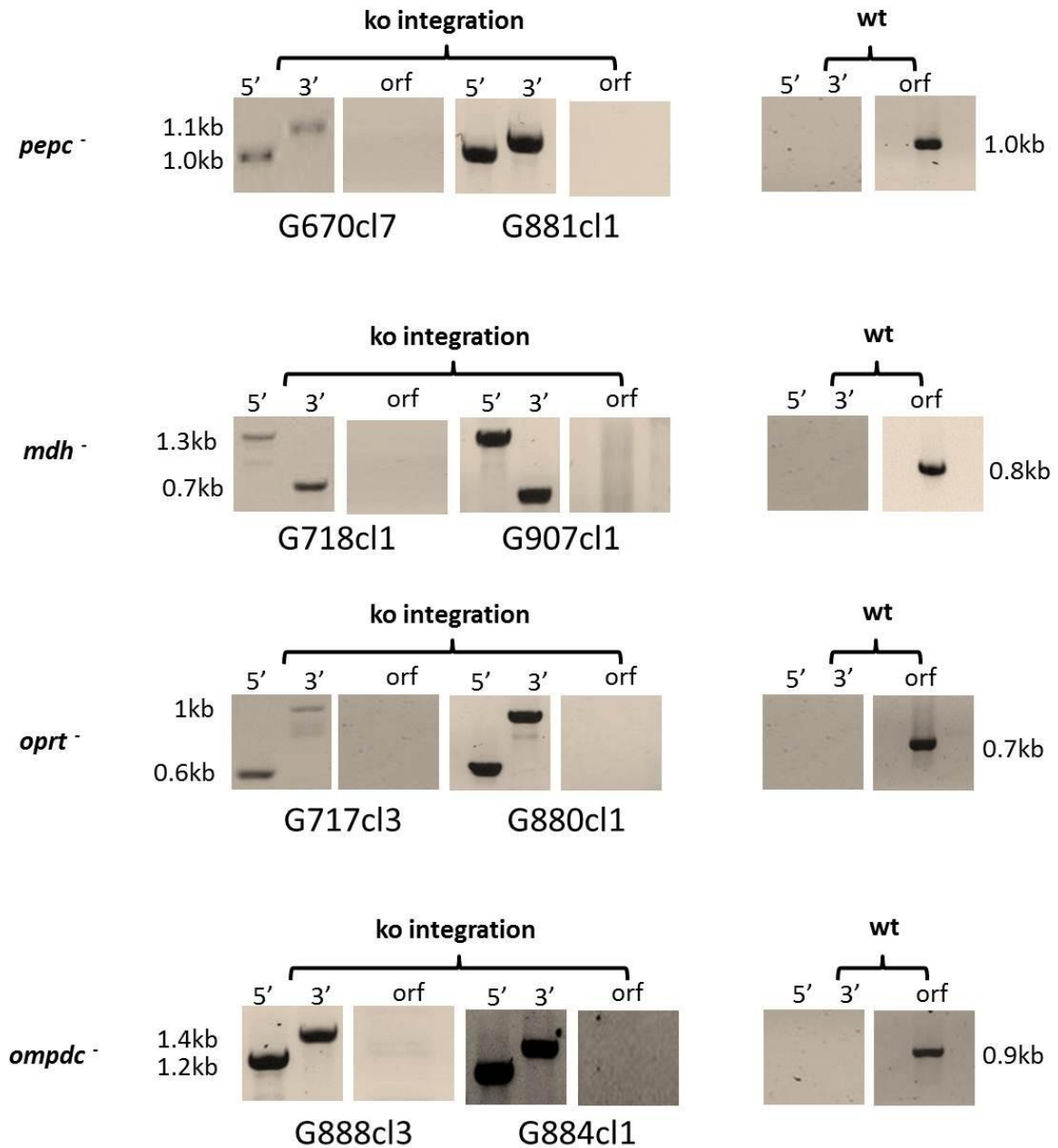
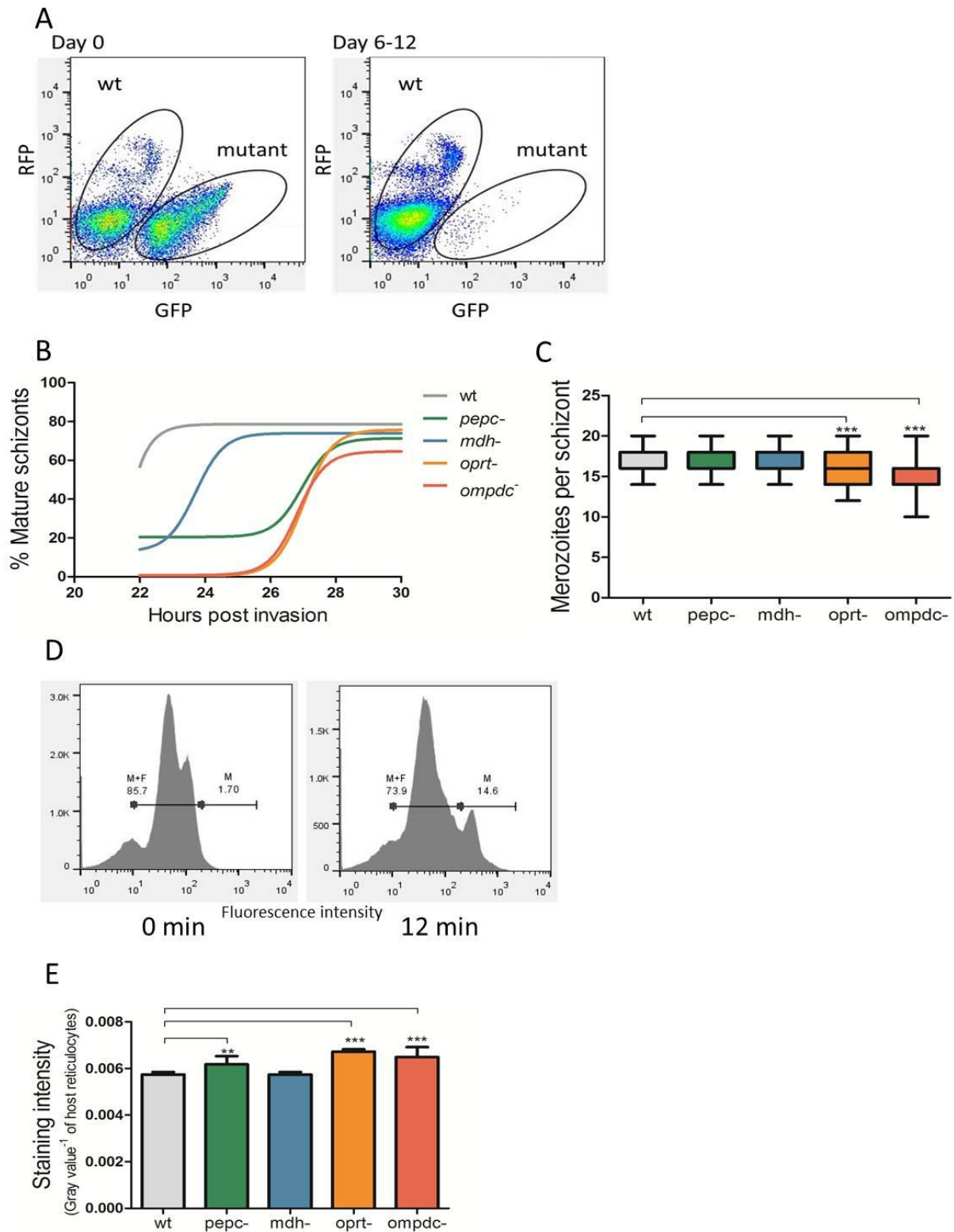


Figure S2A. Schematic representation of gene deletion strategy.



**Figure S2B. Gel electrophoresis of indicated PCR products to confirm integration of selection cassette, disruption of genes and clonality of mutant parasites (i) *pepc* (PBANKA\_101790) (ii) *mdh* (PBANKA\_111770) (iii) *opt* (PBANKA\_111240) (iv) *ompdc* (PBANKA\_050740)**



**Figure S3 Phenotypic characterization of blood stage mutant *P. berghei* parasites**

A. Competition growth assay using FACS analysis. Equal number of parasites ( $10^6$ ) of wt population expressing RFP under constitutive promoter *eef1a* (RMgm-86) and mutant population made in a parent line expressing GFP under the same promoter (RMgm-7) were

mixed and injected into a mouse on day 0 and peripheral blood from the infected mouse was monitored using FACS analyses for the proportion of RFP positive (wt) and GFP positive (mutant) parasites over the next 12 days. Representative FACS screenshots show left panel on day 0 when wt and mutant populations are in equal proportions and right panel shows that over time (by days 6-12), wt population overgrows a slow growing mutant. Infected blood was passaged into a new mouse when multiple infected cells started to appear to allow for optimal growth.

- B. Time taken for asexual parasites to grow to mature schizont stage. Coloured lines indicate non-linear fit of percentage of mature schizonts observed in *in vitro* synchronous cultures of wt and mutant *P. berghei* parasites 22 hours post invasion. Data representative of n=3 independent biological replicates. *pepc*<sup>-</sup>, *opr*<sup>t</sup> and *ompc*<sup>-</sup> mutants took 4-5 hours longer to mature to schizonts compared to wt.
- C. Number of merozoites per schizont grown in *in vitro* cultures as counted in giemsa stained smears. The error is given as the SD of n ≥ 40 schizonts. Data representative of 3 independent biological replicates. P-values: \*\*\*p<0.0005, unpaired two tailed t-test. The number of merozoites observed in mature schizont stages in both *pepc*<sup>-</sup> (17.02 ± 1.8) and *mdh*<sup>-</sup> (17.41 ± 1.7) mutants are similar to wt (17.4±1.8). Both *opr*<sup>t</sup> mutants (15.9 ± 2.0) and *ompc*<sup>-</sup> mutants (15.2 ± 2.5) were found to generate, on average, significantly fewer merozoites than wt per schizont.
- D. FACS plots showing DNA replication in male gametocytes observed by FACS analysis at the start of and 12 min post activation. DNA content was determined in Hoechst-33258-stained purified gametocytes and fluorescence intensity is displayed on x-axis and cell counts on y-axis. Before activation (0 min) males and females are shown in a gate with the same low DNA content (M+F). At 12 mins, prior to the formation of free male gametes, the DNA content of males increases as shown in gate (M).
- E. Intensity of Giemsa staining in wt and mutant *P. berghei* infected reticulocytes. Intensity of the stain was found to be maximum in youngest reticulocytes. Smears were stained with 12% Giemsa stain for 10 minutes after fixing and air drying with methanol. Image data was processed in ImageJ. Gray values were calculated in minimum 100 pixels across the whole host cell (parasites inside the cells were excluded) and staining intensities (Gray value<sup>-1</sup>) were plotted for n=20 infected cells. P-values: \*\*p<0.005, \*\*\*p<0.0005, paired two tailed t-test.

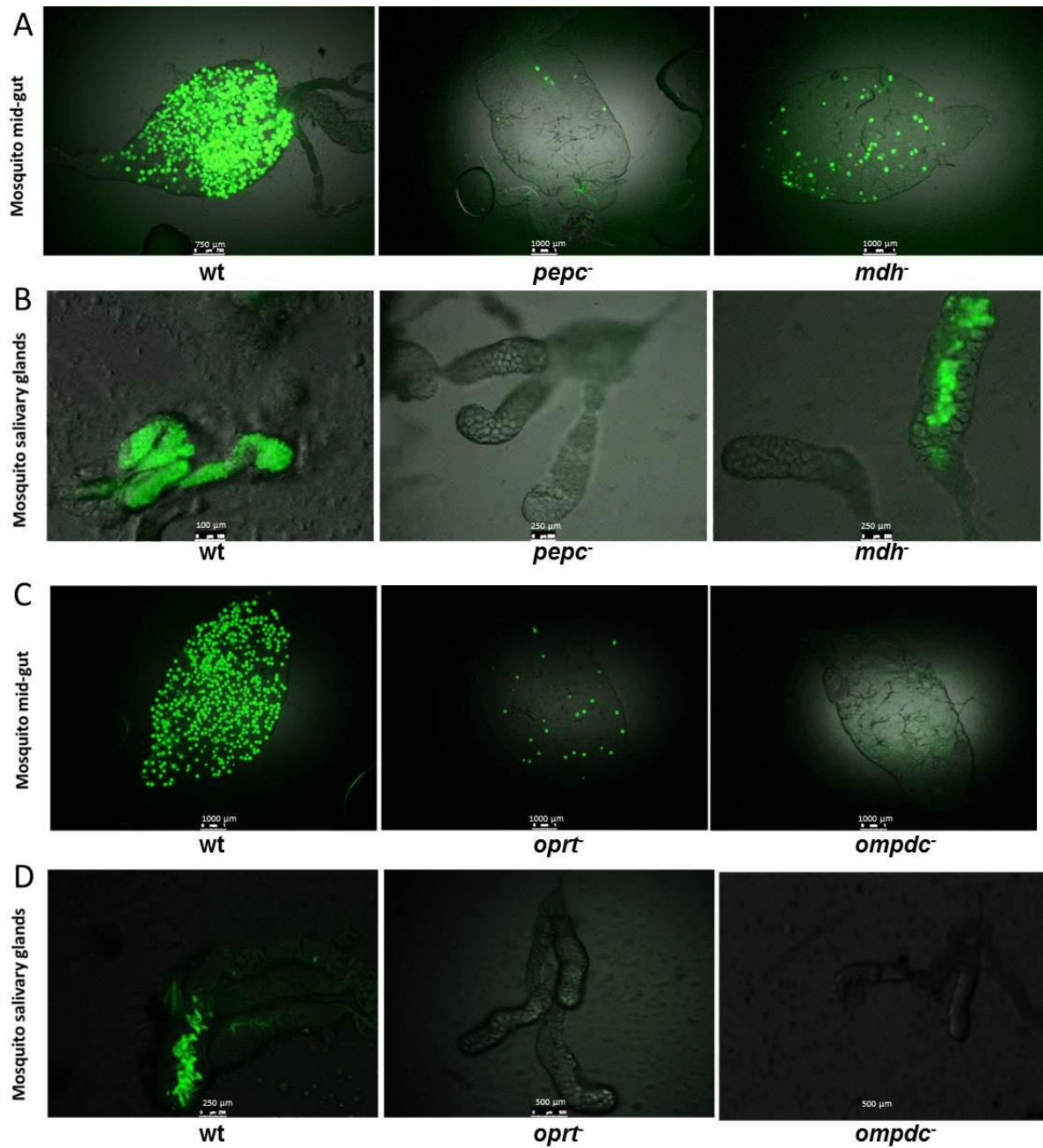


**Figure S4. *P. berghei* infected mosquito midguts and salivary glands as observed on a Leica M205 FA fluorescence stereomicroscope**

- A. Mosquito mid guts showing mature oocysts at day 14 post infection in *wt*, *pepc*<sup>-</sup> and *mdh*<sup>-</sup> *P.berghei* infected mosquitoes.
- B. Mosquito salivary glands showing sporozoites at day 21 post infection in *wt*, *pepc*<sup>-</sup> and *mdh*<sup>-</sup> *P.berghei* infected mosquitoes.
- C. Mosquito mid guts showing mature oocysts at day 14 post infection in *wt*, *opr*<sup>-</sup> and *ompc*<sup>-</sup> *P.berghei* infected mosquitoes.

- D. Mosquito salivary glands showing sporozoites at day 21 post infection in wt, *opr1*<sup>-</sup> and *ompdc*<sup>-</sup> *P.berghei* infected mosquitoes.

Figure S5

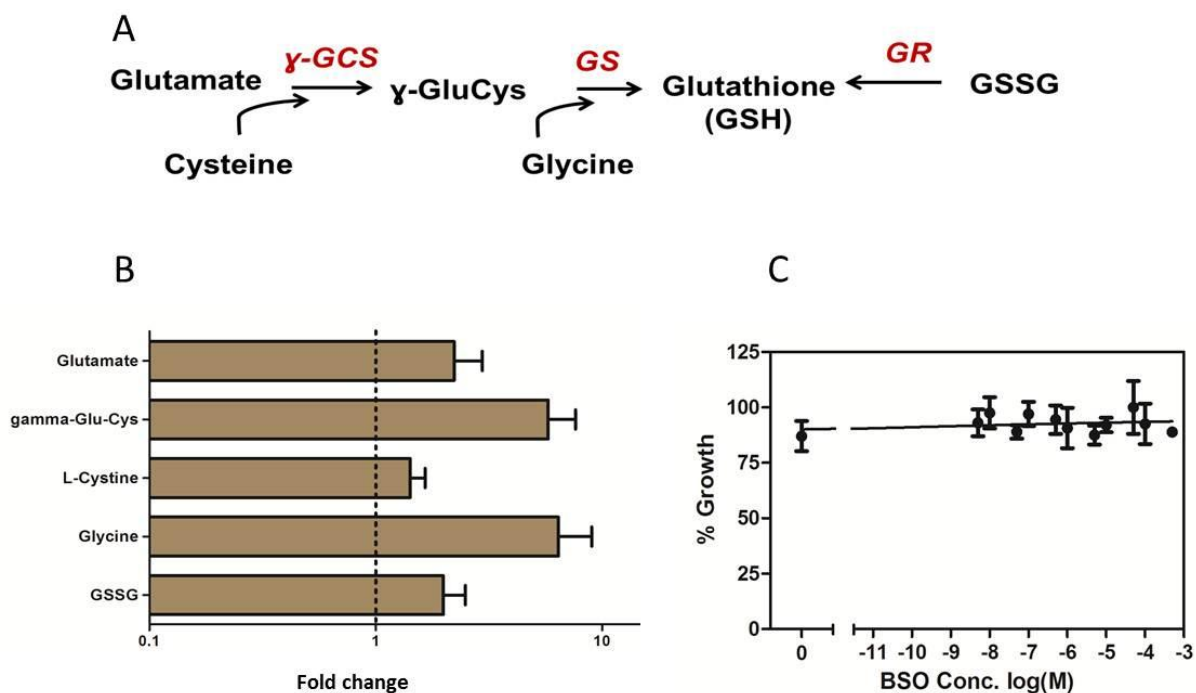


**Figure S5. Glutathione biosynthesis pathway in *Plasmodium***

- A. Schematic representation of glutathione synthesis pathway in *Plasmodium*.  $\gamma\text{-GCS}$  ( $\gamma$ -glutamylcysteine synthetase), *GS* (glutathione synthetase), *GR* (glutathione reductase)  $\gamma\text{-GluCys}$  ( $\gamma$ -L-glutamyl-L-cysteine), GSSG (glutathione disulphide).
- B. Fold change of relative levels (peak intensities) of metabolites of glutathione biosynthesis in rodent reticulocytes compared to normocytes. Dotted line indicates no change and error bars indicate R.S.D. (Relative Standard Deviation) of peak intensities from reticulocyte samples multiplied to the fold change values from n=3 independent biological replicates. It is expected that under these metabolomics extraction conditions the oxidised forms of cystine and glutathione disulphide likely represent the sum of both oxidised and reduced forms of cysteine and glutathione.
- C. *P. berghei* inhibition experiment with buthionine sulfoximine (BSO) *in vitro*. Error bars indicate S.D. from n=2 biological replicates.

